NEUROIMAGING AND INFORMATICS FOR SUCCESSFUL AGING

EDITED BY: Toshiharu Nakai, Eric Tatt Wei Ho, Henning Müller, Fanpei G. Yang and Hanna Lu

PUBLISHED IN: Frontiers in Human Neuroscience, Frontiers in Aging Neuroscience, Frontiers in Aging and Frontiers in Neuroinformatics

frontiers Research Topics

frontiers

ISSN 1664-8714
ISBN 978-2-88976-897-4
DOI 10.3389/978-2-88976-897-4

About Frontiers

Frontiers is more than just an open-access publisher of scholarly articles: it is a pioneering approach to the world of academia, radically improving the way scholarly research is managed. The grand vision of Frontiers is a world where all people have an equal opportunity to seek, share and generate knowledge. Frontiers provides immediate and permanent online open access to all its publications, but this alone is not enough to realize our grand goals.

Frontiers Journal Series

The Frontiers Journal Series is a multi-tier and interdisciplinary set of open-access, online journals, promising a paradigm shift from the current review, selection and dissemination processes in academic publishing. All Frontiers journals are driven by researchers for researchers; therefore, they constitute a service to the scholarly community. At the same time, the Frontiers Journal Series operates on a revolutionary invention, the tiered publishing system, initially addressing specific communities of scholars, and gradually climbing up to broader public understanding, thus serving the interests of the lay society, too.

Dedication to Quality

Each Frontiers article is a landmark of the highest quality, thanks to genuinely collaborative interactions between authors and review editors, who include some of the world's best academicians. Research must be certified by peers before entering a stream of knowledge that may eventually reach the public - and shape society; therefore, Frontiers only applies the most rigorous and unbiased reviews.
Frontiers revolutionizes research publishing by freely delivering the most outstanding research, evaluated with no bias from both the academic and social point of view. By applying the most advanced information technologies, Frontiers is catapulting scholarly publishing into a new generation.

What are Frontiers Research Topics?

Frontiers Research Topics are very popular trademarks of the Frontiers Journals Series: they are collections of at least ten articles, all centered on a particular subject. With their unique mix of varied contributions from Original Research to Review Articles, Frontiers Research Topics unify the most influential researchers, the latest key findings and historical advances in a hot research area! Find out more on how to host your own Frontiers Research Topic or contribute to one as an author by contacting the Frontiers Editorial Office: frontiersin.org/about/contact

NEUROIMAGING AND INFORMATICS FOR SUCCESSFUL AGING

Topic Editors:
Toshiharu Nakai, Osaka University, Japan
Eric Tatt Wei Ho, Universiti Teknologi PETRONAS, Malaysia
Henning Müller, University of Applied Sciences and Arts of Western Switzerland, Switzerland
Fanpei G. Yang, National Tsing Hua University, Taiwan
Hanna Lu, The Chinese University of Hong Kong, China

Citation: Nakai, T., Ho, E. T. W., Müller, H., Yang, F. G., Lu, H., eds. (2022). Neuroimaging and Informatics for Successful Aging. Lausanne: Frontiers Media SA. doi: 10.3389/978-2-88976-897-4

Table of Contents

frontiers | Frontiers in Human Neuroscience

TYPE Editorial
PUBLISHED 28 July 2022
DOI 10.3389/fnhum.2022.976524

OPEN ACCESS

EDITED AND REVIEWED BY
Leonhard Schilbach,
Ludwig Maximilian University of Munich, Germany

*CORRESPONDENCE
Toshiharu Nakai
nakai.iniinf@gmail.com

SPECIALTY SECTION
This article was submitted to Brain Health and Clinical Neuroscience, a section of the journal Frontiers in Human Neuroscience

RECEIVED 23 June 2022
ACCEPTED 12 July 2022
PUBLISHED 28 July 2022

CITATION
Nakai T, Ho ETW, Müller H, Yang FG and Lu H (2022) Editorial: Neuroimaging and informatics for successful aging.
Front. Hum. Neurosci. 16:976524.
doi: 10.3389/fnhum.2022.976524

Editorial: Neuroimaging and informatics for successful aging

Toshiharu Nakai[1,2]*, Eric Tatt Wei Ho[3], Henning Müller[4,5], Fanpei G. Yang[6,7] and Hanna Lu[8]

[1]Institute of NeuroImaging and Informatics, Obu, Japan, [2]Department of Dental Radiology, Graduate School of Dentistry, Osaka University, Suita, Japan, [3]Center for Intelligent Signal and Imaging Research, Universiti Teknologi Petronas, Perak, Malaysia, [4]Institute of Information Systems, University of Applied Sciences and Arts of Western Switzerland HES-SO Valais-Wallis, Sierre, Switzerland, [5]Département de Radiologie et Informatique Médicale, Université de Genève, Geneva, Switzerland, [6]Department of Foreign Languages and Literature, National Tsing Hua University, Hsinchu, Taiwan, [7]Center for Cognition and Mind Sciences, National Tsing Hua University, Hsinchu, Taiwan, [8]Department of Psychiatry, The Chinese University of Hong Kong, Shatin, Hong Kong SAR, China

KEYWORDS

neuroinformatics, older adults, aging, neuroimaging, cognitive intervention, cohort study, neurotechnology, BrainConnects

Editorial on the Research Topic
Neuroimaging and informatics for successful aging

Aging of adults usually involves cognitive decline due to various neuronal pathologies and neurophyonsiological changes, resulting in the so-called "geriatric syndrome" in aging. This puts older adults beyond a certain age at a high risk of getting lost and of falling due to declined attention levels, memorization, visuospatial processing and judgments. In this perspective, the increase in life expectancy around the world must be accompanied by health maintenance, social and intellectual participation and individual security toward "successful aging" that aims at limiting some of the negative effects and risks. In order to achieve a better quality of life, various social programs promoting physical activities for older adults are widely organized depending on the social backgrounds and cultures in each country. However, the outcomes of cognitive and physical interventions have been controversial among behavioral studies because of instability and reduced capacity of cognitive functions under progressive cognitive decline as well as difficulty of methodological standardization. Since physical and cognitive intervention protocols are designed based on the popularity of the activity and physical potential of the participants, the response to the interventions may vary among individuals. This renders objective evaluation very complex and prone to evaluation errors due to the high intra-variability reflecting individual differences and often small effect sizes in studies. Thus, we need to develop an objective approach to extract and classify important factors to maintain to support cognitive function and physical activity. This should include not only structured data but should really mix imaging data on neural activities and decline as well as structured data and possibly other measurements. The importance is to find and analyze the links between the data systematically.

In this respect, we recognize that successful aging strongly depends on successful brain aging, and functional and structural neuroimaging are excellent tools to objectively evaluate and (quantitatively) measure specific factors such as plastic change, i.e., compensation, reorganization, and remodeling of aging brains undergoing cognitive and

physical decline. Integration of different types of information, such as fMRI, DTI, EEG, or NIRS, as well as neurofeedback from performance or physiological monitoring to optimize learning can enhance the precision. Larger studies with quantitative measures could also really advance this field, as well as inclusion of other factors that can have an influence on cognitive decline, for example behavioral changes (smoking, alcohol, sports, …). The goal of this Research Topic is to explore the role of functional and structural neuroimaging together with neuroinformatics and neurotechnologies to reach "successful brain aging" and further develop an emerging and multidisciplinary field of "aging neuroinformatics."

This Research Topic, "*Neuroimaging and Informatics for Successful Aging*," is a result of a long standing international annual research workshop called BrainConnects that started in 2014. The 7th annual meeting, BrainConnects 2020, was transformed into a special issue in Frontiers to overcome the on-going SARS-CoV-2 pandemic. The main goal of this scientific collaboration is to develop and exchange methods and technologies for delaying and modulating neurocognitive changes due to aging that can help enhance and accelerate the projects promoted by the participants from various countries. Our annual interdisciplinary workshop provides an opportunity to introduce and review the ongoing investigations of the dynamics of neuronal circuits in response to cognitive interventions, as well as to promote collaboration among the participating research groups and to nurture young investigators.

Sixteen papers including 3 reviews by 115 authors from 11 countries were judged by 39 reviewers from 18 countries and published across 4 journals in this Research Topic. The study type of the papers can be summarized as the following; four cohort studies evaluated the dependency of a resting state network (RSN) on aging as a biomarker of cognitive performance (Maesawa et al.; Watanabe et al.) and morphologic change (Dominguez et al.; Md Ashraf et al.). Two papers used blood samples to investigate the relationship between plasma amyloid concentration and PET findings (Huang et al.) or biochemical data and brain activation detected by fMRI (You et al.). As neurophysiological studies, the age-related changes of basal ganglia in motor control were explored (Rodorigez-Sabata et al.) and EEG characteristics of Alzheimer disease were reviewed (Yu et al.). As a cellular level approach, an automata model of the aging brain was proposed (Ramos et al.). Brain-wide measures of good cognition in healthy aged brains serve as a potential target for a variety of healthy aging interventions. The RSN patterns identified by Maesawa et al. could be especially meaningful for developing neurofeedback interventions whereas the cortical thickness parameters obtained by Dominguez et al. are relevant to lifestyle-related interventions such as cognitive activities and nutrition.

Six papers reported the effects of cognitive/physical interventions, such as mindful training (Sevinc et al.), verbal training (Fong et al.; Yang et al.; Yoske et al.), musical training (Yamashita, Ohsawa, et al.) or physical training (Yamashita, Suzuki, et al.) on behavioral and neuroimaging outcome and their correlations. The concern regarding verbal training as a method of intervention for older adults may come from its familiarity with the subjects, raising the motivation to train, since languages have an essential role in social participation and human relationships. The use of verbal training as a method of intervention has shown to improve network connectivity and enhance frontal-temporal network activity. Neurotechnology is emerging as an alternative therapy to behavioral interventions and here, state-of-art research into the applications of deep brain stimulation to ameliorate the symptoms of neurodegenerative disease in aging was reviewed by Silverio and Silverio with an emphasis on the electronic circuit technologies required to implement the therapy.

To summarize, these papers span four thematic areas : (i) characterizing the neurodegenerative aspects of aging on the brain (Md Ashraf et al.; Huang et al.; Ramos et al.; Rodriguez-Sabate et al.; Watanabe et al.; Yu et al.; You et al.) (ii) measures of healthy aging in the brain (Maesawa et al.; Dominguez et al.) (iii) evidence of behavioral interventions toward promoting healthy aging in the brain (Fong et al.; Sevinc et al.; Yang et al.; Yeske et al.; Yamashita, Ohsawa, et al.; Yamashita, Suzuki, et al.) and (iv) prospects for a neurotechnology-based therapy to address aspects of aging-linked neurodegenerative disease (Silverio et al.). The papers in area (i) are mostly from clinical side, however, two papers have strong background of engineering science (Md Ashraf et al.; Ramos et al.). Area (ii) is cohort study, studies in area (iii) are approaches from cognitive neuroscience, and area (iv) is engineering science.

The collection of papers in this Research Topic originated from several continents, demonstrating the strong commitment of BrainConnects to link scientists from various disciplines to continue our scientific discourse with a larger community interested in the neurobiology of aging and ways to influence it. We hope that these research articles will share our excitement and enthusiasm for further research collaborations and discussions amongst our readership. We aim to continue research investigations that will bring about meaningful outcomes to answer some of the pressing questions related to cognitive and mental health in aging. Together, we have the common goals of using neurotechnologies and informatics based on solid data to understand and develop innovative methods for successful aging. Expertise in neuroinformatics, such as computational modeling and simulation, data structuring and management, signal recording and processing, atlasing, and ontologies will further evolve aging research to find solutions for the limitations as discussed in each article in this Research Topic.

Author contributions

All authors listed have made a substantial, direct, and intellectual contribution to the work and approved it for publication.

Acknowledgments

The Guest Editors would like to express their profound gratitude to Prof S. H. Annabel Chen (Nanyang Technological University), Dr. Jacqueline Dominguez (St Luke's Medical Center) and Dr. Huong Thi Thanh Ha (Vietnam National University in Ho Chi Minh City) from the BrainConnects community. BrainConnects is acknowledged as a special interest group of International Neuroinformatics Coordinating Facility (incf).

Conflict of interest

The authors declare that the research was conducted in the absence of any commercial or financial relationships that could be construed as a potential conflict of interest.

Publisher's note

frontiers in Aging Neuroscience

ORIGINAL RESEARCH
published: 27 August 2021
doi: 10.3389/fnagi.2021.702796

Mindfulness Training Improves Cognition and Strengthens Intrinsic Connectivity Between the Hippocampus and Posteromedial Cortex in Healthy Older Adults

Gunes Sevinc[1]†, Johann Rusche[1,2†], Bonnie Wong[3], Tanya Datta[1], Robert Kaufman[1], Sarah E. Gutz[1,4], Marissa Schneider[1], Nevyana Todorova[1,5], Christian Gaser[6], Götz Thomalla[2], Dorene Rentz[3,7], Bradford D. Dickerson[1,3] and Sara W. Lazar[1]*

[1] Department of Psychiatry, Massachusetts General Hospital, Harvard Medical School, Boston, MA, United States, [2] Kopf- und Neurozentrum, Department of Neurology, University Medical Center Hamburg-Eppendorf, Hamburg, Germany, [3] Department of Neurology, Massachusetts General Hospital, Harvard Medical School, Boston, MA, United States, [4] Program in Speech and Hearing Bioscience and Technology, Harvard Medical School, Boston, MA, United States, [5] Department of Behavioral Neuroscience, College of Science, Northeastern University, Boston, MA, United States, [6] Department of Psychiatry and Neurology, Jena University Hospital, Jena, Germany, [7] Department of Neurology, Brigham and Women's Hospital, Harvard Medical School, Boston, MA, United States

OPEN ACCESS

Edited by:
Hanna Lu, The Chinese University of Hong Kong, China

Reviewed by:
Atsunobu Suzuki, The University of Tokyo, Japan
Sindhuja T. Govindarajan, University of Pennsylvania, United States

***Correspondence:**
Gunes Sevinc
guenessevinc@gmail.com

† These authors have contributed equally to this work and share first authorship

Received: *29 April 2021*
Accepted: *09 August 2021*
Published: *27 August 2021*

Citation:
Sevinc G, Rusche J, Wong B, Datta T, Kaufman R, Gutz SE, Schneider M, Todorova N, Gaser C, Thomalla G, Rentz D, Dickerson BD and Lazar SW (2021) Mindfulness Training Improves Cognition and Strengthens Intrinsic Connectivity Between the Hippocampus and Posteromedial Cortex in Healthy Older Adults. Front. Aging Neurosci. 13:702796. doi: 10.3389/fnagi.2021.702796

Maintaining optimal cognitive functioning throughout the lifespan is a public health priority. Evaluation of cognitive outcomes following interventions to promote and preserve brain structure and function in older adults, and associated neural mechanisms, are therefore of critical importance. In this randomized controlled trial, we examined the behavioral and neural outcomes following mindfulness training (n = 72), compared to a cognitive fitness program (n = 74) in healthy, cognitively normal, older adults (65–80 years old). To assess cognitive functioning, we used the Preclinical Alzheimer Cognitive Composite (PACC), which combines measures of episodic memory, executive function, and global cognition. We hypothesized that mindfulness training would enhance cognition, increase intrinsic functional connectivity measured with magnetic resonance imaging (MRI) between the hippocampus and posteromedial cortex, as well as promote increased gray matter volume within those regions. Following the 8-week intervention, the mindfulness training group showed improved performance on the PACC, while the control group did not. Furthermore, following mindfulness training, greater improvement on the PACC was associated with a larger increase in intrinsic connectivity within the default mode network, particularly between the right hippocampus and posteromedial cortex and between the left hippocampus and lateral parietal cortex. The cognitive fitness training group did not show such effects. These findings demonstrate that mindfulness training improves cognitive performance in cognitively intact older individuals and strengthens connectivity within the default mode network, which is particularly vulnerable to aging affects.

Clinical Trial Registration: [https://clinicaltrials.gov/ct2/show/NCT02628548], identifier [NCT02628548].

Keywords: aging, resting state – fMRI, mindfulness, cognitive composite, intervention

INTRODUCTION

As maintaining optimal cognitive functioning throughout the lifespan has become a public health priority, a number of interventions that aim to slow or reverse normal age-related decline have been proposed (Anguera et al., 2013; Rebok et al., 2014; Banducci et al., 2017; Foster et al., 2019). Among those, mindfulness training has been suggested to be an efficacious method for enhancing cognitive functions that decline with age (Gard et al., 2014; Fountain-Zaragoza and Prakash, 2017). Here, in a randomized controlled longitudinal study, we investigated cognitive outcomes and associated neural mechanisms following an 8-week mindfulness meditation- based training program compared to a "brain games" mental training program in cognitively normal older adults. An enhanced understanding of the mechanisms through which these interventions may counteract age-related decline can provide novel insights into training based cognitive improvements and enhance our understanding of neural plasticity in aging.

Current interventions aim to help older adults maintain optimal cognitive functioning either through explicit training regimens that engage specific cognitive functions such as memory (Requena et al., 2016), or use various techniques such as transcranial direct current stimulation (Passow et al., 2017) and neurofeedback (Reis et al., 2016; Jiang et al., 2017). Other interventions aim to improve cognitive capacities indirectly through exercise and diet programs (Colcombe and Kramer, 2003). In addition to limitations associated with their near- and far-transferability (Shipstead et al., 2010; Melby-Lervåg and Hulme, 2016; Grönholm-Nyman et al., 2017), these interventions are also limited in terms of their availability to a broader population of older adults.

More recently, mindfulness training have been proposed as an efficacious intervention to enhance cognitive functions in healthy older adults (Chiesa et al., 2011; Gard et al., 2014; Lao et al., 2016; Fountain-Zaragoza and Prakash, 2017; Cásedas et al., 2020). In line with enhanced attentional performance and preserved gray matter volume in long term meditators (Pagnoni and Cekic, 2007), mindfulness meditation-based interventions have been associated with improvements in attention, memory, executive function, processing speed, as well as general cognition. However, neural mechanisms associated with these improvements have yet to be discovered. Mindfulness meditation emphasizes the skill of meta-awareness to monitor distracting external or internal events such as arising thoughts, in order to maintain attention on the meditative object and prevent the mind from wandering, enhancing meta-cognitive monitoring and meta-cognitive control capacity (Schooler, 2002; Schooler et al., 2011). By targeting these domains through mindfulness training, we hypothesize training-specific, measurable cognitive performance effects through mechanisms that are distinctive from other cognitive training programs that use complex exogenous stimuli to capture and maintain attention (Mozolic et al., 2011).

In the absence of external task-demands, the spontaneous fluctuations in the blood-oxygen-level-dependent signal (BOLD) have been shown to display temporally coherent activity patterns within functional and anatomic systems of the brain (Biswal et al., 1995; Greicius et al., 2003; Seeley et al., 2007). This spontaneous during rest have already been associated with individual variability in human behavior. In older adults, particularly, decreases in cognition have been linked to decreases in intrinsic connectivity of the default network. Neurocognitive aging is associated with reduced deactivation of the default network during task-positive states as well as with decreased within-network connectivity during rest (Ferreira and Busatto, 2013; Madhyastha and Grabowski, 2013; Dennis and Thompson, 2014; Persson et al., 2014; Vidal-Piñeiro et al., 2014). Among default mode network structures, posteromedial cortices that are strongly functionally connected to the medial temporal lobes, are selectively vulnerable to pathology (Sperling et al., 2010). Critically, intrinsic connectivity between these regions, particularly between the posteromedial cortex (PMC) and hippocampus, has been associated with individual differences in memory performance among cognitively intact older individuals (Dickerson and Eichenbaum, 2010; Wang et al., 2010; Ferreira et al., 2016). Morphological investigations of preserved cognitive function in aging corroborate the critical role of these regions in preserving cognitive functioning as well (Good et al., 2001; Bakkour et al., 2013). The rate of cortical thinning in the posteromedial cortex, along with other loci, is strongly associated with the rate of cognitive decline (Dickerson and Wolk, 2012), as well as with progression from mild cognitive impairment to Alzheimer's dementia (Chételat et al., 2005).

Mindfulness training-related increases in brain structure and function partly overlap with the neural regions implicated in age-related cognitive decline outlined above, in particular the posterior cingulate cortex (PCC) and hippocampus. Morphological investigations of mindfulness training have documented increases in gray matter density in PCC and hippocampus (Hölzel et al., 2011; Wells et al., 2013; Greenberg et al., 2017). Alterations in hippocampal (Engström et al., 2010; Yang et al., 2016) and PCC activity (Hasenkamp and Barsalou, 2012; Garrison et al., 2013; Ellamil et al., 2016), as well as increased connectivity between these regions during both meditation and while resting have also been reported (Brewer et al., 2011; Kilpatrick et al., 2011; Taylor et al., 2013; Wells et al., 2013; Brewer and Garrison, 2014; Garrison et al., 2015; Kral et al., 2019).

Although mindfulness training has been proposed as an efficacious intervention for healthy aging, a mechanistic account of mindfulness training alterations in cognition in older adults is still lacking. Here we aimed to investigate neural mechanisms associated with mindfulness training dependent changes in cognition. To this end, we used a composite test battery that combines measures of episodic memory, executive function, and global cognition, that was developed to track normal age-related cognitive decline as well as to predict early cognitive changes in neurodegenerative diseases (Donohue et al., 2014; Papp et al., 2017). Relying on the overlap in neural regions implicated in age-related cognitive decline and mindfulness training-related changes in neural functioning, we hypothesized an association between increases in cognition and enhanced intrinsic connectivity between the hippocampus and PMC. We specifically hypothesized that a mindfulness-based intervention

would improve cognitive function across multiple domains in cognitively normal older adults relative to an active control group, and that these improvements would be associated with: (i) increased intrinsic connectivity between the PMC and hippocampus; and (ii) increased gray matter volumes in these regions.

MATERIALS AND METHODS

Recruitment, Randomization and Blinding

Participants responded to advertising for a "Brain Training Study" and were recruited via a direct mail campaign as well as through various email list-servers. Following completion of all baseline testing as specified below, the randomization module within REDCap was used to randomize participants 1:1 into the two training programs in permuted groups of six, by gender. Study staff conducting subsequent testing visits were blind to group status. Importantly, participants were told that both training programs were effective for promoting cognition and that the goal of the study was to determine differential neural mechanisms, in order to minimize expectation and bias.

Participants

Potential participants were screened using the Telephone Interview for Cognitive Status (TICS; Brandt et al., 1988) to determine preliminary eligibility. Inclusion criteria were 65–80 years of age; right-handedness; ability to speak and read English; stable medication usage for at least 30 days; willingness to complete 40 min of homework per day during the 8-week program, motivation to attend all eight classes, presence in the area and availability during the follow-up testing periods. Exclusion criteria included: any non-MRI compatible metal in body; uncontrolled high blood pressure; any cardiovascular disease; a past stroke, congestive heart failure (subjects with well-controlled vascular risk factors, such as treated hypertension or treated hyperlipidemia were included, as were subjects with a history of cerebrovascular problems but no persistent neurological deficits); uncontrolled diabetes or insulin-treated diabetes [well-controlled Type II diabetes (glucose levels $<$250) were included]; active hematological, renal, pulmonary, endocrine, or hepatic disorders; history of neurological disease or injury, including a history of seizures or significant head trauma (i.e., extended loss of consciousness, bleeding in the brain, Parkinson's disease, stroke); received treatment for cancer within the last 2 years; diagnosis of schizophrenia, posttraumatic stress disorder, bipolar disorder, or psychotic disorder at any point during lifetime; any axis I psychiatric disorder within the last 12 months; any neurological or medical conditions that would interfere with study procedures or confound results, such as conditions that alter cerebral blood flow or metabolism; use of psychotropic medications or medications with CNS effects including cholinesterase inhibitors, memantine, and benzodiazepines within 12 months prior to study [medications taken on an occasional as needed basis (prn) were allowed, e.g., allergy relief]. Over the counter supplements, such as Gingko and fish oil, were also allowed; any other medications as reviewed by our team's neurologist (BD) on a case-by-case basis. Individuals were also excluded if they engaged in current regular practice of meditation, yoga, tai chi, Feldenkrais or other mind-body practices on more than six 30-min-long sessions within the last 6 months. Any other significant prior mind-body experience was evaluated on a case-by-case basis by SL and decided upon based on frequency, duration, recency, and type of mind-body practice, with a general guideline of not more than 3 months of regular practice in the last 5 years, or more than 12 months of practice in their lifetime. Participants were also screened for physical activity levels using the Godin-Shephard Leisure-time Physical Activity questionnaire, sleep-related issues using Pittsburgh Sleep Quality Index (Buysse et al., 1989).

While familiarity with leisure activities such as crossword puzzles and sudoku, was not an exclusion criterion, participants who had prior experience with a structured cognitive fitness program such as Lumosity were excluded. Out of 74 participants that were randomized to the or Cognitive Fitness Training program, 45 had some prior experience (n = 27 with crossword puzzles, n = 15 with sudoku, n = 6 word jumbles, and word search, n = 23 with others such as solitaire, board games, or trivia games). While 10 participants had experience with two types of puzzles, none had experience with all four types trained in the course. Similarly, out of the 72 participants who were randomized to the Mindfulness Training, 28 had prior experience with yoga, tai-chi, or mantra meditation, however, the frequency of their practice was below our exclusion threshold.

Potential participants were invited to the laboratory, consented, and then underwent a structured clinical interview with our team's neuropsychologist (BW) who performed a cognitive and functional assessment to determine final eligibility. Cognitively normal participants were determined on the basis of both an absence of cognitive symptoms and absence of impairment on cognitive testing (CDR Rating = 0; MMSE 27–30; normal performance on Trail-making Test, verbal fluency measures based on age- and education matched norms). Participants received the programs for free and were remunerated up to $275 for their participation if they completed all testing visits. Informed consent followed the guidelines of the MGH IRB.

Out of 1472 people who were screened, 146 eligible participants were found eligible and randomized into either Mindfulness Training (n = 72) or Cognitive Fitness Training (n = 74) programs. Cognitive testing and neuroimaging were conducted within a 3-week period before and after the interventions (approximately a 3-month interval). The data reported here are part of a longitudinal study with 2-year follow-up. Only baseline and post-intervention performance in our cognitive outcome measure are reported here. There was no evidence of selective attrition. Please see CONSORT diagram for additional information, including retention.

Cognitive Outcome Measure

Our primary cognitive outcome was the Alzheimer's Disease Cooperative Study Preclinical Alzheimer's Cognitive Composite (PACC; Donohue et al., 2014) which consists of: (1) the Total Recall score from the Free and Cued Selective Reminding Test

(FCSRT) (0–48) (Grober et al., 1988); (2) the Delayed Recall score from the Logical Memory IIa subtest from the Wechsler Memory Scale (0–25) (Wechsler, 1987); (3) the Digit Symbol Substitution Test (DSST) from the Wechsler Adult Intelligence Scale-Revised (0–93) (Wechsler, 1981); and the Mini Mental State Exam (MMSE) total score (0–30) (Folstein et al., 1975). To reduce practice effects, we administered alternate test versions at each time-point. The cognitive composite score, PACC, is determined from its components using an established normalization method (Cutter et al., 1999). Each of the four component change scores (post-pre) is divided by the baseline sample standard deviation of that component, to form standardized z scores. These z scores are summed using the following item weights as previously reported (Donohue et al., 2014): $0.72 \times$ (FCSRT) $+ 0.14 \times$ (Logical Memory IIa) $+ 0.12 \times$ (MMSE) $+ 0.03 \times$ (DSST). The composite score represents a standardized change score based on within-participants alterations in cognition. According to Donohue et al. (2014), the minimum treatment difference of 0.5 units is large enough to suggest a benefit to the patients and also incorporates a possible delay in later clinical deterioration.

Cognitive Training Programs

Mindfulness Training Program

The Mindfulness Training (MT) program is an 8-week program that teaches mindfulness meditation exercises as a means to enhance attention and memory. The program is derived from Mindfulness-Based Stress Reduction (MBSR; Kabat-Zinn, 1990), but with an emphasis on concentration and focus rather than stress reduction. Weekly meetings lasted 1 h: 45 min meditation practice and 15 min of check-in, practice instruction, and Q&A. Participants were instructed to practice meditation at home for 45 min daily and were given guided audio recordings to facilitate practice. Weekly mindfulness instruction consisted of: Weeks 1 and 2: breath meditation and body scan; Week 3: walking meditation; Week 4: mental noting; Week 5: focus on the five physical senses and sensations; Week 6: standing meditation; Week 7: mindful eating and the five senses; Week 8: review all techniques. Participants were allowed to practice any learned technique in subsequent weeks if they desired. On average, participants attended 7.05 of eight classes and practiced 4.01 h per week at home. The program was taught by Greg Topakian, Ph.D. who has 30 years of meditation practice including 20 weeks of intensive retreat practice. He has 20 years of experience teaching in academia as well as 6 years of experience teaching secular mindfulness programs.

Cognitive Fitness Training Program

The Cognitive Fitness Training (CFT) program is an active control condition matched to the MT program for amount of class time and home practice. Like the MT program, class was divided into 45 min of group puzzle solving and 15 min of check-in, practice instruction, and Q&A. Weekly instruction consisted of: Week 1: word search and crossword puzzles; Weeks 2 and 3: Sudoku; Week 4: word jumbles; Weeks 5 and 6: KenKen; Weeks 7 and 8: review. Participants were given packets of puzzles to take home and instructed to practice for 45 min each day. Importantly, there was a range of difficulty available for each type of puzzle during the first week it was introduced in order to accommodate participants with different puzzle solving abilities. However, our goal was to minimize the effectiveness of this program, and so each participant continued to receive only puzzles at that chosen difficulty level for the remainder of the program, to limit development of novel strategies. On average, participants attended 6.64 of eight classes and practiced 5.99 h per week at home. The program was taught by Elisabeth Osgood-Campbell who holds a master's degree in education and has 13 years of experience teaching in academic settings.

MRI Data Acquisition and Analysis

Data Acquisition Parameters

MRI imaging was conducted in a 3T scanner (Siemens Prisma) with a 32-channel gradient head coil at the Athinoula A. Martinos Center for Biomedical Imaging in Charlestown, MA, United States. All subjects were scanned in the same scanner at both time points, i.e., within 2 weeks before (pre-scan) and within 2 weeks (post-scan) after participating in the 8-week program (∼3-month interval). We acquired T1 structural MRI images (sagittal MP-RAGE) for all subjects using the following parameters: TA = 9:14; voxel size = 1.1 mm × 1.1 mm × 1.2 mm; Rel.SNR = 1.00; slice oversampling = 0%; slices per slab = 176; TR = 2300 ms; TE = 2.01 ms; field of view = 270 mm. Subsequently, resting state functional magnetic resonance imaging (rsfMRI) were acquired using a gradient-echo echo-planar pulse sequence sensitive to the blood-oxygen-level-dependent signal (BOLD) with the following parameters: TR = 3000 ms; voxel size = 3.0 mm isotropic voxels; Rel.SNR = 1.00; interleaved slice order, slice oversampling = 0%; slice thickness = 3 mm; TE = 30 ms; Flip Angle = 85°; TA = 6:12; 46 slices, field of view = 216 mm.

Structural Image Processing With Voxel Based Morphometry (VBM)

Prior to preprocessing, the MP-RAGE data from 118 program participants completing both scans were visually investigated with regards to scanner artifacts as well as clinical abnormalities. After preprocessing, the scans underwent an automated quality check with the Computational Anatomy Toolbox's (CAT12.6-rc1; v1426; Structural Brain Mapping Group, Jena, Germany) combining both measurements of noise and spatial resolution to translate into an index of weighted overall image quality. The resulting boxplot enabled a closer visual assessment of potential outliers. Moreover, the covariance between all normalized modulated images was assessed. Thereby we were able to ensure sample homogeneity.

The preprocessing for the voxel-based morphometry was conducted with CAT12's longitudinal processing stream, which was implemented in SPM12 (Wellcome Centre for Human Neuroimaging, London, United Kingdom) running on MATLAB (R2018b) (Mathworks Inc., Natick, MA, United States). In this updated version, CAT12 is optimized to identify subtle volumetric effects resulting from training over short time periods. Default parameters were used unless specified otherwise. Individual T1-weighted MRI images for both time-points were processed by a series of steps, i.e., intra-subject alignment,

bias correction, and segmentation. For the subsequent spatial normalization, we used CAT12's template for the high-dimensional DARTEL registration with 1.5 mm (Ashburner and Friston, 2001). This approach renders a higher sensitivity for detecting regional differences (Bergouignan et al., 2009) as well as an improved normalization power because of a better inter-subject alignment (Yassa and Stark, 2009). As we were interested to investigate the actual GM values locally and to detect potential volumetric changes, images were modulated, i.e., each tissue class image was multiplied by the Jacobian determinant from the normalization matrix. Finally, images were smoothed with an 8 mm FWHM isotropic Gaussian kernel via a SPM12 standard module. Smoothed images translate into an improved normal distribution of the data, which is necessary to honor the underlying assumption for parametric statistical comparisons (Worsley et al., 1996). For the investigation of GM volume change we extracted GM values and conducted statistical analysis of our *a priori* seeds described below using SPSS version 25.

Seed-Based Connectivity Analyses

Resting state functional connectivity analyses were performed using the CONN toolbox v.18b (Whitfield-Gabrieli and Nieto-Castanon, 2012). Preprocessing consisted of realignment and unwarping of functional images, slice timing correction and motion correction. The functional images were resliced using a voxel size of 2 mm × 2 mm × 2 mm and smoothed using an 8-mm FWHM isotropic Gaussian kernel. ART was used detect frames with fluctuations in global signal and motion outliers. Intermediate level thresholds, which were set to reject 3% of the normative sample data, were used. The frames with motion outliers that exceeded 0.9 mm or fluctuations in global signal >5 standard were considered outliers. To address the confounding effects of participant movement and physiological noise the CompCor method (Behzadi et al., 2007) was used. The structural images were segmented into cerebrospinal fluid (CSF), white matter (WM), and GM. The principal components related to the segmented CSF and WM were extracted and were included as confound regressors in a first-level analysis along with movement parameters. The data were linearly detrended and band-pass filtered to 0.008–0.09 Hz, without regressing the global signal. Quality assessment included inspection of the sample in terms of maximum inter-scan motion, number of valid scans per subject, and scan-to-scan change in global BOLD signal and removal of outliers based on the aforementioned criteria ($n = 20$).

For the determination of seeds, an initial seed located at the posteromedial cortex seed/or in posterior cingulate/retrosplenial cortex (MNI coordinates $x = -1$, $y = -52$, $z = 26$) with an 8 mm radius was selected based on previous literature that investigated large-scale networks in older adults (Andrews-Hanna et al., 2007). The hippocampal seeds were determined based on the pattern of correlations at baseline for the whole sample using posterior cingulate/retrosplenial cortex (pC/rsp) seed. After a voxel level correction at $p < 0.001$, and a cluster level at p-FWE < 0.05, spherical ROIs with a radius of 8 mm were defined around the following peak coordinates within the hippocampi (hippocampus/R 30 −16 −14; hippocampus/L −26 −28 −14).

In order to assess group differences in alterations in intrinsic connectivity between our *a priori* seeds, we first examined connectivity estimates between *a priori* hippocampus and posterior cingulate/retrosplenial cortex (pC/rsp) seeds at each time point. In order to further delineate within-group changes in intrinsic connectivity in relation to changes in cognition, follow-up gPPI analyses were conducted for each group. For each group, a generalized psychophysiological interaction (gPPI) analysis computed the level of changes in functional connectivity strength between hippocampal seeds (R/L) and every voxel in the brain (post-pre), covarying with changes in cognition (PACC).

Statistical Analysis Methods for Behavioral and Neural Outcome Measures

To assess within group differences for PACC, a one-sample *t*-test was conducted for each group, where group means were compared to a mean equal to zero, indicating no change in PACC. To assess differences in PACC between mindfulness-based and cognitive fitness trainings, an independent samples *t*-test was used. The connectivity estimates reflect the change in connectivity associated with training-dependent increases in cognition. Group differences in changes in connectivity estimates between *a priori* hippocampus and posterior cingulate/retrosplenial cortex (pC/rsp) seeds were evaluated using a repeated measures ANOVA. To assess changes in hippocampal connectivity strength covarying with changes in cognition (PACC), separate gPPI models were used for the right and the left hippocampal connectivity. For each participant (within-participants level), whole brain time series data were regressed onto the ROI signal to generate connectivity maps at each time point (baseline and post-intervention). Post intervention bivariate regression coefficient maps were then subtracted from baseline maps to create a map of whole-brain connectivity changes with each hippocampal seed for each participant. At the second (between-participants) level, these change maps were then regressed onto PACC scores to create a map of regions whose connectivity change significantly correlated with PACC. To explore changes related to MT, first the gPPI analysis was run on participants from the MT group, followed by the CFT group alone. Both gPPI statistics were evaluated via SPM 8 using a voxel level threshold at $p < 0.001$, and a cluster level threshold at p-FWE < 0.05 for multiple comparisons. Bivariate regression coefficients were then extracted from all participants at each time-point to allow for comparison of MT changes relative to the CFT group.

RESULTS

Cognitive Outcomes

In the MT group, PACC scores increased after the intervention compared to baseline [0.21 mean increase ± 0.68 standard deviations (SD); $t(60) = 2.44$, $p = 0.018$, CI (0.04–0.39), Cohen's d 0.31]. In the CFT group, PACC scores did not increase relative to baseline following the intervention [0.10 mean increase ± 0.64

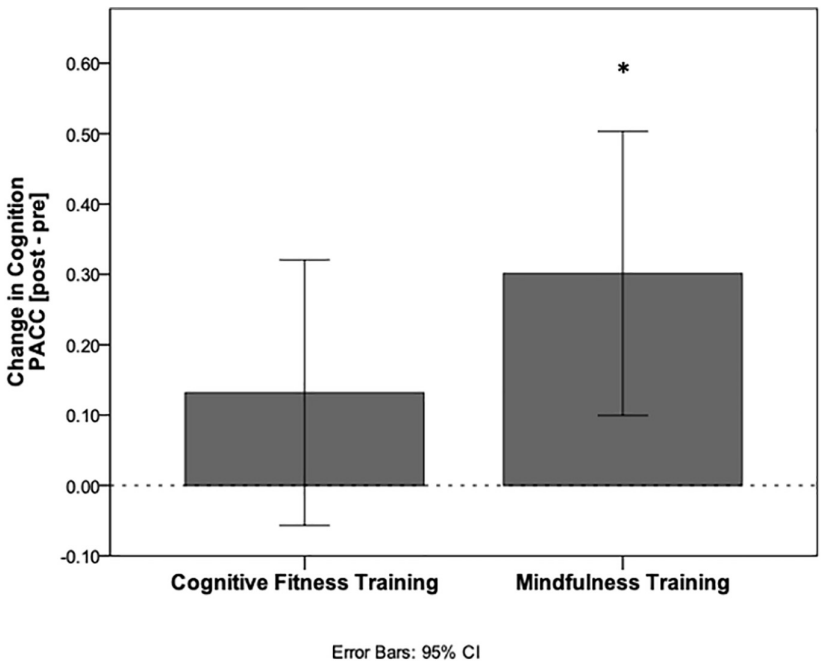

FIGURE 1 | Cognitive improvement relative to baseline performance. PACC scores calculated as change from baseline following the interventions for each group. Mindfulness training resulted in a significant within-group increase in cognition (*$p < 0.05$), while cognitive fitness training did not.

SD; $t(64) = 1.30$, $p = 0.20$, CI (−0.06 to 0.26), Cohen's d 0.16]. Despite these findings, the between-group comparison was not statistically significant [$t(124) = 0.942$, $p = 0.348$, CI (−0.121, 0.342), neuroimaging sample $t(95) = 1.235$, $p = 0.220$, CI (−0.103, 0.442), **Figure 1**].

Baseline characteristics of the whole sample are presented in **Table 1**. Performance on PACC as well as performance on each cognitive test at each time point are presented in **Table 2**. There were no differences between groups in FCSRT [$t(124) = 0.142$, $p = 0.888$], in Logical Memory IIa [$t(124) = -0.040$, $p = 0.968$], in MMSE [$t(124) = 0.946$, $p = 0.346$], or in DSST [$t(124) = 1.291$, $p = 0.199$] at baseline. The significant improvement in the PACC composite score for the MT group was driven by primarily by an increase in the FCSRT total recall that was not seen in the control group. Both groups improved on LMIIa delayed recall performance and showed slight improvements on digit symbol substitution test. The MMSE was uninformative in this study because many participants performed at ceiling at baseline.

There was no significant difference between groups in terms of their physical activity [$t(130) = 0.890$, $p = 0.375$], or sleep levels [$t(124) = 0.468$, $p = 0.641$] at baseline either. The changes in PSQI scores from baseline to post-testing did not differ between groups [$F(1,126) = 1.194$, $p = 0.277$, $\eta^2 = 0.01$]. Mindfulness Training group had the following PSQI scores at baseline (4.83 ± 3.03), and at post (4.66 ± 2.92), while the Cognitive Fitness Training group had the following PSQI scores at baseline (4.72 ± 3.06), and at post (4.75 ± 2.95). The changes in exercise scores from baseline to post-testing did not differ between groups either [$F(1,114) = 2.748$, $p = 0.100$, $\eta^2 = 0.24$]. Mindfulness Training group had the following Godin exercise scores at baseline (34.89 ± 20.10), and at post (35.75 ± 2157), while the Cognitive Fitness Training group had the following scores at baseline (38.64 ± 27.58), and at post (49.72 ± 35.73).

Mindfulness Training Is Associated With Increased Intrinsic Connectivity Between the Right Hippocampus and Posteromedial Cortex

To assess group differences in alterations in intrinsic connectivity between our *a priori* seeds, we first examined connectivity estimates between *a priori* hippocampus and posterior cingulate/retrosplenial cortex (pC/rsp) seeds at each time point. An investigation of group differences in

TABLE 1 | Baseline characteristics of study participants.

	Mindfulness training	Cognitive fitness training	Statistical test value	*p*	Cohen's *d*
Sample size	70	75			
Age (years)	70.2 ± 4.1 (*n* = 70)	71.0 ± 4.3 (*n* = 75)	$t = -1.10$	0.27	0.19
Gender (% female)	55.7 (*n* = 70)	53.3 (*n* = 75)	$\chi(1) = 0.08$	0.77	
Education (years)	16.7 ± 1.8 (*n* = 69)	16.7 ± 1.9 (*n* = 74)	$t = 0.12$	0.91	0.00
Education (ISCED level)	6.5 ± 1.0 (*n* = 69)	6.5 ± 1.1 (*n* = 74)	$t = 0.10$	0.92	0.00

Numbers denote mean ± standard deviation. p indicates the significance of the group differences on Students' t or chi-square test.

changes connectivity estimates between pC/rsp and left hippocampus seed [$F(1,95) = 0.048$, $p = 0.827$, $\eta^2 = 0.001$], and between pC/rsp and right hippocampus seed [$F(1,95) = 0.011$, $p = 0.916$, $\eta^2 = 0.000$] did not reveal any differences between groups over time.

Next, in order to delineate mindfulness training dependent changes in hippocampal connectivity strength that covary with changes in cognition, we conducted a whole brain gPPI analysis (baseline vs. post-intervention) using PACC scores as regressor and right hippocampus as seed region. This analysis resulted in a significant cluster at right precuneus for the mindfulness training group [MNI coordinates +6 −52 +54, cluster size (k) = 74, p-FWE = 0.037, **Figure 2A**]. Mindfulness-training dependent improvements in cognitive composite scores were associated with increases in intrinsic connectivity between the right hippocampus and right precuneus ($r = 0.526$, $p < 0.001$, **Figure 2B**). A parallel whole brain gPPI analysis (baseline vs. post-intervention) using PACC scores as regressor and right hippocampus as seed region in the CFT group did not yield any results. In order to compare two groups, connectivity estimates between the right hippocampus and the cluster in the precuneus were extracted. While there was no association between improvements in cognitive composite scores and increases in intrinsic connectivity between the right hippocampus and right precuneus in the CFT group ($r = -0.023$, $p = 0.876$, **Figure 2B**), a test for between-group differences was not significant [$F(1,95) = 0.264$, $p = 0.609$, $\eta^2 = 0.003$].

TABLE 2 | Cognitive outcome measures.

	Mindfulness training				
	Pre	**Post**	***t***	***p***	**Cohen's *d***
PACC	$n = 70$ ($n = 61$)	$n = 61$			
Digit symbol	51.8 ± 9.7 (51.3 ± 9.3)	52.6 ± 9.1	−1.66	0.10	0.09
MMSE	29.1 ± 1.0 (26.1 ± 1.1)	29.0 ± 1.3	0.25	0.80	0.09
FCSRT total recall	30.8 ± 5.8 (31.2 ± 5.7)	32.3 ± 4.8	−1.93	0.06	0.28
LMIIa delayed recall	12.2 ± 4.2 (12.3 ± 4.2)	13.9 ± 4.1	−2.70	0.009	0.41
Total PACC change ($n = 61$)	**0.21 ± 0.68**				
	Cognitive fitness training				
	Pre	**Post**	***t***	***p***	**Cohen's *d***
PACC	$n = 75$ ($n = 65$)	$n = 65$			
Digit symbol	49.0 ± 11.0 (48.9 ± 11.6)	50.3 ± 11.1	−1.83	0.07	0.12
MMSE	29.0 ± 1.0 (28.9 ± 1.0)	28.8 ± 1.0	1.14	0.26	0.2
Free recall	31.1 ± 5.1 (31.1 ± 5.2)	31.4 ± 4.9	−0.35	0.73	0.06
Delayed recall	12.5 ± 3.3 (12.3 ± 3.3)	14.7 ± 4.0	−5.12	<0.001	0.6
Total PACC change ($n = 65$)	**0.10 ± 0.64**				

Numbers denote mean ± standard deviation for each cognitive measure, and PACC; p values pertain to paired t-tests between participants with both baseline and follow-up measures.

Mindfulness Training Is Associated With Increased Intrinsic Connectivity Between the Left Hippocampus and the Right Angular Gyrus

A whole brain gPPI analysis (baseline vs. post-intervention) using PACC scores as regressor and left hippocampus as seed region resulted in a significant cluster in the right angular gyrus for the mindfulness training group [MNI coordinates +62 −48 +16, cluster size (k) = 116, p-FWE = 0.003, **Figure 2C**]. Mindfulness-training dependent improvements in cognitive composite scores were associated with increases in intrinsic connectivity between the left hippocampus and the right angular gyrus ($r = 0.538$, $p = 0.000$, **Figure 2D**). A parallel whole brain gPPI analysis (baseline vs. post-intervention) using PACC scores as regressor and left hippocampus as seed region in the CFT group did not yield any results. In order to compare two groups, connectivity estimates between the left hippocampus and angular gyrus were extracted as well. While there was no association between improvements in cognitive composite scores and increases in intrinsic connectivity between the left hippocampus and angular gyrus ($r = 0.232$, $p = 0.108$, **Figure 2D**) for the CFT group, and a test for between-group differences was not significant [$F(1,95) = 1.647$, $p = 0.203$, $\eta^2 = 0.017$].

Our hypotheses about changes in gray matter volume were not supported. There was no main effect of time nor any significant within-group changes within our ROIs for the mindfulness group (all $p > 0.48$). There was a main effect of time in the right hippocampus for the CFT group which did not survive multiple comparisons correction. Moreover, in opposition to our *a priori* hypothesis, we were not able to identify any significant results when correlating GMV change values with PACC change scores.

DISCUSSION

In the present study, we performed a randomized controlled trial to test the hypothesis that mindfulness training can maintain or improve cognitive function in healthy older adults, and we used functional and structural MRI to investigate the neural basis of cognitive outcome. We found that an 8-week mindfulness-based training program improved cognition as assessed by Preclinical Alzheimer's Cognitive Composite (PACC) in cognitively normal older adults, and that these improvements were associated with increased intrinsic connectivity within the default mode network, particularly between the right hippocampus and precuneus and between the left hippocampus and right lateral parietal cortex. Although the active control group did not show these effects, we were not able to demonstrate a statistically significant between-group difference in the primary cognitive outcome measure,

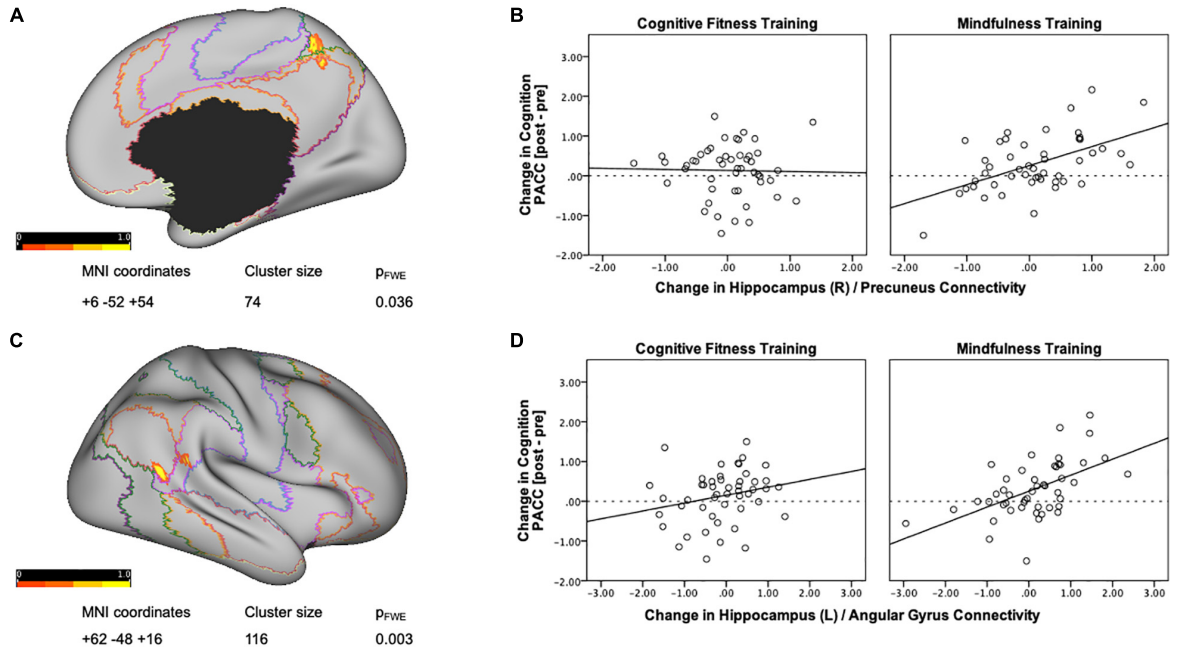

FIGURE 2 | Training-dependent changes in hippocampal connectivity strength that covary with changes in cognition. **(A)** A whole brain gPPI analysis of changes in functional connectivity (baseline vs. post-intervention) using change in PACC scores as regressor and right hippocampus as seed resulted in a significant cluster at the right precuneus for the mindfulness training group. Networks are based on the Yeo seven-network parcellation (Yeo et al., 2011) and are represented by the following colors: violet: visual, blue: somato-motor, green: dorsal attention, pink: ventral attention, cream: limbic, orange: fronto-parietal, and red: default network. **(B)** Mindfulness-training-dependent improvements in PACC cognitive composite scores correlated with increases in intrinsic connectivity between the right hippocampus and the right precuneus, while the Cognitive Fitness Training group showed no association. The connectivity estimates reflect the change in connectivity strength associated with training-dependent increases in cognition, and were plotted using SPSS v.24 (Chart Editor). The fitted regression line reflects the best estimate of the connectivity between the hippocampus and the precuneus in **B**. **(C)** A whole brain gPPI analysis of the changes in functional connectivity (baseline vs. post-intervention) using change in PACC scores as regressor and left hippocampus as seed resulted in a significant cluster at the right angular gyrus for the mindfulness training group. Networks are based on the Yeo seven-network parcellation (Yeo et al., 2011) and are represented by the following colors: violet: visual, blue: somato-motor, green: dorsal attention, pink: ventral attention, cream: limbic, orange: fronto-parietal, and red: default network. **(D)** Mindfulness-training-dependent improvements in cognitive composite scores correlated with increases in intrinsic connectivity between the left hippocampus and the right angular gyrus, while the Cognitive Fitness Training group showed no association. The connectivity estimates reflect the change in connectivity strength associated with training-dependent increases in cognition, and were plotted using SPSS v.24 (Chart Editor). The fitted regression line reflects the best estimate of the connectivity between the left hippocampus and the right angular gyrus in **C**.

likely because the effect size of the mindfulness program was small over this relatively short period of time, control training program was more active than anticipated and/or due to overlaps between the two programs in terms of their utilization of attention and attentional control mechanisms. Nevertheless, these findings suggest that additional longer-term studies of the potential benefits of mindfulness training should be investigated as an activity that could potentially contribute to the prevention of age-related cognitive decline.

The enhanced cognition scores following mindfulness training can be attributed primarily to improved episodic memory performance on both the Free and Cued Selective Reminding Test and the Logical Memory II Delayed Recall Test (Wechsler, 1987; Grober et al., 2008). These findings are consistent with several reviews and meta-analyses which reported moderate effects of mindfulness training on memory specificity (Chiesa et al., 2011; Gard et al., 2014; Lao et al., 2016; Fountain-Zaragoza and Prakash, 2017). The "brain games" practiced by the control group included crossword puzzles and word jumbles, both of which engage semantic memory (Pillai et al., 2011). Thus the lack of between group differences is likely due to the fact that engaging in meaningful mental stimulation and intellectual activity can improve performance on tasks that tap into the same cognitive domain that is trained (Aguirre et al., 2013). Importantly, while neither group exhibited significant levels of improvement in free recall, while the mindfulness training exhibited an improvement that approached significance. Here it is important to note the sensitivity of episodic memory to age-related decline (Donohue et al., 2014). Therefore, an improvement in this ability may be deemed to have potential clinical significance, especially in delaying age-dependent memory decline. Compared to other training programs in healthy older adults that found little to no improvements in memory (Gross et al., 2012), current findings of training-dependent improvements in the PACC, particularly in free recall, further support the use of mindfulness training as an activity to promote successful cognitive aging.

Growing evidence suggests that age-related cognitive decline is associated with changes in functional connectivity within

and between large-scale brain networks (Andrews-Hanna et al., 2007; Ferreira and Busatto, 2013; Damoiseaux, 2017). Relative to younger adults, cognitively intact older adults show reduced functional connectivity within the default mode network at rest (Ward et al., 2015; Damoiseaux, 2017; Staffaroni et al., 2018), as well as less pronounced deactivations during cognitive tasks (Grady et al., 2006; Persson et al., 2014; Spreng et al., 2016). Decreased resting state connectivity between the hippocampus and precuneus/posterior cingulate have been implicated in typical age-related cognitive decline (Wang et al., 2010; Bernard et al., 2015; Li et al., 2020). Although studies with cross-sectional populations suggest that there is a low share for the overall connectivity strength of the default network in explaining the age-related variance across various cognitive domains (Hedden et al., 2016), here, in a large sample of cognitively normal older adults, we report an association between improved cognition and training-dependent increases in the intrinsic connectivity between the right hippocampus and precuneus and between the left hippocampus and right lateral parietal cortex.

The increase in functional connectivity between the posteromedial cortex and hippocampus in the mindfulness training group was strongly associated with increases in episodic memory. This finding supports our initial hypothesis that mindfulness training may improve cognition in part through changed connectivity within the default mode network. Such an interpretation is also congruent with reports of a hippocampal-parietal network that is associated with episodic memory retrieval (Vincent et al., 2006), reports of positive association between default network connectivity and episodic memory (Huo et al., 2018), reports of an association between greater within network functional connectivity and cognitive status in healthy older adults (Sullivan et al., 2019), as well as with reports of mindfulness training dependent connectivity increases within the default mode network (Brewer et al., 2011; Taylor et al., 2013; Wells et al., 2013). The posterior parietal cortex and the precuneus are among the regions most frequently activated during both successful memory formation and episodic memory retrieval (Buckner et al., 2008; Spreng et al., 2009), and are particularly susceptible to neuropathological changes associated with aging and Alzheimer's Dementia (Buckner, 2004). Thus, present findings help substantiate the idea that enhanced intrinsic connectivity between the hippocampus and posteromedial cortex may represent one neural mechanism by which mindfulness training promotes memory function in healthy older adults.

We also identified a mindfulness training related increase in coordinated neural activity between left hippocampus and right angular gyrus. This finding is in accordance with our prior findings of mindfulness training dependent reorganization of hippocampal-cortical networks during retrieval of extinguished fear memories (Sevinc et al., 2019, 2020). Both the precuneus and the angular gyrus are part of the dorsal medial subsystem of the default mode network, that have been associated with metacognitive reflection (D'Argembeau et al., 2014). The dorsomedial and the medial temporal subsystems are closely linked, and both have been shown to be recruited during memory tasks (Andrews-Hanna et al., 2010). Critically, the angular gyrus is part of the ventral parietal cortex that is thought to direct attention to memory contents (Cabeza et al., 2008; Ciaramelli et al., 2008). Although future task-based studies are needed, the results suggest that mindfulness-training based increases in the ability to direct attention to memory contents may be one of the mechanisms through which mindfulness training increases memory performance.

While the design of the present study precludes determining whether the observed memory enhancements resulted from improved encoding or retrieval, consistent with research documenting the relation between mindfulness and attention, we had originally hypothesized that mindfulness training-dependent enhanced awareness of present moment experience would contribute to memory encoding (see Chiesa et al., 2011; Tang et al., 2015, for reviews). The present data suggest that mindfulness training related enhanced connectivity within the default mode network may contribute to improved memory via enhanced encoding or enhanced retrieval mechanisms. These findings are also in agreement with reports of meditation practice moderating aging-related decrements in measures of sustained attention (Zanesco et al., 2018). Conducting more nuanced memory tasks within the MRI scanner will be required to precisely define the impact of mindfulness training on each component of memory encoding and retrieval.

The PACC cognitive composite utilized in the study has been designed to be sensitive to cognitive changes in older adults, especially to the earliest signs of cognitive decline in Alzheimer's disease (AD; Donohue et al., 2014). Test scores that constitute the composite scores have long been used as primary markers of disease progression as well as measure of treatment effects (Amieva et al., 2008, 2019). PACC performance has reliably characterized and quantified the risk for Alzheimer-related cognitive decline among cognitively normal individuals with elevated levels of brain amyloid (Donohue et al., 2017). Consequently, a low score on the Free Recall measure has been suggested as a core neuropsychological marker of prodromal AD (Auriacombe et al., 2010). Similarly, alterations in connectivity between the precuneus/posterior cingulate and the hippocampus during rest have been implicated in MCI and AD patients (Wang et al., 2006; Sperling et al., 2010; Çiftçi, 2011; Vannini et al., 2013). Thus, training dependent increases in precuneus-hippocampal connectivity seen in the current study suggest that mindfulness-training may also be one of the mechanisms through which mindfulness training improves memory in individuals with mild cognitive impairment (Wells et al., 2013; Yang et al., 2016; Wong et al., 2017), and also contribute to discussions around brain regions associated with cognitive reserve in aging (Solé-Padullés et al., 2009).

An important strength of the study was the use of a "stripped down" mindfulness program which focused exclusively on teaching formal mindfulness meditation exercises and did not contain any psycho-education, or cognitive or behavioral therapy elements. Further, we used an engaging, credible, active control condition which was portrayed to the participants as being equally efficacious as the mindfulness program. Together, these study design elements allowed us to identify effects that were specifically attributable to mindfulness practice rather than

to generic effects of participating in a group activity, or to other therapeutic elements that are usually included in clinical mindfulness based interventions (Kabat-Zinn, 1990; Segal and Williams, 2002). As they were no differences between groups in terms of changes in physical activity or sleep quality over time, it is unlikely that the reported changes are due to these potential mediators. Other strengths of the study include the large sample size, blinded outcome of assessors, highly experienced teachers, and excellent participant compliance and retention, all of which have been major issues for many prior mindfulness studies (Chiesa et al., 2011; Tang et al., 2015; van der Velden et al., 2015; Lao et al., 2016; Van Dam et al., 2018).

The primary limitation of the study is that despite our efforts to match the groups on amount of time spent practicing at home, the CFT group practiced considerably more than what was prescribed, while the MT group practiced slightly less than prescribed. Therefore, this study bears the risks of type II errors, i.e., omitting potential group-by-time effects undermined by differential adherence to the study design. However, the within-group analyses help circumvent this issue, as do the differential correlations between brain and cognitive changes. Furthermore, some of the participants in the CFT group were already familiar with the training materials used in the program, which could contribute to smaller effect sizes in the CFT group. Thus, null training effect in the CFT group may be partially explained by their familiarity with some of the training materials prior to enrollment. As such, major limitation of the study is the lack of a significant between-group difference. Future research is needed to assess dissociable cognitive outcomes using more specified attentional measures and associated neural mechanisms of action. Future research may also assess whether the neural changes and cognitive improvements reported in this study are affected from confounding factors such as age, sex, education, whether these gains also translate into tangible gains in everyday life activities, whether the positive effects observed will be maintained over a longer period of time, and to what degree these interventions can delay the onset of various forms of cognitive decline.

DATA AVAILABILITY STATEMENT

The raw data supporting the conclusions of this article will be made available by the authors, without undue reservation.

ETHICS STATEMENT

The studies involving human participants were reviewed and approved by the Mass General Brigham Human Research Committee. The patients/participants provided their written informed consent to participate in this study.

AUTHOR CONTRIBUTIONS

SL and BD contributed to the conception and design of the study. GS, TD, RK, SG, MS, and NT carried out the data collection. GS and JR performed the statistical analysis and wrote the first draft of the manuscript. SL oversaw all the data collection and analysis. CG, GT, DR, and BD oversaw the data analysis. DR, BD, and SL contributed to the interpretation of the results. All authors provided critical feedback, discussed the results, and commented on and approved the submitted manuscript.

FUNDING

We thank the National Institute on Aging for providing primary funding for this study (R01 AG048351 to SL and BD). This research was carried out at the Athinoula A. Martinos Center for Biomedical Imaging at MGH, using resources provided by the Center for Functional Neuroimaging Technologies, P41EB015896, a P41 Biotechnology Resource Grant supported by the National Institute of Biomedical Imaging and Bioengineering (NIBIB), and the Neuroimaging Analysis Center, P41EB015902, a P41 supported by NIBIB. This work also involved the use of instrumentation supported by the National Institutes of Health (NIH) Shared Instrumentation Grant Program; specifically, S10RR017208-01A1, S10RR026666, S10RR022976, S10RR019933, S10RR023043, and S10RR023401.

ACKNOWLEDGMENTS

We would like to thank Clinical Research Coordinators SG, MS, Erin Mulvihill, Burak Cindik, and numerous undergraduate students for their assistance. We would also like to thank our participants for their time and effort, Greg Topakian for teaching the mindfulness program, and Elizabeth Osgood-Campbell for teaching the cognitive fitness training program. Parts of this work were prepared in the context of JR's dissertation at the Faculty of Medicine, University of Hamburg.

SUPPLEMENTARY MATERIAL

The Supplementary Material for this article can be found online at: https://www.frontiersin.org/articles/10.3389/fnagi.2021.702796/full#supplementary-material

REFERENCES

Aguirre, E., Woods, R. T., Spector, A., and Orrell, M. (2013). Cognitive stimulation for dementia: a systematic review of the evidence of effectiveness from randomised controlled trials. *Ageing Res. Rev.* 12, 253–262. doi: 10.1016/j.arr.2012.07.001

Amieva, H., Le Goff, M., Millet, X., Orgogozo, J. M., Pérès, K., Barberger-Gateau, P., et al. (2008). Prodromal Alzheimer's disease: successive emergence of the clinical symptoms. *Ann. Neurol.* 64, 492–498. doi: 10.1002/ana.21509

Amieva, H., Meillon, C., Proust-Lima, C., and Dartigues, J. F. (2019). Is low psychomotor speed a marker of brain vulnerability in late life? Digit symbol substitution test in the prediction of alzheimer, parkinson, stroke, disability,

and depression. *Dement. Geriatr. Cogn. Disord.* 47, 297–305. doi: 10.1159/000500597

Andrews-Hanna, J. R., Reidler, J. S., Sepulcre, J., Poulin, R., and Buckner, R. L. (2010). Functional-anatomic fractionation of the brain's default network. *Neuron* 65, 550–562. doi: 10.1016/j.neuron.2010.02.005

Andrews-Hanna, J. R., Snyder, A. Z., Vincent, J. L., Lustig, C., Head, D., Raichle, M. E., et al. (2007). Disruption of large-scale brain systems in advanced aging. *Neuron* 56, 924–935. doi: 10.1016/j.neuron.2007.10.038

Anguera, J. A., Boccanfuso, J., Rintoul, J. L., Al-Hashimi, O., Faraji, F., Janowich, J., et al. (2013). Video game training enhances cognitive control in older adults. *Nature* 501, 97–101. doi: 10.1038/nature12486

Ashburner, J., and Friston, K. J. (2001). Why voxel-based morphometry should be used. *Neuroimage* 14, 1238–1243. doi: 10.1006/nimg.2001.0961

Auriacombe, S., Helmer, C., Amieva, H., Berr, C., Dubois, B., and Dartigues, J.-F. (2010). Validity of the free and cued selective reminding test in predicting dementia: the 3C study. *Neurology* 74, 1760–1767. doi: 10.1212/WNL.0b013e3181df0959

Bakkour, A., Morris, J. C., Wolk, D. A., and Dickerson, B. C. (2013). The effects of aging and Alzheimer's disease on cerebral cortical anatomy: specificity and differential relationships with cognition. *NeuroImage* 76, 332–344. doi: 10.1016/j.neuroimage.2013.02.059

Banducci, S. E., Daugherty, A. M., Biggan, J. R., Cooke, G. E., Voss, M., Noice, T., et al. (2017). Active experiencing training improves episodic memory recall in older adults. *Front. Aging Neurosci.* 9:133. doi: 10.3389/fnagi.2017.00133

Behzadi, Y., Restom, K., Liau, J., and Liu, T. T. (2007). A component based noise correction method (CompCor) for BOLD and perfusion based fMRI. *NeuroImage* 37, 90–101. doi: 10.1016/j.neuroimage.2007.04.042

Bergouignan, L., Chupin, M., Czechowska, Y., Kinkingnéhun, S., Lemogne, C., Le Bastard, G., et al. (2009). Can voxel based morphometry, manual segmentation and automated segmentation equally detect hippocampal volume differences in acute depression? *NeuroImage* 45, 29–37. doi: 10.1016/j.neuroimage.2008.11.006

Bernard, C., Dilharreguy, B., Helmer, C., Chanraud, S., Amieva, H., Dartigues, J.-F., et al. (2015). PCC characteristics at rest in 10-year memory decliners. *Neurobiol. Aging* 36, 2812–2820. doi: 10.1016/j.neurobiolaging.2015.07.002

Biswal, B., Yetkin, F. Z., Haughton, V. M., and Hyde, J. S. (1995). Functional connectivity in the motor cortex of resting human brain using echo-planar MRI. *Magn. Reson. Med.* 34, 537–541. doi: 10.1002/mrm.1910340409

Brandt, J., Spencer, M., and Folstein, M. (1988). The telephone interview for cognitive status. *Neuropsychiatry Neuropsychol. Behav. Neurol.* 1, 111–117.

Brewer, J. A., and Garrison, K. A. (2014). The posterior cingulate cortex as a plausible mechanistic target of meditation: findings from neuroimaging: the PCC as a target of meditation. *Ann. N.Y. Acad. Sci.* 1307, 19–27. doi: 10.1111/nyas.12246

Brewer, J. A., Worhunsky, P. D., Gray, J. R., Tang, Y.-Y., Weber, J., and Kober, H. (2011). Meditation experience is associated with differences in default mode network activity and connectivity. *Proc. Natl. Acad. Sci. U.S.A.* 108, 20254–20259. doi: 10.1073/pnas.1112029108

Buckner, R. L. (2004). Memory and executive function in aging and AD: multiple factors that cause decline and reserve factors that compensate. *Neuron* 44, 195–208. doi: 10.1016/j.neuron.2004.09.006

Buckner, R. L., Andrews-Hanna, J. R., and Schacter, D. L. (2008). "The brain's default network: anatomy, function, and relevance to disease," in *The Year in Cognitive Neuroscience 2008*, eds A. Kingstone and M. B. Miller (Malden, MA: Blackwell Publishing), 1–38. doi: 10.1196/annals.1440.011

Buysse, D. J., Reynolds, C. F., Monk, T. H., Berman, S. R., and Kupfer, D. J. (1989). The Pittsburgh sleep quality index: a new instrument for psychiatric practice and research. *Psychiatry Res.* 28, 193–213. doi: 10.1016/0165-1781(89)90047-4

Cabeza, R., Ciaramelli, E., Olson, I. R., and Moscovitch, M. (2008). Parietal cortex and episodic memory: an attentional account. *Nat. Rev. Neurosci.* 9, 613–625. doi: 10.1038/nrn2459

Cásedas, L., Pirruccio, V., Vadillo, M. A., and Lupiáñez, J. (2020). Does mindfulness meditation training enhance executive control? A systematic review and meta-analysis of randomized controlled trials in adults. *Mindfulness* 11, 411–424. doi: 10.1007/s12671-019-01279-4

Chételat, G., Landeau, B., Eustache, F., Mézenge, F., Viader, F., de la Sayette, V., et al. (2005). Using voxel-based morphometry to map the structural changes associated with rapid conversion in MCI: a longitudinal MRI study. *Neuroimage* 27, 934–946. doi: 10.1016/j.neuroimage.2005.05.015

Chiesa, A., Calati, R., and Serretti, A. (2011). Does mindfulness training improve cognitive abilities? A systematic review of neuropsychological findings. *Clin. Psychol. Rev.* 31, 449–464. doi: 10.1016/j.cpr.2010.11.003

Ciaramelli, E., Grady, C. L., and Moscovitch, M. (2008). Top-down and bottom-up attention to memory: a hypothesis (AtoM) on the role of the posterior parietal cortex in memory retrieval. *Neuropsychologia* 46, 1828–1851. doi: 10.1016/j.neuropsychologia.2008.03.022

Çiftçi, K. (2011). Minimum spanning tree reflects the alterations of the default mode network during Alzheimer's disease. *Ann. Biomed. Eng.* 39, 1493–1504. doi: 10.1007/s10439-011-0258-9

Colcombe, S., and Kramer, A. F. (2003). Fitness effects on the cognitive function of older adults: a meta-analytic study. *Psychol. Sci.* 14, 125–130. doi: 10.1111/1467-9280.t01-1-01430

Cutter, G. R., Baier, M. L., Rudick, R. A., Cookfair, D. L., Fischer, J. S., Petkau, J., et al. (1999). Development of a multiple sclerosis functional composite as a clinical trial outcome measure. *Brain* 122(Pt. 5), 871–882. doi: 10.1093/brain/122.5.871

D'Argembeau, A., Cassol, H., Phillips, C., Balteau, E., Salmon, E., and Van der Linden, M. (2014). Brains creating stories of selves: the neural basis of autobiographical reasoning. *Soc. Cogn. Affect. Neurosci.* 9, 646–652. doi: 10.1093/scan/nst028

Damoiseaux, J. S. (2017). Effects of aging on functional and structural brain connectivity. *NeuroImage* 160, 32–40. doi: 10.1016/j.neuroimage.2017.01.077

Dennis, E. L., and Thompson, P. M. (2014). Functional brain connectivity using fMRI in aging and Alzheimer's disease. *Neuropsychol. Rev.* 24, 49–62. doi: 10.1007/s11065-014-9249-6

Dickerson, B. C., and Eichenbaum, H. (2010). The episodic memory system: neurocircuitry and disorders. *Neuropsychopharmacology* 35, 86–104. doi: 10.1038/npp.2009.126

Dickerson, B. C., and Wolk, D. A. (2012). MRI cortical thickness biomarker predicts AD-like CSF and cognitive decline in normal adults. *Neurology* 78, 84–90. doi: 10.1212/WNL.0b013e31823efc6c

Donohue, M. C., Sperling, R. A., Petersen, R., Sun, C.-K., Weiner, M. W., Aisen, P. S., et al. (2017). Association between elevated brain amyloid and subsequent cognitive decline among cognitively normal persons. *JAMA* 317:2305. doi: 10.1001/jama.2017.6669

Donohue, M. C., Sperling, R. A., Salmon, D. P., Rentz, D. M., Raman, R., Thomas, R. G., et al. (2014). The preclinical Alzheimer cognitive composite: measuring amyloid-related decline. *JAMA Neurol.* 71, 961–970. doi: 10.1001/jamaneurol.2014.803

Ellamil, M., Fox, K. C. R., Dixon, M. L., Pritchard, S., Todd, R. M., Thompson, E., et al. (2016). Dynamics of neural recruitment surrounding the spontaneous arising of thoughts in experienced mindfulness practitioners. *Neuroimage* 136, 186–196. doi: 10.1016/j.neuroimage.2016.04.034

Engström, M., Pihlsgård, J., Lundberg, P., and Söderfeldt, B. (2010). Functional magnetic resonance imaging of hippocampal activation during silent mantra meditation. *J. Altern. Complement. Med.* 16, 1253–1258. doi: 10.1089/acm.2009.0706

Ferreira, L. K., and Busatto, G. F. (2013). Resting-state functional connectivity in normal brain aging. *Neurosci. Biobehav. Rev.* 37, 384–400. doi: 10.1016/j.neubiorev.2013.01.017

Ferreira, L. K., Regina, A. C. B., Kovacevic, N., Martin, M., da, G. M., Santos, P. P., et al. (2016). Aging effects on whole-brain functional connectivity in adults free of cognitive and psychiatric disorders. *Cereb. Cortex* 26, 3851–3865. doi: 10.1093/cercor/bhv190

Folstein, M. F., Folstein, S. E., and McHugh, P. R. (1975). "Mini-mental state". A practical method for grading the cognitive state of patients for the clinician. *J. Psychiatr. Res.* 12, 189–198. doi: 10.1016/0022-3956(75)90026-6

Foster, P. P., Baldwin, C. L., Thompson, J. C., Espeseth, T., Jiang, X., and Greenwood, P. M. (2019). Editorial: cognitive and brain aging: interventions to promote well-being in old age. *Front. Aging Neurosci.* 11:268. doi: 10.3389/fnagi.2019.00268

Fountain-Zaragoza, S., and Prakash, R. S. (2017). Mindfulness training for healthy aging: impact on attention, well-being, and inflammation. *Front. Aging Neurosci.* 9:11. doi: 10.3389/fnagi.2017.00011

Gard, T., Hölzel, B. K., and Lazar, S. W. (2014). The potential effects of meditation on age-related cognitive decline: a systematic review. *Ann. N. Y. Acad. Sci.* 1307, 89–103. doi: 10.1111/nyas.12348

Garrison, K. A., Scheinost, D., Worhunsky, P. D., Elwafi, H. M., Thornhill, T. A., Thompson, E., et al. (2013). Real-time fMRI links subjective experience with brain activity during focused attention. *Neuroimage* 81, 110–118. doi: 10.1016/j.neuroimage.2013.05.030

Garrison, K. A., Zeffiro, T. A., Scheinost, D., Constable, R. T., and Brewer, J. A. (2015). Meditation leads to reduced default mode network activity beyond an active task. *Cogn. Affect. Behav. Neurosci.* 15, 712–720. doi: 10.3758/s13415-015-0358-3

Good, C. D., Johnsrude, I. S., Ashburner, J., Henson, R. N., Friston, K. J., and Frackowiak, R. S. (2001). A voxel-based morphometric study of ageing in 465 normal adult human brains. *Neuroimage* 14, 21–36. doi: 10.1006/nimg.2001.0786

Grady, C. L., Springer, M. V., Hongwanishkul, D., McIntosh, A. R., and Winocur, G. (2006). Age-related changes in brain activity across the adult lifespan. *J. Cogn. Neurosci.* 18, 227–241. doi: 10.1162/089892906775783705

Greenberg, J., Shapero, B. G., Mischoulon, D., and Lazar, S. W. (2017). Mindfulness-based cognitive therapy for depressed individuals improves suppression of irrelevant mental-sets. *Eur. Arch. Psychiatry Clin. Neurosci.* 267, 277–282. doi: 10.1007/s00406-016-0746-x

Greicius, M. D., Krasnow, B., Reiss, A. L., and Menon, V. (2003). Functional connectivity in the resting brain: a network analysis of the default mode hypothesis. *Proc. Natl. Acad. Sci. U.S.A.* 100, 253–258. doi: 10.1073/pnas.0135058100

Grober, E., Buschke, H., Crystal, H., Bang, S., and Dresner, R. (1988). Screening for dementia by memory testing. *Neurology* 38, 900–903. doi: 10.1212/wnl.38.6.900

Grober, E., Hall, C. B., Lipton, R. B., Zonderman, A. B., Resnick, S. M., and Kawas, C. (2008). Memory impairment, executive dysfunction, and intellectual decline in preclinical Alzheimer's disease. *J. Int. Neuropsychol. Soc.* 14, 266–278. doi: 10.1017/S1355617708080302

Grönholm-Nyman, P., Soveri, A., Rinne, J. O., Ek, E., Nyholm, A., Stigsdotter Neely, A., et al. (2017). Limited effects of set shifting training in healthy older adults. *Front. Aging Neurosci.* 9:69. doi: 10.3389/fnagi.2017.00069

Gross, A. L., Parisi, J. M., Spira, A. P., Kueider, A. M., Ko, J. Y., Saczynski, J. S., et al. (2012). Memory training interventions for older adults: a meta-analysis. *Aging Ment. Health* 16, 722–734. doi: 10.1080/13607863.2012.667783

Hasenkamp, W., and Barsalou, L. W. (2012). Effects of meditation experience on functional connectivity of distributed brain networks. *Front. Hum. Neurosci.* 6:38. doi: 10.3389/fnhum.2012.00038

Hedden, T., Schultz, A. P., Rieckmann, A., Mormino, E. C., Johnson, K. A., Sperling, R. A., et al. (2016). Multiple brain markers are linked to age-related variation in cognition. *Cereb. Cortex* 26, 1388–1400. doi: 10.1093/cercor/bhu238

Hölzel, B. K., Carmody, J., Vangel, M., Congleton, C., Yerramsetti, S. M., Gard, T., et al. (2011). Mindfulness practice leads to increases in regional brain gray matter density. *Psychiatry Res.* 191, 36–43. doi: 10.1016/j.pscychresns.2010.08.006

Huo, L., Li, R., Wang, P., Zheng, Z., and Li, J. (2018). The default mode network supports episodic memory in cognitively unimpaired elderly individuals: different contributions to immediate recall and delayed recall. *Front. Aging Neurosci.* 10:6. doi: 10.3389/fnagi.2018.00006

Jiang, Y., Abiri, R., and Zhao, X. (2017). Tuning up the old brain with new tricks: attention training via neurofeedback. *Front. Aging Neurosci.* 9:52. doi: 10.3389/fnagi.2017.00052

Kabat-Zinn, J. (1990). *Full Catastrophe Living*. New York, NY: Delta Publishing.

Kilpatrick, L. A., Suyenobu, B. Y., Smith, S. R., Bueller, J. A., Goodman, T., Creswell, J. D., et al. (2011). Impact of mindfulness-based stress reduction training on intrinsic brain connectivity. *NeuroImage* 56, 290–298. doi: 10.1016/j.neuroimage.2011.02.034

Kral, T. R. A., Imhoff-Smith, T., Dean, D. C., Grupe, D., Adluru, N., Patsenko, E., et al. (2019). Mindfulness-based stress reduction-related changes in posterior cingulate resting brain connectivity. *Soc. Cogn. Affect. Neurosci.* 14, 777–787. doi: 10.1093/scan/nsz050

Lao, S.-A., Kissane, D., and Meadows, G. (2016). Cognitive effects of MBSR/MBCT: a systematic review of neuropsychological outcomes. *Conscious. Cogn.* 45, 109–123. doi: 10.1016/j.concog.2016.08.017

Li, Q., Dong, C., Liu, T., Chen, X., Perry, A., Jiang, J., et al. (2020). Longitudinal changes in whole-brain functional connectivity strength patterns and the relationship with the global cognitive decline in older adults. *Front. Aging Neurosci.* 12:71. doi: 10.3389/fnagi.2020.00071

Madhyastha, T. M., and Grabowski, T. J. (2013). Age-Related differences in the dynamic architecture of intrinsic networks. *Brain Connect.* 4, 231–241. doi: 10.1089/brain.2013.0205

Melby-Lervåg, M., and Hulme, C. (2016). There is no convincing evidence that working memory training is effective: a reply to Au et al. (2014) and Karbach and Verhaeghen (2014). *Psychon. Bull. Rev.* 23, 324–330. doi: 10.3758/s13423-015-0862-z

Mozolic, J. L., Long, A. B., Morgan, A. R., Rawley-Payne, M., and Laurienti, P. J. (2011). A cognitive training intervention improves modality-specific attention in a randomized controlled trial of healthy older adults. *Neurobiol. Aging* 32, 655–668. doi: 10.1016/j.neurobiolaging.2009.04.013

Pagnoni, G., and Cekic, M. (2007). Age effects on gray matter volume and attentional performance in Zen meditation. *Neurobiol. Aging* 28, 1623–1627. doi: 10.1016/j.neurobiolaging.2007.06.008

Papp, K. V., Rentz, D. M., Orlovsky, I., Sperling, R. A., and Mormino, E. C. (2017). Optimizing the preclinical Alzheimer's cognitive composite with semantic processing: the PACC5. *Alzheimers Dement.* 3, 668–677. doi: 10.1016/j.trci.2017.10.004

Passow, S., Thurm, F., and Li, S.-C. (2017). Activating developmental reserve capacity via cognitive training or non-invasive brain stimulation: potentials for promoting fronto-parietal and hippocampal-striatal network functions in old age. *Front. Aging Neurosci.* 9:33. doi: 10.3389/fnagi.2017.00033

Persson, J., Pudas, S., Nilsson, L.-G., and Nyberg, L. (2014). Longitudinal assessment of default-mode brain function in aging. *Neurobiol. Aging* 35, 2107–2117. doi: 10.1016/j.neurobiolaging.2014.03.012

Pillai, J. A., Hall, C. B., Dickson, D. W., Buschke, H., Lipton, R. B., and Verghese, J. (2011). Association of crossword puzzle participation with memory decline in persons who develop dementia. *J. Int. Neuropsychol. Soc.* 17, 1006–1013. doi: 10.1017/S1355617711001111

Rebok, G. W., Ball, K., Guey, L. T., Jones, R. N., Kim, H.-Y., King, J. W., et al. (2014). Ten-year effects of the advanced cognitive training for independent and vital elderly cognitive training trial on cognition and everyday functioning in older adults. *J. Am. Geriatr. Soc.* 62, 16–24. doi: 10.1111/jgs.12607

Reis, J., Portugal, A. M., Fernandes, L., Afonso, N., Pereira, M., Sousa, N., et al. (2016). An alpha and theta intensive and short neurofeedback protocol for healthy aging working-memory training. *Front. Aging Neurosci.* 8:157. doi: 10.3389/fnagi.2016.00157

Requena, C., Turrero, A., and Ortiz, T. (2016). Six-year training improves everyday memory in healthy older people. randomized controlled trial. *Front. Aging Neurosci.* 8:135. doi: 10.3389/fnagi.2016.00135

Schooler, J. W. (2002). Re-representing consciousness: dissociations between experience and meta-consciousness. *Trends Cogn. Sci.* 6, 339–344. doi: 10.1016/s1364-6613(02)01949-6

Schooler, J. W., Smallwood, J., Christoff, K., Handy, T. C., Reichle, E. D., and Sayette, M. A. (2011). Meta-awareness, perceptual decoupling and the wandering mind. *Trends Cogn. Sci.* 15, 319–326. doi: 10.1016/j.tics.2011.05.006

Seeley, W. W., Menon, V., Schatzberg, A. F., Keller, J., Glover, G. H., Kenna, H., et al. (2007). Dissociable intrinsic connectivity networks for salience processing and executive control. *J. Neurosci.* 27, 2349–2356. doi: 10.1523/JNEUROSCI.5587-06.2007

Segal, Z., and Williams, J. M. G. (2002). *Mindfulness-Based Cognitive Therapy for Depression*. New York, NY: The Guilford Press.

Sevinc, G., Greenberg, J., Hölzel, B. K., Gard, T., Calahan, T., Brunsch, V., et al. (2020). Hippocampal circuits underlie improvements in self-reported anxiety following mindfulness training. *Brain Behav.* 10:e01766. doi: 10.1002/brb3.1766

Sevinc, G., Hölzel, B. K., Greenberg, J., Gard, T., Brunsch, V., Hashmi, J. A., et al. (2019). Strengthened hippocampal circuits underlie enhanced retrieval of extinguished fear memories following mindfulness training. *Biol. Psychiatry* 86, 693–702. doi: 10.1016/j.biopsych.2019.05.017

Shipstead, Z., Redick, T., and Engle, R. (2010). Does working memory training generalize? *Psychol. Belgica* 50, 245–276. doi: 10.5334/pb-50-3-4-245

Solé-Padullés, C., Bartrés-Faz, D., Junqué, C., Vendrell, P., Rami, L., Clemente, I. C., et al. (2009). Brain structure and function related to cognitive reserve variables in normal aging, mild cognitive impairment and Alzheimer's disease. *Neurobiol. Aging* 30, 1114–1124. doi: 10.1016/j.neurobiolaging.2007.10.008

Sperling, R. A., Dickerson, B. C., Pihlajamaki, M., Vannini, P., LaViolette, P. S., Vitolo, O. V., et al. (2010). Functional alterations in memory networks in early Alzheimer's disease. *Neuromol. Med.* 12, 27–43. doi: 10.1007/s12017-009-8109-7

Spreng, R. N., Mar, R. A., and Kim, A. S. N. (2009). The common neural basis of autobiographical memory, prospection, navigation, theory of mind, and the default mode: a quantitative meta-analysis. *J. Cogn. Neurosci.* 21, 489–510. doi: 10.1162/jocn.2008.21029

Spreng, R. N., Stevens, W. D., Viviano, J. D., and Schacter, D. L. (2016). Attenuated anticorrelation between the default and dorsal attention networks with aging: evidence from task and rest. *Neurobiol. Aging* 45, 149–160. doi: 10.1016/j.neurobiolaging.2016.05.020

Staffaroni, A. M., Brown, J. A., Casaletto, K. B., Elahi, F. M., Deng, J., Neuhaus, J., et al. (2018). The longitudinal trajectory of default mode network connectivity in healthy older adults varies as a function of age and is associated with changes in episodic memory and processing speed. *J. Neurosci.* 38, 2809–2817. doi: 10.1523/JNEUROSCI.3067-17.2018

Sullivan, M. D., Anderson, J. A. E., Turner, G. R., and Spreng, R. N. (2019). Intrinsic neurocognitive network connectivity differences between normal aging and mild cognitive impairment are associated with cognitive status and age. *Neurobiology of Aging* 73, 219–228. doi: 10.1016/j.neurobiolaging.2018.10.001

Tang, Y.-Y., Hölzel, B. K., and Posner, M. I. (2015). The neuroscience of mindfulness meditation. *Nat. Rev. Neurosci.* 16, 213–225. doi: 10.1038/nrn3916

Taylor, V. A., Daneault, V., Grant, J., Scavone, G., Breton, E., Roffe-Vidal, S., et al. (2013). Impact of meditation training on the default mode network during a restful state. *Soc. Cogn. Affect. Neurosci.* 8, 4–14. doi: 10.1093/scan/nsr087

Van Dam, N. T., van Vugt, M. K., Vago, D. R., Schmalzl, L., Saron, C. D., Olendzki, A., et al. (2018). Mind the hype: a critical evaluation and prescriptive agenda for research on mindfulness and meditation. *Perspect. Psychol. Sci.* 13, 36–61. doi: 10.1177/1745691617709589

van der Velden, A. M., Kuyken, W., Wattar, U., Crane, C., Pallesen, K. J., Dahlgaard, J., et al. (2015). A systematic review of mechanisms of change in mindfulness-based cognitive therapy in the treatment of recurrent major depressive disorder. *Clin. Psychol. Rev.* 37, 26–39. doi: 10.1016/j.cpr.2015.02.001

Vannini, P., Hedden, T., Sullivan, C., and Sperling, R. A. (2013). Differential functional response in the posteromedial cortices and hippocampus to stimulus repetition during successful memory encoding. *Hum. Brain Mapp.* 34, 1568–1578. doi: 10.1002/hbm.22011

Vidal-Piñeiro, D., Valls-Pedret, C., Fernández-Cabello, S., Arenaza-Urquijo, E. M., Sala-Llonch, R., Solana, E., et al. (2014). Decreased default mode network connectivity correlates with age-associated structural and cognitive changes. *Front. Aging Neurosci.* 6:256. doi: 10.3389/fnagi.2014.00256

Vincent, J. L., Snyder, A. Z., Fox, M. D., Shannon, B. J., Andrews, J. R., Raichle, M. E., et al. (2006). Coherent spontaneous activity identifies a hippocampal-parietal memory network. *J. Neurophysiol.* 96, 3517–3531. doi: 10.1152/jn.00048.2006

Wang, L., LaViolette, P., O'Keefe, K., Putcha, D., Bakkour, A., Van Dijk, K. R. A., et al. (2010). Intrinsic connectivity between the hippocampus and posteromedial cortex predicts memory performance in cognitively intact older individuals. *NeuroImage* 51, 910–917. doi: 10.1016/j.neuroimage.2010.02.046

Wang, L., Zang, Y., He, Y., Liang, M., Zhang, X., Tian, L., et al. (2006). Changes in hippocampal connectivity in the early stages of Alzheimer's disease: evidence from resting state fMRI. *NeuroImage* 31, 496–504. doi: 10.1016/j.neuroimage.2005.12.033

Ward, A. M., Mormino, E. C., Huijbers, W., Schultz, A. P., Hedden, T., and Sperling, R. A. (2015). Relationships between default-mode network connectivity, medial temporal lobe structure, and age-related memory deficits. *Neurobiol. Aging* 36, 265–272. doi: 10.1016/j.neurobiolaging.2014.06.028

Wechsler, D. (1981). *WAIS-R: Manual: Wechsler Adult Intelligence Scale–Revised*. New York, NY: Harcourt Brace Jovanovich [for] Psychological Corp.

Wechsler, D. (1987). *WMS-R: Wechsler Memory Scale–Revised: Manual*. San Antonio, TX: Psychological Corp.: Harcourt Brace Jovanovich.

Wells, R. E., Yeh, G. Y., Kerr, C. E., Wolkin, J., Davis, R. B., Tan, Y., et al. (2013). Meditation's impact on default mode network and hippocampus in mild cognitive impairment: a pilot study. *Neurosci. Lett.* 556, 15–19. doi: 10.1016/j.neulet.2013.10.001

Whitfield-Gabrieli, S., and Nieto-Castanon, A. (2012). Conn: a functional connectivity toolbox for correlated and anticorrelated brain networks. *Brain Connect.* 2, 125–141. doi: 10.1089/brain.2012.0073

Wong, W. P., Coles, J., Chambers, R., Wu, D. B.-C., and Hassed, C. (2017). The effects of mindfulness on older adults with mild cognitive impairment. *J. Alzheimers Dis. Rep.* 1, 181–193. doi: 10.3233/ADR-170031

Worsley, K. J., Marrett, S., Neelin, P., Vandal, A. C., Friston, K. J., and Evans, A. C. (1996). A unified statistical approach for determining significant signals in images of cerebral activation. *Hum. Brain Map.* 4, 58–73. doi: 10.1002/(SICI)1097-019319964:1<58::AID-HBM4<3.0.CO;2-O

Yang, H., Leaver, A. M., Siddarth, P., Paholpak, P., Ercoli, L., St. Cyr, N. M., et al. (2016). Neurochemical and neuroanatomical plasticity following memory training and yoga interventions in older adults with mild cognitive impairment. *Front. Aging Neurosci.* 8:277. doi: 10.3389/fnagi.2016.00277

Yassa, M. A., and Stark, C. E. L. (2009). A quantitative evaluation of cross-participant registration techniques for MRI studies of the medial temporal lobe. *NeuroImage* 44, 319–327. doi: 10.1016/j.neuroimage.2008.09.016

Yeo, B. T., Krienen, F. M., Sepulcre, J., Sabuncu, M. R., Lashkari, D., Hollinshead, M., et al. (2011). The organization of the human cerebral cortex estimated by intrinsic functional connectivity. *J. Neurophysiol.a* 106, 1125–1165. doi: 10.1152/jn.00338.2011

Zanesco, A. P., King, B. G., MacLean, K. A., and Saron, C. D. (2018). Cognitive aging and long-term maintenance of attentional improvements following meditation training. *J. Cogn. Enhanc.* 2, 259–275. doi: 10.1007/s41465-018-0068-1

Conflict of Interest: The authors declare that the research was conducted in the absence of any commercial or financial relationships that could be construed as a potential conflict of interest.

Publisher's Note: All claims expressed in this article are solely those of the authors and do not necessarily represent those of their affiliated organizations, or those of the publisher, the editors and the reviewers. Any product that may be evaluated in this article, or claim that may be made by its manufacturer, is not guaranteed or endorsed by the publisher.

frontiers in Aging Neuroscience

ORIGINAL RESEARCH
published: 04 November 2021
doi: 10.3389/fnagi.2021.751375

Regional Cortical Thickness Predicts Top Cognitive Performance in the Elderly

*Elena Nicole Dominguez[1], Shauna M. Stark[1], Yueqi Ren[2], Maria M. Corrada[3,4], Claudia H. Kawas[1,3] and Craig E. L. Stark[1,2]**

[1] Department of Neurobiology and Behavior, University of California, Irvine, Irvine, CA, United States, [2] Mathematical, Computational and Systems Biology Graduate Program, University of California, Irvine, Irvine, CA, United States, [3] Department of Neurology, University of California, Irvine, Irvine, CA, United States, [4] Department of Epidemiology, University of California, Irvine, Irvine, CA, United States

While aging is typically associated with cognitive decline, some individuals are able to diverge from the characteristic downward slope and maintain very high levels of cognitive performance. Prior studies have found that cortical thickness in the cingulate cortex, a region involved in information processing, memory, and attention, distinguish those with exceptional cognitive abilities when compared to their cognitively more typical elderly peers. Others major areas outside of the cingulate, such as the prefrontal cortex and insula, are also key in successful aging well into late age, suggesting that structural properties across a wide range of areas may better explain differences in cognitive abilities. Here, we aim to assess the role of regional cortical thickness, both in the cingulate and the whole brain, in modeling Top Cognitive Performance (TCP), measured by performance in the top 50th percentile of memory and executive function. Using data from National Alzheimer's Coordinating Center and The 90 + Study, we examined healthy subjects aged 70–100 years old. We found that, while thickness in cingulate regions can model TCP status with some degree of accuracy, a whole-brain, network-level approach out-performed the localist, cingulate models. These findings suggests a need for more network-style approaches and furthers our understanding of neurobiological factors contributing to preserved cognition.

Keywords: cortical thickness, cingulate cortex, top cognitive performer, successful aging, SuperAger, oldest-old

OPEN ACCESS

Edited by:
Henning Müller, University of Applied Sciences and Arts of Western Switzerland, Switzerland

Reviewed by:
Jennifer S. Yokoyama, University of San Francisco, United States
Andrea Stocco, University of Washington, United States

***Correspondence:**
Craig E. L. Stark
cestark@uci.edu

Received: *01 August 2021*
Accepted: *14 October 2021*
Published: *04 November 2021*

Citation:
Dominguez EN, Stark SM, Ren Y, Corrada MM, Kawas CH and Stark CEL (2021) Regional Cortical Thickness Predicts Top Cognitive Performance in the Elderly. Front. Aging Neurosci. 13:751375. doi: 10.3389/fnagi.2021.751375

INTRODUCTION

Advancements in health care and modern technology have led to an increase in life expectancy, such that by 2030, individuals 65 and older will outnumber those under the age of 18. Moreover, between 2000 and 2010, the United States saw a 30.2 and 29 percent increase in individuals aged 90–94 and 95+, respectively (US Census Bureau, 2010, 2018). With more individuals surviving until their ninth and tenth decades, many are interested in successful and healthy older aging. Contrary to those that may experience decline, some elderly individuals are able to remain disease free and maintain their cognitive abilities. Researchers have also identified subsets of individuals in their 70 and 80s that exhibit better-than-normal cognitive performance in comparison to their cognitively normal aged-matched peers. While various definitions of high-performance have been used, a common thread is well-preserved memory and executive functioning.

By examining morphological characteristics of the brain using structural neuroimaging, several studies have attempted to understand trajectories that are associated with avoiding decline and

have started to elucidate what neurobiological factors contribute to preserved cognition throughout advanced aging. One representative group, known as SuperAgers, were distinguished based on their middle-age-like episodic memory, despite being in their eighties (Harrison et al., 2012; Gefen et al., 2015). Upon conducting a whole brain analysis, this high-performing group exhibited significantly greater cortical thickness in the cingulate cortex (Harrison et al., 2012). Note, however, that the modest sample sizes (n = 12 SuperAgers and n = 10 elderly controls) may have impacted their ability to reliably identify a broader range of regions. Following this finding, an *a priori* region-of-interest (ROI)-based analysis revealed that SuperAgers displayed greater cortical thickness in the posterior and caudal anterior cingulate cortex when compared to elderly controls (Gefen et al., 2015).

Studies of successful aging are not limited to the popularized SuperAger cohort and many have examined top performing individuals based on varying neuropsychological performance and tests. One commonality across studies has been highlighting the structural integrity of the cingulate cortex. Seventy-year-old successful agers, defined by high performance in episodic memory, working memory, and processing speed, displayed greater cortical thickness within the right anterior cingulate and prefrontal cortex (Harrison et al., 2018). Additionally, they had greater hippocampal volume and lower white matter hyperintensity volumes. Another study, examining optimal cognitive aging assessed by high performance in visuo-constructive abilities and visual reasoning, found that older individuals with high fluid abilities displayed greater cortical thickness in large areas of the cingulate cortex. Interestingly, they did not find this same relationship when comparing high vs. average performers in younger groups (Fjell et al., 2006).

Though the cingulate has proven to be important in successful aging, the structural integrity of other regions and networks have also been identified in preserved cognitions. For example, Sun et al. (2016) found that younger SuperAgers, aged 60–80, exhibited greater cortical thickness in the midcingulate, dorsomedial prefrontal cortex, angular gyrus, and superior frontal gyrus; all key regions in the default mode and salience networks. Whole brain analyses in high functioning individuals, aged 90 and older, revealed structural preservation in prefrontal and insular areas (Yang et al., 2016). Similarly, 70 + year old Successful Agers, distinguished by high memory scores, exhibited greater cortical thickness in the insula, midcingulate cortex, and the medial prefrontal cortex (Harrison et al., 2018). Thus, while the cingulate appears in each of these studies, several other regions have been implicated as well, suggesting a possible widespread network contributing to the resistance to cognitive decline.

It is important to note that our goal here is not to identify a set of specific cortical biomarkers of successful aging. Rather, the goal of the present study is a more generalized one. Here, we aim to understand how well cortical thickness can be used to model a behavioral outcome like successful aging, whether certain regions are disproportionately involved in this, and whether the cingulate cortex in particular is disproportionately involved. Thus, one hypothesis is that there is a set of specific regions, such as the cingulate regions, where thickness is able to predict cognitive status, while other regions have little or no predictive value (i.e., the cingulate is particularly informative when trying to model cognitive status). A second hypothesis is that the predictive power is distributed as a relatively smooth gradient across regions, with some more predictive than others, but no clear-cut differentiation between predictive and non-predictive regions. Finally, a third, "null" hypothesis is that all regions are equally predictive (or non-predictive) of cognitive status. Using structural and neuropsychological data from the National Alzheimer's Coordinating center (NACC), we evaluated these hypotheses by examining the relationship between cortical thickness the brain and high cognitive performance in measures of episodic memory and executive function; two abilities that are otherwise known as hallmark domains of cognitive impairment and disease progression. We examined individuals aged 70–89, who demonstrated a combined performance at or above the top 50th percentile in both domains, deemed as Top Cognitive Performers (TCP) and we compared logistic regression performance using the cingulate ROIs relative to using the whole brain. To assess reliability of our models and the overall informativeness of individual regions, we performed Monte Carlo sampling of the population, creating logistic regression models for each sample. Finally, we examined the efficacy of these approaches as a function of age as by breaking them down by decade and including data from *The 90 + Study*. Individuals in their 90s display a more marked and rapid decline than those in their 70s in cognitive domains such as memory, perceptual speed, knowledge, and fluency (Singer et al., 2003), making it valuable to understand how the informativeness of these metrics persists into very advanced stages of aging.

EXPERIMENTAL DESIGN AND METHODS

The National Alzheimer's Coordinating Center

Participants

Three hundred and forty-seven individuals were selected from the larger NACC cohort (**Figure 1A**). NACC is a database of patient information collected from multiple Alzheimer disease centers funded by the National Institute on Aging (Beekly et al., 2004). For this analysis, participants were required to be seventy years old and above (70–89 years old) and have at least one T1 MRI scan available within 2 years of their initial UDS visit. Additionally, participants were required to have a NACC status indicating normal cognition and behavior (NORMCOG and NACCUDSD), as determined by a clinician or panel of clinicians based on neuropsychological test scores, CDR, Form B9 (Clinician Judgment of Symptoms), and center specific tests. Individuals who contained missing data in any of the criteria variables, described below, were excluded from the analyses.

Neuropsychological Criteria for Group Inclusion

Previous studies of successfully aging cohorts have used neuropsychological tests with specific criteria based either on performance being consistent with a younger population or

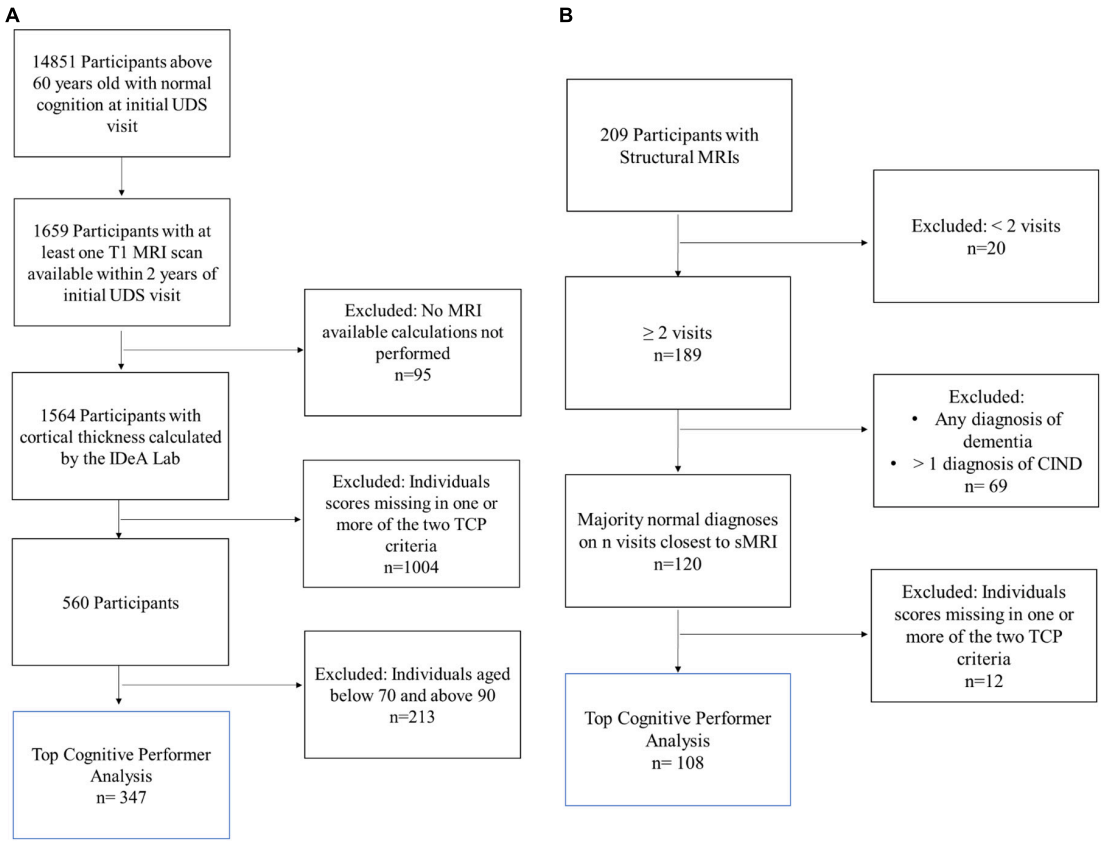

FIGURE 1 | Inclusion flow chart for **(A)** NACC and **(B)** The 90 + Study Participants. Blue box reflects the participants included in the final analysis of top cognitive performers (TCP).

with performance being atypically high for their age group. Following the latter, T were required to be in the top 50th percentile for both the Wechsler Memory Scale-revised Logical Memory IIA-Delayed Recall (WMS-R IIA) and Trails Making Test- Part B (Trails-B). The WMS-R IIA tests verbal and visual modalities and asks participants to recall units of a story after a 15 min delay (Wechsler, 1987). Trails-B engages executive function and processing speed by asking the participant to draw a line that connects an ordered progression of alternating letters and numbers (e.g., 1—A—2—B—3—C. . .) as quickly as possible (Tombaugh, 2004). All individuals that did not fit these criteria were classified as non-Top Cognitive Performers (non-TCP).

MRI Acquisition and Processing

Pre-calculated regional cortical thickness data for NACC MRIs were provided by the IDeA Lab at University of California, Davis. T1-weighted structural MRI (sMRI) scans were obtained from multiple centers using 3.0 and 1.5 Tesla scanners (GE, Siemens, and Phillips). sMRI data from the date closest to the initial UDS visit were processed based on the Advanced Normalization Tools (ANTs) toolkit and thickness pipeline (Das et al., 2009). Modifications to that pipeline for improving GM/WM segmentation used to generate the numbers in NACC are described by Fletcher et al. (2012).

The 90 + Study

Participants

One hundred and eight individuals from the larger *The 90 + Study* cohort were included (**Figure 1B**). The 90 + Study, established in 2003, is an ongoing longitudinal investigation of aging and dementia in individuals aged 90 and above, consisting of the survivors of the Leisure World Cohort Study (Kawas, 2008). Participants were selected based on the availability of a sMRI, two or more neuropsychological visits, and a cognitively normal diagnosis at a majority of their visits (i.e., 2 out of 3 visits or 3 out of 4 visits). Cognitively normal was determined by *The 90 + Study* and refers to a primary diagnosis, determined by neurological examiners, where an individual is deemed as normal, absent of impairment in any cognitive domains, and able to complete Instrumental activities of daily living (IADL). Individuals who contained missing data in any of the criteria variables were excluded from the analyses.

Neuropsychological Criteria for Group Inclusion

While participants in *The 90 + Study* are visited every 6 months by researchers who perform neuropsychological tests, the number of visits for each individual at the time of these analyses varied from 1visit to 23. Thus, based on the available data, median cognitive scores from up to four visits closest to sMRI scan date

were chosen as a more robust measure of cognition that would account possible variance in individual session performance. Following NACC TCP criteria, The 90 + TCP individuals were required to perform at or above the top 50th percentile for their age group on the long-delay recognition portion of the California Verbal Learning Test—short form (CVLT) and at or above the top 50th percentile on completion time for their age group in the Trails-B. All other individuals that did not fit these criteria were classified as non-Top Cognitive Performers (non-TCP).

MRI Acquisition and Processing

T1-weighted structural MRI scans were collected on a 3.0 Tesla GE Discovery MR750w scanner (1 mm isotropic resolution, TE = 3 ms, TR = 7.2 ms, flip angle = 11°). Images were processed using Mindboggle (Klein et al., 2017), which performs atlas registration to the Desikan-Killiany-Tourville (DKT) atlas (Desikan et al., 2006) and cortical thickness estimation using Advanced Normalization Tools (ANTs; its additional FreeSurfer estimates were not used here). ANTs calculates cortical thickness by measuring the distance between gray/white matter boundaries and gray/CSF boundaries by quantifying the amount of registration needed to bring these surfaces together. Thickness was calculated in the original native subject space before being transformed into MNI space. Using DKT regions of interest as masks, we computed the average cortical thickness within each ROI. To reduce edge effects that will be present in these masks (thickness is computed in the cortical sheet and the ROIs will cover voxels not in a particular subject's sheet), thickness maps were clipped at 1mm and the average computed across all resulting non-zero voxels. The average cortical thickness of three bilateral cingulate regions from the DKT atlas (posterior cingulate cortex, caudal anterior cingulate cortex, rostral anterior cingulate cortex) was examined as *a priori* regions based on their previously shown involvement in successful aging (**Figure 2**).

Statistical Analysis of MRI Study Participants and Cortical Thickness

For both datasets, statistical analyses were performed using SAS and both the Statsmodels[1] and skikit-learn[2] libraries in Python. To evaluate the influence of cortical thickness on top cognitive performance (TCP), two logistic regression model were used to model TCP status as a function of regions of interest as follows: (1) 6 bilateral *a priori* cingulate ROIs (rostral anterior, caudal anterior, and posterior segments), and (2) a forward-selection model with 62 whole brain cortical ROIs (cutoff *p*-value for the F statistic, $p = 0.25$). Receiving Operating Characteristic (ROC) curves were created to assess the accuracy of TCP status as a diagnostic marker. Additionally, unpaired *t*-tests were used to evaluate differences in continuous variables (age, education-NACC, and neuropsychological performance) and Fisher's exact test to evaluate gender distribution, across the two subject groups.

[1]https://www.statsmodels.org/

[2]https://scikit-learn.org/

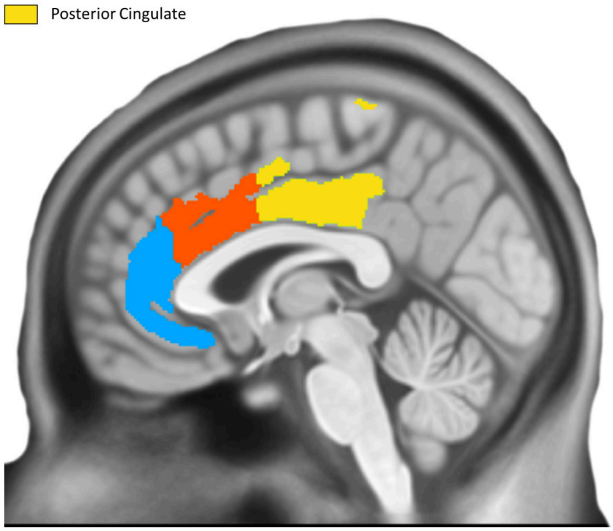

FIGURE 2 | Desikan Killiany Tourville Atlas Three bilateral *a priori* cingulate regions derived from DKT atlas; left hemisphere is shown.

RESULTS

Demographics and Neuropsychological Performance at Baseline

NACC analyses used data from 11 Alzheimer's Disease Research Centers (ADRCs) for UDS visits conducted between September 2005 and December 2020. The average time between initial neuropsychological visit and MRI was 133.3 (189.6) and 138.7 (185.1) days for non-TCP and TCP, respectively. The 347 NACC participants had an average of 15 years of education and were 60.81% female (**Table 1**). TCP and Non-TCP groups did not differ in age in either the 70 [$t(24) = 0.71$, $p = 0.48$] or 80 year old subgroups [$t(1) = 0.98$, $p = 0.33$]. They did, however, differ in education [$t(242) = 5.02$, $p < 0.0001$] and gender distribution (Fisher's exact $p = 0.04$) in the 70 year-olds and education [$t(101) = 2.72$, $p = 0.01$] in the 80 year-olds.

The 108 90 + Study participants were 63.89% female and 47% had a college education (**Table 2**). TCP and Non-TCP did not differ in age [$t(106) = 0.58$, $p = 0.57$], gender distribution (Fisher's exact $p = > 0.999$), or education level at a baseline visit [$X^2(2, n = 108) = 1.88$, $p = 0.39$].

Cortical Thickness in the National Alzheimer's Coordinating Center Sample: *A priori* Cingulate Regions

When considered in isolation, logistic regressions modeling TCP status based on the *a priori* cingulate regions' thickness (**Table 3**) failed to robustly model TCP status. When examining the full NACC 70–89 sample, no cingulate ROI could reliably model TCP status (p's > 0.1, uncorrected for multiple comparisons).

TABLE 1 | NACC demographics.

	All	70 year old's	TCP	Non-TCP	*T*-test/Fisher's exact test	80 Year Old's	TCP	Non-TCP	*T*-test/Fisher's Exact Test
n	347	244	83	161		103	22	81	
Age (SD)	75.94 (4.95)	74.25 (2.72)	74.07 (2.68)	74.34 (2.75)	0.476	83.31 (2.67)	82.82 (2.56)	83.44 (2.70)	0.331
Female (%)	211 (60.81%)	150 (61%)	59 (71%)	91 (56%)	**0.037**	61 (59.22%)	13 (59.09%)	48 (59.26%)	>0.999
Education (SD)	15.00 (3.38)	15.07 (3.35)	16.49 (2.37)	14.33 (3.54)	**<0.0001**	14.82 (3.47)	16.55 (2.54)	14.35 (3.55)	**0.008**

NACC sample subject demographic information with T-test and Fisher's Exact Test comparisons. p value < 0.05.

TABLE 2 | The 90 + study demographics.

	All	TCP	Non-TCP	*T*-test/Fisher's exact test or chi square test
n	108	35	73	
Age (SD)	93.85 (2.60)	94.06 (2.60)	93.75 (2.62)	0.565
Female (%)	69 (63.89)	22 (62.86)	47 (64.38)	>0.999
Education (SD)				0.391
High-school graduate or less (%)	15 (13.89)	3 (8.57)	12 (16.44)	
Some college to college graduate (%)	47 (43.52)	18 (51.43)	29 (39.73)	
Some graduate school or higher (%)	46 (42.59)	14 (40)	32 (43.84)	

The 90 + Study sample subject demographic information with T-Test, Fisher's Exact Test, and Chi square test comparisons.

When restricted to only those in their 70s, the right caudal anterior ($p = 0.04$, uncorrected), and rostral anterior ($p = 0.01$, uncorrected) cingulate showed some predictive power, but this was not the case in the NACC participants in their 80s ($p = 0.15$ and $p = 0.29$, respectively).

We next turned to receiver-operating characteristic (ROC) analysis, using a logistic multiple regression based on all six cingulate ROIs modeling TCP status. Here, we used the area under the curve (AUC) to quantify performance and assess the sensitivity and specificity of the model. Using this, the cingulate regions yielded an estimated AUC of 0.64 across the full age range in NACC (**Figure 3A**). While modest, this AUC was reliably better than chance. Given the combination of the biased base-rate of TCP status and the multiple predictors used (and potential for overfitting), a null value of 0.5 for AUC cannot be assumed. To assess the null and estimate the true alpha, we conducted a permutation analysis, randomly shuffling the TCP/non-TCP labels 10,000 times and running the same logistic regression and AUC estimation to empirically derive an alpha using the same data and the same proportion of TCP status labels. We found the alpha to be ∼0.009, indicating the odds that a large or larger AUC would be generated by chance (**Figure 3D**, blue line).

Cortical Thickness in the National Alzheimer's Coordinating Center Sample: Whole-Brain

To determine whether the cingulate ROIs represented the ideal or near-ideal set of regions for this approach, we next performed a whole-brain forward-selection logistic regression (i.e., using all 62 cortical ROIs). This analysis selected the left caudal anterior cingulate, left caudal middle frontal, left entorhinal, left medial orbitofrontal, left paracentral, right cuneus, and right superior frontal regions with a resulting AUC of 0.74 and a permutation-derived alpha of $p < 0.0001$. Thus, while one of the cingulate regions was present in this model, the optimal model drew upon regions throughout the brain.

We should note that this is not the result of any global difference in cortical thickness across TCP groups. Estimates of average whole-brain cortical thickness were calculated for each individual by weighted averaging of the thickness from all 62 regions (weighted by region volume). Unpaired *t*-tests showed no difference in average whole-brain cortical thickness for the whole cohort or for those in their 70s or 80s separately (all t's < 0.8, all p's > 0.4).

Cortical Thickness Across Age Groups

We next turned to the question of whether our ability to model TCP status was affected by age. To do so, we shifted from thickness values provided by NACC to thickness values derived from ANTs directly as we wanted to include data from The 90 + Study as well to give a broader age range (note, we found that overall, the estimates provided by NACC yielded slightly higher AUCs than those provided by ANTs.) Here, we found that when restricting ourselves to the *a priori* cingulate regions, all three age groups yielded virtually identical ROC curves and 0.68 AUC values (**Figure 3B**). As with the combined data, however, shifting to a whole brain analysis improved performance considerably. The AUCs rose to 0.75 in the cohort in their 70's, 0.88 in those in their 80's, and 0.83 in the 90 + (alpha < 0.0001 in all). ROC contrast estimations comparing AUC's for cingulate vs. forward-selected ROIs revealed a significant difference across all age groups, suggesting a better fit by regional cortical thickness (all $p < 0.02$).

Role of Age, Sex, and Education Covariates

Our primary question here was whether cortical thickness could be used to model TCP status. As such, we excluded typical

TABLE 3 | Fitted logistic regression models.

Age Group	ROI	Fitted Model
70–89	Left Caudal Anterior Cingulate, Left Posterior Cingulate, Left Rostral Anterior Cingulate, Right Caudal Anterior Cingulate, Right Posterior Cingulate, Right Rostral Anterior Cingulate	$\text{Logit(TCP)} = -4.13 + 0.48\ x_{LCaudalAnteriorCingulate} + 0.48\ x_{LPosteriorCingulate} + 0.28\ x_{LRostralAnteriorCingulate} + 0.43\ x_{RCaudalAnteriorCingulate} + 0.33\ x_{RPosteriorCingulate} - 0.61\ x_{RRostralAnteriorCingulate}$
	Left Caudal Anterior Cingulate, Left Caudal Middle Frontal, Left Entorhinal, Left Medial Orbitofrontal, Left Paracentral, Right Cuneus, Right Superior Frontal	$\text{Logit(TCP)} = -2.36 + 0.66\ x_{LCaudalAnteriorCingulate} + 1.72\ x_{LCaudalMiddleFrontal} - 0.62\ x_{LEntorhinal} + 1.28\ x_{LMedialOrbitofrontal} + 1.37\ x_{LParacentral} - 1.00\ x_{RCuneus} - 2.23\ x_{RSuperiorFrontal}$
70s	Left Caudal Anterior Cingulate, Left Posterior Cingulate, Left Rostral Anterior Cingulate, Right Caudal Anterior Cingulate, Right Posterior Cingulate, Right Rostral Anterior Cingulate	$\text{Logit(TCP)} = -3.95 + 0.73\ x_{LCaudalAnteriorCingulate} + 0.28\ x_{LPosteriorCingulate} + 0.51\ x_{LRostralAnteriorCingulate} + 1.05\ x_{RCaudalAnteriorCingulate} + 0.10\ x_{RPosteriorCingulate} - 1.28\ x_{RRostralAnteriorCingulate}$
	Left Entorhinal, Left Inferior Temporal, Left Paracentral, **Left Rostral Anterior Cingulate, Right Caudal Anterior Cingulate**, Right Lingual, **Right Rostral Anterior Cingulate**	$\text{Logit(TCP)} = -4.19 - 0.64\ x_{LEntorhinal} + 1.01\ x_{LInferiorTemporal} + 1.62\ x_{LParacentral} + 1.19\ x_{LRostralAnteriorCingulate} + 1.33\ x_{RCaudalAnteriorCingulate} - 1.50\ x_{RLingual} - 1.39\ x_{RRostralAnteriorCingulate}$
80s	Left Caudal Anterior Cingulate, Left Posterior Cingulate, Left Rostral Anterior Cingulate, Right Caudal Anterior Cingulate, Right Posterior Cingulate, Right Rostral Anterior Cingulate	$\text{Logit(TCP)} = -5.37 - 0.30\ x_{LCaudalAnteriorCingulate} + 1.91\ x_{LPosteriorCingulate} - 0.24 x_{LRostralAnteriorCingulate} - 1.06\ x_{RCaudalAnteriorCingulate} + 0.74\ x_{RPosteriorCingulate} + 0.77\ x_{RRostralAnteriorCingulate}$
	Left Pericalcarine, Left Postcentral, Left Superior Temporal, Left Supramarginal, Right Isthmus Cingulate, Right Parahippocampal, Right Superior Parietal	$\text{Logit(TCP)} = -9.94 + 3.49\ x_{LPericalcarine} + 9.14\ x_{LPostcentral} - 5.33\ x_{LSuperiorTemporal} + 3.95\ x_{LSupramarginal} + 5.76\ x_{RIsthmusCingulate} - 3.72\ x_{RParahippocampal} - 7.79\ x_{RSuperiorParietal}$
90s	Left Caudal Anterior Cingulate, Left Posterior Cingulate, Left Rostral Anterior Cingulate, Right Caudal Anterior Cingulate, Right Posterior Cingulate, Right Rostral Anterior Cingulate	$\text{Logit(TCP)} = -2.67 + 1.51\ x_{LCaudalAnteriorCingulate} + 0.55\ x_{LPosteriorCingulate} - 0.11 x_{LRostralAnteriorCingulate} - 1.28\ x_{RCaudalAnteriorCingulate} + 0.71\ x_{RPosteriorCingulate} - 0.43\ x_{RRostralAnteriorCingulate}$
	Left Isthmus Cingulate, Left Lateral Orbitofrontal, Left Pars Opercularis, Left Transverse Temporal, **Right Caudal Anterior Cingulate**, Right Medial Orbitofrontal, Right Insula	$\text{Logit(TCP)} = -4.21 + 2.31\ x_{LIsthmusCingulate} + 5.41\ x_{LLateralOrbitofrontal} - 6.94\ x_{LParsOpercularis} + 2.25\ x_{LTransverseTemporal} - 2.63\ x_{RCaudalAnteriorCingulate} - 2.77\ x_{RMedialOrbitofrontal} + 2.33\ x_{RInsula}$

First row for each respective age group (70–89, 70s, 80s, and 90s) represents logistic regression models ran with a priori cingulate ROIs as predictors. Second row for each respective age group represents forward selection logistic regression models ran with all 62 cortical ROIs and each region selected; cingulate regions are bolded for reference.

covariates such as age, sex and education that might otherwise predict TCP status and therefore inflate our AUC values. To determine their predictive value beyond cortical thickness, we repeated each of these logistic regression models including these factors. There was a slight increase in AUC's across all age groups when age, sex, and education were added to the model (**Table 4**). The 70 year old group showed the largest improvement, moving from 0.75 to 0.8, while the 80 year old group improved from 0.88 to 0.89 and the 90 year old group from 0.83 to 0.85.

Reliability of Selected Regions

Finally, we turned to the question of the consistency of the generated models. Informally, **Table 3** shows that there is some degree of consistency across models, but that there is significant deviation in the regions chosen as well. These data lead to the hypothesis considered at the outset that, rather than a specific set of ROIs carrying far more predictive value than others, that all ROIs capture some amount of this variance. In this framework, which ROIs are selected in the model might depend, to a large degree, on the specific sample of brains used rather than purely any prior probability of the predictive value of a given region.

Here, we sought to determine the distribution of the predictive value of each ROI across samplings. To do so, we performed a non-parametric bootstrapping analysis that drew 1,000 samples from our 70 to 89 NACC population. Each sample drew the same number of TCP and non-TCP individuals as our final dataset, drawing samples with replacement to arrive at an estimate of the samples one might have outside of our particular population (Wu and Jia, 2013). **Figure 4** shows the resulting distribution of how often each region was selected in the forward-selection logistic along with an inset depicting several possible models. This enables us to determine whether a subset of regions is selected more often than others (e.g., inset, orange line), all regions are equally likely to be selected (inset, blue solid or dashed lines), or

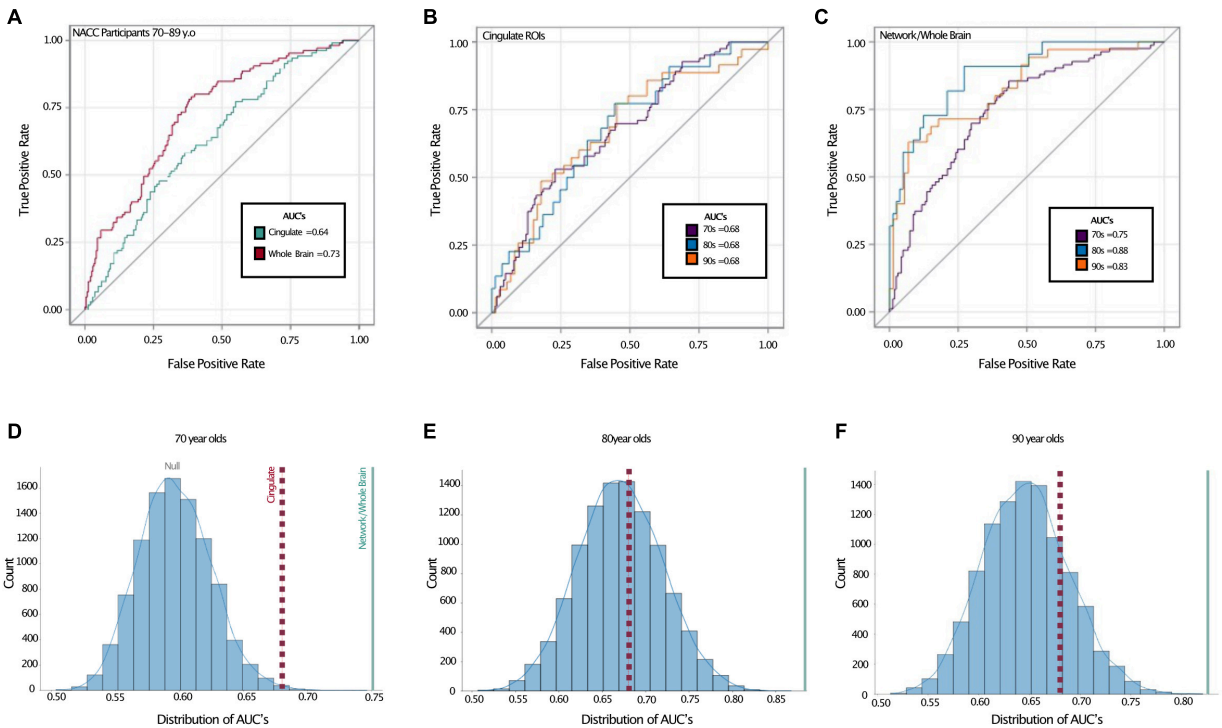

FIGURE 3 | Receiver operating characteristic curves show better TCP predictive performance in whole brain model. Top: ROC curves with area under the curves (AUC) displayed for **(A)** entire NACC sample (ages 70–89), **(B)** *a priori* cingulate regions in all age groups, and **(C)** network/whole-brain forward-selected ROIs across all age groups. Bottom: Permutation analyses where the labeling of TCP vs. non-TCP was shuffled 10,000 times in **(D)** NACC 70 year olds, **(E)** NACC 80 year olds, and **(F)** The 90 + Study 90 year olds. Red dotted lines represent AUC's for *a priori* cingulate ROIS reflected in **(B)** and blue solid lines represent AUC for network/whole-brain forward-selected ROIs reflected in **(C)**. AUC: Area under the curve, 70s: NACC 70 year olds, 80s: NACC 80 year olds, 90s: The 90 + Study 90 year olds.

TABLE 4 | Effects of age, sex, and education on AUC values.

Age group	Forward selected ROIs	Forward selected ROIs + sex	Forward selected ROIs + education	Forward selected ROIs + sex, education	Forward selected ROIs + age, sex, and education
70–89	0.73	0.74	0.77	0.79	0.79
70s	0.75	0.76	0.78	0.80	0.80
80s	0.88	0.89	0.89	0.90	0.89
90s	0.83	0.83	0.84	0.84	0.85

To assess predictive ability beyond cortical thickness, age, sex, and education were added to logistic regression model.

if some in between gradient of predictive value for regions exists (inset, purple line). Results showed a curvilinear distribution that highlighted the relative importance of some regions, but also demonstrated the broad predictive value across the whole brain. In particular, two regions (left entorhinal and right superior frontal) were selected in almost every iteration with two more (left caudal middle frontal and left medial orbitofrontal) selected over 75% of the time. Notably these four ROIs were also included in our initial forward-selection model. Moving down in frequency of selection, 11 ROIs were selected ∼60–70% of the time. This group included three of the *a priori* cingulate ROIs. Note, all of the 62 ROIs were selected at least 22% of the time, although some number of these are at rates expected by chance (determined by 1,000 random shufflings of the TCP/non-TCP labels and repeating the entire process to determine the base rate of region selection). When this analysis was repeated in the 70 year-olds separately, the two of the top four ROIs in the whole group were again in the top 4 here, but the overall distribution was quite linear (**Supplementary Figure 1A**). When repeated in just the 80-year olds, the distribution was again non-linear, but no region was included more than 62% of the iterations and none of the original top four ROIs were present in the top four in this subset (**Supplementary Figure 1B**).

DISCUSSION

The present study aimed to: (1) assess if the cingulate as a localized *a priori* network sufficiently models successful aging, (2) observe if such relationships between cortical thickness and

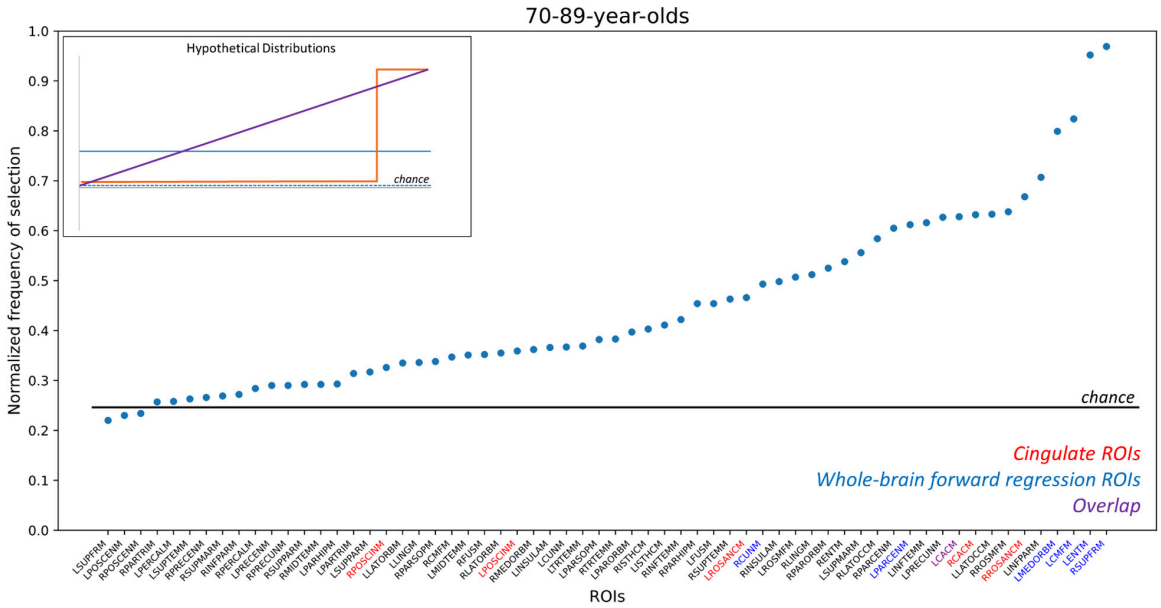

FIGURE 4 | Frequency of ROI selection in bootstrapping analysis. Random samplings of subjects matching our existing TCP rates were repeatedly drawn and analyzed using the same logistic forward regression to determine how often each ROI was selected by the model. ROIs here are sorted by their frequency of being selected, which was normalized by the number of iterations (n = 1,000) to scale from 0 to 1, and ROI names are color-coded by whether they are part of the cingulate *(red)*, were in the original whole-brain model *(blue)*, or both *(purple)*. The horizontal line reflects the chance frequency of selection. ROI names are based on NACC labels. RPOSCINM, Right Posterior Cingulate; LPOSCINM, Left Posterior Cingulate; LROSANCM, Left Rostral Anterior Cingulate; RCUNM, Right Cuneus; LPARCENM, Left Paracentral; LCACM, Left Caudal Anterior Cingulate; RCACM, Right Caudal Anterior Cingulate; RROSANCM, Right Rostral Anterior Cingulate; LMEDORBM, Left Medial Orbital; LCMFM, Left Caudal Middle Frontal; LENTM, Left Entorhinal; RSUPFRM; Right Superior Frontal. For full list, please refer to NACC's Imaging Data Researcher's data dictionary: https://files.alz.washington.edu/documentation/rdd-imaging.pdf. Inset figure: Hypothetical distributions that would arise from different underlying models: *(orange)* distribution that would result if only a small subset of regions were highly predictive; *(purple)* distribution that would result if an even gradient of predictive ability existed across regions; *(blue, dashed)* distribution that would result if no regions' cortical thickness could model TCP status; *(blue, solid)* distribution that would result if all regions had some predictive power but there was no differentiation across regions.

TCP persists in rising age groups, and (3) assess the reliability of various selected networks in the brain in modeling TCP. We were particularly interested in the cingulate cortex based on it recurring role in successful aging literature, as well its role in cognition; including information processing, memory, emotional processing, task engagement, and attention (Vaidya et al., 2007; Pearson et al., 2011; Stanislav et al., 2013). Here, we were able to replicate the finding that the thickness of cingulate cortex can be used to some degree to model TCP status and that this ability was similar across 70s, 80s, and 90 + cohorts (**Figure 3B**). However, we also found that far stronger models could be made when extending the scope of the analysis to the whole brain. Our AUCs from the ROC analyses revealed that, across all age groups, forward selected ROIs from the logistic regression outperformed *a priori* cingulate regions in modeling TCP status. Furthermore, the regions selected by logistic regressions, either on the complete dataset (**Table 4**) or via random sub-sampling of our data (**Figure 4**) often had representation of the cingulate (typically caudal anterior cingulate), but also included representation across the brain.

Thus, while our results continue to implicate structural characteristics of the cingulate cortex in successfully aging individuals, these results suggest that global-style networks, rather than literature driven localized areas, may be better at modeling preserved cognition in the elderly. This is not to suggest a new subset of regions as a model for studying successful aging, but rather to propose examining a more data-driven set of ROIs as a robust approach in modeling superior cognition in memory and executive function.

Similar relationships can be found in other modes of imaging. Seventy-year-old "supernormals," defined by stringent criteria based on 5-year maintenance of episodic memory and executive functioning, displayed stronger functional connectivity between anterior cingulate and the hippocampus, middle cingulate, posterior cingulate, among other regions when compared to healthy elderly controls and those with mild cognitive impairment (MCI) (Lin et al., 2017). More importantly, these researchers identified a functional "Supernormal map," consisting of the right fusiform gyrus, right middle frontal gyrus, right anterior cingulate cortex, left middle temporal gyrus, left precentral gyrus, and left orbitofrontal cortex, which successfully predicted a 1-year change in global cognition and correlated to Alzheimer's pathology (Wang et al., 2019). Similar to possible cortical signatures of successful aging, these findings all suggests a pattern of widespread brain regions that may reflect the neurobiological underpinnings that result in preserved cognition.

This widespread pattern is perhaps best illustrated in **Figure 4** where we aggregated across many random resamplings of our 70–89 year-old population to determine how frequently different regions were included in our logistic model. Under the null hypothesis of all regions being equally uninformative of TCP status (inset, blue dashed), we would have observed a flat

distribution with all regions being included ∼25% of the time. Under a localistic hypothesis in which some subset of regions are informative of TCP status while others are not (inset, orange line), we would have observed a step-function distribution where most regions were uninformative and highly unlikely to be included in the model while others were highly informative and almost always included in the model. Our results were not consistent with either of those hypotheses, instead supporting the view that while cortical thickness is informative of TCP status and while individual regions do vary in their predictive value, there is no specific subset of regions that are the key regions we should use. Instead, the results suggest that many, if not all regions carry the ability to inform modeling of TCP status. Thus, specific set of regions one isolates in a given analysis from a given sample of scans will vary to some degree from what one would arrive at with a different set of scans. However, these results do not arise from simple Type II error as shown by the permutation analyses in **Figures 3D–F** and by the distribution shown in **Figure 4**. Rather, if all regions contain variance that is informative of TCP status to some degree, we would expect that noise and the randomness associated with a particular population (that which we attempted to model in **Figure 4**) will lead to a somewhat different subset of ROIs being chosen in any particular forward selection model, consistent with what we observed in **Table 4**. Therefore, when approaching the problem of modeling TCP status from regional cortical thickness, we must view this as a "brain-wide" problem rather than a "localistic" problem. Rather than approaching a problem such as the relationship between a biomarker like cortical thickness and a behavioral outcome such as TCP status by searching for a critical region or small set of regions, a richer understanding of this relationship might be had by taking a more "distributed" or network-based approach.

While discussing this network-level view of relating regional thickness to TCP status, we should note that a number of the beta coefficients in our models (**Table 3**) are negative. These negative coefficients should not be interpreted as demonstrating a thinner cortex in these regions in TCP individuals. For example, in our 70–89 group, while approximately half of the coefficients in **Table 3** are negative in both the cingulate and the whole-brain analyses, TCP individuals are numerically thicker in all these regions (see also **Figure 3**). The negative coefficients are merely the byproduct of this multiple regression approach.

Finally, we should note that the group analyses in NACC revealed significant differences in sex and education. TCP subjects in their 70s tended to have a higher education and female distribution, while those in their 80s tended to only be more highly educated. All AUCs increased when both sex and education were added into the model, but the gains in AUC appeared quite modest. This is not to say that sex and education are not informative of cognitive status. When examining a cohort of SuperAgers from the Personality and Total Health Through Life (PATH) study, researchers found that SuperAging was both more prevalent in woman and associated to education (Maccora et al., 2021). It is possible that the significant differences in demographics are attributed to TCP group inclusion, which is reflected higher scores in both memory and executive function. Previous studies examining the role of age, sex, and education in elderly cognition revealed that (1) individuals with higher levels of education performed better on cognitive tests and (2) women performed better than men on verbal memory tasks (van Hooren et al., 2007). Additionally, despite there being no group differences in the oldest-old TCP, The 90 + Study previously showed that higher education is associated with lower prevalence rates of dementia in women (Corrada et al., 2008). For example, if education and sex alone are used to model TCP status in the 70–89 group, performance is at least as good as the *a priori* cingulate-only models (AUC = 0.7 vs. the cingulate's AUC of 0.64). However, it is not the case that thickness is merely a very expensive way of determining age and education, as in other groups, performance is far worse (e.g., 90 + Age + Education AUC = 0.52 vs. cingulate AUC = 0.68 or whole-brain AUC = 0.83). Therefore, it is clear that cortical thickness, while potentially correlated with these other factors, can be used to model TCP status irrespective of them.

Limitations

While participants were required to be diagnosed as cognitively normal, and thus determined to be free from MCI or dementia, it is possible that we are capturing some non-TCP individuals who are pre-clinical, defined here as asymptomatic participants with evidence of AD pathology or individuals who display cognitive symptoms that do not meet clinical criteria for MCI. AD-related lesions accumulate in the brain years before cognitive deficits (Morris and Price, 2001; Rowe et al., 2007), with longitudinal studies showing amyloid deposition measured by PET 15 years before symptom onset (Bateman et al., 2012). Thus, it is possible that the effects observed can be attributed to other aging biomarkers not captured on structural MRI, especially given the wide age range. Future studies examining such biomarkers will be informative for better understanding differences in the available data.

We should also point out that the behavioral measures chosen for these analyses were based on previous successful aging studies, which typically use a test of delayed recall [usually CVLT or Rey Auditory Verbal Learning Test (RAVLT)] and executive function (usually Trails B). The WMS-R IIA and CVLT were chosen as tests of delayed recall to mirror this standard as closely as possible, limited by what data is available in each dataset. There are some key differences between these tests of delay recall potentially influencing the differences found between cohorts. The WMS-R IIA requires participants to recall units of a provided story while the CVLT requires participants to recall words from a list. While a narrative will help memory and can be used in both cases, any such narrative must be constructed by the participant in the case of the CVLT, leading to potentially more contamination by executive function in a word list task like the CVLT (Tremont et al., 2000). While these tests are not identical in nature, both are measures of verbal memory and tap into strategic organization of the information to help memory and we find it more likely that the differences observed between cohorts are better explained by additional complex changes the aging brain goes through that may change the importance of structural characteristics of certain brain regions throughout the lifespan, such as amyloid deposition or vascular changes.

It is important to note that differences were also observed within NACC throughout age groups, thus making it less likely that differences are attributed test type.

In addition to the relatively modest sample sizes (particularly in the 80− and 90-year old subgroups), it is important to note the role of volunteer and selection biases these analyses common to many aging studies and potentially all neuroimaging studies. People who are able and willing to participate in imaging tend to be healthier and meet *a priori* selection criteria. One large study examining the nature of volunteer and selection biases found that those who were more likely to participate in studies were also more likely to be cognitively healthy, well-educated, and male compared to their counterparts who were not interested in participating (Ganguli et al., 2015). Inclusion criteria and recruitment, amongst other factors, have led to a more heterogenous population in NACC participants, which tend to be mostly Caucasian and of both high socioeconomic and education status. Given that participants from The 90 + Study are largely survivors of *Leisure World Cohort Study* and recruited from a retirement community in Laguna Woods, California, it is certainly possible that participants are not fully representative of the population. As reported by Melikyan et al. (2019), compared with the oldest-old population in the United States (He and Muenchrath, 2011), the cognitively normal sample in *The 90 + Study* has a higher proportion of Caucasians (98.5% vs. 88%) and a higher percentage of individuals with more than a high school education (78% vs. 28%). Previous research has shown that differences in sex and education may account for cognitive test performance (Hall et al., 2007; van Hooren et al., 2007), and cortical thickness (Seo et al., 2011; Habeck et al., 2020; Steffener, 2021). As reported in **Tables 1**, **2**, the overall TCP NACC sample was 61% female with had an average of 15 years of education, while The 90 + Study sample was 64% female and 46% college educated and above. It is possible that higher education or larger female distributions may be influencing external validity by: (1) introducing a moderation relationship between key demographics, test performance, and cortical thickness that we would not otherwise see in the general public or (2) significantly influencing the distribution of TCP (approximately 32 and 30% for current NACC and The 90 + Study analyses, respectively) that is not representative of all elderly individuals. It is also important to note that, given these potential biases and the fact that percentiles for TCP group inclusion were determined based on a very select subset of each of these cohorts (blue boxes reflected in **Figure 1**), inclusion in the top 50th percentile for each of our cognitive domains may not reflect TCP in the general public. Finally, we should note that the present study cannot identify specific mechanisms that are associated with these differences in cortical thickness.

DATA AVAILABILITY STATEMENT

Publicly available datasets were analyzed in this study. National Alzheimer's Coordinating Center data can be requested here: https://naccdata.org/requesting-data/submit-data-request.

ETHICS STATEMENT

The studies involving human participants were reviewed and approved by the University of California, Institutional Review Board for the 90 + Study. The studies involving data from the NACC were reviewed and approved by their respective IRBs. The patients/participants provided their written informed consent to participate in this study.

AUTHOR CONTRIBUTIONS

CK, CS, and ED conceived of the project. ED, YR, and CS performed data analyses. All authors contributed to writing and editing the manuscript.

FUNDING

This project was funded by R01 AG021055 (PIs: Kawas and Corrada), R01AG034613 (PI: Stark), the UCI ADRC 1P30AG066519 (PI: LaFerla), and by a T32 sub-award to Elena Dominguez (T32 MH119049). The NACC database was funded by NIA/NIH Grant U24 AG072122. NACC data are contributed by the NIA-funded ADRCs: P30 AG019610 (PI Eric Reiman, MD), P30 AG013846 (PI Neil Kowall, MD), P50 AG008702 (PI Scott Small, MD), P50 AG025688 (PI Allan Levey, MD, Ph.D.), P50 AG047266 (PI Todd Golde, MD, Ph.D.), P30 AG010133 (PI Andrew Saykin, PsyD), P50 AG005146 (PI Marilyn Albert, Ph.D.), P50 AG005134 (PI Bradley Hyman, MD, Ph.D.), P50 AG016574 (PI Ronald Petersen, MD, Ph.D.), P50 AG005138 (PI Mary Sano, Ph.D.), P30 AG008051 (PI Thomas Wisniewski, MD), P30 AG013854 (PI Robert Vassar, Ph.D.), P30 AG008017 (PI Jeffrey Kaye, MD), P30 AG010161 (PI David Bennett, MD), P50 AG047366 (PI Victor Henderson, MD, MS), P30 AG010129 (PI Charles DeCarli, MD), P50 AG016573 (PI Frank LaFerla, Ph.D.), P50 AG005131 (PI James Brewer, MD, Ph.D.), P50 AG023501 (PI Bruce Miller, MD), P30 AG035982 (PI Russell Swerdlow, MD), P30 AG028383 (PI Linda Van Eldik, Ph.D.), P30 AG053760 (PI Henry Paulson, MD, Ph.D.), P30 AG010124 (PI John Trojanowski, MD, Ph.D.), P50 AG005133 (PI Oscar Lopez, MD), P50 AG005142 (PI Helena Chui, MD), P30 AG012300 (PI Roger Rosenberg, MD), P30 AG049638 (PI Suzanne Craft, Ph.D.), P50 AG005136 (PI Thomas Grabowski, MD), P50 AG033514 (PI Sanjay Asthana, MD, FRCP), P50 AG005681 (PI John Morris, MD), P50 AG047270 (PI Stephen Strittmatter, MD, Ph.D.).

SUPPLEMENTARY MATERIAL

The Supplementary Material for this article can be found online at: https://www.frontiersin.org/articles/10.3389/fnagi.2021.751375/full#supplementary-material

REFERENCES

Bateman, R. J., Xiong, C., Benzinger, T. L. S., Fagan, A. M., Goate, A., Fox, N. C., et al. (2012). Clinical and Biomarker Changes in Dominantly Inherited Alzheimer's Disease. *N. Engl. J. Med.* 367, 795–804. doi: 10.1056/NEJMoa1202753

Beekly, D. L., Ramos, E. M., van Belle, G., Deitrich, W., Clark, A. D., Jacka, M. E., et al. (2004). The National Alzheimer's Coordinating Center (NACC) Database: an Alzheimer Disease Database. *Alzheimer Dis. Assoc. Disord.* 18, 270–277.

Corrada, M. M., Brookmeyer, R., Berlau, D., Paganini-Hill, A., and Kawas, C. H. (2008). Prevalence of dementia after age 90: results from The 90+ Study. *Neurology* 71, 337–343. doi: 10.1212/01.wnl.0000310773.65918.cd

Das, S. R., Avants, B. B., Grossman, M., and Gee, J. C. (2009). Registration based cortical thickness measurement. *NeuroImage* 45, 867–879. doi: 10.1016/j.neuroimage.2008.12.016

Desikan, R. S., Ségonne, F., Fischl, B., Quinn, B. T., Dickerson, B. C., Blacker, D., et al. (2006). An automated labeling system for subdividing the human cerebral cortex on MRI scans into gyral based regions of interest. *Neuroimage* 31, 968–980. doi: 10.1016/j.neuroimage.2006.01.021

Fjell, A. M., Walhovd, K. B., Reinvang, I., Lundervold, A., Salat, D., Quinn, B. T., et al. (2006). Selective increase of cortical thickness in high-performing elderly—structural indices of optimal cognitive aging. *NeuroImage* 29, 984–994. doi: 10.1016/j.neuroimage.2005.08.007

Fletcher, E., Singh, B., Harvey, D., Carmichael, O., and DeCarli, C. (2012). "Adaptive image segmentation for robust measurement of longitudinal brain tissue change," in *in 2012 Annual International Conference of the IEEE Engineering in Medicine and Biology Society* (San Diego, CA: IEEE), 5319–5322. doi: 10.1109/EMBC.2012.6347195

Ganguli, M., Lee, C.-W., Hughes, T., Snitz, B. E., Jakubcak, J., Duara, R., et al. (2015). Who wants a free brain scan? assessing and correcting for recruitment biases in a population-based smri pilot study. *Brain Imaging Behav.* 9, 204–212. doi: 10.1007/s11682-014-9297-9

Gefen, T., Peterson, M., Papastefan, S. T., Martersteck, A., Whitney, K., Rademaker, A., et al. (2015). Morphometric and Histologic Substrates of Cingulate Integrity in Elders with Exceptional Memory Capacity. *J. Neurosci.* 35, 1781–1791. doi: 10.1523/JNEUROSCI.2998-14.2015

Habeck, C., Gazes, Y., Razlighi, Q., and Stern, Y. (2020). Cortical thickness and its associations with age, total cognition and education across the adult lifespan. *PLoS One* 15:e0230298. doi: 10.1371/journal.pone.0230298

Hall, C. B., Derby, C., LeValley, A., Katz, M. J., Verghese, J., and Lipton, R. B. (2007). Education delays accelerated decline on a memory test in persons who develop dementia. *Neurology* 69, 1657–1664. doi: 10.1212/01.wnl.0000278163.82636.30

Harrison, T. M., Maass, A., Baker, S. L., and Jagust, W. J. (2018). Brain morphology, cognition, and β-amyloid in older adults with superior memory performance. *Neurobiol. Aging* 67, 162–170. doi: 10.1016/j.neurobiolaging.2018.03.024

Harrison, T. M., Weintraub, S., Mesulam, M.-M., and Rogalski, E. (2012). Superior Memory and Higher Cortical Volumes in Unusually Successful Cognitive Aging. *J. Int. Neuropsychol. Soc.* 18, 1081–1085. doi: 10.1017/S1355617712000847

He, W., Muenchrath, M. N. (2011). *Economics and Statistics Administration*. Suitland, MD: U.S. Census Bureau. Available online at: https://www.census.gov/library/publications/2011/acs/acs-17.html

Kawas, C. H. (2008). The oldest old and the 90+ Study. *Alzheimers Dement.* 4, S56–S59. doi: 10.1016/j.jalz.2007.11.007

Klein, A., Ghosh, S. S., Bao, F. S., Giard, J., Häme, Y., Stavsky, E., et al. (2017). Mindboggling morphometry of human brains. *PLoS Comput. Biol.* 13:e1005350. doi: 10.1371/journal.pcbi.1005350

Lin, F., Ren, P., Mapstone, M., Meyers, S. P., Porsteinsson, A., and Baran, T. M. (2017). The Cingulate Cortex of Older Adults with Excellent Memory Capacity. *Cortex* 86, 83–92. doi: 10.1016/j.cortex.2016.11.009

Maccora, J., Peters, R., and Anstey, K. J. (2021). Gender Differences in Superior-memory SuperAgers and Associated Factors in an Australian Cohort. *J. Appl. Gerontol.* 40, 433–442. doi: 10.1177/0733464820902943

Melikyan, Z. A., Corrada, M. M., Dick, M. B., Whittle, C., Paganini-Hill, A., and Kawas, C. H. (2019). Neuropsychological Test Norms in Cognitively Intact Oldest-Old. *J. Int. Neuropsychol. Soc.* 25, 530–545. doi: 10.1017/S1355617719000122

Morris, J. C., and Price, J. L. (2001). Pathologic correlates of nondemented aging, mild cognitive impairment, and early-stage Alzheimer's disease. *J. Mol. Neurosci.* 17, 101–118.

Pearson, J. M., Heilbronner, S. R., Barack, D. L., Hayden, B. Y., and Platt, M. L. (2011). Posterior cingulate cortex: adapting behavior to a changing world. *Trends Cogn. Sci.* 15, 143–151. doi: 10.1016/j.tics.2011.02.002

Rowe, C. C., Ng, S., Ackermann, U., Gong, S. J., Pike, K., Savage, G., et al. (2007). Imaging β-amyloid burden in aging and dementia. *Neurology* 68, 1718–1725.

Seo, S. W., Im, K., Lee, J.-M., Kim, S. T., Ahn, H. J., Go, S. M., et al. (2011). Effects of demographic factors on cortical thickness in Alzheimer's disease. *Neurobiol. Aging* 32, 200–209. doi: 10.1016/j.neurobiolaging.2009.02.004

Singer, T., Verhaeghen, P., Ghisletta, P., Lindenberger, U., and Baltes, P. B. (2003). The fate of cognition in very old age: six-year longitudinal findings in the Berlin Aging Study (BASE). *Psychol. Aging* 18, 318–331. doi: 10.1037/0882-7974.18.2.318

Stanislav, K., Alexander, V., Maria, P., Evgenia, N., and Boris, V. (2013). Anatomical characteristics of cingulate cortex and neuropsychological memory tests performance. *Procedia Soc. Behav. Sci.* 86, 128–133.

Steffener, J. (2021). Education and age-related differences in cortical thickness and volume across the lifespan. *Neurobiol. Aging* 102, 102–110. doi: 10.1016/j.neurobiolaging.2020.10.034

Sun, F. W., Stepanovic, M. R., Andreano, J., Barrett, L. F., Touroutoglou, A., and Dickerson, B. C. (2016). Youthful Brains in Older Adults: preserved Neuroanatomy in the Default Mode and Salience Networks Contributes to Youthful Memory in Superaging. *J. Neurosci.* 36, 9659–9668. doi: 10.1523/JNEUROSCI.1492-16.2016

Tombaugh, T. N. (2004). Trail Making Test A and B: normative data stratified by age and education. *Arch. Clin. Neuropsychol.* 19, 203–214. doi: 10.1016/S0887-6177(03)00039-8

Tremont, G., Halpert, S., Javorsky, D. J., and Stern, R. A. (2000). Differential Impact of Executive Dysfunction on Verbal List Learning and Story Recall. *Clin. Neuropsychol.* 14, 295–302. doi: 10.1076/1385-4046(200008)14:3;1-P;FT295

US Census Bureau. (2010). *The Older Population: 2010*. Available online at: https://www.census.gov/newsroom/press-releases/2018/cb18-41-population-projections.html

US Census Bureau. (2018). *Older People Projected to Outnumber Children*. Suitland, MD: The United States Census Bureau.

Vaidya, J. G., Paradiso, S., Ponto, L. L. B., McCormick, L. M., and Robinson, R. G. (2007). Aging, grey matter, and blood flow in the anterior cingulate cortex. *Neuroimage* 37, 1346–1353.

van Hooren, S. A. H., Valentijn, A. M., Bosma, H., Ponds, R. W. H. M., Boxtel, M. P. J., van, et al. (2007). Cognitive Functioning in Healthy Older Adults Aged 64–81: a Cohort Study into the Effects of Age, Sex, and Education. *Neuropsychol. Dev. Cogn. B Aging Neuropsychol. Cogn.* 14, 40–54. doi: 10.1080/138255890969483

Wang, X., Ren, P., Baran, T. M., Raizada, R. D. S., Mapstone, M., and Lin, F. (2019). Longitudinal Functional Brain Mapping in Supernormals. *Cereb. Cortex* 29, 242–252. doi: 10.1093/cercor/bhx322

Wechsler, D. (1987). *WMS-R: wechsler Memory Scale–Revised: manual*. San Antonio, TX: Psychological Corporation.

Wu, W., and Jia, F. (2013). A New Procedure to Test Mediation With Missing Data Through Nonparametric Bootstrapping and Multiple Imputation. *Multivariate Behav. Res.* 48, 663–691. doi: 10.1080/00273171.2013.816235

Yang, Z., Wen, W., Jiang, J., Crawford, J. D., Reppermund, S., Levitan, C., et al. (2016). Age-associated differences on structural brain MRI in nondemented

individuals from 71 to 103 years. *Neurobiol. Aging* 40, 86–97. doi: 10.1016/j.neurobiolaging.2016.01.006

Conflict of Interest: The authors declare that the research was conducted in the absence of any commercial or financial relationships that could be construed as a potential conflict of interest.

Publisher's Note: All claims expressed in this article are solely those of the authors and do not necessarily represent those of their affiliated organizations, or those of the publisher, the editors and the reviewers. Any product that may be evaluated in this article, or claim that may be made by its manufacturer, is not guaranteed or endorsed by the publisher.

frontiers in Human Neuroscience

ORIGINAL RESEARCH
published: 05 November 2021
doi: 10.3389/fnhum.2021.753836

Resting State Networks Related to the Maintenance of Good Cognitive Performance During Healthy Aging

Satoshi Maesawa[1,2], Satomi Mizuno[3], Epifanio Bagarinao[1], Hirohisa Watanabe[1,4], Kazuya Kawabata[1,5], Kazuhiro Hara[5], Reiko Ohdake[4], Aya Ogura[5], Daisuke Mori[1,6], Daisuke Nakatsubo[2], Haruo Isoda[1], Minoru Hoshiyama[1], Masahisa Katsuno[5], Ryuta Saito[2], Norio Ozaki[1,6] and Gen Sobue[1,7]*

[1] Brain and Mind Research Center, Nagoya University, Nagoya, Japan, [2] Department of Neurosurgery, Nagoya University Graduate School of Medicine, Nagoya, Japan, [3] Department of Rehabilitation Medicine, National Hospital Organization, Nagoya Medical Center, Nagoya, Japan, [4] Department of Neurology, Fujita Health University, Toyoake, Japan, [5] Department of Neurology, Nagoya University Graduate School of Medicine, Nagoya, Japan, [6] Department of Psychiatry, Nagoya University Graduate School of Medicine, Nagoya, Japan, [7] Department of Neurology, Aichi Medical University, Nagakute, Japan

OPEN ACCESS

Edited by:
Eric Tatt Wei Ho, University of Technology Petronas, Malaysia

Reviewed by:
Eleanna Varangis, Columbia University, United States
Colleen Hughes, McGill University, Canada

***Correspondence:**
Satoshi Maesawa
smaesawa@med.nagoya-u.ac.jp

Specialty section:
This article was submitted to Brain Health and Clinical Neuroscience, a section of the journal Frontiers in Human Neuroscience

Received: *05 August 2021*
Accepted: *19 October 2021*
Published: *05 November 2021*

Citation:
Maesawa S, Mizuno S, Bagarinao E, Watanabe H, Kawabata K, Hara K, Ohdake R, Ogura A, Mori D, Nakatsubo D, Isoda H, Hoshiyama M, Katsuno M, Saito R, Ozaki N and Sobue G (2021) Resting State Networks Related to the Maintenance of Good Cognitive Performance During Healthy Aging. Front. Hum. Neurosci. 15:753836. doi: 10.3389/fnhum.2021.753836

Purpose: Maintenance of cognitive performance is important for healthy aging. This study aims to elucidate the relationship between brain networks and cognitive function in subjects maintaining relatively good cognitive performance.

Methods: A total of 120 subjects, with equal number of participants from each age group between 20 and 70 years, were included in this study. Only participants with Addenbrooke's Cognitive Examination – Revised (ACE-R) total score greater than 83 were included. Anatomical T1-weighted MR images and resting-state functional MR images (rsfMRIs) were taken from all participants using a 3-tesla MRI scanner. After preprocessing, several factors associated with age including the ACE-R total score, scores of five domains, sub-scores of ACE-R, and brain volumes were tested. Morphometric changes associated with age were analyzed using voxel based morphometry (VBM) and changes in resting state networks (RSNs) were examined using dual regression analysis.

Results: Significant negative correlations with age were seen in the total gray matter volume (GMV, $r = -0.58$), and in the memory, attention, and visuospatial domains. Among the different sub-scores, the score of the delayed recall (DR) showed the highest negative correlation with age ($r = -0.55$, $p < 0.001$). In VBM analysis, widespread regions demonstrated negative correlation with age, but none with any of the cognitive scores. Quadratic approximations of cognitive scores as functions of age showed relatively delayed decline compared to total GMV loss. In dual regression analysis, some cognitive networks, including the dorsal default mode network, the lateral dorsal attention network, the right / left executive control network, the posterior salience network, and the language network, did not demonstrate negative correlation with age. Some regions in the sensorimotor networks showed positive correlation with the DR, memory, and fluency scores.

Conclusion: Some domains of the cognitive test did not correlate with age, and even the highly correlated sub-scores such as the DR score, showed delayed decline compared to the loss of total GMV. Some RSNs, especially involving cognitive control regions, were relatively maintained with age. Furthermore, the scores of memory, fluency, and the DR were correlated with the within-network functional connectivity values of the sensorimotor network, which supported the importance of exercise for maintenance of cognition.

Keywords: resting state network, aging, healthy cohort, cognition, delayed recall

INTRODUCTION

According to Rowe and Kahn, successful aging consists of three principal components: low risk of disease and disease-related disability, maintenance of high mental, cognitive, and physical functions, and continuous engagement with life, which includes relations with others and productive activity (Rowe and Kahn, 1987, 1997, 2015). During the last two decades, worldwide life expectancy has increased by more than 6.6 years, while healthy life expectancy (HALE), an average period of life-time spent without limitation in daily activities, has also increased by 5.4 years (World Health Organization, 2020). Especially in Japan where the highest aging rate was recorded in the world, the increase in the HALE has exceeded the one in life expectancy (Cabinet Office Japan, 2020). Not only mortality has kept declining, but also years lived with disability has been drastically reduced. Under this global situation, successful aging has gained its importance, and has greatly affected a variety of fields including health science, sociology, economics, and politics.

Cognitive function is an extremely important factor influencing successful aging in the elderly people. It is widely known that cognitive function gradually declines over age even in people who seemed to be healthy. This is especially the case for memory and fluid intelligence, acquired in order to adapt to various circumstances including speed processing, reasoning, working memory, and short term memory (Park et al., 2002). On the other hand, crystalized intelligence, acquired from one's accumulated experience and education and included language abilities, comprehension, and insight, is maintained or improved with age (Baltes et al., 1999). Empirically, when a screening test for cognitive function is performed, unexpected variations in sub-scores can be observed to some extent even if subjects are considered normal in cognitive function based on the total score falling within the normal range.

Morphological studies of the brain using structural magnetic resonance imaging (MRI) have reported wide range of gray matter volume (GMV) decreases with age (Good et al., 2001; Giorgio et al., 2010). The GMV begins to decrease in early adulthood, and continues to decrease approximately linearly throughout the lifespan (Ge et al., 2002; Sowell et al., 2003; Lehmbeck et al., 2006). Although the GMV is generally reduced with age during healthy aging, it still remains unclear whether a cognitive function decline parallels GMV decline. Several studies have been performed about the associations between regional GMV and cognitive scores, but there is no detailed report on the comparison between subtle changes of cognitive test scores in healthy aging and the changes in GMV.

In network analysis using resting state functional MRI (rsfMRI), reduction of the functional connectivity within the default mode network (DMN) with age has been reported in many literatures (Damoiseaux et al., 2008; Koch et al., 2010; Jones et al., 2011). In addition, a within-network decline in functional connectivity has also been reported in other large-scale functional networks, including the salience network (SN), executive control network (ECN), attention network, sensorimotor network (SMN) and the visual network (VN) involved in primary processing (Onoda et al., 2012; Tomasi and Volkow, 2012; Betzel et al., 2014; Geerligs et al., 2015; Huang et al., 2015). Although such canonical networks showed decreases of within-network connectivity, between-network connectivity of some pairs of these networks somewhat increases (Meier et al., 2012; Betzel et al., 2014; Chan et al., 2014; Bagarinao et al., 2019), a possible reflection of the functional network reorganization with aging. Several studies have also reported the relationship between cognitive decline and network changes, e.g., between anterior DMN and executive control function (Damoiseaux et al., 2008), between SN and configuration ability and frontal lobe function (Onoda et al., 2012), and between cingulate network and episodic memory, attentional function, and executive function (Hausman et al., 2020). However, the target age and the number of subjects included were limited in each study, and the findings were inconclusive.

What are the different factors influencing successful aging? Can these factors be identified based on the characteristics of brain-imaging-derived metrics such as brain volume and connectivity? The purpose of this study was to identify such characteristics by investigating the relationship among aging, brain volume, brain network changes, and cognitive function in healthy subjects. For this purpose, healthy individuals who maintained relatively good cognition were enrolled in the study. Within age groups, ranging from 20 to 70 years, an equal number of subjects were included. Although voxel based morphometry (VBM) analysis was performed as the first step, network analysis using rsfMRI represented the main part of this study. RsfMRI is a useful method to visualize various large-scale networks in the brain by examining the synchronization of the blood oxygen level dependent (BOLD) changes in different brain regions during rest, i.e., without performing any tasks, and has been utilized in evaluating changes in brain networks

in aging (Bagarinao et al., 2020) and the pathology of various diseases in the central nervous system from Alzheimer's disease to brain tumors (Greicius et al., 2004; Maesawa et al., 2015; Mulders et al., 2015; Putcha et al., 2015; Abbott et al., 2016). Our hypotheses are as follows: (1) Even in healthy subjects with total score of the cognitive screening test within normal range, some variations of the sub-items in the cognitive test may reflect association with aging. (2) Such sub-items may have a spatiotemporal relationship with the brain's structural differences with age. Some sub-items may show differences with age that parallel with the structural differences, whereas others may show the maintenance of these scores, independent from the structural differences. (3) To help us understand such maintenance, a network-based approach may be necessary aside from the morphological approach, and the analysis using rsfMRI may contribute to the evaluation of the alterations of the RSNs, which may be correlated with the subtle change of cognition observed in our healthy cohort. (4) On the other hand, some networks may be maintained despite of advancing age, which may provide an explanation for the neuronal basis of the maintenance of cognitive function. Through these analyses, we will identify the different conditions necessary for the maintenance of good cognitive function during aging, that is, the different conditions for successful aging.

MATERIALS AND METHODS

Participants

This study was part of the on-going healthy aging cohort study in the Brain & Mind Research Center (BMRC) in Nagoya University, which was approved by the Ethics Committee of Nagoya University Graduate School of Medicine (approval number 2014-0068), and conducted following the Ethical Guidelines for Medical and Health Research Involving Human Subjects as endorsed by the Japanese Government. All participants were healthy volunteers who joined in response to the recruitment using leaflets and the website of the BMRC. Inclusion criteria for the original project were as follows: older than 20 years, not pregnant, had no episode for MRI contraindications, no brain diseases such as cerebrovascular diseases, brain tumor, head injury, depression, and schizophrenia. They provided written informed consent before joining the study. Between 2014 and 2020, more than 1,000 volunteers participated. From the pool of volunteers, a total of 120 participants, consisting of 10 men and 10 women in each of the 6 age groups, 20s, 30s, 40s, 50s, 60s, and 70s, were randomly chosen. Exclusion criteria were as follows: (1) inability to complete the Japanese version of Addenbrooke's Cognitive Examination-Revised (ACE-R) assessment, (2) presence of structural abnormalities (e.g., asymptomatic cerebral infarction, benign brain tumor, white matter abnormalities, etc.) in structural MRI as identified by Japanese board-certified neurologists (HW, KH, and KK) and neurosurgeon (SM), (3) ACE-R total score less than 83, and (4) incomplete imaging data. The mean age for all participants was 48.9 $\pm$ 17.6 (SD) years, 22.7 $\pm$ 2.0 years old for those in the 20s (n = 20), 34.7 $\pm$ 2.9 years old in the 30s (n = 20), 44.5 $\pm$ 2.7 years old in the 40s (n = 20), 53 $\pm$ 2.7 years old in the 50s (n = 20), 63.9 $\pm$ 2.7 years old in the 60s (n = 20), and 74.6 $\pm$ 3 years old in the 70s (n = 20). The average number of years for education was 14.24 $\pm$ 2.52 years. The percentage of participants who smoked were 58.3% in men, 25% in women, and 41.7% in total (**Table 1**). In term of head motion, which typically affect the estimation of the functional connectivity, the mean frame-wise displacement (FD) values (Power et al., 2012) was 0.18 + 0.069 mm on average. The number of subjects with mean FD greater than 0.2 mm was 39 (32.5%) and those with less than 0.2 mm was 81 (67.5%). No participants had mean FD greater than 0.5 mm.

Acquisition of MR Imaging Data

T1 anatomical images and rsfMRI data were obtained from all participants. MRI scanning was performed using a Siemens Magnetom Verio (Siemens, Erlangen, Germany) 3.0-T scanner with a 32-channel head coil at the BMRC in Nagoya University. The high-resolution T1-weighted images (T1-WI) were acquired using a 3D magnetization prepared rapid acquisition gradient echo (MPRAGE) sequence with the following imaging parameters: repetition time (TR) = 2.5 s, echo time (TE) = 2.48 ms, 192 sagittal slices with a distance factor of 50% and 1-mm thickness, field of view (FOV) = 256 mm, 256 $\times$ 256 matrix size, and an in-plane voxel resolution of 1 $\times$ 1 mm2. For the rsfMRI data, a gradient-echo (GE) echo-planar imaging (EPI) sequence was used with the following acquisition parameters: TR = 2.5 s, TE = 30 ms, 39 transversal slices with a 0.5-mm inter-slice interval and 3-mm thickness, FOV = 192 mm, 64 $\times$ 64 matrix dimension, flip angle of 80° and 198 total volumes. During rsfMRI scan, the participants were instructed to close their eyes but to stay awake. The subject's head was tightly fixed with cushions to minimize its motion.

Neuropsychological Test

A Japanese version of ACE-R was performed to evaluate cognitive function for all participants. ACE-R is a brief battery that provides evaluation of five cognitive domains (orientation / attention, memory, verbal fluency, language and visuospatial ability) with a total score of 100 points, and usually requires about 15 min for the examination (Mathuranath et al., 2000; Yoshida et al., 2012). Participants who obtained 82 points or less in total score were excluded from this study because of the possibility of dementia. The sensitivity and specificity of the total ACE-R score was reported to be 99 and 99%, respectively, for dementia when the cut-off score of 82/83 was used, and 87 and 92%, respectively, for MCI, when the cut-off score of 88/89 was used (Yoshida et al., 2012). In addition to the total score, the scores for each of the five cognitive domains, the sub-score of verbal fluency such as semantic or phonological word recall, the sub-score of memory such as memorization, delayed memory, and recognition, and the sub-scores for others were also documented.

Image Preprocessing

Image preprocessing for the anatomical T1WI and rsfMRI dataset was performed using Statistical Parametric Mapping (SPM12, Wellcome Trust Center for Neuroimaging, London,

TABLE 1 | The characteristics of participants and the score of ACE-R test.

	All (*n*=120)		Male (*n*=60)		Female (*n*=60)		20s (*n*=20)		30s (*n*=20)		40s (*n*=20)		50s (*n*=20)		60s (*n*=20)		70s (*n*=20)	
	mean	SD	mean	SD	mean	SD	mean	SD	mean	SD	mean	SD	mean	SD	mean	SD	Mean	SD
Age	48.9	17.6	48.6	17.6	49.1	17.8	22.7	2	34.7	2.9	44.5	2.7	53	2.7	63.9	2.7	74.6	3
The year of education	14.2	2.5	14.5	2.7	14	2.4	15.9	1.4	15	2.8	14.4	3.3	12.9	1.9	14.7	1.8	12.7	2.2
ACE-R total (100)	95.7	3.2	95.9	2.9	95.6	3.6	96.6	1.7	97.4	2.6	96.3	2.4	96.5	2.8	95.2	3.5	92.6	3.8
Attention/orientation (18)	17.9	0.4	17.9	0.3	17.9	0.4	18	0.2	18	0	18	0.2	17.9	0.4	18	0	17.5	0.7
Fluency (14)	13.4	1.2	13.4	1	13.5	1.3	13.8	0.4	13.4	1.4	13.4	1	13.4	1.6	13.3	1.2	13.5	1
Memory (26)	23.6	2	23.7	2.1	23.6	2	24.1	0.9	24.9	1.3	24.2	1.2	24.1	1.6	23.2	2.1	21.5	2.8
Language (26)	25.1	1.1	25.3	0.9	25	1.2	25	1.4	25.4	1	25.3	1	25.4	0.7	25.2	0.8	24.7	1.3
Visuospatial (16)	15.7	0.7	15.7	0.7	15.7	0.7	15.8	0.6	15.9	0.5	15.6	0.7	15.8	0.4	15.5	0.8	15.5	0.9
The rate of smoker	41.7%		58.3%		25%		15%		35%		65%		40%		55%		40%	

United Kingdom) running on Matlab (R2016a, MathWorks, Natick, Mass, United States). The T1WI images were first segmented into component images including gray matter (GM), white matter (WM), and cerebrospinal fluid (CSF), among others, by the segmentation approach included in SPM12. Bias-corrected T1WI and the transformation information from subject space to MNI (Montreal Imaging Institute) space were also obtained during segmentation. For rsfMRI dataset, we excluded the first 5 volumes in the series in order to account for the effects of the initial scanner inhomogeneity. Slice-time correction was then performed relative to the middle slice (slice 20), and the images were realigned to the mean functional volume. The mean volume, together with the realigned functional images, were then co-registered to the bias-corrected T1WI anatomical images. The co-registered functional images were normalized to the MNI space using the transformation information obtained during segmentation, resampled to have an isotropic voxel resolution equal to 2 x 2 x 2 mm^3, and smoothed using an isotropic 8-mm full-width-at-half-maximum (FWHM) 3D Gaussian filter. To correct for head motion and contribution from other nuisance signals, we regressed out 24 motion-related regressors [R_t R_t^2 R_{t-1} R_{t-1}^2], where R = [x, y, z, roll, pitch, yaw] represents the estimated motion parameters (3 translations and 3 rotations). Signals extracted from spherical ROIs within the CSF (center's MNI coordinate = [20, −32, 18], radius = 4 mm) and WM (center's MNI coordinate = [24, −12, 34], radius = 4 mm), the global signal, as well as the signals' derivatives were also removed. Finally, the preprocessed data were then bandpass filtered within 0.01–0.1 Hz. All preprocessing were performed using in-house Matlab scripts as reported previously (Bagarinao et al., 2019). The preprocessed dataset were used in the succeeding analysis.

Data Analysis

A Correlation Analysis and Regression Analysis for Age-Related Factors

In order to identify the factors related to aging, correlation analyses with age were performed using Spearman's rank correlation coefficient method. Variables individually examined included gender, years of education, GMV, WMV, CSFV, and total intracranial volume (TICV) calculated from the anatomical T1WI images, the total score of ACE-R, and the sub-score of each domains (orientation / attention, memory, verbal fluency, language and visuospatial ability). In addition, sub-items of cognitive function in the ACE-R were also examined. Considering the ceiling effects, only sub-items with relatively high variance (SD > 0.5), such as the counts of the correct answer to the serial subtraction of number 7, phonological or semantic word recall score, picture naming score, and delayed recall (DR) score, were included in the analysis. The threshold for statistical significance was set at $p < 0.05$. Next, regression analysis was performed for each factor with significant correlation with age. The statistical significance threshold was set at $p < 0.05$. We examined two regression models. One is linear in age, and the other is quadratic. The appropriate regression model (linear vs. quadratic) was assessed using the coefficient of determination

(R2), the Bayesian information criterion (BIC), and the Akaike's information criterion (AIC).

VBM Analysis With Factors Associated for Aging

The total volumes of GM, WM, and CSF were calculated using the segmented components of the T1-weighted images. Using SPM 12, multiple regression analysis was performed with covariates including age, gender, years of education, and five cognitive domains (orientation/attention, fluency, memory, language, and visuospatial). Global calculation was performed using TICV. The threshold for statistical significance was set at a corrected $p < 0.05$ with a family wise correction (FWE). We also examined the association between GMV and the score of the DR, which showed the highest significant relationship with age in the above correlation analysis, under two different conditions. In one condition, age and the TICV were included as covariates, while in the other condition, age was excluded. Xjview[1] was used to examine regions with significant association with age or the score of delayed memory in the resulting statistical maps. Automatic anatomical labeling (AAL) was used for the anatomical name of the identified region.

Resting State Network Analysis for Aging and the Associated Factors

To evaluate the relationship between factors associated with aging and brain functional networks, we used dual regression analysis. The preprocessed rsfMRI datasets from the 120 subjects were temporally concatenated, and group independent component analysis (ICA) was performed using the MELODIC software from the FSL package (Jenkinson et al., 2012). Thirty independent components (ICs) were derived across the whole sample, extracted, and visually compared to a set of reference RSN templates[2] (Shirer et al., 2012) to identify several well-known RSNs. In dual regression analysis (Filippini et al., 2009), the extracted group ICs were used as spatial regressors and the temporal dynamics associated with each IC for each subject were estimated. These time courses were then used as temporal regressors in a second regression analysis to generate subject-specific maps associated with each group IC. Using the constructed subject-specific maps, regression analysis was performed with the cognitive function scores, year of education, age, gender, and GMV set as regressors. For the cognitive functional scores, in one condition, the scores of the five domains (attention/orientation, fluency, memory, language, visuospatial) were used. In another condition, the DR score was used instead of the memory score. Statistical analysis of each component map was performed using a non-parametric permutation test (5000 permutations), and regions with connectivity showing statistically significant association with each respective factors were identified. All statistical maps were corrected for multiple comparisons using FWE correction with threshold free cluster enhancement. Statistically significance was set at $p < 0.05$.

[1] https://www.alivelearn.net/xjview/

[2] http://findlab.stanford.edu/functional_ROIs.html

RESULTS

A Correlation Analysis and Regression Analysis for Age-Related Factors

In the correlation analysis using a Spearman's rank correlation coefficient, the CSFV was the only factor which showed a significant positive correlation (r = 0.55). On the other hand, significant negative correlations with age were seen in the GMV (r = −0.58), DR score (r = −0.55), ACE-R total score (r = −0.36), attention / orientation score (r = −0.35), memory score (r = −0.38), and visuospatial ability score (r = −0.18) (**Table 2**). The other domains, language and fluency, were not significantly correlated with age. The education year also demonstrated negative correlation with age, which reflect the relatively high college enrollment rate in younger generation and was, therefore, excluded for further regression analysis.

For the regression analysis of each factor with age, we examined two regression models - linear and quadratic. Individual plots for the different factors examined are shown in **Figure 1**, whereas the combined plots for GMV, the DR score, ACE-R total score, attention / orientation, and memory, as functions of age are shown in **Figure 2**. The vertical axis showed the volume and the score of each subject as a standardized z-score, and the horizontal axis is age. The appropriate regression model, shown as solid line, was identified using both AIC, BIC, and R2. The best model was linear for GMV and visuospatial and quadratic for the DR, memory, attention / orientation, and ACE-R total. AIC, BIC, and R2 values for the two regression models of each factor are summarized in **Table 3**. Among the different cognitive function scores, the DR score showed the highest significant relationship with age. GMV showed a relatively steeper slope from the 20s, and fell below the average value (z - score = 0) at around the age of 50. On the other hand, the DR, total ACE-R score, memory and attention score are relatively stable until late 50's and decline sharply afterward. The score of visuospatial ability showed mild linear change with age, but the R2 value was small, and its change was not reliable. The other two cognitive domains (language and fluency) did not show significant relationship with age.

VBM Analysis With Factors Associated With Aging

With VBM, a strong negative correlation with age was observed in many regions across the cerebral cortex. The maximum negative correlation was found in the right posterior central gyrus. Areas with negative correlation with age were widespread and bilaterally observed in the lateral frontal cortices, the lateral temporal cortices, the lateral occipital cortices, the parietal cortices, the cingulate gyrus, the areas surrounding the intraparietal sulcus, and the medial temporal areas including the hippocampus (**Table 4**, upper row in **Figure 3**). In VBM analysis for 5 cognitive domains (attention/orientation, fluency, memory, language, visuospatial ability) and education with age and TICV as covariates, no region survived statistical significance.

VBM analysis for DR and with TICV as the covariate showed positive correlation between DR and gray matter in a relatively

TABLE 2 | A summary of results in correlation analysis.

	Basic information		ACE-R Scores (total and 5 domains)						Subscores of ACE-R				Morphologic information			
	Age	Education year	Total score	Attention/ orientation	Fluency	Memory	Language	Visuospatial	Serial 7	The score of verbal fluency: phonological	The score of verbal fluency: semantic	Naming	Delayed recall	GMV	WMV	CSFV	TICV
Mean	48.9	14.2	95.7	17.9	13.4	23.6	25.1	15.7	4.6	6.7	6.7	11.6	6.2	637.5	432.5	346.4	1416.3
Min.	20	9	83	16	7	15	22	13	1	2	3	8	2	409	298.8	155.6	1058.1
Max.	78	21	100	18	14	26	26	16	5	7	7	12	7	806.6	562.1	803.4	1679.1
S.D.	17.63	2.52	3.24	3.87	1.17	2.02	1.05	0.67	0.75	0.8	0.7	0.8	1.16	75.37	49.54	94.54	140.04
Correlation with age																	
Correlation coefficient; r	N/A	−0.36	−0.36	−0.35	−0.07	−0.38	−0.14	−0.18	−0.15	−0.02	−0.11	0.06	−0.55	−0.58	−0.13	0.55	−0.23
Significant level		<0.01**	<0.01**	<0.01**	0.439	<0.01**	0.132	0.045*	0.092	0.801	0.222	0.548	<0.01**	<0.01**	0.175	<0.01**	0.802

large area including bilateral frontal cortices, bilateral temporal cortices, bilateral insular cortices, and bilateral cingulate cortices ($p < 0.05$, FWE) (**Table 5**, middle row in **Figure 3**). These regions overlapped with the part of the areas showing negative correlation with age (lower row in **Figure 3**). However, in the analysis where the age was also included as a covariate, no region survived.

Resting State Network Analysis for Aging and the Associated Factors

In the first step of the dual regression analysis, 18 resting networks were extracted (**Figure 4**). Those networks included the ventral and dorsal DMN, the right and left ECN, the anterior and posterior SN, the precuneus network, the dorsal attention network (DAN), lateral DAN, the dorsal and ventral SMN, the basal ganglia network (BGN), the language network (LN), the auditory network, the primary, medial, and higher VN, and the cerebellar network. Out of the 18 networks, eight networks exhibited within-network functional connectivity that was negatively correlated with age ($p < 0.05$, FWE), including the primary, medial, and higher VN, dorsal and medial SMN, DAN, anterior SN, and ventral DMN. The negatively correlated regions in each network were shown in **Figure 5**, and the anatomical location and voxel counts of those regions were summarized in **Table 6**. On the other hand, 10 networks did not show significant correlation with age. These networks included the left / right ECN, dorsal DMN, posterior SN, LN, lateral DAN, precuneus, cerebellum, auditory, and BGN.

With regards to the relationship with cognitive function, the score of the domain of memory and the DR was found to be positively correlated with the SMN ($p < 0.05$, FWE). The regions with positive correlation in the SMN were almost the same in the memory and the DR (**Figure 6**, **Table 7**). Furthermore, the score of the fluency was found to be positively correlated with 4 networks, the right ECN, the primary visual, and the dorsal SMN (**Figure 6**, **Table 7**). Longer years of education was weakly associated with higher connectivity in the primary visual network, the precuneus, the DAN, and the ventral DMN, and with lower connectivity in the cerebellar network ($p < 0.05$, FWE).

DISCUSSION

In this study, we evaluated the relationship between aging and cognitive function in a total of 120 healthy subjects consisting of a balanced number of participants within age-groups of 20s, 30s, 40s, 50s, and 70s, who maintained relatively good cognition. Our results were as follows: (1) Among the sub-scores of domains in the cognitive test, the DR, memory, attention/orientation, and visuospatial scores were significantly correlated with age. (2) The score of the DR demonstrated the highest negative correlation with age in this healthy cohort. In the regression analysis, the language and fluency scores did not show significance, whereas other domains (attention/orientation, memory, and visuospatial), and the DR score showed significant relationship with age. A quadratic approximation of the attention/orientation,

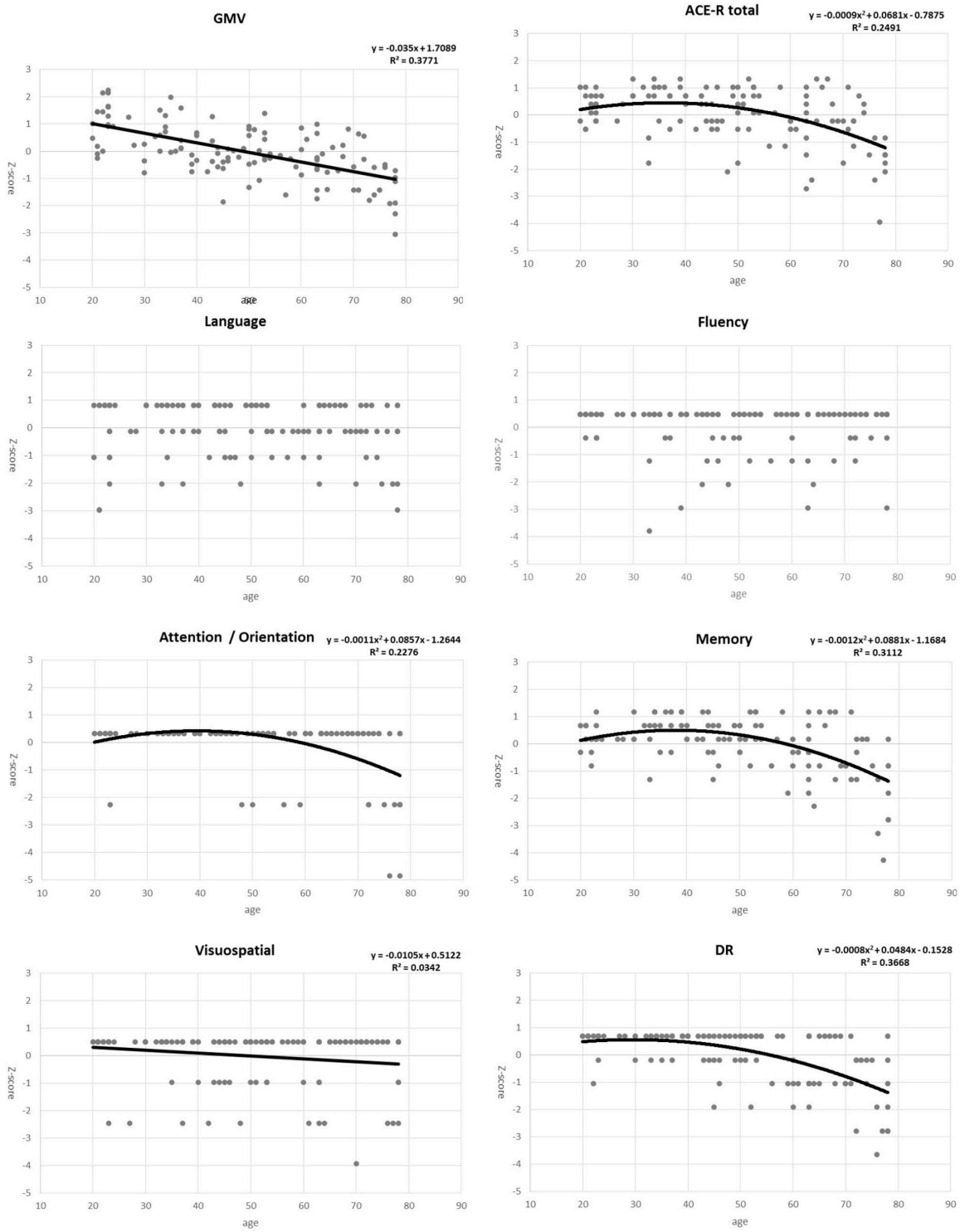

FIGURE 1 | Plots for gray matter volume (GMV), total ACE-R score, five domains of the ACE-R (attention/orientation, memory, fluency, visuospatial, and language), and the delayed recall (DR) score as functions of age. Points represent actual data, whereas solid line/curves represent regression functions.

memory, and the DR scores as functions of age showed relatively delayed decline compared to the total GMV loss. (3) In VBM analysis, widespread brain regions demonstrated negative correlation with age. However, no regions have GM values that correlated with the scores of all domains in the cognitive test when age was included as a covariate. (4) In the analysis for

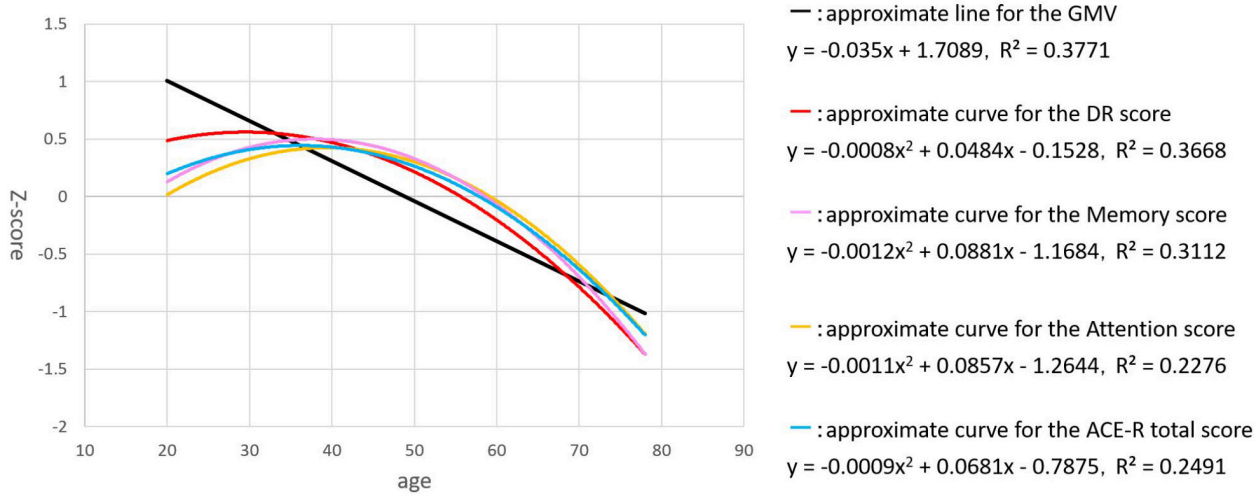

FIGURE 2 | The plots for GMV (black), the DR score (red), ACE-R total score (blue), attention / orientation (yellow), and memory (pink), as functions of age are shown. The vertical axis showed the volume and the score of each subject as a standardized z-score, and the horizontal axis is age.

TABLE 3 | A summary of AIC, BIC, and R2 values for the two regression models of each factor.

	AIC		BIC		R2	
Factor	**Linear**	**Quadratic**	**Linear**	**Quadratic**	**Linear**	**Quadratic**
Attention	327.94	315.55	333.52	323.91	0.1292	0.2276
Fluency	343.94	344.03	349.52	352.39	0.0050	0.0207
Memory	317.93	301.81	323.51	310.17	0.1989	0.3112
Language	343.43	340.02	349.00	348.38	0.0093	0.0529
Visuospatial	340.37	342.37	345.94	350.73	0.0342	0.0342
ACERTotal	321.41	312.16	326.98	320.52	0.1754	0.2491
GMV	287.73	289.72	293.31	298.08	0.3771	0.3772
DRscore	299.88	291.70	305.46	300.07	0.3108	0.3668

TABLE 4 | Anatomical structures correlated with age in VBM.

Peak MNI coordinate	**Peak anatomical structure**	**Peak *T*-value**
‘34 −26 48	Postcentral_R	10.49
Anatomical structures of the clusters (voxel count>100)		
Frontal lobe	Postcentral_L (1781), Postcentral_R (1350), 1278, Frontal_Mid_L (1278), Frontal_Sup_L (1039), Frontal_Inf_Orb_R (1038), Rolandic_Oper_R (983), Frontal_Mid_R (983), Precentral_R (900), Frontal_Inf_Orb_L (807), Frontal_Sup_R (803), Frontal_Inf_Tri_L (796), Rolandic_Oper_L (785), Precentral_L (730), Frontal_Inf_Oper_R (679), Frontal_Inf_Oper_L (676), Frontal_Inf_Tri_R (558), Rectus_R (506), Rectus_L (451), Frontal_Med_Orb_R (323), Frontal_Mid_Orb_R (253), Olfactory_R (228), Frontal_Sup_Orb_L (212), Frontal_Sup_Medial_L (158), Frontal_Med_Orb_L (154), Frontal_Sup_Orb_R (148), Supp_Motor_Area_R (146), Olfactory_L (127), Frontal_Sup_Medial_R (120)	
Temporal lobe	Temporal_Sup_R (2051), Temporal_Sup_L (1876), Temporal_Mid_R (1265), Temporal_Mid_L (873), Temporal_Pole_Sup_L (693), Temporal_Pole_Sup_R (661), Fusiform_R (636), Fusiform_L (571), Temporal_Pole_Mid_R (255), Heschl_R (242), Temporal_Inf_R (225), Heschl_L (210)	
Parietal lobe	Lingual_L (266), Lingual_R (245), Calcarine_L (199), Calcarine_R (141)	
Occipital lobe	Lingual_L(1332), Lingual_R(1317), Calcarine_L(1002), Calcarine_R(701), Cuneus_L(342), Cuneus_R(312)	
Limbic / Insula	Insula_L (1776), Insula_R (1690), Cingulum_Mid_R (1482), Cingulum_Mid_L (1217), Cingulum_Ant_L (770), Cingulum_Ant_R (689), Hippocampus_L (572), ParaHippocampal_R (348), Hippocampus_R (272), ParaHippocampal_L (238), Amygdala_R (222), Amygdala_L (173)	
Subcortical structures	Putamen_R (766), Putamen_L (655), Caudate_L (575), Caudate_R (536), Thalamus_L (195), Thalamus_R (113)	
Cerebellum	Cerebelum_6_R (1060), Cerebelum_6_L (1012), Cerebelum_Crus1_L (413), Cerebelum_8_L (408), Cerebelum_Crus1_R (396), Cerebelum_4_5_L (357), Cerebelum_Crus2_R (352), Cerebelum_4_5_R (295), Cerebelum_Crus2_L (278), Cerebelum_9_L (213), Cerebelum_8_R (197), Vermis_8 (185), Cerebelum_7b_L (150), Vermis_7 (131)	

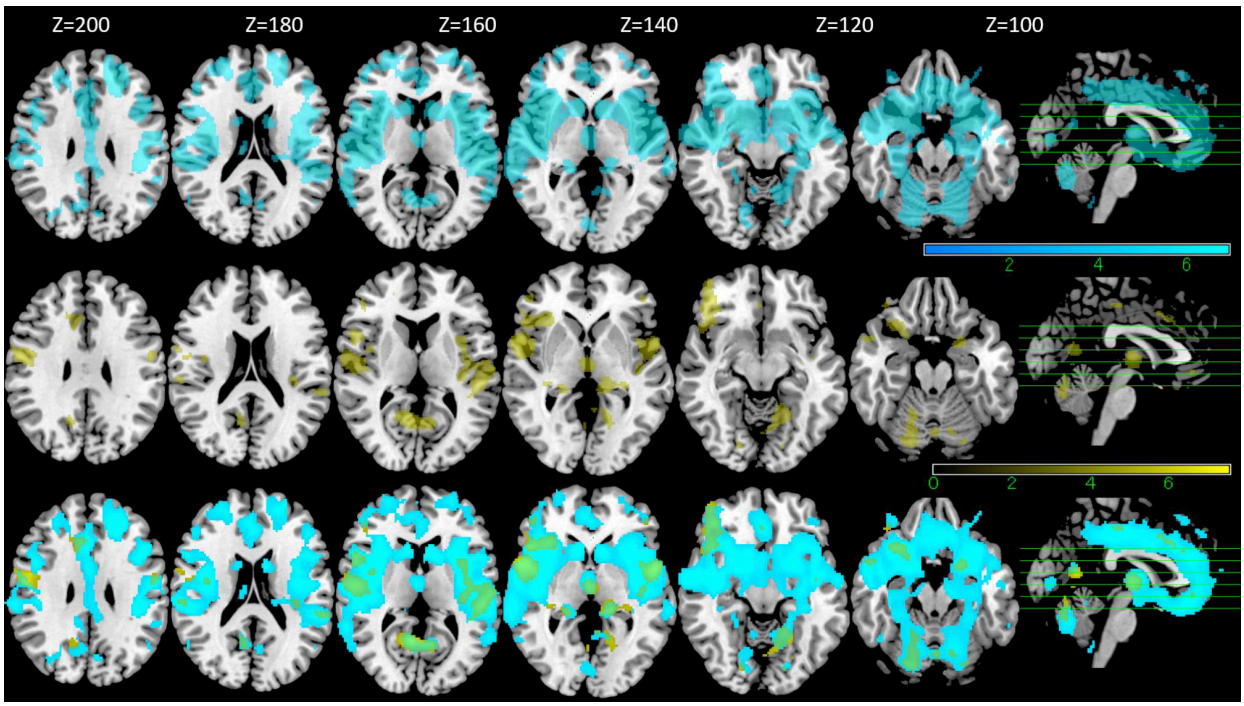

FIGURE 3 | VBM results. Regions with negative correlation with the age are shown in the upper row (blue), those with positive correlation with DR score without age as a covariate are shown in the middle row (yellow) and the overlapped regions between the two are shown in the bottom row (green) (FWE $p < 0.05$).

TABLE 5 | Anatomical structures correlated with age in VBM.

Peak MNI coordinate	Peak anatomical structure	Peak *T*-value
'−56 2 2	Temporal_Sup_L	7.48
Anatomical structures of the clusters (voxel count>100)		
Frontal lobe	Frontal_Inf_Orb_R (664), Precentral_R (348), Rolandic_Oper_R (346), Rolandic_Oper_L (309), Postcentral_R (269), Frontal_Inf_Oper_R (159), Frontal_Inf_Tri_R (154), Frontal_Mid_Orb_R (144)	
Temporal lobe	Temporal_Sup_L (588), Temporal_Sup_R (225), Heschl_L (145), Temporal_Pole_Sup_R (111), Heschl_R (105)	
Parietal lobe	Precuneus_R (142)	
Occipital lobe	Lingual_L (322), Calcarine_R (181), Calcarine_L (179), Lingual_R (127)	
Limbic / Insula	Insula_R (525), Cingulum_Mid_R (290), Cingulum_Mid_L (271), Insula_L (241), Cingulum_Mid_R (236)	
Cerebellum	Cerebelum_6_R (538), Cerebelum_6_L (268), Cerebelum_Crus1_L (266), Cerebelum_Crus1_R (132)	

RSNs, although several networks demonstrated a decrease of within-network functional connectivity with age, such a decrease was not observed in 10 networks including the left / right ECN, dorsal DMN, posterior SN, LN, lateral DAN, precuneus, cerebellum, auditory, and BGN. (5) The SMN was positively correlated with the scores of the domain of memory and fluency, and the DR score.

Morphological Analysis for Aging and Cognition

We selected subjects whose ACE-R score was above the cutoff and was considered normal in cognition. Even in such subjects, ACE-R showed variances in some domains and sub-scores with the DR being the most sensitive sub-score for aging. This finding has a clinical importance to interpret the results of ACE-R. DR purely evaluates short-term memory, not tightly associated with one's experience, and reflects fluid intelligence. Among the five domains of this cognitive screening test, memory, attention/orientation, and visuospatial ability significantly demonstrated negative correlation with age. On the other hand, language and fluency were not significantly correlated with age. These two domains may not be strongly affected by aging in healthy cohort with a relatively maintained cognition, because language ability is more related to one's experiences, knowledge, and vocabulary, that is, crystalized intelligence, and fluency also requires such functionality. These findings support the idea that crystalized intelligence is more maintained than fluid intelligence in healthy aging (Baltes et al., 1999).

In VBM analysis, our results showed that the GMV widely declined with age, even starting from the early 20s. This result

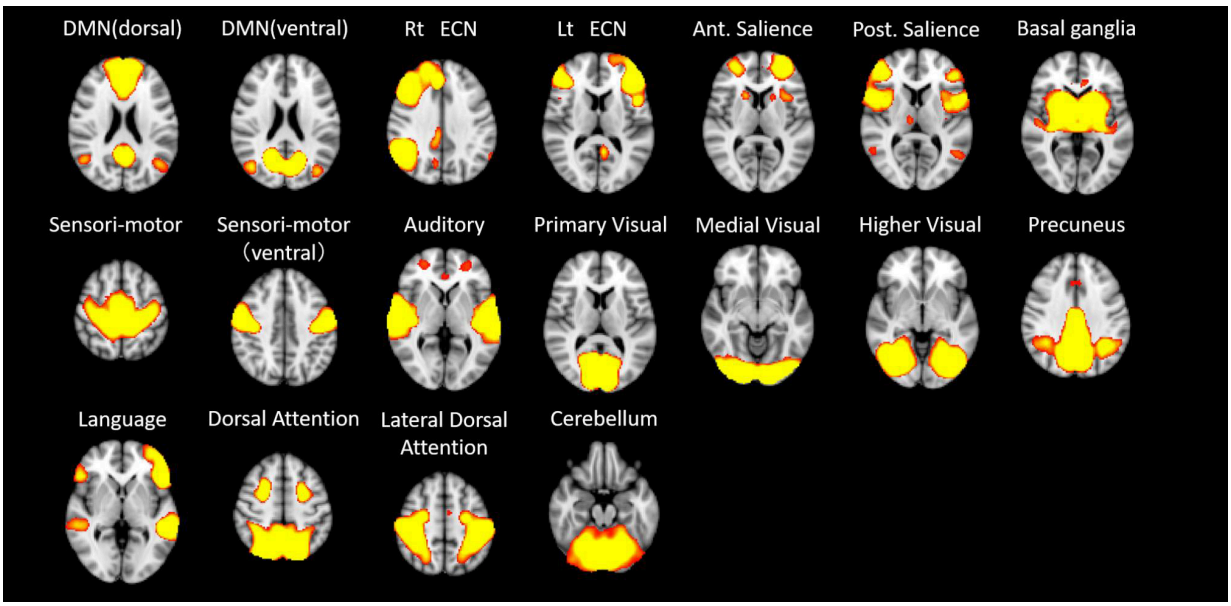

FIGURE 4 | The 18 resting networks extracted at the first step of the dual regression analysis. DMN – default mode network; ECN – executive control network; Rt – right; Ant – anterior; Post – posterior.

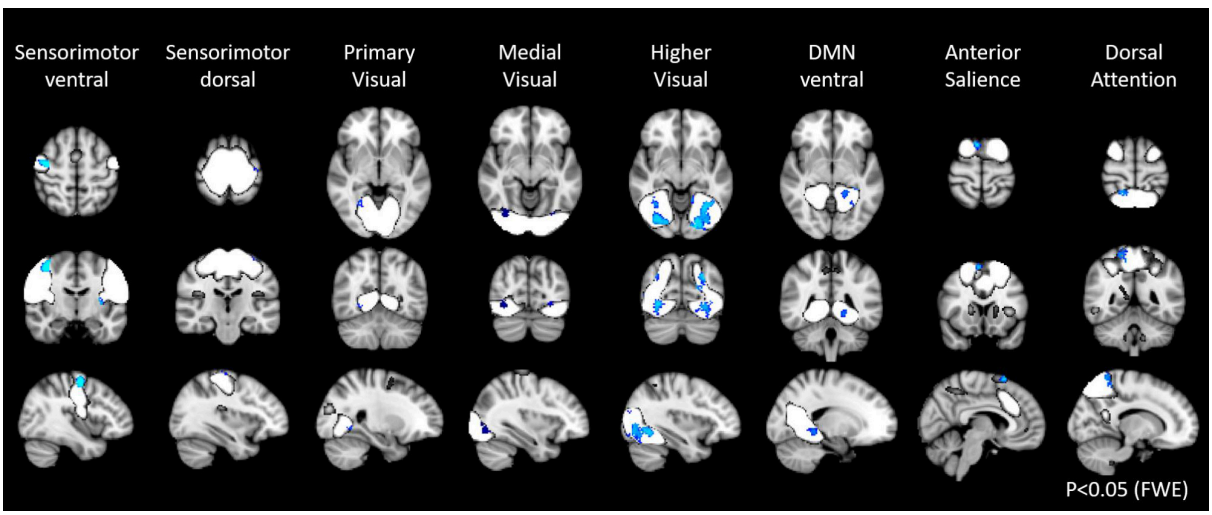

FIGURE 5 | Resting state networks, shown in white, with within-network functional connectivity values that negatively correlated with age. The clusters shown in blue represented the areas with connectivity values showing significant negative correlation with age (FWE $p < 0.05$).

is consistent with many previous studies (Good et al., 2001; Giorgio et al., 2010; Taki et al., 2011). Regarding the location of regions showing negative correlation with age, the areas around the central sulcus and the intraparietal sulcus were commonly reported in several literatures (Good et al., 2001; Giorgio et al., 2010; Taki et al., 2011), but as to deep brain structures such as the hippocampus, the results differed (Good et al., 2001; Giorgio et al., 2010; Taki et al., 2011; Squarzoni et al., 2018). In our study, we found a significantly lower GMV in bilateral regions around the central sulcus and the intraparietal sulcus, and bilateral medial temporal areas including the hippocampus in older adults. In Alzheimer's disease, atrophic changes of GMV have been observed in the medial temporal lobe and the temporo-parietal junction. These changes were also frequently observed even in the stage of mild cognitive impairment (MCI) (Baron et al., 2001; Risacher et al., 2009). We adopted 83 as the cutoff of ACE-R in this study (Mathuranath et al., 2000; Yoshida et al., 2012), and our cohort included four individuals whose total score was between 83 and 89. These individuals may potentially be at the prodromal stage of dementia, that is, MCI, and could have influenced our results. The WMV was known to demonstrate a U-shaped change with age (Bagarinao et al., 2018), and therefore,

TABLE 6 | Anatomical regions decreasing functional connectivity with age in the canonical RSNs.

Primary visual network	Peak MNI coordinate	Peak anatomical region	*P*-value at peak region
	'26 −54 −6	Lingual_R	*P* = 0.0338
	structures (voxel count):		
	23 Lingual_R (23), Fusiform_R (5)		
Sensorimotor network (dorsal)	Peak MNI coordinate	Peak anatomical region	*P*-value at peak region
	'−36 −24 68	Precentral_L	*P* = 0.0392
	structures (voxel count):		
	Precentral_L (15)		
Higher visual network (1)	Peak MNI coordinate	Peak anatomical region	*P*-value at peak region
	'−22 −88 −14	Lingual_L	*P* = 0.0026
	structures (voxel count):		
	Fusiform_L (264), Occipital_Inf_L (241), Lingual_L (190), Occipital_Mid_L (96), Cerebellum_6_L (43), Temporal_Inf_L (8), Temporal_Mid_L (2), Cerebellum_Crus1_L (1)		
Higher visual network (2)	Peak MNI coordinate	Peak anatomical region	*P*-value at peak region
	'48 −84 8	Occipital_Mid_R	*P* = 0.0016
	structures (voxel count):		
	Fusiform_R (457), Occipital_Mid_R (132), Occipital_Inf_R (124), Lingual_R (90), Cerebellum_6_R (60), Temporal_Mid_R (20), Temporal_Inf_R (2)		
Higher visual network (3)	Peak MNI coordinate	Peak anatomical region	*P*-value at peak region
	'−14 −52 −8	Lingual_L	*P* = 0.021
	structures (voxel count):		
	Lingual_L (30), Cerebellum_4_5_L (3)		
Higher visual network (4)	Peak MNI coordinate	Peak anatomical region	*P*-value at peak region
	'−28 −68 34	Occipital_Mid_L	*P* = 0.0066
	structures (voxel count):		
	Occipital_Mid_L (232), Occipital_Sup_L (84), Cuneus_L (41)		
Higher visual network (5)	Peak MNI coordinate	Peak anatomical region	*P*-value at peak region
	'34 −76 36	Occipital_Mid_R	*P* = 0.0228
	structures (voxel count):		
	Occipital_Mid_R (70), Occipital_Sup_R (11)		
Dorsal attention network	Peak MNI coordinate	Peak anatomical region	*P*-value at peak region
	'20 −50 66	Parietal_Sup_R	*P* = 0.0162
	structures (voxel count):		
	Parietal_Sup_R (75), Precuneus_R (34), Postcentral_R (21)		
Anterior salience network	Peak MNI coordinate	Peak anatomical region	*P*-value at peak region
	'6 16 66	Supp_Motor_Area_R	*P* = 0.0162
	structures (voxel count):		
	Supp_Motor_Area_R (57)		
Medial visual network (1)	Peak MNI coordinate	Peak anatomical region	*P*-value at peak region
	'34 −76 −6	Occipital_Inf_R	*P* = 0.03
	structures (voxel count):		
	Occipital_Inf_R (29), Middle Occipital Gyrus, Occipital_Mid_R (11), Fusiform_R (6)		
Medial visual network (2)	Peak MNI coordinate	Peak anatomical region	*P*-value at peak region
	'−26 −76 −4	Occipital_Inf_L	*P* = 0.0118
	structures (voxel count):		
	Occipital_Inf_L (12), Occipital_Mid_L (7), Lingual_L (3), Fusiform_L (2)		
Ventral default mode network (1)	Peak MNI coordinate	Peak anatomical region	*P*-value at peak region
	'−34 −34 −8	Hippocampus_L	*P* = 0.0208
	structures (voxel count):		
	Hippocampus_L (19)		
Ventral default mode network (2)	Peak MNI coordinate	Peak anatomical region	*P*-value at peak region
	'−18 −42 −6	Lingual_L	*P* = 0.0272
	structures (voxel count):		
	Lingual_L (93), ParaHippocampal_L (19), Precuneus_L (8), Fusiform_L (1)		

(Continued)

TABLE 6 | (Continued)

Primary visual network	Peak MNI coordinate	Peak anatomical region	*P*-value at peak region
Ventral sensorimotor network (1)	Peak MNI coordinate '−32 −8 6 structures (voxel count): Insula_L (12)	Peak anatomical region Insula_L	*P*-value at peak region $p = 0.013$
Ventral sensorimotor network (2)	Peak MNI coordinate ' 62 2 34 structures (voxel count): Postcentral_R (14), Precentral_R (10)	Peak anatomical region Postcentral_R	*P*-value at peak region $P = 0.036$
Ventral sensorimotor network (3)	Peak MNI coordinate ' 44 −8 55 structures (voxel count): Precentral_R (161), Frontal_Mid_2_R (66), Frontal_Sup_2_R (11)	Peak anatomical region Precentral_R	*P*-value at peak region $P = 0.001$

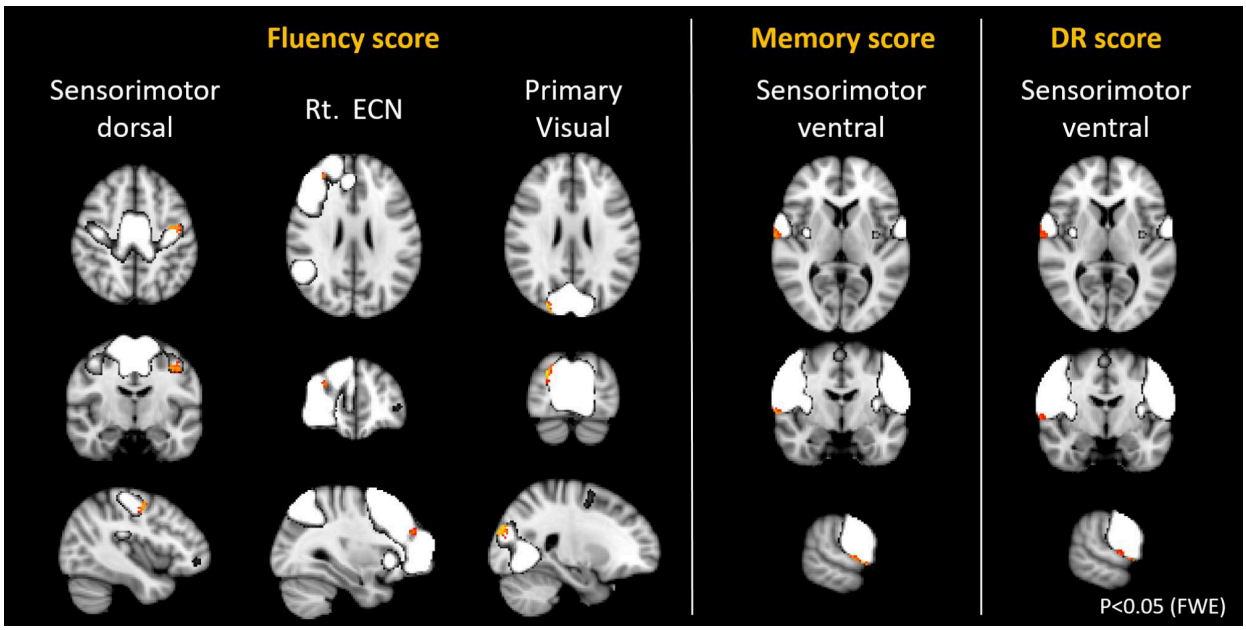

FIGURE 6 | Resting state networks, shown in white, with within-network functional connectivity values that positively correlated with the score of fluency, memory, and delayed recall (DR). The clusters shown in yellow-red represented the areas with connectivity values showing significant positive correlation with the different scores (FWE $p < 0.05$).

we could not find a linear correlation in our analysis. In VBM, we did not find regions with GMV that correlated with the scores of cognitive domain in ACE-R when age was included as a covariate. This result reflects difficulty to evaluate significant relationship between cognition and morphological changes when simultaneously accounting for the influence of age. In the analysis without age as a covariate, the DR score positively correlated with the GMV of a relatively wider brain region that included bilateral frontal cortices, bilateral temporal cortices, bilateral insular cortices, and bilateral cingulate cortices. We assumed that the function of the DR may require activities in a variety of regions including the hippocampus and the nearby medial temporal structures. However, such a topographic characteristic was not observed in our results. These results should be interpreted with care considering the dependence of both DR and GMV with age. In other words, the affected regions may be "related to the decline of the DR score due to aging" and not to the DR function itself. A study by Takeuchi et al., which examined this relationship using a large sample and age-matched healthy young adults with mean age of 20.8 years and SD of 0.8, reported that there was no strong correlations between regional GMV and specific cognitive domains. Diverse cognitive functions may be weakly associated with regional GMV in widespread brain areas, and may be difficult to detect this association in this analysis.

Regarding the relationship between the morphological changes of the brain and cognition with age, Schnack et al. (2015) reported about the relationship between the intelligence quotient (IQ) and the thickness of the cortex over age. Higher IQ was

TABLE 7 | Anatomical regions increasing functional connectivity with cognitive score in the canonical RSNs.

Anatomical regions increasing functional connectivity with Fluency score			
Rt.executive control network	Peak MNI coordinate 32 44 26 Structures (voxel count): Frontal_Mid_2_R (18), Frontal_Sup_2_R(4)	Peak anatomical region Frontal_Mid_2_R	*P*-value at peak region *P* = 0.0274
Primary visual network	Peak MNI coordinate 26 −90 22 structures (voxel count): Occipital_Sup_R(60), Occipital_Mid_R(8)	Peak anatomical region Occipital_Sup_R	*P*-value at peak region *P* = 0.0044
Dorsal sensorimotor network (1)	Peak MNI coordinate '−30 −18 40 Structures (voxel count): Precentral_L(2)	Peak anatomical region Precentral_L	*P*-value at peak region *P* = 0.0306
Dorsal sensorimotor network (2)	Peak MNI coordinate '−40 −8 48 Structures (voxel count): Precentral_L(53), Postcentral_L(31)	Peak anatomical region Precentral_L	*P*-value at peak region *P* = 0.0156
Anatomical regions increasing functional connectivity with Memory score			
Ventral sensorimotor network	Peak MNI coordinate '58 6 −2 Structures (voxel count): Temporal_Sup_R(32), Temporal_Pole_Sup_R(30), Rolandic_Oper_R(4)	Peak anatomical region Temporal_Pole_Sup_R	*P*-value at peak region *P* = 0.0108
Anatomical regions increasing functional connectivity with DR score			
Ventral sensorimotor network (1)	Peak MNI coordinate '60 2 0 Structures (voxel count): Temporal_Pole_Sup_R(18), Temporal_Sup_R(3)	Peak anatomical region Temporal_Pole_Sup_R	*P*-value at peak region *P* = 0.022
Ventral sensorimotor network (2)	Peak MNI coordinate '64 −8 6 Structures (voxel count): Temporal_Sup_R(23), Heschl_R(5), Rolandic_Oper_R(4)	Peak anatomical region Temporal_Sup_R	*P*-value at peak region *P* = 0.0332

associated with larger and thicker surface area until around the age of 20, but this relationship weakened from the age of 40 to 50. They also mentioned that individuals maintaining high IQ may form highly efficient formation of brain networks (Schnack et al., 2015). Although they utilized the IQ, which has four domains including the language, working memory, visuospatial, and performance speed, the results was similar to ours. Our results also demonstrated that the GMV decreased with age from a relatively early stage (20's), whereas the domain of memory and attention, as well as the DR score was maintained to some extent until the late 50s. In healthy aging, a decrease in the GMV and a decrease in cognition showed such temporal dissociation and never showed parallel relationship. The absence of this relationship could not be simply explained by morphological analysis in the brain, and therefore, we supposed that the network analysis was necessary.

More broadly, existing studies have shown that GM continuously declined with age. Thus, it is indeed intriguing that cognitive scores have inverse U-shaped behavior as a function of age, while GMV decreased linearly. Although speculative, this may point to some possible reserve mechanisms at work, where reserve capabilities are accumulated during childhood and young adulthood. The concept of brain or cognitive reserve (Stern, 2002; Satz et al., 2011; Barulli and Stern, 2013) hypothesized the accumulation of neural resources over the years that could lessen the effects of neural decline associated with aging or age-related diseases (Cabeza et al., 2018). Factors such as longer education, greater physical activity, and involvement in demanding leisure activities, among others, affect reserve capacity (Cabeza et al., 2018). This possibly drive the relative preservation in cognitive scores before it peaks and started to decline. Since reserve can also manifest in terms of efficient use of neural resources (Solé-Padullés et al., 2009), large-scale brain networks may also have important roles to play in the maintenance of cognitive functions during aging. To fully understand the association among brain structure, network, and cognition in the aging brain, more studies are needed.

Network Analysis for Aging and Cognition

Previous studies have reported that the connectivity within networks, such as DMN, decreased with age (Damoiseaux et al., 2008; Koch et al., 2010; Jones et al., 2011). Our results

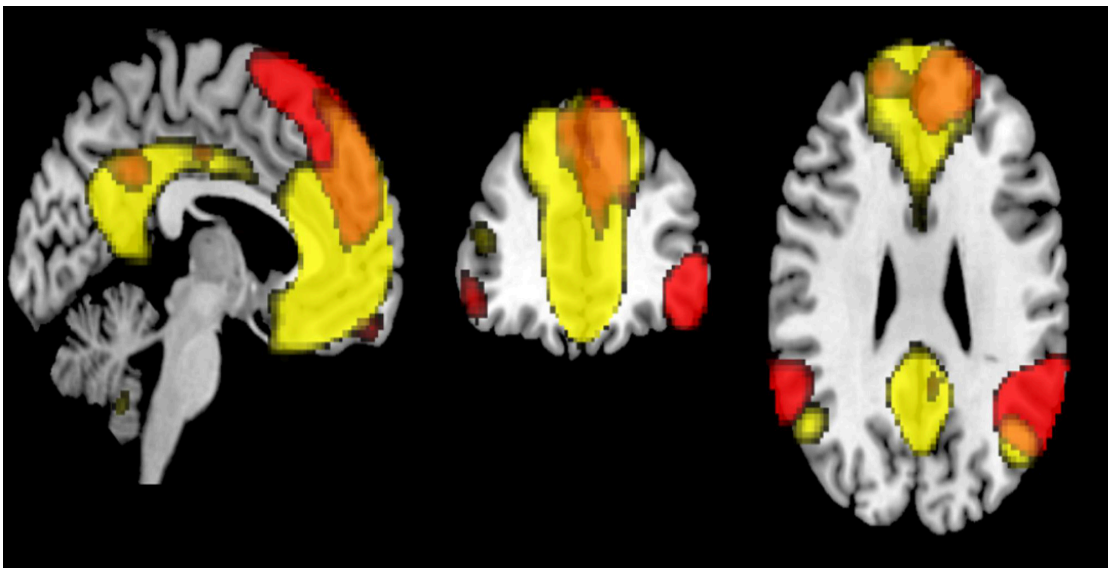

FIGURE 7 | The overlapped regions between the dorsal default mode network (DMN) and the language network (FWE $p < 0.05$).

also demonstrated similar within-network connectivity decreases in 8 out of 18 RSNs. Specifically, the ventral DMN showed significant decrease in functional connectivity, but not the dorsal DMN. Similar results have been previously reported (Campbell et al., 2013; Huang et al., 2015; Bagarinao et al., 2019). The functional difference between the two is currently not well understood. The ventral DMN is more associated with memory, a hippocampus – dependent function (Damoiseaux et al., 2012), and this network may weaken over age as memory declined. Campbell et al. (2013) examined age-related differences in the intrinsic functional connectivity in subsystems of the DMN. Their findings showed that the subsystem involving dorsal posterior cingulate cortex (PCC) to the fronto-parietal regions was relatively maintained in the elderly, whereas that involving the ventral PCC declined in functional connectivity. The dorsal PCC is a core region in the dorsal DMN, and this could be a reason for the observed discrepancy between ventral DMN and dorsal DMN in our study. With regards to the LN, which also showed no association between connectivity and age, we found regional similarity of its connectivity to that of the dorsal DMN. Both networks shared common regions in the dorsal PCC and dorsomedial prefrontal cortex (**Figure 7**). The relative maintenance of the dorsal PCC's connectivity may also explain the relative preservation of LN. In addition, the LN is associated with language ability, an important part of crystalized intelligence. Therefore, this result may be a reflection of the relative maintenance of crystalized intelligence over age. In the absence of supporting literature, more studies examining the association between LN and the network associated with crystallized intelligence are needed. Among the other core cognitive networks, the right / left ECN, lateral dorsal attention, precuneus, and posterior SN have within-network functional connectivity values that did not significantly correlated with age. Previous studies have reported that these networks have decreased within-network functional connectivity (Onoda et al., 2012; Ferreira and Busatto, 2013). However, relative sparing of the functional connectivity in the prefrontal and parietal cortex over age has also been reported (Rajah and D'Esposito, 2005; Reuter-Lorenz and Cappell, 2008; Grady, 2012). These regions are well known to be important for cognitive control, which is a function for the effortful use of cognitive resources to guide, organize, or monitor behavior (Grady, 2012). The networks which were not correlated with age in our study, such as dorsal DMN, the LN, the right / left ECN, lateral dorsal attention, and the posterior salience, included these regions. Some reports suggested that these networks were important for cognitive reserve (Onoda et al., 2012; Chand et al., 2017). Taken together, our results suggest that networks involved with cognitive control were not significantly associated with age. This may reflect the characteristics of our cohort, who had relatively maintained cognition.

Networks associated with primary processing, including ventral and dorsal SMNs and primary VN, demonstrated decrease in functional connectivity with age consistent with previous reports using resting state fMRI and / or task fMRI (Cliff et al., 2013; Roski et al., 2013; Huang et al., 2015; Bagarinao et al., 2019). These results are reasonable considering the vulnerability of the GMV in these areas to aging, physical deterioration, and less external stimulation in the elderly. However, other studies have also demonstrated that the functional connectivity in the primary processing networks is unchanged in advancing age (Geerligs et al., 2015). Therefore, this finding remained inconclusive. The networks related to high-order visual processing also showed negative correlation with age in our study, consistent with previous reports (Yan et al., 2011; Bagarinao et al., 2019).

In terms of the relationship between cognitive functions and functional connectivity within networks, our results

demonstrated that the memory score, the DR score, and the fluency score were positively correlated with the SMN. A close relationship between motor function and cognitive function has been reported in behavioral experiments and epidemiological surveys (Clarkson-Smith and Hartley, 1989; Weuve et al., 2004). Recently, a study has reported that physical exercise improved gait speed, and cognitive performance, through the increasing involvement of motor-related networks (Ji et al., 2018). Voss et al. also reported that cardiorespiratory fitness moderated the adverse effects of aging on cognitively and clinically relevant functional brain networks (Voss et al., 2016). Another study also reported that increased functional connectivity of posterior cingulate gyrus / precuneus in individuals with MCI after excise training possibly increase cognitive reserve (Chirles et al., 2017). The neural basis of exercise as an intervention for the maintenance of cognition is being gradually elucidated by recent network analyses, and this may lead to the development of an effective modality about intervention by exercise to prevent cognitive impairment (Huang et al., 2016). The fluency score also showed positive correlation with the right ECN, and weak correlation with the primary VN. Working memory is related to word phonological fluency, and knowledge and vocabulary are related to word categorization fluency (Ruff et al., 1997; Rende et al., 2002; Stolwyk et al., 2015). This association may reflect the relationship between the score of fluency and the ECN. Other cognitive function scores did not show any significant association with the connectivity of any network.

In terms of education history, longer schooling was associated with higher connectivity in the primary VN, the precuneus network, the DAN, and the ventral DMN. The education history was reported to have a correlation with cognitive reserve. In a study with a 4-year follow up, the group with short education history had a 2.2 times higher risk of developing dementia (Stern et al., 1994; Stern, 2009). A more recent study has shown that the risk is 1.5 times higher (Livingston et al., 2017). Given this, long education history plays an important role to keep cognition within normal range, and the neural basis for this may be related to cognition-related networks such as the DAN and the ventral DMN. These networks may have an important role for cognitive reserve. Although the long history of education negatively correlated to the cerebellar network, there has been no report regarding this finding. Recently, there are some reports about detailed analysis for the RSNs in the cerebellum (Dobromyslin et al., 2012; Kawabata et al., 2020). Further study is warranted.

Limitations

Finally, we enumerated our study's limitations. First, in the VBM analysis for the DR score, the influence of age could not be completely separated. To identify specific regions related to the DR score using VBM, it is necessary to match the age of all participants and examine individual differences in the DR score. Second, ACE-R is typically used for healthy screening, and has a ceiling effect. Under this limitation, we cannot fully discount its contribution in the observed inverse U – shape behavior in some cognitive domains as functions of age. However, such an inverse U-shape curve is not uncommon in aging studies and has been reported for some cognitive scores (Douaud et al., 2014). Moreover, the sensitivity of the sub-score of ACE-R is not well understood. Therefore, the use of specific cognitive batteries is necessary for a more detailed cognitive evaluation. Third, we just examined the strength of the connectivity within networks. Analysis of the interaction among networks is necessary to fully understand how brain networks contribute to preserve cognition from the GMV loss. There are two important hypotheses, the differentiation (Park et al., 2004; Voss et al., 2008; Goh, 2011) and compensation (Grady et al., 1994; Cabeza, 2002; Davis et al., 2008). To evaluate these mechanisms, the between-network analysis will be performed in a future study. Fourth, this study used cross-sectional data collected by each age-group, not a longitudinal observation of individuals. Finally, the effect of head motion during rsfMRI scanning cannot be completely ruled out especially in aging studies (Kato et al., 2020).

CONCLUSION

In our study using a well-balanced healthy cohort in terms of the number of participants and age, we found mixed aging characteristics of brain networks. Among the sub-scores of the cognitive screening test, the DR, memory, attention/orientation, and visuospatial scores were significantly correlated with age, but not language and fluency. Furthermore, the cognitive domains that correlated with age, even the highly correlated sub-scores such as the DR score, showed delayed decline compared to the loss of total GMV. In RSN analysis, the ventral DMN, some networks involving primary processing (the primary VN, the dorsal and ventral SMN), and network related to visual function have within-network connectivity values that negatively correlated with age. On the other hand, some RSNs including the left / right ECN, dorsal DMN, posterior SN, LN, and lateral DAN, have within-network connectivity values that were maintained with age in this cohort. This may reflect a relative preservation in cognitive control function and crystalized intelligence in our cohort. Furthermore, the score of memory, fluency, and the DR was correlated with the sensorimotor network, which supported the importance of the exercise for maintenance of cognition.

DATA AVAILABILITY STATEMENT

The datasets presented in this article are not readily available because of privacy and ethical restrictions. Requests to access the datasets should be directed to SMa, smaesawa@med.nagoya-u.ac.jp.

ETHICS STATEMENT

The studies involving human participants were reviewed and approved by The Ethics Committee of Nagoya University Graduate School of Medicine (approval number 2014-0068). The patients/participants provided their written informed consent to participate in this study.

AUTHOR CONTRIBUTIONS

SMa, SMi, EB, HW, MH, HI, NO, MK, RS, and GS contributed to conception and design of the study. SMa, SMi, DM, DN, KH, KK, RO, AO, MH, and HI were involved in data acquisition, data organization, and data curation. SMa, SMi, EB, HW, and KK contributed to the methodology, analysis, interpretation of the data, and wrote the draft of the manuscript. All authors reviewed and approved the final version of the manuscript.

FUNDING

This work was supported by Grants-in-Aid from the Research Committee of Central Nervous System Degenerative Diseases by the Ministry of Health, Labor, and Welfare and from the Integrated Research on Neuropsychiatric Disorders project carried out under the Strategic Research for Brain Sciences by the Ministry of Education, Culture, Sports, Science, and Technology of Japan. This work was also supported by a Grant-in-Aid for Scientific Research from the Ministry of Education, Culture, Sports, Science, and Technology (MEXT) of Japan (Grant Number: 80569781), and a Grant-in-Aid for Scientific Research on Innovative Areas (Brain Protein Aging and Dementia Control) (Grant Number: 26117002) from MEXT. The funders had no role in study design, data collection, analysis, and interpretation, preparation of the manuscript, or decision to publish.

ACKNOWLEDGMENTS

This is a short text to acknowledge the contributions of specific colleagues, institutions, or agencies that aided the efforts of the authors.

REFERENCES

Abbott, A. E., Nair, A., Keown, C. L., Datko, M., Jahedi, A., Fishman, I., et al. (2016). Patterns of atypical functional connectivity and behavioral links in autism differ between default, salience,and executive networks. *Cereb. Cortex* 26, 4034–4045. doi: 10.1093/cercor/bhv191

Bagarinao, E., Watanabe, H., Maesawa, S., Mori, D., Hara, K., Kawabata, K., et al. (2018). An unbiased data-driven age-related structural brain parcellation for the identification of intrinsic brain volume changes over the adult lifespan. *Neuroimage* 169, 134–144. doi: 10.1016/j.neuroimage

Bagarinao, E., Watanabe, H., Maesawa, S., Mori, D., Hara, K., Kawabata, K., et al. (2019). Reorganization of brain networks and its association with general cognitive performance over the adult lifespan. *Sci. Rep.* 9:11352. doi: 10.1038/s41598-019-47922-x

Bagarinao, E., Watanabe, H., Maesawa, S., Mori, D., Hara, K., Kawabata, K., et al. (2020). Aging impacts the overall connectivity strength of regions critical for information transfer among brain networks. *Front. Aging Neurosci.* 12:592469. doi: 10.3389/fnagi.2020.592469

Baltes, P. B., Staudinger, U. M., and Lindenberger, U. (1999). Lifespan psychology: theory and application to intellectual functioning. *Annu. Rev. Psychol.* 50, 471–507. doi: 10.1146/annurev.psych.50.1.471

Baron, J. C., Chételat, G., Desgranges, B., Perchey, G., Landeau, B., de la Sayette, V., et al. (2001). In vivo mapping of gray matter loss with voxel-based morphometry in mild Alzheimer's disease. *Neuroimage* 14, 298–309. doi: 10.1006/nimg.2001.0848

Barulli, D., and Stern, Y. (2013). Efficiency, capacity, compensation, maintenance, plasticity: emerging concepts in cognitive reserve. *Trends Cogn. Sci.* 17, 502–509. doi: 10.1016/j.tics.2013.08.012

Betzel, R. F., Byrge, L., He, Y., Goñi, J., Zuo, X. N., and Sporns, O. (2014). Changes in structural and functional connectivity among resting-state networks across the human lifespan. *Neuroimage* 102, 345–357. doi: 10.1016/j.neuroimage.2014.07.067

Cabeza, R. (2002). Hemispheric asymmetry reduction in older adults: the HAROLD model. *Psychol. Aging* 17, 85–100. doi: 10.1037//0882-7974.17.1.85

Cabeza, R., Albert, M., Belleville, S., Craik, F. I. M., Duarte, A., Grady, C. L., et al. (2018). Maintenance, reserve and compensation: the cognitive neuroscience of healthy ageing. *Nat. Rev. Neurosci.* 19, 701–710. doi: 10.1038/s41583-018-0068-2

Cabinet Office Japan (2020). *Annual Report on the Ageing Society*. https://www8.cao.go.jp/kourei/english/annualreport/2020/pdf/2020.pdf (accessed July 4, 2021).

Campbell, K. L., Grigg, O., Saverino, C., Churchill, N., and Grady, C. L. (2013). Age differences in the intrinsic functional connectivity of default network subsystems. *Front. Aging Neurosci.* 5:73. doi: 10.3389/fnagi.2013.00073

Chan, M. Y., Park, D. C., Savalia, N. K., Petersen, S. E., and Wig, G. S. (2014). Decreased segregation of brain systems across the healthy adult lifespan. *Proc. Natl. Acad. Sci. U.S.A.* 111, 4997–5006. doi: 10.1073/pnas.1415122111

Chand, G. B., Wu, J., Hajjar, I., and Qiu, D. (2017). Interactions of the salience network and its subsystems with the default-mode and the central-executive networks in normal aging and mild cognitive impairment. *Brain Connect.* 7, 401–412. doi: 10.1089/brain.2017.0509

Chirles, T. J., Reiter, K., Weiss, L. R., Alfini, A. J., Nielson, K. A., and Smith, J. C. (2017). Exercise training and functional connectivity changes in mild cognitive impairment and healthy elders. *J. Alzheimers Dis.* 57, 845–856. doi: 10.3233/JAD-161151

Clarkson-Smith, L., and Hartley, A. A. (1989). Relationships between physical exercise and cognitive abilities in older adults. *Psychol. Aging.* 4, 183–189. doi: 10.1037//0882-7974.4.2.183

Cliff, M., Joyce, D. W., Lamar, M., Dannhauser, T., Tracy, D. K., and Shergill, S. S. (2013). Aging effects on functional auditory and visual processing using fMRI with variable sensory loading. *Cortex* 49, 1304–1313. doi: 10.1016/j.cortex.2012.04.003

Damoiseaux, J. S., Beckmann, C. F., Arigita, E. J., Barkhof, F., Scheltens, P., Stam, C. J., et al. (2008). Reduced resting-state brain activity in the "default network" in normal aging. *Cereb. Cortex* 18, 1856–1864. doi: 10.1093/cercor/bhm207

Damoiseaux, J. S., Prater, K. E., Miller, B. L., and Greicius, M. D. (2012). Functional connectivity tracks clinical deterioration in Alzheimer's disease. *Neurobiol. Aging* 33, 828.e19–828.e30. doi: 10.1016/j.neurobiolaging.2011.06.024

Davis, S. W., Dennis, N. A., Daselaar, S. M., Fleck, M. S., and Cabeza, R. (2008). Que PASA? The posterior-anterior shift in aging. *Cereb. Cortex* 18, 1201–1209. doi: 10.1093/cercor/bhm155

Dobromyslin, V. I., Salat, D. H., Fortier, C. B., Leritz, E. C., Beckmann, C. F., Milberg, W. P., et al. (2012). Distinct functional networks within the cerebellum and their relation to cortical systems assessed with independent component analysis. *Neuroimage* 60, 2073–2085. doi: 10.1016/j.neuroimage.2012.01.139

Douaud, G., Groves, A. R., Tamnes, C. K., Westlye, L. T., Duff, E. P., Engvig, A., et al. (2014). A common brain network links development, aging, and vulnerability to disease. *Proc. Natl. Acad. Sci. U.S.A.* 111, 17648–17653. doi: 10.1073/pnas.1410378111

Ferreira, L. K., and Busatto, G. F. (2013). Resting-state functional connectivity in normal brain aging. *Neurosci. Biobehav. Rev.* 37, 384–400. doi: 10.1016/j.neubiorev.2013.01.017

Filippini, N., MacIntosh, B. J., Hough, M. G., Goodwin, G. M., Frisoni, G. B., Smith, S. M., et al. (2009). Distinct patterns of brain activity in young carriers of the APOE-ε4 allele. *Proc. Natl. Acad. Sci.* 106, 7209–7214. doi: 10.1073/pnas.0811879106

Ge, Y., Grossman, R. I., Babb, J. S., Rabin, M. L., Mannon, L. J., and Kolson, D. L. (2002). Age-related total gray matter and white matter changes in normal

adult brain. Part II: quantitative magnetization transfer ratio histogram analysis. *AJNR Am. J. Neuroradiol.* 23, 1334–1341.

Geerligs, L., Renken, R. J., Saliasi, E., Maurits, N. M., and Lorist, M. M. (2015). A brain-wide study of age-related changes in functional connectivity. *Cereb Cortex* 25, 1987–1999. doi: 10.1093/cercor/bhu012

Giorgio, A., Santelli, L., Tomassini, V., Bosnell, R., Smith, S., De Stefano, N., et al. (2010). Age-related changes in grey and white matter structure throughout adulthood. *Neuroimage* 51, 943–951. doi: 10.1016/j.neuroimage.2010.03.004

Goh, J. O. (2011). Functional dedifferentiation and altered connectivity in older adults: neural accounts of cognitive aging. *Aging Dis.* 2, 30–48.

Good, C. D., Johnsrude, I. S., Ashburner, J., Henson, R. N., Friston, K. J., and Frackowiak, R. S. (2001). A voxel-based morphometric study of ageing in 465 normal adult human brains. *Neuroimage* 14, 21–36. doi: 10.1006/nimg.2001.0786

Grady, C. (2012). The cognitive neuroscience of ageing. *Nat. Rev. Neurosci.* 13, 491–505. doi: 10.1038/nrn3256

Grady, C. L., Maisog, J. M., Horwitz, B., Ungerleider, L. G., Mentis, M. J., Salerno, J. A., et al. (1994). Age-related changes in cortical blood flow activation during visual processing of faces and location. *J. Neurosci.* 14(3 Pt 2), 1450–1462. doi: 10.1523/JNEUROSCI.14-03-01450.1994

Greicius, M. D., Srivastava, G., Reiss, A. L., and Menon, V. (2004). Default-mode network activity distinguishes Alzheimer's disease from healthy aging: evidence from functional MRI. *Proc. Natl. Acad. Sci. U.S.A.* 101, 4637–4642. doi: 10.1073/pnas.0308627101

Hausman, H. K., O'Shea, A., Kraft, J. N., Boutzoukas, E. M., Evangelista, N. D., Van Etten, E. J., et al. (2020). The role of resting-state network functional connectivity in cognitive aging. *Front. Aging Neurosci.* 12:177. doi: 10.3389/fnagi.2020.00177

Huang, C. C., Hsieh, W. J., Lee, P. L., Peng, L. N., Liu, L. K., Lee, W. J., et al. (2015). Age-related changes in resting-state networks of a large sample size of healthy elderly. *CNS Neurosci. Ther.* 21, 817–825. doi: 10.1111/cns.12396

Huang, P., Fang, R., Li, B. Y., and Chen, S. D. (2016). Exercise-Related changes of networks in aging and mild cognitive impairment brain. *Front. Aging Neurosci.* 8:47. doi: 10.3389/fnagi.2016.00047

Jenkinson, M., Beckmann, C. F., Behrens, T. E., Woolrich, M. W., and Smith, S. M. (2012). FSL. *Neuroimage* 62, 782–790. doi: 10.1016/j.neuroimage.2011.09.015

Ji, L., Pearlson, G. D., Zhang, X., Steffens, D. C., Ji, X., Guo, H., et al. (2018). Physical exercise increases involvement of motor networks as a compensatory mechanism during a cognitively challenging task. *Int. J. Geriatr. Psychiatry* 33, 1153–1159. doi: 10.1002/gps.4909

Jones, D. T., Machulda, M. M., Vemuri, P., McDade, E. M., Zeng, G., Senjem, M. L., et al. (2011). Age-related changes in the default mode network are more advanced in Alzheimer disease. *Neurology* 77, 1524–1531. doi: 10.1212/WNL.0b013e318233b33d

Kato, S., Bagarinao, E., Isoda, H., Koyama, S., Watanabe, H., Maesawa, S., et al. (2020). Effects of head motion on the evaluation of age-related brain network changes using resting state functional MRI. *Magn. Reson. Med. Sci.* doi: 10.2463/mrms.mp.2020-0081 [Epub ahead of print].

Kawabata, K., Watanabe, H., Bagarinao, E., Ohdake, R., Hara, K., Ogura, A., et al. (2020). Cerebello-basal ganglia connectivity fingerprints related to motor/cognitive performance in Parkinson's disease. *Parkinsonism Relat. Disord.* 80, 21–27. doi: 10.1016/j.parkreldis.2020.09.005

Koch, W., Teipel, S., Mueller, S., Buerger, K., Bokde, A. L., Hampel, H., et al. (2010). Effects of aging on default mode network activity in resting state fMRI: does the method of analysis matter? *Neuroimage* 51, 280–287. doi: 10.1016/j.neuroimage.2009.12.008

Lehmbeck, J. T., Brassen, S., Weber-Fahr, W., and Braus, D. F. (2006). Combining voxel-based morphometry and diffusion tensor imaging to detect age-related brain changes. *Neuroreport* 17, 467–470. doi: 10.1097/01.wnr.0000209012.24341.7f

Livingston, G., Sommerlad, A., Orgeta, V., Costafreda, S. G., Huntley, J., Ames, D., et al. (2017). Dementia prevention, intervention, and care. *Lancet* 390, 2673–2734. doi: 10.1016/S0140-6736(17)31363-6

Maesawa, S., Bagarinao, E., Fujii, M., Futamura, M., Motomura, K., Watanabe, H., et al. (2015). Evaluation of resting state networks in patients with gliomas: connectivity changes in the unaffected side and its relation to cognitive function. *PLoS One* 10:e0118072. doi: 10.1371/journal.pone.0118072

Mathuranath, P. S., Nestor, P. J., Berrios, G. E., Rakowicz, W., and Hodges, J. R. (2000). A brief cognitive test battery to differentiate Alzheimer's disease and frontotemporal dementia. *Neurology* 55, 1613–1620. doi: 10.1212/01.wnl.0000434309.85312.19

Meier, T. B., Desphande, A. S., Vergun, S., Nair, V. A., Song, J., Biswal, B. B., et al. (2012). Support vector machine classification and characterization of age-related reorganization of functional brain networks. *Neuroimage* 60, 601–613. doi: 10.1016/j.neuroimage.2011.12.052

Mulders, P. C., van Eijndhoven, P. F., Schene, A. H., Beckmann, C. F., and Tendolkar, I. (2015). Resting-state functional connectivity in major depressive disorder: a review. *Neurosci. Biobehav. Rev.* 56, 330–344. doi: 10.1016/j.neubiorev.2015.07.014

Onoda, K., Ishihara, M., and Yamaguchi, S. (2012). Decreased functional connectivity by aging is associated with cognitive decline. *J. Cogn. Neurosci.* 24, 2186–2198. doi: 10.1162/jocn_a_00269

Park, D. C., Lautenschlager, G., Hedden, T., Davidson, N. S., Smith, A. D., and Smith, P. K. (2002). Models of visuospatial and verbal memory across the adult life span. *Psychol. Aging* 17, 299–320.

Park, D. C., Polk, T. A., Park, R., Minear, M., Savage, A., and Smith, M. R. (2004). Aging reduces neural specialization in ventral visual cortex. *Proc. Natl. Acad. Sci. U.S.A.* 101, 13091–13095. doi: 10.1073/pnas.0405148101

Power, J. D., Barnes, K. A., Snyder, A. Z., Schlaggar, B. L., and Petersen, S. E. (2012). Spurious but systematic correlations in functional connectivity MRI networks arise from subject motion. *Neuroimage* 59, 2142–2154. doi: 10.1016/j.neuroimage.2011.10.018

Putcha, D., Ross, R. S., Cronin-Golomb, A., Janes, A. C., and Stern, C. E. (2015). Altered intrinsic functional coupling between core neurocognitive networks in Parkinson's disease. *Neuroimage Clin.* 7, 449–455. doi: 10.1016/j.nicl.2015.01.012

Rajah, M. N., and D'Esposito, M. (2005). Region-specific changes in prefrontal function with age: a review of PET and fMRI studies on working and episodic memory. *Brain* 128, 1964–1983. doi: 10.1093/brain/awh608

Rende, B., Ramsberger, G., and Miyake, A. (2002). Commonalities and differences in the working memory components underlying letter and category fluency tasks: a dual-task investigation. *Neuropsychology* 16, 309–321. doi: 10.1037//0894-4105.16.3.309

Reuter-Lorenz, P. A., and Cappell, K. A. (2008). Neurocognitive aging and the compensation hypothesis. *Curr. Dir. Psychol. Sci.* 17, 177–182.

Risacher, S. L., Saykin, A. J., West, J. D., Shen, L., Firpi, H. A., and McDonald, B. C. (2009). Baseline MRI predictors of conversion from MCI to probable AD in the ADNI cohort, Alzheimer's Disease neuroimaging initiative (ADNI). *Curr. Alzheimer Res.* 6, 347–361. doi: 10.2174/156720509788929273

Roski, C., Caspers, S., Langner, R., Laird, A. R., Fox, P. T., Zilles, K., et al. (2013). Adult age-dependent differences in resting-state connectivity within and between visual-attention and sensorimotor networks. *Front. Aging Neurosci.* 5:67. doi: 10.3389/fnagi.2013.00067

Rowe, J. W., and Kahn, R. L. (1987). Human aging: usual and successful. *Science* 237, 143–149. doi: 10.1126/science.3299702

Rowe, J. W., and Kahn, R. L. (1997). Successful aging. *Gerontologist* 37, 433–440. doi: 10.1093/geront/37.4.433

Rowe, J. W., and Kahn, R. L. (2015). Successful aging 2.0: conceptual expansions for the 21st Century. *J. Gerontol. B Psychol. Sci. Soc. Sci.* 70, 593–596. doi: 10.1093/geronb/gbv025

Ruff, R. M., Light, R. H., Parker, S. B., and Levin, H. S. (1997). The psychological construct of word fluency. *Brain Lang.* 57, 394–405. doi: 10.1006/brln.1997.1755

Satz, P., Cole, M. A., Hardy, D. J., and Rassovsky, Y. (2011). Brain and cognitive reserve: mediator(s) and construct validity, a critique. *J. Clin. Exp. Neuropsychol.* 33, 121–130. doi: 10.1080/13803395.2010.493151

Schnack, H. G., van Haren, N. E., Brouwer, R. M., Evans, A., Durston, S., Boomsma, D. I., et al. (2015). Changes in thickness and surface area of the human cortex and their relationship with intelligence. *Cereb. Cortex* 25, 1608–1617. doi: 10.1093/cercor/bht357

Shirer, W. R., Ryali, S., Rykhlevskaia, E., Menon, V., and Greicius, M. D. (2012). Decoding subject-driven cognitive states with whole-brain connectivity patterns. *Cereb. Cortex* 22, 158–165. doi: 10.1093/cercor/bhr099

Solé-Padullés, C., Bartrés-Faz, D., Junqué, C., Vendrell, P., Rami, L., Clemente, I. C., et al. (2009). Brain structure and function related to cognitive reserve variables

in normal aging, mild cognitive impairment and Alzheimer's disease. *Neurobiol. Aging* 30, 1114–1124. doi: 10.1016/j.neurobiolaging.2007.10.008

Sowell, E. R., Peterson, B. S., Thompson, P. M., Welcome, S. E., Henkenius, A. L., and Toga, A. W. (2003). Mapping cortical change across the human life span. *Nat. Neurosci.* 6, 309–315. doi: 10.1038/nn1008

Squarzoni, P., Duran, F. L. S., Busatto, G. F., and Alves, T. C. T. F. (2018). Reduced gray matter volume of the thalamus and hippocampal region in elderly healthy adults with no impact of apoe ϵ4: a longitudinal voxel-based morphometry study. *J. Alzheimers Dis.* 62, 757–771. doi: 10.3233/JAD-161036

Stern, Y. (2002). What is cognitive reserve? Theory and research application of the reserve concept. *J. Int. Neuropsychol. Soc.* 8, 448–460.

Stern, Y. (2009). Cognitive reserve. *Neuropsychologia* 47, 2015–2028. doi: 10.1016/j.neuropsychologia.2009.03.004

Stern, Y., Gurland, B., Tatemichi, T. K., Tang, M. X., Wilder, D., and Mayeux, R. (1994). Influence of education and occupation on the incidence of Alzheimer's disease. *JAMA* 271, 1004–1010.

Stolwyk, R., Bannirchelvam, B., Kraan, C., and Simpson, K. (2015). The cognitive abilities associated with verbal fluency task performance differ across fluency variants and age groups in healthy young and old adults. *J. Clin. Exp. Neuropsychol.* 37, 70–83. doi: 10.1080/13803395.2014.988125

Taki, Y., Thyreau, B., Kinomura, S., Sato, K., Goto, R., Kawashima, R., et al. (2011). Correlations among brain gray matter volumes, age, gender, and hemisphere in healthy individuals. *PLoS One* 6:e22734. doi: 10.1371/journal.pone.0022734

Tomasi, D., and Volkow, N. D. (2012). Aging and functional brain networks. *Mol. Psychiatry* 5, 549–558. doi: 10.1038/mp.2011.81

Voss, M. W., Erickson, K. I., Chaddock, L., Prakash, R. S., Colcombe, S. J., Morris, K. S., et al. (2008). Dedifferentiation in the visual cortex: an fMRI investigation of individual differences in older adults. *Brain Res.* 1244, 121–131. doi: 10.1016/j.brainres.2008.09.051

Voss, M. W., Weng, T. B., Burzynska, A. Z., Wong, C. N., Cooke, G. E., Clark, R., et al. (2016). Fitness, but not physical activity, is related to functional integrity of brain networks associated with aging. *Neuroimage* 131, 113–125. doi: 10.1016/j.neuroimage.2015.10.044

Weuve, J., Kang, J. H., Manson, J. E., Breteler, M. M., Ware, J. H., and Grodstein, F. (2004). Physical activity, including walking, and cognitive function in older women. *JAMA* 292, 1454–1461. doi: 10.1001/jama.292.12.1454

World Health Organization (2020). *Grobal Health Estimates*. https://www.who.int/data/gho/data/themes/mortality-and-global-health-estimates/ghe-life-expectancy-and-healthy-life-expectancy (accessed July 5, 2021).

Yan, L., Zhuo, Y., Wang, B., and Wang, D. J. (2011). Loss of coherence of low frequency fluctuations of bold fmri in visual cortex of healthy aged subjects. *Open Neuroimag. J.* 5, 105–111.

Yoshida, H., Terada, S., Honda, H., Kishimoto, Y., Takeda, N., Oshima, E., et al. (2012). Validation of the revised addenbrooke's cognitive examination (ACE-R) for detecting mild cognitive impairment and dementia in a Japanese population. *Int. Psychogeriatr.* 24, 28–37. doi: 10.1017/S1041610211001190

Conflict of Interest: The handling editor declared a past co-authorship with one of the author GS.

The remaining authors declare that the research was conducted in the absence of any commercial or financial relationships that could be construed as a potential conflict of interest.

Publisher's Note: All claims expressed in this article are solely those of the authors and do not necessarily represent those of their affiliated organizations, or those of the publisher, the editors and the reviewers. Any product that may be evaluated in this article, or claim that may be made by its manufacturer, is not guaranteed or endorsed by the publisher.

frontiers in Aging Neuroscience

REVIEW
published: 22 November 2021
doi: 10.3389/fnagi.2021.747359

Characteristics of Neural Network Changes in Normal Aging and Early Dementia

Hirohisa Watanabe[1,2], Epifanio Bagarinao[2,3], Satoshi Maesawa[2,4], Kazuhiro Hara[5], Kazuya Kawabata[5], Aya Ogura[5], Reiko Ohdake[1,2], Sayuri Shima[1], Yasuaki Mizutani[1], Akihiro Ueda[1], Mizuki Ito[1], Masahisa Katsuno[5] and Gen Sobue[2,6]*

[1] Department of Neurology, Fujita Health University, Toyoake, Japan, [2] Brain and Mind Research Center, Nagoya University, Nagoya, Japan, [3] Department of Integrated Health Sciences, Nagoya University Graduate School of Medicine, Nagoya, Japan, [4] Department of Neurosurgery, Nagoya University Graduate School of Medicine, Nagoya, Japan, [5] Department of Neurology, Nagoya University Graduate School of Medicine, Nagoya, Japan, [6] Aichi Medical University, Nagakute, Japan

To understand the mechanisms underlying preserved and impaired cognitive function in healthy aging and dementia, respectively, the spatial relationships of brain networks and mechanisms of their resilience should be understood. The hub regions of the brain, such as the multisensory integration and default mode networks, are critical for within- and between-network communication, remain well-preserved during aging, and play an essential role in compensatory processes. On the other hand, these brain hubs are the preferred sites for lesions in neurodegenerative dementias, such as Alzheimer's disease. Disrupted primary information processing networks, such as the auditory, visual, and sensorimotor networks, may lead to overactivity of the multisensory integration networks and accumulation of pathological proteins that cause dementia. At the cellular level, the brain hub regions contain many synapses and require a large amount of energy. These regions are rich in ATP-related gene expression and had high glucose metabolism as demonstrated on positron emission tomography (PET). Importantly, the number and function of mitochondria, which are the center of ATP production, decline by about 8% every 10 years. Dementia patients often have dysfunction of the ubiquitin-proteasome and autophagy-lysosome systems, which require large amounts of ATP. If there is low energy supply but the demand is high, the risk of disease can be high. Imbalance between energy supply and demand may cause accumulation of pathological proteins and play an important role in the development of dementia. This energy imbalance may explain why brain hub regions are vulnerable to damage in different dementias. Here, we review (1) the characteristics of gray matter network, white matter network, and resting state functional network changes related to resilience in healthy aging, (2) the mode of resting state functional network disruption in neurodegenerative dementia, and (3) the cellular mechanisms associated with the disruption.

Keywords: resting state network (RSN), anatomical networks, MRI, aging, dementia, network hub, energy failure

OPEN ACCESS

Edited by:
Hanna Lu,
The Chinese University of Hong Kong, China

Reviewed by:
Pravir Kumar,
Delhi Technological University, India
Vinita Ganesh Chittoor,
Stanford University, United States

****Correspondence:***
Hirohisa Watanabe
nabe@med.nagoya-u.ac.jp

Received: *26 July 2021*
Accepted: *18 October 2021*
Published: *22 November 2021*

Citation:
Watanabe H, Bagarinao E, Maesawa S, Hara K, Kawabata K, Ogura A, Ohdake R, Shima S, Mizutani Y, Ueda A, Ito M, Katsuno M and Sobue G (2021) Characteristics of Neural Network Changes in Normal Aging and Early Dementia. Front. Aging Neurosci. 13:747359. doi: 10.3389/fnagi.2021.747359

INTRODUCTION

Patients with dementia have limitations in activities of daily living due to impaired memory, language comprehension, executive function, visuospatial function, and judgment. These functions also decline with normal aging, but without limitations in activities of daily living. This is because "intelligence," the ability to act purposefully and with reason as well as effectively interact with the environment to solve problems, is well-preserved (Deary, 2012; Park and Bischof, 2013). Interestingly, primary sensations (hearing, touch, and smell), motor function, memory, calculation, and intuition peak at around 20 years of age, followed by a gradual decline; concentration and emotional cognition peak at around 45 years of age, while comprehension, vocabulary, and judgment peak at around 60 years (Hartshorne and Germine, 2015). Considering the aging population, relationships between memory and aging should be determined.

Alzheimer's disease (AD), dementia with Lewy bodies (DLB), and frontotemporal lobar degeneration (FTLD) develop in the elderly population and share the accumulation of pathological proteins (tau and amyloid-β in AD, α-synuclein in DLB, and TDP-43, tau, and FUS in FTLD). However, many older adults with brain atrophy demonstrate normal higher mental functions and intelligence. The accumulation of tau and amyloid-β in AD patients begins more than 20 years before the disease onset, and there is a long asymptomatic or pre-clinical period despite accumulation of pathological proteins (Jack et al., 2013; Masters et al., 2015). In addition, some patients with mild cognitive impairment (MCI) return to the preclinical stage of the disease (with memory impairment but no limitations in activities of daily living) (Ding et al., 2016). In contrast, some asymptomatic patients have pathological accumulation of proteins that is suggestive of AD (Snowdon, 2003).

To understand the plasticity and adaptation of brain, the following facts should be considered:

1. Various aspects of intelligence peak after the age of 45 years,
2. Pathological protein accumulation and brain atrophy do not always correlate with the symptoms, and
3. Patients may transition between the preclinical and MCI stages.

Although various recent studies have provided perspectives to answer these questions in terms of the balance between energy demand and supply in the brain (Camandola and Mattson, 2017; Mattson and Arumugam, 2018; Vandoorne et al., 2018; Diederich et al., 2019), these studies mainly focused at the cellular level, and only a limited number of studies have focused on the relationship between energy and large-scale networks in the brain.

Techniques to analyze brain networks using magnetic resonance imaging (MRI) (Suárez et al., 2020), magnetoencephalography and electroencephalography (Prichep, 2007; de Haan et al., 2009) have become widely available in recent years, which has improved our understanding of the relationships between aging and dementia. Measures of structural and functional brain connectivity using MRI have become widely used as reliable indicators in assessing brain reserve and incompatibility, and in predicting progression to dementia (Farb et al., 2013; Teipel et al., 2016). In our large aging cohort study, we have also employed MRI data to investigate age-related changes in anatomical circuits (Bagarinao et al., 2018), brain volumes (Bagarinao et al., 2018), white matter fiber tracts (Choy et al., 2020), and resting-state functional circuits (Bagarinao et al., 2019, 2020a,b). We have recruited a total of more than 1,500 healthy adult volunteers aged 20–80 years from Nagoya, which is Japan's fourth most populated city, and neighboring areas to elucidate age-related changes in brain networks. We have also collected demographic data, including education, past medical history, medication, drinking and smoking habits, and family history of neurodegenerative diseases, Mini-Mental State Examination (MMSE) and Addenbrooke's Cognitive Examination-Revised (ACE-R) for general cognition. ACE-R evaluates five cognitive subdomains, including orientation/attention, memory, verbal fluency, language and visuospatial ability (Mioshi et al., 2006), and has been reported to have excellent sensitivities and specificities (>0.8) for the diagnosis of MCI and dementia (Livingston et al., 2017). In addition to aging studies, we have also employed similar brain network analysis to examine network alterations in patients with neurodegenerative disorders such as AD (Yokoi et al., 2018), amyotrophic lateral sclerosis (ALS) FTLD (Ogura et al., 2019; Imai et al., 2020), Parkinson's disease with mild cognitive decline (Kawabata et al., 2018) and others.

In this review, we summarize our findings as well as existing evidence from other studies on the characteristics of brain networks of healthy older adults and patients with early dementia and discuss the backgrounds of the potential mechanism at the cellular level of the transition from healthy aging to dementia.

WIDESPREAD ATROPHIC CHANGES AND NETWORK ALTERATIONS IN THE BRAIN'S GRAY MATTER WITH AGING

Several MRI studies measuring brain atrophic changes with aging have shown a global decline in gray matter volume (**Figure 1A**; Good et al., 2001; Allen et al., 2005; Smith et al., 2007; Bagarinao et al., 2018). However, the rate of gray matter volume decline across the whole brain varies. In one study (Bagarinao et al., 2018), we identified regions with similar patterns of age-related brain atrophy in a data-driven approach using independent component analysis (ICA), a method that can be used to separate multivariate signals into multiple additive components, assuming that the observed data is a linear superposition of independent components (**Figure 1C**; Bagarinao et al., 2018). We have identified 192 regions, which interestingly closely resembled that of the conventional anatomical structures and Brodmann's brain map areas. Among these regions, the volume of 174 (90.6%) negatively correlated with age, especially the central posterior gyrus (**Figure 1D**), cerebellum, central gyrus, and inferior frontal gyrus. On the other hand, the thalamus (**Figure 1E**), regions located in the medial frontal lobe, and

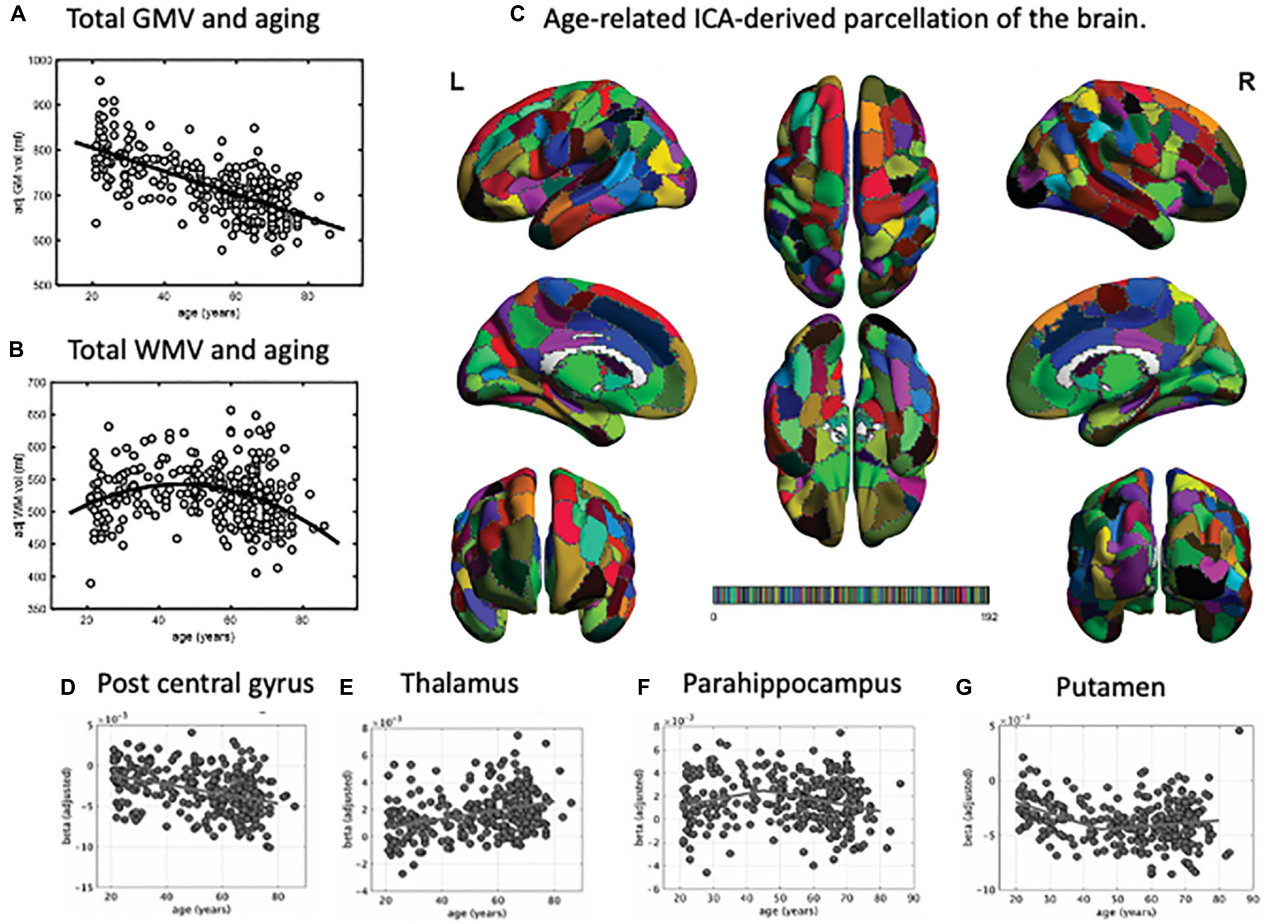

FIGURE 1 | Parcellation map for the unbiased, data-driven, age-related brain structure. Total gray matter volume decreased with aging **(A)**. However, the total white matter volume peaked at around 50 years of age, followed by a decrease **(B)**. Using independent component analysis, we extracted 192 brain regions related to aging **(C)**. Based on this parcellation map, we identified regions where brain volume decreased with age (e.g., post central gyrus, **D**), remained stable (e.g., thalamus, **E**), or peaked at around 45 years of age and then decreased (e.g., parahippocampus, **F**, and putamen, **G**). GMV, gray matter volume; WMV, white matter volume; ICA, independent component analysis. This figure is adapted from Bagarinao et al. (2018).

the superior frontal gyrus demonstrated relatively preserved volumes. In addition, the volumes of regions such as the parahippocampal gyrus (**Figure 1F**) had an inverted U-shape relationship with age, with the maximum volume at 45–50 years. A similar U-shaped relationship was also observed with the volume of the putamen (**Figure 1G**).

In the same study, we also examined the relationships between age and gray matter network properties, including integration and efficiency, using graph theory. We used the ICA-identified regions as network "nodes," the correlations of gray matter values between nodes as "edges," and the entire brain as a set of vertices and edges that form a network. Estimated hub indices, which indicate overall brain integration, and the indices associated with network efficiency exhibited a U-shaped or inverted U-shaped relationship with age, with a peak at around 45–50 years of age. These spatially connected intrinsic brain volume changes and network reconfiguration associated with the increase in network segregation and integration after 50 years of age may provide the needed maintenance of normal social and cognitive status of the elderly and may also lead to the onset of age-related neurodegenerative diseases.

AGING AND CHANGES IN WHITE MATTER VOLUME AND NETWORK

Studies investigating age-related changes in the brain's white matter have shown that the total white matter volume had an inverted U-shape relationship with age, characterized by an initial increase in volume until around 45–50 years of age, followed by a decrease (**Figure 1B**; Allen et al., 2005; Fjell et al., 2013; Bagarinao et al., 2018). Aside from the total volume, more recent studies have also examined age-related microstructural changes in the white matter's fiber tracts. Diffusion-weighted MRI (dMRI) is a technique based on the diffusion of water molecules in tissues and can be used to evaluate white matter fibers. Using dMRI, scalar quantities such as diffusion anisotropy (fractional anisotropy, FA) and mean diffusivity (MD) can be estimated and used as indirect

measures of white matter integrity. Generally, FA decreases with age, while MD increases, indicating a general decline of white matter integrity with age. These metrics, however, do not consider the influence of crossing and kissing fibers in a voxel, which could affect the analysis (Jeurissen et al., 2013).

In another study (Choy et al., 2020), we used the recently developed fixel-based analysis (FBA) (Raffelt et al., 2017), which employed a more advanced diffusion model to resolve multiple fiber populations in a single voxel, to evaluate specific structural changes in each nerve fiber tract. Using FBA, we examined the relationships between age and FBA parameters, such as fiber density (FD), fiber cross-section (FC), and the combined measure of fiber density and cross section called FDC (FD × FC), in 293 healthy participants aged 21–86 years (Choy et al., 2020). We also performed tract-level analysis using the Johns Hopkins University (JHU) white matter tractography atlas, which consists of 11 major fiber tracts, including the anterior thalamic radiation (ATR), cingulum (cingulate gyrus, CCG), cingulum (hippocampus, CH), corticospinal tract (CST), forceps major (FMaj), forceps minor (FMin), inferior fronto-occipital fasciculus (IFOF), inferior longitudinal fasciculus (ILF), superior longitudinal fasciculus (SLF), superior longitudinal fasciculus (temporal, SLTem), and uncinate fasciculus (UF) (**Figure 2**).

Our findings showed that FD decreased significantly with age in 5 of the 11 major fiber tracts (ATR, CCG, CH, FMin, and SLF). This decrease is consistent with previous histopathological reports that white matter axons in the corpus callosum are damaged with age (Hou and Pakkenberg, 2012). On the other hand, the FD of 6 of the 11 fiber tracts did not show a significant negative correlation with age, and the FD of FMaj, IFOF, and ILF only showed a small, but insignificant, change with age. Interestingly, the FC of CH significantly increased with age, whereas that of ATR and UF showed an increasing trend with age but not significant. This may be explained by the fact that the white matter volume peaks at around 45–50 years of age, and the volumes of the middle frontal gyrus, thalamus, parahippocampal gyrus, and superior frontal gyrus remain relatively preserved. A recent meta-analysis reported that aerobic exercise could prevent the age-related decrease in hippocampal volume (Firth et al., 2018). The relationships between exercise and the associated changes in white matter fibers and brain volume during healthy aging still require further investigation. FDC, representing a comprehensive index that evaluates both FD and FC, negatively correlated with age in 6 of the 11 fiber tracts (ATR, CCG, CST, FMin, IFOF, and ILF). As for the CCG and FMin, which are mainly located in the frontal lobe, the FD, FC and FDC were negatively correlated with age.

Age-related changes in white matter fibers are not uniform, as is the case with brain volume, and about half of the major white matter circuits, especially those located posteriorly, are unaffected by aging, which may relate to the preserved cognitive function and intelligence.

As shown, some gray matter areas and white matter volumes did not uniformly decrease with age, and the volumes of white matter and some gray matter regions were not only considerably maintained until 45–50 years of age, but also tended to increase. These volume changes have important implications for the pathogenesis of various cognitive functions and intelligence in middle-aged and older adults.

In monkeys, the decrease in gray matter volume was a result of decreased dendrites and synapses, rather than neurons (Page et al., 2002), which explains why a U-shaped relationship does not occur during their aging process. A recent study has demonstrated that myelin fragmentations were gradually released from aging myelin sheaths and were subsequently cleared by microglia resulting in the formation of insoluble, lipofuscin-like lysosomal inclusions in microglia (Safaiyan et al., 2016). In a study that quantified the density of HLA-DR-positive activated microglia in the white matter of postmortem samples of cognitively normal young adults, cognitively normal older adults, and "super-agers" aged 80 years or older whose memory test scores were equivalent to or higher than those of people aged 50–65 years, the statistical significant differences in microglia density were evident between normal young adults and cognitively normal old but not between normal young adults and SuperAgers (Gefen et al., 2019). A more recent study identified white matter-associated microglia, which form in a TREM2-dependent but APOE-independent manner in aging white matter, where they form nodules that are engaged in phagocytosing damaged myelin (Safaiyan et al., 2021). These findings suggest that there are dynamic changes in the white matter of the brain that regenerate and manage degenerated myelin during aging, which may be associated with healthy cognitive function and toward disease progression.

AGE-RELATED CHANGES IN THE BRAIN'S FUNCTIONAL NETWORKS

Resting-state functional MRI (rsfMRI) is a non-invasive imaging modality that can measure spontaneous low-frequency fluctuations in the blood oxygenation level-dependent (BOLD) signal. The BOLD effect is a phenomenon in which local neural activity changes the binding of blood hemoglobin to oxygen, resulting in a change in magnetism in the same region, which in turn causes a change in the MRI signal (Ogawa and Lee, 1990). Using rsfMRI, various resting-state networks (RSNs) representing spatially distinct areas of the brain that demonstrate synchronous BOLD fluctuations at rest can be identified (Biswal et al., 1995). Typical methods for studying RSNs include ICA, seed-based analysis, and graph theory. These methods examine the relationships between specific regions and the whole brain. ICA for the whole brain is useful to identify large-scale networks, such as the default mode (which activates when the participant is concentrating on an internally oriented task related to cognitive function), primary information processing-related (motor sensory, visual, and auditory networks) and multisensory integration (executive control, salience, and dorsal attention networks) networks.

In our analysis of large-scale brain networks of normal individuals (Bagarinao et al., 2019), within large-scale network connectivity was significantly reduced with age, whereas increased connectivity was observed with regions outside the network. General higher mental functions, assessed by the ACE-R

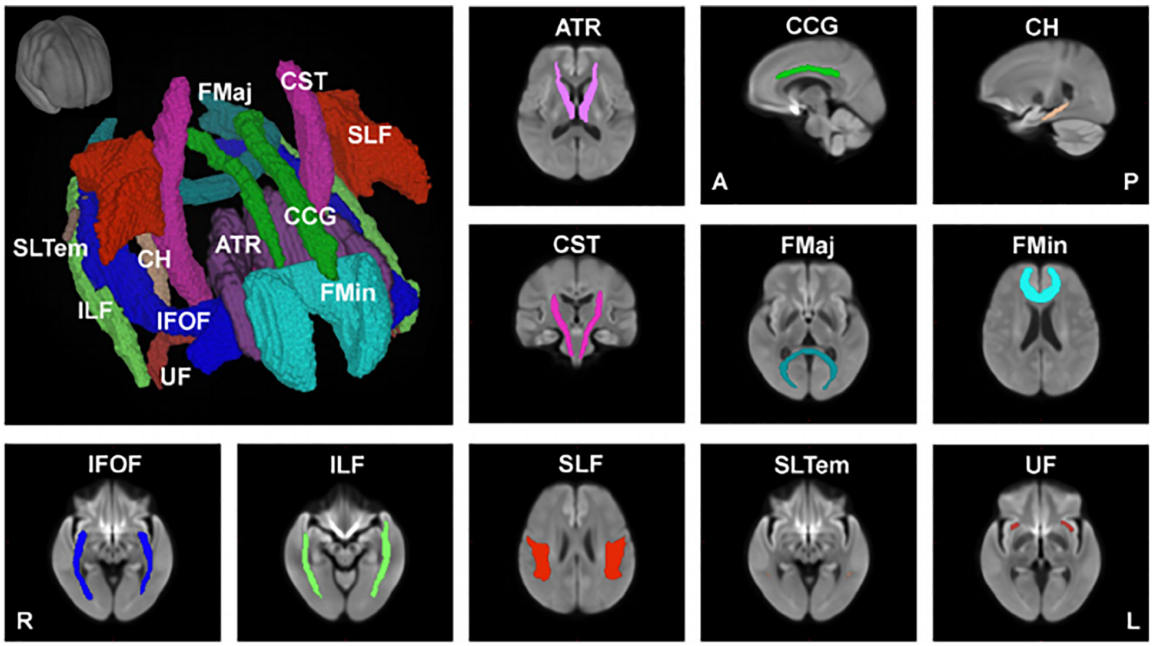

FIGURE 2 | Major anatomical tracts of the brain. Major fiber tracts based on the Johns Hopkins University – International Consortium for Brain Mapping (JHU-ICBM) atlas, warped onto the study's population template space were used for the tract-level analyses of fiber density (FD), fiber cross-section (FC), and combined measure of fiber density and cross-section (FDC). ATR, anterior thalamic radiation; CCG, cingulum (cingulate gyrus); CH, cingulum (hippocampus); CST, corticospinal tract; FMaj, forceps major; FMin, forceps minor; IFOF, inferior fronto-occipital fasciculus; ILF, inferior longitudinal fasciculus; SLF, superior longitudinal fasciculus; SLTem, superior longitudinal fasciculus (temporal); UF, uncinate fasciculus. This figure is reproduced with permission from Choy et al. (2020).

score, were higher for patients with preserved connections within primary information processing-related networks such as auditory and primary visual networks.

In addition, older adults demonstrated a stronger connectivity in the dorsal attention network (which belongs to the multisensory integration network, is active during spontaneous attention and reorientation to unexpected events, and integrates multiple primary information processing), primary information processing-related network (sensorimotor and primary visual networks), default mode network (precuneus network), and the multisensory integration network (salience network). The strength of connections among the default mode, executive control, and salience networks (also called the neurocognitive networks) correlated with higher general cognitive function. On the other hand, stronger connections of the primary information processing networks (sensorimotor, primary visual, and higher visual networks) with the salience and basal ganglia networks were associated with lower general cognitive function.

An analysis of the integrity of large-scale networks in elderly and young participants (<30 years of age) demonstrated decrease in the integrity of most large-scale networks with age. Interestingly, cognitive functions were higher in participants with preserved integrity of the primary visual, higher visual, sensorimotor, and dorsal attention networks.

Using a parcellation map that subdivides the brain into 499 regions of interest (Shirer et al., 2012), we also performed network analysis using graph theory with each region of interest used as a node, and functional connections between nodes considered as edges. Our findings showed that the shortest path length decreased, the overall efficiency increased, and the network integration increased with age.

We further evaluated whether connectivity measures associated with resting-state functional networks or age affects the ACE-R scores, using mediation analysis, and observed that changes in a resting-state functional network had a stronger influence on ACE-R scores compared to age. Recent studies have demonstrated that an enhanced connectivity between resting-state functional networks plays a vital role in patients with preserved motor and higher brain functions in adulthood, despite hemisection of the brain in childhood (Kliemann et al., 2019). Additionally, in patients with glioma in the left hemisphere, enhanced executive control network on the right side was associated with preserved higher mental functions (Maesawa et al., 2015). These results support the idea that resting-state functional network connectivity is related to cognitive function.

Overall, these findings suggest that intra-network connectivity decreases and extra-network connectivity increases in human large-scale functional networks with age, and the integrity of many large-scale networks diminishes in older age. These findings are consistent with those reported previously from Europe and the United States (Betzel et al., 2014a,b), and across different ethnicities. Additionally, the connectivity of dorsal attention (Ptak et al., 2017) and large-scale networks related to primary information processing enhanced with age. However, it is interesting that the general cognitive function is

better if the integrity of primary information-related network is preserved. Epidemiological studies have reported hearing loss in middle age and lack of exercise are observed in 9% and 3% of patients with dementia, respectively (Livingston et al., 2017), and reduced contrast sensitivity is a risk factor for cognitive decline in women (Ward et al., 2018). It is essential to clarify the relationships between risk factors for dementia related to primary information processing networks and resting-state functional networks. Because the strength of connections between networks plays a central role in cognitive function [such as executive control, salience, and default mode (Menon, 2011) and ACE-R scores], lifestyle habits that promote increased connectivity between these networks may help prevent dementia.

DEMENTIA AND FUNCTIONAL NETWORKS: POSITIONING OF HUBS

As described above, healthy aging is characterized by a decline in the function of primary information processing-related networks, and retention and enhancement of multisensory integration networks. The multisensory integration network is considered the "hub" of the brain because it integrates the dispersed neural activities, thereby allowing efficient cognitive functions (Stam, 2014; Lynn and Bassett, 2019). Outside the multisensory integration network, cerebral hubs exist mainly in the default mode network (Bagarinao et al., 2020b). Hubs that integrate large networks with different functions are also called connector hubs, which are robust to aging (Bagarinao et al., 2020a), and may compensate for the loss of function of subordinate networks. In other words, connector hubs may provide robustness and resilience to the healthy aging brain.

The existing data suggest that selective hub vulnerability is responsible for the preferential accumulation of Aβ in the medial hubs of the default mode network and the preferential accumulation of tau in medial temporal lobe hubs in preclinical AD (Yu et al., 2021). In our study of early AD patients with significant amyloid-β deposition demonstrated by positron emission tomography (PET), the relationships between the distribution of THK5351 PET accumulation (reflecting tau burden), inflammation, and the resting-state functional network disruption were examined (Yokoi et al., 2018). Tau and inflammation accumulated in the precuneus (Utevsky et al., 2014) and posterior cingulate gyrus (Leech and Sharp, 2014), which are the hubs of the default mode network; the associated network disruption correlated with disease onset.

Similar findings were observed in patients with FTLD (Ogura et al., 2019; Rittman et al., 2019; Chen et al., 2020; Imai et al., 2020). We also studied patients with ALS, which is thought to reflect the early stage of FTLD. In these patients, the severity of the deficits was associated with a decrease in functional connectivity between the right spindle and lingual gyrus (the hub of speech production) as well as reduced semantic memory and word recognition (Ogura et al., 2019). In addition, we examined the decision-making disorder characteristic of FTLD, using probability inversion learning, and found that significantly more ALS patients selected a decision-making style that seemed to go their way. The degree of abnormality was associated with decreased functional connectivity of the anterior cingulate gyrus/frontal pole, a typical hub (Imai et al., 2020).

In a study of PD without dementia, which is closely related to DLB, patients with mild amnesia had impairments in the precuneus and posterior cingulate cortex, corresponding to the hub of the default mode network (Kawabata et al., 2018; Nagano-Saito et al., 2019). Intriguingly, Kanel et al. (2020) performed PET with [18F]-fluoroethoxybenzovesamicol ([18F]-FEOBV), a radioligand for vesicular acetylcholine transporter (VAChT), in patients with DLB to determine cholinergic vulnerability topography. The results showed that cholinergic vulnerability in DLB consists of important neural centers involved in the networks of tonic arousal (cingulate gyrus), attention (insular cortex), visual attention (visual thalamus), and spatial navigation (limbic and corpus callosum). This study showed that disruption of brain hub function may be associated with the development of dementia, even at the neurotransmitter level.

POSSIBLE CELLULAR MECHANISMS OF HUB VULNERABILITY IN THE AGING BRAIN AND NEURODEGENERATION

Hubs are presumed to be rich in synapses, including those on long axons. It is believed that 64% of the energy used by the brain is spent on synaptic transmission (Sengupta et al., 2013), and genes related to ATP synthesis and metabolic regulation are expressed in a coordinated manner in the mouse hub region (Fulcher and Fornito, 2016). Glucose metabolism is also active in the human hub region (Tomasi et al., 2013). On the other hand, the number and function of human mitochondria decrease by about 8% every 10 years (Short et al., 2005). Therefore, in advanced age, the hub region is always on the verge of an energy crisis. Importantly, the hub region was the preferred site of lesions of early-stage neurodegenerative dementia in our study.

Although the etiology of neurodegenerative diseases remains a mystery, there is much consensus on the effects of reduced energy metabolism, excitotoxicity, and oxidative damage on their pathogenesis (Beal, 2005; Sas et al., 2007; Fan et al., 2017; Toda et al., 2017). Regarding energy metabolism, the human brain consumes about 20% of the biological energy, even though its volume is only about 2% of the body mass (Mink et al., 1981; Attwell and Laughlin, 2001). Neurons are in a post-mitotic excitatory state and require very high energy to generate and transmit action potentials, release neurotransmitters at synapses, set static gradients of ion concentration, dispose of soluble proteins, and remove metabolites (Rangaraju et al., 2019). In addition, the metabolic cost of performing and maintaining neural functions is very high, especially for the billions of incessant synaptic transmissions, which use 80% of the energy required for the functioning of the neuronal network (Rangaraju et al., 2019). For this reason, impaired energy metabolism is considered an important trigger in aging of the central nervous system (Błaszczyk, 2020).

Oxidation of glucose, which is a fast generator of ATP, is the most important energy source for the brain, and the mitochondrial oxidative phosphorylation system plays a major role (Schönfeld and Reiser, 2013). On the other hand, the number and function of mitochondria are known to decline with age (Short et al., 2005), and mitochondrial dysfunction leads to decreased ATP production, decreased glycolysis, increased oxidative stress, limited neuronal self-repair capacity, and excessive neuronal apoptosis (Grimm and Eckert, 2017; Wang et al., 2020). Accumulation of damaged mitochondria is a universal feature of aging, and increased oxidative damage to mtDNA, mitochondrial lipids, and proteins correlates with the accumulation of dysfunctional, damaged organelles (Mecocci et al., 1993; López-Otín et al., 2013). These sequence of events can be most likely to affect neurons in the cortex, hippocampus, and basal ganglia, which have long unmyelinated axons, numerous synaptic connections, and high energy metabolism (Camandola and Mattson, 2017; Mattson and Arumugam, 2018; Vandoorne et al., 2018; Diederich et al., 2019).

In addition, accumulation of reactive oxygen species (ROS) as well as damaged mitochondria has been observed in the aging brain (López-Otín et al., 2013), and the age-related increase rate of 8′-hydroxy-2′-deoxyguanosine (OH8dG) in the cerebral cortex is more pronounced in mtDNA and a significant 15-fold increase was observed in those aged 70 years and older (Mecocci et al., 1993). ROS are involved in immune response, inflammation, synaptic plasticity, learning, and memory, and their excessive production causes oxidative stress, protein and DNA damage, and lipid peroxidation reactions (Kishida and Klann, 2007; Marinho et al., 2014). Mitochondria, in their hyperactivity, also induce excessive ROS production. Excitotoxicity is known to be associated with many pathological conditions such as stroke, epilepsy, hearing impairment due to exposure to excessive noise, and neurodegenerative diseases (Armada-Moreira et al., 2020). Under normal conditions, antioxidant enzymes such as superoxide dismutase, glutathione peroxidase, glutaredoxin, thioredoxin, and catalase regulate the levels of ROS. However, with aging, nitration and oxidation of proteins progresses, and decreased activity of SOD, catalase, and GSH reductase, as well as decreased GSH have been reported (Venkateshappa et al., 2012).

Autophagy is a fundamental cellular process that promotes homeostasis, differentiation, development, and survival by degrading molecules and intracellular elements such as nucleic acids, proteins, lipids, and organelles via lysosomes. In health and aging, autophagy plays a multifaceted role, including protein homeostasis, regulation of macromolecular availability, mitophagy, ER-phagy, nucleophagy, lysophagy, and xenophagy. Recently, the impairment of autophagy in aging and in neurodegenerative diseases has also received much attention. However, the relationship between autophagy and aging and diseases is very complex and has not yet been fully clarified (Aman et al., 2021).

Fluorodeoxyglucose (FDG) PET studies have shown that the hub region of the brain requires a lot of energy (Tomasi et al., 2013). FDG PET studies have also shown that the hub region of the brain is rich in genes related to energy (Fulcher and Fornito, 2016). While the load on the hub region increases due to age-related disturbances in the primary information processing network, energy disturbances, mainly mitochondrial disturbances, can disrupt the energy balance and oxidative stress balance in the hub region, resulting in a combination of increased ROS and disruption of autophagy. The process of dementia development, including the accumulation of pathological proteins, may be accelerated. In AD, PD, and FTLD, abnormalities in energy, mitochondria, excitotoxicity, reactive oxygen species, and autophagy beyond normal aging have been reported, and many reports indicate that these may cause accumulation of pathological proteins alone or in combination (Grimm and Eckert, 2017; Wang et al., 2020). In addition to the fact that aging is the most important risk factor for neurodegenerative diseases, it is urgent to elucidate the series of pathological conditions caused by the disruption of brain energy metabolism.

The dendritic spine of the synapse is the site of excitatory synaptic input, and is the basis for synaptic plasticity, including long-term potentiation and depression. The dendritic spine requires large quantities of ATP to support the rapid membrane pumping activity required to restore the ion gradient after synaptic activation. Therefore, in cases where the ability of a neuron to generate sufficient ATP is impaired (e.g., aging, ischemia, or neurodegenerative diseases), synapses are vulnerable to dysfunction and degeneration (Harris et al., 2012). In neurodegenerative diseases, increased activity occurs in various networks and neurons before the onset of disease, and acts as a compensatory mechanism (Gregory et al., 2017). Compensation by the hub, which is hierarchically located at the upper level of the disrupted lower network, may increase the energy requirements of the same region, and contribute to energy failure and accumulation of pathological proteins (Saxena and Caroni, 2011; de Haan et al., 2012). Treatment with febuxostat and inosine increased blood hypoxanthine and ATP in healthy adults, and a preliminary trial in 30 patients with Parkinson's disease demonstrated symptomatic improvement (Watanabe et al., 2020).

LIMITATIONS AND FUTURE DIRECTIONS

In this review, we discussed the relationship between aging and brain network changes on individuals with normal cognition assessed mainly by general cognitive function test such as ACE-R. Since the current definition of dementia is the limitation of daily life activities due to the decline of cognitive functions, the use of general cognitive function tests to define "normal" general cognitive function will be sufficient in delineating the boundary between healthy aging and dementia. However, decline in episodic memory is a typical clinical manifestation of AD, but it is also observed early in normal aging. Interestingly, different neurocognitive processes were known to develop to compensate for this decline both in early AD and in normal aging (Tromp et al., 2015). Among different types of episodic memories, autobiographical episodic detail generation has been reported to be a good indicator for capturing

minor cognitive dysfunction associated with AD (Grilli et al., 2018). Spatial navigation has also been reported to better reflect the early pathology of AD (Lithfous et al., 2013). Furthermore, processing speed, mental flexibility, digit span memory test, visual scanning, motor processes, and so on, are some of the tests that can be used to extensively evaluate the cognitive effects of aging (Hartshorne and Germine, 2015). And these indicators which are closely related to intelligence and wisdom acquired by humans with aging (Deary, 2012; Park and Bischof, 2013), may be related to the U curve phenomenon observed in gray matter and white matter volume analysis of the brain, as well as the enhancement of efficiency observed in functional networks identified using graph analysis. Changes in the default mode network have been reported even in cognitively healthy older adults, which some believe reflect processes that have enhanced cognitive function and promoted social and emotional well-being and stability in life (Andrews-Hanna et al., 2019). Changing the framework for interpreting alterations in internal cognitive function with aging may shed important light on the neurocognitive mechanisms that distinguish between normal and pathological aging and provide a more complete picture of the complexity of the aging brain. Large scale prospective observational studies with specific tasks which provide the information of early cognitive, social, and behavioral changes are essential to elucidate the relationship between healthy aging and dementia considering the inter-hemispheric and intra-hemispheric interaction and gender differences.

The inverse U-shaped change in white matter volume between the ages of 40 and 50 has been shown in several papers including ours. However, the mechanism is not fully understood. It has been shown that the peak of human cognitive function varies depending on its content. Elucidation of the relationship between these age-dependent peaks in cognitive function and gray matter, white matter, and functional circuits may provide important insights into whether the inverted U-shaped changes are compensatory or not. On the other hand, we may just be looking at the results of white matter aging and its response to changes at the molecular and cellular levels. Interestingly, Pichet Binette et al. (2020) used large multicohort structural MRI data from young to cognitively preserved elderly to derive morphological networks using ICA and extracted gray matter volumes in each derived network. In their study, the preservation of whole-brain gray matter patterns was associated with a lower

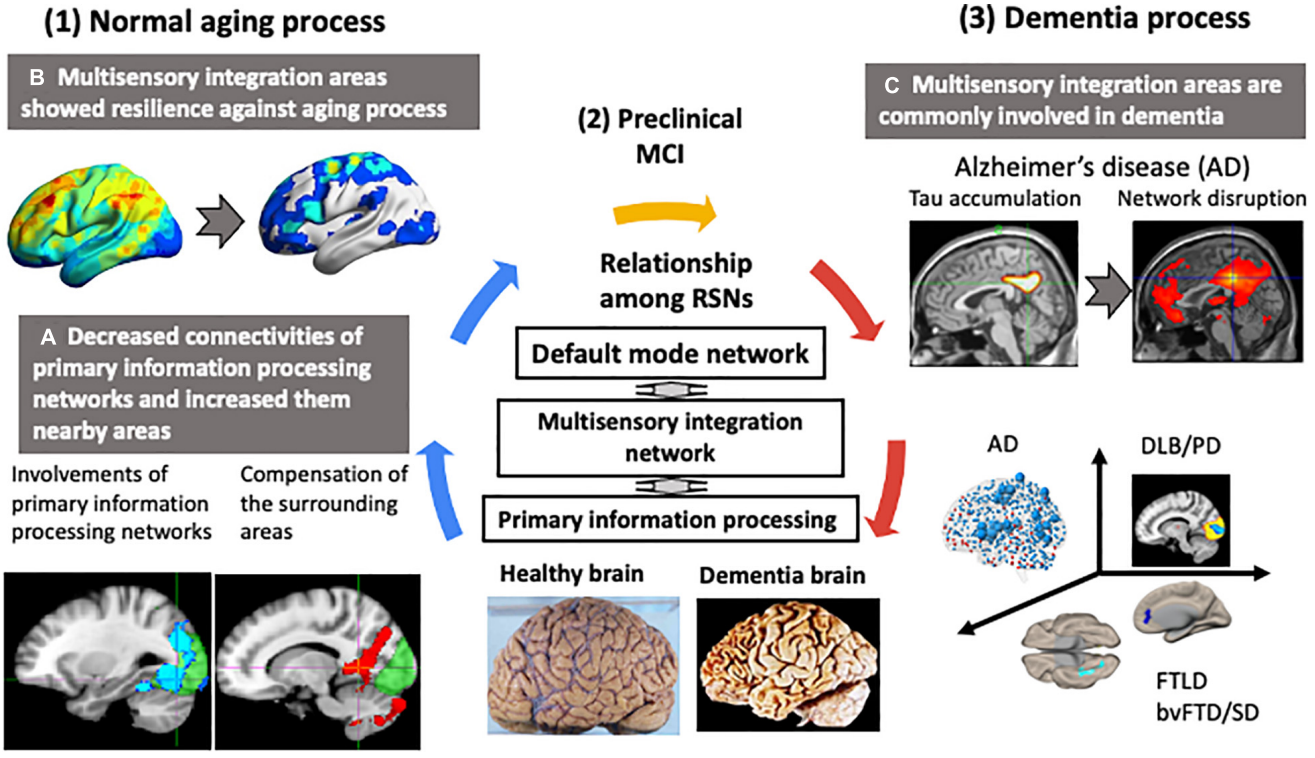

FIGURE 3 | Changes in functional networks with normal aging and dementia. Neurodegenerative dementias are commonly associated with impairments in the connector hub. In the resting state networks (RSNs) of the brain, a multisensory integration network connects each primary information processing network to the default mode network. The multisensory integration networks are closely connected to each other. In normal aging, the functional connectivity of the primary information processing networks decreased and connectivity of the surrounding regions centered on the multisensory integration networks increased. The functional connectivity of the multisensory integration networks was well-preserved with age. In contrast, in dementia, hub regions, such as the multisensory integration networks and the default mode network, were the preferred sites of lesions. Early-stage Alzheimer's disease was characterized by tau accumulation and disrupted functional connectivity in the posterior cingulate gyrus and precuneus, which are the hubs of the default mode network. This vulnerability of the hub region to disruption was also seen in Parkinson's disease with mild cognitive decline and in amyotrophic lateral sclerosis with behavior disorder and semantic impairment.

risk of developing cognitive impairment than the preservation of gray matter volume.

CONCLUSION

Figure 3 summarizes the differences in functional networks between normal aging and dementia. Our basic premise is that age-related changes in brain structure and function are widespread and yet elderly participants remained cognitively normal. This suggests high degree of resilience in the brain, which possibly drives functional reorganization with hub regions playing critical roles. Structurally, there is extensive gray matter atrophy, but the rate of atrophy is not uniform across the entire brain. Similar changes can also be observed in the major white matter fiber tracts, with the fiber density exhibiting an overall decrease and fiber cross-section in some areas exhibiting an increase with age. Despite these structural changes, general cognitive performance in the elderly remains well-preserved, suggesting a high degree of resilience in the brain. This resilience may be responsible for the changes observed in the functional architecture of the brain. With aging, there is reduced connectivity within the large-scale functional networks. However, aging is also accompanied by increased connectivity of large-scale networks with outside regions, which could potentially serve as an important compensatory mechanism. Many regions, including integrative hub regions, may compensate to maintain normal cognitive function. Therefore, well-functioning hub regions may be critical for the normal general cognitive performance during healthy aging (karoshi – "death from overwork"). Failure of hub regions to compensate, due to inadequate energy supply or accumulation of pathological proteins, could trigger a cascade of network dysfunction, leading to cognitive impairment and/or dementia.

AUTHOR CONTRIBUTIONS

HW contributed to the acquisition and analysis of data, study supervision and coordination, review of manuscript, and study concept and design. EB contributed to the review of manuscript, interpretation of data, drafting/revising manuscript for content, study coordination and sample analyses, and authoring first draft of manuscript. SM contributed to the acquisition and analysis of data, acquisition, analysis, or interpretation of data, scientific oversight, identification and recruitment of subjects, advice on sample analysis and sample handling, review of data, and review and edit of manuscript. KH contributed to the acquisition and analysis of data, identification and recruitment of subjects, advice on sample analysis and sample handling, review of data, and review and edit of manuscript. KK and AO contributed to the acquisition and analysis of data, interpretation of data, and study coordination and sample analyses. RO contributed to the acquisition and analysis of data, and study coordination and sample analyses. SS, AU, and MI contributed to the review of manuscript and interpretation of data. YM contributed to the review of manuscript, interpretation of data, and edit of manuscript. MK contributed to the review of manuscript, review of data, and edit of manuscript. GS contributed to the study supervision and coordination, review of manuscript, study concept and design, and study supervision. All authors contributed to the article and approved the submitted version.

FUNDING

This research was supported by AMED under Grant Number JP21wm0425016.

REFERENCES

Allen, J. S., Bruss, J., Brown, C. K., and Damasio, H. (2005). Normal neuroanatomical variation due to age: the major lobes and a parcellation of the temporal region. *Neurobiol. Aging* 26, 1245–1260. doi: 10.1016/j.neurobiolaging.2005.05.023

Aman, Y., Schmauck-Medina, T., Hansen, M., Morimoto, R. I., Simon, A. K., Bjedov, I., et al. (2021). Autophagy in healthy aging and disease. *Nat. Aging* 1, 634–650. doi: 10.1038/s43587-021-00098-4

Andrews-Hanna, J. R., Grilli, M. D., and Irish, M. (2019). *A Review and Reappraisal of the Default Network in Normal Aging and Dementia*. Oxford: Oxford University Press.

Armada-Moreira, A., Gomes, J. I., Pina, C. C., Savchak, O. K., Gonçalves-Ribeiro, J., Rei, N., et al. (2020). Going the extra (Synaptic) mile: excitotoxicity as the road toward neurodegenerative diseases. *Front. Cell Neurosci.* 14:90. doi: 10.3389/fncel.2020.00090

Attwell, D., and Laughlin, S. B. (2001). An energy budget for signaling in the grey matter of the brain. *J. Cereb. Blood Flow Metab.* 21, 1133–1145. doi: 10.1097/00004647-200110000-00001

Bagarinao, E., Watanabe, H., Maesawa, S., Mori, D., Hara, K., Kawabata, K., et al. (2018). An unbiased data-driven age-related structural brain parcellation for the identification of intrinsic brain volume changes over the adult lifespan. *Neuroimage* 169, 134–144. doi: 10.1016/j.neuroimage.2017.12.014

Bagarinao, E., Watanabe, H., Maesawa, S., Mori, D., Hara, K., Kawabata, K., et al. (2019). Reorganization of brain networks and its association with general cognitive performance over the adult lifespan. *Sci. Rep.* 9:11352. doi: 10.1038/s41598-019-47922-x

Bagarinao, E., Watanabe, H., Maesawa, S., Mori, D., Hara, K., Kawabata, K., et al. (2020b). Identifying the brain's connector hubs at the voxel level using functional connectivity overlap ratio. *Neuroimage* 222:117241. doi: 10.1016/j.neuroimage.2020.117241

Bagarinao, E., Watanabe, H., Maesawa, S., Mori, D., Hara, K., Kawabata, K., et al. (2020a). Aging impacts the overall connectivity strength of regions critical for information transfer among brain networks. *Front. Aging Neurosci.* 12:592469. doi: 10.3389/fnagi.2020.592469

Beal, M. F. (2005). Mitochondria take center stage in aging and neurodegeneration. *Ann. Neurol.* 58, 495–505. doi: 10.1002/ana.20624

Betzel, R. F., Byrge, L., He, Y., Goñi, J., Zuo, X. N., and Sporns, O. (2014a). Changes in structural and functional connectivity among resting-state networks across the human lifespan. *Neuroimage* 102, 345–357. doi: 10.1016/j.neuroimage.2014.07.067

Betzel, R. F., Byrge, L., He, Y., Goñi, J., Zuo, X. N., and Sporns, O. (2014b). Decreased segregation of brain systems across the healthy adult lifespan. *Proc. Natl. Acad. Sci. U.S.A.* 111, E4997–E5006. doi: 10.1073/pnas.1415122111

Biswal, B., Yetkin, F. Z., Haughton, V. M., and Hyde, J. S. (1995). Functional connectivity in the motor cortex of resting human brain using echo-planar MRI. *Magn. Reson. Med.* 34, 537–534. doi: 10.1002/mrm.1910340409

Błaszczyk, J. W. (2020). Energy metabolism decline in the aging brain-pathogenesis of neurodegenerative disorders. *Metabolites* 10:450. doi: 10.3390/metabo10110450

Camandola, S., and Mattson, M. P. (2017). Brain metabolism in health, aging, and neurodegeneration. *EMBO J.* 36, 1474–1492. doi: 10.15252/embj.201695810

Chen, Y., Huang, L., Chen, K., Ding, J., Zhang, Y., Yang, Q., et al. (2020). White matter basis for the hub-and-spoke semantic representation: evidence from semantic dementia. *Brain* 143, 1206–1219. doi: 10.1093/brain/awaa057

Choy, S., Bagarinao, E., Watanabe, H., Ho, E. T., Maesawa, S., Mori, D., et al. (2020). Changes in white matter fiber density and morphology across the adult lifespan: a cross-sectional fixel-based analysis. *Hum. Brain Mapp.* 41, 3198–3211. doi: 10.1002/hbm.25008

de Haan, W., Mott, K., van Straaten, E. C., Scheltens, P., and Stam, C. J. (2012). Activity dependent degeneration explains hub vulnerability in Alzheimer's disease. *PLoS Comput. Biol.* 8:e1002582. doi: 10.1371/journal.pcbi.1002582

de Haan, W., Pijnenburg, Y. A., Strijers, R. L., van der Made, Y., van der Flier, W. M., Scheltens, P., et al. (2009). Functional neural network analysis in frontotemporal dementia and Alzheimer's disease using EEG and graph theory. *BMC Neurosci.* 10:101. doi: 10.1186/1471-2202-10-101

Deary, I. J. (2012). Intelligence. *Annu. Rev. Psychol.* 63, 453–482.

Diederich, N. J., James Surmeier, D., Uchihara, T., Grillner, S., and Goetz, C. G. (2019). Parkinson's disease: is it a consequence of human brain evolution? *Mov. Disord.* 34, 453–459. doi: 10.1002/mds.27628

Ding, D., Zhao, Q., Guo, Q., Liang, X., Luo, J., Yu, L., et al. (2016). Progression and predictors of mild cognitive impairment in Chinese elderly: a prospective follow-up in the Shanghai Aging Study. *Alzheimers Dement.* 4, 28–36. doi: 10.1016/j.dadm.2016.03.004

Fan, J., Dawson, T. M., and Dawson, V. L. (2017). Cell death mechanisms of neurodegeneration. *Adv. Neurobiol.* 15, 403–425. doi: 10.1007/978-3-319-57193-5_16

Farb, N. A., Grady, C. L., Strother, S., Tang-Wai, D. F., Masellis, M., Black, S., et al. (2013). Abnormal network connectivity in frontotemporal dementia: evidence for prefrontal isolation. *Cortex* 49, 1856–1873. doi: 10.1016/j.cortex.2012.09.008

Firth, J., Stubbs, B., Vancampfort, D., Schuch, F., Lagopoulos, J., Rosenbaum, S., et al. (2018). Effect of aerobic exercise on hippocampal volume in humans: a systematic review and meta-analysis. *Neuroimage* 166, 230–238. doi: 10.1016/j.neuroimage.2017.11.007

Fjell, A. M., Westlye, L. T., Grydeland, H., Amlien, I., Espeseth, T., Reinvang, I., et al. (2013). Critical ages in the life course of the adult brain: nonlinear subcortical aging. *Neurobiol. Aging* 34, 2239–2247. doi: 10.1016/j.neurobiolaging.2013.04.006

Fulcher, B. D., and Fornito, A. (2016). A transcriptional signature of hub connectivity in the mouse connectome. *Proc. Natl. Acad. Sci. U.S.A.* 113, 1435–1440. doi: 10.1073/pnas.1513302113

Gefen, T., Kim, G., Bolbolan, K., Geoly, A., Ohm, D., Oboudiyat, C., et al. (2019). Activated microglia in cortical white matter across cognitive aging trajectories. *Front. Aging Neurosci.* 11:94. doi: 10.3389/fnagi.2019.00094

Good, C. D., Johnsrude, I. S., Ashburner, J., Henson, R. N. A., Friston, K. J., and Frackowiak, R. S. J. (2001). A voxel-based morphometric study of ageing in 465 normal adult human brains. *Neuroimage* 14, 21–36. doi: 10.1006/nimg.2001.0786

Gregory, S., Long, J. D., Klöppel, S., Razi, A., Scheller, E., Minkova, L., et al. (2017). Operationalizing compensation over time in neurodegenerative disease. *Brain* 140, 1158–1165. doi: 10.1093/brain/awx022

Grilli, M. D., Wank, A. A., Bercel, J. J., and Ryan, L. (2018). Evidence for reduced autobiographical memory episodic specificity in cognitively normal middle-aged and older individuals at increased risk for Alzheimer's disease dementia. *J. Int. Neuropsychol. Soc.* 24, 1073–1083. doi: 10.1017/S1355617718000577

Grimm, A., and Eckert, A. (2017). Brain aging and neurodegeneration: from a mitochondrial point of view. *J. Neurochem.* 143, 418–431. doi: 10.1111/jnc.14037

Harris, J. J., Jolivet, R., and Attwell, D. (2012). Synaptic energy use and supply. *Neuron* 75, 762–777. doi: 10.1016/j.neuron.2012.08.019

Hartshorne, J. K., and Germine, L. T. (2015). When does cognitive functioning peak? The asynchronous rise and fall of different cognitive abilities across the life span. *Psychol. Sci.* 26, 433–443. doi: 10.1177/0956797614567339

Hou, J., and Pakkenberg, B. (2012). Age-related degeneration of corpus callosum in the 90+ years measured with stereology. *Neurobiol. Aging* 33:1009. doi: 10.1016/j.neurobiolaging.2011.10.017

Imai, K., Masuda, M., Watanabe, H., Ogura, A., Ohdake, R., Tanaka, Y., et al. (2020). The neural network basis of altered decision-making in patients with amyotrophic lateral sclerosis. *Ann. Clin. Transl. Neurol.* 7, 2115–2126. doi: 10.1002/acn3.51185

Jack, C. R. Jr., Knopman, D. S., Jagust, W. J., Petersen, R. C., Weiner, M. W., Aisen, P. S., et al. (2013). Tracking pathophysiological processes in Alzheimer's disease: an updated hypothetical model of dynamic biomarkers. *Lancet Neurol.* 12, 207–216. doi: 10.1016/S1474-4422(12)70291-0

Jeurissen, B., Leemans, A., Tournier, J. D., Jones, D. K., and Sijbers, J. (2013). Investigating the prevalence of complex fiber configurations in white matter tissue with diffusion magnetic resonance imaging. *Hum. Brain Mapp.* 34, 2747–2766. doi: 10.1002/hbm.22099

Kanel, P., Müller, M. L. T. M., van der Zee, S., Sanchez-Catasus, C. A., Koeppe, R. A., Frey, K. A., et al. (2020). Topography of cholinergic changes in dementia with lewy bodies and key neural network hubs. *J. Neuropsychiatry Clin. Neurosci.* 32, 370–375. doi: 10.1176/appi.neuropsych.19070165

Kawabata, K., Watanabe, H., Hara, K., Bagarinao, E., Yoneyama, N., Ogura, A., et al. (2018). Distinct manifestation of cognitive deficits associate with different resting-state network disruptions in non-demented patients with Parkinson's disease. *J. Neurol.* 265, 688–700. doi: 10.1007/s00415-018-8755-5

Kishida, K. T., and Klann, E. (2007). Sources and targets of reactive oxygen species in synaptic plasticity and memory. *Antioxid. Redox Signal.* 9, 233–244. doi: 10.1089/ars.2007.9.ft-8

Kliemann, D., Adolphs, R., Tyszka, J. M., Fischl, B., Yeo, B. T. T., Nair, R., et al. (2019). Intrinsic functional connectivity of the brain in adults with a single cerebral hemisphere. *Cell Rep.* 29, 2398–2407. doi: 10.1016/j.celrep.2019.10.067

Leech, R., and Sharp, D. J. (2014). The role of the posterior cingulate cortex in cognition and disease. *Brain* 137(Pt 1), 12–32. doi: 10.1093/brain/awt162

Lithfous, S., Dufour, A., and Després, O. (2013). Spatial navigation in normal aging and the prodromal stage of Alzheimer's disease: insights from imaging and behavioral studies. *Ageing Res. Rev.* 12, 201–213. doi: 10.1016/j.arr.2012.04.007

Livingston, G., Sommerlad, A., Orgeta, V., Costafreda, S. G., Huntley, J., Ames, D., et al. (2017). Dementia prevention, intervention, and care. *Lancet* 390, 2673–2734.

López-Otín, C., Blasco, M. A., Partridge, L., Serrano, M., and Kroemer, G. (2013). The hallmarks of aging. *Cell* 153, 1194–1217.

Lynn, C. W., and Bassett, D. S. (2019). The physics of brain network structure, function and control. *Nat. Rev. Phys.* 1, 318–332. doi: 10.1038/s42254-019-0040-8

Maesawa, S., Bagarinao, E., Fujii, M., Futamura, M., Motomura, K., Watanabe, H., et al. (2015). Evaluation of resting state networks in patients with gliomas: connectivity changes in the unaffected side and its relation to cognitive function. *PLoS One* 10:e0118072. doi: 10.1371/journal.pone.0118072

Marinho, H. S., Real, C., Cyrne, L., Soares, H., and Antunes, F. (2014). Hydrogen peroxide sensing, signaling and regulation of transcription factors. *Redox Biol.* 2, 535–562. doi: 10.1016/j.redox.2014.02.006

Masters, C. L., Bateman, R., Blennow, K., Rowe, C. C., Sperling, R. A., and Cummings, J. L. (2015). Alzheimer's disease. *Nat. Rev. Dis. Primers* 1:15056.

Mattson, M. P., and Arumugam, T. V. (2018). Hallmarks of brain aging: adaptive and pathological modification by metabolic states. *Cell Metab.* 27, 1176–1199. doi: 10.1016/j.cmet.2018.05.011

Mecocci, P., MacGarvey, U., Kaufman, A. E., Koontz, D., Shoffner, J. M., Wallace, D. C., et al. (1993). Oxidative damage to mitochondrial DNA shows marked age-dependent increases in human brain. *Ann. Neurol.* 34, 609–616. doi: 10.1002/ana.410340416

Menon, V. (2011). Large-scale brain networks and psychopathology: a unifying triple network model. *Trends Cogn. Sci.* 15, 483–506. doi: 10.1016/j.tics.2011.08.003

Mink, J. W., Blumenschine, R. J., and Adams, D. B. (1981). Ratio of central nervous system to body metabolism in vertebrates: its constancy and functional basis. *Am. J. Physiol.* 241, R203–R212. doi: 10.1152/ajpregu.1981.241.3.R203

Mioshi, E., Dawson, K., Mitchell, J., Arnold, R., and Hodges, J. R. (2006). The Addenbrooke's cognitive examination revised (ACE-R): a brief cognitive test battery for dementia screening. *Int. J. Geriatr. Psychiatry* 21, 1078–1085. doi: 10.1002/gps.1610

Nagano-Saito, A., Bellec, P., Hanganu, A., Jobert, S., Mejia-Constain, B., Degroot, C., et al. (2019). Why is aging a risk factor for cognitive impairment in

Parkinson's disease?-A resting state fMRI study. *Front. Neurol.* 10:267. doi: 10.3389/fneur.2019.00267

Ogawa, S., and Lee, T. M. (1990). Magnetic resonance imaging of blood vessels at high fields: in vivo and in vitro measurements and image simulation. *Magn. Reson. Med.* 16, 9–18. doi: 10.1002/mrm.1910160103

Ogura, A., Watanabe, H., Kawabata, K., Ohdake, R., Tanaka, Y., Masuda, M., et al. (2019). Semantic deficits in ALS related to right lingual/fusiform gyrus network involvement. *EBioMedicine* 47, 506–517. doi: 10.1016/j.ebiom.2019.08.022

Page, T. L., Einstein, M., Duan, H., He, Y., Flores, T., Rolshud, D., et al. (2002). Morphological alterations in neurons forming corticocortical projections in the neocortex of aged Patas monkeys. *Neurosci. Lett.* 317, 37–41. doi: 10.1016/s0304-3940(01)02428-4

Park, D. C., and Bischof, G. N. (2013). The aging mind: neuroplasticity in response to cognitive training. *Dialog. Clin. Neurosci.* 15, 109–119. doi: 10.31887/dcns.2013.15.1/dpark

Pichet Binette, A., Gonneaud, J., Vogel, J. W., La Joie, R., Rosa-Neto, P., Collins, D. L., et al. (2020). Morphometric network differences in ageing versus Alzheimer's disease dementia. *Brain* 143, 635–649. doi: 10.1093/brain/awz414

Prichep, L. S. (2007). Quantitative EEG and electromagnetic brain imaging in aging and in the evolution of dementia. *Ann. N.Y. Acad. Sci.* 1097, 156–167. doi: 10.1196/annals.1379.008

Ptak, R., Schnider, A., and Fellrath, J. (2017). The dorsal frontoparietal network: a core system for emulated action. *Trends Cogn. Sci.* 21, 589–599. doi: 10.1016/j.tics.2017.05.002

Raffelt, D. A., Tournier, J. D., Smith, R. E., Vaughan, D. N., Jackson, G., Ridgway, G. R., et al. (2017). Investigating white matter fibre density and morphology using fixel-based analysis. *Neuroimage* 144(Pt A), 58–73. doi: 10.1016/j.neuroimage.2016.09.029

Rangaraju, V., Lauterbach, M., and Schuman, E. M. (2019). Spatially stable mitochondrial compartments fuel local translation during plasticity. *Cell* 176, 73–84. doi: 10.1016/j.cell.2018.12.013

Rittman, T., Borchert, R., Jones, S., van Swieten, J., Borroni, B., Galimberti, D., et al. (2019). Functional network resilience to pathology in presymptomatic genetic frontotemporal dementia. *Neurobiol. Aging* 77, 169–177. doi: 10.1016/j.neurobiolaging.2018.12.009

Safaiyan, S., Besson-Girard, S., Kaya, T., Cantuti-Castelvetri, L., Liu, L., Ji, H., et al. (2021). White matter aging drives microglial diversity. *Neuron* 109, 1100–1117. doi: 10.1016/j.neuron.2021.01.027

Safaiyan, S., Kannaiyan, N., Snaidero, N., Brioschi, S., Biber, K., Yona, S., et al. (2016). Age-related myelin degradation burdens the clearance function of microglia during aging. *Nat. Neurosci.* 19, 995–998. doi: 10.1038/nn.4325

Sas, K., Robotka, H., Toldi, J., and Vécsei, L. (2007). Mitochondria, metabolic disturbances, oxidative stress and the kynurenine system, with focus on neurodegenerative disorders. *J. Neurol. Sci.* 257, 221–239. doi: 10.1016/j.jns.2007.01.033

Saxena, S., and Caroni, P. (2011). Selective neuronal vulnerability in neurodegenerative diseases: from stressor thresholds to degeneration. *Neuron* 71, 35–48. doi: 10.1016/j.neuron.2011.06.031

Schönfeld, P., and Reiser, G. (2013). Why does brain metabolism not favor burning of fatty acids to provide energy? Reflections on disadvantages of the use of free fatty acids as fuel for brain. *J. Cereb. Blood Flow Metab.* 33, 1493–1499. doi: 10.1038/jcbfm.2013.128

Sengupta, B., Stemmler, M. B., and Friston, K. J. (2013). Information and efficiency in the nervous system–a synthesis. *PLoS Comput. Biol.* 9:e1003157. doi: 10.1371/journal.pcbi.1003157

Shirer, W. R., Ryali, S., Rykhlevskaia, E., Menon, V., and Greicius, M. D. (2012). Decoding subject-driven cognitive states with whole-brain connectivity patterns. *Cereb. Cortex* 22, 158–165. doi: 10.1093/cercor/bhr099

Short, K. R., Bigelow, M. L., Kahl, J., Singh, R., Coenen-Schimke, J., Raghavakaimal, S., et al. (2005). Decline in skeletal muscle mitochondrial function with aging in humans. *Proc. Natl. Acad. Sci. U.S.A.* 102, 5618–5623. doi: 10.1073/pnas.0501559102

Smith, C. D., Chebrolu, H., Wekstein, D. R., Schmitt, F. A., and Markesbery, W. R. (2007). Age and gender effects on human brain anatomy: a voxel-based morphometric study in healthy elderly. *Neurobiol. Aging* 28, 1075–1087. doi: 10.1016/j.neurobiolaging.2006.05.018

Snowdon, D. A. (2003). Healthy aging and dementia: findings from the Nun Study. *Ann. Intern. Med.* 139(5 Pt 2), 450–454. doi: 10.7326/0003-4819-139-5_part_2-200309021-00014

Stam, C. J. (2014). Modern network science of neurological disorders. *Nat. Rev. Neurosci.* 15, 683–695. doi: 10.1038/nrn3801

Suárez, L. E., Markello, R. D., Betzel, R. F., and Misic, B. (2020). Linking structure and function in macroscale brain networks. *Trends Cogn. Sci.* 24, 302–315. doi: 10.1016/j.tics.2020.01.008

Teipel, S., Grothe, M. J., Zhou, J., Sepulcre, J., Dyrba, M., Sorg, C., et al. (2016). Measuring cortical connectivity in Alzheimer's disease as a brain neural network pathology: toward clinical applications. *J. Int. Neuropsychol. Soc.* 22, 138–163. doi: 10.1017/S1355617715000995

Toda, C., Santoro, A., Kim, J. D., and Diano, S. (2017). POMC neurons: from birth to death. *Annu. Rev. Physiol.* 79, 209–236. doi: 10.1146/annurev-physiol-022516-034110

Tomasi, D., Wang, G. J., and Volkow, N. D. (2013). Energetic cost of brain functional connectivity. *Proc. Natl. Acad. Sci. U.S.A.* 110, 13642–13647. doi: 10.1073/pnas.1303346110

Tromp, D., Dufour, A., Lithfous, S., Pebayle, T., and Després, O. (2015). Episodic memory in normal aging and Alzheimer disease: insights from imaging and behavioral studies. *Ageing Res. Rev.* 24(Pt B), 232–262. doi: 10.1016/j.arr.2015.08.006

Utevsky, A. V., Smith, D. V., and Huettel, S. A. (2014). Precuneus is a functional core of the default-mode network. *J. Neurosci.* 34, 932–940. doi: 10.1523/jneurosci.4227-13.2014

Vandoorne, T., De Bock, K., and Van Den Bosch, L. (2018). Energy metabolism in ALS: an underappreciated opportunity? *Acta Neuropathol.* 135, 489–509. doi: 10.1007/s00401-018-1835-x

Venkateshappa, C., Harish, G., Mahadevan, A., Srinivas Bharath, M. M., and Shankar, S. K. (2012). Elevated oxidative stress and decreased antioxidant function in the human hippocampus and frontal cortex with increasing age: implications for neurodegeneration in Alzheimer's disease. *Neurochem. Res.* 37, 1601–1614. doi: 10.1007/s11064-012-0755-8

Wang, W., Zhao, F., Ma, X., Perry, G., and Zhu, X. (2020). Mitochondria dysfunction in the pathogenesis of Alzheimer's disease: recent advances. *Mol. Neurodegener.* 15:30.

Ward, M. E., Gelfand, J. M., Lui, L. Y., Ou, Y., Green, A. J., Stone, K., et al. (2018). Reduced contrast sensitivity among older women is associated with increased risk of cognitive impairment. *Ann. Neurol.* 83, 730–738. doi: 10.1002/ana.25196

Watanabe, H., Hattori, T., Kume, A., Misu, K., Ito, T., Koike, Y., et al. (2020). Improved Parkinsons disease motor score in a single-arm open-label trial of febuxostat and inosine. *Medicine* 99:e21576. doi: 10.1097/MD.0000000000021576

Yokoi, T., Watanabe, H., Yamaguchi, H., Bagarinao, E., Masuda, M., Imai, K., et al. (2018). Involvement of the precuneus/posterior cingulate cortex is significant for the development of Alzheimer's disease: a PET (THK5351, PiB) and resting fMRI study. *Front. Aging Neurosci.* 10:304. doi: 10.3389/fnagi.2018.00304

Yu, M., Sporns, O., and Saykin, A. J. (2021). The human connectome in Alzheimer disease - relationship to biomarkers and genetics. *Nat. Rev. Neurol.* 17, 545–563. doi: 10.1038/s41582-021-00529-1

Conflict of Interest: The authors declare that the research was conducted in the absence of any commercial or financial relationships that could be construed as a potential conflict of interest.

Publisher's Note: All claims expressed in this article are solely those of the authors and do not necessarily represent those of their affiliated organizations, or those of the publisher, the editors and the reviewers. Any product that may be evaluated in this article, or claim that may be made by its manufacturer, is not guaranteed or endorsed by the publisher.

frontiers in Aging Neuroscience

ORIGINAL RESEARCH
published: 22 November 2021
doi: 10.3389/fnagi.2021.750621

Differences in Diffusion Tensor Imaging White Matter Integrity Related to Verbal Fluency Between Young and Old Adults

Benjamin Yeske[1†], Jiancheng Hou[1,2†], Nagesh Adluru[1,3], Veena A. Nair[1] and Vivek Prabhakaran[1,4,5]*

[1] Department of Radiology, School of Medicine and Public Health, University of Wisconsin–Madison, Madison, WI, United States, [2] Center for Cross-Strait Cultural Development, Fujian Normal University, Fuzhou, China, [3] Waisman Center, University of Wisconsin–Madison, Madison, WI, United States, [4] Department of Psychology, Department of Psychiatry, University of Wisconsin–Madison, Madison, WI, United States, [5] Neuroscience Training Program, University of Wisconsin–Madison, Madison, WI, United States

Throughout adulthood, the brain undergoes an array of structural and functional changes during the typical aging process. These changes involve decreased brain volume, reduced synaptic density, and alterations in white matter (WM). Although there have been some previous neuroimaging studies that have measured the ability of adult language production and its correlations to brain function, structural gray matter volume, and functional differences between young and old adults, the structural role of WM in adult language production in individuals across the life span remains to be thoroughly elucidated. This study selected 38 young adults and 35 old adults for diffusion tensor imaging (DTI) and performed the Controlled Oral Word Association Test to assess verbal fluency (VF). Tract-Based Spatial Statistics were employed to evaluate the voxel-based group differences of diffusion metrics for the values of fractional anisotropy (FA), mean diffusivity (MD), axial diffusivity (AD), radial diffusivity (RD), and local diffusion homogeneity (LDH) in 12 WM regions of interest associated with language production. To investigate group differences on each DTI metric, an analysis of covariance (ANCOVA) controlling for sex and education level was performed, and the statistical threshold was considered at $p < 0.00083$ (0.05/60 labels) after Bonferroni correction for multiple comparisons. Significant differences in DTI metrics identified in the ANCOVA were used to perform correlation analyses with VF scores. Compared to the old adults, the young adults had significantly (1) increased FA values on the bilateral anterior corona radiata (ACR); (2) decreased MD values on the right ACR, but increased MD on the left uncinate fasciculus (UF); and (3) decreased RD on the bilateral ACR. There were no significant differences between the groups for AD or LDH. Moreover, the old adults had only a significant correlation between the VF score and the MD on the left UF. There were no significant correlations between VF score and DTI metrics in the young adults. This study adds to the growing body of research that WM areas involved in language production are sensitive to aging.

Keywords: diffusion tensor imaging (DTI), aging, tract-based spatial statistics (TBSS), white matter integrity, verbal fluency

OPEN ACCESS

Edited by:
Toshiharu Nakai, Osaka University, Japan

Reviewed by:
Yuto Uchida, Nagoya City University, Japan
S. H. Annabel Chen, Nanyang Technological University, Singapore

***Correspondence:**
Benjamin Yeske
byeske@wisc.edu

† These authors have contributed equally to this work and share first authorship

Received: *30 July 2021*
Accepted: *14 October 2021*
Published: *22 November 2021*

Citation:
Yeske B, Hou J, Adluru N, Nair VA and Prabhakaran V (2021) Differences in Diffusion Tensor Imaging White Matter Integrity Related to Verbal Fluency Between Young and Old Adults. Front. Aging Neurosci. 13:750621. doi: 10.3389/fnagi.2021.750621

INTRODUCTION

Throughout adulthood, the brain undergoes an array of structural and functional changes during the typical aging process (Caserta et al., 2009). These changes involve decreased brain volume, reduced synaptic density, and alterations in white matter (WM; Masliah et al., 1993; Jernigan et al., 2001; Resnick et al., 2003). The structural deterioration of the brain is thought to be the reason for cognitive decline seen in the aging process; therefore, correlational studies comparing changes to brain structure and function are increasingly common. These neuroimaging studies have repeatedly shown age-related cortical network re-organization, specifically a reduction of hemispheric specialization toward more bilateral activation. This reduction of hemispheric specialization, known as the hemispheric asymmetry reduction in older adults (HAROLD) model (Cabeza, 2002), is well documented in studies using various imaging modalities, namely, electro-encephalography (Bellis et al., 2000), near-infrared spectroscopy (Herrmann et al., 2006), functional magnetic resonance imaging (fMRI; Cabeza, 2002; La et al., 2016), and diffusion tensor imaging (DTI; Ardekani et al., 2007). In addition to the reduction of hemispheric specialization, an anteroposterior gradient of the loss of WM integrity has also been observed, with the anterior regions of the brain being disproportionately affected in the aging process compared to the posterior regions (Pfefferbaum et al., 2005; Ardekani et al., 2007; Madden et al., 2009; Bennett et al., 2010; Sullivan et al., 2010).

Extensive research has been conducted to explore the aging declines seen in cognitive abilities, namely, working memory (Nyberg et al., 2012; Vaqué-Alcázar et al., 2020), executive function (Fjell et al., 2017; Webb et al., 2020), and language function (Wingfield and Grossman, 2006; Kantarci et al., 2011; Kemmotsu et al., 2012; Baciu et al., 2016). Previous neuroimaging studies concerning language function have measured the ability of adult language production and its correlations to brain function (Pihlajamäki et al., 2000), used fMRI to study language function (Wingfield and Grossman, 2006; Meinzer et al., 2009; Baciu et al., 2016), and studied structural gray matter volume involved in language function (Zhang et al., 2013); however, the structural role of WM in adult language production in individuals across the life span remains to be thoroughly elucidated.

One non-invasive MRI technique for *in vivo* mapping of the structures of WM is DTI, which provides detailed information on the underlying fiber tract architecture as reflected by diffusion patterns of water molecules (Sundaram et al., 2008; Pugliese et al., 2009). Fractional anisotropy (FA, a scalar measure of the directional constraint of water diffusion) and mean diffusivity (MD, the mean of three eigenvectors that each reflects separate directions of minimal and maximal diffusion) are the most frequently used metrics to investigate WM fiber tract integrity. More recently, studies on aging have included axial diffusivity (AD, a scalar measure of diffusivity along the length of an axon; see Thomason and Thompson, 2011) and radial diffusivity (RD, measure of water diffusion perpendicular to the axons and is associated with demyelination and neuro-inflammation with edema and macrophage infiltration; see Budde et al., 2011; Rayhan et al., 2013) in their analyses, as they are more specific to neural changes commonly involved in aging, namely, axonal damage or loss (AD; Song et al., 2003; Budde et al., 2007) and the degree of myelination (RD) (Song et al., 2002, 2003, 2005; Nair et al., 2005; Budde et al., 2007). Using these two metrics, some patterns have been identified to describe the differential aging associations in WM fiber tracts. For example, in some WM tracts, age-related decreases in FA are associated with increases only in RD, but not in AD (Bhagat and Beaulieu, 2004; Davis et al., 2009; Madden et al., 2009; Zhang et al., 2010). Other patterns observed are that decreases in FA are associated with significant increases in both RD and AD (Sullivan and Pfefferbaum, 2006; Zahr et al., 2009; Sullivan et al., 2010) and decreases in FA are associated with increases in RD and decreases in AD (Bennett et al., 2010). These patterns suggest that there may be differential aging processes occurring in different brain regions. Currently, these patterns remain unstudied in their relationship to age-related language production. Additionally, a novel inter-voxel metric called local diffusion homogeneity (LDH), which quantifies the local coherence of water molecule diffusion in a model-free manner, was also examined in our analyses (Gong, 2013). Using the LDH metric to describe the WM fiber tracts is still in its infancy and several studies have reported it as being complementary to FA and MD in detecting changes in WM (Gong, 2013; Liu et al., 2017; Liang et al., 2019).

Currently, there are no studies using LDH to assess language production or brain aging more broadly; however, there are a handful of studies that have taken advantage of other DTI metrics to assess the structural role of WM in typically aging adults and language production. Stamatakis et al. (2011) identified that FA of the superior longitudinal fasciculus (SLF) and inferior longitudinal fasciculus (ILF) was positively correlated with accuracy in naming famous individuals. Madhavan et al. (2014) observed increased FA values on the SLF and increased age were positively associated with the performance in verbal fluency (VF) and word retrieval, respectively. They also identified a relationship between gender and FA values on the SLF tract and reported a linear decrease in FA in males and increase in FA in females until age 40, followed by a gradual decline. Houston et al. (2019) reported the performance on a word-retrieval task was associated with increased FA within the inferior fronto-occipital fasciculus (IFOF), in addition to the SLF, and observed increased FA within the corpus callosum that was associated with lower VF scores. Troutman and Diaz (2020) observed among all adult age groups that better performance on a naming with distractors task was associated with lower RD across dorsal, ventral, and fronto-striatal tracts as well as higher FA along dorsal tracts but was unable to find an association when covarying for age groups. Teubner-Rhodes et al. (2016) looked at age-related performance in acquisition and retrieval of lexical and semantic information and found age-related declines in arcuate fasciculus (AF) microstructure were related to cognitive processing speed, but not to vocabulary retrieval. Interestingly, FA on the left AF was significantly

related to individual variability in vocabulary independent of age, suggesting that the orientation and organization of the AF tract are stable with aging (Teubner-Rhodes et al., 2016). Taken together, these studies suggest that the dorsal stream pathway, specifically the SLF, may have a significant contribution to age-related differences in language production, but further research is needed.

Other tracts have also been identified to be key language comprehension and production pathways by studying patients suffering from diseases that afflict language function, namely, aphasia and strokes. In these patient populations, several WM tracts have been identified for being involved in language comprehension, namely, the IFOF (Ivanova et al., 2016; Hula et al., 2020), uncinate fasciculi (UF; Hula et al., 2020), middle longitudinal fasciculi (Hula et al., 2020), corona radiata (Grönholm et al., 2016; Sul et al., 2019), and external capsule (EC; Chen et al., 2015), and in language production, namely, the AF (Ivanova et al., 2016), middle longitudinal fasciculi (Hula et al., 2020), corona radiata (Grönholm et al., 2016; Sul et al., 2019), and EC (Chen et al., 2015). It is evident that injury to the aforementioned areas is known to affect language function; however, it is less understood how these regions are affected by the typical aging process and what effect this process has on language function.

This study employs Tract-Based Spatial Statistics (TBSS) to examine the regional brain differences related to language function (see the "Region of Interest Selection" in the "Materials and Methods" section for detailed regions) between young and old adults. TBSS is applied to perform automated analysis of WM integrity. TBSS uses a fine-tuned non-linear registration method followed by a projection onto a mean FA skeleton. This skeleton represents the centers of all tracts common to the group and the resulting data fed into voxel-wise cross-subject statistics. Thus, TBSS combines the strength of both voxel-based and tractographic analyses to overcome the limitations of conventional methods, namely, standard registration algorithms and spatial smoothing (Dunst et al., 2014). Moreover, TBSS is assumed to improve the sensitivity, objectivity, and interpretability of multi-subject diffusion imaging studies (Smith et al., 2006; Dunst et al., 2014).

The VF task, which has traditionally been administered as a clinical neuropsychological paradigm to assess linguistic and executive function abilities, was used as behavioral testing in this study; it is one of the most widely used paradigms because of its simplicity and ease of administration. The cognitive components assessed by the VF task include executive functions, namely, initiation, inhibition, planning, updating, and shifting as well as verbal long-term memory (word knowledge) and lexical–semantic linguistic processes (Shao et al., 2014).

Using group differences seen on WM metrics (i.e., FA, MD, AD, RD, and LDH) in old vs. young adults, as well as group performance on the VF task, we hope to elucidate the impact aging has on the WM integrity and its relationship to language function. Portions of this manuscript have been previously presented (Hou et al., 2018).

MATERIALS AND METHODS

Participants

Notably, 38 young adults (21 men and 17 women, mean age = 23.58 ± 3.35 years) and 35 old adults (19 men and 16 women, mean age = 60.91 ± 5.25 years) were recruited from the Madison, Wisconsin, campus community. They were free of any medical, neurological, or psychiatric disorders and had at least 14 years of education. A subset of the participants ($n = 44$) received the Mini Mental State Examination (MMSE; Folstein et al., 1975) and had scores ≥29. For participants with educational level of high school graduate, a score on the MMSE of ≤25 was considered cognitively impaired. The Edinburgh Handedness Inventory (Oldfield, 1971) was administered to all participants. A score greater than +40 was considered right-handed, between −40 and +40 was considered ambidextrous, and less than −40 was considered left-handed. Based on these criteria, there were 64 right, 7 left, and 2 ambidextrous in the study sample. **Table 1** provides the basic demographic information of participants. All participants provided written informed consent. The experimental protocols were approved by the Institutional Review Board (IRB) of the School of Medicine and Public Health, University of Wisconsin–Madison.

Behavioral Testing

We administered the phonemic VF task [the Controlled Oral Word Association Test (COWAT); Benton and Hamsher, 1976] to test cognitive function. The COWAT has been extensively used in both clinical and non-clinical populations because of its face validity (Sauzéon et al., 2011), assessment

TABLE 1 | Demographic data and differences of VF testing.

Characteristics	Young	Old	*t*	*p*
Number	38	35		
Age (years) [range]	23.58 (3.35) [18–32]	60.91 (5.25) [55–77]	28.64	0.000
Education (years) [range]	16.79 (2.22) [12–21]	17.43 (2.87) [12–22]	1.068	0.289
Sex (male/female)	21/17	19/16	0.678	0.878
VF z-score	−0.28 (1.03)	0.35 (1.23)	2.355	0.021
Handedness (right/left/amb)	33/3/2	31/4/0	8.574	0.127

Standard deviations are shown in parentheses. VF, verbal fluency; amb, ambidextrous.

of both verbal cognitive ability and executive control (Fisk and Sharp, 2004), and high correlation with measures of attention, verbal memory, and word knowledge (Ruff et al., 1997). Participants were required to produce words beginning with the letters "F," "A," and "S" in three 1-min trials, respectively. Raw VF scores were based on the total correct responses over the three trials, which were then used to compute age and education corrected VF z-scores based on a normative database (Tombaugh et al., 1999). This corrected VF z-score was used to quantify performance of VF for each participant.

Magnetic Resonance Imaging Data Acquisition

Diffusion-weighted images were acquired using a spin-echo based, single-shot, echo-planar diffusion sequence lasting 10 min on a GE750 3 T MRI scanner. The specific parameters of

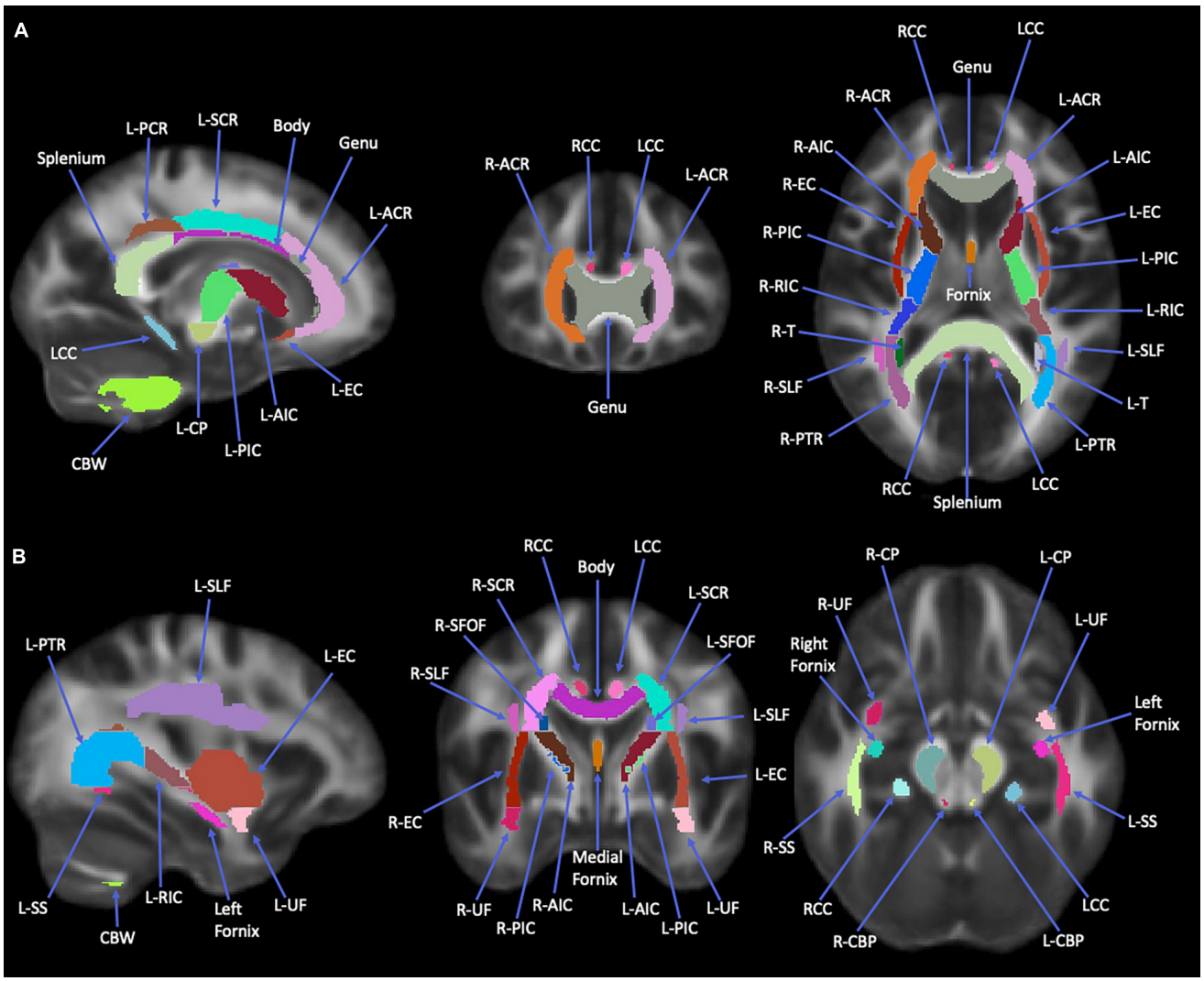

FIGURE 1 | Images of Johns Hopkins University (JHU)-ICBM-DTI-81 white matter (WM) atlas. This atlas was used to obtain the 12 regions of interest used in study analyses. Images are all WM tracts available in this atlas. **(A)** Orientations from left to right: sagittal, coronal, axial. **(B)** Orientations from left to right: sagittal, coronal, axial. Splenium, splenium of corpus callosum; Body, body of corpus callosum; Genu, genu of corpus callosum; L-ACR, left anterior corona radiata; R-ACR, right anterior corona radiata; L-SCR, left superior corona radiata; L-PCR, left posterior corona radiata; RCC, right cingulum cortex; LCC, left cingulum cortex; L-EC, left external capsule; L-AIC, left anterior limb of internal capsule; R-AIC, right anterior limb of internal capsule; L-PIC, left posterior limb of internal capsule; R-PIC, right posterior limb of internal capsule; L-RIC, left retrolenticular part of internal capsule; R-RIC, right retrolenticular part of internal capsule; L-CP, left cerebral peduncle; L-PTR, left posterior thalamic radiation; R-PTR, right posterior thalamic radiation; L-T, left tapetum; R-T, right tapetum; CBW, cerebellar white matter; L-UF, left uncinate fasciculus; R-UF, right uncinate fasciculus; R-EC, right external capsule; L-SLF, left superior longitudinal fasciculus; L-SS, left sagittal stratum; R-SS, right sagittal stratum; R-SCR, right superior corona radiata; L-SFOF, left superior fronto-occipital fasciculus; R-SFOF, right superior fronto-occipital fasciculus; R-CP, right cerebral peduncle; L-CBP, left cerebellar peduncle; R-CBP, right cerebellar peduncle. The regional masks were filtered with the white matter skeleton mask from TBSS (see **Figure 2**).

MRI were as follows: repetition time (TR) = 9,000 ms; echo time (TE) = 76.6 ms; single average (NEX = 1); field of view = 100 mm × 100 mm; matrix size = 256 × 256; in-plane resolution = 1 mm × 1 mm; 75 axial slices with no gap between slices and slice thickness = 2 mm; excitation flip angle $\alpha = 90°$; 56 gradient encoded directions b-value = 1,000 s/mm^2, 10 volumes with b-value = 0 s/mm^2. A high-resolution three-dimensional T1-weighted BRAVO, IR-prepared Fast Spoiled Gradient Echo (FSPGR), MRI sequence with 156 axial slices was performed for each participant using the following parameters: TR = 8.132 ms; TE = 3.18 ms, inversion time (TI) = 450 ms; field of view = 256 mm × 256 mm; matrix size = 256 × 256; in-plane resolution = 1 mm × 1 mm; slice thickness = 1.0 mm; excitation flip angle $\alpha = 12°$.

Data Preprocessing

All diffusion data were processed using the "Pipeline for Analyzing braiN Diffusion images" (PANDA): a toolbox implemented in MATLAB[1] (Cui et al., 2013). This software employs several neuroimaging processing modules, namely, the FMRIB Software Library (FSL), the Pipeline System for Octave and Matlab (PSOM), the Diffusion Toolkit, and the MRIcron to automatically perform a series of steps (i.e., skull removal, correction of eddy current distortion, build diffusion tensor models) (Cui et al., 2013; Kashfi et al., 2017; Hou et al., 2020).

Diffusion metrics such as FA, MD, AD, RD (Smith et al., 2006; Smith and Nichols, 2009; Cui et al., 2013), and LDH (Gong, 2013) for each participant were extracted for 50 tracts identified from the Johns Hopkins University (JHU)-ICBM-DTI-81 WM atlas (Mori et al., 2008; Cui et al., 2013). **Figures 1**, **2** illustrate the representative images of WM tracts for this atlas. These region masks were filtered by applying the TBSS WM skeleton. Each global mean metric (i.e., FA, MD, AD, RD, and LDH) for each participant was obtained by averaging across the 50 labels, with the diffusion metric for each label being divided by this global mean to account for any variability between participants. This standardized metric was used in our statistical analysis.

Region of Interest Selection

Based on prior studies on WM organization of the brain, six WM labels in each hemisphere implicated in language function (Smits et al., 2014; Friederici, 2015) were selected as regions of interests (ROIs), namely, ACR, superior corona radiata (SCR), posterior corona radiata (PCR), EC, UF, and SLF.

Statistical Analysis

A chi-square test was performed for handedness group differences, which did not identify a statistically significant difference between the two groups (see **Table 1** for details). As a result, all handedness variations (right, left, and ambidextrous) were kept in the participant sample.

To investigate group differences on each DTI metric, an analysis of covariance (ANCOVA) controlling for sex and educational years was performed, and the statistical threshold for significance was considered at $p < 0.00083$ (0.05/60 labels) after Bonferroni correction for multiple comparison. This analysis identified tracts in which the diffusivity metrics were significantly different between the groups. Pearson's correlation analysis, with sex as a covariate, was performed between the diffusivity metrics in the significant tracts and VF scores using IBM SPSS version 27 and considered significant at uncorrected $p < 0.05$.

[1]http://www.nitrc.org/projects/panda/

RESULTS

The VF testing demonstrated old adults have significantly higher VF z-scores than young adults (see **Table 1**). Compared to the old adults, the young adults had significantly (1) increased FA values on the bilateral ACR; (2) increased MD value on the left UF; and (3) decreased RD on the bilateral ACR. There were no significant differences between the groups for AD or LDH (**Table 2** and **Figures 3**, **4**). Moreover, the old adults had only a significant positive correlation between the VF z-score and the MD on the left UF [$r_{(35)} = 0.383$, $p = 0.025$], with sex as a covariate (see **Figure 5**). There were no significant correlations between VF score and DTI metrics in young adults.

DISCUSSION

As reported previously in the literature, our study identified age-related reductions in FA and increases in RD on the bilateral ACR as well as an increase in MD on the right ACR (Barrick et al., 2010; Bennett et al., 2010; Ly et al., 2014). Additionally, MD on the left UF showed significant group differences adding to the growing body of research that WM areas indicated in language function are sensitive to aging.

Hemispheric asymmetry with aging is well known (Cabeza, 2002). Specifically, the left lateralized language pattern seen in young adults changes with age to a more bi-hemispheric pattern in older adults, which could be a compensatory mechanism to

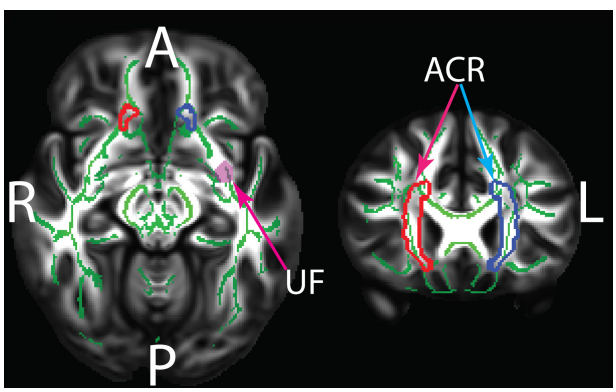

FIGURE 2 | The JHU white matter regions showing statistically significant group differences between old and young adults. ACR, anterior corona radiata; UF, uncinate fasciculus. The underlay shows the TBSS white matter skeleton which was masked by the JHU regions in the statistical analyses. The TBSS skeleton and the JHU regions are overlaid on the HCP 1065 FA template. Green: White matter skeleton; Red: right ACR; Blue: left ACR; pink: left UF.

TABLE 2 | Significant difference between DTI metrics and tract by group comparisons.

	Tracts	Mean difference (young–old)	Standard error	*p*	95% confidence interval for difference	
					Lower bound	Upper bound
FA	Right ACR	0.0454	0.0080	0.0000	0.0175	0.0732
	Left ACR	0.0511	0.0083	0.0000	0.0221	0.0802
MD	Right ACR	−0.195	0.0053	0.0005	−0.0380	−0.0009
	Left UF	0.0291	0.0078	0.0004	0.0018	0.0564
RD	Right ACR	−0.0415	0.0084	0.0000	−0.0709	−0.0121
	Left ACR	−0.0424	0.0094	0.0000	−0.0752	−0.0097

All DTI metric values are $p < 0.00083$ (Bonferroni multiple comparison 0.05/60 labels) after controlling for sex and education. FA, fractional anisotropy; MD, mean diffusivity (unit: $\mu m^2/ms$); RD, radial diffusivity (unit: $\mu m^2/ms$); ACR, anterior corona radiata; UF, uncinate fasciculus.

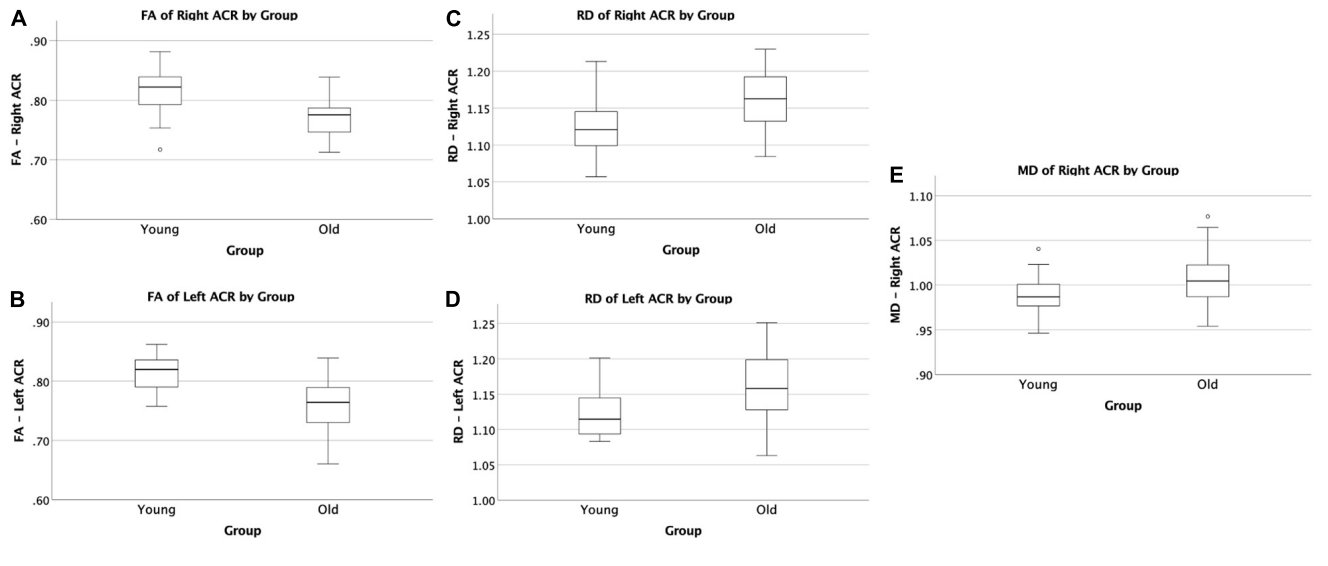

FIGURE 3 | Significant difference in ACR by group comparisons. **(A)** Boxplot showing significant reduction in FA in old adults compared to young adults on the right ACR. **(B)** Boxplot showing significant reduction in FA in old adults compared to young adults on the left ACR. **(C)** Boxplot showing significant increase in RD in old adults compared to young adults on the right ACR. **(D)** Boxplot showing significant increase in RD in old adults compared to young adults on the left ACR. **(E)** Boxplot showing significant increase in MD in old adults compared to young adults on the right ACR. All relationships are considered at $p < 0.00083$ (Bonferroni multiple comparison 0.05/60 labels) after controlling for sex and education. FA, fractional anisotropy; RD, radial diffusivity; MD, mean diffusivity.

maintain behavioral performance. This study observed decreased MD on the left UF and increased MD on the right ACR in the old adults group, suggesting an improvement of the UF integrity and a decrease in the ACR. However, a decrease in left UF integrity would be predicted by the HAROLD model if the left hemispheric predominance of language function were to be reduced toward more bilateral activation (Cabeza, 2002). While this finding may seem to contradict the HAROLD model, it is difficult to assess the reduction of hemispheric specialization with only two non-bilateral group differences. Additionally, in this study, we only included one test of language/executive function. The asymmetry pattern is best investigated using a specific battery of language tests and will be explored in a future study.

This study did find evidence for another model of the aging brain, the anteroposterior model. Since the ACR resides more anteriorly than the other brain regions we studied, our findings for the ACR agree with prior evidence for the existence of an anteroposterior model for loss of WM integrity in the aging brain (Pfefferbaum et al., 2005; Ardekani et al., 2007; Madden et al., 2009; Bennett et al., 2010). Since the UF is located inferiorly to the ACR, our findings of increased MD on the UF in old adults compared to young adults seem to contradict this assertion of anteroposterior aging. However, there is evidence to suggest that superiorly located fiber systems demonstrate age effects earlier than inferior systems (Sullivan et al., 2010) and this finding is additional evidence that there are brain regions with differential aging processes in aging adults. In addition, the significant increase in RD on the ACR signifies an age-related demyelination effect of that tract, based on previous animal and human studies investigating RD and its relationship to neural networks (Song et al., 2002, 2003, 2005; Nair et al., 2005; Budde et al., 2007), as well as evidence supporting typical aging is accompanied by myelin damage and loss (Peters, 2002). Our study did not find any association between ACR and VF, but Troutman and Diaz (2020) observed that higher RD across dorsal, ventral, and fronto-striatal tracts was associated with poorer performance on a naming with distractors task, suggesting that demyelination can result in poorer language performance.

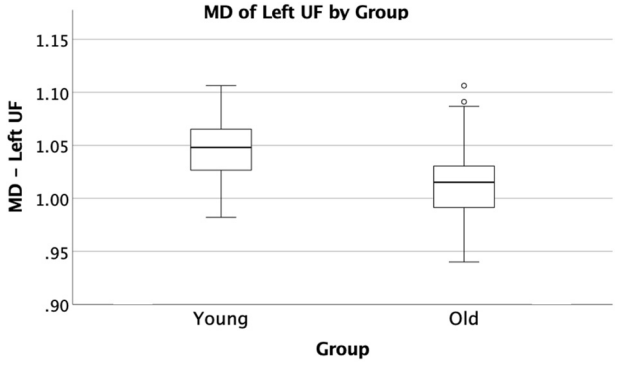

FIGURE 4 | Significant difference in UF by group comparison. Boxplot showing significant decrease in MD in old adults compared to young adults on the left UF. All relationships are considered at $p < 0.00083$ (Bonferroni multiple comparison 0.05/60 labels) after controlling for sex and education.

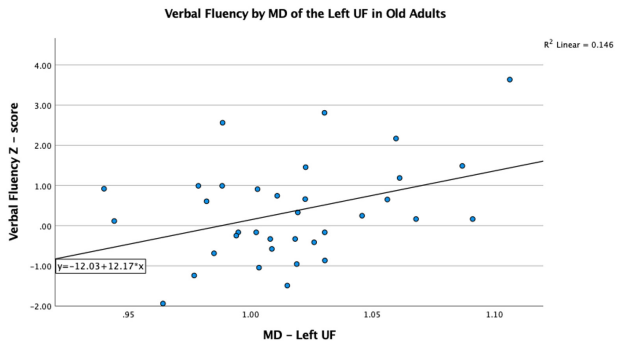

FIGURE 5 | Significant correlation between VF and MD on the left UF in older adults, after controlling for sex, $p < 0.05$.

Compared to young adults, the significantly higher VF score we observed in the old adults group, in conjunction with the age-related demyelination and loss of WM integrity, could be evidence for the use of compensatory strategies to maintain performance. For instance, the HAROLD model purports that certain cognitive functions, namely, language production (La et al., 2016; Kim et al., 2018), lose their hemispheric specialization as one ages to counteract age-related neurocognitive deficits (Cabeza et al., 1997; Cabeza, 2002). Additionally, the compensation view of the HAROLD model has evidence to support recovery of language function after brain injuries (Cao et al., 1999) and resections (Jehna et al., 2017). Studies looking at temporal lobe resections in patients with epilepsy observed post-operative increases in FA in ipsilateral WM regions, such as the corona radiata and external and internal capsule, that were associated with a smaller fall in language proficiency after surgery (Yogarajah et al., 2010; Pustina et al., 2014). While age-related WM alterations may be different than the plastic changes occurring as a compensatory mechanism after regional brain insults, these studies still provide evidence that the brain has the capacity to rewire language pathways. Knowing this, perhaps age-related WM structural changes have a rewiring process to compensate for WM structures prone to degeneration allowing for preserved language function.

In our study, MD on the left UF of the old adult group was positively correlated with VF score, which is in contrast to what we would predict, since a higher MD typically indicates less WM integrity, and less WM integrity typically results in worse tract function. As a group, old adults have lower MD than young adults; however, within the old adult group, it is those with the higher MD values that score better on the VF task. Perhaps this indicates that the UF is becoming better organized to perform this task as we age, but only to a certain threshold, and perhaps the increased MD value in the older adults resulting in better performance is an indication of better compensation in those individuals by other WM tracts involved in VF performance. While we did not find other tract associations with the VF score that could attest to this postulation, Madhavan et al. (2014) did demonstrate a relationship with increased FA on the SLF and stronger language function in an aging population, suggesting some compensatory changes occurring in that tract. However, without other tract associations from this study, it is difficult to ascertain what the explanation for this may be, but future analyses involving a larger sample size may help elucidate this finding.

As previously mentioned, the demyelination and loss of WM integrity in the ACR, in addition to these UF findings, provides evidence that there may be differential aging processes in various WM tracts involved in language production that preserves this function with age. However, a few studies contradict this assertion by reporting losses of WM integrity in the UF with increasing age (Stamatakis et al., 2011; Kemmotsu et al., 2012; Gong, 2013). Taking this into account, it is difficult to interpret considering the sample sizes of the contradictory studies are all smaller than our current study. Further research will be needed to help resolve the discrepancy.

We did not identify any group differences for the AD and LDH DTI metrics, nor correlations of the VF score with the ACR, nor observe any significant group differences in the additional tracts we identified *a priori*. The lack of associations could have been a result of our small sample size and repeating this study with a larger population could elucidate more findings. While LDH is sensitive to diffusion properties among neighboring voxels and offers complementary information to FA, MD, and RD, for this study, it is possible that the metric is not as sensitive to the brain aging process (Sullivan et al., 2001; Pfefferbaum et al., 2005; Sullivan and Pfefferbaum, 2006; Westlye et al., 2010; Lamar et al., 2014; Madhavan et al., 2014; Houston et al., 2019; Troutman and Diaz, 2020).

DATA AVAILABILITY STATEMENT

The original contributions presented in the study are included in the article/supplementary material, further inquiries can be directed to the corresponding author/s.

ETHICS STATEMENT

The studies involving human participants were reviewed and approved by the Institutional Review Board (IRB) of the School of Medicine and Public Health, University of Wisconsin–Madison.

The patients/participants provided their written informed consent to participate in this study.

AUTHOR CONTRIBUTIONS

VP conceived and designed the experiments. VN helped with data acquisition. JH preprocessed the data and wrote the Materials and Methods section of the manuscript. BY and JH analyzed the data. BY wrote the Introduction, Results, and Discussion sections of the manuscript. VN, NA, and VP provided guidance for data analysis, and manuscript writing and editing. All authors contributed to the article and approved the submitted version.

FUNDING

This study was supported by the NIH grants NINDS R01NS117568-01A1, RO1NS111022-01A1, R01NS105646, and NIMH RC1MH090912-01. NIH core grant Waisman Center from the National Institute of Child Health and Human Development (IDDRC U54 HD 090256) is also acknowledged. Funding for trainee, BY was provided by UW–Madison SMPH's Shapiro Summer Research Scholarship.

ACKNOWLEDGMENTS

Portions of this work were presented at the Organization of Human Brain Mapping Annual Meeting (OHBM) 2018.

REFERENCES

Ardekani, S., Kumar, A., Bartzokis, G., and Sinha, U. (2007). Exploratory voxel-based analysis of diffusion indices and hemispheric asymmetry in normal aging. *Magn. Reson. Imaging* 25, 154–167. doi: 10.1016/j.mri.2006.09.045

Baciu, M., Boudiaf, N., Cousin, E., Perrone-Bertolotti, M., Pichat, C., Fournet, N., et al. (2016). Functional MRI evidence for the decline of word retrieval and generation during normal aging. *Age* 38:3. doi: 10.1007/s11357-015-9857-y

Barrick, T. R., Charlton, R. A., Clark, C. A., and Markus, H. S. (2010). White matter structural decline in normal ageing: a prospective longitudinal study using tract-based spatial statistics. *Neuroimage* 51, 565–577. doi: 10.1016/j.neuroimage.2010.02.033

Bellis, T. J., Nicol, T., and Kraus, N. (2000). Aging affects hemispheric asymmetry in the neural representation of speech sounds. *J. Neurosci.* 20, 791–797.

Bennett, I. J., Madden, D. J., Vaidya, C. J., Howard, D. V., and Howard, J. H. (2010). Age-related differences in multiple measures of white matter integrity: a diffusion tensor imaging study of healthy aging. *Hum. Brain. Mapp.* 31, 378–390. doi: 10.1002/hbm.20872

Benton, A., and Hamsher, K. (1976). *Multilingual Aphasia Examination*. Iowa City: University of Iowa.

Bhagat, Y. A., and Beaulieu, C. (2004). Diffusion anisotropy in subcortical white matter and cortical gray matter: changes with aging and the role of CSF-suppression. *J. Magn. Reson. Imaging* 20, 216–227. doi: 10.1002/jmri.20102

Budde, M. D., Janes, L., Gold, E., Turtzo, L. C., and Frank, J. A. (2011). The contribution of gliosis to diffusion tensor anisotropy and tractography following traumatic brain injury: validation in the rat using Fourier analysis of stained tissue sections. *Brain* 134, 2248–2260. doi: 10.1093/brain/awr161

Budde, M. D., Kim, J. H., Liang, H. F., Schmidt, R. E., Russell, J. H., Cross, A. H., et al. (2007). Toward accurate diagnosis of white matter pathology using diffusion tensor imaging. *Magn. Reson. Med.* 57, 688–695. doi: 10.1002/mrm.21200

Cabeza, R. (2002). Hemispheric asymmetry reduction in older adults: the HAROLD model. *Psychol. Aging* 17, 85–100. doi: 10.1037//0882-7974.17.1.85

Cabeza, R., Grady, C. L., Nyberg, L., McIntosh, A. R., Tulving, E., Kapur, S., et al. (1997). Age-related differences in neural activity during memory encoding and retrieval: a positron emission tomography study. *J. Neurosci.* 17, 391–400.

Cao, Y., Vikingstad, E. M., George, K. P., Johnson, A. F., and Welch, K. M. (1999). Cortical language activation in stroke patients recovering from aphasia with functional MRI. *Stroke* 30, 2331–2340. doi: 10.1161/01.str.30.11.2331

Caserta, M. T., Bannon, Y., Fernandez, F., Giunta, B., Schoenberg, M. R., and Tan, J. (2009). Normal brain aging clinical, immunological, neuropsychological, and neuroimaging features. *Int. Rev. Neurobiol.* 84, 1–19. doi: 10.1016/S0074-7742(09)00401-2

Chen, Y., Wang, A., Tang, J., Wei, D., Li, P., Chen, K., et al. (2015). Association of white matter integrity and cognitive functions in patients with subcortical silent lacunar infarcts. *Stroke* 46, 1123–1126. doi: 10.1161/STROKEAHA.115.008998

Cui, Z., Zhong, S., Xu, P., He, Y., and Gong, G. (2013). PANDA: a pipeline toolbox for analyzing brain diffusion images. *Front. Hum. Neurosci.* 7:42. doi: 10.3389/fnhum.2013.00042

Davis, S. W., Dennis, N. A., Buchler, N. G., White, L. E., Madden, D. J., and Cabeza, R. (2009). Assessing the effects of age on long white matter tracts using diffusion tensor tractography. *Neuroimage* 46, 530–541. doi: 10.1016/j.neuroimage.2009.01.068

Dunst, B., Benedek, M., Koschutnig, K., Jauk, E., and Neubauer, A. C. (2014). Sex differences in the IQ-white matter microstructure relationship: a DTI study. *Brain Cogn.* 91, 71–78. doi: 10.1016/j.bandc.2014.08.006

Fisk, J. E., and Sharp, C. A. (2004). Age-related impairment in executive functioning: updating, inhibition, shifting, and access. *J. Clin. Exp. Neuropsychol.* 26, 874–890. doi: 10.1080/13803390490510680

Fjell, A. M., Sneve, M. H., Grydeland, H., Storsve, A. B., and Walhovd, K. B. (2017). The Disconnected Brain and Executive Function Decline in Aging. *Cereb. Cortex* 27, 2303–2317. doi: 10.1093/cercor/bhw082

Folstein, M. F., Folstein, S. E., and McHugh, P. R. (1975). Mini-mental state". A practical method for grading the cognitive state of patients for the clinician. *J. Psychiatr. Res.* 12, 189–198. doi: 10.1016/0022-3956(75)90026-6

Friederici, A. D. (2015). White-matter pathways for speech and language processing. *Handb. Clin. Neurol.* 129, 177–186. doi: 10.1016/B978-0-444-62630-1.00010-X

Gong, G. (2013). Local diffusion homogeneity (LDH): an inter-voxel diffusion MRI metric for assessing inter-subject white matter variability. *PLoS One* 8:e66366. doi: 10.1371/journal.pone.0066366

Grönholm, E. O., Roll, M. C., Horne, M. A., Sundgren, P. C., and Lindgren, A. G. (2016). Predominance of caudate nucleus lesions in acute ischaemic stroke patients with impairment in language and speech. *Eur. J. Neurol.* 23, 148–153. doi: 10.1111/ene.12822

Herrmann, M. J., Walter, A., Ehlis, A. C., and Fallgatter, A. J. (2006). Cerebral oxygenation changes in the prefrontal cortex: effects of age and gender. *Neurobiol. Aging* 27, 888–894. doi: 10.1016/j.neurobiolaging.2005.04.013

Hou, J., Dodd, K., Nair, V. A., Rajan, S., Beniwal-Patel, P., Saha, S., et al. (2020). Alterations in brain white matter microstructural properties in patients with Crohn's disease in remission. *Sci. Rep.* 10:2145. doi: 10.1038/s41598-020-59098-w

Hou, J., Nair, V., Sinha, A., and Prabhakaran, V. (2018). "Differences in white matter integrity related to language production between young and old adults," in *The 24th International Conference of Human Brain Mapping*, (Singapore: Organization for Human Brain Mapping).

Houston, J., Allendorfer, J., Nenert, R., Goodman, A. M., and Szaflarski, J. P. (2019). White Matter Language Pathways and Language Performance in Healthy Adults Across Ages. *Front. Neurosci.* 13:1185. doi: 10.3389/fnins.2019.01185

Hula, W. D., Panesar, S., Gravier, M. L., Yeh, F. C., Dresang, H. C., Dickey, M. W., et al. (2020). Structural white matter connectometry of word production in aphasia: an observational study. *Brain* 143, 2532–2544. doi: 10.1093/brain/awaa193

Ivanova, M. V., Isaev, D. Y., Dragoy, O. V., Akinina, Y. S., Petrushevskiy, A. G., Fedina, O. N., et al. (2016). Diffusion-tensor imaging of major white matter tracts and their role in language processing in aphasia. *Cortex* 85, 165–181. doi: 10.1016/j.cortex.2016.04.019

Jehna, M., Becker, J., Zaar, K., von Campe, G., Mahdy Ali, K., Reishofer, G., et al. (2017). Symmetry of the arcuate fasciculus and its impact on language performance of patients with brain tumors in the language-dominant hemisphere. *J. Neurosurg.* 127, 1407–1416. doi: 10.3171/2016.9.JNS161281

Jernigan, T. L., Archibald, S. L., Fennema-Notestine, C., Gamst, A. C., Stout, J. C., Bonner, J., et al. (2001). Effects of age on tissues and regions of the cerebrum and cerebellum. *Neurobiol. Aging* 22, 581–594. doi: 10.1016/s0197-4580(01)00217-2

Kantarci, K., Senjem, M. L., Avula, R., Zhang, B., Samikoglu, A. R., Weigand, S. D., et al. (2011). Diffusion tensor imaging and cognitive function in older adults with no dementia. *Neurology* 77, 26–34. doi: 10.1212/WNL.0b013e31822313dc

Kashfi, K., Al-Khalil, K., Hou, J., Fang, D., Anderson, R., Rajmohan, R., et al. (2017). Hyper-brain connectivity in binge drinking college students: a diffusion tensor imaging study. *Neurocase* 23, 179–186. doi: 10.1080/13554794.2017.1347264

Kemmotsu, N., Girard, H. M., Kucukboyaci, N. E., McEvoy, L. K., Hagler, D. J., Dale, A. M., et al. (2012). Age-related changes in the neurophysiology of language in adults: relationship to regional cortical thinning and white matter microstructure. *J. Neurosci.* 32, 12204–12213. doi: 10.1523/JNEUROSCI.0136-12.2012

Kim, I. S., Millin, N. J., Hwang, J., Kim, I. S., Millin, N. J., and Hwang, J. (2018). Word retrieval by verbal fluency tasks for young and old people: an fNIR study. *Clin. Arch. Commun. Disord.* 3, 52–58.

La, C., Garcia-Ramos, C., Nair, V. A., Meier, T. B., Farrar-Edwards, D., Birn, R., et al. (2016). Age-Related Changes in BOLD Activation Pattern in Phonemic Fluency Paradigm: an Investigation of Activation, Functional Connectivity and Psychophysiological Interactions. *Front. Aging Neurosci.* 8:110. doi: 10.3389/fnagi.2016.00110

Lamar, M., Zhou, X. J., Charlton, R. A., Dean, D., Little, D., and Deoni, S. C. (2014). In vivo quantification of white matter microstructure for use in aging: a focus on two emerging techniques. *Am. J. Geriatr. Psychiatry* 22, 111–121. doi: 10.1016/j.jagp.2013.08.001

Liang, Y., Zhang, H., Tan, X., Liu, J., Qin, C., Zeng, H., et al. (2019). Local Diffusion Homogeneity Provides Supplementary Information in T2DM-Related WM Microstructural Abnormality Detection. *Front. Neurosci.* 13:63. doi: 10.3389/fnins.2019.00063

Liu, G., Tan, S., Dang, C., Peng, K., Xie, C., Xing, S., et al. (2017). Motor Recovery Prediction With Clinical Assessment and Local Diffusion Homogeneity After Acute Subcortical Infarction. *Stroke* 48, 2121–2128. doi: 10.1161/STROKEAHA.117.017060

Ly, M., Canu, E., Xu, G., Oh, J., McLaren, D. G., Dowling, N. M., et al. (2014). Midlife measurements of white matter microstructure predict subsequent regional white matter atrophy in healthy adults. *Hum. Brain Mapp.* 35, 2044–2054. doi: 10.1002/hbm.22311

Madden, D. J., Spaniol, J., Costello, M. C., Bucur, B., White, L. E., Cabeza, R., et al. (2009). Cerebral white matter integrity mediates adult age differences in cognitive performance. *J. Cogn. Neurosci.* 21, 289–302. doi: 10.1162/jocn.2009.21047

Madhavan, K. M., McQueeny, T., Howe, S. R., Shear, P., and Szaflarski, J. (2014). Superior longitudinal fasciculus and language functioning in healthy aging. *Brain Res.* 1562, 11–22. doi: 10.1016/j.brainres.2014.03.012

Masliah, E., Mallory, M., Hansen, L., DeTeresa, R., and Terry, R. D. (1993). Quantitative synaptic alterations in the human neocortex during normal aging. *Neurology* 43, 192–197. doi: 10.1212/wnl.43.1_part_1.192

Meinzer, M., Flaisch, T., Wilser, L., Eulitz, C., Rockstroh, B., Conway, T., et al. (2009). Neural signatures of semantic and phonemic fluency in young and old adults. *J. Cogn. Neurosci.* 21, 2007–2018. doi: 10.1162/jocn.2009.21219

Mori, S., Oishi, K., Jiang, H., Jiang, L., Li, X., Akhter, K., et al. (2008). Stereotaxic white matter atlas based on diffusion tensor imaging in an ICBM template. *Neuroimage* 40, 570–582. doi: 10.1016/j.neuroimage.2007.12.035

Nair, G., Tanahashi, Y., Low, H. P., Billings-Gagliardi, S., Schwartz, W. J., and Duong, T. Q. (2005). Myelination and long diffusion times alter diffusion-tensor-imaging contrast in myelin-deficient shiverer mice. *Neuroimage* 28, 165–174. doi: 10.1016/j.neuroimage.2005.05.049

Nyberg, L., Lövdén, M., Riklund, K., Lindenberger, U., and Bäckman, L. (2012). Memory aging and brain maintenance. *Trends Cogn. Sci.* 16, 292–305. doi: 10.1016/j.tics.2012.04.005

Oldfield, R. C. (1971). The assessment and analysis of handedness: the Edinburgh inventory. *Neuropsychologia* 9, 97–113. doi: 10.1016/0028-3932(71)90067-4

Peters, A. (2002). The effects of normal aging on myelin and nerve fibers: a review. *J. Neurocytol.* 31, 581–593. doi: 10.1023/a:1025731309829

Pfefferbaum, A., Adalsteinsson, E., and Sullivan, E. V. (2005). Frontal circuitry degradation marks healthy adult aging: evidence from diffusion tensor imaging. *Neuroimage* 26, 891–899. doi: 10.1016/j.neuroimage.2005.02.034

Pihlajamäki, M., Tanila, H., Hänninen, T., Könönen, M., Laakso, M., Partanen, K., et al. (2000). Verbal fluency activates the left medial temporal lobe: a functional magnetic resonance imaging study. *Ann. Neurol.* 47, 470–476.

Pugliese, L., Catani, M., Ameis, S., Dell'Acqua, F., Thiebaut de Schotten, M., Murphy, C., et al. (2009). The anatomy of extended limbic pathways in Asperger syndrome: a preliminary diffusion tensor imaging tractography study. *Neuroimage* 47, 427–434. doi: 10.1016/j.neuroimage.2009.05.014

Pustina, D., Doucet, G., Evans, J., Sharan, A., Sperling, M., Skidmore, C., et al. (2014). Distinct types of white matter changes are observed after anterior temporal lobectomy in epilepsy. *PLoS One* 9:e104211. doi: 10.1371/journal.pone.0104211

Rayhan, R. U., Stevens, B. W., Timbol, C. R., Adewuyi, O., Walitt, B., VanMeter, J. W., et al. (2013). Increased brain white matter axial diffusivity associated with fatigue, pain and hyperalgesia in Gulf War illness. *PLoS One* 8:e58493. doi: 10.1371/journal.pone.0058493

Resnick, S. M., Pham, D. L., Kraut, M. A., Zonderman, A. B., and Davatzikos, C. (2003). Longitudinal magnetic resonance imaging studies of older adults: a shrinking brain. *J. Neurosci.* 23, 3295–3301.

Ruff, R. M., Light, R. H., Parker, S. B., and Levin, H. S. (1997). The psychological construct of word fluency. *Brain Lang.* 57, 394–405. doi: 10.1006/brln.1997.1755

Sauzéon, H., Raboutet, C., Rodrigues, J., Langevin, S., Schelstraete, M. A., Feyereisen, P., et al. (2011). Verbal Knowledge as a Compensation Determinant of Adult Age Differences in Verbal Fluency Tasks over Time. *J. Adult Dev.* 18, 144–154.

Shao, Z., Janse, E., Visser, K., and Meyer, A. S. (2014). What do verbal fluency tasks measure? Predictors of verbal fluency performance in older adults. *Front. Psychol.* 5:772. doi: 10.3389/fpsyg.2014.00772

Smith, S. M., Jenkinson, M., Johansen-Berg, H., Rueckert, D., Nichols, T. E., Mackay, C. E., et al. (2006). Tract-based spatial statistics: voxelwise analysis of multi-subject diffusion data. *Neuroimage* 31, 1487–1505. doi: 10.1016/j.neuroimage.2006.02.024

Smith, S. M., and Nichols, T. E. (2009). Threshold-free cluster enhancement: addressing problems of smoothing, threshold dependence and localisation in cluster inference. *Neuroimage* 44, 83–98. doi: 10.1016/j.neuroimage.2008.03.061

Smits, M., Jiskoot, L. C., and Papma, J. M. (2014). White matter tracts of speech and language. *Semin. Ultrasound CT MR* 35, 504–516. doi: 10.1053/j.sult.2014.06.008

Song, S. K., Sun, S. W., Ju, W. K., Lin, S. J., Cross, A. H., and Neufeld, A. H. (2003). Diffusion tensor imaging detects and differentiates axon and myelin degeneration in mouse optic nerve after retinal ischemia. *Neuroimage* 20, 1714–1722. doi: 10.1016/j.neuroimage.2003.07.005

Song, S. K., Sun, S. W., Ramsbottom, M. J., Chang, C., Russell, J., and Cross, A. H. (2002). Dysmyelination revealed through MRI as increased radial (but unchanged axial) diffusion of water. *Neuroimage* 17, 1429–1436. doi: 10.1006/nimg.2002.1267

Song, S. K., Yoshino, J., Le, T. Q., Lin, S. J., Sun, S. W., Cross, A. H., et al. (2005). Demyelination increases radial diffusivity in corpus callosum of mouse brain. *Neuroimage* 26, 132–140. doi: 10.1016/j.neuroimage.2005.01.028

Stamatakis, E. A., Shafto, M. A., Williams, G., Tam, P., and Tyler, L. K. (2011). White matter changes and word finding failures with increasing age. *PLoS One* 6:e14496. doi: 10.1371/journal.pone.0014496

Sul, B., Lee, K. B., Hong, B. Y., Kim, J. S., Kim, J., Hwang, W. S., et al. (2019). Association of Lesion Location With Long-Term Recovery in Post-stroke Aphasia and Language Deficits. *Front. Neurol.* 10:776. doi: 10.3389/fneur.2019.00776

Sullivan, E. V., Adalsteinsson, E., Hedehus, M., Ju, C., Moseley, M., Lim, K. O., et al. (2001). Equivalent disruption of regional white matter microstructure in ageing healthy men and women. *Neuroreport* 12, 99–104. doi: 10.1097/00001756-200101220-00027

Sullivan, E. V., and Pfefferbaum, A. (2006). Diffusion tensor imaging and aging. *Neurosci. Biobehav. Rev.* 30, 749–761. doi: 10.1016/j.neubiorev.2006.06.002

Sullivan, E. V., Rohlfing, T., and Pfefferbaum, A. (2010). Quantitative fiber tracking of lateral and interhemispheric white matter systems in normal aging: relations to timed performance. *Neurobiol. Aging* 31, 464–481. doi: 10.1016/j.neurobiolaging.2008.04.007

Sundaram, S. K., Kumar, A., Makki, M. I., Behen, M. E., Chugani, H. T., and Chugani, D. C. (2008). Diffusion tensor imaging of frontal lobe in autism spectrum disorder. *Cereb. Cortex* 18, 2659–2665. doi: 10.1093/cercor/bhn031

Teubner-Rhodes, S., Vaden, K. I., Cute, S. L., Yeatman, J. D., Dougherty, R. F., and Eckert, M. A. (2016). Aging-Resilient Associations between the Arcuate Fasciculus and Vocabulary Knowledge: microstructure or Morphology?. *J. Neurosci.* 36, 7210–7222. doi: 10.1523/JNEUROSCI.4342-15.2016

Thomason, M. E., and Thompson, P. M. (2011). Diffusion imaging, white matter, and psychopathology. *Annu. Rev. Clin. Psychol.* 7, 63–85. doi: 10.1146/annurev-clinpsy-032210-104507

Tombaugh, T. N., Kozak, J., and Rees, L. (1999). Normative data stratified by age and education for two measures of verbal fluency: FAS and animal naming. *Arch. Clin. Neuropsychol.* 14, 167–177.

Troutman, S. B. W., and Diaz, M. T. (2020). White matter disconnection is related to age-related phonological deficits. *Brain Imaging Behav.* 14, 1555–1565. doi: 10.1007/s11682-019-00086-8

Vaqué-Alcázar, L., Sala-Llonch, R., Abellaneda-Pérez, K., Coll-Padrós, N., Valls-Pedret, C., Bargalló, N., et al. (2020). Functional and structural correlates of working memory performance and stability in healthy older adults. *Brain Struct. Funct.* 225, 375–386. doi: 10.1007/s00429-019-02009-1

Webb, C. E., Rodrigue, K. M., Hoagey, D. A., Foster, C. M., and Kennedy, K. M. (2020). Contributions of White Matter Connectivity and BOLD Modulation to Cognitive Aging: a Lifespan Structure-Function Association Study. *Cereb. Cortex* 30, 1649–1661. doi: 10.1093/cercor/bhz193

Westlye, L. T., Walhovd, K. B., Dale, A. M., Bjørnerud, A., Due-Tønnessen, P., Engvig, A., et al. (2010). Life-span changes of the human brain white matter: diffusion tensor imaging (DTI) and volumetry. *Cereb. Cortex* 20, 2055–2068. doi: 10.1093/cercor/bhp280

Wingfield, A., and Grossman, M. (2006). Language and the aging brain: patterns of neural compensation revealed by functional brain imaging. *J. Neurophysiol.* 96, 2830–2839. doi: 10.1152/jn.00628.2006

Yogarajah, M., Focke, N. K., Bonelli, S. B., Thompson, P., Vollmar, C., McEvoy, A. W., et al. (2010). The structural plasticity of white matter networks following anterior temporal lobe resection. *Brain* 133, 2348–2364. doi: 10.1093/brain/awq175

Zahr, N. M., Rohlfing, T., Pfefferbaum, A., and Sullivan, E. V. (2009). Problem solving, working memory, and motor correlates of association and commissural fiber bundles in normal aging: a quantitative fiber tracking study. *Neuroimage* 44, 1050–1062. doi: 10.1016/j.neuroimage.2008.09.046

Zhang, H., Sachdev, P. S., Wen, W., Kochan, N. A., Crawford, J. D., Brodaty, H., et al. (2013). Grey matter correlates of three language tests in non-demented older adults. *PLoS One* 8:e80215. doi: 10.1371/journal.pone.0080215

Zhang, Y., Du, A. T., Hayasaka, S., Jahng, G. H., Hlavin, J., Zhan, W., et al. (2010). Patterns of age-related water diffusion changes in human brain by concordance and discordance analysis. *Neurobiol. Aging* 31, 1991–2001. doi: 10.1016/j.neurobiolaging.2008.10.009

Conflict of Interest: The authors declare that the research was conducted in the absence of any commercial or financial relationships that could be construed as a potential conflict of interest.

Publisher's Note: All claims expressed in this article are solely those of the authors and do not necessarily represent those of their affiliated organizations, or those of the publisher, the editors and the reviewers. Any product that may be evaluated in this article, or claim that may be made by its manufacturer, is not guaranteed or endorsed by the publisher.

frontiers in Aging Neuroscience

ORIGINAL RESEARCH
published: 26 November 2021
doi: 10.3389/fnagi.2021.765185

BrainFD: Measuring the Intracranial Brain Volume With Fractal Dimension

Ghulam Md Ashraf[1,2†], Stylianos Chatzichronis[3,4†], Athanasios Alexiou[4,5*†], Nikolaos Kyriakopoulos[6], Badrah Saeed Ali Alghamdi[1,7,8], Haythum Osama Tayeb[8,9], Jamaan Salem Alghamdi[10], Waseem Khan[11], Manal Ben Jalal[11] and Hazem Mahmoud Atta[12]*

[1] Pre-Clinical Research Unit, King Fahd Medical Research Center, King Abdulaziz University, Jeddah, Saudi Arabia, [2] Department of Medical Laboratory Technology, Faculty of Applied Medical Sciences, King Abdulaziz University, Jeddah, Saudi Arabia, [3] Department of Informatics and Telecommunications, National and Kapodistrian University of Athens, Athens, Greece, [4] Department of Science and Engineering, Novel Global Community Educational Foundation, Hebersham, NSW, Australia, [5] AFNP Med Austria, Vienna, Austria, [6] MRI Department, 251 General Airforce Hospital, Athens, Greece, [7] Department of Physiology, Faculty of Medicine, King Abdulaziz University, Jeddah, Saudi Arabia, [8] The Neuroscience Research Unit, Faculty of Medicine, King Abdulaziz University, Jeddah, Saudi Arabia, [9] Division of Neurology, Department of Internal Medicine, King Abdulaziz University, Jeddah, Saudi Arabia, [10] Department of Diagnostic Radiology, Faculty of Applied Medical Sciences, King Abdulaziz University, Jeddah, Saudi Arabia, [11] Department of Radiology, King Abdulaziz University Hospital, King Abdulaziz University, Jeddah, Saudi Arabia, [12] Department of Clinical Biochemistry, Faculty of Medicine, King Abdulaziz University, Rabigh, Saudi Arabia

OPEN ACCESS

Edited by:
Fanpei G. Yang,
National Tsing Hua University, Taiwan

Reviewed by:
Ioannis Haranas,
Wilfrid Laurier University, Canada
Rekha Khandia,
Barkatullah University, India

***Correspondence:**
Ghulam Md Ashraf
ashraf.gm@gmail.com;
gashraf@kau.edu.sa
Athanasios Alexiou
alextha@yahoo.gr;
alexiou@ngcef.net

† These authors have contributed equally to this work and share first authorship

Received: *26 August 2021*
Accepted: *22 October 2021*
Published: *26 November 2021*

Citation:
Ashraf GM, Chatzichronis S, Alexiou A, Kyriakopoulos N, Alghamdi BSA, Tayeb HO, Alghamdi JS, Khan W, Jalal MB and Atta HM (2021) BrainFD: Measuring the Intracranial Brain Volume With Fractal Dimension. Front. Aging Neurosci. 13:765185. doi: 10.3389/fnagi.2021.765185

A few methods and tools are available for the quantitative measurement of the brain volume targeting mainly brain volume loss. However, several factors, such as the clinical conditions, the time of the day, the type of MRI machine, the brain volume artifacts, the pseudoatrophy, and the variations among the protocols, produce extreme variations leading to misdiagnosis of brain atrophy. While brain white matter loss is a characteristic lesion during neurodegeneration, the main objective of this study was to create a computational tool for high precision measuring structural brain changes using the fractal dimension (FD) definition. The validation of the BrainFD software is based on T1-weighted MRI images from the Open Access Series of Imaging Studies (OASIS)-3 brain database, where each participant has multiple MRI scan sessions. The software is based on the Python and JAVA programming languages with the main functionality of the FD calculation using the box-counting algorithm, for different subjects on the same brain regions, with high accuracy and resolution, offering the ability to compare brain data regions from different subjects and on multiple sessions, creating different imaging profiles based on the Clinical Dementia Rating (CDR) scores of the participants. Two experiments were executed. The first was a cross-sectional study where the data were separated into two CDR classes. In the second experiment, a model on multiple heterogeneous data was trained, and the FD calculation for each participant of the OASIS-3 database through multiple sessions was evaluated. The results suggest that the FD variation efficiently describes the structural complexity of the brain and the related cognitive decline. Additionally, the FD efficiently discriminates the two classes achieving 100% accuracy. It is shown that this classification outperforms the currently existing methods in terms of accuracy and the size of the dataset. Therefore, the FD calculation

for identifying intracranial brain volume loss could be applied as a potential low-cost personalized imaging biomarker. Furthermore, the possibilities measuring different brain areas and subregions could give robust evidence of the slightest variations to imaging data obtained from repetitive measurements to Physicians and Radiologists.

Keywords: aging, biomarkers, fractal dimension, intracranial brain volume, MRI, neuroinformatics, OASIS brain database, VoxelMorph

INTRODUCTION

The quantitative measurement of the human brain volumes using segmentation software is highly correlated with the monitoring of neurodegeneration disorders (Jack et al., 2000; Kovacevic et al., 2009; Alexiou et al., 2017, 2019, 2020; Mantzavinos and Alexiou, 2017; Chatzichronis et al., 2019). Therefore, a few algorithms and online MRI databases are available for the assessment of the brain structure, measuring intrasessions and intersessions for the same subject, also applying procedures for potential manual repositioning differences from longitudinally acquired MRI, identification of artifacts, and segmentation errors (Dale et al., 1999; Fischl et al., 2002; Brewer et al., 2009; Fischl, 2012; Maclaren et al., 2014). While a reliable brain volume decline can be characterized as unbiased if and only if the loss is large enough (Narayanan et al., 2020), and by taking into consideration that brain lesions and brain atrophy associated with mild cognitive impairment (MCI) are higher than the expected decline per year in non-demented older adults (Liu J. Z. et al., 2003; Liu R. et al., 2003; Fotenos et al., 2005, 2008; Maclaren et al., 2014), any sources of high statistical variation, due to technical or physiological fluctuations, could be crucial for the reliability of the MRI results as a dementia biomarker (Caramanos et al., 2010; Fonov et al., 2010; Borghi and Van Gulick, 2018; Narayanan et al., 2020). In contrast, recent clinical studies suggest that the cortical functional connectivity networks show fractal properties and that any fluctuations to the fractal dimension (FD) of the brain gray and white matter are highly correlated with cognitive decline (Ha et al., 2005; Im et al., 2006; Li et al., 2007; King et al., 2009; Mustafa et al., 2012; Varley et al., 2020).

Biological structures similar to the brain gray matter usually have rough surfaces and are characterized by heterogenicity and self-similar structures. This mathematical self-similarity is the repetitive display of the whole structure after lowering the scaling. When the scale is altered, the structures are changed repeatedly, implying that the biological networks follow self-similarity patterns (Cerofolini et al., 2008). As the scale diminishes, the fractal becomes more complex (Kazemi Korayem et al., 2018). The definition of FD gives the complexity of these structures. The FD can reveal the properties and the mechanisms for the roughness of a structure. For example, if a fractal shape has a dimension of 2.3, it is more simplified than a 3D cube but more complicated than a 2D square. This non-Euclidean approach can be applied to minimize errors in the visualization of brain gray matter. One of the most common algorithms for calculating the FD and detecting image details is the box-counting algorithm. First, the fractal object is covered by a grid structured with small boxes of equal size. Each box should contain at least one region belonging to the fractal. Then, the number of boxes is counted. The next step is to design the grid again with the same properties but smaller square boxes. The abovementioned procedure is the traditional method where no lattices between squares or overlaps exist (Yadav and Nishikanta, 2010).

In amyotrophic lateral sclerosis (ALS), it is proved that the FD of brain white matter skeleton and general structure is significantly different between ALS patients with corticospinal tract hyperintensity and those with frontotemporal dementia groups (Rajagopalan et al., 2013; Di leva et al., 2015). Furthermore, while the numerical identification of differences

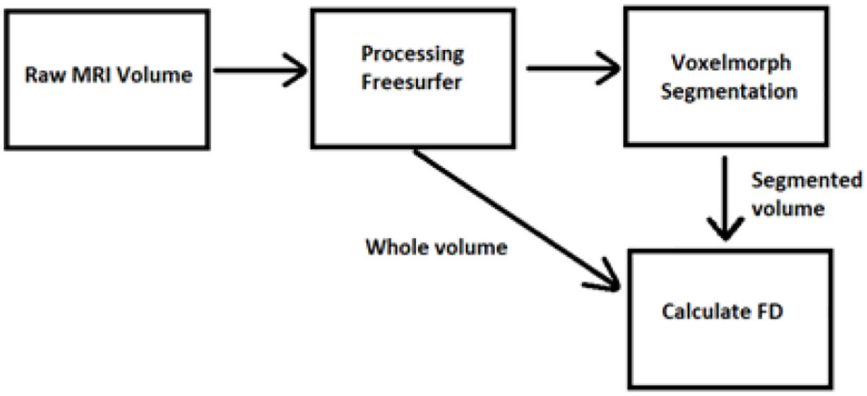

FIGURE 1 | The algorithm of the proposed method – software.

in brain FD is still an open problem (Varley et al., 2020) and simultaneously could be a very strong evidence biomarker of consciousness disorder, we present new software in this study for handling MRI images and measuring FD of brain volume. We trained a learning-based registration tool using data obtained from the Open Access Series of Imaging Studies (OASIS) database (Marcus et al., 2007, 2010). The latest version of this database, i.e., the OASIS-3 (LaMontagne et al., 2019), includes a longitudinal neuroimaging, clinical, cognitive, and biomarker dataset for normal aging and Alzheimer's disease (AD) from 2,168 MRI sessions and 1,608 PET sessions to more than 100 participants (LaMontagne et al., 2019). The participants in this database were classified according to their Clinical Dementia Rating (CDR). The brain MRI

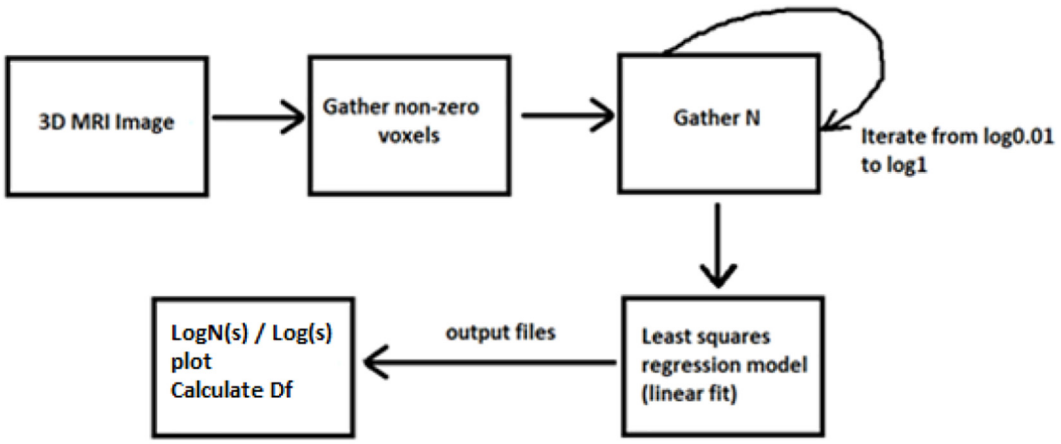

FIGURE 2 | Visualization of computing fractal dimension (FD).

TABLE 1 | Fractal dimension calculation software.

Software	Approach	Main properties
BENOIT	Measures the FD and hurst exponent of datasets using various methods to analyze self-similar patterns and self-affine traces, also applying a white noise filter	There are two main versions, for Windows and Matlab. The input data formats can be only: For 1D traces and size-frequency data, text format or MS-Excel format, for 2D patterns: BMP files and for 3D objects (available only in Matlab) BMP files, where the 3D object should be represented as a number of 2D slices.
Fracdim (Fractal Dimension Java Applet)	Calculates the box-counting dimension using a Monte Carlo algorithm.	This Java Applet imports only a set of points in a CSV file or an image, but the user is prompt to supply an image that has been thresholded to show where the fractal pattern is.
FracLac (Fractal Dimension and Lacunarity, part of ImageJ)	Describes morphology details represented in binary or grayscale digital images, using mass and box-counting FD and multi-fractal analysis data	Provide calculations and graphs. This plugin works on binary images and grayscale images or grayscale images converted to RGB. The images must be thresholded before analysis to ensure that only the pixels of interest are assessed.
Fractal analysis system for Windows	Calculates FD by the method of box-counting after preprocessing	This software calculates FD from rjb, png, pcx, jpg, and thinning images after preprocessing.
Fractal Dimension Estimator	Measures the FD of a 2D image using the box-counting method	This software measures the FD of a 2D image using the box-counting method after applying an RGB threshold to convert the image into binary data.
Fractaldim-package	Estimates an FD of the given data, using different methods regarding the type of dimensional time series	The package provides tools for estimating the FD of 1d or 2d data.
Fractalyse (Fractal Analysis Software)	Computes the FD of the black and white image, curve, and network	It is a software application for computing FD of 2D bitmap images, vector images, and networks.
Gwyddion	A modular program for scanning probe microscopy (SPM) data visualization and analysis	It is a modular program for several SPM data formats visualization and analysis.
HarFA (Harmonic and Fractal Image Analysis)	Performs harmonic and wavelet analysis of digitized images and calculations their fractal parameters	The software provides tools for estimating the FD and other statistical parameters of 2D images.
Hausdorff (Box-Counting) **Fractal Dimension**	Returns the Hausdorff FD of an object represented by its binary image	A MATLAB module returns the Hausdorff fractal dimension of an object represented by a binary image.
UJA-3DFD	Computes the 3D FD from brain MRI, calculating the 3D box-counting of the brain's entire volume and 3D skeletonization	This software calculates the FD in 3D images. However, it offers only FD calculation for the whole brain volume and not each brain region separately.

imaging sessions include T1-weighted (T1w), T2-weighted (T2w), fluid attenuated inversion recovery (FLAIR), arterial spin labeled (ASL), susceptibility weighted imaging (SWI), time of flight, resting-state blood oxygenation level dependent (BOLD), diffusion tensor imaging (DTI) sequences, PET imaging from three different tracers, C-Pittsburgh compound B (PIB), amyloid imaging tracer (AV45), and fluorodeoxyglucose (FDG) (LaMontagne et al., 2019). In the following sections, the algorithms for measuring the intracranial brain volume using the FD will be described based on the MRI brain data (**Figures 1**, **2**).

MATERIALS AND METHODS

There is a rapidly increasing interest in box-counting algorithms in biology and medicine, such as applying fractal geometry for efficient recognition and capture of circulating cancer cells (Zhang et al., 2013; Maipas et al., 2018) and the correlation between the fractal property distribution and aging (Varley et al., 2020). Fractals have the property of self-similarity in various scales, and when the scale is altered, the structures are changed repeatedly. Furthermore, biological structures present complex fractal patterns similar to brain structures (Hofman, 1991; Varley et al., 2020). Therefore, depending on the image resolution and noise, FD may evaluate the condition of specific tissues such as the cerebral cortex (Blanton et al., 2001; Todoroff et al., 2014). In addition, the FD can influence the neurodegeneration analysis progression (Carstensen and Franchini, 1993; Jelinek and Fernandez, 1998; Pereira, 2010). While brain white matter loss is one of the characteristic lesions during neurodegeneration and other related disorders, measuring any structural brain change with high precision will act as a very effective and low-cost personalized imaging biomarker. Additionally, any geometric structural brain changes could be an excellent factor in measuring variations in the

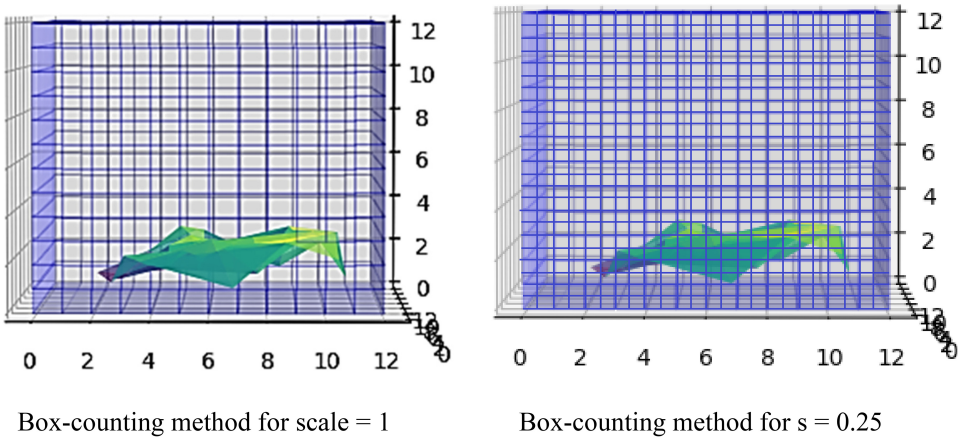

FIGURE 3 | The algorithm calculating FD in 3D examples.

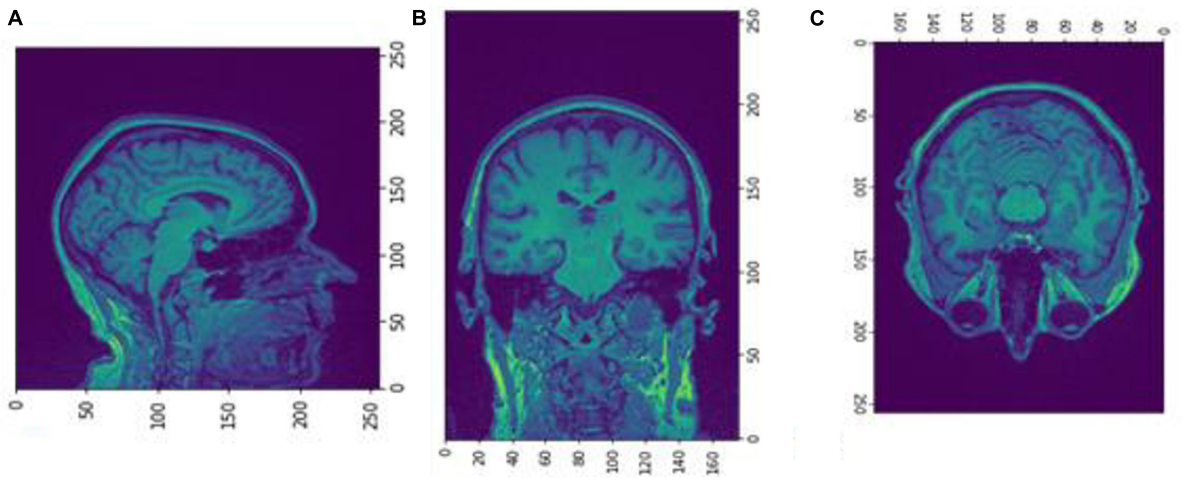

FIGURE 4 | Slices **(A)** Sagittal, **(B)** coronal, and **(C)** axial planes. The output of FreeSurfer of session OAS30001_MR_d0129. This volume is imported in FreeSurfer and later exported as a.mgz file. The images are shown using NiBabel library version 3.2.1 (https://zenodo.org/record/4295521#.YCpJqeqxWMI).

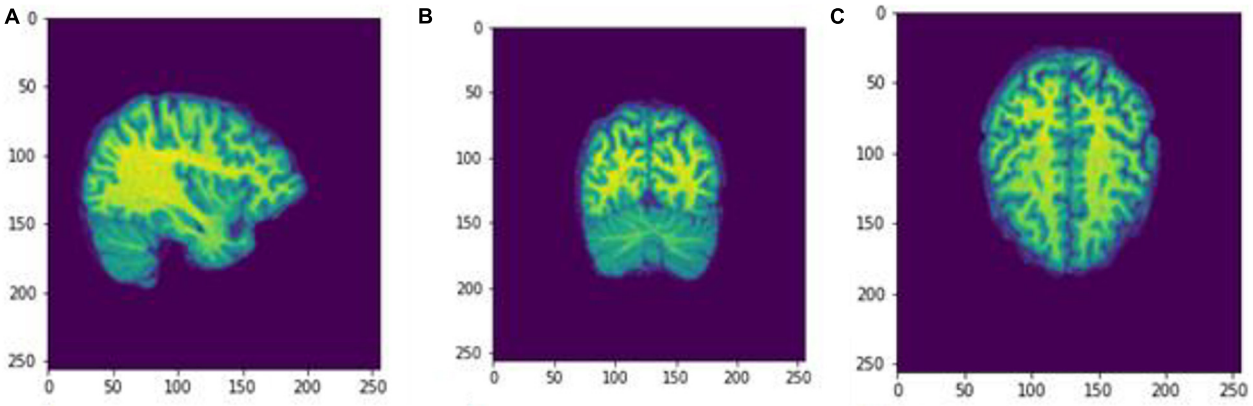

FIGURE 5 | Slices **(A)** Sagittal, **(B)** coronal, and **(C)** axial planes. The output of FreeSurfer of session OAS30001_MR_d0129 as NIfTI files. This volume shall be imported later as a cropped image.npz file into the Box-Counting FD calculator. The images are shown using NiBabel library version 3.2.1 (https://zenodo.org/record/4295521#.YCpJqeqxWMI).

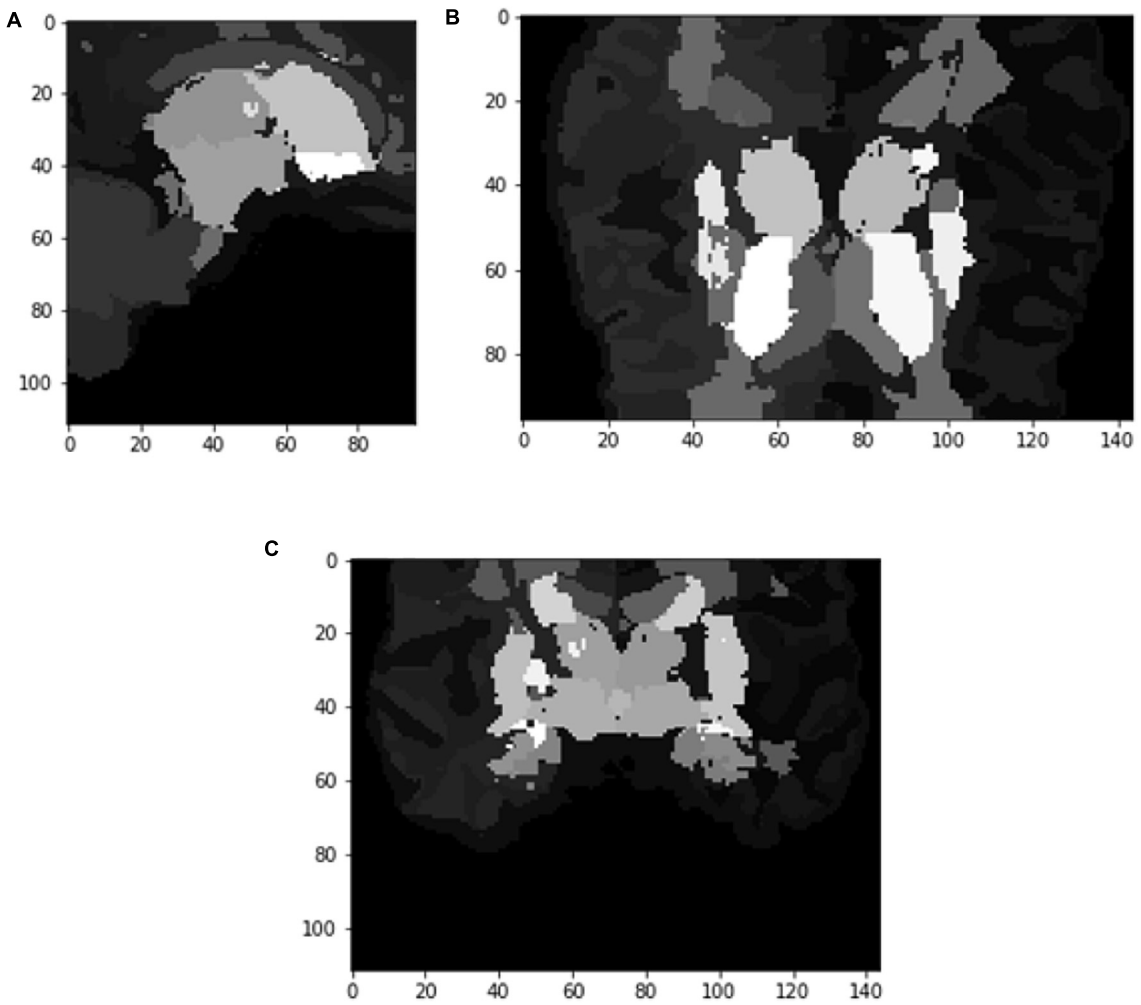

FIGURE 6 | Slices **(A)** Sagittal, **(B)** coronal, and **(C)** axial planes. The output of VoxelMorph of session OAS30319_MR_d0043. Each brain structure has a unique label with grayscale values varying from 0 to 40. Later with filtering, each region is separated, and the Box-Counting FD is calculated. The images are shown using NiBabel library version 3.2.1 (https://zenodo.org/record/4295521#.YCpJqeqxWMI).

structural neural plasticity, while FD measures the roughness of surfaces, and software can be used to calculate the FD of an image (**Table 1**).

Compared to other tools, we succeeded in implementing the image segmentation of brain regions in a 3D fashion.

The box-counting algorithm is the most commonly used technique for FD measurement (Schaefer et al., 1991; Fernández-Martínez and Sánchez-Granero, 2014; Joosten et al., 2016; Soltanifar, 2021), calculating the Minkowski–Bouligand dimension as follows:

$$D_{\text{box}}(S) = \lim_{g \to 0} \left(\frac{\log N(\varepsilon)}{\log\left(\frac{1}{\varepsilon}\right)} \right), \quad (1)$$

$D_{box}(S)$ is the FD of the box, S is the fractal, $N(\varepsilon)$ is the number of boxes, and ε is the scaling factor. The parameter ε is computed with the formula $\varepsilon = \frac{1}{s}$ where s is the length of each box. The majority of related studies mainly introduce the FD calculation from 2D MRI images, while others apply the multifractal analysis to examine different dynamics in the system. In our case, we have only calculated FD with a box-counting algorithm for the 3D brain structures. By calculating a whole 3D image instead of 2D scans, we ensure better accuracy in results.

The concept of this algorithm in our study is to divide the 3D image into cubes. The 3D image includes a region of interest (ROI). Then, we calculate the number of N cubes with length ε of each box as part of the ROI. By applying equation (1) in each iteration, we calculate the FD. If the variable D in every iteration has a slight deviation, then logN/logs are stable, which means a linear correlation between logN and logs. In that case, the complexity of the structure can be efficiently described by FD. If not, the multifractal analysis is required to effectively describe the structure while other

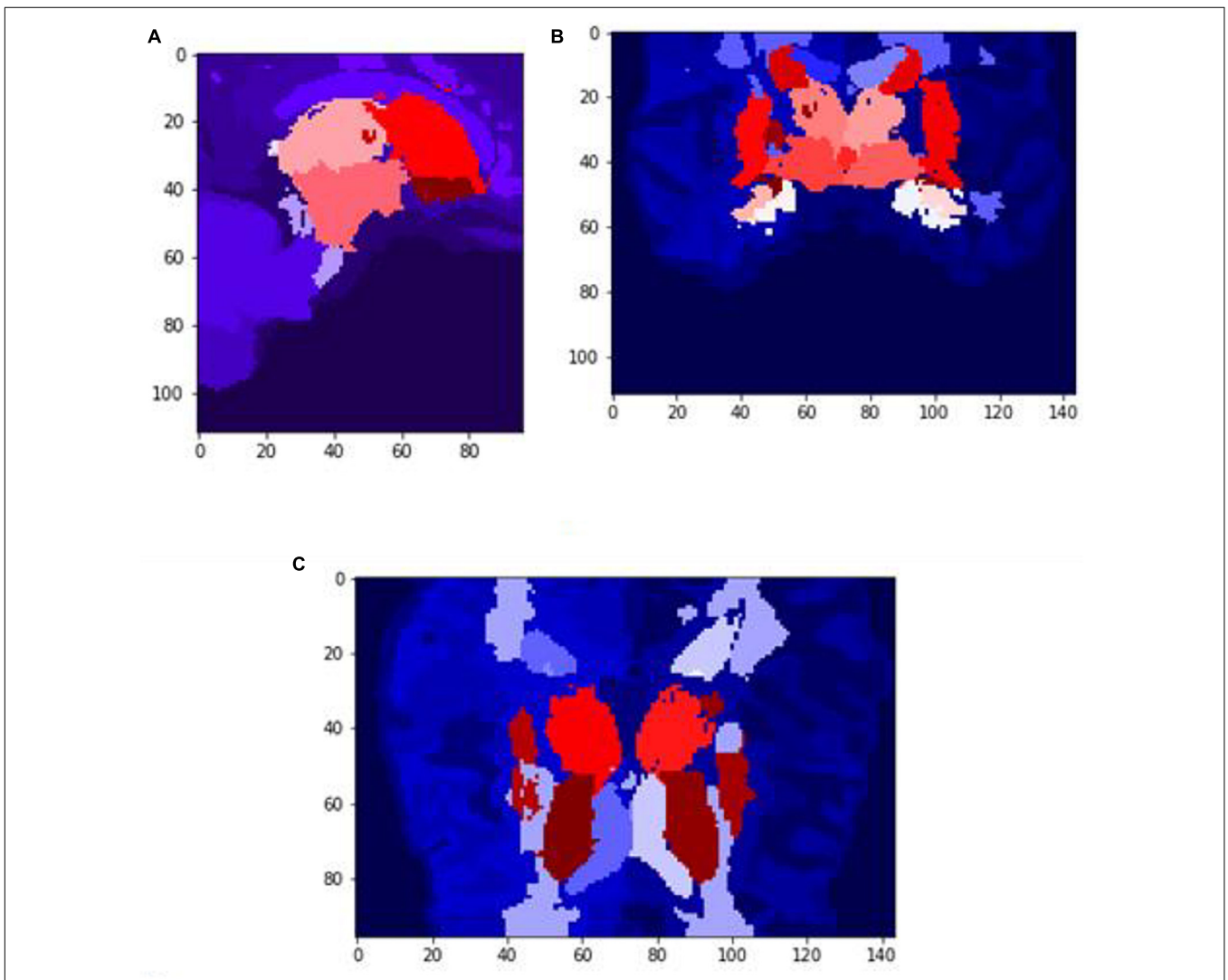

FIGURE 7 | Slices **(A)** Sagittal, **(B)** coronal, and **(C)** axial planes. The output of VoxelMorph of session OAS30319_MR_d0043. Each brain structure has been colored differently.rgb values. The images are shown using NiBabel library version 3.2.1 (https://zenodo.org/record/4295521#.YCpJqeqxWMl).

dynamics are included in the system in which FD cannot efficiently describe (**Figure 3**).

The data have been acquired from OASIS-3 (LaMontagne et al., 2019), which includes MRI (Berger, 2002; Grover et al., 2015; Chow et al., 2017) and PET (Willemsen and van den Hoff, 2002) data. We have used T1w MRI images (Chavhan et al., 2009; Yokoo et al., 2010), which have been later imported into the FreeSurfer (Fischl, 2012) for further image processing (Deserno Né Lehmann et al., 2013; Uchida, 2013). Then, the data were cropped to fit into the VoxelMorph software (Dalca et al., 2019) to perform image segmentation (Karsch et al., 2009; Despotović et al., 2015; Bui et al., 2017; Mondal et al., 2018; Buda et al., 2019; Dalca et al., 2019; Dolz et al., 2019; Rickmann et al., 2019, 2020; Cerri et al., 2020, 2021).

Our study has included 609 adults with normal cognitive ability (controls) and 489 multiple-staging dementia subjects aged from 42 to 95 years old, totaling 1,961 scan sessions. Each subject had multiple scan sessions, and each session included raw images from the MRI scanner. Some of them may have an additional file processed by FreeSurfer. Those files are already processed, so they are used in our next stage, avoiding image processing. The raw data obtained from the OASIS-3 brain dataset (LaMontagne et al., 2019) in the form of T1w 3D MRI images following the Neuroimaging Informatics Technology Initiative (NIfTI) format (Larobina and Murino, 2014), while the processed files by FreeSurfer follows the.mgz format. The FreeSurfer has been used for the initial image processing (Fischl, 2012), such as Motion Correction and Conform Non-Uniform intensity normalization, Talairach transform computation, Intensity Normalization, Skull Stripping, Linear volumetric registration, and CA Intensity normalization. The abovementioned methods export the data into the preprocessed images of (256, 256, 256) resolution. However, all the processing and post-processing steps of FreeSurfer were not executed to reduce time complexity, while VoxelMorph is more efficient for image segmentation. Furthermore, the image files are converted from.mgz to.npz format and then cropped to fit the (160, 192, 224) dimensions required to apply the VoxelMorph algorithm to the segmentation of brain volumes.

There are many segmentation algorithms based on supervised learning, but with high complexity, similar to the FreeSurfer. Their training procedures rely on labeled images, which means that they are accurate for specific scenarios. However, when a new dataset is tested with different contrast levels, additional training is required. Other methods include convolutional neural networks, which perform better during the testing, but they lose accuracy when changes occur in the intensity distribution of the tested images. In contrast, VoxelMorph is an UNet architecture using an unsupervised Bayesian approach, which tackles the drawbacks of those methods and has faster performance. To train a model, a brain atlas with multiple 3D MRI scans with no manual delineations is required. Instead, each voxel of the atlas has a vector with prior probabilities for each segmented label. Thus, when importing a new dataset with distinct unobserved contrast, the VoxelMorph algorithm does not require training the network again for new labels. Instead, it is automatically adapted due to its unsupervised

TABLE 2 | The iteration steps to calculate the box-counting FD for the whole volume of session OAS30001_MR_d0129.

Scale	*N*
1.023292992280754	6.84523
1.146832521422478	4.85708
1.285286659943615	3.45522
1.440456010246376	2.45680
1.614358556826486	1.75729
1.809255910253820	1.26666
2.027682719521282	8.95650
2.272479635270844	6.40170
2.546830252585041	4.54770
2.854302513786581	3.25020
3.198895109691398	2.35480
3.585089482765549	1.63960
4.017908108489400	1.15920
4.502979812880891	8.62700
5.046612975635284	6.18900
5.655877570891540	4.14000
6.338697112569270	3.11100
7.103951700029557	2.23500
7.961593504173188	1.62600
8.922776195878269	1.10200

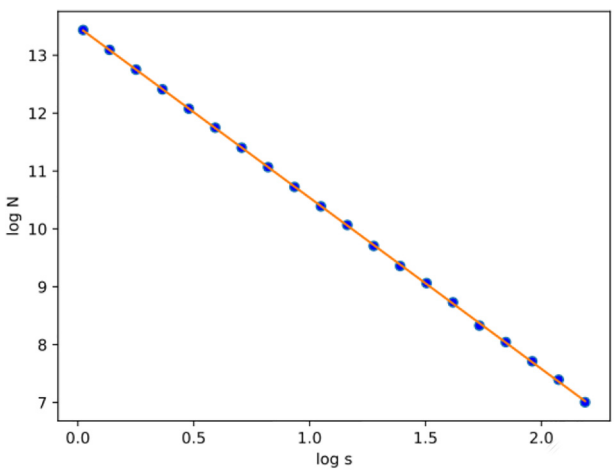

FIGURE 8 | After calculating the logN/logs plot spots using the least square error, the fitted line is estimated for subject OAS30001_MR_d0129. Experiments have shown that at least 20 iterations were enough to estimate FD. Also, the linear relation of logN and logs suggests that FD efficiently describes the complexity of the structure; therefore, the multifractal analysis is not required. Root-mean-square error (RMSE) can describe how well a linear regression model describes the data. For data points close to the output line of the regression model, RMSE is expected to be low; therefore, the estimated FD is close to the theoretical solution. The two variables used in the linear regression model are the number of boxes (*N*) and the current scale (s). If a linear relationship describes the two variables, then the structure can be described by FD. If not, the structure is considered to have multifractal properties.

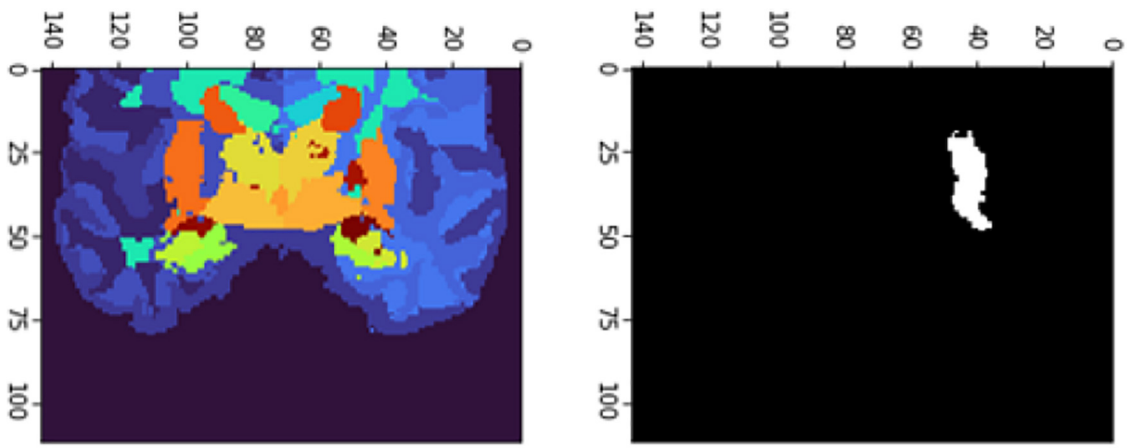

FIGURE 9 | 2D scan from the output volume of subject OAS30319_MR_d0043. We have chosen the third ventricle of the brain structure with an intensity value of 26.

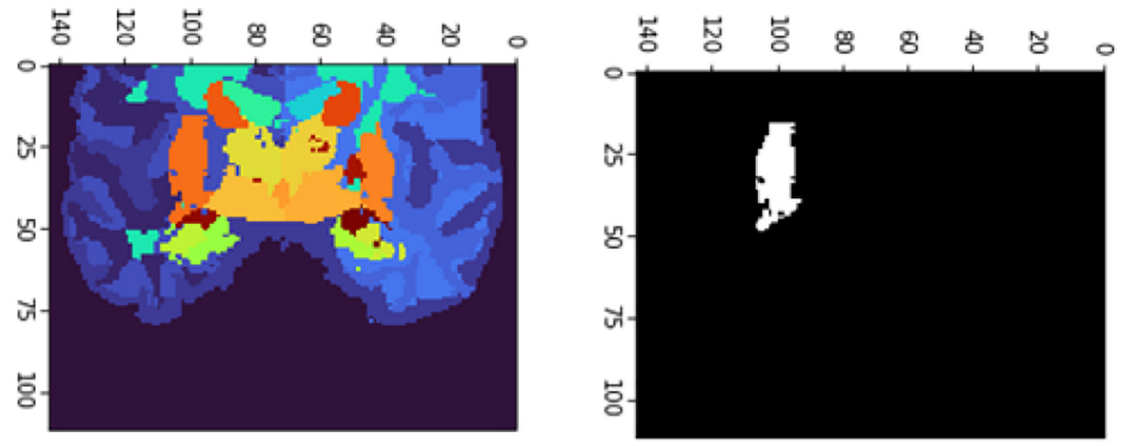

FIGURE 10 | 2D scan from the output volume of subject OAS30319_MR_d0043. We have chosen the right putamen of the brain structure whose intensity value equals 27.

nature. VoxelMorph has been mainly tested on T1w MRI scans. The brain structures delineated from VoxelMorph are the cerebral cortex, white matter, lateral ventricle, cerebellar cortex, white matter, thalamus, caudate, putamen, pallidum, brain stem, hippocampus, and amygdala. One exclusive session from each patient is used to train the model to avoid including dependent measurements.

TABLE 3 | Box-counting FD testing on multiple sessions corresponding to various subjects.

Session	FD		
	Whole volume	Third ventricle	Right putamen
OAS30319_MR_d0043	2.95129	2.37498	2.59033
OAS30524_MR_d0198	2.95208	2.35327	2.50763
OAS31101_MR_d0076	2.95413	2.36024	2.52151
OAS31170_MR_d2410	2.95321	2.34761	2.54668

RESULTS

We executed two experiments. The first was a cross-sectional study that separated data into two CDR classes, 0 and greater than 1. VoxelMorph is used to train a model for each class. In the second experiment, we trained a model on multiple heterogeneous data and evaluated the FD development for each subject through multiple sessions. Random subjects have been chosen, and their development through FD metrics was assessed. In the following tables and figures for the OAS30001_MR_d0129 session, the whole process is implemented. The id of the session is defined from the id of the patient, i.e., 30001 and 0129, in the days since the subject was included in the study. OAS stands for OASIS database and MR for MRI. The raw data images from the MRI scan were imported on the software (**Figure 4**). The output is shown in **Figure 5**. We imported the images into VoxelMorph with a pretrained model run in Kaggle Kernel (i.e., 120 epochs, batch size of 1, and 19 sessions) to distinguish the brain areas. These

Kaggle Kernel parameters were chosen only due to the restrictions of memory.

Figures 6, **7** show the segmented brain, with each region having a unique value ranging from 0 to 40. After segmentation, the FD is calculated for the brain regions, as shown in **Table 2**. Multiple experiments have shown that 20 iterations gave an efficient convergence to the box-counting FD, resulting in less time complexity (**Figure 8**). Iterations are related to the number of data points produced for each regression model. For example, 20 iterations correspond to 20 data points that are used to estimate the FD. During experimentation, it was observed that fewer iterations led to slightly different results. Using 20 or 25 iterations, the estimated FD was similar. However, more data points require more time to estimate. Therefore, choosing 20 data points is an efficient choice to balance time complexity and accuracy for the estimation of FD.

The FD is calculated for the brain regions corresponding to 26 and 27 intensity values (**Figures 9**, **10**) separately for four

TABLE 4 | Box-counting FD testing on multiple sessions of the same subject OAS30109.

Session	FD		
	Whole volume	**Third ventricle**	**Right putamen**
OAS30109_MR_d0270	2.946480299699088	2.3627751053697	2.5383689529296
OAS30109_MR_d0432	2.956639640069534	2.3414306913102	2.5583078971937
OAS30109_MR_d0997	2.957821984011597	2.3122620327539	2.5603106683312
OAS30109_MR_d2310	2.954899003322276	2.2987594704108	2.5215747308024

TABLE 5 | Box-counting FD testing on multiple sessions of the same subject OAS30052.

Session	FD			
	Whole volume	**Right thalamus proper**	**Left ventral DC**	**Clinical diagnosis**
OAS30052_MR_d0693	2.95047009894	2.519209063	2.397232208	No MCI Depression
OAS30052_MR_d1296	2.9475385443	2.518800477	2.407069774	No MCI No Depression
OAS30052_MR_d2709	2.9478168557	2.505436960	2.383144328	No MCI Depression
OAS30052_MR_d2737	2.9484438042	2.500205780	2.384530171	No MCI Depression

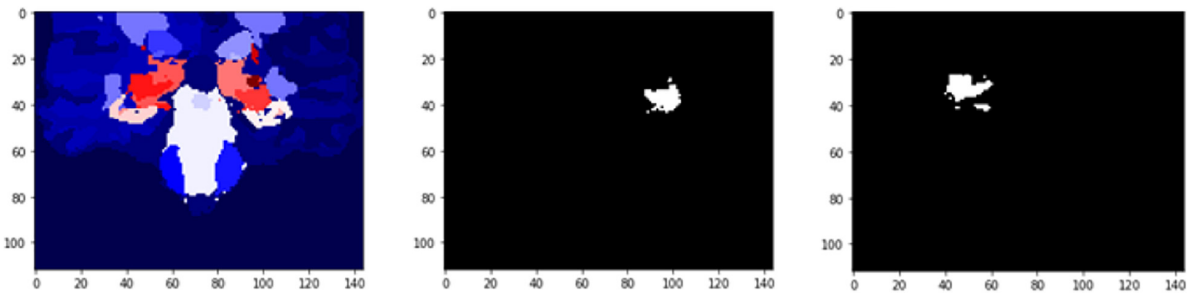

FIGURE 11 | 2D scan from the output volume of subject OAS30052_MR_d0693. Right Thalamus Proper and Left Ventral DC equal to 23 and 24 intensity values.

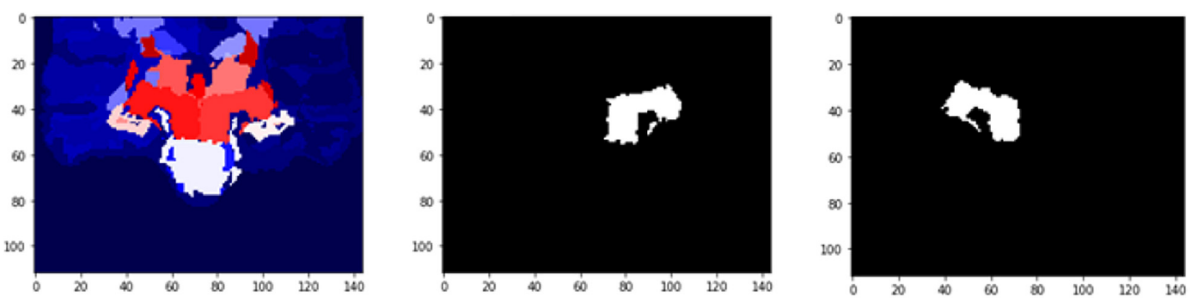

FIGURE 12 | 2D scan from the output volume of subject OAS30052_MR_d0693. We have chosen the Right Thalamus Proper and Left Ventral DC of the brain structures equal to 23 and 24 intensity values. The 2D scans are from different axial slices of the same subject compared with the 2D scans in **Figure 11**.

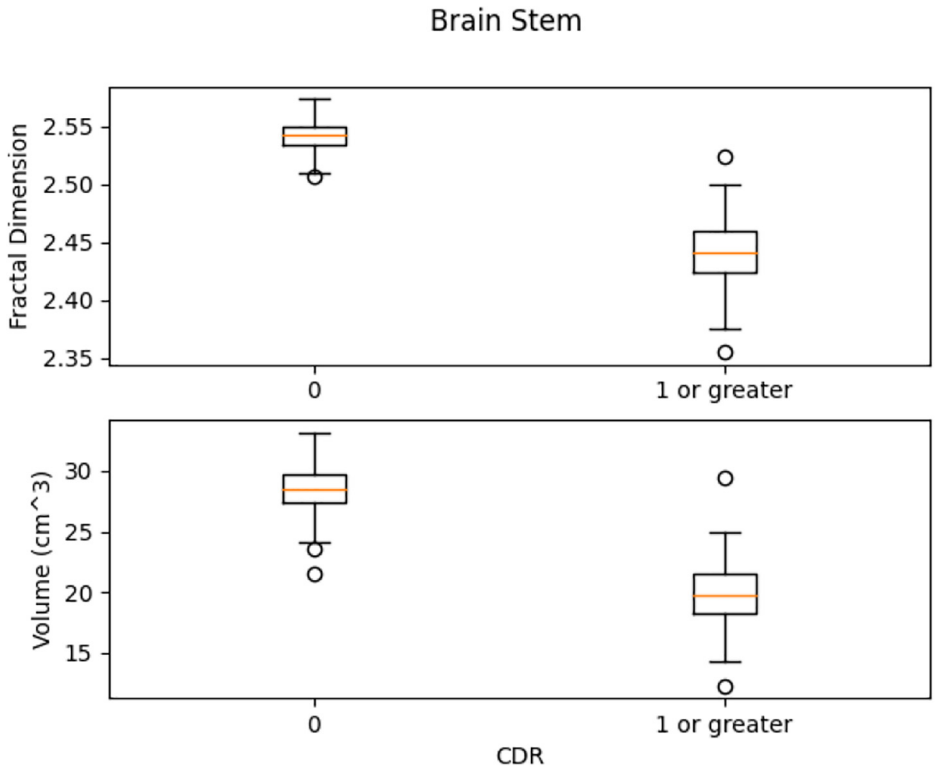

FIGURE 13 | Comparison of the distribution of health vs. control group. There is a slight overlap of the two classes in both features.

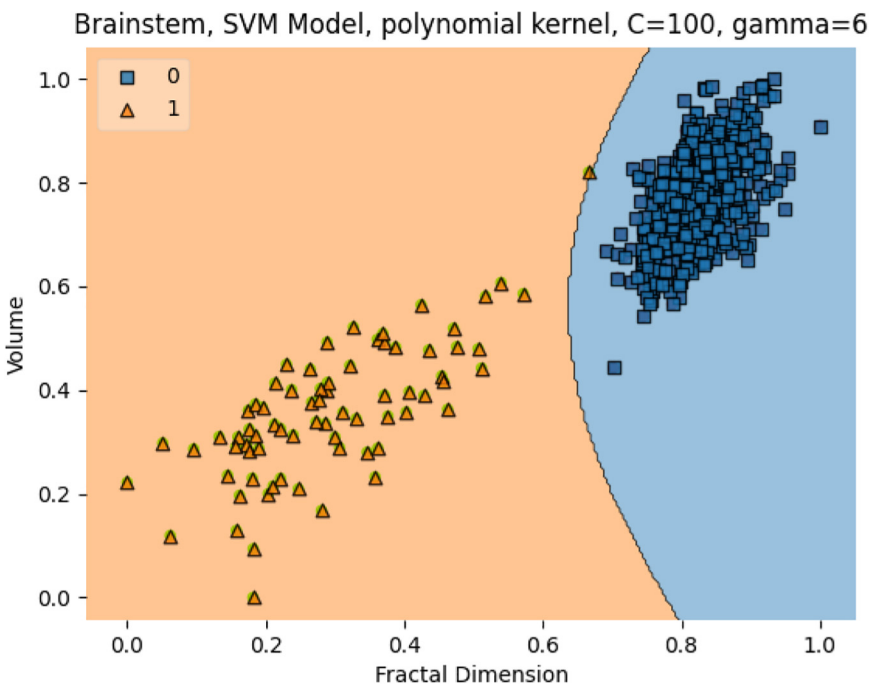

FIGURE 14 | The SVM model separating the two groups. Features are Volume and FD. Hyperparameters are regularization hyperparameter C = 100 and gamma = 6 with polynomial kernel.

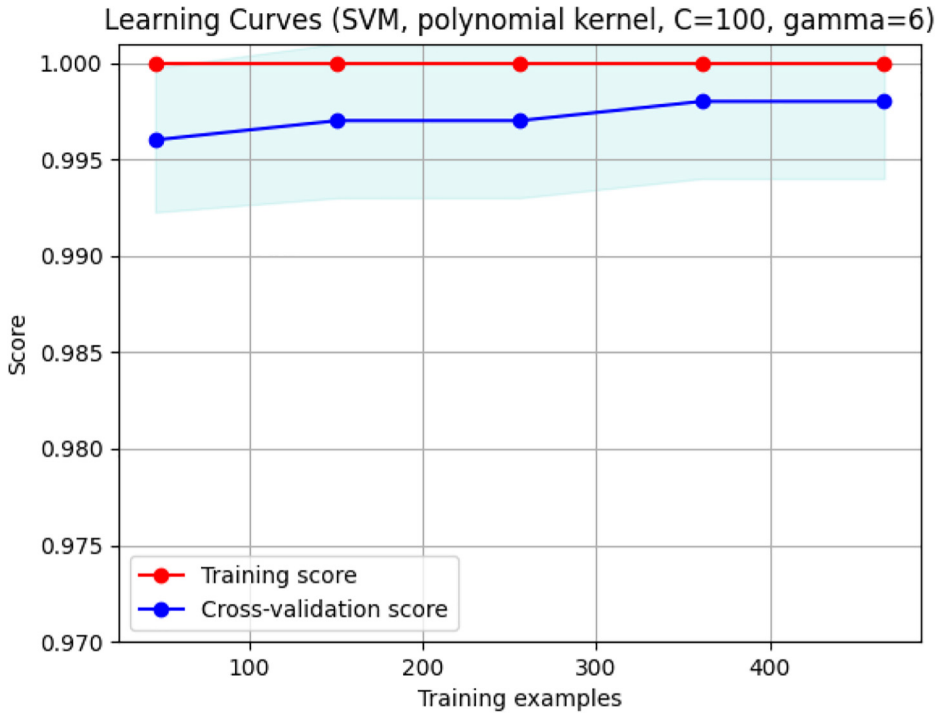

FIGURE 15 | The validation plot. It shows that for a training sample of approximately 480, maximum accuracy with no overfitting is achieved. With FD and Volume, the two groups are separated efficiently with 99.5% accuracy.

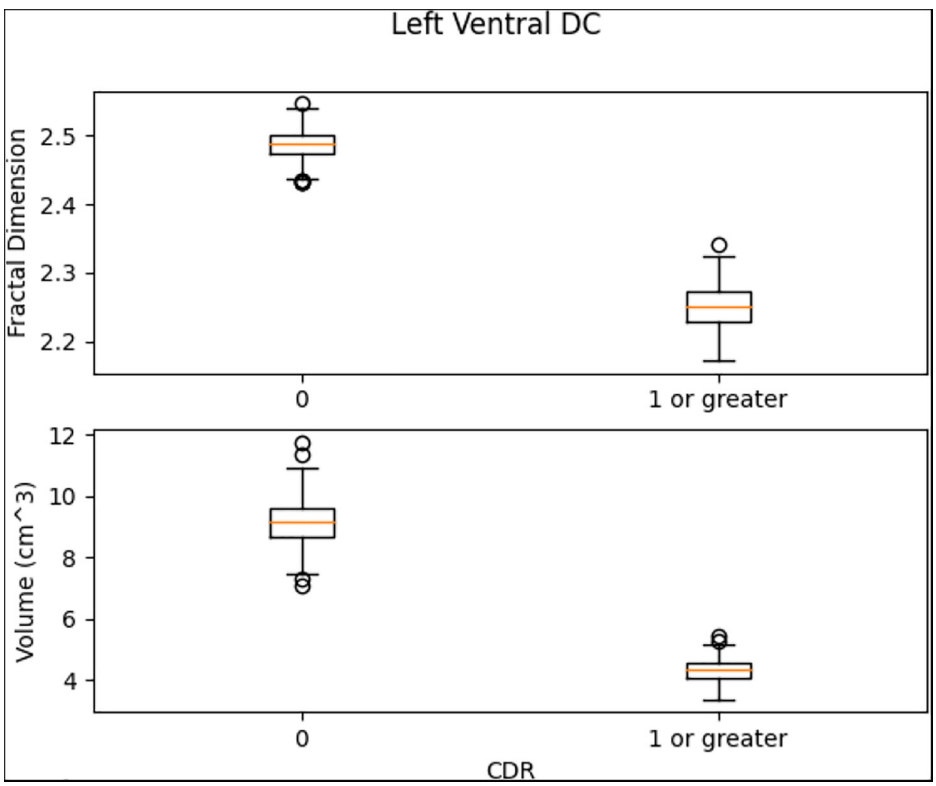

FIGURE 16 | The box plots for Left Ventral DC region.

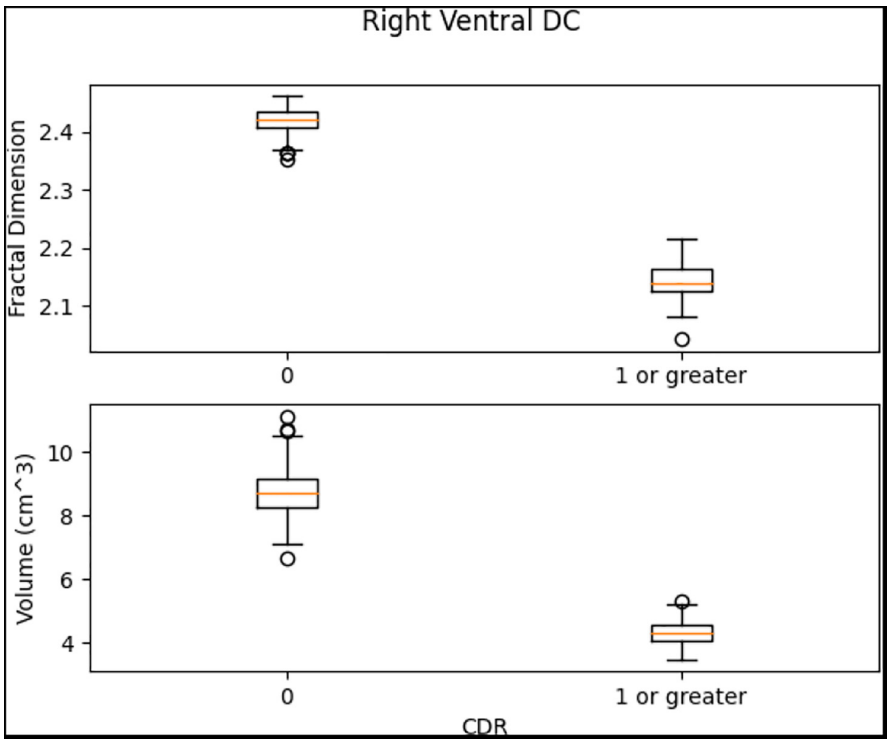

FIGURE 17 | The box plots for Right Ventral DC region.

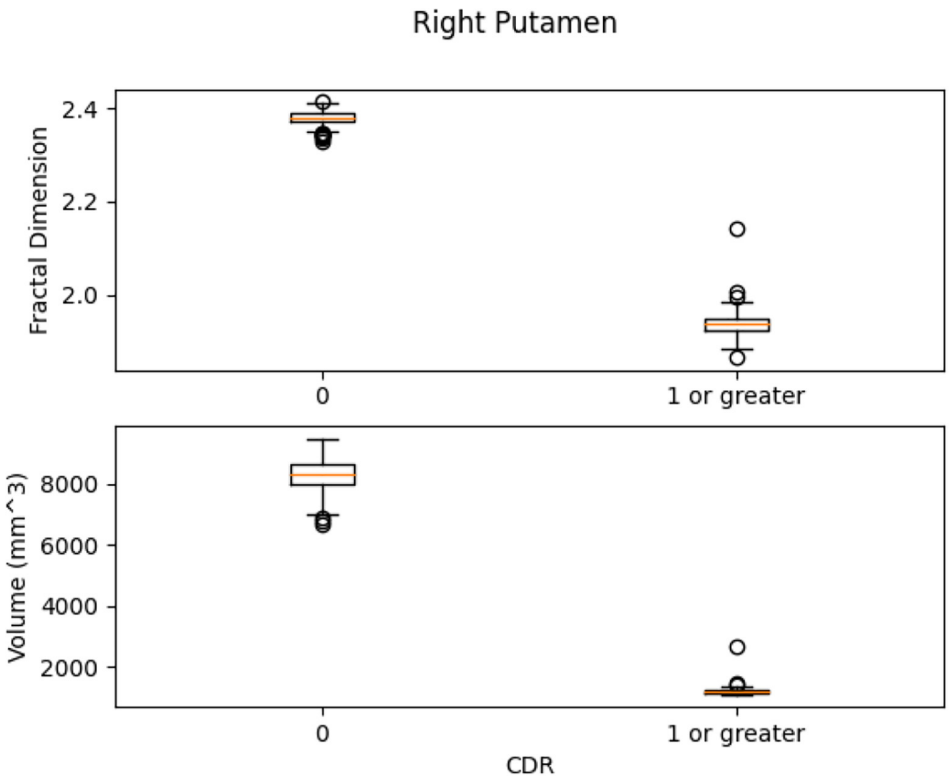

FIGURE 18 | The box plots for Right Putamen.

different subjects, namely, OAS30319, OAS30524, OAS31101, and OAS31170 (**Table 3**). In addition, the software has the functionality of measuring the FD for different subjects on the same brain regions, with high accuracy and resolution, offering the ability to compare brain data regions from different subjects and on multiple sessions.

Extending the functionality described in **Table 3**, the software calculates and compares FD for the same subject and repetitive MRI measurements. This procedure is not yet presented widely (Krohn et al., 2019). **Table 4** calculates the FD of the whole brain volume for the Third Ventricle and Right Putamen, respectively, of the same subject, OAS30109, and four different MRI sessions. OAS30109 is recorded at the initial clinical diagnosis as Female, Aged 72.27, Handedness Right, Education level 13, and Caucasian Race. During the repeated clinical evaluations for OAS30109 on days 1,102, 2,237, and 3,000, there was no report for MCI, dementia, or other neurological conditions, resulting in cognitive impairment or neuropsychological problems. We observed an average of 0.3% variation from the minimal variation of FD.

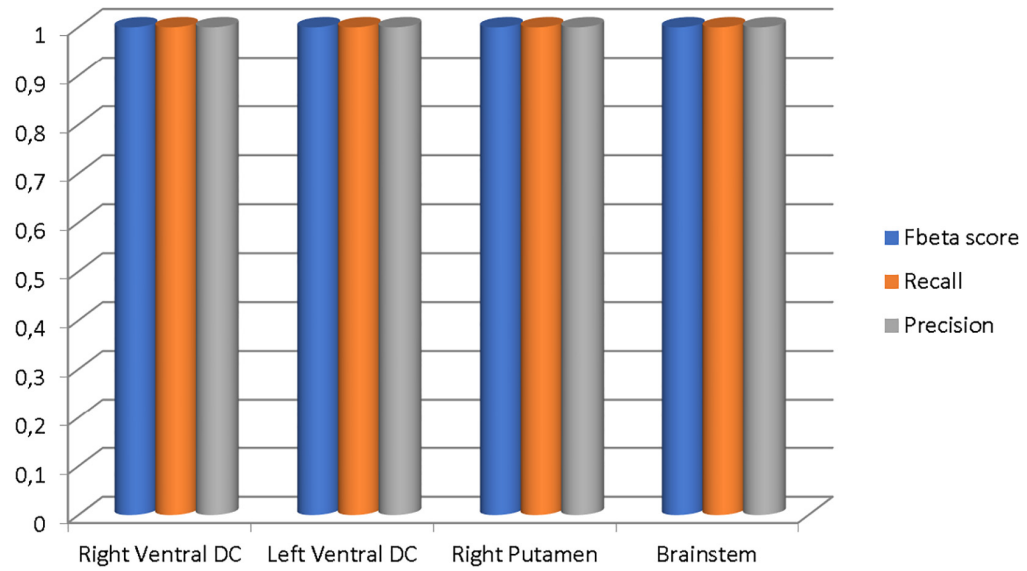

FIGURE 19 | The Fbeta score, recall, and precision metrics of the classifications performed in each brain region.

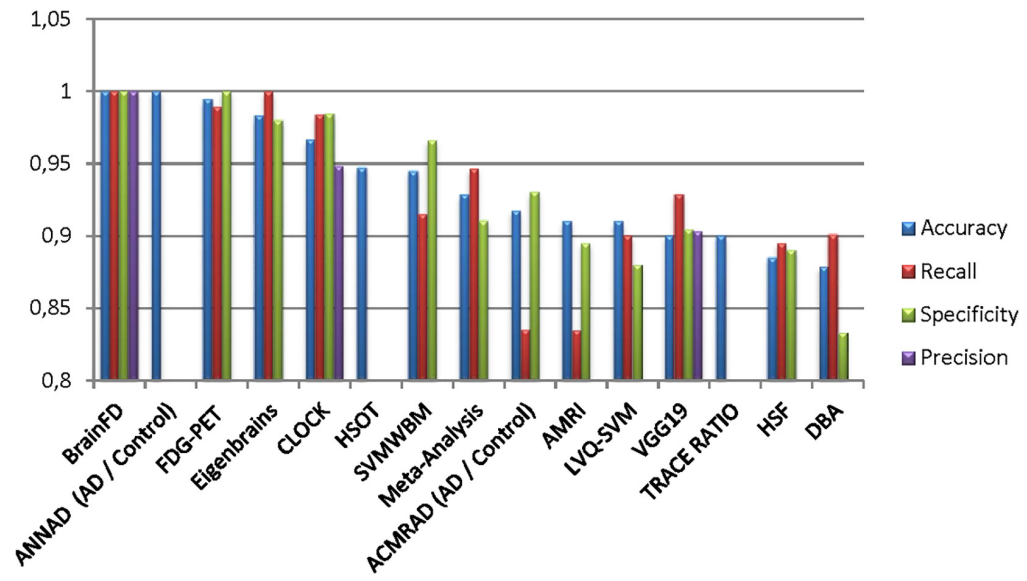

FIGURE 20 | Comparison of the current classification (BrainFD) with other methods. Each compared method corresponds to the following bibliography, respectively (Huang et al., 2008; Kloppel et al., 2008; Magnin et al., 2009; Desikan et al., 2009; Lopez, 2009; Ortiz et al., 2013; Dukart et al., 2013; Yong et al., 2014; Bharanidharan and Rajaguru, 2018; Chen et al., 2020).

OAS30052 is also recorded at the initial clinical diagnosis as Female, Aged 59.02, Handedness Right, Education level 18, and Caucasian Race, diagnosed with depression. However, during the repeated clinical evaluations for OAS30052 on days 0728, 1,512, 2,650, and 3,028, there was no report for MCI, dementia, or other neurological conditions. Still, there was a report for depression, except for the clinical diagnosis on day 1,512.

The results (**Table 5**) are verified from the corresponding variation of FD concerning the whole brain volume and the regions corresponding to Left Ventral DC and Right Thalamus Proper (**Figures 11**, **12**). There was an increase of FD of more than 0.4% during the first and the second clinical assessment and again a continuous decrease. **Figures 11**, **12** correspond to 2D scans from different axial slices of the same subject, even though the FD calculation has been obtained, as in every case, from the 3D brain model for maximizing the accuracy. Thus, even though the pathophysiology of depression may be identified in many brain regions (Pandya et al., 2012), we have chosen the Right Thalamus Proper and Left Ventral DC as the subareas of the thalamus. Recent researches have revealed that brain areas implicated in depression are the amygdala, the hippocampus, and the thalamus, even though an exact formula of the correlation between volumetric abnormalities in these regions and the development of depression is not yet proved (Sheline et al., 1998; Kronmuller et al., 2008; MacQueen et al., 2008; Lorenzetti et al., 2009).

This experiment removed repeated sessions from each subject to delete any within-subject factor and perform a cross-sectional study. As a cross-sectional study, each session corresponded to one patient and *vice versa*. The subjects were separated into the classes of CDR = 0 (control group) and CDR $\leq$ 1 (patients with at least mild dementia). MRI sessions were not labeled, while CDR sessions are usually performed on different dates from the MRI sessions. Therefore, to label each MRI session, some criteria had to be applied. First, each MRI session had to have occurred between two CDR sessions of the same score. If the MRI session took place between two different CDR sessions with different MRI scores, the score from the closest CDR session could be selected, considering that the chosen CDR session was performed no further than 45 days from the MRI session. In the MRI session being close to only one CDR session, the threshold of 45 days had again been chosen to ensure that the dementia level was correctly assessed. In any other scenario, subjects were dropped out of this study. The control group consisted of 593 subjects and 73 subjects with at least mild dementia.

After labeling the data, we trained a segmentation model using VoxelMorph for each class. Then, each volume was segmented into brain regions with its corresponding class model. Second, using Python and scikit-learn package (Pedregosa et al., 2011), we trained efficient support vector machine (SVM) classifiers in Left Ventral DC, Right Ventral DC, Right Putamen, and Brain Stem to diagnose subjects with at least mild dementia (CDR = 1) and to discriminate them from the control group. Other regions within the ROI did not show any significant differences. Finally, we used SVM models with radial basis function (RBF) kernels to find the margin between the two classes and evaluated the results with five-fold validation. Figures suggest that even measurement with one variable, either volume or FD, subjects can be accurately classified with a precision of 100%.

In **Figure 13**, the box plots imply an overlap of the volumetric and fractal measurements of the brain stem. Two linear SVM models were trained. Volume and FD were used as features for each case. It is shown that the FD feature discriminates more efficiently between the two classes (**Figures 14**, **15**). The increased nature of the decision boundary may imply a constant increase in FD during the years.

Left Ventral DC, Right Ventral DC, and Right Putamen box plots have shown significant differences in volume and FD

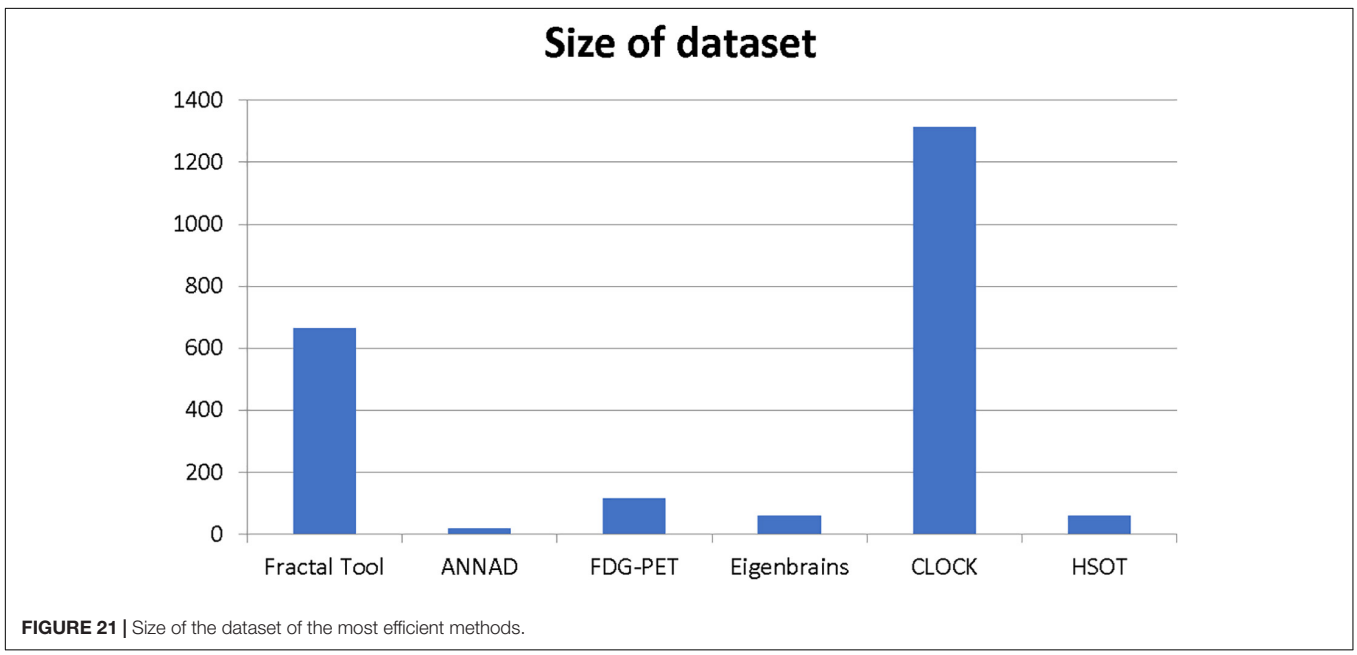

FIGURE 21 | Size of the dataset of the most efficient methods.

(**Figures 16–18**). Linear SVM classifiers using volume and FD as features achieve 100% precision and recall due to the vast distance between the two groups.

Our results suggest state-of-the-art performance in classifying healthy and dementia subjects, as shown in **Figure 19**. Since the dataset was unbalanced and the control group had a size of 8.25 greater than the dementia class, the Fbeta score metric has been used with factor $\beta = 8.25$ instead of precision. Another reason for penalizing more the errors in the dementia class is that it is significant to minimize type I error by maximizing recall. Furthermore, it is crucial to identify the patient group efficiently in medical problems and avoid assigning a patient wrongly to the control group. In **Figures 20**, **21**, a comparison of our classification with the other existing methods is displayed. Our method outperforms all other methods in terms of the accuracy and size of the dataset. More precisely, although the first three algorithms have similar performance with our classification, they yield results from smaller datasets.

CONCLUSION

This study presents a new software using the OASIS brain database for brain volume measurement using the definition of FD. The possibilities measuring different brain areas and subregions could give robust evidence of the slightest variations to imaging data obtained from repetitive measurements to Physicians and Radiologists.

Three experiments on the OASIS brain dataset have shown the use of FD as a tool for the diagnosis and prediction of early dementia. The first experiment trained the segmentation model on a heterogeneous dataset to ensure its universal validity for repeated measurements. The second experiment showed different imaging profiles on the early stages of dementia. The third is a classification to distinguish healthy subjects from patients of various dementia stages. The latter shows high accuracy compared to any existing method.

Each segmentation model is trained on an online Kaggle Kernel with a 16 GB NVIDIA TESLA P100 GPU. The primary limitation of the procedure is that the algorithm required more memory to allocate images of (160, 192, 224) resolution; therefore, we manually reduced them. The corresponding atlas to (144, 112, 96) dimensions the specific regions of the brain. Due to these memory constraints, the model has also been executed with a batch size of 1 and 120 epochs for both experiments. The programming code for the FD calculation can be found in the following GitHub link: https://github.com/BrainLabVol/BrainFD and basic instructions of the Graphical User Interface in the **Appendix**.

Future study is planned to validate this model for control and dementia groups, using R correlation to validate the FD and more data to train and validate the cross-sectional study. Also, an improved computational system will perform the segmentation of the whole brain volume instead of an ROI and will adequately evaluate the trained segmentation model.

DATA AVAILABILITY STATEMENT

Publicly available datasets were analyzed in this study. This data can be found here: https://www.oasis-brains.org/. The programming code for the FD calculation can be found here: https://github.com/BrainLabVol/BrainFD.

ETHICS STATEMENT

Ethical review and approval was not required for the study on human participants in accordance with the local legislation and institutional requirements. The patients/participants provided their written informed consent to participate in this study.

AUTHOR CONTRIBUTIONS

All authors made a significant contribution to the study reported, whether that is in the conception, study design, execution, acquisition of data, analysis, and interpretation, or in all these areas, took part in drafting, revising, or critically reviewing the article, and gave final approval of the version to be published.

FUNDING

This study was financially supported by the Research and Development Office (RDO) at the Ministry of Education, Kingdom of Saudi Arabia (Grant No. HIQ1-49-2019).

ACKNOWLEDGMENTS

The authors acknowledge the Research and Development Office (RDO-KAU) at the King Abdulaziz University for the technical support.

REFERENCES

Alexiou, A., Chatzichronis, S., and Ashraf, G. M. (2020). "The prediction of Alzheimer's disease," in *Diagnosis and Management in Dementia: the Neuroscience of Dementia, Edition*, Vol 1, eds C. Martin and V. Preedy (Amsterdam: Elsevier).

Alexiou, A., Kamal, M. A., and Ashraf, G. M. (2019). Editorial: the Alzheimer's disease challenge. *Front. Neurosci.* 13:768.

Alexiou, A., Matzavinos, V., Greig, N. H., and Kamal, M. A. (2017). A Bayesian model for the early prediction and diagnosis of Alzheimer's disease. *Front. Aging Neurosci.* 9:77.

Berger, A. (2002). Magnetic resonance imaging. *BMJ* 324:35.

Bharanidharan, N., and Rajaguru, H. (2018). "Classification of dementia using harmony search optimization technique," in *2018 IEEE Region 10 Humanitarian Technology Conference*, (Piscataway, NJ: IEEE).

Blanton, R. E., Levitt, J. G., Thompson, P. M., Narr, K. L., Capetillo-Cunliffe, L., and Nobel, A. (2001). Mapping cortical asymmetry and complexity patterns in normal children. *Psychiatry Res.* 107, 29–43. doi: 10.1016/s0925-4927(01)00091-9

Borghi, J. A., and Van Gulick, A. E. (2018). Data management and sharing in neuroimaging: practices and perceptions of MRI researchers. *PLoS One* 13:e0200562. doi: 10.1371/journal.pone.0200562

Brewer, J. B., Magda, S., Airriess, C., and Smith, M. E. (2009). Fully-automated quantification of regional brain volumes for improved detection of focal atrophy in Alzheimer disease. *AJNR Am. J. Neuroradiol.* 30, 578–580. doi: 10.3174/ajnr.A1402

Buda, M., Saha, A., and Mazurowski, M. A. (2019). Association of genomic subtypes of lower-grade gliomas with shape features automatically extracted by a deep learning algorithm. *Comput. Biol. Med.* 109, 218–225. doi: 10.1016/j.compbiomed.2019.05.002

Bui, T., Shin, J., and Moon, T. (2017). 3D densely convolutional networks for volumetric segmentation. *ArXiv*. Available Online at: https://arxiv.org/abs/1709.03199 (accessed October 1, 2021).

Caramanos, V. S., Fonov, S. J., Francis, S., Narayanan, G. B., Pike, D. L., Collins, D. L., et al. (2010). Gradient distortions in MRI: characterizing and correcting for their effects on SIENA-generated measures of brain volume change. *Neuroimage* 49, 1601–1611. doi: 10.1016/j.neuroimage.2009.08.008

Carstensen, J. T., and Franchini, M. (1993). The use of fractal geometry in pharmaceutical systems. *Drug Dev. Ind. Pharm.* 19, 85–100. doi: 10.3109/03639049309038762

Cerofolini, G. F., Narducci, D., Amato, P., and Romano, E. (2008). Fractal nanotechnology. *Nanoscale Res. Lett.* 3, 381–385.

Cerri, S., Hoopes, A., Greve, D. N., Mühlau, M., and Van Leemput, K. (2020). "A longitudinal method for simultaneous whole-brain and lesion segmentation in multiple sclerosis," in *Clinical Neuroimaging and Radiogenomics in Neuro-oncology. MLCN 2020, RNO-AI 2020. Lecture Notes in Computer Science*, Vol. 12449, eds S. M. Kia and Machine Learning (Berlin: Springer).

Cerri, S., Puonti, O., Meier, D. S., Wuerfel, J., Mühlau, M., Siebner, H. R., et al. (2021). A contrast-adaptive method for simultaneous whole-brain and lesion segmentation in multiple sclerosis. *Neuroimage* 225:117471. doi: 10.1016/j.neuroimage.2020.117471

Chatzichronis, S., Alexiou, A., Simou, P., Mantzavinos, V., Vasileios, T., Perveen, A., et al. (2019). Neurocognitive assessment software for enrichment sensory environments. *J. Proteomics Bioinform* 12, 018–028.

Chavhan, G. B., Babyn, P. S., Thomas, B., Shroff, M. M., and Haacke, E. M. (2009). Principles, techniques, and applications of T2*-based MR imaging and its special applications. *Radiographics* 29, 1433–1449. doi: 10.1148/rg.295095034

Chen, S., Stromer, D., Alabdalrahim, H. A., Schwab, S., Weih, M., and Maier, A. (2020). Automatic dementia screening and scoring by applying deep learning on clock-drawing tests. *Sci. Rep.* 10:20854. doi: 10.1038/s41598-020-74710-9

Chow, M. S., Wu, S. L., Webb, S. E., Gluskin, K., and Yew, D. T. (2017). Functional magnetic resonance imaging and the brain: a brief review. *World J. Radiol.* 9, 5–9. doi: 10.4329/wjr.v9.i1.5

Dalca, A. V., Yu, E., Golland, P., Fischl, B., Sabuncu, M. R., and Iglesias, J. E. (2019). Unsupervised deep learning for bayesian brain MRI segmentation. *Med. Image Comput. Comput Assist. Interv.* 11766, 356–365. doi: 10.1007/978-3-030-32248-9_40

Dale, A. M., Fischl, B., and Sereno, M. I. (1999). Cortical surface-based analysis. i. segmentation and surface reconstruction. *Neuroimage* 9, 179–194.

Deserno Né Lehmann, T. M., Handels, H., Maier-Hein Né Fritzsche, K. H., Mermann, S., Palm, C., Tolxdoff, T., et al. (2013). Viewpoints on medical image processing: from science to application. *Curr. Med. Imaging Rev.* 9, 79–88. doi: 10.2174/1573405611309020002

Desikan, R. S., Cabral, H. J., Hess, C. P., Dillon, W. P., Glastonbury, C. M., and Weiner, M. W. (2009). Automated MRI measures identify individuals with mild cognitive impairment and Alzheimer's disease. *Brain* 132, 2048–2057.

Despotović, I., Goossens, B., and Philips, W. (2015). MRI segmentation of the human brain: challenges, methods, and applications. *Comput. Math. Methods Med.* 2015:450341. doi: 10.1155/2015/450341

Di Ieva, A., Esteban, F. J., Grizzi, F., Klonowski, W., and Martín-Landrove, M. (2015). Fractals in the neurosciences, Part II: clinical applications and future perspectives. *Neuroscientist* 21, 30–43. doi: 10.1177/1073858413513928

Dolz, J., Gopinath, K., Yuan, J., Lombaert, H., Desrosiers, C., and Ben Ayed, I. (2019). HyperDense-Net: a hyper-densely connected CNN for multi-modal image segmentation. *IEEE Trans. Med. Imaging* 38, 1116–1126. doi: 10.1109/TMI.2018.2878669

Dukart, J., Mueller, K., Barthel, H., Villringer, A., Sabri, O., and Schroeter, M. P. (2013). Meta-analysis based SVM classification enables accurate detection of Alzheimer's disease across different clinical centers using FDG-PET and MRI. *Psychiatry Res. Neuroimaging* 212, 230–236. doi: 10.1016/j.pscychresns.2012.04.007

Fernández-Martínez, M., and Sánchez-Granero, M. A. (2014). Fractal dimension for fractal structures: a Hausdorff approach revisited. *J. Math. Anal. Appl.* 409, 321–330. doi: 10.1016/j.jmaa.2013.07.011

Fischl, B. (2012). FreeSurfer. *Neuroimage* 62, 774–781.

Fischl, B., Salat, D. H., Busa, E., Albert, M., Dieterich, M., and Haselgrove, C. (2002). Whole brain segmentation: automated labeling of neuroanatomical structures in the human brain. *Neuron* 33, 341–355.

Fonov, V. S., Janke, A., Caramanos, Z., Arnold, D. L., Narayanan, S., Pike, G. B., et al. (2010). "Improved precision in the measurement of longitudinal global and regional volumetric changes via a novel MRI gradient distortion characterization and correction technique," in *Medical Imaging and Augmented Reality*, eds H. Liao, P. J. Edwards, X. Pan, and Y. Fan (Berlin: Springer).

Fotenos, A. F., Mintun, M. A., Snyder, A. Z., Morris, M. D., and Buckner, R. L. (2008). Brain volume decline in aging: evidence for a relation between socioeconomic status, pre-clinical Alzheimer's disease, and reserve. *Arch Neurol.* 65, 113–120. doi: 10.1001/archneurol.2007.27

Fotenos, A. F., Snyder, A. Z., Girton, L. E., Morris, J. C., and Buckner, R. L. (2005). Normative estimates of cross-sectional and longitudinal brain volume decline in aging and AD. *Neurology* 64, 1032–1039. doi: 10.1212/01.WNL.0000154530.72969.11

Grover, V. P., Tognarelli, J. M., Crossey, M. M., Cox, I. J., Taylor-Robinson, S. D., and McPhail, M. J. (2015). Magnetic resonance imaging: principles and techniques: lessons for clinicians. *J. Clin. Exp. Hepatol.* 5, 246–255.

Ha, T. H., Yoon, U., Lee, K. J., Shin, Y. W., Lee, J. M., Kim, I. Y., et al. (2005). Fractal dimension of cerebral cortical surface in schizophrenia and obsessive–compulsive disorder. *Neurosci. Lett.* 384, 172–176. doi: 10.1016/j.neulet.2005.04.078

Hofman, M. A. (1991). The fractal geometry of convoluted brains. *J. Hirnforsch.* 32, 103–111.

Huang, C., Yan, B., Jiang, H., and Wang, D. (2008). "Combining voxel-based morphometry with artifical neural network theory in the application research of diagnosing Alzheimer's disease," in *Proceedings of the 2008 International Conference on BioMedical Engineering and Informatics*, Sanya, 250–254.

Im, K., Lee, J. M., Yoon, U., Shin, Y. W., Hong, S. B., Kim, I. Y., et al. (2006). Fractal dimension in human cortical surface: multiple regression analysis with cortical thickness, sulcal depth, and folding area. *Hum. Brain Mapp.* 27, 994–1003. doi: 10.1002/hbm.20238

Jack, C. R., Petersen, R. C., Xu, Y., O'Berin, P. C., Smith, G., Ivnik, R. J., et al. (2000). Rates of hippocampal atrophy correlate with change in clinical status in aging and AD. *Neurology* 55, 484–489. doi: 10.1212/wnl.55.4.484

Jelinek, H. F., and Fernandez, E. (1998). Neurons and fractals: how reliable and useful are calculations of fractal dimensions? *J. Neurosci. Methods* 81, 9–18. doi: 10.1016/s0165-0270(98)00021-1

Joosten, J. J., Soler-Toscano, F., and Zenil, H. (2016). Fractal dimension versus process complexity. *Adv. Math. Phys.* 2016:5030593.

Karsch, K., He, Q., and Duan, Y. (2009). "A fast, semi-automatic brain structure segmentation algorithm for magnetic resonance imaging," in *2009 IEEE International Conference on Bioinformatics and Biomedicine*, (Washington, DC).

Kazemi Korayem, A., Ghamami, S., and Bahrami, Z. (2018). Fractal properties and morphological investigation of Nano hydrochlorothiazide is used to treat hypertension. *BMC Pharmacol. Toxicol.* 19:70. doi: 10.1186/s40360-018-0259-5

King, R. D., George, A. T., Jeon, T., Hynan, L. S., Youn, T. S., and Kennedy, D. N. (2009). Characterization of atrophic changes in the cerebral cortex using fractal dimensional analysis. *Brain Imaging Behav.* 3, 154–166. doi: 10.1007/s11682-008-9057-9

Kloppel, S., Stonnington, C. M., Chu, C., Draganski, B., Scahill, R. I., Rohrer, J. D., et al. (2008). Automatic classification of MR scans in Alzheimer's disease. *Brain* 131, 681–689. doi: 10.1093/brain/awm319

Kovacevic, S., Rafii, M. S., and Brewer, J. B. (2009). High-throughput, fully automated volumetry for prediction of MMSE and CDR decline in mild cognitive impairment. *Alzheimer Dis. Assoc. Disord.* 23, 139–145. doi: 10.1097/WAD.0b013e318192e745

Krohn, S., Froeling, M., Leemans, A., Ostwald, D., Villoslada, P., Finke, C., et al. (2019). Evaluation of the 3D fractal dimension as a marker of structural brain complexity in multiple-acquisition MRI. *Hum. Brain Mapp.* 40, 3299–3320. doi: 10.1002/hbm.24599

Kronmuller, K. T., Pantel, J., Kohler, S., Victor, D., Giesel, F., Magnotta, V. A., et al. (2008). Hippocampal volume and 2-year outcome in depression. *Br. J. Psychiatry* 192, 472–473. doi: 10.1192/bjp.bp.107.040378

LaMontagne, P. J., Benzinger, T. L. S., Morris, J. C., Keefe, S., Hornbeck, R., and Xiong, C. (2019). OASIS-3: longitudinal neuroimaging, clinical, and cognitive dataset for normal aging and Alzheimer disease. *medRxiv* doi: 10.1101/2019.12.13.19014902

Larobina, M., and Murino, L. (2014). Medical image file formats. *J. Digit. Imaging* 27, 200–206. doi: 10.1007/s10278-013-9657-9

Li, X., Jiang, J., Zhu, W., Yu, C., Sui, M., Wang, Y., et al. (2007). Asymmetry of prefrontal cortical convolution complexity in males with attention-deficit/hyperactivity disorder using fractal information dimension. *Brain Dev.* 29, 649–655. doi: 10.1016/j.braindev.2007.04.008

Liu, J. Z., Zhang, L. D., and Yue, G. H. (2003). Fractal dimension in human cerebellum measured by magnetic resonance imaging. *Biophys. J.* 85, 4041–4046. doi: 10.1016/s0006-3495(03)74817-6

Liu, R., Lemieux, L., Bell, G. S., Sisodiya, S. M., Shorvon, S. D., Sander, J. W., et al. (2003). A longitudinal study of brain morphometrics using quantitative magnetic resonance imaging and difference image analysis. *Neuroimage* 20, 22–33. doi: 10.1016/s1053-8119(03)00219-2

Lopez, C. G. (2009). "Automatic system for Alzheimer's disease diagnosis using eigenbrains and bayesian classification rules," in *Bio-Inspired Systems: Computational and Ambient Intelligence*, eds J. Cabestany, F. Sandoval, and A. Prieto (Berlin: Springer), 949–956. doi: 10.1007/978-3-642-02478-8_119

Lorenzetti, V., Allen, N. B., Fornito, A., and Yucel, M. (2009). Structural brain abnormalities in major depressive disorder: a selective review of recent MRI studies. *J. Affect. Disord.* 117, 1–17. doi: 10.1016/j.jad.2008.11.021

Maclaren, J., Han, Z., Vos, S. B., Fischbein, N., and Bammer, R. (2014). Reliability of brain volume measurements: a test-retest dataset. *Sci. Data* 1:140037.

MacQueen, G. M., Yucel, K., Taylor, V. H., Macdonald, K., and Joffe, R. (2008). Posterior hippocampal volumes are associated with remission rates in patients with major depressive disorder. *Biol. Psychiatry* 64, 880–883. doi: 10.1016/j.biopsych.2008.06.027

Magnin, B., Mesrob, L., Kinkingnéhun, S., Pélégrini-Issac, M., Colliot, O., and Sarazin, M. (2009). Support vector machine-based classification of Alzheimerâ€™s disease from whole-brain anatomical MRI. *Neuroradiology* 51, 73–83. doi: 10.1007/s00234-008-0463-x

Maipas, S., Nonni, A., Politi, E., Sarlanis, H., and Kavantzas, N. G. (2018). The Goodness-of-fit of the fractal dimension as a diagnostic factor in breast cancer. *Cureus* 10:e3630. doi: 10.7759/cureus.3630

Mantzavinos, V., and Alexiou, A. (2017). Biomarkers for Alzheimer's disease diagnosis. *Curr. Alzheimer Res.* 14, 1149–1154.

Marcus, D. S., Fotenos, A. F., Csernansky, J. G., Morris, J. C., and Buckner, R. L. (2010). Open access series of imaging studies: longitudinal MRI data in nondemented and demented older adults. *J. Cogn. Neurosci.* 22, 2677–2684. doi: 10.1162/jocn.2009.21407

Marcus, D. S., Wang, T. H., Parker, J., Csernansky, J. G., Morris, J. C., and Buckner, R. L. (2007). Open Access Series of Imaging Studies (OASIS): cross-sectional MRI data in young, middle aged, nondemented, and demented older adults. *J. Cogn. Neurosci.* 19, 1498–1507. doi: 10.1162/jocn.2007.19.9.1498

Mondal, A. K., Dolz, J., and Desrosiers, C. (2018). Few-shot 3D multi-modal medical image segmentation using generative adversarial learning. *arXiv*. Available Online at: https://arxiv.org/abs/1810.12241 (accessed October 1, 2021).

Mustafa, N., Ahearn, T. S., Waiter, G. D., Murray, A. D., Whalley, L. J., and Staff, R. T. (2012). Brain structural complexity and life course cognitive change. *NeuroImage* 61, 694–701. doi: 10.1016/j.neuroimage.2012.03.088

Narayanan, S., Nakamura, K., Fonov, V. S., Maranzano, J., Caramanos, Z., and Giacomini, P. S. (2020). Brain volume loss in individuals over time: source of variance and limits of detectability. *NeuroImage* 214:116737. doi: 10.1016/j.neuroimage.2020.116737

Ortiz, A., Gorriz, J. M., Ramirez, J., and Martinez-Murcia, F. J. (2013). LVQ-SVM based CAD tool applied to structural MRI for the diagnosis of the Alzheimerâ€™s disease. *Pattern Recognit. Lett.* 34, 1725–1733. doi: 10.1016/j.patrec.2013.04.014

Pandya, M., Altinay, M., Malone, D. A., and Anand, A. (2012). Where in the brain is depression? *Curr. Psychiatry Rep.* 14, 634–642. doi: 10.1007/s11920-012-0322-7

Pedregosa, F., Varoquaux, G., Gramfort, A., Michel, V., Thirion, B., and Grisel, O. (2011). Scikit-learn: machine learning in python. *J. Mach. Learn. Res.* 12, 2825–2830.

Pereira, L. M. (2010). Fractal pharmacokinetics. *Comput. Math. Methods Med.* 11, 161–184. doi: 10.1080/17486700903029280

Rajagopalan, V., Liu, Z., Allexandre, D., Zhang, L., Wang, X.-F., Pioro, E. P., et al. (2013). Brain white matter shape changes in Amyotrophic Lateral Sclerosis (ALS): a fractal dimension study. *PLoS One* 8:e73614. doi: 10.1371/journal.pone.0073614

Rickmann, A.-M., Roy, A. G., Sarasua, I., and Wachinger, C. (2020). Recalibrating 3D ConvNets with project &excite. *IEEE Trans. Med. Imaging* 39, 2461–2471. doi: 10.1109/TMI.2020.2972059

Rickmann, A.-M., Roy, A. G., Sarasua, I., Navab, N., and Wachinger, C. (2019). *Project & Excite' Modules for Segmentation of Volumetric Medical Scans*. Berlin: Springer.

Schaefer, A., Kong, R., Gordon, E. M., Laumann, T. O., Zuo, X. N., Holmes, A. J., et al. (1991). Local-global parcellation of the human cerebral cortex from intrinsic functional connectivity MRI. *Cereb. Cortex* 28, 3095–3114. doi: 10.1093/cercor/bhx179

Sheline, Y. I., Gado, M. H., and Price, J. L. (1998). Amygdala core nuclei volumes are decreased in recurrent major depression. *NeuroReport* 9, 2023–2028. doi: 10.1097/00001756-199806220-00021

Soltanifar, M. (2021). A generalization of the hausdorff dimension theorem for deterministic fractals. *Mathematics* 9:1546. doi: 10.3390/math9131546

Todoroff, N., Kunze, J., Schreuder, H., Hessler, G., Baringhaus, K. H., and Schneider, G. (2014). Fractal dimensions of macromolecular structures. *Mol. Inform.* 33, 588–596. doi: 10.1002/minf.201400090

Uchida, S. (2013). Image processing and recognition for biological images. *Dev. Growth. Differ.* 55, 523–549. doi: 10.1111/dgd.12054

Varley, T. F., Craig, M., Adapa, R., Finoia, P., Williams, G., Allanson, J., et al. (2020). Fractal dimension of cortical functional connectivity networks & severity of disorders of consciousness. *PLoS One* 15:e0223812. doi: 10.1371/journal.pone.0223812

Willemsen, A. T., and van den Hoff, J. (2002). Fundamentals of quantitative PET data analysis. *Curr. Pharm. Des.* 8, 1513–1526. doi: 10.2174/1381612023394359

Yadav, J. B., and Nishikanta, J. K. (2010). Fractal dimension as a measure of the scale of Homogeneity. *Mon. Not. R. Astron. Soc.* 405, 2009–2015.

Yokoo, T., Bae, W. C., Hamilton, G., Karimi, A., Borgstede, J. P., and Bowen, B. C. (2010). A quantitative approach to sequence and image weighting. *J. Comput. Assist. Tomogr.* 34, 317–331. doi: 10.1097/rct.0b013e3181d3449a

Yong, X., Lu, S., Wen, L., Eberl, S., Fulham, M., and Feng, D. D. (2014). Automated identification of dementia using FDG-PET imaging. *BioMed Res. Int.* 2014, 1–8. doi: 10.1155/2014/421743

Zhang, P., Chen, L., Xu, T., Liu, H., Liu, X., Meng, J., et al. (2013). Programmable fractal nanostructured interfaces for specific recognition and electrochemical release of cancer cells. *Adv. Mater.* 25, 3566–3570. doi: 10.1002/adma.201300888

Conflict of Interest: The authors declare that the research was conducted in the absence of any commercial or financial relationships that could be construed as a potential conflict of interest.

Publisher's Note: All claims expressed in this article are solely those of the authors and do not necessarily represent those of their affiliated organizations, or those of the publisher, the editors and the reviewers. Any product that may be evaluated in this article, or claim that may be made by its manufacturer, is not guaranteed or endorsed by the publisher.

APPENDIX

Documentation

Installation guide

Necessary libraries:

– pip install VoxelMorph
– pip install TensorFlow

GUI

Option	Description
Single File	Manipulate a single file
Choose subject	Select a file
Raw Data	Select a NIfTI, DICOM file to perform Image Segmentation with FreeSurfer
Fs file (Norm.mgz)	Load a mgz file, this file is extracted after Image Segmentation
Fs file (npz)	Load a npz file that has been previously converted from mgz to npz
Vxm file	Load the output npz file that VoxelMorph outputs after segmentation
Fd file	Load the npz file produced after Fractal analysis
Mgz to npz	The mgz file is converted into npz format
VoxelMorph	After importing npz files, perform image segmentation with VoxelMorph
Estimate Df and L	Estimate Fractal Dimension of the imported npz file

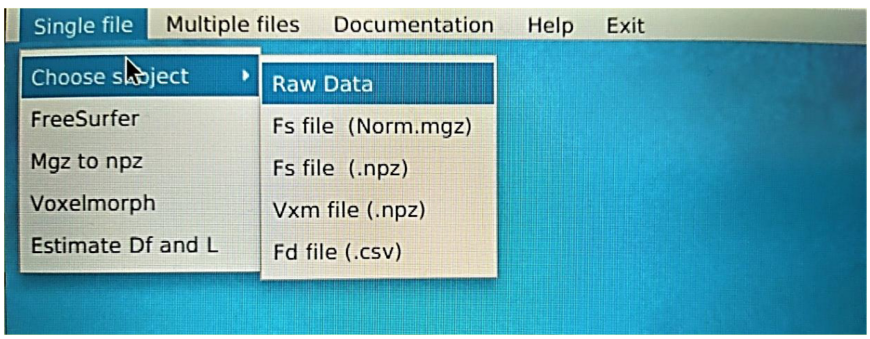

Option	Description
Multiple Files	Manipulate multiple files
Choose subjects	Select a parent folder containing NIfTI or DICOM files
Raw Data	Select a folder with NIfTI, DICOM files to perform Image Segmentation with FreeSurfer
Fs file (Norm.mgz)	Load a folder with mgz files, those files are extracted after Image Segmentation
Fs file (npz)	Load a folder with npz files that have been previously converted from mgz to npz
Vxm file	Load a folder with the output npz files that VoxelMorph outputs after segmentation
Fd file	Load a folder with the npz files produced after Fractal analysis
Mgz to npz	After importing mgz files convert them into npz format
Train a segmentation model with VoxelMorph	After importing npz files, train a segmentation model with VoxelMorph
Segment with VoxelMorph	Import previous trained model and previously imported npz files to perform image segmentation with VoxelMorph
Estimate Df and L	Estimate Fractal Dimension of the imported npz files, the output is a folder for each file
Create a dataset	Select a folder containing the output of Estimate Df and L, to create a dataset from multiple images

- The folder and the directories shall follow the hierarchical file structure of XNAT.

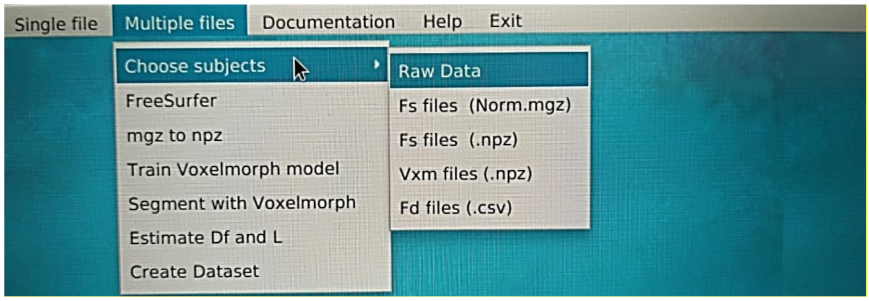
Single file
Multiple files
Documentation
Help
Exit
Choose subjects
FreeSurfer
mgz to npz
Train Voxelmorph model
Segment with Voxelmorph
Estimate Df and L
Create Dataset
Raw Data
Fs files (Norm.mgz)
Fs files (.npz)
Vxm files (.npz)
Fd files (.csv)

frontiers in Human Neuroscience

REVIEW
published: 30 November 2021
doi: 10.3389/fnhum.2021.747077

Electrophysiological Biomarkers of Epileptogenicity in Alzheimer's Disease

*Tingting Yu[1,2], Xiao Liu[1,2], Jianping Wu[1,2,3] and Qun Wang[1,2,4]**

[1] Department of Neurology, Beijing Tiantan Hospital, Capital Medical University, Beijing, China, [2] China National Clinical Research Center for Neurological Diseases, Beijing, China, [3] Advanced Innovation Center for Human Brain Protection, Capital Medical University, Beijing, China, [4] Collaborative Innovation Center for Brain Disorders, Beijing Institute of Brain Disorders, Capital Medical University, Beijing, China

Cortical network hyperexcitability is an inextricable feature of Alzheimer's disease (AD) that also might accelerate its progression. Seizures are reported in 10–22% of patients with AD, and subclinical epileptiform abnormalities have been identified in 21–42% of patients with AD without seizures. Accurate identification of hyperexcitability and appropriate intervention to slow the compromise of cognitive functions of AD might open up a new approach to treatment. Based on the results of several studies, epileptiform discharges, especially those with specific features (including high frequency, robust morphology, right temporal location, and occurrence during awake or rapid eye movement states), frequent small sharp spikes (SSSs), temporal intermittent rhythmic delta activities (TIRDAs), and paroxysmal slow wave events (PSWEs) recorded in long-term scalp electroencephalogram (EEG) provide sufficient sensitivity and specificity in detecting cortical network hyperexcitability and epileptogenicity of AD. In addition, magnetoencephalogram (MEG), foramen ovale (FO) electrodes, and computational approaches help to find subclinical seizures that are invisible on scalp EEGs. We performed a comprehensive analysis of the aforementioned electrophysiological biomarkers of AD-related seizures.

Keywords: Alzheimer's disease, epileptogenesis, seizure, electrophysiology, biomarkers

OPEN ACCESS

Edited by:
Henning Müller, University of Applied Sciences and Arts of Western Switzerland, Switzerland

Reviewed by:
Anna Szucs, Semmelweis University, Hungary
Angel Nunez, Autonomous University of Madrid, Spain
Qing Yun Wang, Beihang University, China
James Tao, University of Chicago, United States

****Correspondence:***
Qun Wang
wangq@ccmu.edu.cn

Specialty section:
This article was submitted to Brain Health and Clinical Neuroscience, a section of the journal Frontiers in Human Neuroscience

Received: *25 July 2021*
Accepted: *01 November 2021*
Published: *30 November 2021*

Citation:
Yu T, Liu X, Wu J and Wang Q (2021) Electrophysiological Biomarkers of Epileptogenicity in Alzheimer's Disease. Front. Hum. Neurosci. 15:747077. doi: 10.3389/fnhum.2021.747077

INTRODUCTION

Brain rhythms are fundamental in maintaining normal cognition and behavior, and neuronal hyperexcitability has emerged as an important electrical abnormality that could not only lead to memory failure in the early stage of Alzheimer's disease (AD) but also contribute to the progression of the disease (Noebels, 2011; Vossel et al., 2013; Busche and Konnerth, 2015, 2016; Palop and Mucke, 2016). Once neuronal hyperexcitability of the cerebral cortex is established, it can manifest as epileptic seizures or subclinical epileptiform discharges. Seizures are reported in 10–22% of patients with AD (Friedman et al., 2011; Vossel et al., 2013; Cretin et al., 2016; Sarkis et al., 2016),

Abbreviations: 5xFAD, 5x familial AD; AD, Alzheimer's disease; AEDs, antiepileptic drugs; aMCI, amnesic mild cognitive impairment; APOE4, the E4 variant of apolipoprotein E; AUROC, area under receiver operating characteristic; BBBd, blood-brain barrier dysfunction; EEG, electroencephalogram; eLORETA, exact low-resolution brain electromagnetic tomography; FO, foramen ovale; MEG, magnetoencephalogram; mTL, mesial temporal lobe; PSWEs, paroxysmal slow wave events; REM, rapid eye moment; SSS, small sharp spikes; TIRDA, temporal inter mitten rhythmic delta activity.

and subclinical epileptiform activities have been found in more than 40% of patients with AD in a recent prospective electroencephalogram (EEG) study (Vossel et al., 2016).

The presence of seizure and subclinical epileptiform activities have been shown to contribute to impaired memory and attention, especially cognitive fluctuation (Palop and Mucke, 2009; Vossel et al., 2016). A greater extent of neuronal hyperactivity tends to occur in the earliest stages of AD compared with later stages, which has been shown from both fMRI studies in humans and neuronal activity studies in mouse models of AD (Zott et al., 2018). "Antiepileptogenic" therapies in AD appear to be feasible in order to delay the progression of the disease. Although they are easy to implement, performing these treatments in all patients with AD presents a problem as the majority of patients with AD would not have any benefit, though the subset of patients with AD who have epileptiform activity might benefit greatly from early treatment with antiepileptic drugs (AEDs). Hence, effective treatment first requires the detection and suppression of seizures and subclinical epileptiform activity. In this study, we performed a comprehensive analysis of the potential electrophysiological biomarkers of AD-related seizures in humans and discuss their feasibility in clinical practice and their potential to predict the subsequent development of clinical seizures and epilepsy.

SCALP ELECTROENCEPHALOGRAM

Epileptiform Discharges

The best-known biomarker of hyperexcitability in humans is the epileptiform discharge, which is defined as a paroxysmal EEG graphoelement (spike or sharp wave) with a duration of 20–200 ms that is clearly distinct from ongoing background EEG activity followed by slow waves (Noachtar and Remi, 2009) (**Figure 1A**). On scalp EEGs, visible subclinical epileptiform discharges occur in 9–21% of patients with AD who had no prior history of epilepsy or seizure, a higher rate than 0–5% of healthy controls (Vossel et al., 2016; Brunetti et al., 2020; Lam et al., 2020). Long-term EEG detection has found that epileptiform discharges in patients with AD mainly occur during a sleep state and are largely lateralized to the temporal lobe, especially the left temporal lobe.

Epileptiform discharges that had more robust morphological features including significantly larger trough voltage, peak-to-trough voltage, and slope of falling half-wave of the peak are more strongly associated with clinical seizures in AD (Lam et al., 2020). The guiding significance of robust epileptiform discharges is similar to giant spikes (simultaneous spikes in all channels, with massive voltages $> \pm 10$ SD from the filtered baseline in at least one channel) observed in transgenic mice with APP/PS1 mutations (Gureviciene et al., 2019). The same indicative effect being strongly associated with clinical seizures has also been seen in right temporal epileptiform discharges (100% specificity and 43% sensitivity) (Lam et al., 2020).

The detection rate of epileptic discharges in patients with AD by scalp EEG is significantly correlated with recording time. Approximately, 62% of patients with AD showed epileptic discharges in EEG recordings lasting 24 h (Horvath et al., 2018) and only 3% in 20 min of eyes-closed EEG recordings (Liedorp et al., 2010). Most epileptiform discharges from patients with AD occur during sleep, requiring overnight EEG monitoring for detection. Epileptiform discharges occurred most frequently during N2 sleep, while awake and rapid eye moment (REM) states are the least permissive states for the expression of epileptiform discharges in patients with focal epilepsy (Sammaritano et al., 1991; Malow et al., 1997; Diaz-Negrillo, 2013), and the results of EEG monitoring in patients with AD are consistent with this. While epileptiform discharges detected during awake or REM states were suggestive for clinical seizures (85.7% specificity and 85.7% sensitivity) (Lam et al., 2020), the study by Lam et al. (2020) also pointed out that patients with AD who had high frequencies of epileptiform discharges were more likely to have generalized convulsions.

Lam et al. (2017a) found that spikes (sharply contoured transients, clearly distinguishable from, and usually interrupting background activities, with a duration of <70 ms) from patients with aMCI were largely lateralized to the left mesial temporal lobe (mTL), whereas they were largely lateralized to the right mTL in moderate patients with AD. Thus, they proposed that there might be left hemisphere hyperactivity predisposition and left mTL susceptibility in the early stages of AD. Data from anatomical and functional connectivity modalities also support this; the result may also be mediated in part by the E4 variant of apolipoprotein E (APOE4) allele (Thompson et al., 2003; Damoiseaux et al., 2009; Donix et al., 2013; Wessa et al., 2016; Yang et al., 2017; Liu et al., 2018; Zott et al., 2018).

Studies in animal models with AD have established a direct link between neuronal hyperactivity and propagation of amyloid and tau pathology (Cirrito et al., 2005; Busche et al., 2012; Pooler et al., 2013; Wu et al., 2016). Reyes-Marin and Nunez (2017) also found that the frequency of epileptiform-like discharges was significantly correlated with the number of amyloid-β plaques in APP/PS1 mice. The results of these animal studies illustrate that the asymmetry in temporal lobe hyperexcitability might be related to an asymmetric cascade of AD pathology.

Finally, there is growing evidence that scalp EEG epileptiform discharges in patients with AD have a variable association with clinical seizures (Vossel et al., 2016; Lam et al., 2020). With an infrequent frequency (<10 per 24 h), these epileptiform discharges typically arise locally from the lateral temporal cortex or propagate to the surface from deep mTL foci (Bakker et al., 2012; Lam et al., 2017a). Thus, to some extent, scalp EEG epileptiform discharges alone are limited, and they may not be the optimal biomarkers for epileptogenicity in AD.

Small Sharp Spikes

Small sharp spikes (SSSs), also known as benign sporadic sleep spikes (White et al., 1977), are low amplitude (30–50 uV), short duration (<50 ms) spikes that occur during early drowsiness, and N1 and N2 sleep stages (**Figure 1B**). They are widely distributed in bilateral brain hemispheres typically seen independently over the bi-frontotemporal regions but can also occur unilaterally. In addition, SSSs are usually considered as a benign variant of EEG, which has no association with epilepsy. However, recent studies

have indicated that SSS-like waveforms in the scalp might be related to mTL epileptiform discharges, especially unilateral SSS-like waveforms (Lam et al., 2017a; Issa et al., 2018). According to the study by Lam et al. (2020) unilateral (left or right temporal region) SSS-like waveforms with high frequency (>100 per 24 h) are associated with clinical seizure in AD. However, pinpointing SSSs as an electrophysiological biomarker of seizure in patients with AD requires further validation in more well-designed studies to distinguish pathological SSSs from benign SSSs.

Temporal Intermittent Rhythmic Delta Activity

Temporal intermittent rhythmic delta activity (TIRDA) refers to the delta activity distributed in the temporal lobe with a frequency of 2.5–3.0 Hz and a sinusoidal or serrated waveform that occurs repeatedly and intermittently and has a strong association with mesial temporal lobe epilepsy (mTLE) (Reiher et al., 1989; Gambardella et al., 1995; Normand et al., 1995; Gennaro et al., 2003) (**Figure 1C**). TIRDA occurs in 26% of patients with AD-related epilepsy (Lam et al., 2020). Although occurring at a lower frequency in patients with AD without epilepsy, TIRDA has been associated with higher diagnostic confidence compared to epileptiform discharges (positive predictive value for determining epileptiform, 83.3 vs. 61.5%) (Lam et al., 2020). Like epileptiform discharges, TIRDA is more likely to occur during N2 sleep and in the left temporal location, while TIRDA that does occur during awake or REM states is more strongly associated with clinical seizures in AD (Lam et al., 2020). What is more, the lateralization of TIRDA matches that of epileptiform discharges in patients with AD. However, because of its low frequency (<10 per 24 h) of occurrence in AD, the utility of TIRDA as a quantitative biomarker is somewhat limited (Lam et al., 2020).

Paroxysmal Slow Cortical Activity

Slowing of scalp EEG activity has been observed in AD by studying early quantitative EEG power changes in patients with AD (Musaeus et al., 2018), and the EEG slowing correlates with decreased cognition in patients with AD and unimpaired older adults (Stomrud et al., 2010; Musaeus et al., 2018). The EEG slowing might be a potential sign of neural network dysfunction. Milikovsky et al. (2019) analyzed the temporal characteristics of EEG slowing from patients with AD and found that cortical slowing is in part composed of transient paroxysmal slowing of the cortical network. This transient paroxysmal slowing of the cortical network is called paroxysmal slow wave events (PSWEs), which refer to "events" when the median power frequency is lower than 6 Hz for at least 5 consecutive s on the scalp EEG (Milikovsky et al., 2019) (**Figure 1D**). These PSWEs were also obtained in patients with epilepsy, animal models of AD, and animal models of epilepsy.

Investigating PSWE characteristics in aged mice, young 5xFAD mice, and young rats with epilepsy, Milikovsky et al. (2019) found that there was a spatial correlation between PSWEs and blood-brain barrier dysfunction (BBBd). They also observed a causal link between BBBd and PSWE in animal models by infusing albumin into the lateral ventricle of rats and then detecting the PSWEs in epidural recordings after a month of infusion. Their results indicate that PSWEs can be an indicator for the subclinical seizure-like activity that reflects microvascular pathology. Hence, PSWE detection in routine scalp EEG recordings might be an affordable and sensitive diagnostic indicator for subclinical seizures among patients with AD and as a pharmacodynamic measure for AEDs. However, we must realize that seizure and epileptiform activity mostly occur in the mTL in patients with AD and are often undetectable by scalp EEG recording. Thus, more effective approaches that can detect epileptiform discharges in the mTL are needed to improve the efficiency of scalp EEG monitoring.

MAGNETOENCEPHALOGRAPHY

Magnetoencephalography (MEG), which is thought to be more sensitive to discharges of tangential sulcal sources than EEG with a high temporal and spatial resolution (Oishi et al., 2002), has also been widely used as a non-invasive tool to assess mTL activity and localized epileptogenic lesions in an epilepsy non-invasive tool (Enatsu et al., 2008; Kaiboriboon et al., 2010; Wennberg et al., 2011; Wennberg and Cheyne, 2014). Although the main application field of MEG is the presurgical evaluation of drug-resistant epilepsy, MEG also provides a complementary approach to scalp EEG in detecting cortical network dysfunction in patients with AD. Vossel et al. (2016) prospectively assessed the epileptiform activities in 33 patients with AD and 19 age-matched healthy controls, by 1-h resting MEG recordings and overnight scalp EEG recordings. Vossel et al. (2016) found that visible epileptiform discharges on MEG occurred in 33.3% of patients with AD, much higher than that of 21.1% on overnight scalp EEGs. Although the specificity of MEG might not be as high as that of overnight EEG (11% of healthy controls had epileptiform discharges visible on MEG while had them on overnight EEG), patients with epileptiform activity on MEG or overnight EEG had significantly faster rates of cognitive decline than those without epileptiform activity (Vossel et al., 2016). These findings suggest that MEG is an effective electrophysiological biomarker of cortical hyperexcitability in patients with AD with much higher sensitivity than scalp EEG. Interestingly, epileptiform discharges detected by MEG were more right-sided compared with the more left-sided epileptiform discharges detected by scalp-EEG (Vossel et al., 2016). Different detection capabilities or different interpretation techniques may contribute to the discordance, but the principle behind this remains unclear.

Importantly, epileptiform discharges in patients with AD mainly occur during a sleep state, while the MEG recording cannot exceed a few hours at a time. Thus, it is nearly impossible to capture natural sleep or paroxysmal events during a sleep state by MEG. Considering the high requirement of equipment maintenance and the high costs of MEG examination, it is difficult to carry out MEG as a routine examination in general patients with AD. However, for patients with high suspicion of cortical hyperexcitability without visible epileptiform discharge on scalp EEG, MEG examination can be chosen to individually guide the usage of AEDs.

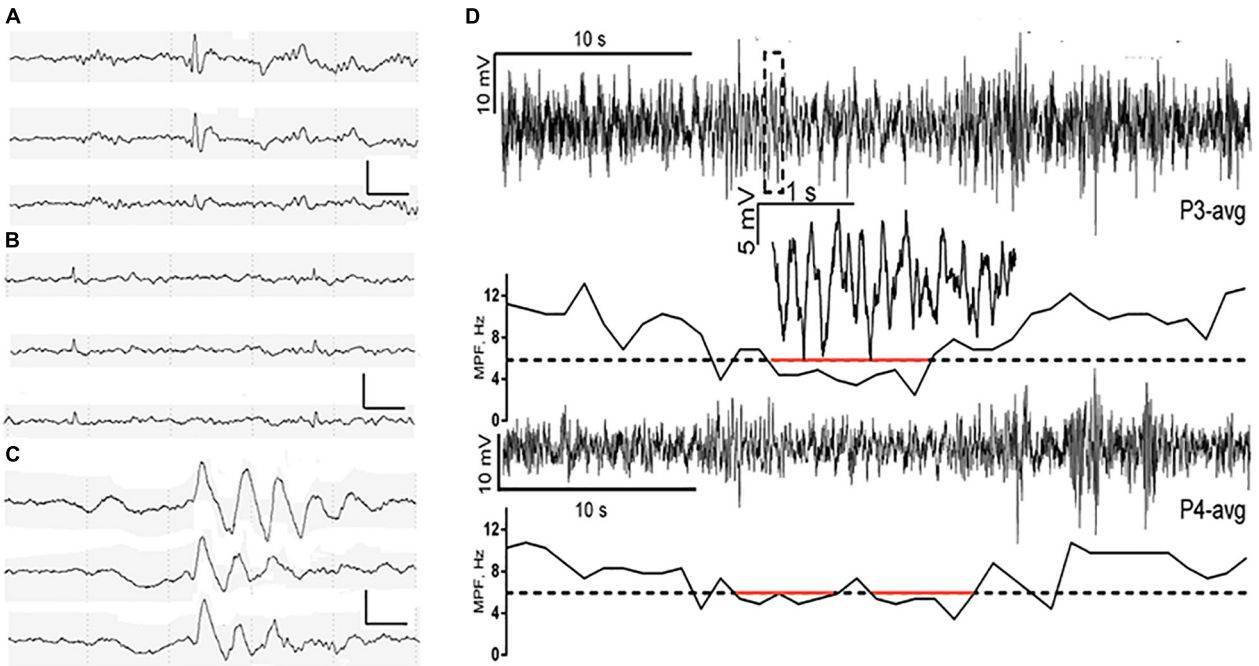

FIGURE 1 | Characterization of spike, small sharp spike (SSS), temporal intermittent rhythmic delta activities (TIRDA), and paroxysmal slow-wave event (PSWE). **(A–C)** Representative examples of spike, SSS, and TIRDA from the right temporal region in three patients with AD from our own ward, respectively. Scalp electrodes were placed using the international 10–20 system, sampling at 200 Hz. EEG channels (top to bottom): F8-ave, T4-ave, and T6-ave. Calibration bars: 100 μV and 500 ms. **(D)** A PSWE detected in a patient with AD. Traces from electrodes P3 (upper trace) and P4 (averaged as reference) are shown. The segment within the dashed rectangle of P3 is shown magnified. The median power frequency is presented below each trace. Segments below 6 Hz (dashed line) are marked in red. From Milikovsky et al. (2019). Reprint with permission from The American Association for the Advancement of Science (AAAS).

TABLE 1 | Electrophysiological biomarkers of AD-related increase of cortical excitability.

	Characteristics associated with clinical seizure	Advantages	Disadvantages	
Scalp EEG		Non-invasive		
Epileptiform discharges	Robust morphology, right temporal location, occur during awake or REM state, and higher frequency	Simple to implement in clinical work	Required long recording time and insensitive to epileptic discharges from deep mTL foci	Liedorp et al., 2010; Bakker et al., 2012; Vossel et al., 2016; Lam et al., 2017a, 2020; Horvath et al., 2018
SSSs	Unilateral SSS-like waveforms and frequent frequency (>100 per 24 h)	Simple to implement in clinical work	Hard to distinguish pathologic from benign SSSs	Lam et al., 2017a, 2020; Issa et al., 2018
TIRDA	Occur during awake or REM state	High diagnostic confidence	Infrequently frequency (<10 per 24 h)	Lam et al., 2020
PSWEs	–	No requirement for long recording time	Hard to distinguish	Milikovsky et al., 2019
MEG	–	Non-invasive and sensitive to discharges of tangential sulcal sources	Low specificity, high requirement of equipment, and only be monitored for a short time at a time	Oishi et al., 2002; Vossel et al., 2016
FO electrodes	Occur during non-REM sleep state	High quality, long-term recording, capture samples from deep temporal activities, and no skull defect	High cost, semi-invasive, and request for good neurosurgical skills of electrode placement	Sheth et al., 2014; Lam et al., 2017a, 2019
Computational approaches	–	Non-invasive and short monitoring time	Request for validation with large clinical data sets	Lam et al., 2016, 2017b; Babiloni et al., 2020

AD, Alzheimer's disease; SSS, small sharp spikes; TIRDA, temporal inter mitten rhythmic delta activity; PSWEs, paroxysmal slow wave events; EEG, electroencephalogram; MEG, magnetoencephalogram; FO, foramen ovale; mTL, mesial temporal lobe; REM, rapid eye moment.

FORAMEN OVALE ELECTRODES

Foramen ovale (FO) electrodes are a semi-invasive alternative to stereo-EEG electrodes. After general endotracheal anesthesia is induced, a single multi-contact FO electrode is positioned adjacent to each mTL inserted through the cheek skin to the ipsilateral natural aperture (FO) in the skull (Sheth et al., 2014). High-quality, long-term recordings can be obtained directly from the mTL using FO electrodes (Sperling et al., 1986; Fernández Torre et al., 1999). As FO electrodes will cause no skull defect, scalp EEG recording can be carried out simultaneously with FO electrodes. Furthermore, as mentioned above, since the mTL is the most affected location in patients with AD and FO electrodes that are accurate in capturing samples from deep temporal activities might be the best method for assessing subclinical discharges in patients with AD (Lam et al., 2019).

Lam et al. (2017a) used bilateral FO electrode recordings in two patients with AD (one had aMCI and another had moderate dementia; both had cerebrospinal fluid biomarker-confirmed AD) for the first time. The FO electrode recordings of both patients with AD demonstrated abundant, sleep-activated (especially non-REM sleep) spikes, and over 95% of the spikes were invisible on the simultaneous scalp EEG. In addition, three silent mTL seizures were captured on FO electrode recordings, while no visible evidence was found on scalp EEG in the patient with aMCI. They also found that mTL spikes on FO electrode recordings in the patient with aMCI occurred at up to a 10-fold rate compared with the patient with moderate dementia, supporting the concept that a greater extent of neuronal hyperactivity had developed during the earliest stages of AD rather than later stages (Zott et al., 2018). Existing studies indicate that mTL epileptiform discharges detected by FO electrodes mostly occur during a sleep state in both humans and mouse AD models (Lam et al., 2017a; Brown et al., 2018) but non-REM sleep in humans (Lam et al., 2017a; Brown et al., 2018) and REM sleep in mouse models with AD (Kam et al., 2016; Brown et al., 2018). Although FO electrodes offer high quality and long-term recordings of mTL activity, their utility as a screening tool for epileptiform discharges in patients with AD is limited because of their high cost, potential risks (for example, central nervous system infection and bleeding), and the requirement of good neurosurgical skills for electrode placement.

COMPUTATIONAL APPROACHES

For patients with AD, routine scalp EEG monitoring (20–40 min) is both necessary and feasible for the purpose of observing brain rhythms, but it is less helpful in recording epileptiform activity (Liedorp et al., 2010). However, performing overnight EEG, MEG, or FO electrode recordings is not feasible for the reasons of hospital resources, willingness to monitor patients, and high costs. As such, scientists have developed non-invasive and inexpensive methods, which can be widely implemented for diagnosing epileptiform activity.

Many studies have demonstrated that though there is a lack of visible epileptiform activity on scalp EEG, non-specific subtle and quantitative changes in local or long-distance networks induced by mTL spikes or seizures (Tyvaert et al., 2009; Vulliemoz et al., 2011; Cunningham et al., 2012; Aghakhani et al., 2015; Khoo et al., 2017; Naftulin et al., 2018) can be detected indirectly using artificial intelligence approaches. In a proof-of-principle study, Lam et al. (2016) analyzed the EEG data of 25 patients with epilepsy who underwent scalp EEG recording and FO electrode recording. By dividing scalp EEG recording into epochs and extracting coherence features of each epoch, they trained a seizure detector which correctly identified 40% of scalp-negative seizures (seizures detected by FO electrode recording but invisible on the scalp EEG), with a positive predictive value of 75% (Lam et al., 2016). In another publication by the same authors (Lam et al., 2017b), they extracted scalp EEG spectral power as an input feature and trained a machine learning algorithm that correctly identified 50% of scalp-negative seizures, with a positive predictive value of 94%. Studies by other researchers (Nayak et al., 2004; Koessler et al., 2015) also pointed out that mTL spikes or seizures might be detected by quantitative EEG signatures though they are invisible on a scalp EEG. Babiloni et al. (2020) found that higher temporal delta source activities are more strongly associated with clinical seizures in AD by estimating regional EEG cortical sources using exact low-resolution brain electromagnetic tomography (eLORETA) freeware. They used the area under receiver operating characteristic (AUROC) curves to index the accuracy of eLORETA solutions in identifying seizures and found an accuracy of 69% (Babiloni et al., 2020).

Development of computational approaches that accurately identify spikes or seizures from scalp EEG or MEG is underway (Lam et al., 2016, 2017b; Spyrou et al., 2016; Pizzo et al., 2019). However, this might be difficult to validate with large clinical data sets of combined scalp EEG/MEG and intracranial (especially FO electrode) recordings. Once the computational approaches become established, patients with AD may obtain more accurate guidance on antiepileptic therapy.

DISCUSSION

Patients with AD have an increased risk of seizures, compared to an age-matched control population, and they are over 10 times more likely to develop epilepsy, especially patients with early onset familial AD (Amatniek et al., 2006; Pandis and Scarmesa, 2012). The significance of interictal epileptiform activities in patients with AD is still controversial, and they are biomarkers of hyperexcitability, but their relation to seizures is actually unknown. Interictal epileptiform activities may compromise memory formation and consolidate themselves, even in the absence of seizures. There are also studies that contend that seizures might be a critical part of AD pathogenesis (Scarmeas et al., 2009). Numerous studies (Reyes-Marin and Nunez, 2017; Gureviciene et al., 2019) in animal models also suggest the importance of detecting these events, finding that a high number of interictal spikes increases the risk of seizures.

However, one thing most studies agree on is that patients with AD with seizures or subclinical epileptiform activity

experience faster cognitive declines over time (Vossel et al., 2016), and patients with AD might benefit from antiepileptic therapy. Moreover, the identification of biomarkers of epileptogenesis in patients with AD is a prerequisite for designing and developing targeted therapeutic approaches.

CONCLUSION

To date, human studies have identified several candidate EEG biomarkers as follows: epileptiform discharges (especially those with specific features, including high frequency, robust morphology, right temporal location, and occurrence during awake or REM states), frequent SSSs, TIRDA, and PSWEs recorded by scalp EEG (**Table 1**). In addition, MEG, FO electrodes, and computational approaches help to find subclinical seizures that are invisible on scalp EEG electrodes in patients with AD (**Table 1**). However, these findings require further study in humans as well as in animals to validate them and determine which are reliable and feasible electrophysiological biomarkers of epileptogenicity in patients with AD.

AUTHOR CONTRIBUTIONS

TY chose the search term, determined the methodology of the review, and drafted the manuscript. XL helped to choose the search term and determined the methodology of the review. JW and QW revised the manuscript and commented on previous versions of the manuscript. All authors read and approved the final manuscript.

FUNDING

This study was supported by the National Key R&D Program of China 2017YFC1307500 and Capital Healthy Development Research Funding 2016-1-2011 and 2020-1-2013.

ACKNOWLEDGMENTS

The authors thank AiMi Academic Services (www.aimieditor.com) for the English language editing and review services.

REFERENCES

Aghakhani, Y., Beers, C. A., Pittman, D. J., Gaxiola-Valdez, I., Goodyear, B. G., and Federico, P. (2015). Co-localization between the BOLD response and epileptiform discharges recorded by simultaneous intracranial EEG-fMRI at 3 T. *Neuroimage Clin.* 7, 755–763. doi: 10.1016/j.nicl.2015.03.002

Babiloni, C., Noce, G., Di Bonaventura, C., Lizio, R., Pascarelli, M. T., Tucci, F., et al. (2020). Abnormalities of cortical sources of resting state delta electroencephalographic rhythms are related to epileptiform activity in patients with amnesic mild cognitive impairment not due to Alzheimer's disease. *Front. Neurol.* 11:514136. doi: 10.3389/fneur.2020.514136

Bakker, A., Krauss, G. L., Albert, M. S., Speck, C. L., Jones, L. R., Stark, C. E., et al. (2012). Reduction of hippocampal hyperactivity improves cognition in amnestic mild cognitive impairment. *Neuron* 74, 467–474. doi: 10.1016/j.neuron.2012.03.023

Brown, R., Lam, A. D., Gonzalez-Sulser, A., Ying, A., Jones, M., Chou, R. C., et al. (2018). Circadian and brain state modulation of network hyperexcitability in Alzheimer's disease. *eNeuro* 5:ENEURO.0426-17.2018. doi: 10.1523/ENEURO.0426-17.2018

Brunetti, V., D'Atri, A., Della Marca, G., Vollono, C., Marra, C., Vita, M. G., et al. (2020). Subclinical epileptiform activity during sleep in Alzheimer's disease and mild cognitive impairment. *Clin. Neurophysiol.* 131, 1011–1018. doi: 10.1016/j.clinph.2020.02.015

Busche, M. A., and Konnerth, A. (2015). Neuronal hyperactivity – a key defect in Alzheimer's disease? *BioEssays* 37, 624–632. doi: 10.1002/bies.201500004

Busche, M. A., and Konnerth, A. (2016). Impairments of neural circuit function in Alzheimer's disease. *Philos. Trans. R. Soc. Lond. B Biol. Sci.* 371:20150429. doi: 10.1098/rstb.2015.0429

Busche, M. A., Chen, X., Henning, H. A., Reichwald, J., Staufenbiel, M., Sakmann, B., et al. (2012). Critical role of soluble amyloid-β for early hippocampal hyperactivity in a mouse model of Alzheimer's disease. *Proc. Natl. Acad. Sci. U.S.A.* 109, 8740–8745. doi: 10.1073/pnas.1206171109

Cirrito, J. R., Yamada, K. A., Finn, M. B., Sloviter, R. S., Bales, K. R., May, P. C., et al. (2005). Synaptic activity regulates interstitial fluid amyloid-beta levels in vivo. *Neuron* 46, 913–922. doi: 10.1016/j.neuron.2005.10.028

Amatniek, J. C., Hauser, W. A., DelCastillo-Castaneda, C., Jacobs, D. M., Marder, K., Bell, K., et al. (2006). Incidence and predictors of seiures in patients with Alzheimer's disease. *Epilepsia* 47, 867–872. doi: 10.1111/j.1528-1167.2006.00554.x

Cretin, B., Sellal, F., Philippi, N., Bousiges, O., Di Bitonto, L., Martin-Hunyadi, C., et al. (2016). Epileptic prodromal Alzheimer's disease, a retrospective study of 13 new cases: expanding the spectrum of Alzheimer's disease to an epileptic variant? *J. Alzheimers Dis.* 52, 1125–1133. doi: 10.3233/JAD-150096

Cunningham, C. B., Goodyear, B. G., Badawy, R., Zaamout, F., Pittman, D. J., Beers, C. A., et al. (2012). Intracranial EEG-fMRI analysis of focal epileptiform discharges in humans. *Epilepsia* 53, 1636–1648. doi: 10.1111/j.1528-1167.2012.03601.x

Damoiseaux, J. S., Smith, S. M., Witter, M. P., Sanz-Arigita, E. J., Barkhof, F., Scheltens, P., et al. (2009). White matter tract integrity in aging and Alzheimer's disease. *Hum. Brain Mapp.* 30, 1051–1059. doi: 10.1002/hbm.20563

Diaz-Negrillo, A. (2013). Influence of sleep and sleep deprivation on ictal and interictal epileptiform activity. *Epilepsy Res. Treat.* 2013:492524. doi: 10.1155/2013/492524

Donix, M., Burggren, A. C., Scharf, M., Marschner, K., Suthana, N. A., Siddarth, P., et al. (2013). APOE associated hemispheric asymmetry of entorhinal cortical thickness in aging and Alzheimer's disease. *Psychiatry Res.* 214, 212–220. doi: 10.1016/j.pscychresns.2013.09.006

Enatsu, R., Mikuni, N., Usui, K., Matsubayashi, J., Taki, J., Begum, T., et al. (2008). Usefulness of MEG magnetometer for spike detection in patients with mesial temporal epileptic focus. *Neuroimage* 41, 1206–1219. doi: 10.1016/j.neuroimage.2008.03.038

Fernández Torre, J. L., Alarcón, G., Binnie, C. D., and Polkey, C. E. (1999). Comparison of sphenoidal, foramen ovale and anterior temporal placements for detecting interctal epileptiform discharges in presutgical assessment for temporal lobe epilepsy. *Clin. Neurophysiol.* 110, 895–904. doi: 10.1016/s1388-2457(99)00039-5

Friedman, D., Honig, L. S., and Scarmeas, N. (2011). Seizures and epilepsy in Alzheimer's disease. *CNS Neurosci. Ther.* 18, 285–294. doi: 10.1111/j.1755-5949.2011.00251.x

Gambardella, A., Gotman, J., Cendes, F., and Andermann, F. (1995). Focal intermittent delta activity in patient with mesiotemporal atrophy: a reliable marker of the epileptogenic focus. *Epilepsia* 36, 122–129. doi: 10.1111/j.1528-1157.1995.tb00970.x

Gennaro, G. D., Quarato, P. P., Onorati, P., Colazza, G. B., Mari, F., Grammaldo, L. G., et al. (2003). Localizing significance of temporal intermittent rhythmic delta activity (TIRDA) in drug-resistant focal epilepsy. *Clin. Neurophysiol.* 114, 70–78. doi: 10.1016/s1388-2457(02)00332-2

Gureviciene, I., Ishchenko, I., Ziyatdinova, S., Jin, N., Lipponen, A., Gurevicius, K., et al. (2019). Characterization of epileptic spiking associated with brain amyloidosis in APP/PS1 mice. *Front. Neurol.* 12:1151. doi: 10.3389/fneur.2019.01151

Horvath, A., Szucs, A., Csukly, G., Sakovics, A., Stefanics, G., and Kamondi, A. (2018). EEG and ERP biomarkers of Alzheimer's disease: a critical review. *Front. Biosci.* 23, 183–220. doi: 10.2741/4587

Issa, N. P., Wu, S., Rose, S., Towle, V. L., Warnke, P. C., and Tao, J. X. (2018). Small sharp spikes as EEG markers of mesiotemporal lobe epilepsy. *Clin. Neurophysiol.* 129, 1796–1803. doi: 10.1016/j.clinph.2018.06.011

Kaiboriboon, K., Nagarajan, S., Mantle, M., and Kirsch, H. E. (2010). Interictal MEG/MSI in intractable mesial temporal lobe epilepsy: spike yield and characterization. *Clin. Neurophysiol.* 121, 325–331. doi: 10.1016/j.clinph.2009.12.001

Kam, K., Duffy, A. M., Moretto, J., LaFrancois, J. J., and Scharfman, H. E. (2016). Interictal spikes during sleep are an early defect in the Tg2576 mouse model of β-amyloid neuropathology. *Sci. Rep.* 9:20119. doi: 10.1038/srep20119

Khoo, H. M., von Ellenrieder, N., Zazubovits, N., Dubeau, F., and Gotman, J. (2017). Epileptic networks in action: synchrony between distant hemodynamic responses. *Ann. Neurol.* 82, 57–66. doi: 10.1002/ana.24973

Koessler, L., Cecchin, T., Colnat-Coulbois, S., Vignal, J. P., Jonas, J., Vespignani, H., et al. (2015). Catching the invisible: mesial temporal source contribution to simultaneous EEG and SEEG recordings. *Brain Topogr.* 28, 5–20. doi: 10.1007/s10548-014-0417-z

Lam, A. D., Cole, A. J., and Cash, S. S. (2019). New approaches to studying silent mesial temporal lobe seizures in Alzheimer's disease. *Front. Neurol.* 10:959. doi: 10.3389/fneur.2019.00959

Lam, A. D., Deck, G., Goldman, A., Eskandar, E. N., Noebels, J., and Cole, A. J. (2017a). Silent hippocampal seizures and spikes identified by foramen ovale electrodes in Alzheimer's disease. *Nat. Med.* 23, 678–680. doi: 10.1038/nm.4330

Lam, A. D., Maus, D., Zafar, S. F., Cole, A. J., and Cash, S. S. (2017b). SCOPE-mTL: a noninvasive tool for identifying and lateralizing mesial temporal lobe seizures prior to scalp EEG ictal onset. *Clin. Neurophysiol.* 128, 1647–1655. doi: 10.1016/j.clinph.2017.06.040

Lam, A. D., Sarkis, R. A., Pellerin, K. R., Jing, J., Dworetzky, B. A., Hoch, D. B., et al. (2020). Association of epileptiform abnormalities and seizures in Alzheimer disease. *Neurology* 20, e2259–e2270. doi: 10.1212/WNL.0000000000010612

Lam, A. D., Zepeda, R., Cole, A. J., and Cash, S. S. (2016). Widespread changes in network activity allow noninvasive detection of mesial temporal lobe seizures. *Brain* 139, 2679–2693. doi: 10.1093/brain/aww198

Liedorp, M., Stam, C. J., van der Flier, W. M., Pijnenburg, Y. A. L., and Scheltens, P. (2010). Prevalence and clinical significance of epileptiform EEG discharges in a large memory clinic cohort. *Dement. Geriatr. Cogn. Disord.* 29, 432–437. doi: 10.1159/000278620

Liu, H., Zhang, L., Xi, Q., Zhao, X., Wang, F., Wang, X., et al. (2018). Changes in brain lateralization in patients with mild cognitive impairment and Alzheimer's disease: a resting-state functional magnetic resonance study from Alzheimer's disease neuroimaging initiative. *Front. Neurol.* 9:3. doi: 10.3389/fneur.2018.00003

Malow, B. A., Kushwaha, R., Lin, X., Morton, K. J., and Aldrich, M. S. (1997). Relationship of interictal epileptiform discharges to sleep depth in partial epilepsy. *Electroencephalogr. Clin. Neurophysiol.* 102, 20–26. doi: 10.1016/s0013-4694(96)96028-9

Milikovsky, D. Z., Ofer, J., Senatorov, V. V. Jr., Friedman, A. R., Prager, O., Sheintuch, L., et al. (2019). Paroxysmal slow cortical activity in Alzheimer's disease and epilepsy is associated with blood-brain barrier dysfunction. *Sci. Transl. Med.* 11:eaaw8954. doi: 10.1126/scitranslmed.aaw8954

Musaeus, C. S., Engedal, K., Hogh, P., Jelic, V., Morup, M., Naik, M., et al. (2018). EEG theta power is an early marker of cognitive decline in dementia due to Alzheimer's disease. *J. Alzheimers Dis.* 64, 1359–1371. doi: 10.3233/JAD-180300

Naftulin, J. S., Ahmed, O. J., Piantoni, G., Eichenlaub, J. B., Martinet, L. E., Kramer, M. A., et al. (2018). Ictal and preictal power changes outside of the seizure focus correlate with seizure generalization. *Epilepsia* 59, 1398–1409. doi: 10.1111/epi.14449

Nayak, D., Valentin, A., Alarcon, G., Garcia Seoane, J. J., Brunnhuber, F., Juler, J., et al. (2004). Characteristics of scalp electrical fields associated with deep medial temporal epileptiform discharges. *Clin. Neurophysiol.* 115, 1423–1435. doi: 10.1016/j.clinph.2004.01.009

Noachtar, S., and Remi, J. (2009). The role of EEG in epilepsy: a critical review. *Epilepsy Behav.* 15, 22–33. doi: 10.1016/j.yebeh.2009.02.035

Noebels, J. (2011). A perfect storm: converging paths of epilepsy and Alzheimer's dementia intersect in the hippocampal formation. *Epilepsia* 52(Suppl. 1), 39–46. doi: 10.1111/j.1528-1167.2010.02909.x

Normand, M. M., Wszolek, Z. K., and Klass, D. W. (1995). Temporal intermittent rhythmic delta activity in electroencephalograms. *J. Clin. Neurophysiol.* 12, 280–284. doi: 10.1097/00004691-199505010-00005

Oishi, M., Otsubo, H., Kameyama, S., Morota, N., Masuda, H., Kitayama, M., et al. (2002). Epileptic spikes: magnetoencephay versus simultaneous electrocorticography. *Epilepsia* 43, 1390–1395. doi: 10.1046/j.1528-1157.2002.10702.x

Palop, J. J., and Mucke, L. (2009). Epilepsy and cognitive impairments in Alzheimer disease. *Arch. Neurol.* 66, 435–440. doi: 10.1001/archneurol.2009.15

Palop, J. J., and Mucke, L. (2016). Network abnormalities and interneuron dysfunction in Alzheimer disease. *Nat. Rev. Neurosci.* 17, 777–792. doi: 10.1038/nrn.2016.141

Pandis, D., and Scarmesa, N. (2012). Seizures in Alzheimer disease: clinical and epidemiological data. *Epilepsy Curr.* 12, 184–187. doi: 10.5698/1535-7511-12.5.184

Pizzo, F., Roehri, N., Medina Villalon, S., Trebuchon, A., Chen, S., Lagarde, S., et al. (2019). Deep brain activities can be detected with magnetoencephalography. *Nat. Commun.* 10:971. doi: 10.1038/s41467-019-08665-5

Pooler, A. M., Phillips, E. C., Lau, D. H., Noble, W., and Hanger, D. P. (2013). Physiological release of endogenous tau is stimulated by neuronal activity. *EMBO Rep.* 14, 389–394. doi: 10.1038/embor.2013.15

Reiher, J., Beaudry, M., and Leduc, C. P. (1989). Temporal intermittent rhythmic delta activity (TIRDA) in the diagnosis of complex partial epilepsy: sensitivity, specificity and predictive value. *Can. J. Neurol. Sci.* 16, 398–401. doi: 10.1017/s0317167100029450

Reyes-Marin, K. E., and Nunez, A. (2017). Seizure susceptibility in the APP/PS1 mouse model of Alzheimer's disease and relationship with amyloid β plaques. *Brain Res.* 15, 93–100. doi: 10.1016/j.brainres.2017.09.026

Sammaritano, M., Gigli, G. L., and Gotman, J. (1991). Interictal spiking during wakefulness and sleep and the localization of foci in temporal lobe epilepsy. *Neurology* 41, 290–297. doi: 10.1212/wnl.41.2_part_1.290

Sarkis, R. A., Dickerson, B. C., Cole, A. J., and Chemali, Z. N. (2016). Clinical and neurophysiologic characteristics of unprovoked seizures in patients diagnosed with dementia. *J. Neuropsychiatry Clin. Neurosci.* 28, 56–61. doi: 10.1176/appi.neuropsych.15060143

Scarmeas, N., Honig, L. S., Choi, H., Cantero, J., Brandt, J., Blacker, D., et al. (2009). Seizures in Alzheimer disease: who, when, and how common? *Arch. Neurol.* 66, 992–997. doi: 10.1001/archneurol.2009.130

Sheth, S. A., Aronson, J. P., Shafi, M. M., Phillips, H. W., Velez-Ruiz, N., Walcott, B. P., et al. (2014). Utility of foramen ovale electrodes in mesial temporal lobe epilepsy. *Epilepsia* 55, 713–724. doi: 10.1111/epi.12571

Sperling, M. R., Mendius, J. R., and Engel, J. Jr. (1986). Mesial temporal spikes: a simultaneous comparison of sphenidal, nasopharyngeal, and ear electrodes. *Epilepsia* 27, 81–86. doi: 10.1111/j.1528-1157.1986.tb03505.x

Spyrou, L., Martin-Lopez, D., Valentin, A., Alarcon, G., and Sanei, S. (2016). Detection of intracranial signatures of interictal epileptiform discharges from concurrent scalp EEG. *Int. J. Neural Syst.* 26:1650016. doi: 10.1142/S0129065716500167

Stomrud, E., Hansson, O., Minthon, L., Blennow, K., Rosen, I., and Londos, E. (2010). Slowing of EEG correlates with CSF biomarkers and reduced cognitive speed in elderly with normal cognition over 4 years. *Neurobiol. Aging* 31, 215–223. doi: 10.1016/j.neurobiolaging.2008.03.025

Thompson, P. M., Hayashi, K. M., Zubicaray, G. D., Janke, A. L., Rose, S. E., Semple, J., et al. (2003). Dynamics of gray matter loss in Alzheimer's disease. *J. Neurosci.* 23, 994–1005. doi: 10.1523/JNEUROSCI.23-03-00994.2003

Tyvaert, L., LeVan, P., Dubeau, F., and Gotman, J. (2009). Noninvasive dynamic imaging of seizures in epileptic patients. *Hum. Brain Mapp.* 30, 3993–4011. doi: 10.1002/hbm.20824

Vossel, K. A., Beagle, A. J., Rabinovici, G. D., Shu, H., Lee, S. E., Naasan, G., et al. (2013). Seizures and epileptiform activity in the early stages of Alzheimer disease. *JAMA Neurol.* 70, 1158–1166. doi: 10.1001/jamaneurol.2013.136

Vossel, K. A., Ranasinghe, K. G., Beagle, A. J., Mizuiri, D., Honma, S. M., Dowling, A. F., et al. (2016). Incidence and impact of subclinical epileptiform activity in Alzheimer's disease. *Ann. Neurol.* 80, 858–870. doi: 10.1002/ana.24794

Vulliemoz, S., Carmichael, D. W., Rosenkranz, K., Diehl, B., Rodionov, R., Walker, M. C., et al. (2011). Simultaneous intracranial EEG and fMRI of interictal epileptic discharges in humans. *Neuroimage* 54, 182–190. doi: 10.1016/j.neuroimage.2010.08.004

Wennberg, R., and Cheyne, D. (2014). Reliability of MEG source imaging of anterior temporal spikes: analysis of an intracranially characterized spike focus. *Clin. Neurophysiol.* 125, 903–918. doi: 10.1016/j.clinph.2013.08.032

Wennberg, R., Valiante, T., and Cheyne, D. (2011). EEG and MEG in mesial temporal lobe epilepsy: where do the spikes really come from? *Clin. Neurophysiol.* 122, 1295–1313. doi: 10.1016/j.clinph.2010.11.019

Wessa, M., King, A. V., Meyer, P., Frolich, L., Flor, H., Poupon, C., et al. (2016). Impaired and preserved aspects of feedback learning in aMCI: contributions of structural connectivity. *Brain Struct. Funct.* 221, 2831–2846. doi: 10.1007/s00429-015-1075-y

White, J. C., Langston, J. W., and Pedley, T. A. (1977). Benign epileptiform transients of sleep. Clarification of the small sharp spike controversy. *Neurology* 27, 1061–1068. doi: 10.1212/wnl.27.11.1061

Wu, J. W., Hussaini, S. A., Bastille, I. M., Rodriguez, G. A., Mrejeru, A., Rilett, K., et al. (2016). Neuronal activity enhances tau propagation and tau pathology in vivo. *Nat. Neurosci.* 19, 1085–1092. doi: 10.1038/nn.4328

Yang, C., Zhong, S., Zhou, X., Wei, L., Wang, L., and Nie, S. (2017). The abnormality of topological asymmetry between hemispheric brain white matter networks in Alzheimer's disease and mild cognitive impairment. *Front. Aging Neurosci.* 9:261. doi: 10.3389/fnagi.2017.00261

Zott, B., Busche, M. A., Sperling, R. A., and Konnerth, A. (2018). What happens with the circuit in Alzheimer's disease in the mice and humans. *Annu. Rev. Neurosci.* 41, 277–297. doi: 10.1146/annurev-neuro-080317-061725

Conflict of Interest: The authors declare that the research was conducted in the absence of any commercial or financial relationships that could be construed as a potential conflict of interest.

Publisher's Note: All claims expressed in this article are solely those of the authors and do not necessarily represent those of their affiliated organizations, or those of the publisher, the editors and the reviewers. Any product that may be evaluated in this article, or claim that may be made by its manufacturer, is not guaranteed or endorsed by the publisher.

frontiers in Human Neuroscience

ORIGINAL RESEARCH
published: 08 December 2021
doi: 10.3389/fnhum.2021.766935

Impact of Early-Commenced and Continued Sports Training on the Precuneus in Older Athletes

*Masatoshi Yamashita[1], Maki Suzuki[2,3], Toshikazu Kawagoe[3,4], Kohei Asano[5,6], Masatoshi Futada[3], Ryusuke Nakai[6], Nobuhito Abe[6] and Kaoru Sekiyama[1,3]**

[1]Graduate School of Advanced Integrated Studies in Human Survivability, Kyoto University, Kyoto, Japan, [2]Department of Behavioral Neurology and Neuropsychiatry, Osaka University United Graduate School of Child Development, Osaka, Japan, [3]Faculty of Letters, Kumamoto University, Kumamoto, Japan, [4]Liberal Arts Education Center, Kyushu Campuses, Tokai University, Kumamoto, Japan, [5]Faculty of Child Care and Education, Osaka University of Comprehensive Children Education, Osaka, Japan, [6]Kokoro Research Center, Kyoto University, Kyoto, Japan

Intervention studies on sedentary older adults have demonstrated that commencing physical exercise at an older age has a positive effect on brain structure. Although this suggests that older athletes with lifelong sports training have larger gray matter volume (GMV) in some brain regions compared to age-matched non-athletes, evidence in the literature is scarce. Moreover, it remains unclear whether a larger GMV is associated with training intensity or period of training in life. To address these gaps in the literature, we compared regional brain GMV between 24 older athletes (mean age, 71.4 years; age at the commencement of sports training, 31.2 years, continuous sports training, 40.0 years; current training time, 7.9 h/week) and 24 age-matched non-athletes (mean age, 71.0 years). The period of sports training and the current training time of the athletes were assessed. Both groups were evaluated for physical activity intensity as well as cognitive and motor performance. Although no group differences were noted in cognitive and motor performance, athletes reported higher physical activity intensity than non-athletes. Whole-brain structural analysis revealed a significantly larger GMV in several brain regions in athletes. Notably, the GMV of the precuneus in athletes was positively correlated with earlier commencement of sports training and training duration but was negatively correlated with current training time. Our findings demonstrate that early-commenced and continued sports training predicts structural maintenance of the precuneus in old age. Our results also suggest that excessive training time in old age may have a negative impact on the GMV of the precuneus; thereby delineating how the precuneus is associated with lifelong sports training in older athletes.

Keywords: older athletes, precuneus, aging, early-commenced sports training, excessive training

OPEN ACCESS

Edited by:
Fanpei G. Yang,
National Tsing Hua University, Taiwan

Reviewed by:
Sze Chai Kwok,
Duke Kunshan University, China
Ayşe İkinci Keleş,
Aksaray University, Turkey

****Correspondence:***
Kaoru Sekiyama
sekiyama.kaoru.8a@kyoto-u.ac.jp

Specialty section:
This article was submitted to Brain Health and Clinical Neuroscience, a section of the journal Frontiers in Human Neuroscience

Received: *30 August 2021*
Accepted: *12 October 2021*
Published: *08 December 2021*

Citation:
Yamashita M, Suzuki M, Kawagoe T, Asano K, Futada M, Nakai R, Abe N and Sekiyama K (2021) Impact of Early-Commenced and Continued Sports Training on the Precuneus in Older Athletes. Front. Hum. Neurosci. 15:766935. doi: 10.3389/fnhum.2021.766935

INTRODUCTION

Magnetic resonance imaging (MRI) studies have revealed key structural characteristics of the aging brain. For example, the gray matter volume (GMV) of the frontal cortex, cingulate cortex, hippocampus, cerebellum, basal ganglia, and parietal lobe (e.g., supramarginal gyrus and precuneus) decreases with age (Raz et al., 2004, 2010; Ramanoël et al., 2018; Eyme et al., 2019; Hahm et al., 2019). Atrophy of these brain regions is associated

with age-related decline in various behavioral measures of cognitive function (Seidler et al., 2010; Nyberg et al., 2012). Given the rise in aging-associated issues in current society, identifying lifestyle habits that effectively mitigate age-related cognitive decline and brain atrophy is essential.

Continued physical exercise is a candidate lifestyle factor in this regard, given its association with a reduced risk of dementia (Rovio et al., 2005; Larson et al., 2006; Tanaka et al., 2020) and mild cognitive impairment (Geda et al., 2010). Previous studies have reported that 6- to 12-month walking programs in sedentary older adults were associated with increased GMV of the hippocampus and frontal lobes, including the anterior cingulate cortex, supplementary motor area, and inferior frontal gyrus, compared to control participants who performed stretching as a non-aerobic exercise (Colcombe et al., 2006; Erickson et al., 2011). In addition, greater walking distance is associated with a larger GMV in the prefrontal and temporal regions, which reduces the risk of cognitive impairment (Erickson et al., 2010). These findings suggest that a physically active lifestyle predicts structural maintenance and related cognitive maintenance. Nevertheless, it remains unclear whether the effects of a physically active lifestyle are cross-sectionally evident in masters athletes relative to non-athletes.

Masters athletes are an excellent model of older adults who have participated in lifelong sports training and maintain high levels of motor skills. Several cross-sectional behavioral studies have reported higher levels of verbal memory, visuospatial processing, and attention in young (Lobjois et al., 2006; Tarumi et al., 2013) and older athletes (Lobjois et al., 2006; Tseng et al., 2013; Zhao et al., 2016) compared to that in age-matched non-athletes. These favorable characteristics of athletes may be underscored by physical fitness (e.g., muscle strength and cardiovascular endurance) as well as motor fitness (e.g., speed, balance, and fine motor coordination). The vigorous sports training of athletes may improve perceptual and motor processes associated with the mapping of sensation to action, which enables efficient spatial orientation and reactions to moving objects/persons. Moreover, metacognition in athletes is thought of as an essential component of self-regulation, proper strategies, and motor coordination monitoring to excel in sports (MacIntyre et al., 2014). Thus, sports training may lead to greater effects on cognitive function and brain structure compared to simple physical exercises, such as walking. Nevertheless, there is a paucity of studies on the effects of lifelong sports training on brain structure. One study reported that young athletes had larger GMV in the inferior parietal lobule, middle temporal gyrus, precentral gyrus, and frontal cortex compared to non-athletes (Fukuo et al., 2020). Another study reported larger GMV in the right parietal lobe (e.g., precuneus), occipital lobe, and cerebellum in a small group of older athletes compared to that in sedentary elderly individuals (Tseng et al., 2013). These findings suggest that the beneficial structural changes in the brains of athletes involve both motor-related and perception-related areas, highlighting the involvement of coordination between cognitive and motor processes when playing sports. Moreover, a study reported that current maximal oxygen consumption was positively correlated with the GMV of several brain structures, including the precuneus, frontal, and occipital lobes in older athletes (Tseng et al., 2013). However, these findings were based on a small sample. Further, the correlation was only observed between the current physical status of athletes and brain structure, and the study lacked information about the correlation between past athletic training and brain maintenance. Of note, previous studies have demonstrated that early-commenced physical training is associated with the strength of structural and functional connectivity in frontoparietal and default mode networks as well as related cognitive enhancement in middle-aged adults who have participated in regular sports training (Dik et al., 2003; Ferro et al., 2016; Ishihara et al., 2021). These findings suggest that early commencement of sports training may contribute to neural changes and related cognitive maintenance in later life and that the beneficial structural changes in the brains of athletes are affected not only by the amount of current physical activity (e.g., maximal oxygen consumption and current training time) but also by the length of experience, such as early-commenced and continued sports training. However, no study to date has identified the contribution of the length of sports experience to brain structure in older athletes.

This cross-sectional study aimed to address two research questions. First, we aimed to replicate the previously reported finding that the GMV in several brain regions was larger in older athletes compared to older non-athletes (Tseng et al., 2013) using a larger sample. Second, we aimed to determine whether the favorable structural changes in the brains of athletes, if any, were associated with the length of sports experience in life and/or the amount of current physical activity. To address these questions, we compared brain structure between older athletes and age-matched non-athletes. Based on the structural differences between groups, we further examined the associations between GMV in regions of interest (ROIs) and sports traits [age of commencement, years of training, current training time, and International Physical Activity Questionnaire (IPAQ) score]. We hypothesized that athletes would have increased the GMV in one or more brain regions (the precuneus, occipital lobe, and cerebellum) and that this increase would be correlated with the length of sports experience.

MATERIALS AND METHODS

Participants

The Psychological Research Ethics Committee of Kumamoto University approved the protocol, and all study participants provided informed consent. In total, 49 older adults (25 athletes and 24 non-athletes, aged 65–79 years) participated in this study. Athletes were defined as those who had received sports training for at least 15 years, based on a previous study (Tseng et al., 2013). Athletes were recruited *via* the Kyoto City Silver Human Resources Center, Kyoto Kendo Hall, and personal connections associated with tennis, golf clubs, and dance schools. Non-athletes with less than 3 years of sports experience were recruited from the Kyoto City Silver Human Resources Center. All the participants were right-handed.

The exclusion criteria were cognitive impairments [**Table 1**; Mini-Mental State Examination (MMSE) score $\geq$ 25], a history of neurological, cardiovascular, or psychiatric illness, and/or contraindications for MRI. One athlete was excluded due to physical deconditioning. The final analysis comprised 24 athletes (12 men and 12 women) and 24 non-athletes (12 men and 12 women).

The athletes had commenced sports training between the ages of 7 and 57 years (**Table 2**; mean = 31.2 years) and had been practicing sports for more than 19 years at the time the study was conducted (**Table 2**; mean = 40.0 years, range = 19–65 years). The current training time of the athletes was between 0.5 and 36.0 h per week (**Table 2**; mean = 7.9 h/week). The sports included tennis, kendo, golfing, dancing, cycling, and swimming. These sports, compared to simple physical exercises, such as walking and running, highlight the need for perceptual (e.g., visuospatial processing and attention shift) and motor (e.g., speed and balance) processing associated with sensation-to-action mapping.

Measures of Physical Activity

Physical activity intensity levels were assessed using the Japanese version of the IPAQ-Short Form, which contains seven questions (Craig et al., 2003; Inoue et al., 2009). In the IPAQ, participants were instructed to record their physical activity intensity levels (vigorous-intensity activity, moderate-intensity activity, walking, and sitting) over the previous 7 days.

Behavioral Measurements

Cognitive and motor function and physical activity levels were measured and compared between athletes and non-athletes. Cognitive tests consisted of the Japanese versions of parts A and B of the trail-making test (TMT; Reitan and Wolfson, 1993) and logical memory-I and -II subtests of the Wechsler Memory Scale-Revised edition (WMS-R; Wechsler, 1997; Sugishita, 2000). Motor tests consisted of timed up and go (TUG; Podsiadlo and Richardson, 1991) and pegboard (Guo et al., 2020) tasks.

TABLE 1 | Demographics of athletes and non-athletes.

Total (n = 48)	Athletes (n = 24)	Non-athletes (n = 24)	P-value
Sex (male/female)	12/12	12/12	1.000
Age (years)	71.4 (3.4)	71.0 (3.5)	0.737
Education (years)	14.2 (2.2)	13.0 (2.3)	0.077
Body height (cm)	160.1 (7.3)	159.9 (8.4)	0.913
Body weight (kg)	56.9 (9.0)	58.1 (13.6)	0.728
MMSE (score)	28.9 (1.2)	28.9 (0.9)	0.891
IPAQ (score)	3479.9 (2133.1)	991.4 (1406.8)	<0.001

The parameters are presented as mean (SD). P-values for age, education, body height and weight, MMSE, and IPAQ are from t-tests for group differences. P-value for sex ratio is from Chi-square test for group differences. MMSE, Mini-Mental State Examination; IPAQ, International Physical Activity Questionnaire; SD, standard deviation.

TABLE 2 | Sports training status in athletes.

Athletes (n = 24)	Mean (SD)	Range
Age of commencement	31.2 (15.0)	7–57
Years of training	40.0 (15.5)	19–65
Current training time (hours/week)	7.9 (7.2)	0.5–36

SD, standard deviation.

Parts A and B of the TMT were used to evaluate executive function. In TMT-A, participants were instructed to draw lines to sequentially connect 25 numbers in ascending order. In TMT-B, participants were instructed to draw lines alternately between numbers and letters (1, A, 2, B, etc.). The logical memory-I and -II subtests of the WMS-R were conducted to evaluate verbal memory. In the logical memory-I subtest, participants were instructed to immediately recall two stories sequentially. In the logical memory-II subtest, participants were instructed to recall the two stories 30 min later. The TUG and pegboard tasks were conducted to evaluate motor function. In the TUG test, participants were instructed to stand up from a standard chair, walk 3 m up and back, and sit down. In the pegboard task, participants were instructed to turn over 20 pegs (diameter $\times$ height = 0.5 $\times$ 3.5 cm) in 20 holes carved on a square board (length $\times$ width $\times$ thickness = 15 $\times$ 18 $\times$ 2 cm; SAKAI Medical Co., Ltd., Japan) using the right hand.

Statistical Analysis of Behavioral Data

IPAQ scores and behavioral data were compared between athletes and non-athletes using a two-sample t-test for each of the seven measures. IBM-SPSS Statistics for Windows, version 25 (IBM corporation, Armonk, NY, USA) was used for statistical analysis. However, multiple t-tests may induce type I errors (overestimation of significant effects without correction) or type II errors (underestimation of significant effects under conservative correction, such as that using the Bonferroni method). The sampling method (e.g., permutation) can be used to estimate adjusted P-values while avoiding parametric assumptions about the joint distribution of the test statistics (Dudoit et al., 2003). A permutation test (Camargo et al., 2008) was conducted using MATLAB R2020a (The Mathworks Inc., United States) with a statistics and machine-learning toolbox. For each behavioral measure, all 48 observed samples (24 athletes and 24 non-athletes) were randomized together and resampled to obtain a dummy t-value. This procedure was repeated 10,000 times for each of the seven behavioral measures. A total of 70,000 t-values (10,000 resampling $\times$ 7 behavioral measures) were pooled and a unique permutation t-distribution was created to obtain a single adjusted α-level threshold (the top five percentile rank in the distribution).

Image Acquisition

Scanning was performed using a 3T Siemens MAGNETOM Verio MR scanner (Siemens, Erlangen, Germany). The participants' head was immobilized using a scanner head-coil (12 channels). High-resolution structural images were acquired using an axial T1-weighted magnetization-prepared rapid gradient-echo pulse sequence (TR = 2,250 ms; TE = 3.51 ms; TI = 900 ms; field of view = 256 $\times$ 256; matrix size = 256 $\times$ 256; voxel size = 1 $\times$ 1 $\times$ 1 mm; 208 slices).

Image Preprocessing and Statistical Analysis of Structural Data

Voxel-based morphometry (VBM; Ashburner and Friston, 2000) was performed using the statistical parametric mapping software SPM12 (Wellcome Department of Cognitive Neurology,

London) and MATLAB R2018a. Structural T1-weighted images were first segmented to separate the different types of tissues: gray matter, white matter, cerebrospinal fluid, soft tissue, and skull. The segmented images (gray matter and white matter) were then spatially normalized using the Diffeomorphic Anatomical Registration using Exponentiated Lie algebra (Ashburner, 2007). To preserve the absolute volume of gray matter, modulation was performed on normalized gray matter images by multiplying the Jacobian determinants derived from spatial normalization. Finally, the modulated gray matter images were smoothed with an 8-mm full-width at half-maximum Gaussian kernel.

For the VBM statistical analysis, we used threshold-free cluster enhancement (TFCE), which was introduced to enhance voxel-based analysis sensitivity, by applying 5,000 permutations (Smith method; Smith and Nichols, 2009; Salimi-Khorshidi et al., 2011; Nenadic et al., 2021). First, we tested the GMV differences between groups using a general linear model in the SPM software, with total brain volume defined as a nuisance variable. An explicit mask was used to exclude noisy voxels from the statistical analysis. Based on the TFCE analysis, the statistical thresholds were set at $P < 0.001$, uncorrected for multiple comparisons, and $P < 0.05$ family-wise error corrected for multiple comparisons. Thereafter, we identified the cluster location obtained from structural data using the anatomy toolbox in SPM12 (Eickhoff et al., 2005).

Next, the associations between sports traits and the GMVs in the ROIs were investigated. Based on the structural result differences between the groups, we used MarsBaR software (Brett et al., 2002) to extract spherical ROIs that centered on the local maximal peaks of the significant clusters (we used sub-clusters for overly large clusters) that were located within a 10-mm radius of the regions identified in the aforementioned analysis (Guo et al., 2020). Correlation analyses were conducted using the Pearson's correlation coefficient. For these multiple coefficients, validation tests for correlation were performed using a permutation test in MATLAB R2020a. To examine the correlation for a given pair of variables (e.g., age at commencement of sports training and the GMV in the precuneus), a dummy coefficient was obtained by correlating the two variables randomly across participants. This procedure was repeated 10,000 times for each of the five correlations. A total of 50,000 dummy coefficients (10,000 resamplings × 5 correlations) were pooled and a unique permutation coefficient distribution was created to obtain a single adjusted α-level threshold (the top five percentile ranks in the distribution). For all analyses, statistical significance was set at $P < 0.05$.

RESULTS

Demographics

Demographic data are presented in **Table 1**. No significant group differences were observed in age, years of education, body height and weight, and MMSE scores, indicating that the two groups were comparable, with the exception of sports traits. Welch's *t*-test was used to analyze IPAQ scores due to heteroscedasticity. The results revealed a significant difference between groups ($t_{(41.69)} = 4.66$, $P < 0.001$, $d = 1.32$). This *t*-value was higher than the adjusted significance level threshold ($t_{(47)} = 2.00$) obtained in the permutation test, indicating that physical activity intensity levels were higher in athletes than in non-athletes.

TABLE 3 | Behavioral results in both groups.

Total (n = 48)	Athletes (n = 24)	Non-athletes (n = 24)	*P*-value
TMT-A (second)	37.9 (10.0)	36.5 (9.7)	0.625
TMT-B (second)	87.7 (18.7)	100.2 (43.4)	0.203
Logical memory-I (score)	18.3 (5.6)	18.8 (6.2)	0.811
Logical memory-II (score)	14.6 (5.9)	13.5 (5.0)	0.497
TUG (second)	6.0 (0.8)	6.3 (0.8)	0.265
Pegboard (second)	28.0 (4.2)	26.3 (4.2)	0.155

The parameters are presented as mean (SD). P-values were obtained using t-tests for group differences. TMT, Trail-Making Test; Logical memory-I, immediate recall; Logical memory-II, delayed recall; TUG, time up and go; SD, standard deviation.

Behavioral Scores

Behavioral data are presented in **Table 3** as mean ± standard deviation (*SD*). Based on a Student's *t*-test, no significant between-group differences were identified in the TMT-A and -B, logical memory-I and -II subtests, TUG test, and pegboard task, indicating that behavioral performance was comparable between athletes and non-athletes in this study.

Sports Experience-Related Structural Changes

The whole-brain voxel-based gray matter analyses revealed significantly larger GMVs in the left middle cingulate gyrus, left posterior cingulate gyrus, right precuneus, left superior frontal gyrus, right frontal pole, left posterior and anterior insula, and right superior frontal gyrus (**Table 4** and **Figure 1**). GMVs of ROIs in these regions in athletes were extracted, and the associations between GMV and sports traits were investigated (**Figure 2**). Age of commencement and continuous sports training were correlated with the GMV of the precuneus in athletes (age of commencement: $r = -0.50$, $P = 0.014$; years of training: $r = 0.50$, $P = 0.013$). In addition, GMV of the precuneus was negatively correlated with current training time ($r = -0.45$, $P = 0.027$). These Pearson's *r*-values were higher in absolute value than the adjusted significance level threshold ($|r| = 0.40$) obtained in the permutation test. In contrast, no significant correlation between the GMV of the precuneus and IPAQ scores was observed in athletes ($r = -0.27$, $P = 0.20$) or in non-athletes ($r = -0.049$, $P = 0.82$). GMV of the precuneus was greater in athletes with earlier training commencement and longer training duration, highlighting the influence of lifelong sports training.

DISCUSSION

This study compared the brain structure in older athletes with that in age-matched non-athletes. The correlation between GMV in athletes and sports traits was also investigated. Although no significant differences in cognitive and motor performance were observed between athletes and non-athletes, athletes demonstrated higher physical activity intensity levels, as measured using the IPAQ, compared to that of non-athletes.

TABLE 4 | Brain areas with significantly larger gray matter volume in athletes than in non-athletes (TFCE analysis, $P < 0.05$, FWE corrected).

Location	MNI coordinates			*P*-value	Cluster size
	x	*y*	*z*		
Left middle cingulate gyrus	−2	−23	42	0.030	1,860
Left posterior cingulate gyrus	0	−39	30	0.031	
Right precuneus	11	−53	53	0.038	
Left superior frontal gyrus	−12	54	2	0.034	1,740
Right frontal pole	6	62	−18	0.038	
Left posterior insula	−35	−17	8	0.037	1,576
Left anterior insula	−42	−2	−2	0.040	
Right superior frontal gyrus	2	47	26	0.046	352

For overly large clusters, we also showed sub-clusters. TFCE, threshold-free cluster enhancement; FWE, family-wise error; MNI, Montreal Neurological Institute.

Compared to the non-athletes, the GMVs were larger in several of the brain regions in the athletes. Notably, the GMV of the precuneus was correlated with the early commencement of sports training and training duration. In contrast, the GMV of the precuneus in athletes was negatively correlated with current training time. IPAQ scores, which reflect the total intensity levels of multiple types of physical activity, were not correlated with the GMV of the precuneus. These findings suggest that early-commenced and continued sports training, rather than the amount of current physical activity, predict the structural integrity of the precuneus in old age. Additionally, the negative correlation between GMV of the precuneus and current training time implies that excessive physical training in old age may be detrimental. Since the aim of this study was to clarify

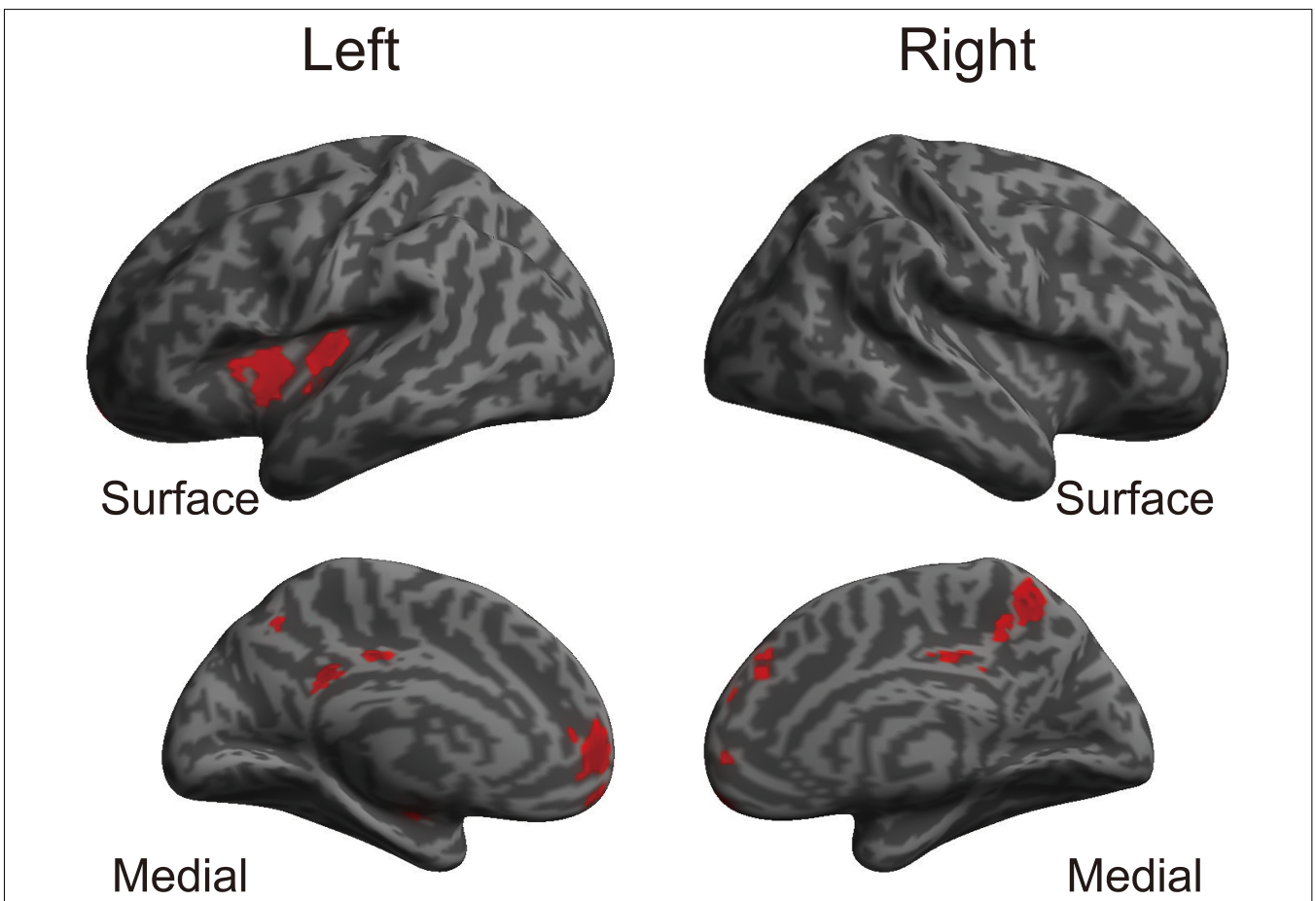

FIGURE 1 | Brain regions where athletes showed larger GMVs than non-athletes. Using a TFCE analysis, the athletes showed increased GMVs in various brain regions compared to the non-athletes. **Table 4** shows the brain regions where the athletes showed gray matter enlargement. TFCE, threshold-free cluster enhancement; GMV, gray matter volume.

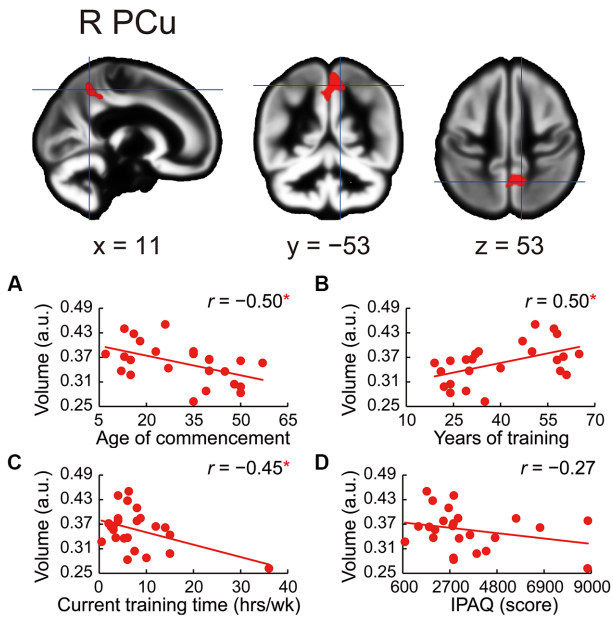

FIGURE 2 | Correlations between precuneus volume and sports traits in the athletes. GMV in the right precuneus was larger in athletes than in non-athletes. Using ROIs in the precuneus, **(A)** age at the commencement of sports training was negatively correlated with GMV of the precuneus in athletes. **(B)** GMV of the precuneus was positively correlated with the number of years of sports training in athletes. **(C)** GMV of the precuneus was negatively correlated with current training time in athletes. **(D)** No significant correlation between GMV of the precuneus and IPAQ scores in athletes was noted. *$P < 0.05$, GMV, gray matter volume; ROI, region of interest; R PCu, right precuneus; a.u., arbitrary units; hrs/wk, hours per week; IPAQ, International Physical Activity Questionnaire.

which essential brain regions are associated with lifelong sports training, the present discussion is restricted to our findings regarding the correlation between sports experience traits and the precuneus in older athletes.

In contrast to previous studies reporting that young and older athletes exhibit better verbal memory and executive function performance (Tarumi et al., 2013; Tseng et al., 2013), no significant differences in WMS-R and TMT task performance were observed between athletes and non-athletes in this study. A possible reason for this discrepancy is the involvement of other lifestyle factors such as frequency of cognitive activity and social interaction; these factors were not controlled between the groups, which may have weakened the effect of sports. In this study, participants in the control group were recruited from the Kyoto City Silver Human Resources Center, i.e., they were working part-time. Therefore, they may have been more active than sedentary older adults. Another possible reason for the discrepant findings is the age difference between the groups. In the study by Tseng et al. (2013), the mean ages of athletes and non-athletes were 72.4 and 74.6 years old, respectively. In contrast, the mean ages of athletes and non-athletes in the current study were 71.4 and 71.0 years, respectively. Thus, in the study by Tseng et al. (2013), compared to the athlete group, the non-athlete group may have included more participants that were older than 75 years. In this regard, an advanced decline in executive function tends to occur at this age (Suzuki et al., 2018).

Although no significant differences in behavioral performance were observed between athletes and non-athletes in this study, the GMVs of the various brain regions were larger in the athletes than in the non-athletes. Of note, the GMV of the precuneus was significantly associated with sports experience traits in athletes. Specifically, larger GMV of the precuneus in athletes was associated with earlier commencement of sports training and training duration. These findings suggest that lifelong sports training may result in beneficial structural changes in the brain. These findings are consistent with previous studies. For instance, our results extend the findings from a previous study of young athletes (Fukuo et al., 2020) to include older populations. This consistency suggests that the precuneus is an essential region affected by sports training. Further, the GMV of the precuneus in older athletes was positively correlated with early commencement and duration of sports training. This extends a previous finding in middle-aged athletes (Eyme et al., 2019) to the older population. In agreement with the well-established aging-related deterioration of the precuneus (Eyme et al., 2019; Hahm et al., 2019), our findings validate the analogous effects of sports in older athletes (≥65 years). The current results also highlight the benefits of commencing sports training in early life and continuing training into old age to maintain the structural integrity of the precuneus.

The precuneus is involved in self-awareness, metacognitive efficiency, and attentional shift (Nagahama et al., 1999; Gilboa et al., 2004; Ye et al., 2019) and plays an important role in visuospatial imagery for body movement control (Ogiso et al., 2000; Suchan et al., 2002; Tian et al., 2019). Malouin et al. (2003) reported activation of the precuneus in imagery tasks of walking with obstacles through a virtual environment, suggesting the involvement of the precuneus in the efficient predictive adaptation of postural control, motor coordination, spatial orientation, and reaction to moving objects/persons. Moreover, the precuneus has been implicated in the processing capacity of visuospatial information in athletes (Guo et al., 2017). The accumulation of training in motor skills may strongly influence the precuneus in old age, presumably because visuospatial processing, self-awareness, metacognition, and attentional shift are essential for playing sports. The increased GMV of the precuneus and its association with the length of sports experience observed in our study suggests that athletes may maintain motor skills involving high cognitive demand at an old age.

In addition, the current findings highlight the potential effects of sports on the default mode network. The precuneus and posterior cingulate cortex comprise the functional core of the default mode network (Wang et al., 2006; Utevsky et al., 2014). Connectivity in the default mode network at rest has been reported to decrease with age (Damoiseaux et al., 2008; Ferreira and Busatto, 2013), and this suppression may be associated with a reduction in cognitive control (Dik et al., 2003; Ferro et al., 2016; Ishihara et al., 2021). In contrast, early-commenced motor training is associated with the strength of structural connectivity, including that in the

default mode network, in middle-aged adults (Dik et al., 2003; Ferro et al., 2016; Ishihara et al., 2021). In our study, a positive change in the GMV of the precuneus was observed in athletes due to long-term sports experience. Future research should investigate the relationship between the maintenance of the GMV of the precuneus and connectivity in the default mode network.

Previous studies have reported that a higher amount of physical activity (maximal oxygen consumption) is associated with a larger GMV of the precuneus (Prakash et al., 2010; Tseng et al., 2013; Boots et al., 2015; Castells-Sánchez et al., 2021). In contrast, the present study revealed a negative association between the GMV and current training time, suggesting that the GMV of the precuneus in athletes decreased with prolonged training time. A relevant concept in this regard is the U-shaped function of the relationship between physical exercise intensity and cardiovascular state, whereby moderate physical exercise is better than no exercise, but vigorous physical exercise is associated with adverse cardiovascular events (Merghani et al., 2016). The latter may be due to the metabolic activation of the tryptophan-kynurenine pathway in the brain as a result of prolonged physical activity and intense physical exercise, which can lead to central fatigue (Strasser et al., 2016; Yamashita, 2020). These neuroactive metabolites are associated with cognitive decline and brain deterioration (Yamashita and Yamamoto, 2017; Yamashita, 2020). Moreover, several studies have demonstrated that central fatigue may influence the reduction in the GMV in the cortical and subcortical regions (de Lange et al., 2005; Riccitelli et al., 2011; Arm et al., 2019). Higher concentrations of tryptophan and kynurenine have been observed in younger and older adults during prolonged physical exercise (Melancon et al., 2012; Strasser et al., 2016; Trepci et al., 2020). Prolonged physical activity and its high load in older athletes may be associated with structural deterioration due to central fatigue. If the relationship between the amount of current physical exercise and GMV of the precuneus is underpinned by a U-shaped function, moderate sports training may have beneficial effects on brain health. To interpret previous reports (Prakash et al., 2010; Tseng et al., 2013; Boots et al., 2015; Castells-Sánchez et al., 2021) and the current findings uniformly in accordance with a U-shaped function, maximal oxygen consumption may be a useful physical measure to distinguish lower amounts of physical exercise, whereas current training time may indicate a higher amount of exercise.

Our study has several limitations. First, our study was cross-sectional; thus, causal relationships between sports training and changes in GMV in athletes could not be drawn conclusively. Second, the present study was unable to recruit a sufficient number of athletes for each sport to investigate the effects of sports type on brain structure and cognitive function. Therefore, the effects of sports type on the current results remain unclear. Third, the present study did not observe significant differences in cognitive and motor performance between athletes and non-athletes, presumably because extraneous variables may have weakened the effects of sports training. Therefore, future research should control for lifestyle factors, such as the frequency of cognitive activity and social interaction.

CONCLUSION

Compared to age-matched non-athletes, older athletes exhibited beneficial structural changes in the precuneus, and the GMV of the precuneus was significantly associated with sports traits. Although no significant group differences in cognitive and motor performance were observed between athletes and non-athletes, athletes exhibited lower levels of brain atrophy in the precuneus. Moreover, early-commenced and continued sports training were associated with a larger GMV in the precuneus. However, excessive sports training may have negative effects on the GMV in the precuneus. The present findings shed new light on the effects of lifelong sports training on the maintenance of brain health in old age.

DATA AVAILABILITY STATEMENT

The raw data supporting the conclusions of this article will be made available by the authors, without undue reservation.

ETHICS STATEMENT

The studies involving human participants were reviewed and approved by The Psychological Research Ethics Committee of Kumamoto University. The patients/participants provided their written informed consent to participate in this study.

AUTHOR CONTRIBUTIONS

KS and MS designed the research. MS, TK, and MF performed the research. MY, MS, TK, KA, MF, RN, NA, and KS contributed experimental materials and tools. MY and MS analyzed the data. MY and KS wrote the original manuscript. MY, MS, TK, KA, MF, RN, NA, and KS revised the manuscript. All authors contributed to the article and approved the submitted version.

FUNDING

This work was supported by the Japan Society for the Promotion of Science through Grants-in-Aid for Scientific Research (KAKENHI) grant numbers 16H06325 and 21H04422 to KS.

ACKNOWLEDGMENTS

We are grateful to the Kyoto City Silver Human Resources Center and other key individuals who provided support for recruiting older participants. We thank Yuki Otsuka for assisting with the data collection for behavioral measures. This study was conducted using an MRI scanner and related facilities at the Kokoro Research Center, Kyoto University.

REFERENCES

Arm, J., Ribbons, K., Lechner-Scott, J., and Ramadan, S. (2019). Evaluation of MS related central fatigue using MR neuroimaging methods: scoping review. *J. Neurol. Sci.* 400, 52–71. doi: 10.1016/j.jns.2019.03.007

Ashburner, J. (2007). A fast diffeomorphic image registration algorithm. *Neuroimage* 38, 95–113. doi: 10.1016/j.neuroimage.2007.07.007

Ashburner, J., and Friston, K. J. (2000). Voxel-based morphometry—the methods. *Neuroimage* 11, 805–821. doi: 10.1006/nimg.2000.0582

Boots, E. A., Schultz, S. A., Oh, J. M., Larson, J., Edwards, D., Cook, D., et al. (2015). Cardiorespiratory fitness is associated with brain structure, cognition and mood in a middle-aged cohort at risk for Alzheimer's disease. *Brain Imaging Behav.* 9, 639–649. doi: 10.1007/s11682-014-9325-9

Brett, M., Anton, J.-L., Valabregue, R., and Poline, J.-B. (2002). "Region of interest analysis using an SPM toolbox [abstract]," in *Presented at the 8th International Conference on Functional Mapping of the Human Brain, June 2-6, 2002* (Sendai, Japan).

Camargo, A., Azuaje, F., Wang, H., and Zheng, H. (2008). Permutation - based statistical tests for multiple hypotheses. *Source Code Biol. Med.* 3:15. doi: 10.1186/1751-0473-3-15

Castells-Sánchez, A., Roig-Coll, F., Dacosta-Aguayo, R., Lamonja-Vicente, N., Sawicka, AK., Torán-Monserrat, P., et al. (2021). Exercise and fitness neuroprotective effects: molecular, brain volume and psychological correlates and their mediating role in healthy late-middle-aged women and men. *Front. Aging Neurosci.* 13:615247. doi: 10.3389/fnagi.2021.615247

Colcombe, S. J., Erickson, K. I., Scalf, P. E., Kim, J. S., Prakash, R., McAuley, E., et al. (2006). Aerobic exercise training increases brain volume in aging humans. *J. Gerontol. A. Biol. Sci. Med. Sci.* 61, 1166–1170. doi: 10.1093/gerona/61.11.1166

Craig, C. L., Marshall, A. L., Sjostrom, M., Bauman, A. E., Booth, M. L., and Ainsworth, B. E. (2003). International physical activity questionnaire: 12 country reliability and validity. *Med. Sci. Sports Exerc.* 35, 1381–1395. doi: 10.1249/01.MSS.0000078924.61453.FB

Damoiseaux, J. S., Beckmann, C. F., Arigita, E. J., Barkhof, F., Scheltens, P., Stam, C. J., et al. (2008). Reduced resting-state brain activity in the "default network" in normal aging. *Cereb. Cortex* 18, 1856–1864. doi: 10.1093/cercor/bhm207

de Lange, F. P., Kalkman, J. S., Bleijenberg, G., Hagoort, P., van der Meer, J. W., and Toni, I. (2005). Gray matter volume reduction in the chronic fatigue syndrome. *Neuroimage* 26, 777–781. doi: 10.1016/j.neuroimage.2005.02.037

Dik, M., Deeg, D. J., Visser, M., and Jonker, C. (2003). Early life physical activity and cognition at old age. *J. Clin. Exp. Neuropsychol.* 25, 643–653. doi: 10.1076/jcen.25.5.643.14583

Dudoit, S., Shaffer, J. P., and Boldrick, J. C. (2003). Multiple hypothesis testing in microarray experiments. *Stat. Sci.* 18, 71–103. doi: 10.1214/ss/1056397487

Eickhoff, S. B., Stephan, K. E., Mohlberg, H., Grefkes, C., Fink, G. R., Amunts, K., et al. (2005). A new SPM toolbox for combining probabilistic cytoarchitectonic maps and functional imaging data. *Neuroimage* 25, 1325–1335. doi: 10.1016/j.neuroimage.2004.12.034

Erickson, K. I., Raji, C. A., Lopez, O. L., Becker, J. T., Rosano, C., Newman, A. B., et al. (2010). Physical activity predicts gray matter volume in late adulthood: the cardiovascular health study. *Neurology* 75, 1415–1422. doi: 10.1212/WNL.0b013e3181f88359

Erickson, K. I., Voss, M. W., Prakash, R. S., Basak, C., Szabo, A., Chaddock, L., et al. (2011). Exercise training increases size of hippocampus and improves memory. *Proc. Natl. Acad. Sci. U S A* 108, 3017–3022. doi: 10.1073/pnas.1015950108

Eyme, K. M., Domin, M., Gerlach, F. H., Hosten, N., Schmidt, C. O., Gaser, C., et al. (2019). Physically active life style is associated with increased grey matter brain volume in a medial parieto-frontal network. *Behav. Brain Res.* 359, 215–222. doi: 10.1016/j.bbr.2018.10.042

Ferreira, L. K., and Busatto, G. F. (2013). Resting-state functional connectivity in normal brain aging. *Neurosci. Biobehav. Rev.* 37, 384–400. doi: 10.1016/j.neubiorev.2013.01.017

Ferro, D. A., Deijen, J. B., Koppes, L. L., van Mechelen, W., Twisk, J. W., and Drent, M. L. (2016). The effects of physical activity and fitness in adolescence on cognition in adulthood and the role of insulin-like growth factor I. *J. Phys. Activ. Health* 13, 392–402. doi: 10.1123/jpah.2014-0594

Fukuo, M., Kamagata, K., Kuramochi, M., Andica, C., Tomita, H., Waki, H., et al. (2020). Regional brain gray matter volume in world-class artistic gymnasts. *J. Physiol. Sci.* 70:43. doi: 10.1186/s12576-020-00767-w

Geda, Y. E., Roberts, R. O., Knopman, D. S., Christianson, T. J., Pankratz, V. S., Ivnik, R. J., et al. (2010). Physical exercise, aging, and mild cognitive impairment: a population-based study. *Arch. Neurol.* 67, 80–86. doi: 10.1001/archneurol.2009.297

Gilboa, A., Winocur, G., Grady, C. L., Hevenor, S. J., and Moscovitch, M. (2004). Remembering our past: functional neuroanatomy of recollection of recent and very remote personal events. *Cereb. Cortex* 14, 1214–1225. doi: 10.1093/cercor/bhh082

Guo, Z., Li, A., and Yu, L. (2017). "Neural efficiency" of athletes' brain during visuo-spatial task: an fMRI study on table tennis players. *Front. Behav. Neurosci.* 11:72. doi: 10.3389/fnbeh.2017.00072

Guo, X., Yamashita, M., Suzuki, M., Ohsawa, C., Asano, K., Abe, N., et al. (2020). Musical instrument training program improves verbal memory and neural efficiency in novice older adults. *Hum. Brain Mapp.* 42, 1359–1375. doi: 10.1002/hbm.25298

Hahm, S., Lotze, M., Domin, M., and Schmidt, S. (2019). The association of health-related quality of life and cerebral gray matter volume in the context of aging: a voxel-based morphometry study with a general population sample. *Neuroimage* 191, 470–480. doi: 10.1016/j.neuroimage.2019.02.035

Inoue, S., Murase, N., Shimomitsu, T., Ohya, Y., Odagiri, Y., Takamiya, T., et al. (2009). Association of physical activity and neighborhood environment among Japanese adults. *Prev. Med.* 48, 321–325. doi: 10.1016/j.ypmed.2009.01.014

Ishihara, T., Miyazaki, A., Tanaka, H., Fujii, T., Takahashi, M., Nishina, K., et al. (2021). Childhood exercise predicts response inhibition in later life *via* changes in brain connectivity and structure. *Neuroimage* 237:118196. doi: 10.1016/j.neuroimage.2021.118196

Larson, E. B., Wang, L., Bowen, J. D., McCormick, W. C., Teri, L., Crane, P., et al. (2006). Exercise is associated with reduced risk for incident dementia among persons 65 years of age and older. *Ann. Intern. Med.* 144, 73–81. doi: 10.7326/0003-4819-144-2-200601170-00004

Lobjois, R., Benguigui, N., and Bertsch, J. (2006). The effect of aging and tennis playing on coincidence-timing accuracy. *J. Aging Phys. Activ.* 14, 74–97. doi: 10.1123/japa.14.1.74

MacIntyre, T. E., Igou, E. R., Campbell, M. J., Moran, A. P., and Matthews, J. (2014). Metacognition and action: a new pathway to understanding social and cognitive aspects of expertise in sport. *Front. Psychol.* 5:1155. doi: 10.3389/fpsyg.2014.01155

Malouin, F., Richards, C. L., Jackson, P. L., Dumas, F., and Doyon, J. (2003). Brain activations during motor imagery of locomotor-related tasks: a PET study. *Hum. Brain Mapp.* 19, 47–62. doi: 10.1002/hbm.10103

Melancon, M. O., Lorrain, D., and Dionne, I. J. (2012). Exercise increases tryptophan availability to the brain in older men age 57–70 years. *Med. Sci. Sports Exerc.* 44, 881–887. doi: 10.1249/MSS.0b013e31823ede8e

Merghani, A., Malhotra, A., and Sharma, S. (2016). The U-shaped relationship between exercise and cardiac morbidity. *Trends Cardiovasc. Med.* 26, 232–240. doi: 10.1016/j.tcm.2015.06.005

Nagahama, Y., Okada, T., Katsumi, Y., Hayashi, T., Yamauchi, H., Sawamoto, N., et al. (1999). Transient neural activity in the medial superior frontal gyrus and precuneus time locked with attention shift between object features. *Neuroimage* 10, 193–199. doi: 10.1006/nimg.1999.0451

Nenadic, I., Lorenz, C., and Gaser, C. (2021). Narcissistic personality traits and prefrontal brain structure. *Sci. Rep.* 11:15707. doi: 10.1038/s41598-021-94920-z

Nyberg, L., Lövdén, M., Riklund, K., Lindenberger, U., and Bäckman, L. (2012). Memory aging and brain maintenance. *Trends Cogn. Sci.* 16, 292–305. doi: 10.1016/j.tics.2012.04.005

Ogiso, T., Kobayashi, K., and Sugishita, M. (2000). The precuneus in motor imagery: a magnetoencephalographic study. *Neuroreport* 11, 1345–1349. doi: 10.1097/00001756-200004270-00039

Podsiadlo, D., and Richardson, S. (1991). The timed "Up & Go": a test of basic functional mobility for frail elderly persons. *J. Am. Geriatr. Soc.* 39, 142–148. doi: 10.1111/j.1532-5415.1991.tb01616.x

Prakash, R. S., Snook, E. M., Motl, R. W., and Kramer, A. F. (2010). Aerobic fitness is associated with gray matter volume and white matter

integrity in multiple sclerosis. *Brain Res.* 1341, 41–51. doi: 10.1016/j.brainres.2009.06.063

Ramanoël, S., Hoyau, E., Kauffmann, L., Renard, F., Pichat, C., Boudiaf, N., et al. (2018). Gray matter volume and cognitive performance during normal aging. A voxel-based morphometry study. *Front. Aging Neurosci.* 10:235. doi: 10.3389/fnagi.2018.00235

Raz, N., Ghisletta, P., Rodrigue, K. M., Kennedy, K. M., and Lindenberger, U. (2010). Trajectories of brain aging in middle-aged and older adults: regional and individual differences. *Neuroimage* 51, 501–511. doi: 10.1016/j.neuroimage.2010.03.020

Raz, N., Gunning-Dixon, F., Head, D., Rodrigue, K. M., Williamson, A., and Acker, J. D. (2004). Aging, sexual dimorphism and hemispheric asymmetry of the cerebral cortex: replicability of regional differences in volume. *Neurobiol. Aging* 25, 377–396. doi: 10.1016/S0197-4580(03)00118-0

Reitan, R. M., and Wolfson, D. (1993). *Halstead-Reitan Neuropsychological Battery*. Tuscon, AZ: Neuropsychology Press.

Riccitelli, G., Rocca, M. A., Forn, C., Colombo, B., Comi, G., and Filippi, M. (2011). Voxelwise assessment of the regional distribution of damage in the brains of patients with multiple sclerosis and fatigue. *Am. J. Neuroradiol.* 32, 874–879. doi: 10.3174/ajnr.A2412

Rovio, S., Kåreholt, I., Helkala, E. L., Viitanen, M., Winblad, B., Tuomilehto, J., et al. (2005). Leisure-time physical activity at midlife and the risk of dementia and Alzheimer's disease. *Lancet Neurol.* 4, 705–711. doi: 10.1016/S1474-4422(05)70198-8

Salimi-Khorshidi, G., Smith, S. M., and Nichols, T. E. (2011). Adjusting the effect of nonstationarity in cluster-based and TFCE inference. *Neuroimage* 54, 2006–2019. doi: 10.1016/j.neuroimage.2010.09.088

Seidler, R. D., Bernard, J. A., Burutolu, T. B., Fling, B. W., Gordon, M. T., Gwin, J. T., et al. (2010). Motor control and aging: links to age-related brain structural, functional and biochemical effects. *Neurosci. Biobehav. Rev.* 34, 721–733. doi: 10.1016/j.neubiorev.2009.10.005

Smith, S. M., and Nichols, T. E. (2009). Threshold-free cluster enhancement: addressing problems of smoothing, threshold dependence and localisation in cluster inference. *Neuroimage* 44, 83–98. doi: 10.1016/j.neuroimage.2008.03.061

Strasser, B., Geiger, D., Schauer, M., Gatterer, H., Burtscher, M., and Fuchs, D. (2016). Effects of exhaustive aerobic exercise on tryptophan-kynurenine metabolism in trained athletes. *PLoS One* 11:e0153617. doi: 10.1371/journal.pone.0153617

Suchan, B., Yaguez, L., Wunderlich, G., Canavan, A. G., Herzog, H., Tellmann, L., et al. (2002). Hemispheric dissociation of visual-pattern processing and visual rotation. *Behav. Brain Res.* 136, 533–544. doi: 10.1016/s0166-4328(02)00204-8

Sugishita, M. (2000). *Wechsler Memory Scale—Revised.* Tokyo, Japan: Nihon Bunka Kagakusha.

Suzuki, M., Kawagoe, T., Nishiguchi, S., Abe, N., Otsuka, Y., Nakai, R., et al. (2018). Neural correlates of working memory maintenance in advanced aging: evidence from fMRI. *Front. Aging Neurosci.* 10:358. doi: 10.3389/fnagi.2018.00358

Tanaka, H., Tarumi, T., and Rittweger, J. (2020). Aging and physiological lessons from master athletes. *Compr. Physiol.* 10, 261–296. doi: 10.1002/cphy.c180041

Tarumi, T., Gonzales, M. M., Fallow, B., Nualnim, N., Pyron, M., Tanaka, H., et al. (2013). Central artery stiffness, neuropsychological function and cerebral perfusion in sedentary and endurance-trained middle-aged adults. *J. Hypertens.* 31, 2400–2409. doi: 10.1097/HJH.0b013e328364decc

Tian, Q., Resnick, S. M., Davatzikos, C., Erus, G., Simonsick, E. M., Studenski, S. A., et al. (2019). A prospective study of focal brain atrophy, mobility and fitness. *J. Intern. Med.* 286, 88–100. doi: 10.1111/joim.12894

Trepci, A., Imbeault, S., Wyckelsma, V. L., Westerblad, H., Hermansson, S., Andersson, D. C., et al. (2020). Quantification of plasma kynurenine metabolites following one bout of sprint interval exercise. *Int. J. Tryptophan Res.* 13:1178646920978241. doi: 10.1177/1178646920978241

Tseng, B. Y., Uh, J., Rossetti, H. C., Cullum, C. M., Diaz-Arrastia, R. F., Levine, B. D., et al. (2013). Masters athletes exhibit larger regional brain volume and better cognitive performance than sedentary older adults. *J. Magn. Reson. Imaging* 38, 1169–1176. doi: 10.1002/jmri.24085

Utevsky, A. V., Smith, D. V., and Huettel, S. A. (2014). Precuneus is a functional core of the default-mode network. *J. Neurosci.* 34, 932–940. doi: 10.1523/JNEUROSCI.4227-13.2014

Wang, L., Zang, Y., He, Y., Liang, M., Zhang, X., Tian, L., et al. (2006). Changes in hippocampal connectivity in the early stages of Alzheimer's disease: evidence from resting state fMRI. *Neuroimage* 31, 496–504. doi: 10.1016/j.neuroimage.2005.12.033

Wechsler, D. (1997). *Manual for the Wechsler Adult Intelligence Scale III.* San Antonio, TX: Harcourt Assessment.

Yamashita, M. (2020). Potential role of neuroactive tryptophan metabolites in central fatigue: establishment of the fatigue circuit. *Int. J. Tryptophan Res.* 13:1178646920936279. doi: 10.1177/1178646920936279

Yamashita, M., and Yamamoto, T. (2017). Tryptophan circuit in fatigue: from blood to brain and cognition. *Brain Res.* 1675, 116–126. doi: 10.1016/j.brainres.2017.09.002

Ye, Q., Zou, F., Dayan, M., Lau, H., Hu, Y., and Kwok, S. C. (2019). Individual susceptibility to TMS affirms the precuneal role in meta-memory upon recollection. *Brain Struct. Funct.* 224, 2407–2419. doi: 10.1007/s00429-019-01909-6

Zhao, E., Tranovich, M. J., DeAngelo, R., Kontos, A. P., and Wright, V. J. (2016). Chronic exercise preserves brain function in masters athletes when compared to sedentary counterparts. *Phys. Sportsmed.* 44, 8–13. doi: 10.1080/00913847.2016.1103641

Conflict of Interest: The authors declare that the research was conducted in the absence of any commercial or financial relationships that could be construed as a potential conflict of interest.

frontiers in Human Neuroscience

ORIGINAL RESEARCH
published: 14 December 2021
doi: 10.3389/fnhum.2021.735063

Neurodegeneration and Vascular Burden on Cognition After Midlife: A Plasma and Neuroimaging Biomarker Study

Kuo-Lun Huang[1], Ing-Tsung Hsiao[2,3], Ting-Yu Chang[1], Shieh-Yueh Yang[4], Yeu-Jhy Chang[1], Hsiu-Chuan Wu[1], Chi-Hung Liu[1], Yi-Ming Wu[5], Kun-Ju Lin[2,3], Meng-Yang Ho[1,6] and Tsong-Hai Lee[1]**

[1]Department of Neurology, Linkou Chang Gung Memorial Hospital, and College of Medicine, Chang Gung University, Taoyuan, Taiwan, [2]Department of Nuclear Medicine and Molecular Imaging Center, Linkou Chang Gung Memorial Hospital, Taoyuan, Taiwan, [3]Healthy Aging Research Center and Department of Medical Imaging and Radiological Sciences, College of Medicine, Chang Gung University, Taoyuan, Taiwan, [4]MagQu Co., Ltd., New Taipei City, Taiwan, [5]Department of Radiology, Linkou Chang Gung Memorial Hospital, Taoyuan, Taiwan, [6]Graduate Institute of Behavioral Sciences, Chang Gung University, Taoyuan, Taiwan

OPEN ACCESS

Edited by:
Fanpei G. Yang, National Tsing Hua University, Taiwan

Reviewed by:
Man Mohan Mehndiratta, BLK-Max Super Specialty Hospital, India
Seonjoo Lee, Columbia University, United States

***Correspondence:**
Tsong-Hai Lee
thlee@adm.cgmh.org.tw
Meng-Yang Ho
myho@mail.cgu.edu.tw

Specialty section:
This article was submitted to Brain Health and Clinical Neuroscience, a section of the journal Frontiers in Human Neuroscience

Received: *02 July 2021*
Accepted: *19 November 2021*
Published: *14 December 2021*

Citation:
Huang K-L, Hsiao I-T, Chang T-Y, Yang S-Y, Chang Y-J, Wu H-C, Liu C-H, Wu Y-M, Lin K-J, Ho M-Y and Lee T-H (2021) Neurodegeneration and Vascular Burden on Cognition After Midlife: A Plasma and Neuroimaging Biomarker Study. Front. Hum. Neurosci. 15:735063. doi: 10.3389/fnhum.2021.735063

Background and Objectives: Neurodegeneration and vascular burden are the two most common causes of post-stroke cognitive impairment. However, the interrelationship between the plasma beta-amyloid (Aβ) and tau protein, cortical atrophy and brain amyloid accumulation on PET imaging in stroke patients is undetermined. We aimed to explore: (1) the relationships of cortical thickness and amyloid burden on PET with plasma Aβ40, Aβ42, tau protein and their composite scores in stroke patients; and (2) the associations of post-stroke cognitive presentations with these plasma and neuroimaging biomarkers.

Methods: The prospective project recruited first-ever ischemic stroke patients around 3 months after stroke onset. The plasma Aβ40, Aβ42, and total tau protein were measured with the immunomagnetic reduction method. Cortical thickness was evaluated on MRI, and cortical amyloid plaque deposition was evaluated by ^{18}F-florbetapir PET. Cognition was evaluated with Mini-Mental State Examination (MMSE), Geriatric Depression Scale (GDS), Dementia Rating Scale-2 (DRS-2).

Results: The study recruited 24 stroke patients and 13 normal controls. The plasma tau and tau*Aβ42 levels were correlated with mean cortical thickness after age adjustment. The Aβ42/Aβ40 ratio was correlated with global cortical ^{18}F-florbetapir uptake value. The DRS-2 and GDS scores were associated with mean cortical thickness and plasma biomarkers, including Aβ42/Aβ40, tau, tau*Aβ42, tau/Aβ42, and tau/Aβ40 levels, in stroke patients.

Conclusion: Plasma Aβ, tau, and their composite scores were associated with cognitive performance 3 months after stroke, and these plasma biomarkers were correlated with corresponding imaging biomarkers of neurodegeneration. Further longitudinal studies with a larger sample size are warranted to replicate the study results.

Keywords: cognition, amyloid plaque, PET, post-stroke cognitive impairment, plasma biomarker, tau protein

INTRODUCTION

Neurodegeneration and vascular pathology are the two most common causes of cognitive impairment in the elderly. Post-stroke cognitive impairment (PSCI) is a special condition of vascular cognitive impairment (VCI) and refers to the presence of cognitive impairment after stroke. PSCI is noted in about one-third of stroke survivors, which usually manifest 3–6 months after stroke occurrence (Pendlebury and Rothwell, 2009; Gottesman and Hillis, 2010). The occurrence of PSCI can be attributed to vascular injury, pre-existing neurodegenerative substrates, and a combination of both (Mijajlović et al., 2017). Besides, stroke patients with co-existing beta-amyloid (Aβ) plaque tend to present steeper cognitive declines in longitudinal follow-up (Liu et al., 2015).

Regarding the *in vivo* detection of neurodegenerative pathology in stroke patients, positron emission tomography (PET) imaging, cerebrospinal fluid (CSF) and blood examination have been developed in the past decades. PET imaging can yield an excellent visual resolution of the topographical distribution of Aβ pathology and tau protein, but it is expensive with limited availability and requires multiple scanning sessions if different pathological substrates are to be detected. The concentrations of Aβ protein and tau protein in CSF have been shown highly correlated with brain pathological changes and clinical presentations, but the invasive nature of lumbar puncture limits its clinical application. Compared to PET and CSF studies, blood biomarkers of neurodegeneration have the advantage of more convenient accessibility with no risk for radiation exposure and invasive procedures (Blennow, 2017). Detection of plasma neurodegeneration markers, such as Aβ40, Aβ42, and tau protein, has been shown feasible and reliable by the immunomagnetic reduction (IMR) technique (Yang et al., 2011). Patients with Alzheimer's disease (AD) had lower plasma Aβ40 and higher plasma Aβ42 and tau protein levels than patients with mild cognitive impairment (MCI) and healthy controls (Chiu et al., 2013, 2014). Regarding the reliability of plasma neurodegenerative biomarkers, the CSF and plasma Aβ42 were shown correlated in a recent AD study (Teunissen et al., 2018). Moreover, plasma Aβ40 and Aβ42 levels were significantly correlated with amyloid accumulation on Pittsburgh compound B (PiB) PET (Tzen et al., 2014).

Detection of fluid biomarkers of amyloid plaque and tau protein has been applied in stroke patients, and their levels would vary according to sampling time point, vascular lesion characteristics, and coexisting neurodegeneration states (Hesse et al., 2000; Zhang et al., 2010; Bielewicz et al., 2011; Skillback et al., 2015). Previous studies have shown that there is no significant change in amyloid plaque accumulation after acute stroke (Hesse et al., 2000; Sahathevan et al., 2016). On the other hand, tau protein level has an abrupt increase within 5–10 days after acute stroke, and then gradually decreases to a stable level in the following 3 months after stroke (Hesse et al., 2000; Kaerst et al., 2013). Therefore, plasma amyloid peptide and tau protein levels measured 3 months after stroke would be within a relatively stable condition and may represent the overall neurodegenerative condition in stroke patients.

Although plasma Aβ42 and tau protein levels have been recently reported to have significant associations with VCI presentations (Tang et al., 2018; Chi et al., 2019), there is limited literature on the relationship between the imaging and blood biomarkers of neurodegeneration in the context of PSCI. In this study, we aimed to explore: (1) the associations of plasma Aβ40, Aβ42, and tau protein levels with cognitive presentations around 3 months after first-ever ischemic stroke; and (2) the relationships of plasma Aβ40, Aβ42, and tau protein with the relevant imaging markers, such as cortical atrophy on MRI and amyloid burden on PET imaging.

METHODS

Participants

We conducted a prospective, cross-sectional study to screen patients with recent first-ever ischemic stroke (around 3 months after onset) from the Department of Neurology and Stroke Center at Linkou Chang Gung Memorial Hospital, Taiwan, as previously described (Huang et al., 2018b). These stroke patients were recruited based on the following criteria: (1) a diagnosis of acute ischemic stroke confirmed on magnetic resonance imaging (MRI) at stroke onset; (2) education years at least 6 years; (3) no history of old stroke, dementia, tauopathy diseases, substantial traumatic brain injury or epilepsy before the index stroke; (4) without recurrent stroke occurring between the index stroke and the study screening procedure; and (5) without persistent moderate to severe dysphasia, which was defined as a score of >1 point in the language score of the National Institutes of Health Stroke Scale (NIHSS; Srikanth et al., 2006). The NIHSS scores were recorded at stroke onset and 3 months after stroke. In addition, age- and education-matched elderly normal controls were also recruited, and they had: (1) education at least 6 years; (2) no subjective cognitive complaint; (3) no major neurological and psychiatric disease; and (4) the sum of Clinical Dementia Rating sub-scores was 0.

The study protocol and procedure for obtaining informed consent were compliant with the Helsinki Declaration and were approved by the Institutional Review Board of Chang Gung Memorial Hospital (IRB No. 201601092B0, 201601675A0, 103-7584A). All participants provided written informed consent.

Cognitive Assessment

Cognitive assessment was administered on all participants around 3 months after the occurrence of the index stroke. The assessment entailed the Mini-Mental State Examination (MMSE), the Clinical Dementia Rating (CDR) and the Dementia Rating Scale-2 (DRS-2). The subtests of the DRS-2, including attention, initiation and perseveration (IP), conceptualization, memory and construction, were applied to evaluate domain-specific cognitive function. The 15-item Geriatric Depression Scale (GDS) was used to evaluate mood condition. All of these tests have been used in our previous studies (Huang et al., 2017, 2018a).

Blood Sample Collection and Preparation

Every participant was asked to provide a 10-ml non-fasting venous blood sample (K3 EDTA, lavender-top tube). The blood samples were centrifuged (3,000 *g* for 20 min) within 1 h of collection, and plasma was aliquoted into cryotubes and stored at −80°C before measurement. The laboratory staff were blinded to the demographic, clinical and imaging data of each participant.

IMR Measurements

Measurements of plasma Aβ40, Aβ42 and total tau protein with immunomagnetic reduction (IMR) have been reported in our previous study (Lin et al., 2019). In brief, the reagents used to determine plasma Aβ40, Aβ42, and tau protein levels in this study consisted of dextran-coated Fe_3O_4 nanoparticles functionalized with antibodies. Immunomagnetic reduction assays were the method used to probe the associations of plasma magnetic nanoparticles with Aβ40, Aβ42, and tau protein reagents. This technique mainly detected the percentage reduction in an alternating current that reflects the magnetic susceptibility (*X*ac) of a reagent due to the interactions of functionalized magnetic nanoparticles and target proteins. The percentage reductions of immunomagnetic signals were then converted to target protein concentrations using the standard curves of the respective analytes.

Stroke Volume and Brain Atrophy Evaluation

Brain CT and MRI were performed at stroke onset to assess acute stroke lesions. The MRI scanning protocol included fluid-attenuated inversion recovery (FLAIR), diffusion-weighted imaging (DWI), and T1-weighted (T1W) sequences. The stroke volume was delineated on the DWI maps using the PMOD software (version 3.7; PMOD Technologies Ltd., Zurich, Switzerland). We normalized stroke lesion volume according to the head size, which was measured using the FreeSurfer software (version 6.0.0).

Brain atrophy was evaluated based on the follow-up brain MRI scans performed around 3 months after stroke onset. Axial three-dimensional T1W-MPRAGE (Magnetization Prepared Rapid Gradient Echo) and FLAIR sequences were acquired on a Siemens 3T MRI system as previously described (Huang et al., 2018b). We measured the cortical thickness on the T1W-MPRAGE images using the FreeSurfer software (Becker et al., 2011). We evaluated hippocampal atrophy using the Schelten medial temporal lobe atrophy (MTA) score (Scheltens and van de Pol, 2012; Huang K. L. et al., 2019).

Amyloid PET Image Acquisition and Analysis

An ^{18}F-florbetapir PET scan was performed using Biograph mMR PET/magnetic resonance scanner (Siemens Medical Solutions, Malvern, PA, USA) about 3 months after stroke onset. A 10-min PET scan of ^{18}F-florbetapir was acquired at 50 min post-injection of 384 ± 13 MBq. ^{18}F-florbetapir PET images were reconstructed using point-spread function reconstruction with two iterations and 21 subsets, as well as MR-based attenuation correction and scatter and random corrections. The final reconstructed ^{18}F-florbetapir PET images were of 344 × 344 × 127 matrix size (0.834 × 0.834 × 1.2 mm voxel size).

PET data were motion-corrected, and then spatially normalized into MNI space using MR-based spatial normalization. Image processing was performed using PMOD software (version 3.7; PMOD Technologies Ltd, Zurich, Switzerland) by previously reported protocols (Huang C.-C. et al., 2019). Then, the SUVR (standardized uptake value ratio) image was calculated by using the cerebellar gray matter as the reference region. Amyloid plaque positivity was visually evaluated on ^{18}F-florbetapir PET images (Johnson et al., 2013).

Study Procedures and Statistical Analyses

Cognitive performance, plasma neurodegenerative biomarkers, mean cortical thickness on brain MRI, and ^{18}F-florbetapir SUVR as amyloid burden were measured around 3 months after acute stroke. Firstly, we evaluated the influence of plasma neurodegenerative markers, such as Aβ40, Aβ42, and tau protein, on PSCI performance. Secondly, we evaluated the associations of plasma neurodegenerative markers with the corresponding neuroimaging markers, including mean cortical thickness and ^{18}F-florbetapir SUVR.

For descriptive statistics, we performed the two-sample t-test, chi-square test, and Fisher's exact test for group comparisons. Further, we performed Pearson's correlation analyses to investigate the correlations among the mean cortical thickness, ^{18}F-florbetapir SUVR, and plasma biomarker values. Moreover, we analyzed the partial correlations of cognitive performance with plasma biomarker and other relevant factors after adjusting for age and education.

RESULTS

The study recruited 24 patients with first-ever ischemic stroke and 13 age- and education-matched normal controls. Stroke patients had higher proportions of hypertension and dyslipidemia than those of the controls. There were no differences between the two groups in mean cortical thickness, plasma levels of Aβ40, Aβ42, tau, or the composite scores for Aβ42/Aβ40, tau/Aβ40, tau*Aβ42, and tau*Aβ42/Aβ40 (**Table 1**). The median days of blood sampling, neurocognition assessment, and neuroimaging evaluation were 96 (86–105, interquartile range), 98 (88–110), and 100 (87–118) days after stroke occurrence for stroke patients, and these intervals were highly correlated (r = 0.48–0.68, p values < 0.03). These evaluations were performed within 15 days for the controls.

Age was negatively correlated with mean cortical thickness in all participants (r = −0.35, p value = 0.04), and plasma tau protein level and tau-related composite scores were correlated with mean cortical thickness after age adjustment. Subgroup analyses were then performed to evaluate associations between plasma biomarkers and mean cortical thickness in stroke patients and normal controls, respectively. In stroke patients, plasma tau, tau*Aβ42, and tau/Aβ42 levels were correlated with mean cortical thickness, but not with stroke volume (**Figure 1**). However, such correlations were not observed in normal controls (**Table 2**).

TABLE 1 | Comparisons of demographic data and plasma Aβ40, Aβ42, tau protein and their composite scores between normal controls and patients with ischemic stroke.

	NC, *n* = 13	Stroke, *n* = 24	Effect size	*p* value
Categorical variables	n (%)	n (%)	Odds Ratio	
Male	7 (54)	20 (83)	4.3 (0.9–19.8)	0.12
APOE4 carrier	0 (0)	3 (13)	NA	0.54
Hypertension	6 (46)	21 (88)	8.2 (1.6–41.6)	0.02
Diabetes mellitus	3 (23)	7 (29)	1.4 (0.3–6.5)	1.00
Dyslipidemia	5 (38)	18 (75)	4.8 (1.1–20.5)	0.04
Gout	1 (8)	5 (21)	3.2 (0.3–30.4)	0.39
Continuous variables	Mean (SD)	Mean (SD)	Cohen's d	
Age, y	64.8 (6.3)	62.0 (8.5)	0.37	0.29
Education, y	10.5 (3.5)	10.5 (3.3)	0.01	0.97
Mean cortical thickness, mm	2.40 (0.06)	2.41 (0.07)	0.15	0.66
MTA score	0.9 (1.0)	0.7 (0.9)	0.03	0.58
Aβ40, pg/ml	53.2 (3.2)	53.1 (6.8)	0.01	0.98
Aβ42, pg/ml	16.5 (0.5)	16.3 (1.4)	0.14	0.61
Tau, pg/ml	21.4 (2.5)	19.7 (4.5)	0.42	0.16
Aβ42/Aβ40	0.31 (0.03)	0.31 (0.07)	0.06	0.82
Tau/Aβ40	0.40 (0.06)	0.39 (0.14)	0.15	0.59
Tau/Aβ42	1.30 (0.12)	1.20 (0.20)	0.54	0.08
Tau*Aβ42	353.5 (50)	326.7 (95.1)	0.32	0.27
Tau*Aβ42/Aβ40	6.70 (1.17)	6.45 (2.79)	0.10	0.71
MMSE	26.9 (1.7)	26.7 (2.1)	0.13	0.71
GDS	1.3 (1.7)	2.0 (2.5)	0.31	0.38
DRS-2 total	131.9 (7.2)	129.4 (10.1)	0.28	0.43
DRS-2 attention	35.3 (1.4)	36.0 (1.0)	0.64	0.07
DRS-2 IP	31.8 (3.9)	29.5 (5.6)	0.45	0.20
DRS-2 Conceptualization	36.2 (2.2)	35.4 (4.0)	0.25	0.41
DRS-2 Memory	22.6 (1.9)	22.4 (2.1)	0.10	0.78
DRS-2 Construction	5.9 (0.3)	6.0 (0.0)	0.47	0.34
CDR SOB	0 (0)	0.3 (0.4)	0.79	0.01
Stroke volume, 10^{-6}	NA	3.92 (5.36)	NA	NA
NIHSS score at onset	NA	2.6 (1.4)	NA	NA
NIHSS score at 3M	NA	1.7 (1.1)	NA	NA

NC, normal controls; APOE, apolipoprotein E; MTA, medial temporal atrophy; MMSE, Mini-Mental State Examination; GDS, Geriatric Depression Scale; DRS-2, Dementia Rating Scale-2; IP, Initiation and Perseveration; CDR SOB, sum of boxes of Clinical Dementia Rating Scale; NIHSS, National Institutes of Health Stroke Scale; NA, not applicable.

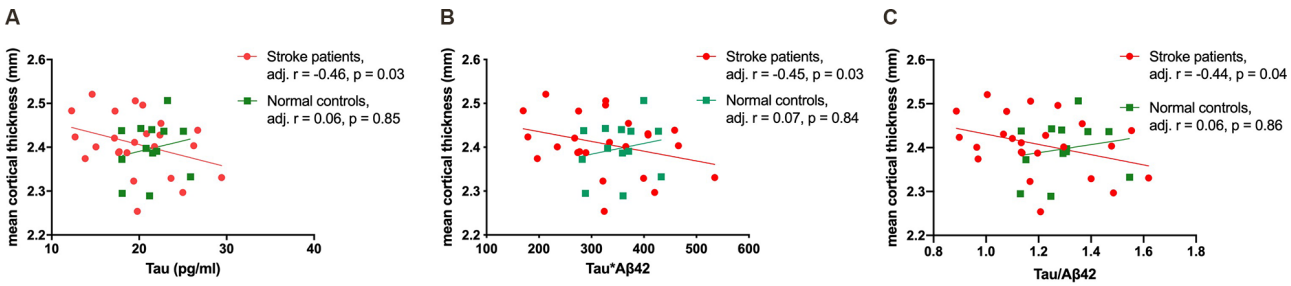

FIGURE 1 | The correlations of mean cortical thickness with plasma tau **(A)**, tau*Aβ42 **(B)**, and tau/Aβ42 **(C)** in stroke patients and normal controls.

In all participants, plasma levels of Aβ40, Aβ42/Aβ40, tau/Aβ40, and tau*Aβ42/Aβ40 were all significantly correlated with the GDS and DRS-2 total scores, respectively, and remained significant after controlling for age and education (**Table 3**). Similarly, in stroke patients alone, the plasma Aβ42/Aβ40, tau, tau/Aβ42, tau/Aβ40, and tau*Aβ42/Aβ40 levels were significantly correlated with the GDS score, DRS-2 total score, and DRS-2 I/P subtest score after age and education adjustment (**Figure 2**). The correlations of stroke volume with the NIHSS, MMSE, GDS and DRS-2 total scores were not significant.

An ^{18}F-florbetapir PET scanning was done in 19 of 24 stroke patients and 11 of 13 controls. There were no differences in age, education, or cognitive test scores between participants with and without ^{18}F-florbetapir PET scanning. The ^{18}F-florbetapir PET imaging was visually negative for amyloid plaque in all participants. The ^{18}F-florbetapir SUVR was positively and moderately correlated with Aβ42/Aβ40 (r = 0.42, p value = 0.07) in stroke patients (**Figure 3**), but was not significantly correlated with any cognitive test scores in either group.

TABLE 2 | Partial correlations of mean cortical thickness with plasma Aβ40, Aβ42, and tau protein and their composite scores after adjustment for age.

	Aβ42	Aβ40	Aβ42/Aβ40	Tau	Tau*Aβ42	Tau/Aβ42	Tau/Aβ40	Tau*Aβ42/Aβ40
All subjects	−0.31	0.25	−0.30	−0.34*	−0.34*	−0.31	−0.33*	−0.34*
Stroke	−0.39	0.27	−0.34	−0.46*	−0.45*	−0.44*	−0.41	0.41
NC	0.06	0.18	−0.09	0.06	0.07	0.06	−0.01	0.01

*$P < 0.05$.

DISCUSSION

PSCI is not a single disease entity; rather, it describes an unspecified cognitive decline that usually occurs 3–6 months after stroke onset (Tuladhar and de Leeuw, 2010). In this study, we checked plasma Aβ42, Aβ40, and tau protein levels as well as structural MRI and amyloid PET scanning around 3 months after the occurrence of first-ever ischemic stroke. We found that plasma tau protein level and tau-related composite scores were correlated with mean cortical thickness. In addition, the Aβ42/Aβ40 ratio was moderately correlated with ^{18}F-florbetapir PET SUVR. Furthermore, plasma Aβ42, Aβ40, tau protein and their composite scores were correlated with cognitive performance 3 months after stroke. All these findings suggest plasma biomarkers of Aβ42, Aβ40, and tau protein may be associated with the development of PSCI.

Amyloid plaque is a pathognomonic marker of Alzheimer's disease and could be present for decades before the manifestations of cognitive impairment (Jack et al., 2013). Although vascular lesions and Aβ pathology frequently coexist in stroke patients, previous CSF or amyloid PET studies have shown that stroke itself would not induce amyloid plaque accumulation (Hesse et al., 2000; Sahathevan et al., 2016). Nonetheless, the presence of co-existing amyloid plaque has been implicated as a risk factor for PSCI development (Thiel et al., 2014; Skillback et al., 2015). Therefore, detection of both vascular injury and neurodegeneration pathology would be helpful to disentangle the complex etiologies of PSCI. Our study found that plasma Aβ proteins were correlated with PSCI performance. Of note, the Aβ42/Aβ40 ratio was more sensitive to PSCI than Aβ42 or Aβ40 alone in our study. It has been proposed that the Aβ42/Aβ40 ratio could compensate for general inter-individual variations than Aβ42 or Aβ40 alone (Hansson et al., 2019), and the Aβ42/Aβ40 ratio in either CSF and blood studies had adequate accuracy and reliability to differentiate AD patients from controls (Chiu et al., 2012; Hansson et al., 2019).

The correlations of VCI with plasma Aβ42, Aβ40, and tau protein have been recently reported (Tang et al., 2018; Chi et al., 2019). Tang et al. (2018) found elevated plasma Aβ42 was associated with worse cognitive performance in stroke patients. However, the intervals from stroke occurrence to cognitive evaluation ranged from acute stroke stage to more than 10 years after stroke in their study, and disparity in evaluation intervals may limit the ability to elucidate the temporal relationship between vascular and neurodegenerative contributions to the PSCI development. In our study, the plasma biomarker collection, cognitive evaluation and neuroimaging studies were performed around 3 months after stroke, and we found the plasma Aβ42/Aβ40 ratio and tau-related composite scores were correlated with PSCI presentations. This finding implies the potential role of these markers in signifying the development of PSCI. On the other hand, we found that stroke volume was not correlated with PSCI severity in this study. This could be partly related to the relatively minor stroke severity in our cases, whose NIHSS scores were 2.6 ± 1.4 points at stroke onset and 1.7 ± 1.1 points 3 months after stroke, respectively.

Both plasma and CSF Aβ42/Aβ40 ratios have been reported as surrogate biomarkers of cortical amyloid plaque deposition on PET (Fandos et al., 2017; Alcolea et al., 2019). Although the ^{18}F-florbetapir PET results were visually rated negative for Aβ pathology in our stroke patients, the plasma Aβ42/Aβ40 ratio had a moderate correlation with global ^{18}F-florbetapir SUVR. In agreement with the previous studies, our results showed that the plasma Aβ42/Aβ40 ratio was correlated with cognitive performance as well as the ^{18}F-florbetapir SUVR even under the condition of low Aβ burden on PET imaging.

Tau is a microtubule-associated protein involved in stabilizing the axonal cytoskeleton and is deemed as a potential marker of axonal injury (Seco et al., 2012). Previous CSF and serum studies have shown that tau protein level has an abrupt elevation in the acute ischemic stroke stage, with a peak increase within 5–10 days after stroke onset, followed by a gradual normalization after 3 months. Therefore, the interval from stroke onset to blood collection may have an influence on the plasma tau protein level. In our study, plasma tau protein was collected around 3 months after stroke, and intervals from stroke onset to plasma collection were not correlated with plasma tau level or its composite scores (data not shown). Furthermore, the tau protein level in the acute stage is correlated with stroke volume, implying the role in direct neuronal injury severity (Hesse et al., 2000; Bitsch et al., 2002; Bielewicz et al., 2011; Kaerst et al., 2013). However, the relationship between acute tau protein level and post-stroke cognitive performance has not been well investigated. In a recent study, a single measurement of plasma tau protein which was done within 1 week after stroke onset has not revealed an association with cognitive performance 3 months or 1 year after stroke. Since a steep elevation of tau protein level may occur within days after stroke onset, multiple and intensive sampling of tau protein levels in the acute stroke stage should be more reliable when investigating its influence on long-term neurological and cognitive deficits in future studies.

On the other hand, since the plasma tau protein was detected around 3 months after stroke in our study, its concentration might be more related to either pre-existing or stroke-related neurodegeneration, rather than the direct neuronal injury effect (Chen and Jiang, 2019). Furthermore, we found plasma tau protein level and its composite scores were associated with mean cortical thickness and cognitive performance in stroke patients.

TABLE 3 | The correlations of cognitive results with cortical thickness, stroke volume, plasma Aβ42, Aβ40, tau, and their composite scores.

Cognitive tests	Groups	Cortical thickness	Aβ42	Aβ40	Aβ42/Aβ40	Tau	Tau*Aβ42	Tau/Aβ42	Tau/Aβ40	Tau*Aβ42/Aβ40	Stroke volume
MMSE	All	0.32	0.03	0.23	−0.15	−0.08	−0.05	−0.12	−0.15	−0.12	NA
	IS	0.37	0.02	0.29	−0.19	−0.04	−0.02	−0.07	−0.16	−0.12	−0.09
	NC	0.20	0.10	−0.03	0.09	−0.30	−0.23	−0.40	−0.20	−0.14	NA
GDS	All	−0.37*	0.23	−0.35*†	0.38*†	0.31†	0.32†	0.29	0.41*†	0.40*†	NA
	IS	−0.41*	0.31	−0.41*	0.44*†	0.48*†	0.46*†	0.48*†	0.52*†	0.51*†	−0.16
	NC	−0.33	−0.22	−0.04	−0.06	−0.29	−0.28	−0.30	−0.22	−0.21	NA
DRS-2 Total	All	0.33*	−0.18	0.39*†	−0.38*†	−0.27*†	−0.26†	−0.28	−0.39*†	−0.37*†	NA
	IS	0.41*	−0.23	0.47*	−0.44*†	−0.41*†	−0.38†	−0.44*†	−0.50*†‡	−0.46*†‡	−0.13
	NC	0.17	0.10	0.01	0.02	0.16	0.16	0.16	0.12	0.12	NA
DRS-2 Attention	All	0.32	−0.09	0.26	−0.19	−0.14	−0.13	−0.14	−0.19	−0.18	NA
	IS	0.23	−0.04	0.25	−0.20	−0.14	−0.12	−0.16	−0.22	−0.20	−0.31
	NC	0.44	−0.24	0.45	−0.40	0.03	−0.03	0.10	−0.16	−0.17	NA
DRS-2 IP	All	0.27	−0.23†	0.35*†	−0.35*†	−0.26	−0.26†	−0.25	−0.34*†	−0.32*†	NA
	IS	0.37	−0.32†‡	0.44*†‡	−0.43*†‡	−0.46*†‡	−0.43*†‡	−0.47*†‡	−0.48*†‡	−0.45*†‡	−0.21
	NC	0.07	0.27	−0.15	0.19	0.34	0.34	0.33	0.33	0.32	NA
DRS-2 Conceptualization	All	0.21	−0.09	0.25	−0.27	−0.16	−0.15	−0.16	−0.28	−0.27	NA
	IS	0.23	−0.11	0.29	−0.30	−0.21	−0.19	−0.22	−0.32	−0.30	0.22
	NC	0.20	−0.04	0.03	−0.06	−0.05	−0.05	−0.05	−0.07	−0.07	NA
DRS-2 Memory	All	0.27	0.00	0.29†	−0.23†	−0.19†	−0.16	−0.24†	−0.29†	−0.26†	NA
	IS	0.41*	−0.02	0.38†	−0.30	−0.27†	−0.22	−0.33†	−0.38†	−0.34†	−0.33
	NC	−0.04	0.10	−0.06	0.09	0.02	0.04	−0.01	0.04	0.04	NA
DRS-2 Construction	All	−0.09	−0.10	0.08	−0.07	−0.20	−0.19	−0.22	−0.15	−0.14	NA
	IS	NA	NA	NA	NA	NA	NA	NA	NA	NA	NA
	NC	−0.19	−0.35	0.25	−0.30	−0.44	−0.45	0.42	−0.46	−0.45	NA
NIHSS	All	0.01	−0.08	−0.09	0.07	−0.05	−0.05	−0.05	0.05	0.04	NA
	IS	−0.07	−0.05	−0.13	0.06	0.14	0.09	0.20	0.14	0.11	−0.11
	NC	NA	NA	NA	NA	NA	NA	NA	NA	NA	NA
CDR SOB	All	−0.31	0.06	−0.17	0.13	0.03	0.04	0.02	0.09	0.09	NA
	IS	−0.44*	0.10	−0.19	0.14	0.13	0.11	0.14	0.14	0.12	0.00
	NC	NA	NA	NA	NA	NA	NA	NA	NA	NA	NA

*$P < 0.05$; †$P < 0.05$ after age and education adjustment; ‡$P < 0.05$ after age, education and GDS adjustment; NA, not applicable; MMSE, Mini-Mental State Examination; GDS, Geriatric Depression Scale; DRS-2, Dementia Rating Scale-2; IP, Initiation and Perseveration; NIHSS, National Institutes of Health Stroke Scale; CDR SOB, the sum of boxes of Clinical Dementia Rating Scale; IS, ischemic stroke; NC, normal controls.

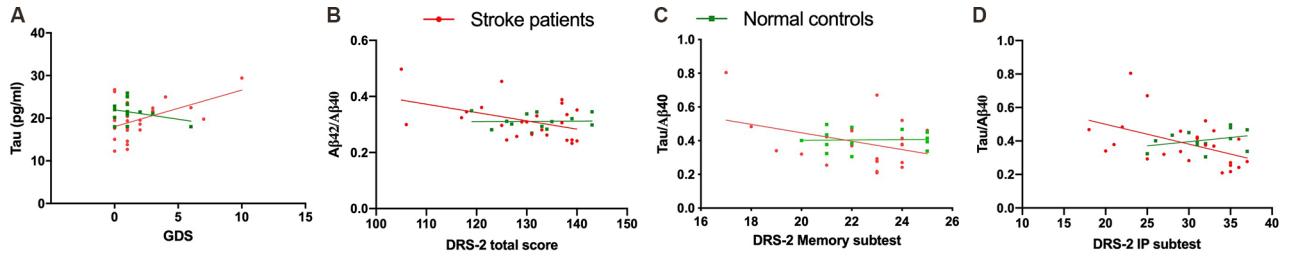

FIGURE 2 | The correlations among cognitive results and plasma biomarkers. Geriatric Depression Score (GDS) vs. tau **(A)**. Dementia Rating Scale-2 (DRS-2) total score vs. Aβ42/Aβ40 ratio **(B)**. DRS-2 memory subtest score vs. tau/Aβ40 **(C)**. DRS-2 initiation and perseveration (DRS IP) subtest score vs. tau/Aβ40 **(D)**.

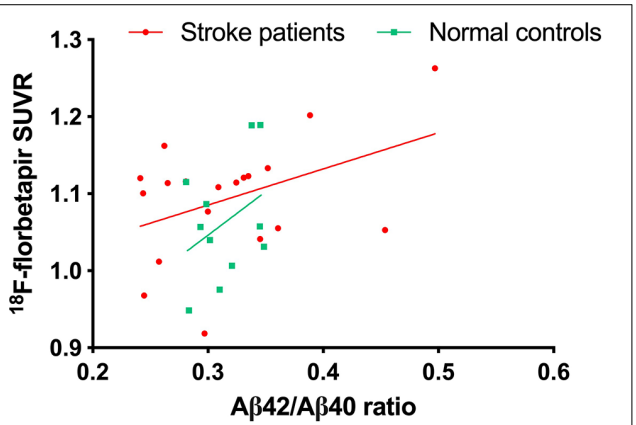

FIGURE 3 | The correlation between plasma Aβ42/Aβ40 ratio and cortical amyloid accumulation burden on ^{18}F-florbetapir PET.

Similar findings were also noted in previous studies. Tau protein level is associated with brain atrophy severity in both stroke patients and normal controls (Ihle-Hansen et al., 2017; Harrison et al., 2021). However, stroke patients have a greater brain atrophy rate than normal controls (Brodtmann et al., 2020), and the correlation between CSF tau protein level and brain atrophy severity is still significant 1 year after stroke, suggesting stroke may enhance or trigger tau-linked neurodegeneration with loss of neurons (Ihle-Hansen et al., 2017).

Various combinations of plasma Aβ42, Aβ40, and tau levels have shown better correlations with cognition than single biomarkers in patients with either AD or VCI (Lue et al., 2017; Chen et al., 2019; Chi et al., 2019). During the neurodegenerative process, Aβ tends to elevate during the MCI stage and reaches a plateau towards the demented stage, while tau protein increases as AD progresses. Therefore, the combination of these biomarkers could be synergistically representative of the neurodegeneration profile. For example, the product of plasma Aβ42 and tau has better accuracy for clinically diagnosed AD than either biomarker alone (Lue et al., 2017; Jiao et al., 2020). Moreover, the plasma tau/Aβ42 ratio showed a stronger association with brain tau accumulation than tau alone (Park et al., 2019). Indeed, the characteristic of an inverse relationship between plasma tau and Aβ40 during the neurodegeneration process (Fan et al., 2018) was also epitomized in our study that the tau/Aβ40 ratio had the strongest correlation with cognitive performance among the other plasma biomarkers and their composite scores.

PSCI development is subject to multiple factors, and the underlying mechanisms are not fully understood. In addition to AD-specific biomarkers, there is a considerable number of fluid and imaging biomarkers associated with vascular cognitive impairment. Previous studies have shown elevated CSF/blood albumin ratio, CSF matrix metalloproteinase (MMP) level, CSF neurofilament, and blood inflammatory cytokines and adhesion molecules are associated with worse cognitive performance, which could be attributed to disruption of blood-CSF/brain barriers and breakdown of white matter fibers and extracellular matrix (Wallin et al., 2017). Furthermore, neuroimaging measures, such as total gray matter volume, leukoaraiosis severity, stroke location, CSF volume, and neuroinflammatory presentations, have been implicated in PSCI development (Thiel et al., 2014; Molad et al., 2019; Huang et al., 2020). Therefore, multi-modality studies are required to investigate the relationships among fluid and imaging biomarkers and their composite influence on PSCI prognosis.

There were several limitations of this study that should be considered. First, the sample size was relatively small, and it should be cautious to generalize the study results. A larger sample size is required to validate the influence of plasma Aβ and tau protein on the PSCI development. Second, additional studies may be required to investigate the interactions among stroke location, stroke severity, and plasma AD biomarkers on the PSCI presentations. Since CSF biomarker analysis has been a more direct measure of the CNS condition than blood analysis, the correlations between CSF and blood measurement of neurodegeneration biomarkers, especially for tau protein, in stroke patients may be needed in future studies. Finally, this was a cross-sectional study, and further longitudinal study is deemed necessary to determine the long-term influence of plasma AD biomarkers on PSCI development.

CONCLUSION

In this study, we found that plasma Aβ42/Aβ40 ratio was correlated with amyloid cortical deposition on ^{18}F-florbetapir SUVR and the total tau protein value was correlated with mean cortical thickness 3 months after stroke. The plasma Aβ42/Aβ40 ratio, tau protein, and tau-related composite scores

were correlated with cognitive performance. The relationship of plasma Aβ40, Aβ42, and tau protein with the long-term post-stroke structural and cognitive changes requires further studies in larger populations.

DATA AVAILABILITY STATEMENT

The datasets presented in this article are not readily available because the used consent does not allow for the public sharing of the data. Requests to access the datasets should be directed to thlee@adm.cgmh.org.tw.

ETHICS STATEMENT

The studies involving human participants were reviewed and approved by The institutional review board at Linkou Chang Gung Memorial Hospital. The patients/participants provided their written informed consent to participate in this study.

AUTHOR CONTRIBUTIONS

K-LH wrote the initial draft, performed neurologic examinations, took part in the data collection and analysis, and scientific interpretation of data. K-JL conceptualized the study design, carried out PET imaging analysis, and wrote a portion of the draft. S-YY conceptualized the study design, took part in scientific interpretation of data, and critical review of the manuscript. T-YC, Y-JC, H-CW, and C-HL performed the data collection, neurologic examination, and scientific interpretation of data. I-TH and Y-MW performed the MRI analysis, took part in data interpretation, and critical review of the manuscript. M-YH conceptualized the study design, wrote a portion of the draft, conducted the cognitive evaluation, took part in data analysis, and critical review of the manuscript. T-HL conceptualized the study design, took part in critical review of the manuscript, and edited the manuscript for content. All authors contributed to the article and approved the submitted version.

FUNDING

This study was supported from Research Fund of Chang Gung Memorial Hospital (CPRPG3H0012, CMRPG3F2183, BMRP611, CMRPG3J0371, EMRPD1L0451, CMRPD1H0393, BMRP488) and Ministry of Science and Technology, Taiwan (MOST 107-2410-H-182-008-MY3, 110-2314-B-182A-073-MY3, 109-2314-B182-019-MY3).

ACKNOWLEDGMENTS

We thank Clinical Trial Center of Chang Gung Memorial Hospital for administrative assistance under support from the Ministry of Health and Welfare, Taiwan.

REFERENCES

Alcolea, D., Pegueroles, J., Muñoz, L., Camacho, V., López-Mora, D., Fernández-León, A., et al. (2019). Agreement of amyloid PET and CSF biomarkers for Alzheimer's disease on lumipulse. *Ann. Clin. Transl. Neurol.* 6, 1815–1824. doi: 10.1002/acn3.50873

Becker, J. A., Hedden, T., Carmasin, J., Maye, J., Rentz, D. M., Putcha, D., et al. (2011). Amyloid-β associated cortical thinning in clinically normal elderly. *Ann. Neurol.* 69, 1032–1042. doi: 10.1002/ana.22333

Bielewicz, J., Kurzepa, J., Czekajska-Chehab, E., Stelmasiak, Z., and Bartosik-Psujek, H. (2011). Does serum tau protein predict the outcome of patients with ischemic stroke? *J. Mol. Neurosci.* 43, 241–245. doi: 10.1007/s12031-010-9403-4

Bitsch, A., Horn, C., Kemmling, Y., Seipelt, M., Hellenbrand, U., Stiefel, M., et al. (2002). Serum tau protein level as a marker of axonal damage in acute ischemic stroke. *Eur. Neurol.* 47, 45–51. doi: 10.1159/000047946

Blennow, K. (2017). A review of fluid biomarkers for Alzheimer's disease: moving from CSF to blood. *Neurol. Ther.* 6, 15–24. doi: 10.1007/s40120-017-0073-9

Brodtmann, A., Khlif, M. S., Egorova, N., Veldsman, M., Bird, L. J., and Werden, E. (2020). Dynamic regional brain atrophy rates in the first year after ischemic stroke. *Stroke* 51, e183–e192. doi: 10.1161/STROKEAHA.120.030256

Chen, T.-B., Lee, Y.-J., Lin, S.-Y., Chen, J.-P., Hu, C.-J., Wang, P.-N., et al. (2019). Plasma Aβ42 and total tau predict cognitive decline in amnestic mild cognitive impairment. *Sci. Rep.* 9:13984. doi: 10.1038/s41598-019-50315-9

Chen, X., and Jiang, H. (2019). Tau as a potential therapeutic target for ischemic stroke. *Aging (Albany NY)* 11, 12827–12843. doi: 10.18632/aging.102547

Chi, N.-F., Chao, S.-P., Huang, L.-K., Chan, L., Chen, Y.-R., Chiou, H.-Y., et al. (2019). Plasma amyloid beta and tau levels are predictors of post-stroke cognitive impairment: a longitudinal study. *Front. Neurol.* 10:715. doi: 10.3389/fneur.2019.00715

Chiu, M.-J., Chen, Y.-F., Chen, T.-F., Yang, S.-Y., Yang, F.-P. G., Tseng, T.-W., et al. (2014). Plasma tau as a window to the brain—negative associations with brain volume and memory function in mild cognitive impairment and early Alzheimer's disease. *Hum. Brain Mapp.* 35, 3132–3142. doi: 10.1002/hbm.22390

Chiu, M. J., Yang, S. Y., Chen, T. F., Chieh, J. J., Huang, T. Z., Yip, P. K., et al. (2012). New assay for old markers-plasma beta amyloid of mild cognitive impairment and Alzheimer's disease. *Curr. Alzheimer Res.* 9, 1142–1148. doi: 10.2174/156720512804142967

Chiu, M.-J., Yang, S.-Y., Horng, H.-E., Yang, C.-C., Chen, T.-F., Chieh, J.-J., et al. (2013). Combined plasma biomarkers for diagnosing mild cognition impairment and Alzheimer's disease. *ACS Chem. Neurosci.* 4, 1530–1536. doi: 10.1021/cn400129p

Fan, L.-Y., Tzen, K.-Y., Chen, Y.-F., Chen, T.-F., Lai, Y.-M., Yen, R.-F., et al. (2018). The relation between brain amyloid deposition, cortical atrophy and plasma biomarkers in amnesic mild cognitive impairment and Alzheimer's disease. *Front. Aging Neurosci.* 10:175. doi: 10.3389/fnagi.2018.00175

Fandos, N., Perez-Grijalba, V., Pesini, P., Olmos, S., Bossa, M., Villemagne, V. L., et al. (2017). Plasma amyloid beta 42/40 ratios as biomarkers for amyloid beta cerebral deposition in cognitively normal individuals. *Alzheimers Dement (Amst)* 8, 179–187. doi: 10.1016/j.dadm.2017.07.004

Gottesman, R. F., and Hillis, A. E. (2010). Predictors and assessment of cognitive dysfunction resulting from ischaemic stroke. *Lancet Neurol.* 9, 895–905. doi: 10.1016/S1474-4422(10)70164-2

Hansson, O., Lehmann, S., Otto, M., Zetterberg, H., and Lewczuk, P. (2019). Advantages and disadvantages of the use of the CSF Amyloid beta (Abeta) 42/40 ratio in the diagnosis of Alzheimer's disease. *Alzheimers Res. Ther.* 11:34. doi: 10.1186/s13195-019-0485-0

Harrison, T. M., Du, R., Klencklen, G., Baker, S. L., and Jagust, W. J. (2021). Distinct effects of beta-amyloid and tau on cortical thickness in cognitively healthy older adults. *Alzheimers Dement.* 17, 1085–1096. doi: 10.1002/alz.12249

Hesse, C., Rosengren, L., Vanmechelen, E., Vanderstichele, H., Jensen, C., Davidsson, P., et al. (2000). Cerebrospinal fluid markers for Alzheimer's disease evaluated after acute ischemic stroke. *J. Alzheimer's Dis.* 2, 199–206. doi: 10.3233/jad-2000-23-402

Huang, K.-L., Chang, T.-Y., Chang, C.-H., Liu, H.-L., Chang, Y.-J., Liu, C.-H., et al. (2017). Asymmetric cerebrovascular collateral supply affects cognition in patients with unilateral carotid artery stenosis. *Curr. Neurovasc. Res.* 14, 347–358. doi: 10.2174/1567202614666171005141716

Huang, K.-L., Chang, T.-Y., Ho, M.-Y., Chen, W.-H., Yeh, M.-Y., Chang, Y.-J., et al. (2018a). The correlation of asymmetrical functional connectivity with cognition and reperfusion in carotid stenosis patients. *Neuroimage Clin.* 20, 476–484. doi: 10.1016/j.nicl.2018.08.011

Huang, K.-L., Hsu, J.-L., Lin, K.-J., Chang, C.-H., Wu, Y.-M., Chang, T.-Y., et al. (2018b). Visualization of ischemic stroke-related changes on 18F-THK-5351 positron emission tomography. *EJNMMI Res.* 8:62. doi: 10.1186/s13550-018-0417-1

Huang, K.-L., Hsiao, I.-T., Ho, M.-Y., Hsu, J.-L., Chang, Y.-J., Chang, T.-Y., et al. (2020). Investigation of reactive astrogliosis effect on post-stroke cognitive impairment. *J. Neuroinflammation* 17:308. doi: 10.1186/s12974-020-01985-0

Huang, C.-C., Hsiao, I.-T., Huang, C.-Y., Weng, Y.-C., Huang, K.-L., Liu, C.-H., et al. (2019). Tau PET with 18F-THK-5351 Taiwan patients with familial Alzheimer's disease with the APP p.D678H mutation. *Front. Neurol.* 10:503. doi: 10.3389/fneur.2019.00503

Huang, K.-L., Hsiao, I.-T., Kuo, H.-C., Hsieh, C.-J., Hsieh, Y.-C., Wu, Y.-M., et al. (2019). Correlation between visual association memory test and structural changes in patients with Alzheimer's disease and amnestic mild cognitive impairment. *J. Formos. Med. Assoc.* 118, 1325–1332. doi: 10.1016/j.jfma.2018.12.001

Ihle-Hansen, H., Hagberg, G., Fure, B., Thommessen, B., Fagerland, M. W., Øksengård, A. R., et al. (2017). Association between total-Tau and brain atrophy one year after first-ever stroke. *BMC Neurol.* 17:107. doi: 10.1186/s12883-017-0890-6

Jack, C. R., Knopman, D. S., Jagust, W. J., Petersen, R. C., Weiner, M. W., Aisen, P. S., et al. (2013). Tracking pathophysiological processes in Alzheimer's disease: an updated hypothetical model of dynamic biomarkers. *Lancet Neurol.* 12, 207–216. doi: 10.1016/S1474-4422(12)70291-0

Jiao, F., Yi, F., Wang, Y., Zhang, S., Guo, Y., Du, W., et al. (2020). The validation of multifactor model of plasma Aβ42 and total-tau in combination with MoCA for diagnosing probable Alzheimer disease. *Front. Aging Neurosci.* 12:212. doi: 10.3389/fnagi.2020.00212

Johnson, K. A., Sperling, R. A., Gidicsin, C. M., Carmasin, J. S., Maye, J. E., Coleman, R. E., et al. (2013). Florbetapir (F18-AV-45) PET to assess amyloid burden in Alzheimer's disease dementia, mild cognitive impairment and normal aging. *Alzheimer's Dement.* 9, S72–S83. doi: 10.1016/j.jalz.2012.10.007

Kaerst, L., Kuhlmann, A., Wedekind, D., Stoeck, K., Lange, P., and Zerr, I. (2013). Cerebrospinal fluid biomarkers in Alzheimer's disease, vascular dementia and ischemic stroke patients: a critical analysis. *J. Neurol.* 260, 2722–2727. doi: 10.1007/s00415-013-7047-3

Lin, S.-Y., Lin, K.-J., Lin, P.-C., Huang, C.-C., Chang, C.-C., Lee, Y.-C., et al. (2019). Plasma amyloid assay as a pre-screening tool for amyloid positron emission tomography imaging in early stage Alzheimer's disease. *Alzheimer's Res. Ther.* 11:111. doi: 10.1186/s13195-019-0566-0

Liu, W., Wong, A., Au, L., Yang, J., Wang, Z., Leung, E. Y. L., et al. (2015). Influence of amyloid-beta on cognitive decline after stroke/transient ischemic attack - three-year longitudinal study. *Stroke* 46, 3074–3080. doi: 10.1161/STROKEAHA.115.010449

Lue, L.-F., Sabbagh, M.N., Chiu, M.-J., Jing, N., Snyder, N. L., Schmitz, C., et al. (2017). Plasma levels of Aβ42 and tau identified probable Alzheimer's dementia: findings in two cohorts. *Front. Aging Neurosci.* 9:226. doi: 10.3389/fnagi.2017.00226

Mijajlović, M. D., Pavlović, A., Brainin, M., Heiss, W.-D., Quinn, T. J., Ihle-Hansen, H. B., et al. (2017). Post-stroke dementia–a comprehensive review. *BMC Med.* 15:11. doi: 10.1186/s12916-017-0779-7

Molad, J., Hallevi, H., Korczyn, A. D., Kliper, E., Auriel, E., Bornstein, N. M., et al. (2019). Vascular and neurodegenerative markers for the prediction of post-stroke cognitive impairment: results from the TABASCO study. *J. Alzheimers Dis.* 70, 889–898. doi: 10.3233/JAD-190339

Park, J.-C., Han, S.-H., Yi, D., Byun, M. S., Lee, J. H., Jang, S., et al. (2019). Plasma tau/amyloid-β1–42 ratio predicts brain tau deposition and neurodegeneration in Alzheimer's disease. *Brain* 142, 771–786. doi: 10.1093/brain/awy347

Pendlebury, S. T., and Rothwell, P. M. (2009). Prevalence, incidence and factors associated with pre-stroke and post-stroke dementia: a systematic review and meta-analysis. *Lancet Neurol.* 8, 1006–1018. doi: 10.1016/S1474-4422(09)70236-4

Sahathevan, R., Linden, T., Villemagne, V. L., Churilov, L., Ly, J. V., Rowe, C., et al. (2016). Positron emission tomographic imaging in stroke: cross-sectional and follow-up assessment of amyloid in ischemic stroke. *Stroke* 47, 113–119. doi: 10.1161/STROKEAHA.115.010528

Scheltens, P., and van de Pol, L. (2012). Atrophy of medial temporal lobes on MRI in "probable" Alzheimer's disease and normal ageing: diagnostic value and neuropsychological correlates. *J. Neurol. Neurosurg. Psychiatry* 83, 1038–1040. doi: 10.1136/jnnp-2012-302562

Seco, M., Edelman, J. J., Wilson, M. K., Bannon, P. G., and Vallely, M. P. (2012). Serum biomarkers of neurologic injury in cardiac operations. *Ann. Thorac. Surg.* 94, 1026–1033. doi: 10.1016/j.athoracsur.2012.04.142

Skillback, T., Farahmand, B. Y., Rosen, C., Mattsson, N., Nagga, K., Kilander, L., et al. (2015). Cerebrospinal fluid tau and amyloid-beta1–42 in patients with dementia. *Brain* 138, 2716–2731. doi: 10.1093/brain/awv181

Srikanth, V. K., Quinn, S. J., Donnan, G. A., Saling, M. M., and Thrift, A. G. (2006). Long-term cognitive transitions, rates of cognitive change and predictors of incident dementia in a population-based first-ever stroke cohort. *Stroke* 37, 2479–2483. doi: 10.1161/01.STR.0000239666.46828.d7

Tang, S.-C., Yang, K.-C., Chen, C.-H., Yang, S.-Y., Chiu, M.-J., Wu, C.-C., et al. (2018). Plasma β-amyloids and tau proteins in patients with vascular cognitive impairment. *Neuromol. Med.* 20, 498–503. doi: 10.1007/s12017-018-8513-y

Teunissen, C. E., Chiu, M.-J., Yang, C.-C., Yang, S.-Y., Scheltens, P., Zetterberg, H., et al. (2018). Plasma amyloid-β (Aβ 42) correlates with cerebrospinal fluid Aβ 42 in Alzheimer's disease. *J. Alzheimer's Dis.* 62, 1857–1863. doi: 10.3233/JAD-170784

Thiel, A., Cechetto, D. F., Heiss, W.-D., Hachinski, V., and Whitehead, S. N. (2014). Amyloid burden, neuroinflammation and links to cognitive decline after ischemic stroke. *Stroke* 45, 2825–2829. doi: 10.1161/STROKEAHA.114.004285

Tuladhar, A. M., and de Leeuw, F. E. (2010). Poststroke dementia--what's in a name? *Nat. Rev. Neurol.* 6, 63–64. doi: 10.1038/nrneurol.2009.229

Tzen, K.-Y., Yang, S.-Y., Chen, T.-F., Cheng, T.-W., Horng, H.-E., Wen, H.-P., et al. (2014). Plasma Aβ but not tau is related to brain PiB retention in early Alzheimer's disease. *ACS Chem. Neurosci.* 5, 830–836. doi: 10.1021/cn500101j

Wallin, A., Kapaki, E., Boban, M., Engelborghs, S., Hermann, D. M., Huisa, B., et al. (2017). Biochemical markers in vascular cognitive impairment associated with subcortical small vessel disease - A consensus report. *BMC Neurol.* 17:102. doi: 10.1186/s12883-017-0877-3

Yang, C.-C., Yang, S.-Y., Chieh, J.-J., Horng, H.-E., Hong, C.-Y., Yang, H.-C., et al. (2011). Biofunctionalized magnetic nanoparticles for specifically detecting biomarkers of Alzheimer's disease *in vitro*. *ACS Chem. Neurosci.* 2, 500–505. doi: 10.1021/cn200028j

Zhang, T., Pan, B. S., Sun, G. C., Sun, X., and Sun, F. Y. (2010). Diabetes synergistically exacerbates poststroke dementia and tau abnormality in brain. *Neurochem. Int.* 56, 955–961. doi: 10.1016/j.neuint.2010.04.003

Conflict of Interest: S-YY is an employee and a shareholder of MagQu Co., Ltd.

The remaining authors declare that the research was conducted in the absence of any commercial or financial relationships that could be construed as a potential conflict of interest.

Publisher's Note: All claims expressed in this article are solely those of the authors and do not necessarily represent those of their affiliated organizations, or those of the publisher, the editors and the reviewers. Any product that may be evaluated in this article, or claim that may be made by its manufacturer, is not guaranteed or endorsed by the publisher.

frontiers in Human Neuroscience

ORIGINAL RESEARCH
published: 03 January 2022
doi: 10.3389/fnhum.2021.765451

Is There Any Relationship Between Biochemical Indices and Anthropometric Measurements With Dorsolateral Prefrontal Cortex Activation Among Older Adults With Mild Cognitive Impairment?

Yee Xing You[1], Suzana Shahar[1], Mazlyfarina Mohamad[2], Nor Fadilah Rajab[3], Normah Che Din[4], Hui Jin Lau[5] and Hamzaini Abdul Hamid[6]*

[1] Dietetics Program and Center for Healthy Aging and Wellness (H-Care), Faculty of Health Sciences, Universiti Kebangsaan Malaysia, Kuala Lumpur, Malaysia, [2] Diagnostic Imaging and Radiotherapy Program, Faculty of Health Sciences, Universiti Kebangsaan Malaysia, Kuala Lumpur, Malaysia, [3] Biomedical Sciences Program and Center for Healthy Aging and Wellness (H-Care), Faculty of Health Sciences, Universiti Kebangsaan Malaysia, Kuala Lumpur, Malaysia, [4] Health Psychology Program, Centre of Rehabilitation and Special Needs, Faculty of Health Sciences, Universiti Kebangsaan Malaysia, Kuala Lumpur, Malaysia, [5] Nutritional Sciences Program and Center for Healthy Aging and Wellness (H-Care), Faculty of Health Sciences, Universiti Kebangsaan Malaysia, Kuala Lumpur, Malaysia, [6] Department of Radiology, Faculty of Medicine, Universiti Kebangsaan Malaysia Medical Center, Kuala Lumpur, Malaysia

OPEN ACCESS

Edited by:
Fanpei G. Yang, National Tsing Hua University, Taiwan

Reviewed by:
Murat Çetin Rağbetli, Karamanoğlu Mehmetbey University, Turkey
Manal Badrasawi, An-Najah National University, Palestine

***Correspondence:**
Suzana Shahar
suzana.shahar@ukm.edu.my

Specialty section:
This article was submitted to Brain Health and Clinical Neuroscience, a section of the journal Frontiers in Human Neuroscience

Received: *27 August 2021*
Accepted: *03 November 2021*
Published: *03 January 2022*

Citation:
You YX, Shahar S, Mohamad M, Rajab NF, Che Din N, Lau HJ and Abdul Hamid H (2022) Is There Any Relationship Between Biochemical Indices and Anthropometric Measurements With Dorsolateral Prefrontal Cortex Activation Among Older Adults With Mild Cognitive Impairment? Front. Hum. Neurosci. 15:765451. doi: 10.3389/fnhum.2021.765451

Working memory is developed in one region of the brain called the dorsolateral prefrontal cortex (DLPFC). The dysfunction of this region leads to synaptic neuroplasticity impairment. It has been reported that several biochemical parameters and anthropometric measurements play a vital role in cognition and brain health. This study aimed to investigate the relationships between cognitive function, serum biochemical profile, and anthropometric measurements using DLPFC activation. A cross-sectional study was conducted among 35 older adults (≥60 years) who experienced mild cognitive impairment (MCI). For this purpose, we distributed a comprehensive interview-based questionnaire for collecting sociodemographic information from the participants and conducting cognitive tests. Anthropometric values were measured, and fasting blood specimens were collected. We investigated their brain activation using the task-based functional MRI (fMRI; N-back), specifically in the DLPFC region. Positive relationships were observed between brain-derived neurotrophic factor (BDNF) ($\beta = 0.494$, $p < 0.01$) and Mini-Mental State Examination (MMSE) ($\beta = 0.698$, $p < 0.01$); however, negative relationships were observed between serum triglyceride ($\beta = -0.402$, $p < 0.05$) and serum malondialdehyde (MDA) ($\beta = -0.326$, $p < 0.05$) with right DLPFC activation ($R^2 = 0.512$) while the participants performed 1-back task after adjustments for age, gender, and years of education. In conclusion, higher serum triglycerides, higher oxidative stress, and lower neurotrophic factor were associated with lower right DLPFC activation among older adults with MCI. A further investigation

needs to be carried out to understand the causal-effect mechanisms of the significant parameters and the DLPFC activation so that better intervention strategies can be developed for reducing the risk of irreversible neurodegenerative diseases among older adults with MCI.

Keywords: anthropometry, biochemical, biomarkers, brain activation, cognitive

INTRODUCTION

Functional MRI (fMRI) is a noninvasive process that can be used for measuring brain activities since it detects changes related to blood flow (Wright and Wise, 2018). fMRI is regarded as an important tool that helped in detecting the changes that took place in the neural mechanisms of older adults (Belleville and Bherer, 2012). This technique includes several features, which could be used as effective surrogate markers for investigating the cognitive status among older adults (Belleville and Bherer, 2012; Clément and Belleville, 2012). The human brain includes a region called the dorsolateral prefrontal cortex (DLPFC). This region is located in the middle frontal gyrus of the human brain, which is a part of the lateral region in Brodmann's area 9 and 46 (Barbey et al., 2013). Impaired synaptic neuroplasticity occurs due to a DLPFC dysfunction (Kumar et al., 2017). At present, the site that was most frequently targeted among older adults with mild cognitive impairment (MCI) was the DLPFC as reported in recent studies, which is important for working memory (Wang et al., 2014; Badhwar et al., 2017; Taylor et al., 2019).

Several risk factors have been identified, which indicate cognitive declines such as increased age of adults, inadequate nutrient intake, low educational level, presence of comorbidities, and a lack of physical and social activities (Sachdev et al., 2013; Baumgart et al., 2015; Boyle et al., 2016; Kobe et al., 2016). Additionally, a higher body mass index (BMI) was also associated with a poor cognitive status. Previous studies have also reported that the greater BMI and higher body fat percentage were closely related to poor cognitive status among older adults (Malek Rivan et al., 2019). Cognitive deterioration was also associated with the biochemical profiles of the participants such as the serum lipid profiles. Current evidence suggests that lipids help in regulating the neural functions in the central nervous system since they participate in many local mechanisms associated with the systemic lipid metabolism (Weinstock-Guttman et al., 2011; Hottman et al., 2014). A previous Malaysian study reported that hypertriglyceridemia was related to an increased risk of poor cognitive among older adults with cognitive impairment (Rivan et al., 2020). Although previous studies have focused on the relationship between these parameters with brain activities, however, not all parameters were systematically included in one study among older adults with MCI.

In addition, Revel et al. (2015) reported that oxidative stress-related damage would accelerate the aging process and lead to an age-related cognitive decline. Malondialdehyde (MDA) was observed to be an important biomarker of the lipid peroxidation process, which plays a vital role in progressing dementia (García-Blanco et al., 2017; He et al., 2017; Luo et al., 2020). Age-related oxidative brain damage was significantly increased by lipid peroxidation products, protein oxidation mechanisms, and the oxidative changes that take place in the mitochondrial and nuclear DNA (Zabel et al., 2018). All these factors can lead to irreversible neurodegenerative diseases (García-Blanco et al., 2017; Luo et al., 2020). It is necessary to identify possible biomarkers that can serve better in determining their relationship with cognitive function and can potentially be used as a molecular signature for targeted interventions in the future among older adults with MCI so that their condition could be reversed to successful aging.

A majority of the earlier local studies made use of neuropsychological batteries for assessing the cognitive functions and defining the potential predictors, which led to a decrease in cognitive functioning (Vanoh et al., 2017; Rivan et al., 2020; You et al., 2020). The fMRI technique could measure the changes occurring in the blood flow levels in response to some memory challenges. Hence, it helps in understanding the differences in brain activation levels among older adults. At present, several methods were used to predict the progression of MCI, such as fMRI (Lau et al., 2018; Wright and Wise, 2018), and the analysis of biomarkers in the cerebrospinal fluid and peripheral blood (Hermida et al., 2012). In this study, we aimed to determine the relationship between the various biochemical parameters, anthropometric values, and cognitive function with working memory related to the DLPFC function among the older adults with MCI. We hypothesized that there is a relationship between biochemical parameters, anthropometric values, and cognitive function with working memory related to the DLPFC function among the older adults with MCI.

MATERIALS AND METHODS

Study Design

This is a cross-sectional study that involved 35 community-dwelling older adults with MCI aged 60 years and above as recruited involving two cohorts prior to nutritional intervention studies involving local traditional vegetables (You et al., 2021) and herbs (Lau et al., 2020). They were screened for eligibility based on the inclusion and exclusion criteria. This study was approved by the Medical Research and Ethics Committee of the Universiti Kebangsaan Malaysia (UKM; NN-2019-137), and written informed consent was obtained from all the participants prior to data collection. In this study, the inclusion criteria included older adults aged 60 years and above with MCI based on the criteria described by Petersen et al. (2014) and who were able to communicate in Malay, English, Chinese, or Tamil language participated in the study. The criteria described by Petersen et al. (2014) are stated as follows:

(1) Currently not receiving any clinical judgments on dementia.
(2) Have no or very minimal limitations in instrumental activities of daily livings (IADL) with a score of ≤1.5 SD from the mean norm.
(3) Essentially preserved general cognitive functioning by scoring ≥19 in Mini-Mental State Examination (MMSE).
(4) Objective memory impairment with a score of at least 1.5 SD below the mean average in one or more cognitive tests [Rey Auditory Verbal Learning Test (RAVLT) (immediate recall) or Digit Span] (Vanoh et al., 2017).
(5) Subjective memory complaints.

The exclusion criteria were a history of mental health illness (i.e., Alzheimer's disease, schizophrenia, and history of stroke), score >5 in the Geriatric Depression Scale (GDS), physical disabilities, alcohol and drug users, being claustrophobic, and having internal metallic or electronic implants.

The sample size was calculated using the formula as follows (Hulley et al., 2013):

$$n = [\frac{(Z\alpha+Z\beta)}{C}]^2 + 3$$

where Z_α = 95% CI = 1.96; Z_β = 80% power = 0.842; $C = 0.5 \times \ln[(1+r)/(1-r)] = 0.61$; r = correlation coefficient = 0.515 (Lau et al., 2018), and additional dropout 20%; thus, the total sample size was 35 participants.

Data Collection

Data collection was carried out at the Center of Healthy Aging and Wellness, UKM and the Hospital Canselor Tuanku Muhriz, UKM. The data that were collected included sociodemographic information, self-reported medical condition, anthropometric measurements, biochemical profiles, neuropsychological tests, and fMRI analysis. The participants signed the informed consent prior to the data collection. A total of five trained field-workers from dietetics, nutrition, and biomedical backgrounds joined the data collection. All field-workers were trained by experienced researchers on anthropometric measurements, blood sample collection, and neuropsychological batteries prior to data collection. No pretesting of the questionnaire was conducted as we used validated questionnaires for all parameters.

The anthropometric measurements such as weight, height, waist circumference, and hip circumference were carried out after informed consent was obtained from the participants. All the measurements were carried out according to the standard procedure (Gibson, 1990). Every measurement was repeated two times, and later, the average value was calculated. BMI was calculated to determine the weight status of the participants. BMI was obtained by dividing weight (kg) with (height)^2 (m^2). Equipment was calibrated prior to the measurements.

Participants were asked to fast overnight for at least 10 h to collect blood samples. A total of 20 ml peripheral venous blood was collected and stored in an icebox immediately for delivery purpose. All the basic biochemical profile analyses such as fasting blood sugar, lipid profile, liver function test, and renal profile were analyzed at the medical laboratory (Pathlab Malaysia Sdn Bhd). Serum was isolated by centrifugation and stored at −80°C for 1 month before the biomarker analysis was carried out using commercial ELISA kits. The oxidative stress biomarkers (i.e., MDA), inflammatory biomarkers [i.e., inducible nitric oxide synthase (iNOS) and cyclooxygenase-2 (COX-2)], and brain-derived neurotrophic factor (BDNF) were measured.

We utilized four validated neuropsychological batteries [i.e., MMSE (Ibrahim et al., 2009), Digit Span, Digit Symbol (Weshsler, 1997), and RAVLT (Jamaluddin et al., 2009)] in assessing the global cognitive function, working memory, processing speed, and verbal memory of the participants. The scaled Digit Span and Digit Symbol scores were calculated based on the age-specific tables of the manual (Weshsler, 1997).

A qualified field-worker explained the procedures involved in fulfilling the N-back task. To ensure a clear understanding of the assignment at hand, the participants were provided with a diagram of the task blocks, and the protocol was clearly explained by the field-worker. The two conditions of the N-back task, which were used in this study, had consisted of 0-back and 1-back that were employed by previous studies (Lau et al., 2018; You et al., 2019), which had been created and displayed by using the SuperLab 5 (Cedrus, Los Angeles, CA, United States). N-back holds four blocks for every 0-back and 1-back condition. **Figure 1** displays the 0-back and 1-back paradigms. During the 0-back condition, the participants were obliged to react to the stimulus provided and to distinguish if it is similar to the position of the target at the start of the block (i.e., pre-demarcated stimulus). As for the 1-back condition, the participants were called on to decide if the position of the target exhibited is similar to the one previous to it. A radiographer performed a 3-min anatomical scan of the brain, which was followed by approximately 9 min of N-back tasks. The duration of each block was 30 s; there was a 30-s rest between blocks, and the total duration to complete the task was 510 s.

Single-shot spin-echo echo planar imaging (EPI) was obtained; the fMRI data and the fMRI images were performed on a 3.0-tesla magnetic resonance (MR) scanner (MAGNETOM, Trio, Siemens, Erlangen, Germany) with each of the subjects being subjected to a high resolution of T1-weighted anatomical images [repetition time (TR) = 1,900 ms, echo time (TE) = 2.35 ms, voxel dimensions = 1.0 × 1.0 × 1.0 mm, 250 × 250 voxels, 176 slices, slice thickness = 1 mm], while those of the N-back task had been conducted *via* the T2*-weighted imaging data (TR = 3,000 ms, TE = 30 ms, 3-mm isotropic voxels, flip angle = 90°, 27 slices, slice thickness = 4 mm).

The percentage of accuracy and the mean response time (RT) on the N-back task of each participant were then recorded in the calculation of the average data. Correct response (CR) is the percentage of CR from the total response performed by each participant. An index $\frac{\text{Reaction time}}{\text{Reaction accuracy}}$ was used to analyze the behavioral performance of the data (You et al., 2019).

Preprocessing of the Functional Data and First-Level Analysis

The preprocessing and data analysis stage utilized the statistical parametric mapping (SPM12) software that was implemented in MATLAB 9.4.0 R2018a (MathWorks Inc., Natick, MA, United States). The functional images were first slice time corrected followed by realignment. These functional images would then be co-registered to the mean T1-weighted image

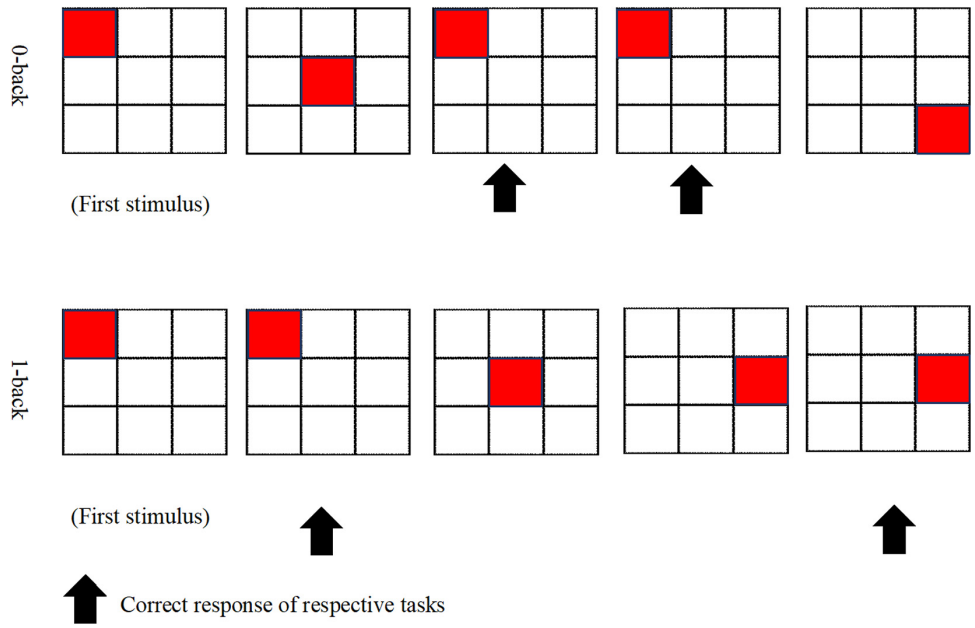

FIGURE 1 | 0-back and 1-back paradigms.

of the subject and estimated against a standardized Montreal Neurological Institute (MNI) stereotaxic space, where the spatial normalization procedure would involve a 6-parameter affine transformation with a spatial transformation matrix. After undergoing the normalization process, all of the functional volumes were then be subjected to spatial smoothing with a 6-mm full-width half-maximum of isotropic Gaussian kernel as a way of increasing the signal-to-noise level through the removal of the high-frequency information and the reduction of its intersubject variability.

The DLPFC is a key node in the cognitive control network that supports working memory, executive function, attention, planning, and decision-making. Many researchers used the N-back task for evaluating the DLPFC function (Townsend et al., 2010; Diamond, 2013; Lau et al., 2018; You et al., 2019). The DLPFC mask was selected, and it had been defined by the WFU PickAtlas (Maldjian et al., 2003) with Brodmann's area 9 and 46. Previous studies had identified this volume of interest (VOI) as being responsible for generating the working memory and executive function of the human brain (Townsend et al., 2010; Lau et al., 2018; You et al., 2019). Individual analysis of the participants was performed to determine VOIs within bilateral DLPFC areas to extract averaged percent change of blood oxygen level dependency (BOLD) representing significant activation [$p < 0.05$, family-wise error (FWE) corrected] using MarsBaR toolbox (Brett et al., 2002).

Statistical Analysis

In this study, the Statistical Package for Social Sciences (SPSS) version 23.0 software was used for carrying out all statistical analyses. The Shapiro–Wilk test was used for determining the data normality ($p > 0.05$). The demographic data of the participants were presented as a percentage value with appropriate SDs. The Pearson's correlation was used for analyzing the relationship between the demographic characteristics (age, gender, and years of education), biochemical parameters, anthropometric values, and neuropsychological test scores with regard to DLPFC activation (i.e., percent signal change extracted from SPM software). To control for the inflated FWE rates that result from performing multiple tests on the same data, the significance of this partial correlation at a Bonferroni-adjusted alpha level was performed. Furthermore, to make adjustment, the family-wise alpha level (0.05) was divided by the total numbers of variables. In addition, the relationships between significant variables from the Pearson's correlation analysis and dependent variable (i.e., percent signal change as DLPFC activation) were modeled using the multiple linear regression after adjustments for age, gender, and years of education.

RESULTS

Profiles of the Participants

A total of 35 participants comprising of 10 men and 25 women with a mean age of 65 years participated in this study. All the mean values of both the anthropometric measurements and the biochemical parameters were within the normal range except systolic blood pressure, which was higher than the normal values (**Table 1**).

Functional MRI Brain Activation

The activated brain region in DLPFC (middle frontal gyrus and Brodmann's area 9 and 46) when performing the N-back task

TABLE 1 | Demographic characteristics of total participants [expressed in mean ± SD or number (%)].

Parameters	Total participants (n = 35)	Reference range [a,b,c,d,e]
Age (years) [a]	65.03 ± 3.36	69.5
Gender (men, %) [a]	10 (28.60)	N/A
Education (years) [a]	9.26 ± 4.07	5.5
Household income (USD/month) [a]	402.24 ± 183.43	336
Hypertension (n, %) [b]	15 (42.90)	37%
Type 2 Diabetes Mellitus (n, %)[b]	6 (17.10)	41.5%
Hyperlipidemia (n, %)[b]	15 (42.90)	60.8%
Height (cm)	156.73 ± 7.83	N/A
Weight (kg)[a]	64.40 ± 10.48	62.4
Body mass index (kg/m^2)[c]	26.12 ± 3.01	22–27
Waist circumference (cm)[d]	88.33 ± 8.39	<90
Systolic blood pressure (mmHg) [d]	132.91 ± 16.05	120
Diastolic blood pressure (mmHg)[d]	72.63 ± 10.02	80
Fasting blood glucose (mmol/L)[e]	5.46 ± 1.17	3.9–5.6
Total cholesterol (mmol/L)[e]	5.40 ± 0.96	<5.2
Low density lipoprotein (mmol/L)[e]	3.27 ± 0.90	<2.6
High density lipoprotein (mmol/L)[e]	1.52 ± 0.37	>1.04
Triglyceride (mmol/L)[e]	1.38 ± 0.55	<1.7
Sodium (mmol/L)[e]	141.51 ± 3.06	137–150
Potassium (mmol/L)[e]	4.45 ± 0.52	3.5–5.3
Urea (mmol/L)[e]	4.34 ± 1.11	1.7–8.4
Creatinine (μmol/L)[e]	69.31 ± 18.16	62–115
Uric acid (μmol/L)[e]	0.35 ± 0.01	0.20–0.42
Total protein (g/L)[e]	72.51 ± 6.20	57–82
Albumin (g/L)[e]	43.91 ± 2.38	32–48
Globulin (g/L)[e]	28.63 ± 6.53	20–50
Total bilirubin (μmol/L)[e]	11.86 ± 4.77	3–19
Alkaline phosphatase (U/L)[e]	74.54 ± 17.11	39–117
Alanine aminotransferase (ALT) (U/L)[e]	20.20 ± 11.19	0–40
Aspartate aminotransferase (AST) (U/L)[e]	22.71 ± 5.43	0–40
Inducible nitric oxide synthase (iNOS) (pg/ml)	182.31 ± 29.21	N/A
Cyclooxygenase-2 (COX-2) (ng/ml)	1.34 ± 0.70	N/A
Brain-derived neurotrophic factor (BDNF) (pg/ml)	114.52 ± 53.56	N/A
Malondialdehyde (MDA) (ng/ml)	211.22 ± 50.27	N/A
Neuropsychological batteries		
MMSE [a]	25.94 ± 2.18	19
Digit Span (Scaled score)[a]	13.14 ± 1.90	7.7
RAVLT immediate recall [a]	6.83 ± 1.47	7
RAVLT delayed recall[a]	6.11 ± 2.01	6
Digit Symbol (Scaled score)[a]	7.63 ± 2.43	8
fMRI behavioral performance		
Reaction accuracy (N-back) (%)	62.07 ± 10.59	N/A
Reaction time (N-back) (ms)	2245.95 ± 297.87	N/A
RT/RA index	37.35 ± 8.87	N/A
fMRI brain activation		
0-back mean percent signal change (%) Left DLPFC	0.73 ± 0.52	N/A
0-back mean percent signal change (%) Right DLPFC	0.83 ± 0.40	N/A
1-back mean percent signal change (%) Left DLPFC	0.82 ± 0.49	N/A
1-back mean percent signal change (%) Right DLPFC	0.94 ± 0.40	N/A

[a] *Nationwide aging population research in Malaysia (Shahar et al., 2016).*
[b] *National Health and Morbidity Survey 2019 in Malaysia.*
[c] *Body mass index for older adults (Winter et al., 2014).*
[d] *WHO cutoff guidelines (World Health Organisation, 2011).*
[e] *Normal range values from the accredited biomedical laboratory.*
DLPFC, dorsolateral prefrontal cortex; fMRI, functional MRI; MMSE, Mini-Mental State Examination; RAVLT, Rey Auditory Verbal Learning Test; RA, reaction accuracy; and RT, reaction time.

($p < 0.05$, FWE corrected) is presented in **Table 2**. The total voxels activated in DLPFC for 0-back and 1-back being 5,141 and 7,915 voxels, respectively, with the highest activation observed in the right middle frontal gyrus (rMFG) for both 0-back and 1-back tasks ($p < 0.05$, FWE corrected). **Figure 2** demonstrates that the middle frontal gyrus, precentral gyrus, superior frontal gyrus, and inferior frontal gyrus were activated while the participants performed 0-back and 1-back tasks.

Relationship Between Demographic Characteristics, Anthropometric Measurements, Biochemical Profiles, Biomarkers, Cognitive Tests, and Brain Activation

Table 3 shows the relationship between demographic characteristics, anthropometric measurements, biochemical indices, and cognitive tests with DLPFC. Women participants demonstrated higher right DLPFC activation compared to men participants while performing the 1-back task ($p < 0.05$). Significant positive correlations were observed between years of education ($r = 0.400$, $p < 0.05$), high density lipoprotein ($r = 0.431$, $p < 0.01$), serum BDNF ($r = 0.407$, $p < 0.0125$), MMSE ($r = 0.466$, $p < 0.01$), and RAVLT immediate recall ($r = 0.451$, $p < 0.01$) with right DLPFC activation while the participants performed the 1-back task. However, significant negative correlations were observed between age ($r = -0.340$, $p < 0.05$), serum triglyceride for female ($r = -0.450$, $p < 0.01$), and serum MDA ($r = -0.455$, $p < 0.0125$) with right DLPFC activation while the participants performed the 1-back task. Further analysis using the multivariate linear regression is demonstrated in **Table 4**. The findings showed positive relationships between BDNF ($\beta = 0.494$, $p < 0.01$) and MMSE ($\beta = 0.698$, $p < 0.01$); however, negative relationships were observed between serum triglyceride ($\beta = -0.402$, $p < 0.05$) and serum MDA ($\beta = -0.326$, $p < 0.05$) with right DLPFC activation ($R^2 = 0.512$) while the participants performed the 1-back task after adjustments for age, gender, and years of education.

DISCUSSION

In this study, we have successfully determined the relationship between the various biochemical parameters, anthropometric values, and neuropsychological test scores with the DLPFC activation among the older adults with MCI. The results of our study showed that older participants with MCI had lower DLPFC activation, which was associated with increased lipid peroxidation and oxidative stress. A few earlier studies indicated that lipid peroxidation led to oxidative degradation of the polyunsaturated fatty acids in cells. This could cause a release of many inflammatory and pro-inflammatory factors that promote cell proliferation or apoptosis (Libetta et al., 2011; Redza-Dutordoir and Averill-Bates, 2016). Additionally, the brain shows a higher oxidative metabolism that can lead to the production of a higher concentration of reactive oxygen species (ROS; Redza-Dutordoir and Averill-Bates, 2016; Salim, 2017; You et al., 2018).

TABLE 2 | Activated brain regions during 0-back and 1-back task [$p < 0.05$, family-wise error (FWE) corrected].

Anatomical region	L/R	Coordinates			Voxels activated	Maximum *T*-value
		x	*y*	*z*		
0-back						
Middle frontal gyrus	R	44	10	14	2,922	16.47
	L	−34	0	50	2,188	14.83
Precentral gyrus	L	−36	4	30	3	10.58
Inferior frontal gyrus	L	−42	42	−2	26	5.31
Superior frontal gyrus	R	4	40	38	2	4.72
1 back						
Middle frontal gyrus	R	46	12	38	4,269	17.66
	L	−40	8	34	3,551	16.78
Superior frontal gyrus	R	4	30	38	73	9.14
	L	−6	30	38	18	7.73
Inferior frontal gyrus	R	50	40	2	2	5.89
Precentral gyrus	R	62	6	26	2	4.99

L, left; R, right.

ROS molecules induce neuronal death and further decrease the activation potential value of the neurons, which could decrease the local demand for the oxygenation process. This, in turn, decreased the blood volume supply or perfusion (Belaïch et al., 2015). Thereafter, the intensity of the BOLD images collected from the activated cortical regions in the brain was decreased. This was based on the fact that community-dwelling older adults showed significant oxidative stress (Belaïch et al., 2015). Thus, it could be concluded that oxidative stress might directly affect brain activation as the ROS molecules were involved in the neurodegenerative metabolic process (Numakawa et al., 2011; Salim, 2017).

Additionally, serum BDNF showed a positive association with right DLPFC activation. Phillips (2017) showed that an adequate BDNF level modulated neuronal plasticity, which helped in maintaining the neuronal functions and promoted the adaptation to the exogenous and endogenous stressors particularly during chronic stress or depression. The strongest evidence for the role of BDNF in cognitive performance comes from the relatively large body of literature using a human model to elucidate the role of BDNF on spatial memory (Erickson et al., 2010; Piepmeier and Etnier, 2015). Correlational evidence with older adults has shown that serum BDNF was associated with hippocampal volume and spatial memory (Piepmeier and Etnier, 2015; Lau et al., 2020). Erickson et al. (2010) utilized MRI, ELISA, and measures of spatial memory to assess the association between age-related decreases in brain volume, BDNF, and memory in older adults. Results indicated that subjects with MCI had significantly lower concentrations of BDNF, smaller hippocampal volumes, and worse performance on spatial memory tasks as compared to successful aging participants (Erickson et al., 2010). In another study, Mattson et al. (2004) stated that the age-dependent impairment in the cognitive functions could be due to a decrease in the BDNF expression in the primary areas of the brain, which were affected by the aging-related issues (Mattson et al., 2004). Thus, it was concluded that BDNF is an important biomarker that was closely associated with brain activation among older adults with MCI.

In this study, we noted a negative relationship between serum triglyceride levels and brain activation. Similar results were reported earlier by Parthasarathy et al. (2017) who observed that the serum triglyceride levels were related to the brain function of the healthy older participants.

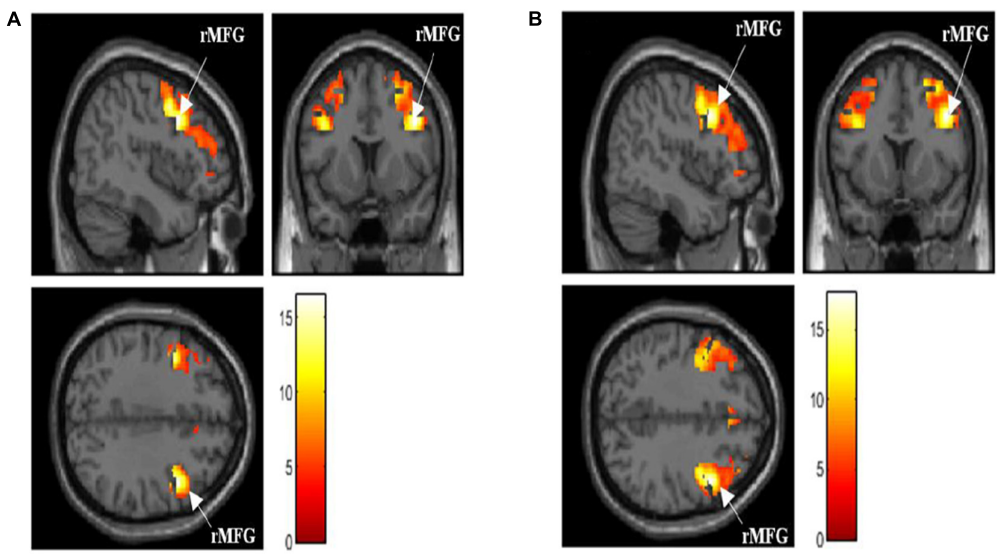

FIGURE 2 | (A) Activated brain region in dorsolateral prefrontal cortex (DLPFC) when performing 0-back task [$p < 0.05$, family-wise error (FWE) corrected]. **(B)** Activated brain region in DLPFC when performing 1-back task [$p < 0.05$, FWE corrected]. rMFG, right middle frontal gyrus; activation intensity: Red to White (low to high).

TABLE 3 | Relationship between demographic characteristics, anthropometric measurements, biochemical indices, and cognitive tests with dorsolateral prefrontal cortex (DLPFC) activation (n = 35).

		0-back right DLPFC activation	0-back left DLPFC activation	1-back right DLPFC activation	1-back left DLPFC activation
		Participants (n = 35)	Participants (n = 35)	Participants (n = 35)	Participants (n = 35)
Age [a]	r	−0.118	−0.031	−0.340*	−0.020
	p	0.500	0.860	0.045	0.908
Gender [b]	p	0.171	0.630	0.042*	0.629
Education years [a]	r	0.131	0.107	0.400*	0.119
	p	0.453	0.539	0.017	0.496
Anthropometric measurements [a]					
Body mass index	r	−0.226	−0.264	−0.166	−0.413
	p	0.479	0.407	0.606	0.182
Biochemical profiles [c]					
Fasting blood glucose	r	−0.304	−0.010	−0.047	−0.190
	p	0.075	0.954	0.790	0.275
Total cholesterol	r	−0.158	−0.252	−0.022	−0.167
	p	0.365	0.144	0.900	0.337
Low density lipoprotein	r	−0.166	−0.263	−0.121	−0.097
	p	0.340	0.127	0.487	0.579
High density lipoprotein	r	0.111	0.163	0.431*	0.187
	p	0.526	0.349	0.009	0.281
Triglyceride	r	−0.082	−0.176	−0.450*	−0.007
	p	0.638	0.311	0.008	0.967
Biomarkers [d]					
Inducible nitric oxide synthase	r	−0.300	−0.281	−0.258	−0.156
	p	0.080	0.102	0.135	0.372
Cyclooxygenase-2	r	−0.120	−0.061	−0.363	−0.006
	p	0.671	0.829	0.183	0.982
Brain-derived neurotrophic factor	r	0.063	0.026	0.407*	0.085
	p	0.718	0.881	0.018	0.629
Malondialdehyde	r	−0.384	−0.270	−0.455*	−0.172
	p	0.023	0.117	0.008	0.323
Neuropsychological batteries [c]					
Mini-Mental State Examination	r	0.105	0.273	0.466*	0.206
	p	0.548	0.112	0.005	0.236
Digit Span	r	0.114	0.015	0.252	0.067
	p	0.516	0.933	0.144	0.704
RAVLT immediate recall	r	0.291	0.328	0.451*	0.233
	p	0.090	0.055	0.008	0.177
RAVLT delayed recall	r	0.243	0.136	0.105	0.093
	p	0.160	0.436	0.547	0.595
Digit symbol	r	0.081	0.081	0.077	0.086
	p	0.643	0.642	0.659	0.625

Significant at [a]$p < 0.05$, [c]$p < 0.01$*, [d]$p < 0.0125$* using the Pearson's correlation after the Bonferroni correction.*
Significant at [b]$p < 0.05$ using the independent t-test.*
DLPFC, dorsolateral prefrontal cortex; fMRI, functional MRI; and RAVLT, Rey Auditory Verbal Learning Test.

Hence, in this study, we hypothesized that there could be a significant relationship between the serum triglyceride levels and brain activation in older adults with MCI. The serum triglycerides can pass the blood-brain barrier (BBB; Banks et al., 2018) and can regulate the transport of insulin and gastrointestinal hormones across BBB, which could negatively affect brain activation (Urayama and Banks, 2008; Banks, 2012; Parthasarathy et al., 2017). Hypertriglyceridemia can trigger the production of ROS molecules in the mitochondrial electron system, which causes lipid peroxidation in the cell membranes and leads to the generation of lipid peroxide and other radicals. An increase in the lipid peroxidation mechanism was attributed to oxidative stress and could lead to a cognitive decline (Bradley-Whitman and Lovell, 2015; You et al., 2018). Thus, it was concluded that the actual effect of the serum triglyceride levels on brain activation has not been explained clearly, and further studies need to be carried out to determine their actual relationship with neuron function in the DLPFC.

Furthermore, another highlight of the outcomes of this study is the positive relationship between the MMSE scores and DLPFC activation among participants with MCI. MMSE is a validated neuropsychological test that assesses global cognitive functions (i.e., visuospatial, attention, and executive functions). It is highly sensitive to the functions of the frontal lobe (Ibrahim et al., 2009). DLPFC also plays a vital role in controlling the verbal and working memory, particularly, manipulating the stimuli,

TABLE 4 | Multiple linear regression model of biochemical profiles, biomarkers, cognitive tests, and DLPFC activation.

Parameter	1-back right DLPFC activation			
	R^2	Adjusted odd ratio (95% CI)	*t*	*p*-value
High density lipoprotein	0.512	0.197 (−0.183–0.205)	0.981	0.336
Triglyceride		−0.402 (−0.552 to −0.332)*	−2.301	0.029
Brain-derived neurotrophic factor		0.494 (0.301–0.606)**	2.902	0.007
Malondialdehyde		−0.326 (−0.354 to −0.305)	−2.175	0.038
Mini-Mental State Examination		0.698 (0.591–0.796)**	3.912	0.001
RAVLT immediate recall		0.071 (0.059–0.082)	1.641	0.113

Significant at $p < 0.05$ and $p < 0.01$** using multiple linear regression (MLR). MLR model was adjusted by age, gender, and years of formal education. DLPFC, dorsolateral prefrontal cortex; RAVLT, Rey Auditory Verbal Learning Test.*

integrating all the collected information, selecting the best response while making decisions, and temporarily storing vital information (Barbey et al., 2013; Bosch et al., 2013; Buckholtz et al., 2015; You et al., 2019). These characteristics are supported by the fact that the cognitive functions and the verbal memory were associated with the structure of the white matter tracts related to the DLPFC (Turken et al., 2008).

Some researchers also investigated the association between anthropometric values and cognitive function with brain activation (Papachristou et al., 2015; Won et al., 2017). However, this study did not observe any relationship of these parameters with brain activation. This could be attributed to the activation that may have occurred in different regions in the brain, which was not studied.

In addition, the maximal DLPFC activation was observed in the rMFG region when the participants performed the N-back task. This was attributed to the fact that they showed a right-hemispheric dominance during the visual-spatial processing phase when they performed the N-back task (Pisella et al., 2011). Generally, the prefrontal cortex regions, such as the rMFG, left superior frontal gyrus, and inferior frontal gyrus, control the working memory, attention, and executive functioning in humans (Lara and Wallis, 2015; Koyama et al., 2017). A few earlier studies proved that the middle frontal gyrus was involved in various working memory tasks such as numerical operations or word reading (Koyama et al., 2017; Lau et al., 2018; You et al., 2019).

The strength of this article is the use of the fMRI approach that helped in investigating all underlying changes that affected the cerebral hemodynamic responses to the anthropometric values, biochemical profiles, and blood biomarkers. As fMRI is noninvasive and does not involve the use of ionizing radiation, it is suitable for older adults. The limitation of this study is that the significant findings were not shown in men, probably due to a smaller sample size, as compared to women. In addition, the brain activation was analyzed using the VOI analysis (i.e., DLPFC); however, the whole-brain analysis is recommended to investigate the biochemical and anthropometric variables related to other activated brain regions in the future. We also suggest that a longitudinal study should be conducted to examine the association between the biochemical indices and anthropometric measurements with brain activation and the inclusion of a healthy control group using the whole-brain analysis in future study.

CONCLUSION

Abnormal lipid profile as indicated by a higher level of serum triglycerides, oxidative stress, and lipid peroxidation and also as indicated by a higher serum MDA and a lower BDNF was associated with poorer brain activation as assessed using the right DLPFC activation, particularly in women subjects. A further investigation needs to be carried out for understanding the mechanisms affecting the relationships between all the above mentioned parameters and the DLPFC activation so that better intervention strategies can be developed to reduce the risk of irreversible neurodegenerative diseases among older adults with MCI.

DATA AVAILABILITY STATEMENT

The original contributions presented in the study are included in the article/supplementary material, further inquiries can be directed to the corresponding author.

ETHICS STATEMENT

The studies involving human participants were reviewed and approved by the Medical Research and Ethics Committee of the Universiti Kebangsaan Malaysia (NN-2019-137). The patients/participants provided their written informed consent to participate in this study. Written informed consent was obtained from the individual(s) for the publication of any potentially identifiable images or data included in this article.

AUTHOR CONTRIBUTIONS

YXY contributed to the drafting of the manuscript, acquisition and analysis of data, project administration, interpreting and validation of the results, and operations. SS contributed to study conception and design, acquisition and analysis of data, interpreting and validation of the results, and supervision. MM contributed to the design of paradigms and data processing and analysis of data. NFR contributed to interpreting and validation of the results as well as supervision. NCD contributed to the acquisition of data and operations. HJL contributed to interpreting and validation of the results as well as operations. HAH contributed to interpreting and validation of the results.

All authors contributed to the manuscript and approved the submitted version.

FUNDING

This study was supported by the Fundamental Research Grant Scheme (FGRS) provided by the Ministry of Education Malaysia (Grant No. FRGS/1/2019/SKK02/UKM/01/1) and the Dana Impak Perdana, Universiti Kebangsaan Malaysia (Grant No. DIP-2019-029).

ACKNOWLEDGMENTS

We would like to express our gratitude to all field-workers, local authorities, enumerators, UKM statisticians, and participants for their involvement in this study.

REFERENCES

Badhwar, A., Tam, A., Dansereau, C., Orban, P., Hoffstaedter, F., and Bellec, P. (2017). Resting-state network dysfunction in Alzheimer's disease: a systematic review and meta-analysis. *Alzheimers Dement. (Amst.)* 8, 73–85. doi: 10.1016/j.dadm.2017.03.007

Banks, W. A. (2012). Role of the blood-brain barrier in the evolution of feeding and cognition. *Ann. N. Y. Acad. Sci.* 1264, 13–19. doi: 10.1111/j.1749-6632.2012.06568.x

Banks, W. A., Farr, S. A., Salameh, T. S., Niehoff, M. L., Rhea, E. M., Morley, J. E., et al. (2018). Triglycerides cross the blood-brain barrier and induce central leptin and insulin receptor resistance. *Int. J. Obesity (2005)* 42, 391–397. doi: 10.1038/ijo.2017.231

Barbey, A. K., Koenigs, M., and Grafman, J. (2013). Dorsolateral prefrontal contributions to human working memory. *Cortex* 49, 1195–1205. doi: 10.1016/j.cortex.2012.05.022

Baumgart, M., Snyder, H. M., Carrillo, M. C., Fazio, S., Kim, H., and Johns, H. (2015). Summary of the evidence on modifiable risk factors for cognitive decline and dementia: a population-based perspective. *Alzheimers Dement.* 11, 718–726. doi: 10.1016/j.jalz.2015.05.016

Belaïch, R., Boujraf, S., Housni, A., Maaroufi, M., Batta, F., Magoul, R., et al. (2015). Assessment of hemodialysis impact by Polysulfone membrane on brain plasticity using BOLD-fMRI. *Neuroscience* 288, 94–104. doi: 10.1016/j.neuroscience.2014.11.064

Belleville, S., and Bherer, L. (2012). Biomarkers of cognitive training effects in aging. *Curr. Transl. Geriatr. Exp. Gerontol. Rep.* 1, 104–110. doi: 10.1007/s13670-012-0014-5

Bosch, O. G., Wagner, M., Jessen, F., Kühn, K.-U., Joe, A., Seifritz, E., et al. (2013). Verbal memory deficits are correlated with prefrontal hypometabolism in (18)FDG PET of recreational MDMA users. *PLoS One* 8:e61234. doi: 10.1371/journal.pone.0061234

Boyle, P. A., Yu, L., Fleischman, D. A., Leurgans, S., Yang, J., Wilson, R. S., et al. (2016). White matter hyperintensities, incident mild cognitive impairment, and cognitive decline in old age. *Ann. Clin. Transl. Neurol.* 3, 791–800. doi: 10.1002/acn3.343

Bradley-Whitman, M. A., and Lovell, M. A. (2015). Biomarkers of lipid peroxidation in Alzheimer disease (AD): an update. *Arch. Toxicol.* 89, 1035–1044. doi: 10.1007/s00204-015-1517-6

Brett, M., Anton, J.-L., Valabregue, R., and Poline, J.-B. (2002). "Region of interest analysis using an SPM toolbox," in *Proceedings of the 8th International Conference on Functional Mapping of the Human Brain*, Sendai.

Buckholtz, J. W., Martin, J. W., Treadway, M. T., Jan, K., Zald, D. H., Jones, O., et al. (2015). From blame to punishment: disrupting prefrontal cortex activity reveals norm enforcement mechanisms. *Neuron* 87, 1369–1380. doi: 10.1016/j.neuron.2015.08.023

Clément, F., and Belleville, S. (2012). Effect of disease severity on neural compensation of item and associative recognition in mild cognitive impairment. *J. Alzheimers Dis.* 29, 109–123. doi: 10.3233/jad-2012-110426

Diamond, A. (2013). Executive functions. *Annu. Rev. Psychol.* 64, 135–168. doi: 10.1146/annurev-psych-113011-143750

Erickson, K. I., Prakash, R. S., Voss, M. W., Chaddock, L., Heo, S., McLaren, M., et al. (2010). Brain-derived neurotrophic factor is associated with age-related decline in hippocampal volume. *J. Neurosci.* 30, 5368–5375. doi: 10.1523/jneurosci.6251-09.2010

García-Blanco, A., Baquero, M., Vento, M., Gil, E., Bataller, L., and Cháfer-Pericás, C. (2017). Potential oxidative stress biomarkers of mild cognitive impairment due to Alzheimer disease. *J. Neurol. Sci.* 373, 295–302. doi: 10.1016/j.jns.2017.01.020

Gibson, R. S. (1990). *Principles of Nutritional Assessment*. New York, NY: Oxford University Press.

He, W., Wang, C., Chen, Y., He, Y., and Cai, Z. (2017). Berberine attenuates cognitive impairment and ameliorates tau hyperphosphorylation by limiting the self-perpetuating pathogenic cycle between NF-κB signaling, oxidative stress and neuroinflammation. *Pharmacol. Rep.* 69, 1341–1348. doi: 10.1016/j.pharep.2017.06.006

Hermida, A. P., McDonald, W. M., Steenland, K., and Levey, A. (2012). The association between late-life depression, mild cognitive impairment and dementia: is inflammation the missing link? *Expert Rev. Neurother.* 12, 1339–1350. doi: 10.1586/ern.12.127

Hottman, D. A., Chernick, D., Cheng, S., Wang, Z., and Li, L. (2014). HDL and cognition in neurodegenerative disorders. *Neurobiol. Dis.* 72(Pt A), 22–36. doi: 10.1016/j.nbd.2014.07.015

Hulley, S. B., Cummings, S. R., Browner, W. S., Grady, D. G., and Newman, T. B. (2013). *Designing Clinical Research*, 4th Edn. San Francisco, CA: Lippincott Williams & Wilkins.

Ibrahim, N. M., Shohaimi, S., Chong, H. T., Rahman, A. H., Razali, R., Esther, E., et al. (2009). Validation study of the mini-mental state examination in a Malay-speaking elderly population in Malaysia. *Dement. Geriatr. Cogn. Disord.* 27, 247–253. doi: 10.1159/000203888

Jamaluddin, R., Othman, Z., Musa, K. I., and Alwi, M. N. M. (2009). Validation of the malay version of auditory verbal learning test (Mvavlt) among schizophrenia patients in hospital Universiti Sains Malaysia (Husm), Malaysia. *ASEAN J. Psychiatry* 10, 54–74.

Kobe, T., Witte, A. V., Schnelle, A., Lesemann, A., Fabian, S., Tesky, V. A., et al. (2016). Combined omega-3 fatty acids, aerobic exercise and cognitive stimulation prevents decline in gray matter volume of the frontal, parietal and cingulate cortex in patients with mild cognitive impairment. *Neuroimage* 131, 226–238. doi: 10.1016/j.neuroimage.2015.09.050

Koyama, M. S., O'Connor, D., Shehzad, Z., and Milham, M. P. (2017). Differential contributions of the middle frontal gyrus functional connectivity to literacy and numeracy. *Sci. Rep.* 7:17548. doi: 10.1038/s41598-017-17702-6

Kumar, S., Zomorrodi, R., Ghazala, Z., Blumberger, D., Fischer, C., Daskalakis, Z., et al. (2017). Dorsolateral prefrontal cortex neuroplasticity deficits in Alzheimer's disease. *Biol. Psychiatry* 81:S148. doi: 10.1016/j.biopsych.2017.02.378

Lara, A. H., and Wallis, J. D. (2015). The role of prefrontal cortex in working memory: a mini review. *Front. Syst. Neurosci.* 9:173. doi: 10.3389/fnsys.2015.00173

Lau, H., Shahar, S., Mohamad, M., Rajab, N. F., Yahya, H. M., Din, N. C., et al. (2018). Relationships between dietary nutrients intake and lipid levels with functional MRI dorsolateral prefrontal cortex activation. *Clin. Intervent. Aging* 14, 43–51. doi: 10.2147/CIA.S183425

Lau, H., Shahar, S., Mohamad, M., Rajab, N. F., Yahya, H. M., Din, N. C., et al. (2020). The effects of six months Persicaria minor extract supplement among older adults with mild cognitive impairment: a double-blinded, randomized, and placebo-controlled trial. *BMC Complement. Med. Ther.* 20:315. doi: 10.1186/s12906-020-03092-2

Libetta, C., Sepe, V., Esposito, P., Galli, F., and Dal Canton, A. (2011). Oxidative stress and inflammation: implications in uremia and hemodialysis. *Clin. Biochem.* 44, 1189–1198. doi: 10.1016/j.clinbiochem.2011.06.988

Luo, J., Mills, K., le Cessie, S., Noordam, R., and van Heemst, D. (2020). Ageing, age-related diseases and oxidative stress: what to do next? *Ageing Res. Rev.* 57:100982. doi: 10.1016/j.arr.2019.100982

Maldjian, J. A., Laurienti, P. J., Kraft, R. A., and Burdette, J. H. (2003). An automated method for neuroanatomic and cytoarchitectonic atlas-based interrogation of fMRI data sets. *Neuroimage* 19, 1233–1239. doi: 10.1016/s1053-8119(03)00169-1

Malek Rivan, N. F., Shahar, S., Rajab, N. F., Singh, D. K. A., Din, N. C., Hazlina, M., et al. (2019). Cognitive frailty among Malaysian older adults: baseline findings from the LRGS TUA cohort study. *Clin. Intervent. Aging* 14, 1343–1352. doi: 10.2147/CIA.S211027

Mattson, M. P., Maudsley, S., and Martin, B. (2004). BDNF and 5-HT: a dynamic duo in age-related neuronal plasticity and neurodegenerative disorders. *Trends Neurosci.* 27, 589–594. doi: 10.1016/j.tins.2004.08.001

Numakawa, T., Matsumoto, T., Numakawa, Y., Richards, M., Yamawaki, S., and Kunugi, H. (2011). Protective action of neurotrophic factors and estrogen against oxidative stress-mediated neurodegeneration. *J. Toxicol.* 2011:405194. doi: 10.1155/2011/405194

Papachristou, E., Ramsay, S. E., Lennon, L. T., Papacosta, O., Iliffe, S., Whincup, P. H., et al. (2015). The relationships between body composition characteristics and cognitive functioning in a population-based sample of older British men. *BMC Geriatr.* 15:172. doi: 10.1186/s12877-015-0169-y

Parthasarathy, V., Frazier, D. T., Bettcher, B. M., Jastrzab, L., Chao, L., Reed, B., et al. (2017). Triglycerides are negatively correlated with cognitive function in nondemented aging adults. *Neuropsychology* 31, 682–688. doi: 10.1037/neu0000335

Petersen, R. C., Caracciolo, B., Brayne, C., Gauthier, S., Jelic, V., and Fratiglioni, L. (2014). Mild cognitive impairment: a concept in evolution. *J. Int. Med.* 275, 214–228. doi: 10.1111/joim.12190

Phillips, C. (2017). Brain-Derived Neurotrophic Factor, Depression, and Physical Activity: Making the Neuroplastic Connection. *Neural Plast.* 2017:7260130. doi: 10.1155/2017/7260130

Piepmeier, A. T., and Etnier, J. L. (2015). Brain-derived neurotrophic factor (BDNF) as a potential mechanism of the effects of acute exercise on cognitive performance. *J. Sport Health Sci.* 4, 14–23. doi: 10.1016/j.jshs.2014.11.001

Pisella, L., Alahyane, N., Blangero, A., Thery, F., Blanc, S., and Pelisson, D. (2011). Right-hemispheric dominance for visual remapping in humans. *Philos. Trans. R. Soc. B Biol. Sci.* 366, 572–585. doi: 10.1098/rstb.2010.0258

Redza-Dutordoir, M., and Averill-Bates, D. A. (2016). Activation of apoptosis signalling pathways by reactive oxygen species. *Biochim. Biophys. Acta (BBA) Mol. Cell Res.* 1863, 2977–2992. doi: 10.1016/j.bbamcr.2016.09.012

Revel, F., Gilbert, T., Roche, S., Drai, J., Blond, E., Ecochard, R., et al. (2015). Influence of oxidative stress biomarkers on cognitive decline. *J. Alzheimers Dis.* 45, 553–560. doi: 10.3233/jad-141797

Rivan, N. F. M., Shahar, S., Rajab, N. F., Singh, D. K. A., Che Din, N., Mahadzir, H., et al. (2020). Incidence and predictors of cognitive frailty among older adults: a community-based longitudinal study. *Int. J. Environ. Res. Public Health* 17:1547.

Sachdev, P. S., Lipnicki, D. M., Crawford, J., Reppermund, S., Kochan, N. A., Trollor, J. N., et al. (2013). Factors predicting reversion from mild cognitive impairment to normal cognitive functioning: a population-based study. *PLoS One* 8:e59649. doi: 10.1371/journal.pone.0059649

Salim, S. (2017). Oxidative stress and the central nervous system. *J. Pharmacol. Exp. Ther.* 360, 201–205. doi: 10.1124/jpet.116.237503

Shahar, S., Omar, A., Vanoh, D., Hamid, T. A., Mukari, S. Z., Din, N. C., et al. (2016). Approaches in methodology for population-based longitudinal study on neuroprotective model for healthy longevity (TUA) among Malaysian older adults. *Aging Clin. Exp. Res.* 28, 1089–1104. doi: 10.1007/s40520-015-0511-4

Taylor, J. L., Hambro, B. C., Strossman, N. D., Bhatt, P., Hernandez, B., Ashford, J. W., et al. (2019). The effects of repetitive transcranial magnetic stimulation in older adults with mild cognitive impairment: a protocol for a randomized, controlled three-arm trial. *BMC Neurol.* 19:326. doi: 10.1186/s12883-019-1552-7

Townsend, J., Bookheimer, S. Y., Foland-Ross, L. C., Sugar, C. A., and Altshuler, L. L. (2010). fMRI abnormalities in dorsolateral prefrontal cortex during a working memory task in manic, euthymic and depressed bipolar subjects. *Psychiatry Res.* 182, 22–29. doi: 10.1016/j.pscychresns.2009.11.010

Turken, A., Whitfield-Gabrieli, S., Bammer, R., Baldo, J. V., Dronkers, N. F., and Gabrieli, J. D. (2008). Cognitive processing speed and the structure of white matter pathways: convergent evidence from normal variation and lesion studies. *Neuroimage* 42, 1032–1044. doi: 10.1016/j.neuroimage.2008.03.057

Urayama, A., and Banks, W. A. (2008). Starvation and triglycerides reverse the obesity-induced impairment of insulin transport at the blood-brain barrier. *Endocrinology* 149, 3592–3597. doi: 10.1210/en.2008-0008

Vanoh, D., Shahar, S., Din, N. C., Omar, A., Vyrn, C. A., Razali, R., et al. (2017). Predictors of poor cognitive status among older Malaysian adults: baseline findings from the LRGS TUA cohort study. *Aging Clin. Exp. Res.* 29, 173–182. doi: 10.1007/s40520-016-0553-2

Wang, J. X., Rogers, L. M., Gross, E. Z., Ryals, A. J., Dokucu, M. E., Brandstatt, K. L., et al. (2014). Targeted enhancement of cortical-hippocampal brain networks and associative memory. *Science* 345, 1054–1057. doi: 10.1126/science.1252900

Weinstock-Guttman, B., Zivadinov, R., Mahfooz, N., Carl, E., Drake, A., Schneider, J., et al. (2011). Serum lipid profiles are associated with disability and MRI outcomes in multiple sclerosis. *J. Neuroinflamm.* 8:127. doi: 10.1186/1742-2094-8-127

Weshsler, D. (1997). *Wechsler Adult Intelligence Scale-III*. San Antonio, TX: The Psychological Corporation.

Winter, J. E., MacInnis, R. J., Wattanapenpaiboon, N., and Nowson, C. A. (2014). BMI and all-cause mortality in older adults: a meta-analysis. *Am. J. Clin. Nutr.* 99, 875–890. doi: 10.3945/ajcn.113.068122

Won, H., Abdul, M. Z., Mat Ludin, A. F., Omar, M. A., Razali, R., and Shahar, S. (2017). The cut-off values of anthropometric variables for predicting mild cognitive impairment in Malaysian older adults: a large population based cross-sectional study. *Clin. Intervent. Aging* 12, 275–282. doi: 10.2147/CIA.S118942

World Health Organisation (2011). *Waist Circumference and Waist–Hip Ratio: Report of a WHO Expert Consultation*. Geneva: World Health Organisation.

Wright, M. E., and Wise, R. G. (2018). Can blood oxygenation level dependent functional magnetic resonance imaging be used accurately to compare older and younger populations? a mini literature review. *Front. Aging Neurosci.* 10:371. doi: 10.3389/fnagi.2018.00371

You, Y. X., Shahar, S., Haron, H., Yahya, H. M., and Che Din, N. (2020). High traditional Asian vegetables(ulam) intake relates to better nutritional status, cognition and mood among aging adults from low-income residential areas. *Br. Food J.* 122, 3179–3191. doi: 10.1108/BFJ-01-2020-0009

You, Y. X., Shahar, S., Mohamad, M., Yahya, H. M., Haron, H., and Abdul Hamid, H. (2019). Does traditional asian vegetables (ulam) consumption correlate with brain activity using fMRI? A study among aging adults from low-income households. *J. Magn. Reson. Imaging* 51, 1142–1153. doi: 10.1002/jmri.26891

You, Y. X., Shahar, S., Rajab, N. F., Haron, H., Yahya, H. M., Mohamad, M., et al. (2021). Effects of 12 weeks *Cosmos caudatus* supplement among older adults with mild cognitive impairment: a randomized, double-blind and placebo-controlled trial. *Nutrients* 13:434. doi: 10.3390/nu13020434

You, Y., Shahar, S., Haron, H., and Yahya, H. (2018). More ulam for your brain: a review on the potential role of ulam in protecting against cognitive decline. *Sains Malaysiana* 47, 2713–2729. doi: 10.17576/jsm-2018-4711-15

Zabel, M., Nackenoff, A., Kirsch, W. M., Harrison, F. E., Perry, G., and Schrag, M. (2018). Markers of oxidative damage to lipids, nucleic acids and proteins and antioxidant enzymes activities in Alzheimer's disease brain: a meta-analysis in human pathological specimens. *Free Radic. Biol. Med.* 115, 351–360. doi: 10.1016/j.freeradbiomed.2017.12.016

Conflict of Interest: The authors declare that the research was conducted in the absence of any commercial or financial relationships that could be construed as a potential conflict of interest.

Publisher's Note: All claims expressed in this article are solely those of the authors and do not necessarily represent those of their affiliated organizations, or those of the publisher, the editors and the reviewers. Any product that may be evaluated in this article, or claim that may be made by its manufacturer, is not guaranteed or endorsed by the publisher.

frontiers in Human Neuroscience

ORIGINAL RESEARCH
published: 05 January 2022
doi: 10.3389/fnhum.2021.784026

Neural Advantages of Older Musicians Involve the Cerebellum: Implications for Healthy Aging Through Lifelong Musical Instrument Training

*Masatoshi Yamashita[1], Chie Ohsawa[2], Maki Suzuki[3], Xia Guo[4,5], Makiko Sadakata[6], Yuki Otsuka[7], Kohei Asano[7,8], Nobuhito Abe[7] and Kaoru Sekiyama[1]**

[1] Graduate School of Advanced Integrated Studies in Human Survivability, Kyoto University, Kyoto, Japan, [2] School of Music, Mukogawa Women's University, Hyogo, Japan, [3] Department of Behavioral Neurology and Neuropsychiatry, Osaka University United Graduate School of Child Development, Osaka, Japan, [4] Graduate School of Social and Cultural Sciences, Kumamoto University, Kumamoto, Japan, [5] Japan Society for the Promotion of Science, Tokyo, Japan, [6] Institute for Logic, Language and Computation, University of Amsterdam, Amsterdam, Netherlands, [7] Kokoro Research Center, Kyoto University, Kyoto, Japan, [8] Faculty of Child Care and Education, Osaka University of Comprehensive Children Education, Osaka, Japan

OPEN ACCESS

Edited by:
Toshiharu Nakai, Osaka University, Japan

Reviewed by:
Nadia Justel, Interdisciplinary Laboratory of Cognitive Neuroscience, Argentina
Claude Alain, Rotman Research Institute (RRI), Canada
Delphine Dellacherie, Université Lille Nord de France, France

***Correspondence:**
Kaoru Sekiyama
sekiyama.kaoru.8a@kyoto-u.ac.jp

Specialty section:
This article was submitted to Brain Health and Clinical Neuroscience, a section of the journal Frontiers in Human Neuroscience

Received: *27 September 2021*
Accepted: *01 November 2021*
Published: *05 January 2022*

Citation:
Yamashita M, Ohsawa C, Suzuki M, Guo X, Sadakata M, Otsuka Y, Asano K, Abe N and Sekiyama K (2022) Neural Advantages of Older Musicians Involve the Cerebellum: Implications for Healthy Aging Through Lifelong Musical Instrument Training. Front. Hum. Neurosci. 15:784026. doi: 10.3389/fnhum.2021.784026

This study compared 30 older musicians and 30 age-matched non-musicians to investigate the association between lifelong musical instrument training and age-related cognitive decline and brain atrophy (musicians: mean age 70.8 years, musical experience 52.7 years; non-musicians: mean age 71.4 years, no or less than 3 years of musical experience). Although previous research has demonstrated that young musicians have larger gray matter volume (GMV) in the auditory-motor cortices and cerebellum than non-musicians, little is known about older musicians. Music imagery in young musicians is also known to share a neural underpinning [the supramarginal gyrus (SMG) and cerebellum] with music performance. Thus, we hypothesized that older musicians would show superiority to non-musicians in some of the abovementioned brain regions. Behavioral performance, GMV, and brain activity, including functional connectivity (FC) during melodic working memory (MWM) tasks, were evaluated in both groups. Behaviorally, musicians exhibited a much higher tapping speed than non-musicians, and tapping speed was correlated with executive function in musicians. Structural analyses revealed larger GMVs in both sides of the cerebellum of musicians, and importantly, this was maintained until very old age. Task-related FC analyses revealed that musicians possessed greater cerebellar-hippocampal FC, which was correlated with tapping speed. Furthermore, musicians showed higher activation in the SMG during MWM tasks; this was correlated with earlier commencement of instrumental training. These results indicate advantages or heightened coupling in brain regions associated with music performance and imagery in musicians. We suggest that lifelong instrumental training highly predicts the structural maintenance of the cerebellum and related cognitive maintenance in old age.

Keywords: aging, older musicians, cerebellum, finger tap, music imagery

INTRODUCTION

Normal aging accompanies the age-related decline in various cognitive and motor functions, especially in processing speed, episodic and working memory, and motor speed (Park et al., 2002; Seidler et al., 2010; Nyberg et al., 2012). Magnetic resonance imaging (MRI) studies have shown that the volumes of the cerebellum, hippocampus, basal ganglia, and frontal cortex decrease with normal aging (Raz et al., 2004, 2010; Ramanoël et al., 2018). In a progressively aging society, it is important to identify lifestyles that effectively mitigate age-related cognitive decline and brain atrophy. Playing musical instruments is a candidate for such a lifestyle because it is associated with a reduced risk of dementia (Verghese et al., 2003; Bugos et al., 2007; Hall et al., 2009). Cross-sectional behavioral studies have shown that older instrumental musicians have higher levels of non-verbal visual memory, naming, executive function, and auditory attention compared to non-musicians (Hanna-Pladdy and MacKay, 2011; Parbery-Clark et al., 2011; Hanna-Pladdy and Gajewski, 2012; Amer et al., 2013; White-Schwoch et al., 2013; Zendel and Alain, 2014; Strong and Mast, 2019). Such superiority of musicians may be accounted for by their vigorous musical training with complex physical and mental operations such as the translation of visually presented musical symbols into auditory-motor imagery, high speed and skillful execution of finger movement to realize melodies and musical impressions, and memorization of long musical phrases. However, little is known about the neural characteristics of older musicians, that is, how their brain structure and activity benefit from lifelong training and playing of a musical instrument.

Previous studies on musicians' brains have focused on young musicians. These studies have found larger gray matter volume (GMV) in the auditory cortex, motor cortex, cerebellum, and putamen in young musicians compared to non-musicians (Gaser and Schlaug, 2003; Vaquero et al., 2016; Acer et al., 2018). Among the various brain regions where young musicians show gray matter enlargement, the cerebellum seems to be particularly relevant to behavioral functions. For example, Hutchinson et al. (2003) reported that compared to non-musicians, young keyboard players had a larger cerebellar volume, and there was a correlation between the cerebellar volume and the daily practice intensity. Furthermore, a recent study on young musicians reported that larger GMV in the cerebellum was associated with higher performance in temporal discrimination of musical tones (Paquette et al., 2017). These findings indicate that the cerebellum is critically associated with instrumental music training and musically relevant cognitive skills. As the cerebellum has been implicated in motor control (Buhusi and Meck, 2005; Stoodley and Schmahmann, 2018), accumulating daily training of musical skills may strongly influence the cerebellum. However, investigations of musicians' brains have been limited to young participants. Do the brain regions where enlargement has been found in young musicians (the auditory cortex, motor cortex, cerebellum, and putamen) maintain the musician's superiority into old age? As aging greatly affects the cerebellum (Raz et al., 2010; Ramanoël et al., 2018), it is possible that the musicians' increase in cerebellar volume is not retained in old age.

In addition, there is a growing body of evidence regarding brain activation patterns in young musicians. These studies have reported that compared to non-musicians, musicians show increased activation in various cortical regions during passive listening to piano melodies (Bangert et al., 2001, 2006; Baumann et al., 2007). This increase in activation affected not only auditory-related areas but also motor-related areas such as the primary motor and premotor cortices and the cerebellum, suggesting a degree of audiomotor transformation when listening to music. In addition, musician-specific activation of the supramarginal gyrus (SMG) was observed during passive listening, suggesting the involvement of linguistic processing (Bangert et al., 2006; Baumann et al., 2007). Moreover, Notter et al. (2020) reported that the SMG is a core region of auditory perception. One notion from these findings is that the coupling between audiolinguistic and motor circuits is stronger in the brains of musicians (Bangert et al., 2006; Zatorre et al., 2007; Patel and Iversen, 2014), perhaps because of musical training and practice. In fact, a longitudinal study revealed that young non-musicians showed increased co-activation of the auditory and motor-related areas (supplementary motor area and premotor cortex) not only in instrumental training but also when listening to a learned melody after training (Wollman et al., 2018). Moreover, the notion that auditory-motor coupling is involved in music performance and listening emphasizes the use of music imagery in musicians (Lotze et al., 2003; Meister et al., 2004; Herholz et al., 2012). In general, the way in which music imagery is used by musicians can take several forms, such as mental practice away from the instrument (Johnson, 2011), silent reading of musical scores (Brodsky et al., 2008), and thinking of the ideal sound during the performance (Trusheim, 1991). Meister et al. (2004) revealed activations in the SMG and cerebellum in musicians both when they played a presented piano piece on the keyboard and when they imagined playing the presented piece. This evidence suggests a great overlap between the neural substrates involved in music imagery and music performance, and it contributes to music excellence in collaboration with daily music performance. In addition, the SMG has been implicated in phonological processing (Rauschecker, 2011), suggesting a role in converting auditory pitch information into note names. Given these multimodal properties in music, musical instrument training enhances co-activation of audiolinguistic and motor-related areas, so that the connected circuit is triggered by the auditory input alone. Interestingly, previous studies revealed that young musicians exhibited enhanced resting-state functional connectivity (FC) between the motor and multisensory cortices (e.g., auditory, visual, somatosensory, and multisensory integration regions) compared to non-musicians (Luo et al., 2012; Klein et al., 2016). However, little is known about the functional characteristics of older musicians.

Collectively, the brain structure and activity of instrumental musicians are reorganized through instrumental training over a long period. However, most studies have focused on young musicians, whereas the brain structure and activity of older musicians have received scant attention. Given the superiority in cerebellar volume in young musicians and brain atrophy, especially in the cerebellum and hippocampus, in normal aging, it

is important to clarify whether lifelong involvement in playing an instrument is effective in counteracting age-related brain atrophy.

The present study addresses two research questions. First, is the superiority in brain structure and increased co-activation of audiolinguistic and motor-related areas observed in young musicians maintained in older musicians? Second, if these characteristics are retained in older musicians, does this lead to the superiority of cognitive function measured by using behavioral assessments? To answer these, we investigated brain structure and activity, including FC, during a melodic working memory (MWM) task by comparing older musicians with non-musicians. Although a passive listening task is often used to assess brain activations for music imagery, this study used the MWM task to increase the attentiveness of participants to melodic stimuli. We hypothesized that musicians would have increased activation in one or more of the regions where differences between musicians and non-musicians have been found in young populations, such as the auditory and motor cortices, cerebellum, and SMG.

TABLE 1 | Demographics of musicians and non-musicians.

Total (n = 60)	Musicians (n = 30)	Non-musicians (n = 30)	P-value
Sex (male/female)	11/19	13/17	0.598
Age (years)	70.8 (4.0)	71.4 (4.6)	0.595
Education (years)	15.7 (1.6)	14.9 (2.2)	0.130
Years of cognitive activity	12.7 (19.2)	18.7 (22.6)	0.274
Years of exercise	11.3 (10.6)	7.1 (10.8)	0.142
Frequency of cognitive activity	0.9 (1.6)	1.7 (2.3)	0.116
Frequency of exercise	2.9 (2.4)	2.1 (2.3)	0.154
Frequency of work	2.5 (2.1)	1.8 (1.9)	0.173
Frequency of family care	2.3 (2.9)	2.2 (3.0)	0.923
Frequency of volunteering	0.4 (1.0)	0.4 (1.0)	0.832
MMSE (score)	29.5 (0.9)	29.6 (0.6)	0.868

Parameters are indicated as the mean (SD). P-values for age, education, cognitive activity, exercise, work, family care, volunteering, and MMSE are from t-tests for group differences. P-value for sex ratio is from Chi-square test for group differences. Frequency, days per week; MMSE, Mini-Mental State Examination; SD, standard deviation.

MATERIALS AND METHODS

Participants

The Psychological Research Ethics Committee of Kyoto University approved the protocol (29-P-7), and all study participants gave their informed consent. Seventy older adults (36 musicians and 34 non-musicians, aged 65–81 years) participated in this study. Musicians who had received musical instrument training for at least 20 years were recruited through a music conservatory, an amateur orchestra, and private or volunteer-supported music schools. Non-musicians with no or less than 3 years of musical experience were recruited from the Kyoto City Silver Human Resources Center, a theatrical club, and personal connections in the neighborhood. All participants were right-handed, had no cognitive impairment (**Table 1**; Mini-Mental State Examination [MMSE] score $\geq$ 27), no history of neurological, cardiovascular, or psychiatric illness, and no contraindication for MRI. Six musicians were excluded from the analysis because of claustrophobia during the MRI scan, the presence of a brain lesion, or the use of a tranquilizer. Four non-musicians were excluded because of physical deconditioning and hearing deterioration based on age-appropriate normal hearing threshold levels (35 decibels or less at frequencies of 500, 1,000, 2,000, and 4,000 Hz). In the final analysis, there were 30 instrumental musicians (19 women and 11 men) and 30 non-musicians (17 women and 13 men).

The musicians had commenced musical instrument training between the ages of 3 and 16 years (**Table 2**; mean = 8.6 years). They had at least 22 years of experience playing a musical instrument on a regular basis (**Table 2**; mean = 52.7 years, range 22–70 years) and had been playing a musical instrument for more than 10 years at the time the study was conducted (**Table 2**; mean = 46.4 years, range 10–70 years). All musicians were actively playing an instrument at the time of this study. The instruments included piano, violin, cello, electric guitar, mandolin, wood bass, ukulele, viola, electronic clarinet, and alto saxophone. To control for the influences of other activities, the amount of time spent performing physical exercise and cognitive activities were assessed. The types of physical exercise and cognitive activities per group is elaborated in **Supplementary Table 1**.

TABLE 2 | Musical instrument training status in musicians.

Instrumental musicians (n = 30)	Mean (SD)	Range
Age of commencement	8.6 (3.3)	3–16
Years of musical training	52.7 (14.6)	22–70
Years of continuous musical training	46.4 (20.2)	10–70
Current playing time (hours/day)	1.8 (1.7)	0.1–8.5

SD, standard deviation.

Goldsmiths Musical Sophistication Index

To assess musical skills and behaviors in both instrumental musicians and non-musicians, we used the Japanese translated version of the Goldsmiths Musical Sophistication Index (Gold-MSI) version 1.0 (Müllensiefen et al., 2014). This 39-item scale measures six musical sophistication dimensions: active engagement (e.g., *I spend a lot of my free time doing music-related activities*), perceptual abilities (e.g., *I can compare and discuss differences between two performances or versions of the same piece of music*), emotions (e.g., *Pieces of music rarely evoke emotions for me*), singing abilities (e.g., *I only need to hear a new tune once and I can sing it hours later*), musical training (e.g., *At the peak of my interest, I practiced ___ hours per day on my primary instrument*), and general sophistication (e.g., *I enjoy writing about music, for example, on blogs and forums*). Participants provided responses to each statement on a seven-point scale (1 = *not at all* to 7 = *very*). The results showed that the musicians had higher musical abilities than the non-musicians (**Table 3**).

TABLE 3 | Musical abilities according to the Gold-MSI in both groups.

Total (n = 60)	Musicians (n = 30)	Non-musicians (n = 30)	P-value
Active engagement (score)	36.9 (9.1)	20.9 (7.7)	<0.001
Perceptual abilities (score)	47.5 (7.0)	31.9 (10.2)	<0.001
Musical training (score)	34.3 (6.6)	11.6 (4.6)	<0.001
Singing ability (score)	29.2 (7.1)	16.9 (7.7)	<0.001
Emotions (score)	28.3 (5.7)	20.4 (6.2)	<0.001
General sophistication (score)	81.8 (14.7)	40.5 (15.6)	<0.001
Melody memory accuracy (%)	73.3 (13.0)	65.4 (14.9)	0.033
Memory confidence (score)	18.2 (3.1)	14.6 (3.4)	<0.001

Data are presented as the mean (SD). P-values are from t-tests on between-group differences. Gold-MSI, Goldsmiths Musical Sophistication Index; SD, standard deviation.

Moreover, we administered a memory test using melodies from the Gold-MSI.[1] The melodic memory task consisted of eight-pair trials of two short melodies (containing 10–17 notes per melody), and the second melody was always presented at a different pitch level than the first one. Participants were required to judge whether the two melodies had an identical pitch interval structure and to estimate how confident they felt about their judgment on a three-point scale (1 = *I am guessing*, 2 = *I think so*, 3 = *I am totally sure*). Melodic memory accuracy was defined as the percentage of correct answers. In addition to the identity judgment for the pair of melodies, confidence rating of the judgment was obtained on a three-point scale. The results showed that the melodic memory accuracy and confidence were higher in the musicians than in the non-musicians (**Table 3**). Overall, musicians in this study were shown to have higher levels of musical sophistication and skills. Of note, this melodic memory task in the Gold-MSI was conducted only for behavioral performance (and confidence), and not used in brain imaging, which will be described later.

Behavioral Measurements

Cognitive and motor functions were measured to compare musicians and non-musicians. The cognitive and motor tests consisted of many neuropsychological tests that are likely to detect differences between musicians and non-musicians (Jäncke et al., 1997; Bugos and Mostafa, 2011; Hanna-Pladdy and MacKay, 2011; Hanna-Pladdy and Gajewski, 2012; Amer et al., 2013; Fauvel et al., 2014; Strong and Mast, 2019). Cognitive tests consisted of the Japanese versions of the verbal (letter) fluency task (Lezak et al., 2012), logical memory-I and –II subtests of the Wechsler Memory Scale-Revised edition (WMS-R), visual reproduction-I and –II subtests of the WMS-R (Wechsler, 1997; Sugishita, 2000), and parts A and B of the trail making test (TMT) (Reitan and Wolfson, 1993). Motor tests consisted of finger-tapping and pegboard tasks.

The verbal fluency task was conducted to assess verbal functioning. Participants were given a word-initial sound "KA" and asked to generate as many words as possible in 60 s. The logical memory-I and –II subtests of the WMS-R were conducted to evaluate verbal memory. In the logical memory-I subtest, participants were asked to immediately recall two stories, one after the other. In the logical memory-II subtest, participants were asked to recall the two stories 30 min later. The visual reproduction-I and –II subtests of the WMS-R were conducted to assess non-verbal visual memory. In the visual reproduction-I subtest, participants were presented with a geometric figure on a card (A) for 10 s and asked to draw it immediately after the presentation. Another three cards (B, C, and D) were presented in the same way. In the visual reproduction-II subtest, participants were asked to draw these geometric figures on four cards 30 min later. Parts A and B of the TMT were conducted to evaluate executive function. In TMT-A, participants were asked to draw lines, sequentially connecting 25 numbers in ascending order. In TMT-B, participants were asked to draw lines alternately between numbers and letters (1, A, 2, B, etc.). The finger-tapping and pegboard tasks were conducted to evaluate functional finger dexterity. In the finger-tapping test, by using the MIDI sequencer software Domino version 1.43[2], participants were asked to tap a computer mouse with the index finger of each hand as fast as possible for 20 s. In the pegboard task, participants were asked to turn over 20 pegs (diameter 0.5 cm × height 3.5 cm) in 20 holes carved on a square board (length 15 cm × width 18 cm × thickness 2 cm; SAKAI Medical Co., Ltd., Japan) using just one hand.

Statistical Analysis of Behavioral Data

Behavioral data were compared between musicians and non-musicians using the unpaired two-sample t-test for each of the 11 measures by using IBM SPSS statistics for windows, version 25 (IBM corporation, Armonk, NY, United States).

However, multiple tests may induce type I errors, overestimating significant effects under no correction, or type II errors, underestimating significant effects under conservative correction such as that using the Bonferroni method. The resampling method (e.g., permutation) can be used to estimate adjusted P-values while avoiding parametric assumptions about the joint distribution of the test statistics (Dudoit et al., 2003). Here, we conducted a permutation test (Camargo et al., 2008) using MATLAB R2020a with a statistics and machine learning toolbox. For each behavioral measure, all 60 observed samples (30 musicians and 30 non-musicians) were randomized together and were resampled to obtain a dummy t-value. This procedure was repeated 10,000 times for each of the 11 behavioral measures. We pooled 110,000 t-values (10,000 resamplings × 11 behavioral measures) and created a unique permutation t-distribution to obtain the single adjusted α-level threshold (the top five percentile rank in the distribution).

Finally, correlation analyses (only for behavioral tests in which group differences were significant) were conducted by calculating Spearman's rank-order correlation coefficients using IBM-SPSS. For these multiple coefficients, validation tests for correlations were performed with a permutation test using MATLAB R2020a. To examine the correlation in a given pair of variables (e.g., tapping and TMT-B), a dummy coefficient

[1]https://www.gold.ac.uk/music-mind-brain/gold-msi/download/

[2]http://takabosoft.com/domino

was obtained by correlating the two variables randomly across participants. This procedure was repeated 10,000 times for each of the 11 correlations. We pooled a total of 110,000 dummy coefficients (10,000 resamplings × 11 correlations) and created a unique permutation coefficient distribution to obtain the single adjusted α-level threshold (the top five percentile ranks in the distribution). For all analyses, $P < 0.05$ was considered statistically significant.

Image Acquisition

Scanning was performed using a 3-T Siemens Magnetom Verio MR scanner (Siemens, Erlangen, Germany). The participant's head was immobilized in a scanner head coil (12 channels). Functional images were acquired with a T2-weighted echo-planar image (EPI) (repetition time, 2,000 ms; echo time, 25 ms; flip angle, 75°; acquisition matrix, 64 × 64; field of view, 224 × 224). The EPI volume was acquired in interleaved order and consisted of 39 axial slices with a slice thickness of 3.5 mm (in-plane resolution: 3.5 mm × 3.5 mm). The EPIs were acquired during the MWM task. The first five scans in each run were discarded to allow for T1 equilibration. After the MWM task, a high-resolution structural image was acquired using an axial T1-weighted magnetization-prepared rapid gradient-echo pulse sequence (field of view: 256 × 256; matrix size: 256 × 256; voxel size: 1 mm × 1 mm × 1 mm; 208 slices).

Functional Magnetic Resonance Imaging Tasks

A block-design functional magnetic resonance imaging (fMRI) experiment was conducted with three conditions (1-back: working memory for melodies, 0-back: hearing a melody, and rest). Melodic stimuli were presented with various three-tone equal-interval sequences of piano sounds through a pair of headphones. In the 0-back task, participants were instructed to respond when the melody had finished playing. In the 1-back task, participants were asked to judge whether the melody item was identical to the one immediately preceding it. Thus, there was no working memory required for the 0-back task, while the 1-back task required maintenance of melody information for a short time. During rest, participants were asked to relax and keep their attention on the central fixation point. Instruction and practice for the *n*-back tasks (0-back, 1-back, and rest tasks) for the fMRI experiment were given prior to the scanning, outside the scanner.

Each melody item appeared for 2,000 ms. A central fixation cross was presented throughout the inter-item interval for 2,000 ms. The task period contained twelve task blocks in total, comprising four blocks each for the 0-back and 1-back tasks, and four rest blocks; the blocks were alternated in one fMRI run. Each block lasted for 32 s, and each task block consisted of eight trials. All responses were indicated with either the index ("yes") or middle ("no") finger of the right hand using an MRI-compatible keypad. Participants were instructed to respond as quickly and accurately as possible.

Image Pre-processing and Statistical Analysis of Structural Data

Voxel-based morphometry (Ashburner and Friston, 2000) was performed by using the statistical parametric mapping software SPM12 (Wellcome Department of Cognitive Neurology, London) and MATLAB R2018a (The Mathworks Inc., United States). First, the structural T1-weighted images were segmented to separate the different types of tissues: gray matter, white matter, cerebrospinal fluid, soft tissue, and skull. Thereafter, the segmented images (gray matter and white matter) were spatially normalized with DARTEL, the Diffeomorphic Anatomical Registration using Exponentiated Lie algebra (Ashburner, 2007). To preserve the absolute volume of the gray matter, modulation was performed on the normalized gray matter images by multiplying the Jacobian determinants derived from the spatial normalization. Finally, the modulated gray matter images were smoothed with an 8-mm full-width at half-maximum (FWHM) Gaussian kernel.

The individual smoothed gray matter images were entered into a second-level analysis employing a random-effects analysis within the general linear model. Previous studies have shown that brain volume is related to age, sex, education, exercise, cognitive activity, and social interaction (Erickson et al., 2011; Duan et al., 2012; Mortimer et al., 2012; Cheng, 2016; Boller et al., 2017; Firth et al., 2018; Chen et al., 2019). In order to prevent the potential influence of these factors on brain volume, the two-sample *t*-test was conducted after controlling for the effects of sex, age, educational level, and the levels of cognitive activity, exercise, work, family care, and volunteering (**Table 1**), as previously reported (Ramanoël et al., 2018; Wu et al., 2021). In addition, the total volume of gray matter was included as a nuisance variable to correct for global differences in gray matter, as previously reported (Vaquero et al., 2016). Moreover, an explicit mask was used to exclude noisy voxels in the statistical analysis. The statistical thresholds were set at $P < 0.001$, uncorrected for multiple comparisons at the voxel levels, and $P < 0.05$ family wise error (FWE) corrected for multiple comparisons at the cluster level. Thereafter, we identified the cluster location obtained from structural data using the anatomy toolbox in SPM12 (Eickhoff et al., 2005).

In addition, we investigated associations between age and GMV in regions of interests (ROIs). Based on the difference for structural results between groups, we extracted the ROIs of a cluster using the MarsBaR software (Brett et al., 2002). Correlation analyses were conducted using Spearman's rank-order correlation coefficients. For these multiple coefficients, validation tests for correlation were performed using the same permutation method as described for the behavioral analyses. For correlation analyses, $P < 0.05$ was considered statistically significant.

Image Pre-processing and Statistical Analysis of Task-Related Functional Connectivity

CONN toolbox version 18b (Whitfield-Gabrieli and Nieto-Castanon, 2012) was used to analyze task-related FC during

the MWM tasks (1-back and 0-back). By using default pre-processing, the possible confounding effects of head motion artifacts, as well as cerebrospinal fluid and blood oxygen level-dependent (BOLD) signals, were defined and addressed. For denoising, signals from the white matter, cerebrospinal fluid, and motion parameters were regressed from the functional data. Data were bandpass-filtered (0.008–0.09 Hz), as previously reported (Wollman et al., 2018).

The FC analysis was conducted by using seed-to-voxel analysis. Thereafter, the seeds were set, and the ROIs were obtained from the results of the structural analysis, as previously reported (Wang et al., 2018). For the seed-to-voxel analysis, individual correlation maps were generated throughout the brain by extracting the mean task BOLD time course of each seed and calculating their correlation coefficients with the BOLD time course of each voxel. The correlation was obtained by applying the general linear model and bivariate correlation analysis weighted for the hemodynamic response function. This analysis was conducted directly in the CONN toolbox using the Fisher-transformed connectivity value. In addition to this first-level analysis for each participant, a second-level analysis was conducted for the differences in connectivity between musicians and non-musicians by using the two-sample *t*-test after controlling for the effects of sex, age, educational level, and the levels of cognitive activity, exercise, work, family care and volunteering (**Table 1**). The statistical thresholds were set at $P < 0.001$ uncorrected for multiple comparisons at the voxel levels, and $P < 0.05$ FWE corrected for multiple comparisons at the cluster level. Finally, correlation analyses were conducted between the FC value and behavioral measures using IBM-SPSS after controlling for the effects of age, educational level, and the levels of cognitive activity and exercise. For these multiple correlation coefficients, validation tests for correlation were performed by using the same permutation method as described for the behavioral analyses. For correlation analyses, $P < 0.05$ was considered statistically significant.

Image Pre-processing and Statistical Analysis of Functional Data

The fMRI data pre-processing was carried out using SPM12 and MATLAB R2018a. First, the origin of the EPI was manually set to the anterior–posterior commissure for each participant. The fMRI data were spatially realigned to the first volume of the series and subsequently to the across-run mean volume, after which they were co-registered with the anatomical data. The anatomical data were normalized to the Montreal Neurological Institute (MNI) space using a unified segmentation procedure. Afterward, the resulting deformation parameters were applied to the fMRI data that were resampled into 3 mm × 3 mm × 3 mm voxels and smoothed with an 8-mm FWHM Gaussian kernel.

Activated voxels during MWM activation were identified using a statistical model containing a boxcar function convolved with a canonical hemodynamic response function. A high-pass filter (1/128 Hz) was used to remove low-frequency noise, and an autoregressive (AR (1)) model was employed to correct temporal autocorrelations. The data were analyzed using the two-way ANOVA with groups (musicians and non-musicians) and tasks (0-back, 1-back, and rest tasks) after controlling for the effects of sex, age, educational level, and the levels of cognitive activity, exercise, work, family care and volunteering (**Table 1**), as previously reported (Huang et al., 2020). The statistical thresholds were set at $P < 0.001$ uncorrected for multiple comparisons at the voxel level, and $P < 0.05$ FWE corrected for multiple comparisons at the cluster level. Afterward, we identified the cluster location as described for the structural data analysis.

In addition, we investigated associations between musical traits and task-related parameter estimates of BOLD values in ROIs. Based on the differences between groups for functional results, we extracted the ROIs of a cluster using the MarsBaR software. Significance in Spearman's rank-order correlation coefficients was assumed at $P < 0.05$ in IBM-SPSS. For these multiple correlation coefficients, validation tests for correlation were performed using the same permutation method as described for the behavioral analyses.

RESULTS

Demographics

Demographic data are shown in **Table 1**. There were no significant group differences in age (musicians: 70.8 ± 4.0 years; non-musicians: 71.4 ± 4.6 years), years of education (musicians: 15.7 ± 1.6; non-musicians: 14.9 ± 2.2), MMSE (musicians: 29.5 ± 0.9; non-musicians: 29.6 ± 0.6), sex ratio, or time spent on cognitive activity, exercise, work, family care, and volunteering. These results indicate that the two groups did not significantly differ demographically.

Behavioral Scores

Behavioral data are shown in **Figure 1** and **Table 4** as the mean ± standard deviation (*SD*). Student's *t*-test showed significant differences between groups in right tapping (**Figure 1A**: $t_{(58)} = 4.11$, $P < 0.001$, $d = 1.06$), left tapping (**Figure 1B**: $t_{(58)} = 4.46$, $P < 0.001$, $d = 1.15$), and verbal fluency (**Table 4**: $t_{(58)} = 2.14$, $P = 0.036$, $d = 0.55$). For TMT-B, Welch's *t*-test was used due to heteroscedasticity, and the results showed a significant difference between the groups (**Table 4**: $t_{(44.94)} = 2.33$, $P = 0.024$, $d = 0.60$). These *t*-values were higher than the adjusted significance level threshold $t_{(58)} = 1.99$ obtained in the permutation test. In contrast, there were no significant between-group differences in the logical memory-I and –II subtests, visual reproduction-I and –II subtests, TMT-A, and pegboard task (**Table 4**). These results indicate that musicians had higher levels of verbal functioning, executive control, and tapping speed compared to non-musicians.

In subsequent correlation analyses, tapping scores were negatively correlated with time to perform the TMT-B in musicians (right: $\rho = -0.59$, $P < 0.001$; left: $\rho = -0.49$, $P = 0.006$; **Figure 2**). These Spearman's ρ-values were higher in absolute value than the adjusted significance level threshold $|\rho| = 0.36$ obtained in the permutation test. By contrast, non-musicians did not show such a correlation (right: $\rho = -0.32$, $P = 0.082$; left:

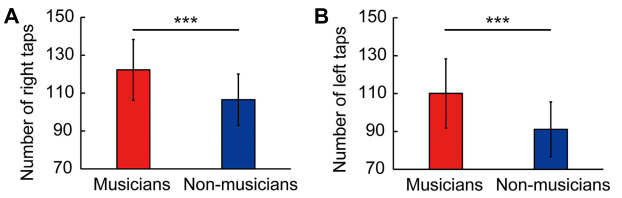

FIGURE 1 | Skillful tapping in musicians. Compared to non-musicians, musicians showed enhanced performances in right tapping speed **(A)** and left tapping speed **(B)**. Parameters are indicated as the mean (*SD*). ***$P < 0.001$ vs. non-musicians. *SD*, standard deviation.

TABLE 4 | Behavioral results in both groups.

Total ($n = 60$)	Musicians ($n = 30$)	Non-musicians ($n = 30$)	*P*-value
Verbal fluency (words)	14.1 (4.0)	12.1 (3.5)	0.036
TMT-A (second)	32.6 (10.5)	38.3 (12.2)	0.059
TMT-B (second)	70.1 (17.9)	85.9 (32.7)	0.024
Logical memory-I (score)	23.9 (6.7)	25.7 (7.4)	0.339
Logical memory-II (score)	20.9 (7.7)	21.4 (8.6)	0.789
Visual reproduction-I (score)	35.2 (5.0)	35.6 (5.6)	0.771
Visual reproduction-II (score)	34.4 (6.1)	32.1 (8.7)	0.235
Right pegboard (second)	37.1 (10.5)	39.1 (6.3)	0.375
Left pegboard (second)	39.9 (9.3)	42.0 (7.1)	0.331

Data are presented as the mean (SD). P-values are from t-tests on group differences. TMT, trail making test; Logical memory-I, immediate recall; Logical memory-II, delayed recall; Visual reproduction-I, immediate recall; Visual reproduction-II, delayed recall; SD, standard deviation.

$\rho = -0.16$, $P = 0.399$; **Figure 2**). These results indicate that for the musicians, higher tapping speeds were linked to more rapid executive control.

Musical Instrument Experience-Related Structural Changes

Whole-brain voxel-based gray matter analyses in both groups showed significantly larger GMVs in crus I of the left and right cerebellum of musicians compared to those of non-musicians (**Figures 3A,B**, and **Supplementary Table 2**). Subsequently, we investigated associations between the GMV of ROIs in bilateral crus I of both sides of the cerebellum and age (**Figures 3C,D**). In non-musicians, the GMVs of crus I of both sides of the cerebellum were negatively correlated with age (left: $\rho = -0.50$, $P = 0.005$; right: $\rho = -0.66$, $P < 0.001$), indicating that in non-musicians, these bilateral regions of the cerebellum are more subject to age-dependent atrophy. These Spearman's ρ-values were higher in absolute value than the adjusted significance level threshold $|\rho| = 0.36$ obtained in the permutation test. By contrast, such correlations with age were not significant in musicians (left: $\rho = -0.27$, $P = 0.147$; right: $\rho = -0.35$, $P = 0.058$). These results show that crus I of both sides of the cerebellum exhibited differential age-related GMV changes between musicians and non-musicians.

Task-Related Functional Connectivity

Structural analyses revealed larger GMVs in both sides of the cerebellum in musicians compared to non-musicians. Therefore, we used ROIs in both sides of the cerebellum as the seed for the FC analyses of the task-related fMRI data. The group differences in FC are shown in **Figure 4A** and listed in **Supplementary Table 3**. Compared to non-musicians, musicians had enhanced FC between the left cerebellum and the right hippocampus. In addition, we investigated the correlation between cerebellar-hippocampal FC and behavioral functions (**Figure 4B**). The task-related cerebellar-hippocampal FC and left tapping speed were significantly correlated in musicians ($\rho = 0.42$, $P = 0.039$). This Spearman's ρ was higher in absolute value than the adjusted significance level threshold $|\rho| = 0.36$ obtained in the permutation test. By contrast, non-musicians did not show such a correlation ($\rho = -0.23$, $P = 0.284$). These results indicate that in musicians, enhancement of the cerebellar-hippocampal FC in MWM processing is linked to a higher tapping speed.

Task-Related Activation

Contrast images for 1-back vs. rest were computed to assess the brain activity during the MWM task in both groups. Non-musicians had increased activation in limited brain regions, whereas musicians had increased activation in extensive brain regions (**Figures 5A,B**). In terms of behavioral performance during the MWM task, there were no significant between-group differences in 1-back task performance (**Figure 5C**). The other between-group differences are shown in **Figure 6A** and

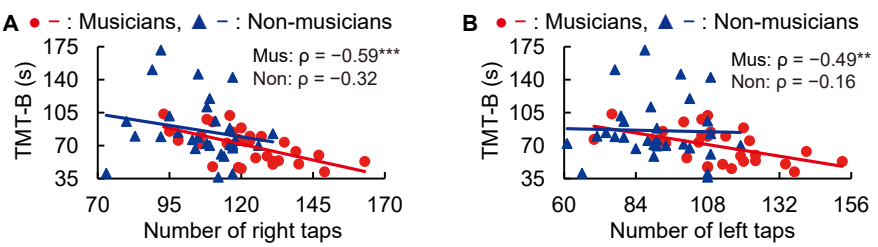

FIGURE 2 | Correlation between tapping and TMT-B. In musicians, the numbers of right **(A)** and left **(B)** tapping (in 20 s) were negatively correlated with the time to complete the TMT-B. By contrast, these correlations with tapping were not statistically significant in non-musicians. **$P < 0.01$, ***$P < 0.001$, Mus, musicians; Non, non-musicians; TMT, trail making test.

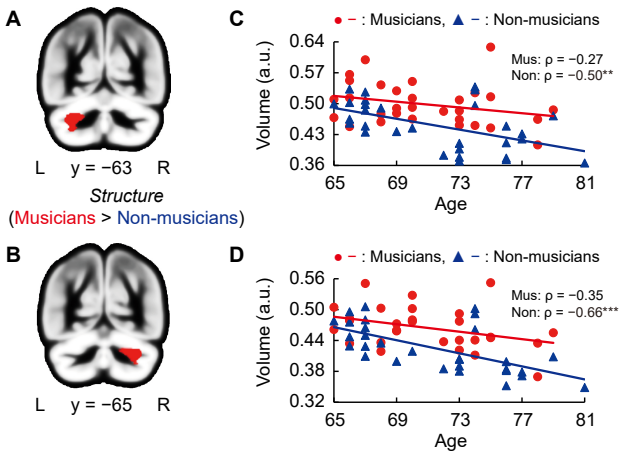

FIGURE 3 | Structural changes related to musical instrument experience. **(A,B)** Musicians had larger GMVs in both sides of the cerebellum compared to non-musicians. **(C,D)** For the cerebellar ROIs in both hemispheres, the non-musicians displayed negative correlations between their GMV and age. In musicians, such correlations (age-related volume reductions) were not significant. $^{**}P < 0.01$, $^{***}P < 0.001$, Mus, musicians; Non, non-musicians; GMV, gray matter volume; ROI, region of interest; L, left; R, right; a.u., arbitrary units.

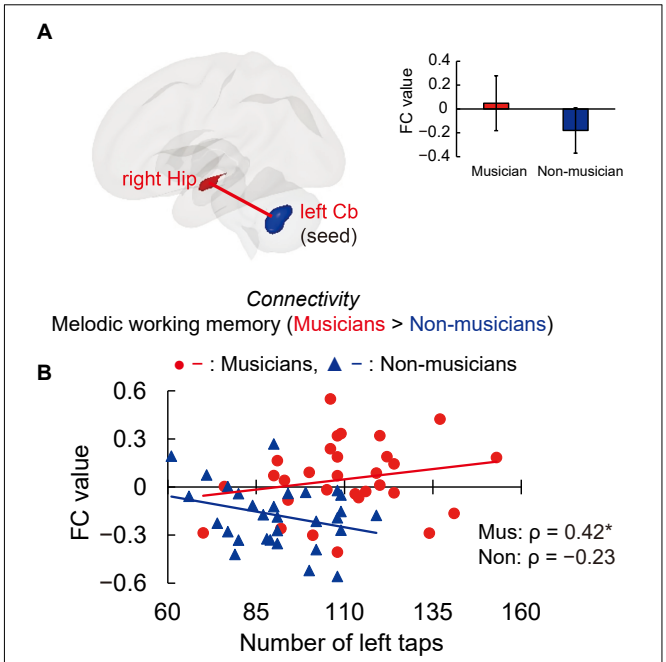

FIGURE 4 | Task-related FC. **(A)** Using ROIs in both sides of the cerebellum as the seed (where musicians showed greater GMV than non-musicians, as illustrated in **Figure 3**), musicians exhibited enhanced FC between the left cerebellum and right hippocampus during the MWM task compared to non-musicians, but no change in FC of the right cerebellum and other regions. **(B)** In the associations between cerebellar-hippocampal FC and behavioral functions, task-related cerebellar-hippocampal FC and left tapping speed were positively correlated in musicians. $^{*}P < 0.05$, Mus, musicians; Non, non-musicians; FC, functional connectivity; ROI, region of interest; GMV, gray matter volume; MWM, melodic working memory; Hip, hippocampus; Cb, cerebellum.

listed in **Supplementary Table 4**. Musicians showed greater activation within the left SMG than non-musicians. However, contrast images for 0-back vs. rest and 1-back vs. 0-back did not show a significant difference between groups. Subsequently, we extracted parameter estimates in the ROI of the left SMG in musicians and investigated the associations between its activation and musical traits (**Figure 6B**). No correlation was found between SMG activation and scores of behavioral performances. One trait, i.e., the age at the commencement of musical training, was negatively correlated with SMG activation ($\rho = -0.41$, $P = 0.026$). This Spearman's ρ was higher in absolute value than the adjusted significance level threshold $|\rho| = 0.36$ obtained in the permutation test. The activation during the MWM task was higher for the musicians with earlier training commencement, indicating an influence of childhood instrumental training.

DISCUSSION

The present work aimed to investigate the association between lifelong instrumental training and age-related cognitive decline and brain atrophy. The main findings revealed that compared to non-musicians, musicians (i) showed enhanced performance in several constructs such as tapping speed (**Figure 1**), verbal fluency, and executive control (**Table 4**); (ii) had larger GMVs in both sides of the cerebellum (**Figure 3**); (iii) exhibited higher task-related FC between the left cerebellum and right hippocampus, with FC being correlated with tapping speed (**Figure 4**); and (iv) exhibited increased activation of the left SMG during the MWM task, with its greater activation being associated with earlier commencement of musical training (**Figure 6**).

The Effect of Lifelong Musical Training: From Skillful Tapping to Cognition

The behavioral results revealed that musicians had higher verbal fluency, TMT-B, and finger-tapping performances compared to non-musicians. Previous studies have reported that young musicians have higher levels of tapping speed (Jäncke et al., 1997), finger tap-related rhythm synchronization (Karpati et al., 2016), and executive function (Bugos and Mostafa, 2011) than young non-musicians. Further studies indicated older musicians' superiority in letter fluency and executive function in cognitive aging (Hanna-Pladdy and MacKay, 2011; Hanna-Pladdy and Gajewski, 2012; Amer et al., 2013; Fauvel et al., 2014; Strong and Mast, 2019; Chan and Alain, 2020), which our results support. Moreover, we provided a correlation between tapping speed of simple finger movement and executive function measured by using the TMT-B in older musicians, in line with a previous study that displayed simple finger taps and executive control association for non-musicians (Mak et al., 2016). In contrast, some studies have reported that complex finger taps in non-musicians had a high load in executive

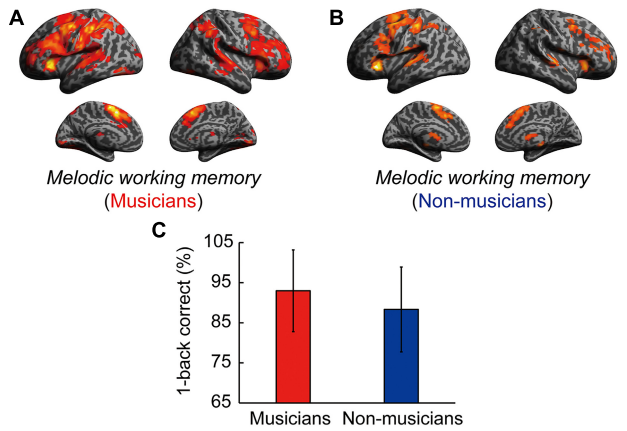

FIGURE 5 | Task-related brain activity in each group. **(A)** Musicians have increased activation of extensive brain regions. **(B)** Non-musicians have increased activation of limited brain regions. **(C)** There were no significant between-group differences in 1-back task performance. For significant between-group differences, see **Supplementary Table 4**, **Figure 6**, and the main text.

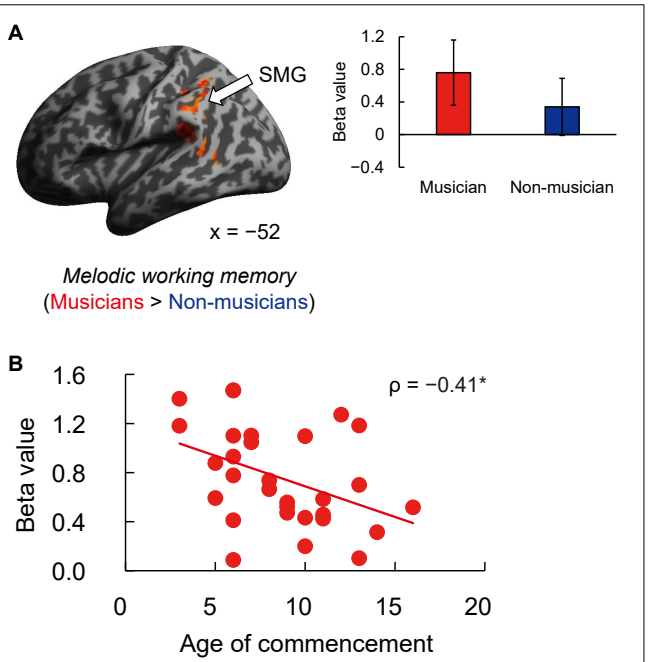

FIGURE 6 | Task-related brain activity. **(A)** Musicians exhibited increased activation of the left SMG during the MWM task (1-back vs. rest), whereas no change was seen in auditory and motor regions. **(B)** Using ROIs in the left SMG, age at commencement of musical training was negatively correlated with task-related SMG activation in musicians. *$P < 0.05$, SMG, supramarginal gyrus; MWM, melodic working memory; ROI, region of interest.

function compared to simple finger taps (Harding et al., 2017; Holm et al., 2017). Because these studies showed within-non-musicians differences in levels of load of executive function for different complexity of tapping, the relationship between the previous findings and our between-groups difference cannot be clearly interpreted. Since musical performance requires motor planning and monitoring of finger movement (Palmer and Drake, 1997; Moreno et al., 2011; Shen et al., 2019; Colombo et al., 2020; Guo et al., 2021), we suggest that musicians perform finger taps with higher executive involvement compared to non-musicians even when they are simple ones. The higher levels of executive function in musicians can be maintained by the same processes to enable masterful temporal and ordinal precision of finger movements, together with fine-grained finger force control. Although aging degrades processing speed and working memory associated with executive function (Park et al., 2002; Nyberg et al., 2012), the preservation of skillful tapping abilities through instrumental training may mitigate such declines in older adults.

In addition, the musicians in our study displayed behavioral superiority in verbal (letter) fluency, in line with previous studies that addressed music and language associations (Anvari et al., 2002; Patel and Iversen, 2007; Wong et al., 2007; Kraus and Chandrasekaran, 2010). Letter fluency has been shown to involve phonological processing (Heim et al., 2008; Shao et al., 2014). Patel and Iversen (2007) reported that musical training strengthens the processing of auditory features common to music and language. Based on these associations, musicians' superior verbal fluency in our study may be explained by the common phonological features in music-making and language production (Patel and Iversen, 2007; Wong et al., 2007). As learning about the acoustic structure of musical pieces involves phonological processing, music-making may facilitate the higher performance of letter fluency in musicians compared to non-musicians. Another study emphasized that music training involves a high working memory load, maintenance of selective attention skills, and learning of the acoustic rules that bind musical sounds together (Kraus and Chandrasekaran, 2010). These cognitive skills are also crucial for speech production (Strait et al., 2011); such an overlap may partly explain this intriguing positive transfer effect from music to language.

Older Musicians' Cerebellar Maintenance

Whole-brain voxel-based GMV analyses revealed significantly larger bilateral GMVs in crus I of the cerebellum in musicians compared to non-musicians. Moreover, we found that the two groups showed different age-related volume changes in cerebellar ROIs; whereas non-musicians' cerebellar GMVs in the ROIs sharply decreased with age, musicians did not show a significant correlation between volume and age. These findings indicate that musical instrument training possibly induces neural structural advantages in two key ways. First, consistent with previous findings of a larger cerebellar GMVs in young musicians compared to non-musicians (Gaser and Schlaug, 2003; Acer et al., 2018), we demonstrated the superiority of older musicians compared to age-matched non-musicians. Second, the cerebellar volume is known to decrease with age (Raz et al., 2010; Ramanoël et al., 2018), and it is important to verify whether lifelong engagement in playing a musical instrument suppresses this reduction. We found that musicians may maintain their

cerebellar volume into old age, whereas the cerebellum of a non-musician is relatively vulnerable to age-related atrophy. These results suggest that the lifelong practice of a musical instrument is associated with structural maintenance of cerebellum in old age.

The cerebellum is known to be involved in some cognitive control processes and play an important role in fine motor activity (Buhusi and Meck, 2005; Hautzel et al., 2009; Stoodley and Schmahmann, 2018). In addition, several studies have proposed that there is a functional topographic organization in the cerebellum such that sensorimotor function is represented predominantly in the anterior lobe (lobules I–V), cognitive processing is associated with posterior lobules VI and VII (including crus I, II, and VIIB), and the cerebellar vermis and fastigial nuclei constitute the limbic cerebellum (Schmahmann, 2004, 2019; Stoodley and Schmahmann, 2009). The cluster of cerebellar GMV that showed between-group differences in our study was located in crus I according to the coordinate system of Eickhoff et al. (2005). Some studies have reported that reduction in GMV of crus I is associated with executive dysfunction (Olivito et al., 2018; Tse et al., 2020), suggesting that such structural changes play an important role in the maintenance of motor planning and monitoring (D'Agata et al., 2011; Stoodley, 2012; Stoodley and Schmahmann, 2018), which are needed for skillful execution of finger movement during music-making. This region also corresponds to an area of musically relevant temporal discrimination in the cerebellum (Baer et al., 2015; Paquette et al., 2017). For efficient predictive adaptation of behavior, the cerebellum is thought to play key roles in the precise encoding of perceived temporal structures (Schwartze and Kotz, 2013). Several studies have pointed out that the cerebellum is involved in optimizing sensory input from the auditory system when stimulated by music (Gao et al., 1996; Penhune et al., 1998). These aspects of musical training could contribute to the structural superiority in crus I of the cerebellum in old age. In particular, crus I enlargement may help to coordinate auditory and motor systems in musicians.

Interestingly, although increased GMVs of the auditory and motor cortices has been reported in young professional musicians (Gaser and Schlaug, 2003; Groussard et al., 2010; Vaquero et al., 2016; Acer et al., 2018), the present study did not find such between-group differences in these regions in older participants. This inconsistency may be explained by differences in the expertise level of musicians (e.g., professional vs. amateur). Of note, our results, based on an uncorrected threshold ($P < 0.001$), showed that older musicians had a larger GMV in the right hippocampus compared to non-musicians (**Supplementary Figure 1A** and **Supplementary Table 5**). Moreover, the hippocampal GMV in the ROIs decreased with age in older participants, including both musicians and non-musicians (**Supplementary Figure 1B**). Although the uncorrected results should be interpreted with caution, these results suggest the possibility that musical instrument training suppresses the reduction in hippocampal volume. Such suppression may be explained by the role of the hippocampus in temporal processing and consonance/dissonance detection (Wieser and Mazzola, 1986; James et al., 2008; Groussard et al., 2010). The regular and sustained practice of musical instruments may affect the cerebellum and hippocampus in old age more strongly than the auditory and motor cortices, presumably because their function in temporal processing is essential for playing an instrument.

Activation of the Cerebellar-Hippocampal Network and Supramarginal Gyrus in Musicians

We found that musicians had enhanced FC between the left cerebellum and right hippocampus in the MWM task compared to non-musicians. Moreover, higher cerebellar-hippocampal FC was associated with greater left tapping speed in musicians, indicating a musician-specific link between processes controlling finger movements and cerebellar-hippocampal FC during the MWM task. This result suggests that musicians try to maintain their MWM by associating a melody with imaginary finger movements.

A few fMRI studies have reported that activation of the cerebellum was observed in imagery tasks involving specific timing and sequential finger coordination, such as imagery of playing the piano and a finger-tapping task (Hanakawa et al., 2003; Meister et al., 2004), suggesting a role of the cerebellum in the imagery of music-related finger movements. Anatomically, the fiber bundles of the posterior cerebellum (e.g., crus I) project to the hippocampus where they play a role in motor control and cognitive function (Arrigo et al., 2014; Bohne et al., 2019). The heightened cerebellar-hippocampal FC and its association with tapping speed in musicians in our study suggest that during MWM tasks, musicians may encode melodies to sequences of finger movements for memory maintenance. Alternatively, the heightened cerebellar-hippocampal FC may be related to music imagery. Alonso et al. (2016) reported that non-musicians had increased activation in the left cerebellum and right hippocampus in a music imagery task in which participants were instructed to bind lyrics and melodies together to encode a song. This finding supports the involvement of the cerebellar-hippocampal FC in music imagery. Thus, it is natural to anticipate that such a music imagery-related network would be strengthened in musicians through musical instrument training.

Another feature of musicians' fMRI data was increased activation of the left SMG in the MWM task compared to non-musicians. Moreover, in musicians, greater activation of the left SMG was associated with earlier commencement of instrumental training. That is, learning a musical instrument from childhood is closely linked to increased activation of the left SMG in MWM processes.

In fMRI studies of music imagery and performance (using fingers), activation of the SMG and cerebellum has been observed in musicians during both imagery and performance conditions (Lotze et al., 2003; Meister et al., 2004; Herholz et al., 2012), indicating that music imagery shares the same neural substrates in these regions with executed music performance. The increased SMG activation in our musicians suggests that musicians evoked music imagery during the MWM task. The SMG has also been implicated in auditory perception (Rauschecker, 2011; Notter

et al., 2020), such as phonological processing. A previous study reported that in young developing children aged 5–6 years, specialization of the left SMG in phonological processing is already evident (Weiss et al., 2018). In addition, several studies have shown that activation of the left SMG is associated with the phonological short-term memory task (Paulesu et al., 1993; Gaab et al., 2003, 2006; Lerub et al., 2021), suggesting that the left SMG is the primary location of the phonological store. Furthermore, SMG activation was observed during both linguistic auditory imagery and listening to novel piano melodies (Hickok et al., 2003; Tsai et al., 2018). In our study, we think that musicians may have encoded auditory pitch information into linguistic labels, such as note names ("C," "D," and "E") during the MWM task for working memory maintenance, more so than non-musicians. This interpretation is also consistent with the correlation between SMG activation and earlier commencement of instrumental training.

Although increased activation of the auditory and motor cortices during melody-listening has been reported in young musicians (Bangert et al., 2001, 2006; Baumann et al., 2007), we did not find such between-group differences in these regions during the MWM task in the older participants of the present study. One possible reason is the difference in stimuli: stimuli in our MWM task were not long phrases from existing musical pieces as in previous studies, but short sequences of three tones in a uniform rhythm, which may have evoked less musical processing. Another possibility is the difference in tasks: the previous studies used a passive listening task, but we used a working memory task.

Taken together, cerebellar-hippocampal FC and the SMG seem to play a role in encoding the melodies to motor (finger movements) and phonetic (note names) information, respectively. This notion indicates musicians' advantages or heightened coupling in brain regions associated with music performance and imagery.

Our study has some limitations. First, our study was cross-sectional; thus, the superiority of musicians observed in several aspects cannot be attributed to musical instrument training in a causal manner. However, our careful control of various confounding factors together with observed correlations between musical traits and cognitive or neural characteristics increase the likelihood that the results support the hypothesis that lifelong musical training is useful in maintaining cognitive function in old age. Second, the musicians in our study started their musical training in relatively early periods, by the age of 16 years at the latest. Therefore, the superiority of brain functions in older individuals who started their musical instrument training beyond the age of 16 remains unknown. Third, the present study was unable to recruit a sufficient number of musicians for each instrument to investigate the effects of musical instrument type on the brain and cognitive functions. Therefore, it is unclear how the musical instrument type influenced the results in this study. However, the participation of a heterogenous group of musicians in our study may improve the generalizability of our results relative to those of previous studies (Gaser and Schlaug, 2003; Hutchinson et al., 2003; Bangert et al., 2006; Acer et al., 2018). Furthermore, as a musicians age, they may display training-related mitigation of subcortical atrophy in additional regions such as the hippocampus. To investigate this hypothesis, longitudinal studies of the brain structure of older musicians are needed.

CONCLUSION

For the first time, we found neural advantages in older musicians compared to age-matched non-musicians. The musicians showed lower levels of age-related cognitive decline and brain atrophy in the cerebellum. Behaviorally, cerebellum-related skillful tapping was associated with the maintenance of executive function in musicians. Moreover, fMRI results during the MWM task indicated musician-specific heightened cerebellar-hippocampal FC and SMG activation, suggesting that musicians may encode melodies into motor and phonetic information for memory maintenance. The present results demonstrate that lifelong active engagement in musical instrument training is related to structural and functional advantages in the neural system involving the cerebellum. The main findings of the present study shed new light on how lifelong musical instrument training potentially influences brain maintenance in old age.

DATA AVAILABILITY STATEMENT

The raw data supporting the conclusions of this article will be made available by the authors, without undue reservation.

ETHICS STATEMENT

The studies involving human participants were reviewed and approved by the Psychological Research Ethics Committee of Kyoto University, (protocol 29-P-7). The patients/participants provided their written informed consent to participate in this study.

AUTHOR CONTRIBUTIONS

KS and CO designed the research. MY, CO, and XG performed the research. MY analyzed the data. MY and KS wrote the manuscript. All authors contributed to the experimental materials and tools, and revised the manuscript.

FUNDING

This work was supported by the Japan Society for the Promotion of Science through Grants-in-Aid for Scientific Research (KAKENHI) grant numbers 16H06325 and 21H04422 to KS.

ACKNOWLEDGMENTS

We are grateful to Chieko Sadakata and Kuniko Harimoto for recruiting the instrumental musicians. We thank Takahiro Soshi,

Ryusuke Nakai, and Ryuhei Ueda for supporting us in the MRI analyses. We also thank Aiko Murai and Maki Terao for supporting us in the MRI scans. This study was conducted using the MRI scanner and related facilities of the Kokoro Research Center, Kyoto University.

SUPPLEMENTARY MATERIAL

The Supplementary Material for this article can be found online at: https://www.frontiersin.org/articles/10.3389/fnhum.2021.784026/full#supplementary-material

REFERENCES

Acer, N., Bastepe-Gray, S., Sagiroglu, A., Gumus, K. Z., Degirmencioglu, L., Zararsiz, G., et al. (2018). Diffusion tensor and volumetric magnetic resonance imaging findings in the brains of professional musicians. *J. Chem. Neuroanat.* 88, 33–40. doi: 10.1016/j.jchemneu.2017.11.003

Alonso, I., Davachi, L., Valabregue, R., Lambrecq, V., Dupont, S., and Samson, S. (2016). Neural correlates of binding lyrics and melodies for the encoding of new songs. *Neuroimage* 127, 333–345. doi: 10.1016/j.neuroimage.2015.12.018

Amer, T., Kalender, B., Hasher, L., Trehub, S. E., and Wong, Y. (2013). Do older professional musicians have cognitive advantages? *PLoS One* 8:e71630. doi: 10.1371/journal.pone.0071630

Anvari, S. H., Trainor, L. J., Woodside, J., and Levy, B. A. (2002). Relations among musical skills, phonological processing, and early reading ability in preschool children. *J. Exp. Child Psychol.* 83, 111–130. doi: 10.1016/s0022-0965(02)00124-8

Arrigo, A., Mormina, E., Anastasi, G. P., Gaeta, M., Calamuneri, A., Quartarone, A., et al. (2014). Constrained spherical deconvolution analysis of the limbic network in human, with emphasis on a direct cerebello-limbic pathway. *Front. Hum. Neurosci.* 8:987. doi: 10.3389/fnhum.2014.00987

Ashburner, J. (2007). A fast diffeomorphic image registration algorithm. *Neuroimage* 38, 95–113. doi: 10.1016/j.neuroimage.2007.07.007

Ashburner, J., and Friston, K. J. (2000). Voxel-based morphometry–the methods. *Neuroimage* 11, 805–821. doi: 10.1006/nimg.2000.0582

Baer, L. H., Park, M. T., Bailey, J. A., Chakravarty, M. M., Li, K. Z., and Penhune, V. B. (2015). Regional cerebellar volumes are related to early musical training and finger tapping performance. *Neuroimage* 109, 130–139. doi: 10.1016/j.neuroimage.2014.12.076

Bangert, M., Haeusler, U., and Altenmüller, E. (2001). On practice: how the brain connects piano keys and piano sounds. *Ann. N.Y. Acad. Sci.* 930, 425–428. doi: 10.1111/j.1749-6632.2001.tb05760.x

Bangert, M., Peschel, T., Schlaug, G., Rotte, M., Drescher, D., Hinrichs, H., et al. (2006). Shared network for auditory and motor processing in professional pianists: evidence from fMRI conjunction. *Neuroimage* 30, 917–926. doi: 10.1016/j.neuroimage.2005.10.044

Baumann, S., Koeneke, S., Schmidt, C. F., Meyer, M., Lutz, K., and Jancke, L. (2007). A network for audio-motor coordination in skilled pianists and non-musicians. *Brain Res.* 1161, 65–78. doi: 10.1016/j.brainres.2007.05.045

Bohne, P., Schwarz, M. K., Herlitze, S., and Mark, M. D. (2019). A new projection from the deep cerebellar nuclei to the hippocampus via the ventrolateral and laterodorsal thalamus in mice. *Front. Neural. Circuits* 13:51. doi: 10.3389/fncir.2019.00051

Boller, B., Mellah, S., Ducharme-Laiberte, G., and Bellevillé, S. (2017). Relationships between years of education, regional grey matter volumes, and working memory-related brain activity in healthy older adults. *Brain Imaging Behav.* 11, 304–317. doi: 10.1007/s11682-016-9621-7

Brett, M., Anton, J.-L., Valabregue, R., and Poline, J.-B. (2002). "Region of Interest Analysis Using an SPM Toolbox," in *[Abstract] Presented at the 8th International Conference on Functional Mapping of the Human Brain, June 2-6, 2002, Sendai, Japan. Retrieved from CD-ROM in Neuroimage 16*, (Sendai).

Brodsky, W., Kessler, Y., Rubinstein, B. S., Ginsborg, J., and Henik, A. (2008). The mental representation of music notation: notational audiation. *J. Exp. Psychol. Hum. Percept. Perform.* 34, 427–445. doi: 10.1037/0096-1523.34.2.427

Bugos, J., and Mostafa, W. (2011). Musical training enhances information processing speed. *Bull. Council. Res. Music Edu.* 187, 7–18. doi: 10.2307/41162320

Bugos, J. A., Perlstein, W. M., McCrae, C. S., Brophy, T. S., and Bedenbaugh, P. H. (2007). Individualized piano instruction enhances executive functioning and working memory in older adults. *Aging Ment. Health* 11, 464–471. doi: 10.1080/13607860601086504

Buhusi, C. V., and Meck, W. H. (2005). What makes us tick? Functional and neural mechanisms of interval timing. *Nat. Rev. Neurosci.* 6, 755–765. doi: 10.1038/nrn1764

Camargo, A., Azuaje, F., Wang, H., and Zheng, H. (2008). Permutation – based statistical tests for multiple hypotheses. *Source Code Biol. Med.* 3:15. doi: 10.1186/1751-0473-3-15

Chan, T. M. V., and Alain, C. (2020). "Theories of cognitive aging: a look at potential benefits of music training on the aging brain," in *Music and the Aging Brain*, eds L. L. Cuddy, S. Belleville, and A. Moussard (Cambridge, MA: Academic Press), 195–220.

Chen, Y., Lv, C., Li, X., Zhang, J., Chen, K., Liu, Z., et al. (2019). The positive impacts of early-life education on cognition, leisure activity, and brain structure in healthy aging. *Aging (Albany NY).* 11, 4923–4942. doi: 10.18632/aging.102088

Cheng, S. T. (2016). Cognitive reserve and the prevention of dementia: the role of physical and cognitive activity. *Curr. Psychiatry Rep.* 18:85. doi: 10.1007/s11920-016-0721-2

Colombo, P. J., Habibi, A., and Alain, C. (2020). Editorial: music training, neural plasticity, and executive function. *Front. Integr. Neurosci.* 14:41. doi: 10.3389/fnint.2020.00041

D'Agata, F., Caroppo, P., Boghi, A., Coriasco, M., Caglio, M., Baudino, B., et al. (2011). Linking coordinative and executive dysfunctions to atrophy in spinocerebellar ataxia 2 patients. *Brain Struct. Funct.* 216, 275–288. doi: 10.1007/s00429-011-0310-4

Duan, X., Liao, W., Liang, D., Qiu, L., Gao, Q., Liu, C., et al. (2012). Large-scale brain networks in board game experts: insights from a domain-related task and task-free resting state. *PLoS One* 7:e32532. doi: 10.1371/journal.pone.0032532

Dudoit, S., Shaffer, J. P., and Boldrick, J. C. (2003). Multiple hypothesis testing in microarray experiments. *Statist. Sci.* 18, 71–103. doi: 10.1214/ss/1056397487

Eickhoff, S. B., Stephan, K. E., Mohlberg, H., Grefkes, C., Fink, G. R., Amunts, K., et al. (2005). A new SPM toolbox for combining probabilistic cytoarchitectonic maps and functional imaging data. *Neuroimage* 25, 1325–1335. doi: 10.1016/j.neuroimage.2004.12.034

Erickson, K. I., Voss, M. W., Prakash, R. S., Basak, C., Szabo, A., Chaddock, L., et al. (2011). Exercise training increases size of hippocampus and improves memory. *Proc. Natl. Acad. Sci. U.S.A.* 108, 3017–3022. doi: 10.1073/pnas.1015950108

Fauvel, B., Groussard, M., Mutlu, J., Arenaza-Urquijo, E. M., Eustache, F., Desgranges, B., et al. (2014). Musical practice and cognitive aging: two cross-sectional studies point to phonemic fluency as a potential candidate for a use-dependent adaptation. *Front. Aging Neurosci.* 6:227. doi: 10.3389/fnagi.2014.00227

Firth, J., Stubbs, B., Vancampfort, D., Schuch, F., Lagopoulos, J., Rosenbaum, S., et al. (2018). Effect of aerobic exercise on hippocampal volume in humans: a systematic review and meta-analysis. *Neuroimage* 166, 230–238. doi: 10.1016/j.neuroimage.2017.11.007

Gaab, N., Gaser, C., and Schlaug, G. (2006). Improvement-related functional plasticity following pitch memory training. *Neuroimage* 31, 255–263. doi: 10.1016/j.neuroimage.2005.11.046

Gaab, N., Gaser, C., Zaehle, T., Jancke, L., and Schlaug, G. (2003). Functional anatomy of pitch memory–an fMRI study with sparse temporal sampling. *Neuroimage* 19, 1417–1426. doi: 10.1016/s1053-8119(03)00224-6

Gao, J. H., Parsons, L. M., Bower, J. M., Xiong, J., Li, J., and Fox, P. T. (1996). Cerebellum implicated in sensory acquisition and discrimination rather than motor control. *Science* 272, 545–547. doi: 10.1126/science.272.5261.545

Gaser, C., and Schlaug, G. (2003). Brain structures differ between musicians and non-musicians. *J. Neurosci.* 23, 9240–9245. doi: 10.1523/JNEUROSCI.23-27-09240.2003

Groussard, M., La Joie, R., Rauchs, G., Landeau, B., Chételat, G., Viader, F., et al. (2010). When music and long-term memory interact: effects of musical expertise on functional and structural plasticity in the hippocampus. *PLoS One* 5:e13225. doi: 10.1371/journal.pone.0013225

Guo, X., Yamashita, M., Suzuki, M., Ohsawa, C., Asano, K., Abe, N., et al. (2021). Musical instrument training program improves verbal memory and neural efficiency in novice older adults. *Hum. Brain Mapp.* 42, 1359–1375. doi: 10.1002/hbm.25298

Hall, C. B., Lipton, R. B., Sliwinski, M., Katz, M. J., Derby, C. A., and Verghese, J. (2009). Cognitive activities delay onset of memory decline in persons who develop dementia. *Neurology* 73, 356–361. doi: 10.1212/WNL.0b013e3181b04ae3

Hanakawa, T., Immisch, I., Toma, K., Dimyan, M. A., Van Gelderen, P., and Hallett, M. (2003). Functional properties of brain areas associated with motor execution and imagery. *J. Neurophysiol.* 89, 989–1002. doi: 10.1152/jn.00132.2002

Hanna-Pladdy, B., and Gajewski, B. (2012). Recent and past musical activity predicts cognitive aging variability: direct comparison with general lifestyle activities. *Front. Hum. Neurosci.* 6:198. doi: 10.3389/fnhum.2012.00198

Hanna-Pladdy, B., and MacKay, A. (2011). The relation between instrumental musical activity and cognitive aging. *Neuropsychology* 25, 378–386. doi: 10.1037/a0021895

Harding, I. H., Corben, L. A., Delatycki, M. B., Stagnitti, M. R., Storey, E., Egan, G. F., et al. (2017). Cerebral compensation during motor function in Friedreich ataxia: the IMAGE-FRDA study. *Mov. Disord.* 32, 1221–1229. doi: 10.1002/mds.27023

Hautzel, H., Mottaghy, F. M., Specht, K., Müller, H. W., and Krause, B. J. (2009). Evidence of a modality-dependent role of the cerebellum in working momory? An fMRI study comparing verbal and abstract n-back tasks. *Neuroimage* 47, 2073–2082. doi: 10.1016/j.neuroimage.2009.06.005

Heim, S., Eickhoff, S. B., and Amunts, K. (2008). Specialisation in Broca's region for semantic, phonological, and syntactic fluency? *Neuroimage* 40, 1362–1368. doi: 10.1016/j.neuroimage.2008.01.009

Herholz, S. C., Halpern, A. R., and Zatorre, R. J. (2012). Neuronal correlates of perception, imagery, and memory for familiar tunes. *J. Cogn. Neurosci.* 24, 1382–1397. doi: 10.1162/jocn_a_00216

Hickok, G., Buchsbaum, B., Humphries, C., and Muftuler, T. (2003). Auditory-motor interaction revealed by fMRI: speech, music, and working memory in area Spt. *J. Cogn. Neurosci.* 15, 673–682. doi: 10.1162/089892903322307393

Holm, L., Karampela, O., Ullén, F., and Madison, G. (2017). Executive control and working memory are involved in sub-second repetitive motor timing. *Exp. Brain Res.* 235, 787–798. doi: 10.1007/s00221-016-4839-6

Huang, Q., Liu, Y., Liao, W., Yang, S., Shen, L., Tang, T., et al. (2020). Disruption of regional brain activity and functional connectivity in patients with asymptomatic vulnerable carotid plaque. *Neurosci. Lett.* 716:134634. doi: 10.1016/j.neulet.2019.134634

Hutchinson, S., Lee, L. H., Gaab, N., and Schlaug, G. (2003). Cerebellar volume of musicians. *Cereb. Cortex* 13, 943–949. doi: 10.1093/cercor/13.9.943

James, C. E., Britz, J., Vuilleumier, P., Hauert, C. A., and Michel, C. M. (2008). Early neuronal responses in right limbic structures mediate harmony incongruity processing in musical experts. *Neuroimage* 42, 1597–1608. doi: 10.1016/j.neuroimage.2008.06.025

Jäncke, L., Schlaug, G., and Steinmetz, H. (1997). Hand skill asymmetry in professional musicians. *Brain Cogn.* 34, 424–432. doi: 10.1006/brcg.1997.0922

Johnson, R. B. (2011). Musical tempo stability in mental practice: a comparison of motor and non-motor imagery techniques. *Res. Stud. Music Edu.* 33, 3–30. doi: 10.1177/1321103X11400501

Karpati, F. J., Giacosa, C., Foster, N. E., Penhune, V. B., and Hyde, K. L. (2016). Sensorimotor integration is enhanced in dancers and musicians. *Exp. Brain Res.* 234, 893–903. doi: 10.1007/s00221-015-4524-1

Klein, C., Liem, F., Hänggi, J., Elmer, S., and Jäncke, L. (2016). The "silent" imprint of musical training. *Hum. Brain Mapp.* 37, 536–546. doi: 10.1002/hbm.23045

Kraus, N., and Chandrasekaran, B. (2010). Music training for the development of auditory skills. *Nat. Rev. Neurosci.* 11, 599–605. doi: 10.1038/nrn2882

Lerub, K. D., Vines, B. W., Shinde, A. B., and Schlaug, G. (2021). Modulating short-term auditory memory with focal transcranial direct current stimulation applied to the supramarginal gyrus. *Neuroreport* 32, 702–710. doi: 10.1097/WNR.0000000000001647

Lezak, M. D., Howieson, D. B., Bigler, E. D., and Tranel, D. (2012). *Neuropsychological Assessment*, 5th Edn. New York, NY: Oxford University Press.

Lotze, M., Scheler, G., Tan, H.-R. M., Braun, C., and Birbaumer, N. (2003). The musician's brain: functional imaging of amateurs and professionals during performance and imagery. *Neuroimage* 20, 1817–1829. doi: 10.1016/j.neuroimage.2003.07.018

Luo, C., Guo, Z. W., Lai, Y. X., Liao, W., Liu, Q., Kendrick, K. M., et al. (2012). Musical training induces functional plasticity in perceptual and motor networks: insights from resting-state FMRI. *PLoS One* 7:e36568. doi: 10.1371/journal.pone.0036568

Mak, M. K., Cheung, V., Ma, S., Lu, Z. L., Wang, D., Lou, W., et al. (2016). Increased cognitive control during execution of finger tap movement in people with Parkinson's Disease. *J. Parkinsons Dis.* 6, 639–650. doi: 10.3233/JPD-160849

Meister, I. G., Krings, T., Foltys, H., Boroojerdi, B., Müller, M., Töpper, R., et al. (2004). Playing piano in the mind–an fMRI study on music imagery and performance in pianists. *Brain Res. Cogn. Brain Res.* 19, 219–228. doi: 10.1016/j.cogbrainres.2003.12.005

Moreno, S., Bialystok, E., Barac, R., Schellenberg, E. G., Cepeda, N. J., and Chau, T. (2011). Short-term music training enhances verbal intelligence and executive function. *Psychol. Sci.* 22, 1425–1433. doi: 10.1177/0956797611416999

Mortimer, J. A., Ding, D., Borenstein, A. R., DeCarli, C., Guo, Q., Wu, Y., et al. (2012). Changes in brain volume and cognition in a randomized trial of exercise and social interaction in a community-based sample of non-demented Chinese elders. *J. Alzheimers Dis.* 30, 757–766. doi: 10.3233/JAD-2012-120079

Müllensiefen, D., Gingras, B., Musil, J., and Stewart, L. (2014). The musicality of no-musicians: an index for assessing musical sophistication in the general population. *PLoS One* 9:e89642. doi: 10.1371/journal.pone.0089642

Notter, M. P., Hanke, M., Murray, M. M., and Geiser, E. (2020). Encoding of auditory temporal gestalt in the human Brain. *Cereb. Cortex* 29, 475–484. doi: 10.1093/cercor/bhx328

Nyberg, L., Lövdén, M., Riklund, K., Lindenberger, U., and Bäckman, L. (2012). Memory aging and brain maintenance. *Trends Cogn. Sci.* 16, 292–305. doi: 10.1016/j.tics.2012.04.005

Olivito, G., Lupo, M., Iacobacci, C., Clausi, S., Romano, S., Masciullo, M., et al. (2018). Structural cerebellar correlates of cognitive functions in spinocerebellar ataxia type 2. *J. Neurol.* 265, 597–606. doi: 10.1007/s00415-018-8738-6

Palmer, C., and Drake, C. (1997). Monitoring and planning capacities in the acquisition of music performance skills. *Can. J. Exp. Psychol.* 51, 369–384. doi: 10.1037/1196-1961.51.4.369

Paquette, S., Fujii, S., Li, H. C., and Schlaug, G. (2017). The cerebellum's contribution to beat interval discrimination. *Neuroimage* 163, 177–182. doi: 10.1016/j.neuroimage.2017.09.017

Parbery-Clark, A., Strait, D. L., Anderson, S., Hittner, E., and Kraus, N. (2011). Musical experience and the aging auditory system: implications for cognitive abilities and hearing speech in noise. *PLoS One* 6:e18082. doi: 10.1371/journal.pone.0018082

Park, D. C., Lautenschlager, G., Hedden, T., Davidson, N. S., Smith, A. D., and Smith, P. K. (2002). Models of visuospatial and verbal memory across the adult life span. *Psychol. Aging* 17, 299–320. doi: 10.1037/0882-7974.17.2.299

Patel, A. D., and Iversen, J. R. (2007). The linguistic benefits of musical abilities. *Trends Cogn. Sci.* 11, 369–372.

Patel, A. D., and Iversen, J. R. (2014). The evolutionary neuroscience of musical beat perception: the action simulation for auditory prediction. *Front. Syst. Neurosci.* 8:57. doi: 10.3389/fnsys.2014.00057

Paulesu, E., Frith, C. D., and Frackowiak, R. S. (1993). The neural correlates of the verbal component of working memory. *Nature* 362, 342–345. doi: 10.1038/362342a0

Penhune, V. B., Zatorre, R. J., and Evans, A. C. (1998). Cerebellar contributions to motor timing: a PET study of auditory and visual rhythm reproduction. *J. Cogn. Neurosci.* 10, 752–765. doi: 10.1162/089892998563149

Ramanoël, S., Hoyau, E., Kauffmann, L., Renard, F., Pichat, C., Boudiaf, N., et al. (2018). Gray matter volume and cognitive performance during normal aging. A voxel-based morphometry study. *Front. Aging Neurosci.* 10:235. doi: 10.3389/fnagi.2018.00235

Rauschecker, J. P. (2011). An expanded role for the dorsal auditory pathway in sensorimotor control and integration. *Hear. Res.* 271, 16–25. doi: 10.1016/j.heares.2010.09.001

Raz, N., Ghisletta, P., Rodrigue, K. M., Kennedy, K. M., and Lindenberger, U. (2010). Trajectories of brain aging in middle-aged and older adults: regional and individual differences. *Neuroimage* 51, 501–511. doi: 10.1016/j.neuroimage.2010.03.020

Raz, N., Gunning-Dixon, F., Head, D., Rodrigue, K. M., Williamson, A., and Acker, J. D. (2004). Aging, sexual dimorphism, and hemispheric asymmetry of the cerebral cortex: replicability of regional differences in volume. *Neurobiol. Aging* 25, 377–396. doi: 10.1016/S0197-4580(03)00118-0

Reitan, R. M., and Wolfson, D. (1993). *Halstead-Reitan Neuropsychological Battery*. Tuscon, AZ: Neuropsychology Press.

Schmahmann, J. D. (2004). Disorders of the cerebellum: ataxia, dysmetria of thought, and the cerebellar cognitive affective syndrome. *J. Neuropsychiatry Clin. Neurosci.* 16, 367–378. doi: 10.1176/jnp.16.3.367

Schmahmann, J. D. (2019). The cerebellum and cognition. *Neurosci. Lett.* 688, 62–75. doi: 10.1016/j.neulet.2018.07.005

Schwartze, M., and Kotz, S. A. (2013). A dual-pathway neural architecture for specific temporal prediction. *Neurosci. Biobehav. Rev.* 37, 2587–2596. doi: 10.1016/j.neubiorev.2013.08.005

Seidler, R. D., Bernard, J. A., Burutolu, T. B., Fling, B. W., Gordon, M. T., Gwin, J. T., et al. (2010). Motor control and aging: links to age-related brain structural, functional, and biochemical effects. *Neurosci. Biobehav. Rev.* 34, 721–733. doi: 10.1016/j.neubiorev.2009.10.005

Shao, Z., Janse, E., Visser, K., and Meyer, A. S. (2014). What do verbal fluency tasks measure? Predictors of verbal fluency performance in older adults. *Front. Psychol.* 5:772. doi: 10.3389/fpsyg.2014.00772

Shen, Y., Lin, Y., Liu, S., Frang, L., and Liu, G. (2019). Sustained effect of music training on the enhancement of executive function in preschool children. *Front. Psychol.* 10:1910. doi: 10.3389/fpsyg.2019.01910

Stoodley, C. J. (2012). The cerebellum and cognition: evidence from functional imaging studies. *Cerebellum* 11, 352–365. doi: 10.1007/s12311-011-0260-7

Stoodley, C. J., and Schmahmann, J. D. (2009). Functional topography in the human cerebellum: a meta-analysis of neuroimaging studies. *Neuroimage* 44, 489–501. doi: 10.1016/j.neuroimage.2008.08.039

Stoodley, C. J., and Schmahmann, J. D. (2018). Functional topography of the human cerebellum. *Handb. Clin. Neurol.* 154, 59–70. doi: 10.1016/B978-0-444-63956-1.00004-7

Strait, D. L., Hornickel, J., and Kraus, N. (2011). Subcortical processing of speech regularities underlies reading and music aptitude in children. *Behav. Brain Funct.* 7:44. doi: 10.1186/1744-9081-7-44

Strong, J. V., and Mast, B. T. (2019). The cognitive functioning of older adult instrumental musicians and non-musicians. *Neuropsychol. Dev. Cogn. B. Aging Neuropsychol. Cogn.* 26, 367–386. doi: 10.1080/13825585.2018.1448356

Sugishita, M. (2000). *Wechsler Memory Scale – Revised*. Tokyo: Nihon Bunka Kagakusha.

Trusheim, W. H. (1991). Audiation and mental imagery: implications for artistic performance. *Q. J. Music Teach. Learn.* 2, 138–147.

Tsai, C. G., Chou, T. L., and Li, C. W. (2018). Roles of posterior parietal and dorsal premotor cortices in relative pitch processing: comparing musical intervals to lexical tones. *Neuropsychologia* 119, 118–127. doi: 10.1016/j.neuropsychologia.2018.07.028

Tse, N. Y., Chen, Y., Irush, M., Cordato, N. J., Landin-Romero, R., Hodges, J. R., et al. (2020). Cerebellar contributions to cognition in corticobasal syndrome and progressive supranuclear palsy. *Brain Commun.* 2:fcaa194. doi: 10.1039/braincomms/fcaa194

Vaquero, L., Hartmann, K., Ripollés, P., Rojo, N., Sierpowska, J., François, C., et al. (2016). Structural neuroplasticity in expert pianists depends on the age of musical training onset. *Neuroimage* 126, 106–119. doi: 10.1016/j.neuroimage.2015.11.008

Verghese, J., Lipton, R. B., Katz, M. J., Hall, C. B., Derby, C. A., Kuslansky, G., et al. (2003). Leisure activities and the risk of dementia in the elderly. *N. Engl. J. Med.* 348, 2508–2516. doi: 10.1056/NEJMoa022252

Wang, Y., Fang, J. L., Cui, B., Liu, J., Song, P., Lang, C., et al. (2018). The functional and structural alterations of the striatum in chronic spontaneous urticaria. *Sci. Rep.* 8:1725. doi: 10.1038/s41598-018-19962-2

Wechsler, D. (1997). *Manual for the Wechsler Adult Intelligence Scale III*. San Antonio, TX: Harcourt Assessment.

Weiss, Y., Cweigenberg, H. G., and Booth, J. R. (2018). Neural specialization of phonological and semantic processing in young children. *Hum. Brain Mapp.* 39, 4334–4348. doi: 10.1002/hbm.24274

White-Schwoch, T., Woodruff Carr, K., Anderson, S., Strait, D. L., and Kraus, N. (2013). Older adults benefit from music training early in life: biological evidence for long-term training-driven plasticity. *J. Neurosci.* 33, 17667–17674. doi: 10.1523/JNEUROSCI.2560-13.2013

Whitfield-Gabrieli, S., and Nieto-Castanon, A. (2012). Conn: a functional connectivity toolbox for correlated and anticorrelated brain networks. *Brain Connect.* 2, 125–141. doi: 10.1089/brain.2012.0073

Wieser, H. G., and Mazzola, G. (1986). Musical consonances and dissonances: are they distinguished independently by the right and left hippocampi? *Neuropsychologia* 24, 805–812. doi: 10.1016/0028-3932(86)90079-5

Wollman, I., Penhune, V., Segado, M., Carpentier, T., and Zatorre, R. J. (2018). Neural network retuning and neural predictors of learning success associated with cello training. *Proc. Natl. Acad. Sci. U.S.A.* 115, E6056–E6064. doi: 10.1073/pnas.1721414115

Wong, P. C., Skoe, E., Russo, N. M., Dees, T., and Kraus, N. (2007). Musical experience shapes human brainstem encoding of linguistic pitch patterns. *Nat. Neurosci.* 10, 420–422. doi: 10.1038/nn1872

Wu, X., Zhang, R., Li, X., Feng, T., and Yan, N. (2021). The moderating role of sensory processing sensitivity in the link between stress and depression: a VBM study. *Neuropsychologia* 150:107704. doi: 10.1016/j.neuropsychologia.2020.107704

Zatorre, R. J., Chen, J. L., and Penhune, V. B. (2007). When the brain plays music: auditory-motor interactions in music perception and production. *Nat. Rev. Neurosci.* 8, 547–558. doi: 10.1038/nrn2152

Zendel, B. R., and Alain, C. (2014). Enhanced attention-dependent activity in the auditory cortex of older musicians. *Neurobiol. Aging* 35, 55–63. doi: 10.1016/j.neurobiolaging.2013.06.022

Conflict of Interest: The authors declare that the research was conducted in the absence of any commercial or financial relationships that could be construed as a potential conflict of interest.

Publisher's Note: All claims expressed in this article are solely those of the authors and do not necessarily represent those of their affiliated organizations, or those of the publisher, the editors and the reviewers. Any product that may be evaluated in this article, or claim that may be made by its manufacturer, is not guaranteed or endorsed by the publisher.

frontiers in Neuroinformatics

ORIGINAL RESEARCH
published: 07 January 2022
doi: 10.3389/fninf.2021.763560

Young and Aged Neuronal Tissue Dynamics With a Simplified Neuronal Patch Cellular Automata Model

Reinier Xander A. Ramos[1], *Jacqueline C. Dominguez*[2,3] *and Johnrob Y. Bantang*[1,4]*

[1] *Instrumentation Physics Laboratory, National Institute of Physics, College of Science, University of the Philippines, Quezon City, Philippines,* [2] *Institute for Neurosciences, St Luke's Medical Center, Quezon City, Philippines,* [3] *Elderly and Dementia Care, Institute for Dementia Care Asia, Quezon City, Philippines,* [4] *Computational Science Research Center, University of the Philippines, Quezon City, Philippines*

Realistic single-cell neuronal dynamics are typically obtained by solving models that involve solving a set of differential equations similar to the Hodgkin-Huxley (HH) system. However, realistic simulations of neuronal tissue dynamics —especially at the organ level, the brain— can become intractable due to an explosion in the number of equations to be solved simultaneously. Consequently, such efforts of modeling tissue- or organ-level systems require a lot of computational time and the need for large computational resources. Here, we propose to utilize a cellular automata (CA) model as an efficient way of modeling a large number of neurons reducing both the computational time and memory requirement. First, a first-order approximation of the response function of each HH neuron is obtained and used as the response-curve automaton rule. We then considered a system where an external input is in a few cells. We utilize a Moore neighborhood (both totalistic and outer-totalistic rules) for the CA system used. The resulting steady-state dynamics of a two-dimensional (2D) neuronal patch of size $1,024 \times 1,024$ cells can be classified into three classes: (1) Class 0–inactive, (2) Class 1–spiking, and (3) Class 2–oscillatory. We also present results for different quasi-3D configurations starting from the 2D lattice and show that this classification is robust. The numerical modeling approach can find applications in the analysis of neuronal dynamics in mesoscopic scales in the brain (patch or regional). The method is applied to compare the dynamical properties of the young and aged population of neurons. The resulting dynamics of the aged population shows higher average steady-state activity $\langle a(t \to \infty) \rangle$ than the younger population. The average steady-state activity $\langle a(t \to \infty) \rangle$ is significantly simplified when the aged population is subjected to external input. The result conforms to the empirical data with aged neurons exhibiting higher firing rates as well as the presence of firing activity for aged neurons stimulated with lower external current.

Keywords: neuronal dynamics, continuous cellular automata, brain, numerical model, activation function, aged neurons

OPEN ACCESS

Edited by:
Toshiharu Nakai,
Osaka University, Japan

Reviewed by:
Andrei Dragomir,
National University of Singapore, Singapore
Ergin Yilmaz,
Bulent Ecevit University, Turkey

***Correspondence:**
Johnrob Y. Bantang
jybantang@up.edu.ph

Received: *25 August 2021*
Accepted: *06 December 2021*
Published: *07 January 2022*

Citation:
Ramos RXA, Dominguez JC and Bantang JY (2022) Young and Aged Neuronal Tissue Dynamics With a Simplified Neuronal Patch Cellular Automata Model. Front. Neuroinform. 15:763560. doi: 10.3389/fninf.2021.763560

1. INTRODUCTION

Since the development of the first neuronal model by Louis Lapicque in 1907, most neuronal models we have today use a set of ordinary differential equations (ODEs) to model the dynamics of neurons (Lapicque, 1907; Brunel and Van Rossum, 2007). The Nobel-prize winning Hodgkin-Huxley (HH) model describes the relationship between the membrane potential of the neuron and

the flow of ions across the membrane normally via the ion channels (Hodgkin and Huxley, 1952; Gerstner et al., 2014). The HH model is successfully used to describe the dynamics of a squid giant axon and even the Purkinje fibers in the heart (Noble, 1962). Other models such as Dalton and FitzHugh (1960), Nagumo et al. (1962) and Morris and Lecar (1981) models were improvisations and simplifications on the HH model. While these models are good representations of a neuronal response, it is a challenge for us to construct a simple model useful in describing the behavior of a large neuronal population. HH neurons can be arbitrarily interconnected (Pang and Bantang, 2015) but simulations for large numbers of neurons take long computational run time and need high computing resources since they require solving many coupled ODEs and saving numerous system variables.

One study involves cortical simulations of 10^9 neurons of a cat using Blue Gene/P supercomputer (Ananthanarayanan et al., 2009). The simulations were powered by 147, 456 CPUs and 144 TB of main memory (roughly $\sim 6 \times 10^3$ neurons/CPU, $\sim$144 KB/neuron). In this study, we propose simple cellular automata models to simulate many interconnected neurons that will help investigate integrated dynamics of up to millions (10^6) of neurons using lower CPU and GPU requirements. Our simulations are powered with 1 CPU and 16 GB of memory (RAM) (roughly $\sim 10^6$ neuron/CPU, $\sim$16 KB/neuron). The Blue Brain project primarily uses the NEURON simulation environment to accomplish their feat. NEURON mainly solves ODE-based models with data-driven parameters. However, solving ODEs differs from the cellular automata (CA)-based models. CA models can employ a look-up-table-based algorithm that is usually faster than solving ODEs.

Cellular automaton modeling paradigm was first developed in the late 1940's by Stanislaw Ulam and John von Neumann (von Neumann, 1966). It became popular after it was used to model Conway's Game of Life in the 1970's. A CA system $\mathcal{A}$ consists of the set $\mathcal{C}$ of agents or "cells" c ($c \in \mathcal{C}$) arranged in a lattice $\mathcal{L}$ with a specified neighborhood set $\mathcal{N} = \mathcal{C}^{n+1}$ where n is the number of neighbors of any given cell. Certain boundary conditions are also applied depending on the properties of the physical system being modeled (Wolfram, 2002; Arciaga et al., 2009). These cells have assigned state s, typically obtained from a finite state binary set such $\mathcal{S} = \{0, 1\}$, being the simplest. The "0" and "1" states usually represent either "dead" or "alive," or for our present case of neuronal dynamics represent "resting" or "spiking" (active), respectively. Each neighborhood has a unique state $\bar{s} \in \mathcal{S}^{n+1}$.

The various dynamics of a CA model also emerge from the rules applied to the lattice. In this work, we investigate a CA system with a first-order linear approximation to the HH neuronal response as our rule for each cell. The activation function is further discussed in section 2.1. We perform different analyses (spatiotemporal, cobweb, bifurcation) on the CA system to classify the observed dynamics. This lays the groundwork of our proposed model that can be extended to future directions. In section 7, we extended our model into a nonlinear activation function, which is used to better fit the response of young and aged neurons of a rhesus monkey (Coskren et al., 2015).

Aged neurons have distinctly less myelin and shorter axon internodal distance leading to reduced conduction velocity (Peters, 2007). Dysregulated signaling pathways in oligodendroglia and the loss of reregenerative capacity of oligodendrocyte progenitor cells are thought to be the major cause for myelin loss (Rivera et al., 2021). At the synapse, dendritic spines where majority of excitatory synaptic processes occur are smaller and lesser (Pannese, 2011) but are functionally intact to make synaptic connections. The connections may be weaker but exhibit lesser capacity for short-term plasticity (Mostany et al., 2013). Presumably, the shrinkage in the density of the dendritic spine impacts excitatory synaptic activity in neuronal circuits and accounts for the cognitive changes observed in older adults even in the absence of pathology. However, in the light of reports of increase in action potential firing rates (excitability) in aged neurons, there is need for studies to further understand the dynamics of cell-to-cell communication and open avenues for potential interventions to mitigate the effects of brain aging. In a study on rhesus monkey prefrontal cortex (Coskren et al., 2015), it was found that aged neurons typically have higher action potential (AP) firing rates compared to younger neurons. The empirical data from the study is used as an application of our CA model.

2. CONTINUOUS CELLULAR AUTOMATA MODEL OF A NEURONAL PATCH

As a CA model, neurons are arranged in a two-dimensional lattice $\mathcal{L}$ composed of $1,024 \times 1,024$ cells. This choice of lattice size is one of the highest possible in a common computing device (without the need of high-performance computing). The resulting dynamics does not change with varying lattice size (Ramos and Bantang, 2018, 2019c). However, the computing performance is compared in section 9. The state of s each neuron is represented by a real number a (stands for activity) which ranges from 0 to 1, thus forming a continuous-state CA. The state of each neuron is initialized by assigning a random value to the CA state drawn from a uniform distribution such that $a_{i,j} \in [0, 1]$ for all CA cells in the system ($i, j \in [1, 1024]$).

At each timestep, the average state of the neighborhood of a given cell is taken as the cell's input a_{in} or stimulus. The response of the current cell is obtained from the mapping of a_{in} into its corresponding output a_{out} or response. A generalized linear activation or response function is shown in **Figure 1**. The various modes of neighborhood and boundary conditions are discussed in section 2.2 and the activation function is discussed in section 2.1 below. We found that a value of 100 timesteps is enough to achieve steady-state for any initial state, and that randomizing the initial location of active cells does not affect the dynamical results of our model (Ramos and Bantang, 2018; Ramos, 2019).

2.1. Activation Function

The activation function used in the CA model is mainly derived from the response function of the HH model. Many other neuronal models such as leaky integrate-and-fire (Tal and Schwartz, 1997; Gerstner et al., 2014) and Wilson-Cowan (Wilson and Cowan, 1972) exhibit a similar trend of neuronal firing

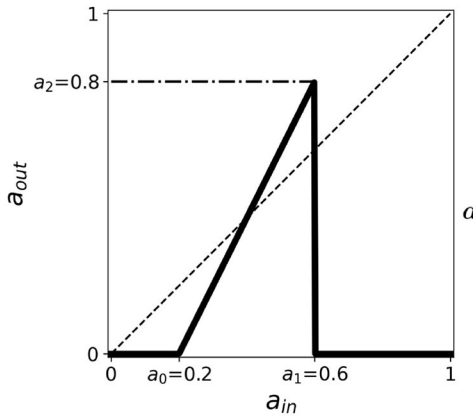

$$a_{\text{out}} = \begin{cases} 0 & a_{\text{in}} < a_0 \\ \frac{a_2(a_{\text{in}}-a_0)}{a_1-a_0} & a_{\text{in}} \in [a_0, a_1] \\ 0 & a_{\text{in}} > a_1 \end{cases}, \quad (1)$$

FIGURE 1 | A simplified neuronal response used for the CA model of neurons. The output a_{out} is related to the probability of the neuron to fire given the input a_{in}. The plot shows such functions for threshold values $a_0 = 0.2$, $a_1 = 0.6$, $a_2 = 0.8$. The dashed line corresponds to $a_{\text{out}} = a_{\text{in}}$ useful in the cobweb analysis.

rate with increasing input current. Three main properties of the activation function can be observed:

1. Two thresholds (a minimum and a maximum) in the input are present indicating that neurons fire only when stimulated by an input current between these two thresholds. We, respectively, assign for these the thresholds a_0 and a_1, the minimum and maximum.
2. The firing rate monotonically increases whenever the input current is between a_0 and a_1; the firing rate is zero otherwise.
3. A maximum threshold in the output is present limiting the firing rate values for the entire range of a_{in}. We assign this as a_2.

The thresholds are incorporated into the activation function and are simplified by taking the first-order approximation as described in **Figure 1**. The parameter thresholds are varied from 0 to 1 with a step size of 0.1. The condition $a_0 = a_1$ results in a trivial mapping $a_{\text{out}} = 0$, for all a_{in}-values. The resulting equation for the neuronal activation function is given by:

$$a_{\text{out}} = \begin{cases} 0 & a_{\text{in}} < a_0 \\ \frac{a_2(a_{\text{in}}-a_0)}{a_1-a_0} & a_{\text{in}} \in [a_0, a_1] \\ 0 & a_{\text{in}} > a_1 \end{cases} \quad (1)$$

We performed an exhaustive search by varying each parameter in $\{a_0, a_1, a_2\}$ from 0 to 1 with increments of 0.1 (Ramos and Bantang, 2018, 2019c). The resulting steady-state dynamics for all possible combinations of $\{a_0, a_1, a_2\}$ in this scheme were classified into one of the types discussed in section 3.

2.2. Neighborhood and Boundary Conditions

Two often used neighborhood configurations in CA models are the von Neumann and the Moore neighborhoods (Wolfram, 2002). **Figure 2A**, on one hand, shows a von Neumann setting. In this case, the central cell of any 3 × 3 subset of the lattice is connected to the adjacent cells in the primary directions (4 neighbors: left, right, top, and bottom) with respect to the cell. **Figure 2B**, on the other hand, shows a Moore neighborhood setting. This time, the central cell is connected to the adjacent cells in the primary and secondary directions (including the diagonal directions, total of 8 neighbors). Moore neighborhood is used in the model since a biological neuron is typically connected to all neighboring cells in the 2D space (Hawick and Scogings, 2011). Two types of Moore neighborhood configurations are considered: totalistic and outer-totalistic. The only difference between these configurations is that the outer-totalistic setting has the central cell of the 3 × 3 subset included in the neighborhood state (see **Figure 2C**).

The boundary conditions describe how the cells at the edge of the lattice behave. Two types of boundary conditions were considered: toroidal and spherical boundaries. With the toroidal boundary condition, the cells on the leftmost column are connected to the rightmost column, and the top row is connected to the bottom row. This produces a wrap-around effect on our automaton as shown in **Figure 3A**. For the spherical setting (Ramos and Bantang, 2019c), the square lattice is projected on the surface of a sphere (Mercator projection) as shown in **Figure 3B**. Observe that the cells in the top (and bottom) row are fully connected to each other becoming a pole, while in the middle rows neighbors wrap around.

2.3. Two-Layered Lattice and the External Input

To analyze a quasi three-dimensional (3D) neighborhood, we extended our analysis to a two-layered automaton for both toroidal and spherical boundary conditions (Ramos and Bantang, 2019a,b). The intra-layer connection has a Moore neighborhood setting, while the inter-layer connection is a direct overlay between the layers. The neighborhood conditions for this two-layer lattice is visualized in **Figure 3C**. For systems with the number of layers greater than two, the topmost and bottommost layer are connected as if the bottommost layer is stacked above the topmost layer.

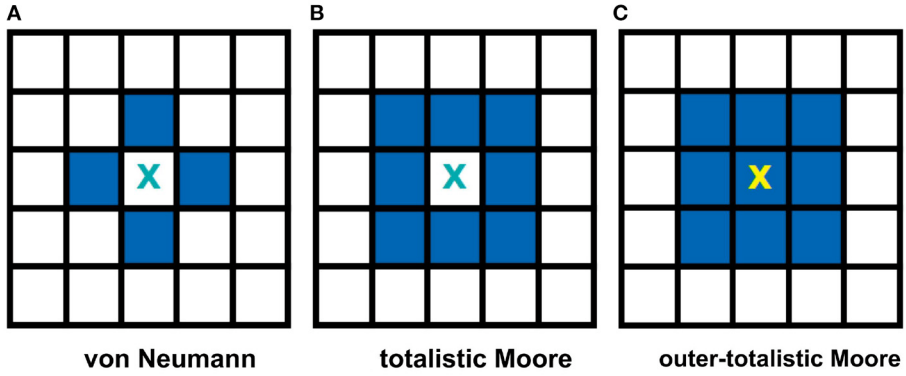

FIGURE 2 | Common neighborhood configurations used in CA theory. The shaded cells show the neighbors of cell X for each type of neighborhood. The von Neumann neighborhood **(A)** of cell X consists of the four cells in the primary directions, while Moore **(B)** extends it to the secondary directions. In an outer-totalistic setting **(C)**, the cell X itself is included in the neighborhood. In this work, Moore neighborhood is used because a biological neuron is typically connected to all neighboring cells in the 2D space.

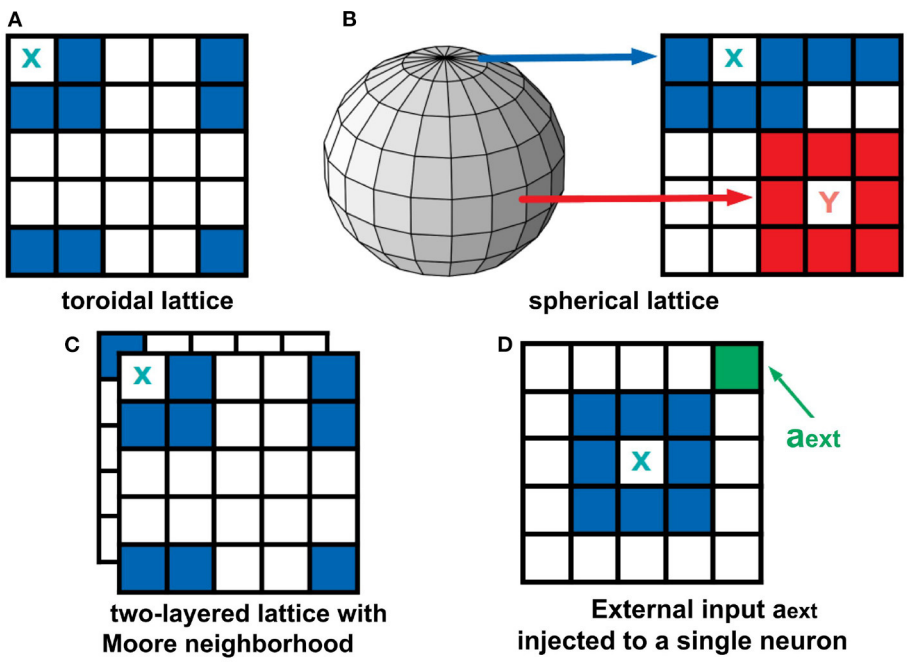

FIGURE 3 | Top row: Boundary conditions used in this study. In a toroidal lattice **(A)**, we wrap-around the top and bottom rows, and the leftmost and rightmost parts of the grid. For the spherical lattice **(B)**, a Mercator projection was used to draw the lattice on the sphere's surface. Bottom row: Extended neighborhood and boundary conditions explored in this work. For the two-layered lattice **(C)**, the intra-layer connection is Moore, but the inter-layer connection is the overlay between layers. For the analysis of external input **(D)**, a fraction of neurons in the population are set to be always active $a_{\text{ext}} = 1$.

A CA system (Ramos and Bantang, 2019a) with a constant external input $a_{\text{in}} = a_{\text{ext}} = 1$ injected to one of the neurons c_{ext}, shown in **Figure 3D**, is also analyzed. In this case, the neuron c_{ext} is always in spiking state since $a = 1$ at all times.

3. NUMERICAL EXPERIMENTS

We first examined the dynamics of the neuronal CA using Moore toroidal boundary condition. The average neuronal patch activity $\langle a \rangle$ is obtained for each timestep and plotted as shown in **Figure 4**. We observed two types of steady-state dynamics: a quiescent or zero steady-state; and a spiking or nonzero steady-state. These steady-state trends are also observed in the HH model (as well as Morris-Lecar) as Type I and Type II neurons, respectively (Hodgkin and Huxley, 1952; Morris and Lecar, 1981; Gerstner et al., 2014). The steady-state dynamics is the same for totalistic and outer-totalistic neighborhoods. Samples of spatiotemporal activity of the neuronal CA are shown in

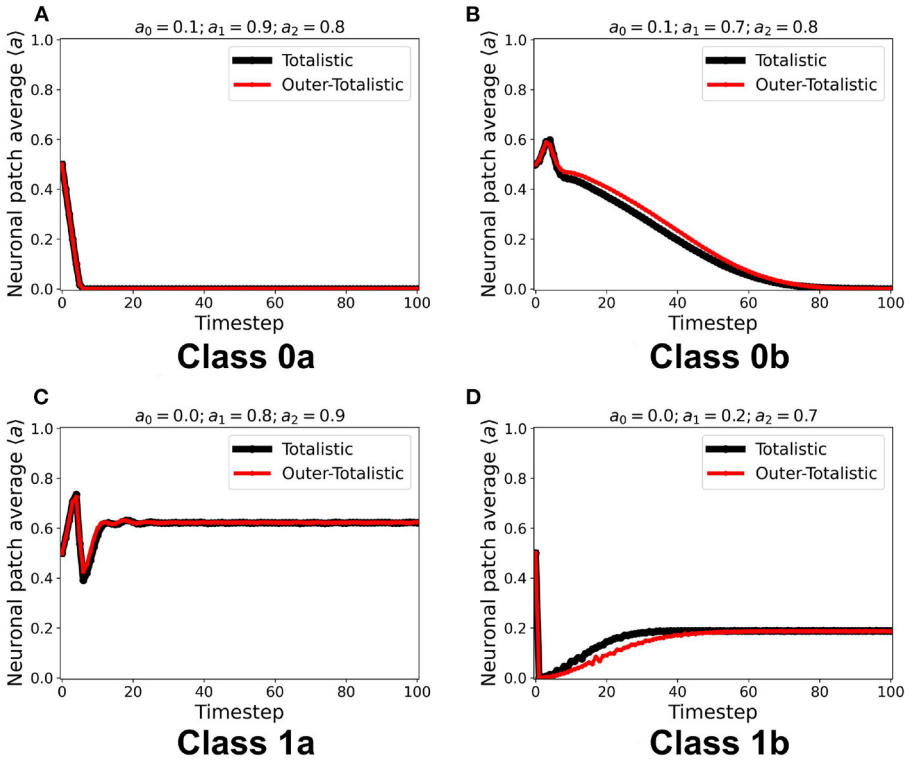

FIGURE 4 | (A–D) Representative steady-state dynamics for each neuronal CA class. The steady-state is taken as the average neuronal activity of the patch at that timestep. The black solid line shows the average neuronal activity using totalistic rules while the red solid line corresponds to the outer-totalistic setting.

Figures 5, **7**, respectively for toroidal and spherical shapes. We observed that a certain subset of the spiking steady-state CA produced exploding patterns before reaching a randomly spiking steady-state. For any given parameter set a_0, a_1, a_2, the dynamics are observed to fall into any one of the following classes.

1. Class 0: Quiescent Steady-State: (a) Fast-decay; (b) Slow-decay.
2. Class 1: Spiking Steady-State: (a) With random patterns; (b) With exploding patterns.

The classification above becomes more obvious as we look at the steady-state trajectory shown in **Figure 6**. Here, we plotted the activity a_{t+1} vs. a_t. With spherical boundary conditions, this steady-state dynamics remains unchanged (see **Supplementary Figure 1**). Hence, the boundary condition in the systems investigated does not affect neuronal CA classification. There is a slight variation on the spatiotemporal evolution of the automaton with the spherical boundary condition as shown in **Figure 7**. The effect of spherical lattice is clearly visible on Class 1b, where the activity signal bounces back from the location of the polar-points (top and bottom rows).

In a previous work (Ramos and Bantang, 2019c), we explored the different regimes in which these CA classes exist in the phase space diagram. We found that a minimum of 20% of the population of the neurons must be active or spiking at $t = 0$ to observe a nonzero steady-state CA (Class 1). As the output threshold a_2 is increased, the systems with parameters that fall near the phase boundary, transitions from Class 0 to Class 1 CA, and thus, increasing the region for which Class

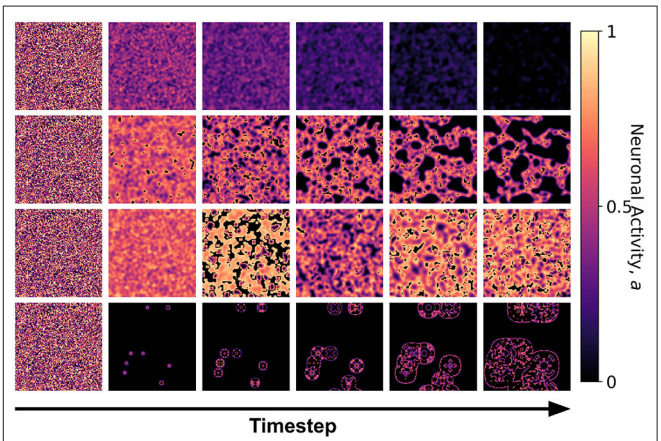

FIGURE 5 | Snapshots of the neuronal CA with toroidal lattice configuration for each class taken at different timesteps of the simulation. The snapshots are taken with increasing timesteps (not necessarily consecutive) to highlight the different dynamics observed. At $t = 0$, the initial state is the same for all classes, but each class evolved into one of the CA classes, depending on the set of parameter thresholds used in the activation function.

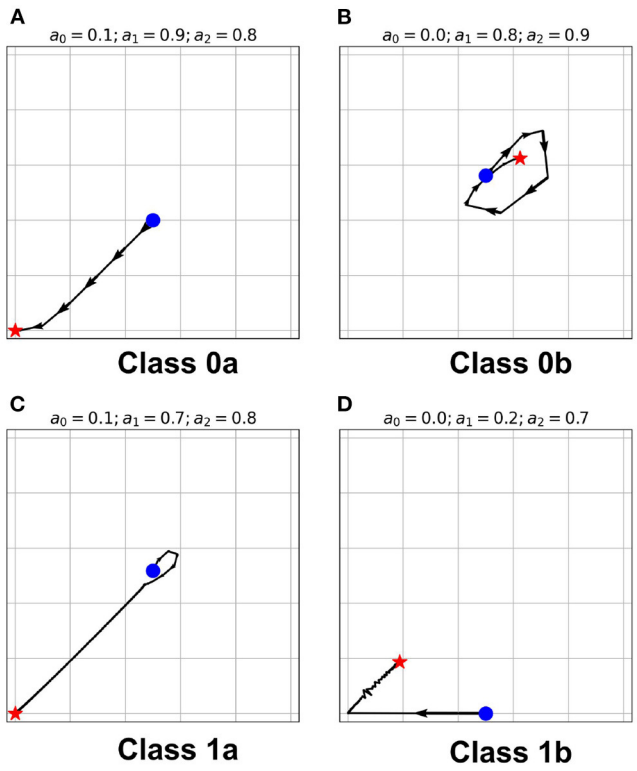

FIGURE 6 | (A–D) State-space trajectories of each of the classes. The • and ⋆ marks the automaton state at $t = 0$ and $t = \infty$, respectively. The arrows show the direction of evolution of the average neuronal steady-state over time.

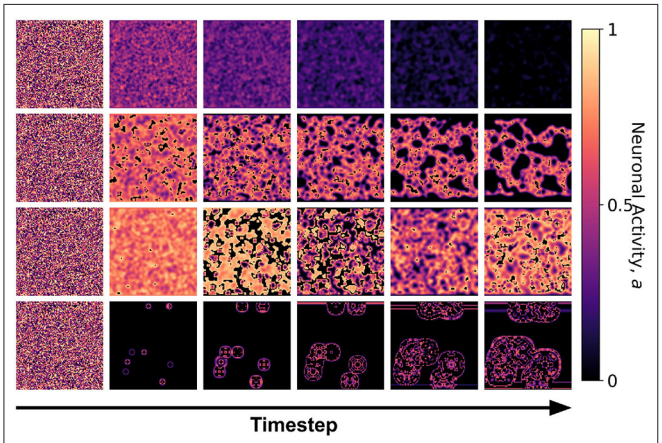

FIGURE 7 | Snapshots of the neuronal CA with spherical lattice configuration for each class taken at different timesteps of the simulation. The snapshots are taken with increasing timesteps (not necessarily consecutive) to highlight the different dynamics observed. At $t = 0$, the initial state is the same for all classes, but each class evolved into one of the CA classes, depending on the set of the parameter threshold used in the activation function.

1 CA is observed. In this work, the chosen set of parameters belong to the stable regions in which the dynamical classification is observed.

4. EFFECT OF EXTERNAL INPUT AND LAYERED LATTICE

Using the same initial state of the automaton, we assigned a certain fraction (1% and 5%) of the neurons in random locations to be c_{ext}, injected with constant $a_{\text{in}} = 1$. It is notable in **Figure 8** that for all steady-state classes, the overall system activity $\langle a \rangle$ becomes typically much greater than the input. Class0b neurons with 5% c_{ext} were found to have similar steady-state dynamics with Class 1a. Furthermore, Class 1b neurons resorted to an oscillating steady-state with 5% c_{ext}.

We implemented the method described in section 2.3 for a two-layered and four-layered CA system. The average steady-state activity remains unchanged across each layer and remains the same for the whole CA system (see **Supplementary Figure 2**). Increasing the number of layers from two to four layers did not change the CA steady-state classification. It is notable in **Figure 9** that increasing the number of layers also increases the number of neurons in the neighborhood state, and consequently delays the transition to quiescent steady-state in Class 0b. The delay is also due to the gradual decrease of the wave amplitude as it travels at least once across the system. This follows the proportionality between the system size and the time taken for the signal to propagate across the system (Wolfram, 2002).

5. COBWEB DIAGRAM ANALYSIS

Cobweb diagrams visualize how a dynamical system behaves over time (Stoop and Steeb, 2006). Consider a CA system response function defined by $a_{\text{out}} = f(a_{\text{in}})$ (see **Figure 1**). We then can draw a cobweb diagram on a plane $(x, y) = (a_{\text{in}}, a_{\text{out}})$ as follows:

1. Given a chosen starting point $(x_{\text{start}}, y_{\text{start}}) = (a_{\text{start}}, 0)$, we trace a vertical line from it to $(a_{\text{start}}, f(a_{\text{start}}))$.
2. We trace a horizontal line from $(a_{\text{start}}, f(a_{\text{start}}))$ until it crosses the dashed line with the equation $a_{\text{out}} = a_{\text{in}}$. This value becomes the new starting point, such that $(x_{\text{start}}, y_{\text{start}}) = (f(a_{\text{start}}), f(a_{\text{start}}))$.
3. Repeat steps 1 and 2 until we reach a sufficient number of steps (here, we use 100).

The resulting cobweb diagrams for the different dynamical classes are shown in **Figure 10** (Ramos and Bantang, 2020). The activation function of Class 0a falls below the line $a_{\text{out}} = a_{\text{in}}$ such that any neuron transitions to quiescent state regardless of its initial state (marked by the blue star ⋆). A collection of neurons of this class approaches a quiescent state in a short amount of timesteps. However, in Class 0b, the activation function crosses the line $a_{\text{out}} = a_{\text{in}}$ once. Any neuron state that starts from the left or right of the intersection point results in a temporary overall active state but the system eventually ends up to be in the quiescent steady-state. If the neuron state starts exactly at the intersection point, its state remains there as a trivial application of the procedure above. Only a few of neurons coincide with this trivial case since the initial state-values of the CA in our numerical experiments is obtained from a uniform random

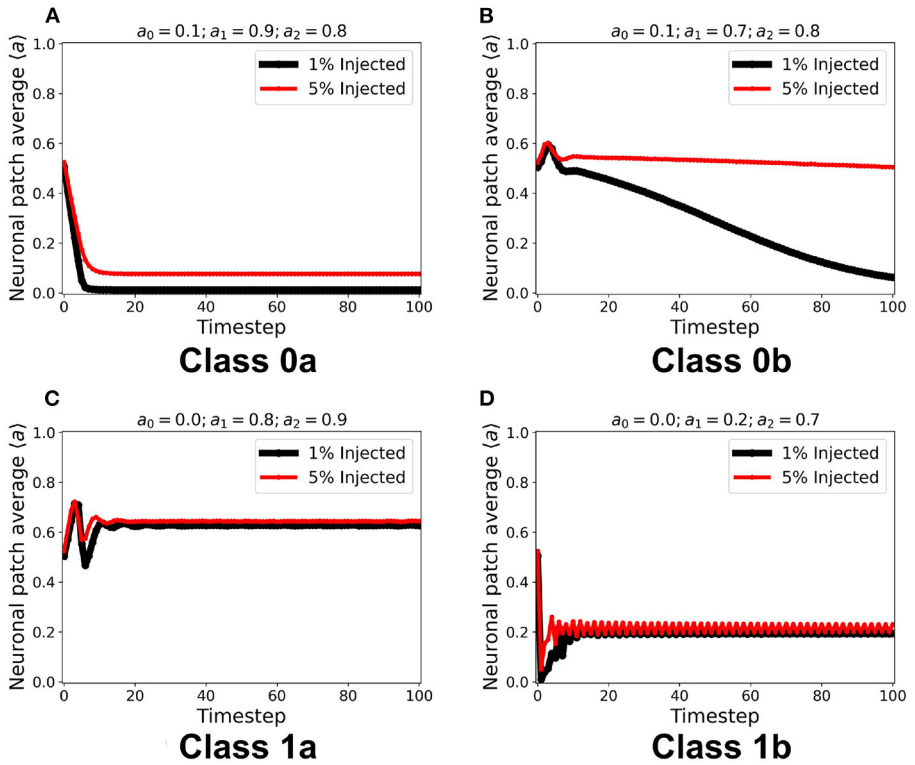

FIGURE 8 | (A–D) Steady-state dynamics for each CA class in a toroidal lattice configuration with external input injected to a fraction of the neuronal population. The black line shows the average steady-state when 1% of the population is injected with external constant input. The red line corresponds to 5% of the neuronal population injected accordingly.

distribution in the range [0, 1]. Collectively, Class 0b neurons go into the quiescent state but at a slower rate compared to Class 0a. Inhibitory neurons (Type I) can therefore be modeled by Class 0 neuronal patch.

If the intersection point is located at the origin (i.e. $a_0 = 0$), the collection of neurons always approaches a spiking steady-state. The greater is the difference $a_1 - a_0$, the higher the average steady-state value $\langle a \rangle$ of the system. Neuronal CAs with lower average steady-state value usually result from exploding patterns (Class 1b). Random patterns (Class 1a) consequently produce higher average steady-state values. Excitatory (Type II) neurons belong to Class 1 in the classification scheme presented.

6. BIFURCATION DIAGRAM ANALYSIS

Bifurcation diagrams show the dynamical trend of the system as we vary a parameter of interest Çelik Karaaslanl (2012). In this work, we chose to investigate the trend for varying a_2-values, holding both a_0 and a_1 at various combinations of constant values. Since 100 timesteps is enough for the simulation to reach steady-state at any given parameter set Ramos and Bantang (2018, 2019c), we obtained the average neuronal patch activity $\langle a \rangle$ only for the last (10) timesteps. The resulting bifurcation diagrams are shown in **Figure 11** (Ramos and Bantang, 2020).

At certain parameter sets, the neuronal CA exhibits period-doubling. This only happens when the activation function is negatively-sloped and strictly satisfies the conditions: $a_1 = 0$ and $a_0 > 0$. Only with this specific constraint will the overall neuron state oscillate as shown in the cobweb diagrams in **Figure 12**. An oscillating overall neuronal state indicates that a significant degree of synchronization happens in the majority fraction of the neurons. Epileptic neurons can be modeled by these negatively-sloped activation functions. This oscillatory behavior is unchanged by any neighborhood and boundary conditions, as shown in **Figure 12**. However, as we increase the fraction of neurons c_{ext} with input, the oscillation becomes underdamped.

7. EXTENDING TO NONLINEAR ACTIVATION FUNCTION

As discussed in section 1, one possible extension of the model is to consider a nonlinear activation function that provides a better approximation of the neuronal response (Hodgkin and Huxley, 1952; Gerstner et al., 2014; Pang and Bantang, 2015). The second-order approximation of the activation function is given by the equation:

$$a_{\text{out}} = \begin{cases} 0 & 0 < a_{\text{in}} < a_0 \\ a_2\left(1 - \left(1 - \frac{a_{\text{in}} - a_0}{1 - a_0}\right)^b\right) & a_{\text{in}} \geq a_0 \end{cases} \quad (2)$$

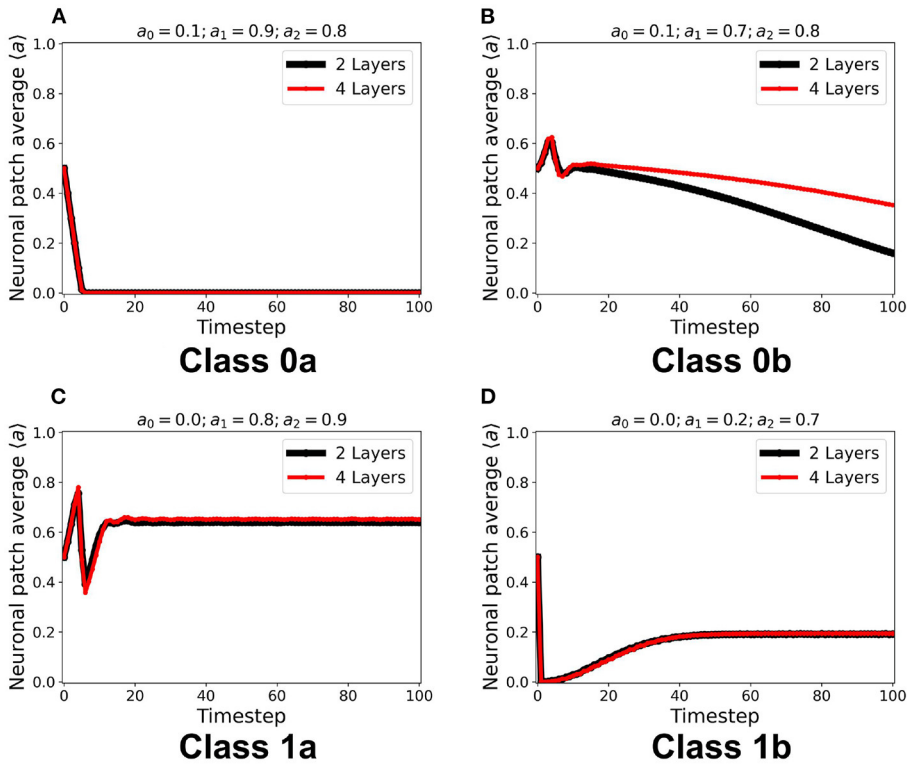

FIGURE 9 | (A–D) Steady-state dynamics of each class in a two-layered (black line) and four-layered (red line) toroidal lattice configuration. The dynamical trend remains the same for each class.

where a_0, a_2 represents the same thresholds as in Equation 1, and b is the nonlinearity parameter. Here, $a_1 = 1$. When $b = 1$, this function reverts to the first-order linear approximation. **Figure 13A** shows how the activation function changes when we increase b. An exhaustive testing of the nonlinear activation function has been done with varying input and output thresholds $a_0, a_2 \in [0, 1]$, and nonlinearity parameter $b \in [0, 40]$ (Ramos and Bantang, 2021). The resulting dynamics are classified below. Representative steady-state dynamics for each class are shown in **Figure 13B**.

1. Class 0: Quiescent Steady-State: (a) Fast-decay; (b) Slow-decay
2. Class 1: Spiking Steady-State: (a) low activation probability; (b) high activation probability.

The conditions for phase transition are presented in a previous work (Ramos and Bantang, 2021). It is notable that the opposing extreme cases ($a_2 = 0.0$ and $a_0 = 1.0$) always belong to Class 0. Whenever $0 \leq b < 1$, the system also falls under Class 0 independent of the other parameters. Once we increase the nonlinearity such that $b > 1$, especially for cases when the corresponding linear activation function lies completely in the region below the $a_{\text{out}} = a_{\text{in}}$ line, the dynamical evolution transitions from Class 0 to Class 1. This transition is caused by the crossing of the activation function to the region above $a_{\text{out}} = a_{\text{in}}$ line as shown in **Figure 13A**. Hence, using the cobweb analysis above, there are individual neurons that will contribute to an overall system spiking steady-state. We also found that, on one hand, the average steady-state activity transitions abruptly when the input threshold a_0 is decreased. On the other hand, the transition is gradual when the output threshold a_2 is increased, with the phase boundary approximated at $b \sim 1/a_2$. Furthermore, increasing the nonlinearity parameter b transitions the neuronal classification from Class 0 to Class 1.

It is notable that the opposing extreme cases ($a_2 = 0.0$ and $a_0 = 1.0$) always belong to Class 0. Whenever $0 \leq b < 1$, the system also falls under Class 0 independent of the other parameters. Once we increase the nonlinearity such that $b > 1$, especially for cases when the corresponding linear activation function lies completely in the region below the $a_{\text{out}} = a_{\text{in}}$ line, the dynamical evolution transitions from Class 0 to Class 1. This transition is caused by the crossing of the activation function to the region above $a_{\text{out}} = a_{\text{in}}$ line as shown in **Figure 13A**. Hence, using the cobweb analysis above, there are individual neurons that will contribute to an overall system spiking steady-state.

8. YOUNG AND AGED NEURONAL SYSTEMS

As an application of the proposed CA modeling paradigm, we obtained an empirical dataset of the single-cell response that shows the dynamical difference between young and aged neurons in response to input signals (Coskren et al., 2015). Data shows higher firing rates from the aged neurons. The dataset is normalized over the range of the input current ($30 - -330$pA) used in the study. When the first-order approximation activation

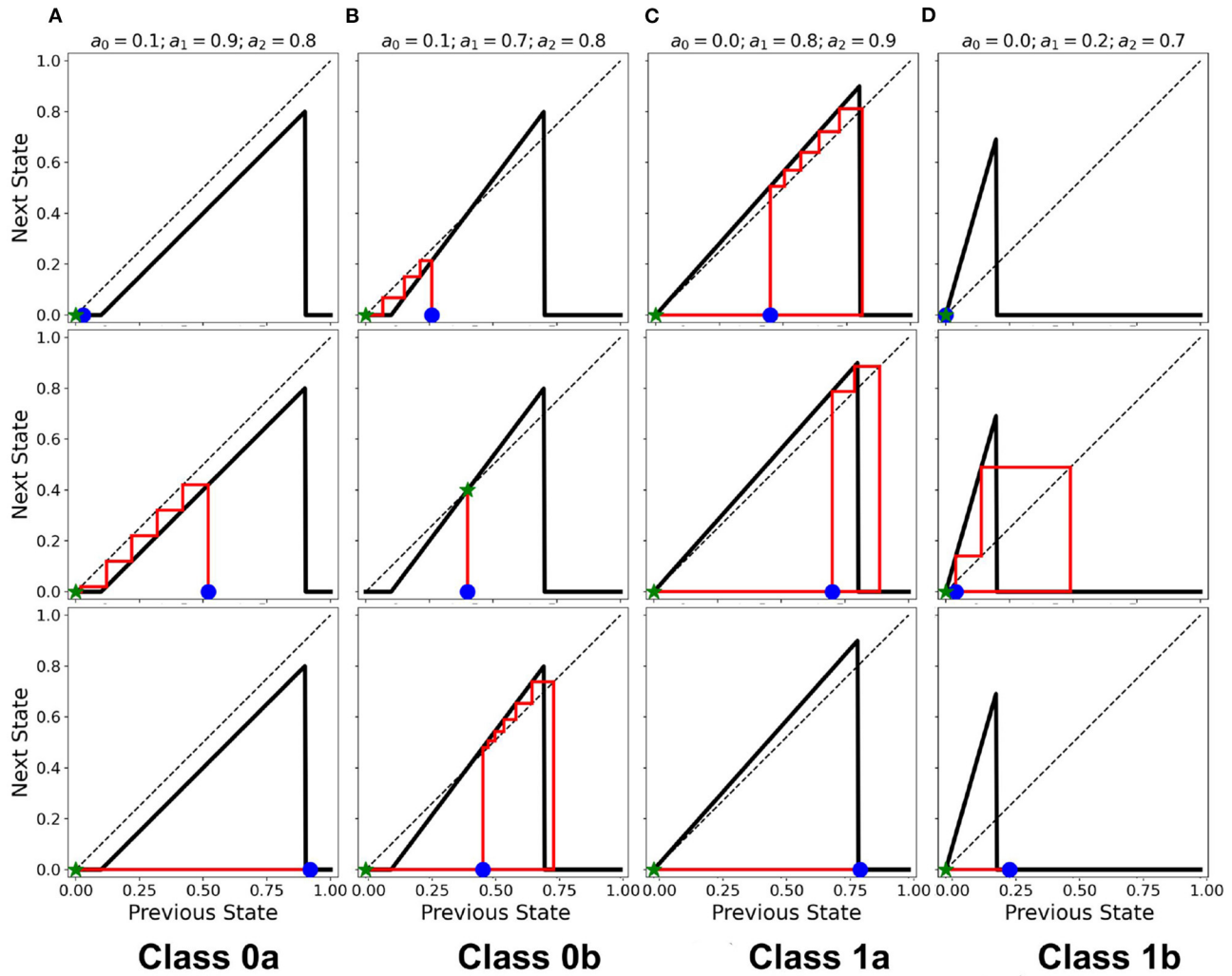

FIGURE 10 | (A–D) Cobweb diagrams showing the behavior of individual neurons for each class. In each column, the individual plots show different cases that a neuron is initialized (marked by •). Each case may not necessarily be the same across all the classes. The ⋆ marks the final state on the x-axis with the red line showing the trajectory of the neuronal state through time.

function $a_{\text{out}} = f(a_{\text{in}})$ given by Equation 1 is used to fit the dataset, both young and aged neuronal system resulted to quiescent steady-state with young neuronal CA decaying faster than the aged ones (see **Supplementary Figure 3**). If injected $a_{\text{ext}} = 1$–5% of the neuronal population, the average steady-state is the same for both young and aged neuronal systems. This result contradicts the observations by Coskren et al. (2015).

A better fitting function to the dataset is the second-order approximation given by Equation 2. **Figure 14A** shows the resulting response curve. Using this response curve, we found a significant difference in the dynamics between young and aged neuronal systems (see **Figure 14B**). The aged neuronal population shows a spiking steady-state with a higher average neuronal response than the younger population. Injecting constant external input ($a_{\text{ext}} = 1$) randomly to 5% of the neuronal population amplifies the average steady-state for both young and aged neuronal systems but with different steady-state values. Hence, the aged neuronal system does not need a very high external input for it to be amplified, unlike the younger population. This result confirms the higher firing rate of aged neurons as well as the presence of spiking states for aged at lower input currents (Coskren et al., 2015). **Figure 14C** shows the actual response of young and aged neuronal patches obtained using the method described in Ramos and Bantang (2018) and Ramos and Bantang (2021). A sample discrete response of a single neuron from the young and aged neuronal patches is shown in **Figure 14D**.

9. COMPUTATIONAL COMPLEXITY

The computational efficiency of using CA to model neuronal patch dynamics is quantified using the time it takes to finish a

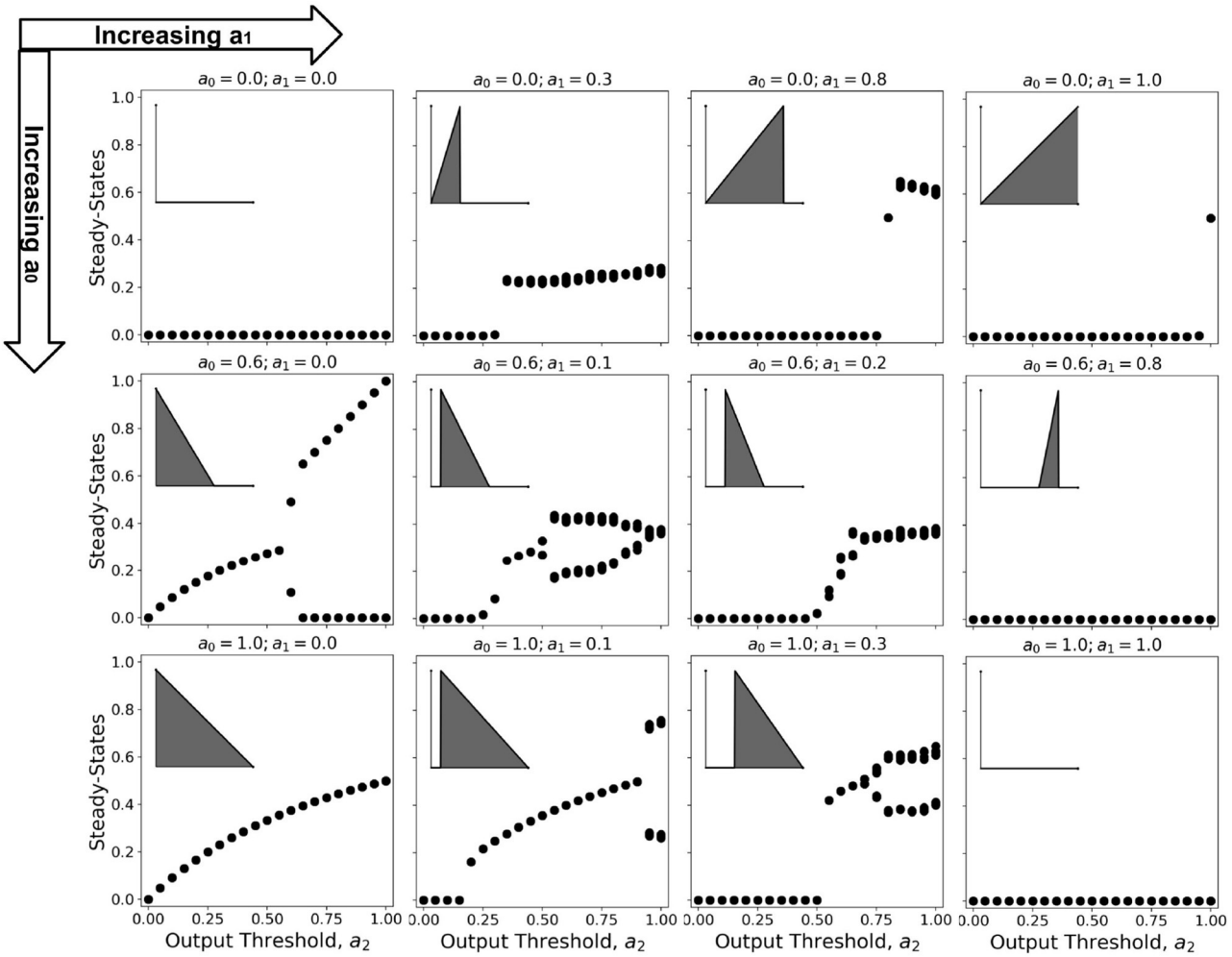

FIGURE 11 | Representative bifurcation diagrams for the neuronal CA system. Each individual plot shows the steady-state values vs. increasing a_2 with constant a_0, a_1 values. From left to right column shows the different steady-state trends with increasing a_1 while from top row to bottom shows increasing a_0. The inset shows the activation function for that parameter set given that $a_2 = 1.0$, for reference.

given simulation. With increasing neuronal population N, the time it takes to finish the simulation T is recorded as the average of three (3) runs or trials for each solver. In general, we find that the time T can be fitted with:

$$T = a(N - b)^c \tag{3}$$

where a, b and c are the fitting parameters. From these parameters, c provides the relevant information for the computational complexity whereby $T \sim O(N^c)$ for large N-values.

Figure 15 shows the comparison of the simulation time using different solvers to the HH ODEs and the CA modeling method presented here. On one hand, solving the ODEs of the HH neuronal network using the forward Euler method yields quadratic time complexity ($T \sim O(N^2)$). Using more accurate solver variants such as Runge-Kutta order-4 (RK4) and Livermore Solver for Ordinary Differential Equations(LSODA) increases the overall magnitude of T yet returns consistent complexity $c \approx 2$. On the other hand, our CA model presents a linear time complexity ($T \sim O(N)$) indicating a much faster computational time than simulating interconnected HH neurons, especially for much larger system size N.

Figure 15 also shows that the T-values for HH neuronal population sizes beyond $N = 4,096$ is absent. Running simulations for larger sizes causes our current computational machines to exceed their memory capacity. The use of our CA model shows significant advantage in simulating up to millions of neurons (more than 10^3 times the other reported approach) before this memory problem happens. The algorithm of the CA model can be more straightforwardly parallelized and GPU-implemented to amplify the neuronal population without increasing the simulation time.

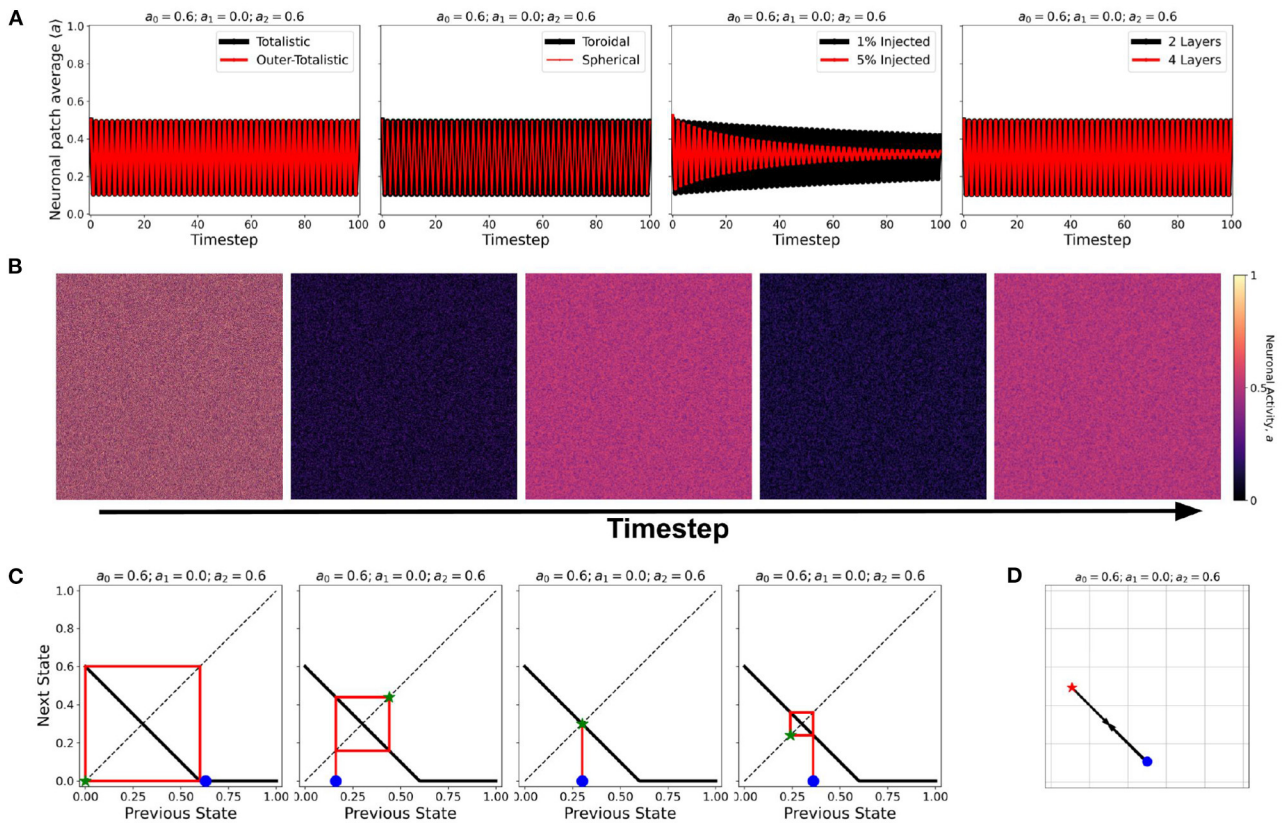

FIGURE 12 | (A) Steady-state dynamics of Class 2 CA using the various neighborhood and boundary conditions aforementioned. **(B)** Snapshots showing spatiotemporal evolution of Class 2 CA. **(C)** Cobweb diagrams for each possible initial condition (marked by •) in a Class 2 CA with threshold values $a_0 = 0.6$, $a_1 = 0.0$, and $a_2 = 0.6$. **(D)** Trajectory of the neuronal steady-state activity in state-space. The average state of the CA are marked at $t = 0$ (•) and at $t = \infty$ (⋆) with the black arrows tracing the trajectory. It is notable that the neuronal CA cycles back and forth along the path of evolution.

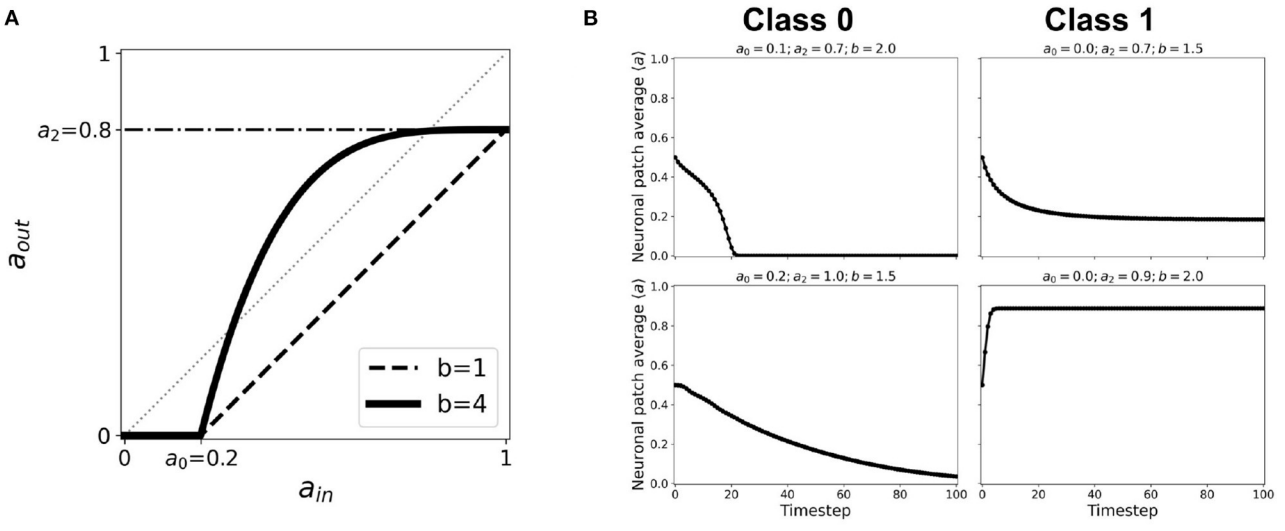

FIGURE 13 | (A) Representative nonlinear activation function ($b = 4$) using the second-order approximation given by Equation 2 with thresholds $a_0 = 0.2$, $a_1 = 1.0$, $a_2 = 0.8$. The black dashed line shows the same thresholds with nonlinearity parameter $b = 1$, which is equivalent to the case of first-order approximated activation function. **(B)** Representative steady-state dynamics for each class using nonlinear activation function ($b > 1$).

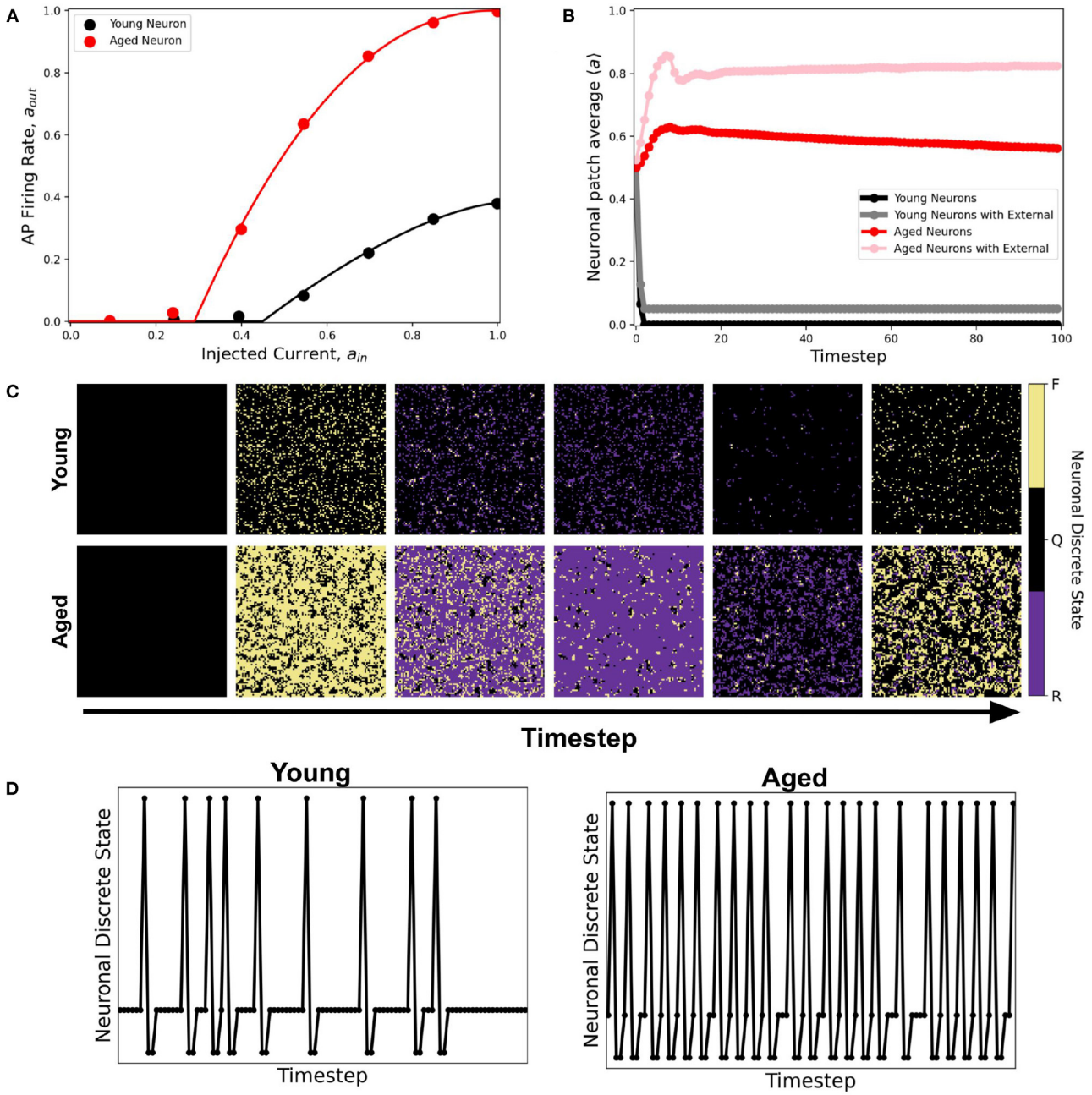

FIGURE 14 | (A) Activation function of young (black) and aged (red) neuronal population derived from empirical data from rhesus monkey prefrontal cortex (Coskren et al., 2015). The dots are the dataset from the study, while the solid lines are the activation function fitted using Equation 2. The parameter thresholds are $a_0 = 0.45$, $a_2 = 0.38$, $b = 1.5$ for the young neuronal system, and $a_0 = 0.29$, $a_2 = 1.0$, $b = 2.2$ for the aged population. **(B)** Corresponding average steady-state dynamics of young and aged neuronal population using the CA model. **(C)** Actual response of young and aged neuronal patch obtained using the method described in Ramos and Bantang (2018) and Ramos and Bantang (2021). The color represents the discrete state the neuron is in: Q (Quiescent), F (Firing), R (Refractory). **(D)** Representative temporal response of a single neuron from the young and aged neuronal patch according to the discrete states in **(C)**.

10. CONCLUSIONS

In this work, we proposed a cellular automata (CA) model as an efficient way of modeling large numbers of neurons that can reduce both computational time and memory requirements in simulation. We implemented neuronal dynamics on a neuronal CA patch of lattice size $1,024 \times 1,024$ using a first-order linear approximation of the resulting activation function of the HH model. The system dynamics is characterized according to the three parameters of the resulting activation function.

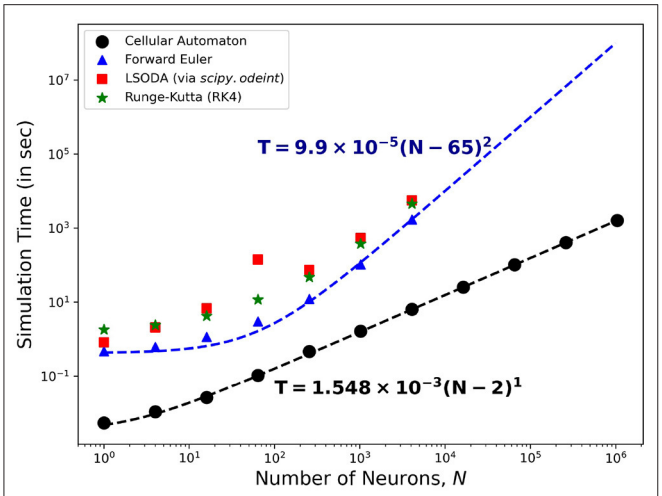

FIGURE 15 | Time complexity of the neuronal model comparing different algorithms for solving the HH dynamics. The forward Euler method (marked ▲) shows quadratic order in time ($\sim O(N^2)$) while the CA model (marked •) presents a linear complexity time ($\sim O(N)$) indicating the efficiency of using the CA model in simulation of neuronal patch dynamics.

The steady-state dynamics are investigated for different lattice configuration (2D and quasi-3D), boundary conditions (toroidal and spherical), layering (one- or two-layered), and Moore neighborhood type (totalistic and outer-totalistic). Cases wherein a fraction (1% and 5%) of neurons have constant activation input (a_{in}) are also explored. We observed the following CA classification:

1. Class 0: Quiescent Steady-State: (a) Fast-decay; (b) Slow-decay
2. Class 1: Spiking Steady-State: (a) With random patterns; (b) With exploding patterns
3. Class 2: Oscillatory Steady-State.

Numerical experiments of CA neuronal systems are shown to conform to this classification. While our analysis of the cobweb diagrams show that individual neuron states will eventually reduce to quiescent state, spiking steady-state can still emerge for a collection of interconnected neurons. Collective oscillatory behavior (Class 2) of the overall neuronal state is observed for the system with significant synchronization among neurons.

The proposed CA model is applied to analyze the resulting dynamical class of young and aged patches of neurons. The response function of individual young and aged neuronal cells are obtained from empirical data and are fitted to a second-order approximation for better semblance. The CA model for aged patch shows dynamics with higher average neuronal steady-state and therefore more robust spiking behavior compared to the younger population. This result conforms to the higher action potential firing rates of aged neurons from the empirical data. On one hand, the average neuronal steady-state is amplified for the aged population when injected with a small external input. On the other hand, the younger population needs higher external input to observe significant amplification of the average neuronal steady-state. This result conforms to the presence of spiking activity in aged neurons stimulated with lower external current. Whether artificially generated spatiotemporal patterns of neuronal patch activity in this work correspond to the activity of actual neuronal systems remains to be determined.

The cellular automata model presented here can easily be extended to model more realistic neuronal systems such as brain patches or even the whole brain. Individual neuronal response data can also be used to improve the choice of the CA activation function $a_{\text{out}} = f(a_{\text{in}})$. The activation function can be modified into similar input-output mapping in frequency domain or voltage-current domain, and can be used as the rule for our CA model. Our computational modeling framework can be utilized for large scale simulation of different neuronal conditions such as Parkinson's disease (Bevan et al., 2002; Kang and Lowery, 2014), Alzheimer's disease, and chronic traumatic encephalopathy (Gabrieli et al., 2020; Wickramaratne et al., 2020).

We presented here that an adult brain shows an increase of neuronal response, even in the presence of constant external input. However, it remains a challenge to understand in which particular biological aspect these changes correspond to. In future studies, we recommend investigating dynamical systems of interconnected neurons, both young and aged, in the following aspects: 1) input-output mapping; 2) spatiotemporal distribution; and 3) connectivity architecture. Learning about the dynamics of these systems would help medical practitioners to detect early signs of ailments or disorders stemming from the aging process and help identify appropriate medicinal (chemical, radiation), behavioral (lifestyle, dietary) and/or surgical intervention.

DATA AVAILABILITY STATEMENT

The original contributions presented in the study are included in the article/**Supplementary Material**, further inquiries can be directed to the corresponding author.

AUTHOR CONTRIBUTIONS

RR did the simulation and wrote the manuscript draft. All authors conceived the research problem and analyzed the results, and edited the final manuscript.

ACKNOWLEDGMENTS

This work was supported by the Institute for Neurosciences, St. Luke's Medical Center. RXAR acknowledges the Department of Science and Technology (DOST) for his Advanced Science and Technology Human Resources Development Program (ASTHRDP) scholarship.

SUPPLEMENTARY MATERIAL

The Supplementary Material for this article can be found online at: https://www.frontiersin.org/articles/10.3389/fninf.2021.763560/full#supplementary-material

REFERENCES

Ananthanarayanan, R., Esser, S. K., Simon, H. D., and Modha, D. S. (2009). "The cat is out of the bag: Cortical simulations with 109 neurons, 1013 synapses," in *Proceedings of the Conference on High Performance Computing Networking, Storage and Analysis, SC '09* (New York, NY: Association for Computing Machinery), 1–12.

Arciaga, M., Pastor, M., Batac, R., Bantang, J., and Monterola, C. (2009). Experimental observation and an empirical model of enhanced heap stability resulting from the mixing of granular materials. *J. Stat. Mech*. 2009, P07040. doi: 10.1088/1742-5468/2009/07/P07040

Bevan, M. D., Magill, P. J., Hallworth, N. E., Bolam, J. P., and Wilson, C. J. (2002). Regulation of the timing and pattern of action potential generation in rat subthalamic neurons *in vitro* by gaba-a ipsps. *J. Neurophysiol*. 87, 1348–1362. doi: 10.1152/jn.00582.2001

Brunel, N., and Van Rossum, M. C. (2007). Quantitative investigations of electrical nerve excitation treated as polarization. *Biol. Cybern*. 97, 341–349. doi: 10.1007/s00422-007-0189-6

Çelik Karaaslanl, C. (2012). "Bifurcation analysis and its applications," in *Numerical Simulation: From Theory to Industry, Chapter 1*, ed M. Andriychuk (London: INTECH Open Access Publisher, Pidstryhach Institute for Applied Problems of Mechanics and Mathematics), 3–34.

Coskren, P. J., Luebke, J. I., Kabaso, D., Wearne, S. L., Yadav, A., Rumbell, T., et al. (2015). Functional consequences of age-related morphologic changes to pyramidal neurons of the rhesus monkey prefrontal cortex. *J. Comput. Neurosci*. 38, 263–283. doi: 10.1007/s10827-014-0541-5

Dalton, J. C., and FitzHugh, R. (1960). Applicability of Hodgkin-Huxley model to experimental data from the giant axon of lobster. *Science* 131, 1533–1534. doi: 10.1126/science.131.3412.1533

Gabrieli, D., Schumm, S. N., Vigilante, N. F., Parvesse, B., and Meaney, D. F. (2020). Neurodegeneration exposes firing rate dependent effects on oscillation dynamics in computational neural networks. *PLoS ONE* 15:e234749. doi: 10.1371/journal.pone.0234749

Gerstner, W., Kistler, W. M., Naud, R., and Paninski, L. (2014). *Neuronal Dynamics: From Single Neurons to Networks and Models of Cognition and Beyond*. Cambridge: Cambridge University Press.

Hawick, K., and Scogings, C. (2011). "Cycles, transients, and complexity in the game of death spatial automaton," in *Proceedings of International Conference on Scientific Computing (CSC-11)*. (Las Vegas, NV: CSREA), 241–247.

Hodgkin, A. L., and Huxley, A. F. (1952). A quantitative description of membrane current and its application to conduction and excitation in nerve. *J. Physiol*. 117, 500–544. doi: 10.1113/jphysiol.1952.sp004764

Kang, G., and Lowery, M. (2014). Effects of antidromic and orthodromic activation of stn afferent axons during dbs in parkinson's disease: a simulation study. *Front. Comput. Neurosci*. 8:32. doi: 10.3389/fncom.2014.00032

Lapicque, L. (1907). Recherches quantitatives sur l'excitation électrique des nerfs traitée comme une polarisation. *J. Physiol. Pathol. Gen*. 9, 620–635.

Morris, C., and Lecar, H. (1981). Voltage oscillations in the barnacle giant muscle fiber. *Biophys. J*. 35, 193–213. doi: 10.1016/S0006-3495(81)84782-0

Mostany, R., Anstey, J. E., Crump, K. L., Maco, B., Knott, G., and Portera-Cailliau, C. (2013). Altered synaptic dynamics during normal brain aging. *J. Neurosci*. 33, 4094–4104. doi: 10.1523/JNEUROSCI.4825-12.2013

Nagumo, J., Arimoto, S., and Yoshizawa, S. (1962). An active pulse transmission line simulating nerve axon. *Proc. IRE* 50, 2061–2070. doi: 10.1109/JRPROC.1962.288235

Noble, D. (1962). A modification of the Hodgkin Huxley equations applicable to Purkinje fibre action and pacemaker potentials. *J. Physiol*. 160, 317–352. doi: 10.1113/jphysiol.1962.sp006849

Pang, J. C. S., and Bantang, J. Y. (2015). Hodgkin huxley neurons with defective and blocked ion channels. *Int. J. Modern Phys. C* 26, 1550112. doi: 10.1142/S0129183115501120

Pannese, E. (2011). Morphological changes in nerve cells during normal aging. *Brain Struct. Funct*. 216, 85–89. doi: 10.1007/s00429-011-0308-y

Peters, A. (2007). "The effects of normal aging on nerve fibers and neuroglia in the central nervous system," in *Brain Aging*. (Boca Raton, FL: CRC Press), 97–126.

Ramos, R., and Bantang, J. (2018). "Proposed cellular automaton model for a neuronal patch with a thresholded linear activation function," in *Proceedings of the Samahang Pisika ng Pilipinas, Vol. 36* (SPP-2018-PB-37), (Puerto Princesa).

Ramos, R., and Bantang, J. (2019a). "Classification of the dynamics of an outer-totalistic 2D and quasi-3D cellular automata simplistic models of neuronal patches," in *16th International Conference on Molecular Systems Biology* (Manila: BST 2019, De La Salle University Poster presentation), Available online at: https://drive.google.com/file/d/1bs655p68uv0SpZmmOcDr8MFV-_bWLvo_/view.

Ramos, R., and Bantang, J. (2019b). "An outer-totalistic 2D and quasi-3D cellular automata simplistic models of neuronal patches," in *Brain Connects 2019 and the 9th Neuroscience International Symposium* (Taguig: St. Luke's Medical Center, Global City. Poster and oral presentation), BC2019-14.

Ramos, R. X., and Bantang, J. (2019c). "Totalistic cellular automata model of a neuronal network on a spherical surface," in *Proceedings of the Samahang Pisika ng Pilipinas, Vol. 37*, (Tagbilaran). SPP-2019-PB-16.

Ramos, R. X. A. (2019). *Dynamics of a neuronal lattice network with a linear activation function using cellular automata modelling* (Bachelor's thesis). National Institute of Physics, College of Science, University of the Philippines, Diliman, Quezon City.

Ramos, R. X. A., and Bantang, J. Y. (2020). "Verhulst and bifurcation analyses of a neuronal network on an outer-totalistic toroidal cellular automata," in *Proceedings of the Samahang Pisika ng Pilipinas, Vol. 38*, (Quezon City). SPP-2020-3C-05.

Ramos, R. X. A., and Bantang, J. Y. (2021). "Simplified cellular automata model of neuronal patch dynamics with generalized non-linear cell response," in *Proceedings of the Samahang Pisika ng Pilipinas, Vol. 39*, (Quezon City). (SPP-2021-PB-03).

Rivera, A. D., Pieropan, F., Chacon-De-La-Rocha, I., Lecca, D., Abbracchio, M. P., Azim, K., et al. (2021). Functional genomic analyses highlight a shift in gpr17-regulated cellular processes in oligodendrocyte progenitor cells and underlying myelin dysregulation in the aged mouse cerebrum. *Aging Cell*. 20:e13335. doi: 10.1111/acel.13335

Stoop, R., and Steeb, W.-H. (2006). *Berechenbares Chaos in Dynamischen Systemen*. Basel: Springer-Verlag.

Tal, D., and Schwartz, E. (1997). Computing with the leaky integrate-and-fire neuron: logarithmic computation and multiplication. *Neural Comput*. 9, 305–318. doi: 10.1162/neco.1997.9.2.305

von Neumann, J. (1966). *Theory of Self-Reproducing Automata*. Champaign, IL: University of Illinois Press.

Wickramaratne, S. D., Mahmud, M. S., and Ross, R. S. (2020). "Use of brain electrical activity to classify people with concussion: a deep learning approach," in *ICC 2020-2020 IEEE International Conference on Communications (ICC)* (Dublin), 1–6.

Wilson, H. R., and Cowan, J. D. (1972). Excitatory and inhibitory interactions in localized populations of model neurons. *Biophys. J*. 12, 1–24. doi: 10.1016/S0006-3495(72)86068-5

Wolfram, S. (2002). *A New Kind of Science*. Champaign, IL: Wolfram Media, Inc. Available online at: https://www.wolframscience.com/nks/.

Conflict of Interest: The authors declare that the research was conducted in the absence of any commercial or financial relationships that could be construed as a potential conflict of interest.

frontiers in Aging Neuroscience

ORIGINAL RESEARCH
published: 12 January 2022
doi: 10.3389/fnagi.2021.785666

The Influence of Aging on the Functional Connectivity of the Human Basal Ganglia

Clara Rodriguez-Sabate[1,2], *Ingrid Morales*[1,2] *and Manuel Rodriguez*[1,2]*

[1] Center for Networked Biomedical Research in Neurodegenerative Diseases, Madrid, Spain, [2] Laboratory of Neurobiology and Experimental Neurology, Department of Basic Medical Sciences, Physiology, Faculty of Medicine, University of La Laguna, San Cristóbal de La Laguna, Spain

Although basal ganglia (BG) are involved in the motor disorders of aged people, the effect of aging on the functional interaction of BG is not well-known. This work was aimed at studying the influence of aging on the functional connectivity of the motor circuit of BG (BGmC). Thirty healthy volunteers were studied (young-group 26.4 ± 5.7 years old; aged-group 63.1 ± 5.8 years old) with a procedure planned to prevent the spurious functional connectivity induced by the closed-loop arrangement of the BGmC. BG showed different functional interactions during the inter-task intervals and when subjects did not perform any voluntary task. Aging induced marked changes in the functional connectivity of the BGmC during these inter-task intervals. The finger movements changed the functional connectivity of the BG, these modifications were also different in the aged-group. Taken together, these data show a marked effect of aging on the functional connectivity of the BGmC, and these effects may be at the basis of the motor handicaps of aged people during the execution of motor-tasks and when they are not performing any voluntary motor task.

Keywords: aging, basal ganglia, functional connectivity, hand motion, resting state

OPEN ACCESS

Edited by:
Henning Müller, University of Applied Sciences and Arts of Western Switzerland, Switzerland

Reviewed by:
Jan Kassubek, University of Ulm, Germany
Kaundinya S. Gopinath, Emory University, United States

***Correspondence:**
Manuel Rodriguez
mrdiaz@ull.edu.es

Specialty section:
This article was submitted to Neurocognitive Aging and Behavior, a section of the journal Frontiers in Aging Neuroscience

Received: *29 September 2021*
Accepted: *14 December 2021*
Published: *12 January 2022*

Citation:
Rodriguez-Sabate C, Morales I and Rodriguez M (2022) The Influence of Aging on the Functional Connectivity of the Human Basal Ganglia. Front. Aging Neurosci. 13:785666. doi: 10.3389/fnagi.2021.785666

HIGHLIGHTS

- The effect of aging on the basal ganglia interactions was studied with neuroimaging methods.
- Aging deteriorates the functional connectivity of basal ganglia.
- Basal ganglia are involved in the motor disorders of aged people.

INTRODUCTION

The decline of motor abilities associated with aging normally occurs parallel to changes in different cortical and subcortical motor centers (Fjell and Walhovd, 2010; Seidler et al., 2010). Although changes in the volume (Seidler et al., 2010; Walhovd et al., 2011) and structural connectivity (Bhagat and Beaulieu, 2004; Wang et al., 2010; De Groot et al., 2015; Cox et al., 2016; Behler et al., 2021) of basal ganglia (**BG**) may be involved in age-associated motor deterioration, the actual role of these changes has not been clearly established. A circumstance that limits the association of the motor handicaps and the BG changes induced by aging is that although motor deterioration is better known (Sun et al., 2012; Ferreira and Busatto, 2013; Mathys et al., 2014; Sala-Llonch et al., 2015; Xiao et al., 2018), the effect of aging on the functional connectivity of BG is less clear. The study of BG activity with magnetic resonance imaging (**MRI**), and particularly with functional connectivity

MRI (**fcMRI**), has reported inconsistent results indicating an increase (Marchand et al., 2011), a decrease (Taniwaki et al., 2007) or no changes (Baudrexel et al., 2011) in the functional connectivity of BG with aging. This low consistency of fcMRI studies may be associated with age-related changes in the neuro-vascular coupling (Riecker et al., 2003), the small size of some BG (which hampers the grouping of data obtained in different subjects), and the closed-loop wiring of BG (the interaction between two centers may reflect the circulation of information across the BG closed-loop circuit more than their direct interaction).

This work was planned to study the influence of aging on the functional connectivity of the BG regions directly involved in the execution of movements, the BG nuclei included in the BG motor circuit (**BGmC**). BGmC is a closed-loop circuit composed of projections from the primary motor cortex (**M1**) to the posterior regions of the putamen (**Put**), and from this center to the external globus pallidum (**GPe**), subthalamic nucleus (**STN**), internal globus pallidum (**GPi**), substantia nigra (**SN**), and the motor thalamus (**MTal**), a thalamic region that sends projections back to the M1 and completes the closed-loop circuit of BG (Alexander et al., 1986; Hoover and Strick, 1993; Delong and Wichmann, 2009). In order to prevent the fcMRI computed between two centers from being "contaminated" by their common interactions with other BG, data used to study the interaction between each two BG were "regressed" with data recorded in all the other BG (partial correlation) (Zhang et al., 2008, 2010). In order to prevent the "contamination" of the blood-oxygen-level-dependent (**BOLD**) data of the smallest BG (e.g., STN) by those of surrounding structures, the data used to represent the activity of each center was computed by averaging voxels included in a volume-of-interest (**VOI**) which was located inside each BG of each subject according to previously reported procedures (Rodriguez-Sabate et al., 2015, 2017b). The partial correlation coefficient (**CC**) was used to estimate the "magnitude" of the functional interaction of BG (Fox and Raichle, 2007), and a block-task paradigm with interleaved "no-motion"/"motion" (hand movements) intervals was used to study the influence of motion on the BG interaction (Fair et al., 2007).

METHODS

Subjects

Thirty healthy volunteers 20–67 years of age (15 men and 15 women; 45.1 ± 12.6 years old; mean ± standard deviation) showing: (1) no acute or chronic illness, (2) no history of neurological diseases (they showed a normal neurological examination and no evidence of motor disorders according to the Hoehn and Yahr, the Schwab and England scales), (3) no history of psychiatric diseases (including no evidence of dementia and normal values in the Montreal Cognitive Assessment and the Mini Mental State examinations), (4) normal values in basic laboratory tests, and (5) Normal MRI scans. Written informed consent was provided by all participants, and all procedures were in accordance with the ethical standards of the Declaration of Helsinki. The study was approved by an institutional review board (Human Studies Committee-La Laguna University). Subjects were divided into two groups, the young-group (26.4 ± 5.7 years old; 8 men with an average age of 25.4 and 7 women with an average age of 27.3) and the aged-group (63.1 ± 5.8 years old; 7 men with an average age of 61.7 and 8 women with an average age of 64.5).

Data Collection

The basic experimental procedures were similar to those previously reported (Rodriguez-Sabate et al., 2015, 2017a). Briefly, the BOLD-fluctuation of BG was used to study the functional connectivity of the BGmC in subjects who performed a motor-task or remained at rest. A block-task paradigm with interleaved "no-motion"/"motion" intervals was used. During the motor-task block, subjects performed a repetitive sequence of finger extensions/flexions with the right-hand (from the little finger to the thumb and back to the little finger). During the no-motion block, subjects did not perform any planned task. The transitions between the no-motion and motion time intervals were orally announced by a single word, "MOVE" to start motion and "STOP" to finish motion. One hundred volumes were recorded in each of the four task-blocks. In order to prevent the effects of the transitions between tasks (the change of the BOLD signal baseline may need seconds) the frames 1–10 of each block were not included in the data analysis.

BOLD-contrast images (64 × 64 sampling matrix with voxels of 4 × 4 × 4 mm) were acquired (GE; 3.0 T) in a coronal plane (250 × 250 mm field of view) with gradient-echo (echo-planar imaging; repetition-time 1,600 ms; echo-time 21.6 ms; flip-angle 90°). fMRI data were co-registered with 3D anatomical images (repetition-time 7.6 ms; echo-time 1.6 ms; flip-angle 12°; 250 × 250 mm field of view; 256 × 256 sampling matrix; voxels of 1 × 1 × 1 mm). Functional and anatomical studies were obtained in a single session and with the head fixed in the same position. Different structural markers were jointly used to decide where to place each ROI in the brain of each subject (Rodriguez-Sabate et al., 2017b). Briefly, ROIs were positioned in each center of each subject by using the Talairach coordinates, the shape of the nucleus, and the anatomical relationship of the nucleus with other structures (external cues) as the main indicators (working with normalized 3D-anatomical images). All centers were identified in coronal slices located 4–27 mm posterior to the anterior commissure. The optic tract, internal capsule, and medial forebrain bundle were used as external cues to identify the putamen, GPe, GPi and MTal. GPi was initially identified ≈6 mm posterior to anterior commissure and just over the optic tract. The ROI for the putamen was located at post-commissural level because the somato-sensorimotor regions primarily project to the posterior putamen. The post-commissural putamen was then identified ≈5 mm posterior to anterior commissure. GPe was located ≈3 mm posterior to the anterior commissure. MTal was located ≈11 mm posterior to anterior commissure (5 mm posterior to the GPi). Special care was taken to identify the STN. Three external cues were used to identify the STN, the oculomotor nerve, cerebral peduncle, and pons. Coronal images were initially moved backwards and forwards (between 10 and 18 mm posterior to anterior commissure) to identify the slice where the oculomotor nerve was trapped in the most medial

region of the contact between the pons and cerebral peduncle. The backward-forward movements of the slices were also used to identify the slice where the oculomotor nerve was trapped between the pons and cerebral peduncle. The STN was identified, in this slice, as the center located 10 mm medial to the optical tract, just above a horizontal line crossing this tract and near the medial boundary of the cerebral peduncle. The STN, in this position, was mainly surrounded by tracts and located anterior to the SN. So as not to mix data on specific centers with those of the surrounding centers, the ROIs were generally small and clearly located within each nucleus. This was not the case of the SN. In humans, SN pars compacta is intermixed with SN pars reticulata and both portions of the SN cannot be clearly segregated in MRI images. Thus, the ROI in this case included the whole SN, and was located between the red nucleus and posterior commissure in slices −22 to −26 mm posterior to the anterior commissure. The M1 representation of the hand was located in the precentral gyrus, just posterior to the junction of the superior frontal sulcus with the precentral sulcus. Depending on the slice level, the hand representation in M1 has a "zig-zag" or "step-like" shape or a "hook" or "Ω" shape. This distribution was generally observed in a position anterior to the protrusion ("knob") of the precentral gyrus toward the central sulcus. The fMRI response was also used to verify the location of M1 (10 voxels showing the maximum BOLD response to finger movements) because the comparison of the BOLD signal between the no-motion and the motion intervals clearly showed an activation in hand representation in M1. This is a time consuming method, but it prevents the mixture of different brain regions when BOLD-data are integrated in an experimental group. All data sets were normalized to the Talairach space.

Data Pre-processing

Data were preprocessed (BrainVoyager software) with a slice scan-time correction, a 3D-motion correction, and a temporal filtering (0.009 Hz high-pass GLM-Fourier filter). No spatial smoothing was performed, and studies with a brain-translation >0.5 mm or a brain-rotation >0.5 degrees were rejected. Residual motion artifacts and physiological signals (respiration, cardiac activity) were diminished by regressing the BOLD-signals with the mean average of the BOLD-signals recorded in white matter and brain ventricles (Power et al., 2014).

Correlation Methods

fcMRI was computed with the mean BOLD-signal of voxels included in each VOI, and values of right and left brain centers were grouped together (Gopinath et al., 2011). The Pearson correlation coefficient (r; $p < 0.001$ two-tailed) was used to estimate the "strength" of the functional connectivity of the BG centers (Statistica-Statsoft, Tulsa). Partial correlations were used to eliminate the collateral influence of the other BG (used as "regressors") on the functional connectivity between two particular centers, a method which is particularly useful in closed-loop networks where the activity of any center may have time-relationships with the activity of all the other centers of the network (Zhang et al., 2008, 2010).

TABLE 1 | Coordinates are shown in mm (Talairach).

	X lateral	Y posterior	Z superior	Size
Primary motor cortex				
Young-group	31.1 ±3.8	−19.6 ±5.2	53.2 ±6.4	40.7 ±8.9
Aged-group	37.3 ±3.9	−19.7 ±5.3	48.3 ±5.3	37.2 ±10.9
Putamen				
Young-group	26.7 ±1.8	−4.8 ±1.2	0.33 ±0.1	21.9 ±4.1
Aged-group	27.1 ±1.3	−5.2 ±1.3	0.41 ±0.4	20.1 ±3.7
External pallidum				
Young-group	14.6 ±5.5	−2.4 ±0.6	2.0 ±1.8	8.5 ±4.0
Aged-group	16.8 ±1.9	−2.3 ±1.3	2.8 ±2.2	7.4 ±3.7
Internal pallidum				
Young-group	13.7 ±2.1	−6.4 ±1.1	−2.1 ±1.7	8.2 ±0.6
Aged-group	14.9 ±1.8	−6.1 ±1.7	−1.4 ±1.9	8.2 ±0.6
Subthalamic nucleus				
Young-group	11.2 ±1.5	−13.8 ±2.0	−3.3 ±2.5	11.3 ±4.6
Aged-group	10.8 ±1.7	−13.1 ±2.2	−5.1 ±2.7	12.1 ±3.6
Substantia nigra				
Young-group	7.3 ±1.6	−19.2 ±1.3	−7.9 ±1.7	224.1 ±31.1
Aged-group	7.2 ±0.7	−18.5 ±1.3	−9.1 ±3.1	217.1 ±29.3
Ventral-anterior thalamus				
Young-group	9.1 ±0.7	−11.0 ±1.0	6.6 ±3.0	22.6 ±6.2
Aged-group	9.6 ±1.2	−11.1 ±1.6	7.5 ±1.9	28.2 ±7.3

The size of the VOIs is shown by the number of their structural voxels.

The motor-task effect and the aging effect on the interaction between two centers were considered to be significant when the change of the partial correlation computed for their BOLD-signals reached statistical significance. Differences between two correlation coefficients were identified by using the r-to-Fisher-z transformation ($r' = 0.5*(ln(1 + r) - ln(1-r)$; *r′ being the Fisher-z transformed r)* and a two-sided t comparison (*mean and standard error of each sample evaluated against the t distribution with df = n1 + n2 – 2 degrees of freedom; n1 and n2 being the sample sizes*) adjusted for multiple comparisons (Greicius et al., 2003).

RESULTS

Table 1 shows the position and size (no. of voxels) of VOIs used to characterize the BOLD activity of BG. No statistical difference was found between the VOI sizes in the young and aged groups.

Functional Connectivity of BG During the No-Motion Intervals

Figure 1 shows the functional connectivity during the no-motion intervals (indicated by the partial correlation coefficient CC) in the young (left) and aged (right) groups. In the **young-group**, the M1 BOLD-activity showed a significant positive CC with the Put and GPe, and a negative correlation with the SN (**Figure 1A**). Positive correlations were also found between Put-STN (**Figure 1C**), GPe-SN (**Figure 1E**), GPe-GPi (**Figure 1E**), and STN-GPi (**Figure 1G**). The GPi, SN, and MTal did not showed any significant correlation between them (**Figure 1G**).

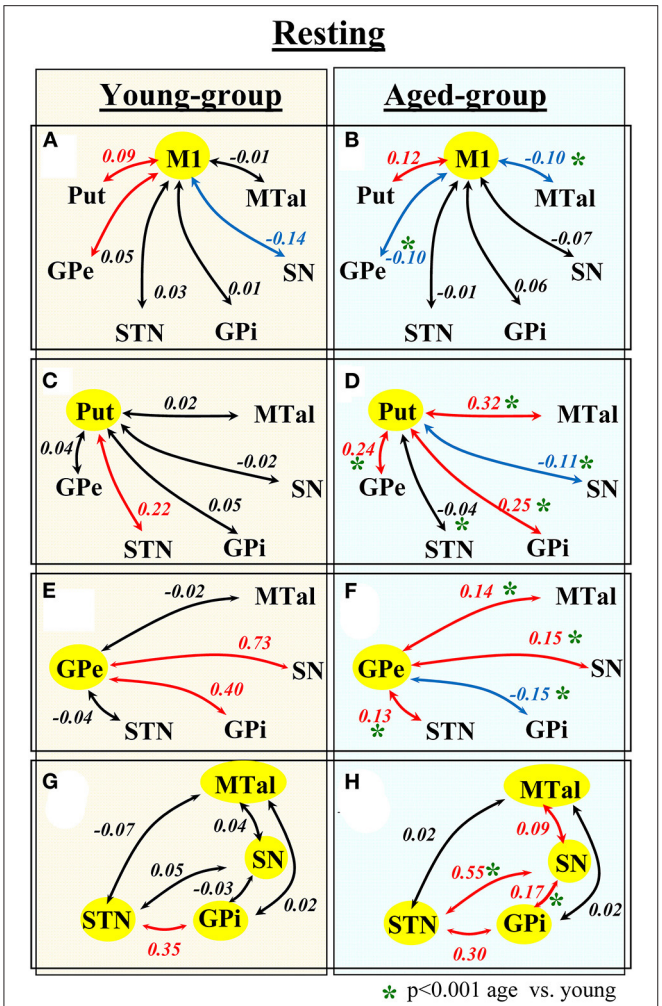

FIGURE 1 | Functional connectivity of BG during task-resting in the young- and aged-groups. Diagrams show the partial correlation coefficient in the young-group (left-hand side) and aged-group (right-hand side). Numbers represent the mean correlation coefficient, in red positive correlations, in blue negative correlations and in black no statistical correlations. Statistical differences between the correlation computed in the young- and aged-groups are shown by green asterisks. M1, primary motor cortex; Put, post-commissural putamen; GPe, external globus pallidum; STN, subthalamic nucleus; GPi, internal globus pallidum; SN, substantia nigral; and MTal, motor thalamus.

The functional connectivity in the **aged-group** was clearly different to that observed in the young-group. In the aged-group, the **M1** showed a significant positive correlation with the Put, and a negative correlation with the GPe and MTal (**Figure 1B**). The **Put** showed a positive correlation with the GPe, GPi, and MTal and a negative correlation with the SN (**Figure 1D**). The **GPe** showed a positive correlation with the STN, SN and MTal, and a negative correlation with the GPi (**Figure 1F**). The **STN** showed a positive correlation with the GPi and SN (**Figure 1H**). The **SN** showed a positive correlation with the GPi and MTal (**Figure 1H**). When compared with the young-group, the aged-group showed a significant increase of positive correlations between Put-GPe, Put-GPi, and Put-MTal (**Figures 1C,D**), GPe-MTal and GPe-STN (**Figures 1E,F**), STN-SN, SN-GPi and SN-MTal (**Figures 1G,H**), and a significant increase of negative correlations between M1-MTal, M1-GPe (**Figures 1A,B**) and Put-SN (**Figures 1C,D**). Some positive correlations found in the young-group vanished (Put-STN; **Figures 1C,D**) or were replaced by negative correlations (GPe-GPi in **Figures 1E,F**) in the aged-group.

Thus, aging induced a marked reconfiguration of BG activity during the no-motion intervals which in many cases increased the synchronicity of BG (positive correlations), but which in some cases increased their anti-synchronic activity (negative correlations) or replaced their synchronic behavior by anti-synchronic behavior. A summary of these changes is shown in **Figure 2**, where the significant synchronicity of two nuclei is shown with red lines, and their anti-synchronicity with blue lines. Three chains of BG connections were found in the young-group during the no-motion intervals (**Figure 2** left), a M1 ↔ Put ↔ STN ↔ GPi synchronic connection (green area), a M1 ↔ GPe ↔ GPi/SN synchronic connection (blue area), and an M1 ↔ SN anti-synchronic connection (orange area). In the aged-group (**Figure 2** right): (1) M1 ↔ Put ↔ STN ↔ GPi synchronicity was replaced by M1 ↔ Put ↔ GPe ↔ STN ↔ GPi synchronicity, (2) M1 ↔ GPe ↔ GPi/SN synchronicity showed a marked decrease of GPe ↔ SN synchronicity and M1 ↔ GPe and GPe ↔ GPi synchronicity were replaced by anti-synchronic activities, and (3) M1-SN anti-synchronicity vanished. These changes were accompanied by a synchronic co-activation of Put-GPi, Put-MTal, GPe-MTal, GPi-SN, SN-MTal, and STN-SN and by an anti-synchronic activation of the Put-SN and MTal-M1.

Functional Connectivity of BG During the Motor-Task

The influence of motion on the functional connectivity of BG was tested by comparing the CC computed during the motion and no-motion intervals. **Figure 3** shows the CC values in the young-group (**Figure 3** left) and aged-group (**Figure 3** right), with the CC values computed for the no-motion and motion intervals shown at the top and bottom of each square, respectively. Red numbers show significant positive correlations, blue numbers significant negative correlations and black numbers non-significant correlations. Significant differences in CC computed between the no-motion and motion intervals (asterisk) indicate the effect of motion on the BG functional connectivity. Only the functional relationships which changed with the motor activity are shown in this figure. Red arrows indicate significant changes of positive CC and blue arrows significant changes of negative CC.

In the young-group, finger-movements increased the M1-STN, M1-MTal, Put-GPi, Put-MTal, STN-MTal, and SN-MTal synchronicity, increased the Put-SN anti-synchronicity, decreased the Put-STN and GPe-SN synchronicity, and decreased the M1-SN anti-synchronicity. The effect of motion was different in the aged-group, which showed an increase of M1-Put, M1-GPi, Put-GPe, and GPi-SN synchronicity, an increase of the M1-STN, M1-MTal, and SN-MTal anti-synchronicity, a

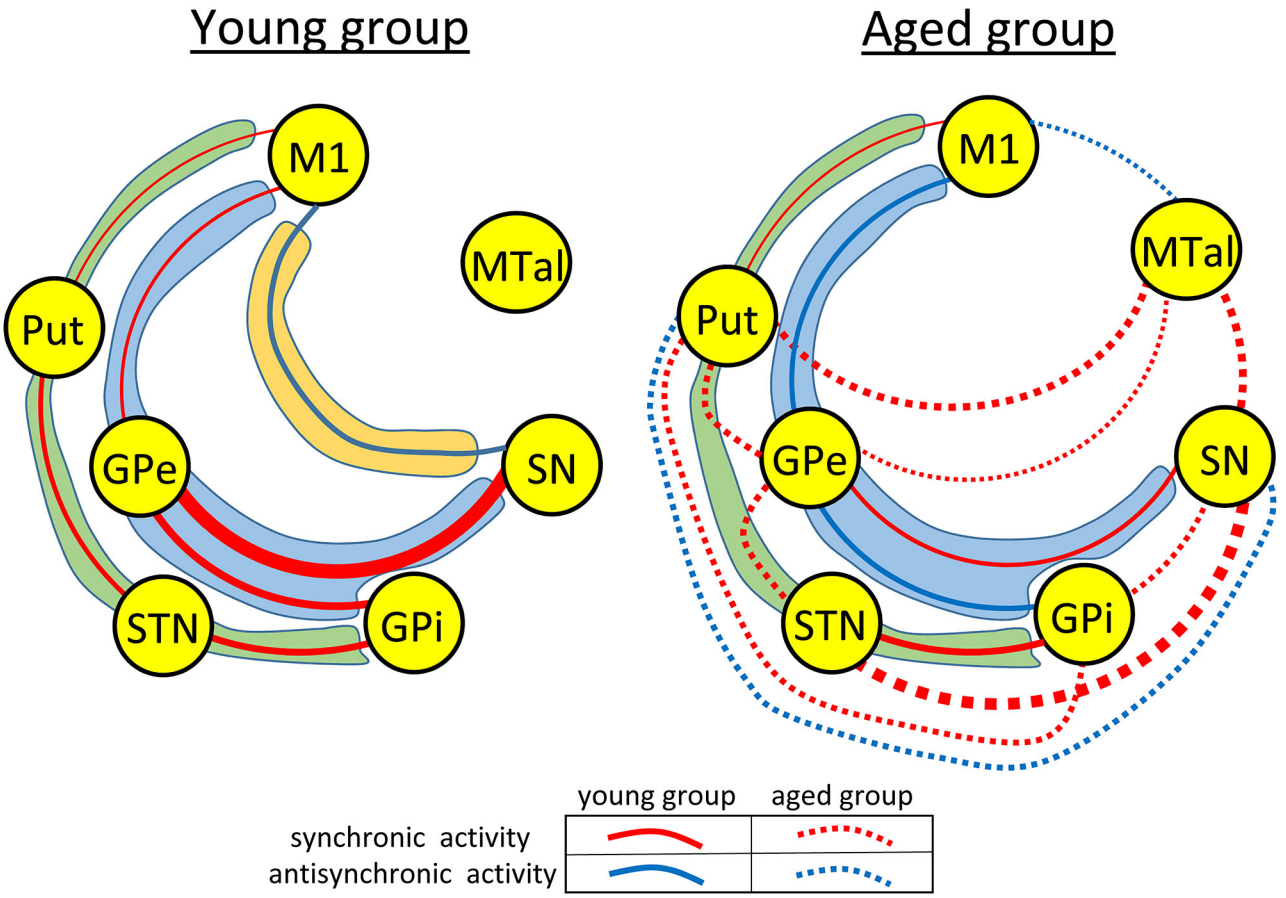

FIGURE 2 | Diagrams showing a summary of the main functional networks of the basal ganglia motor circuit in the young- and aged-groups during the no-motion intervals. Functional relationships with statistical significance are shown with red (synchronic activity) or blue (anti-synchronic activity) lines. The amplitude of correlations is represented by the thickness of the lines connecting the different basal ganglia. In the aged-group (right-side hand), correlations found in both the aged and young groups are shown with continuous lines, and those found in the aged-group but not in the young-group are shown with discontinuous lines. The main functional networks found during the no-motion intervals are grouped within areas of different colors, the M1 ↔ Put ↔ STN ↔ GPi network in green areas, the M1 ↔ GPe ↔ GPi/SN network in blue areas, and the M1-SN network in an orange area. M1, primary motor cortex; Put, post-commissural putamen; GPe, external globus pallidum; STN, subthalamic nucleus; GPi, internal globus pallidum; SN, substantia nigral; and MTal, motor thalamus.

decrease of STN-GPi and STN-SN synchronicity and a decrease of M1-GPe, M1-SN, and GPe-GPi anti-synchronicity.

DISCUSSION

The use of BOLD-data of VOIs located in the main nuclei of the BGmC and of the partial correlation method proved useful to study the effect of aging on the functional interaction of BG. BG showed marked changes in aged people during both the no-motion and motion intervals, suggesting that a different functional connectivity of BGmC nuclei may be at the basis of the motor deterioration induced by aging.

Functional Connectivity of the BGmC in Young People

The classical BG-model is based on excitatory/inhibitory relationships between their nuclei (Alexander et al., 1986; Hoover and Strick, 1993; Delong and Wichmann, 2009). fcMRI does not provide information about the structural connectivity between centers or about the mechanisms involved in their functional interactions. Positive and negative BOLD-correlations do not indicate the existence of excitatory or inhibitory connections, and a high BOLD-correlation between two centers does not necessarily imply their "direct" interaction (the functional connectivity between two centers can be facilitated by other "crossing centers" able to transmit the information between each other). Despite these methodological constraints, fcMRI may reveal some aspects of the functional dynamic of BG that can go unnoticed for the tracing techniques that identify structural connections between brain centers and for the single-unit recordings that identify excitatory-inhibitory interactions between individual neurons of two brain centers. Motor tasks often need seconds to be executed, which allows the identification of *task-positive motor networks* with fcMRI methods (1.6 s is the time-resolution here). Previous studies have identified functional networks by detecting brain centers with synchronous BOLD-signal fluctuations and a positive correlation between the BOLD-signals of their centers (Biswal et al., 1995; Uddin

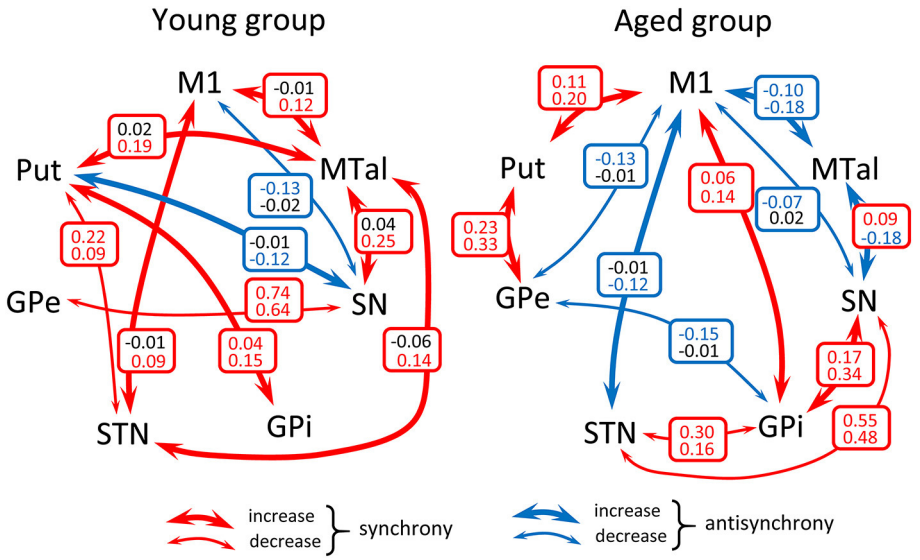

FIGURE 3 | Diagrams showing a summary of the action of motor activity on the functional connectivity of BG in the young- and aged-groups. Numbers show the mean correlation coefficient for each group computed during the no-motion (top of squares) and the motion (bottom of squares) time-intervals in the young-group (left-side hand) and aged-group (right-side hand). Red numbers show significant positive correlations, blue numbers significant negative correlations and black numbers non-significant correlations. Significant differences of the correlation coefficient computed during task-resting and the motor-task are shown by asterisks. Only the functional relationships which changed with the motor activity are shown in this figure (all comparison reached a $p < 0.001$ statistical significance). Red arrows indicate significant changes of positive correlations and blue arrows significant changes of negative correlations. M1, primary motor cortex; Put, post-commissural putamen; GPe, external globus pallidum; STN, subthalamic nucleus; GPi, internal globus pallidum; SN, substantia nigral; and MTal, motor thalamus.

et al., 2009; Tomasi and Volkow, 2010; Van Dijk et al., 2010; Tomasi et al., 2016). From this point of view, two centers showing no significant correlations do not belong to the same functional network (and could work in parallel without disturbing each other), and two centers showing a negative correlation (anti-synchronous BOLD-fluctuation) could belong to different networks with incompatible activities (Fox et al., 2005; Fair et al., 2007; Uddin et al., 2009; Hampson et al., 2010). In addition, motor networks may maintain their activity during the no-motion intervals, also working when subjects are not performing any voluntary motor task. Therefore, fcMRI is more suitable for analyzing the behavior of neuronal networks than for studying its "wiring" or the mechanisms involved in the interaction of their components. fcMRI data are more suitable to identify functional networks that to identify structural networks or to study the excitatory-inhibitory interactions between the centers of structural networks.

The young-group data suggest that the indirect pathway may work following two different functional arrangement, one involving a M1 ↔ Put ↔ STN ↔ GPi functional connectivity and the other involving a M1 ↔ GPe ↔ SN/GPi functional connectivity. M1 showed an anti-synchronous relationship with SN which suggests that the SN activation is followed by an M1 inactivation, a possibility which agrees with both the classical BG model (the GABAergic projections of SN to MTal inhibits the glutamatergic excitatory action of MTal on M1) (Alexander et al., 1986; Delong, 1990; Parent and Hazrati, 1995; Delong and Wichmann, 2009; Yin, 2017), and the fact that the inhibition of the SN activity (e.g., by inhibiting or lesioning the STN), and the fact that the inhibition of the SN activity (e.g., by inhibiting the STN) increases the M1 activity in Parkinson's disease (Obeso et al., 2000, 2017; Delong and Wichmann, 2009; Rodriguez-Rojas et al., 2018). The *functional networks* observed here during the no-motion intervals may be involved in the modulation of muscle tone, in the stabilization of body posture or in any function performed by BG when subjects are not executing voluntary motor patterns. The functional interaction of BG changed with the execution of the motor task. The synchronicity between most BG increased with voluntary movements (left-side **Figure 3**), showing that some nuclei of the BGmC are also involved in *task-positive motor networks*.

Functional Connectivity of the BGmC in Aged People

The aging processes induced a substantial restructuration of the BG activity during the no-motion intervals. In the M1 ↔ Put ↔ STN ↔ GPi network, the Put ↔ STN synchronicity was replaced by the Put ↔ GPe ↔ STN synchronicity. In the M1 ↔ GPe ↔ SN/GPi network, M1 ↔ GPe ↔ GPi synchronicity was replaced by anti-synchronicity, and GPe ↔ SN synchronicity decreased. The SN-M1 anti-synchronicity observed in the young-group vanished in the aged-group. Additional interactions were observed in the aged-group, including a synchronicity between Put-MTal, Put-GPi, STN-SN, GPe-MTal, GPi-SN and SN-MTal, and anti-synchronicity between Put-SN and MTal-M1 (right-side **Figure 3**). The BGmC is involved in the stabilization of

body posture (Takakusaki, 2017) and the modulation of muscle tone (Takakusaki et al., 2004), physiological functions that could be performed when subjects are not performing voluntary motor tasks. In this case, these motor problems of aged people (Woodhull-Mcneal, 1992; Agyapong-Badu et al., 2016) could be caused by a deficient functional connectivity of the *no-motion networks* of the BGmC.

The effect of motion on the BGmC was also different in the young and aged groups. BG synchronicities activated by motion in the young groups vanished in the aged group, with a number of anti-synchronicities and some new synchronicities not observed in the young group emerging in the aged-group (**Figure 3**). The BGmC is involved in the execution of unsupervised automatic motor patterns (Lehericy et al., 2005) which also decline with aging (Hellmers et al., 2018). The deficient functional connectivity of the *task-positive motor networks* of the BGmC observed here in the age-group could be at the basis of this behavioral problem.

The aged-group had an average age of 63 years old which was enough to find age-related differences with the young-group. These differences could be greater for older people but some misleading variables (e.g., instability of the motor task during the MRI study) could hamper the analysis of results, and therefore no person with more than 70 years of age was included in the study. The young and aged groups had similar compositions of men and women (8 men and 7 women in the young-group and 7 men and 8 women in the aged-group), and differences observed between the young and aged groups cannot be attributed to effects associated with gender. This does not mean that the effect of aging on BGmC is the same in both sexes, a possibility that would require a specific study. Different aged-related neurodegenerative diseases present muscle tone and motor behavior disorders. This is the case of Parkinson's disease, which normally shows slowness movements and muscle rigidity. It has been suggested that Parkinson's disease is produced by an accelerated aging of the brain, and particularly of the dopaminergic cells which control the basal ganglia motor circuit studied here (Rodriguez et al., 2014, 2015). Thus, it is possible that an increase of the aging effects on the basal ganglia motor circuit found here may be at the basis of some of the motor disorders of Parkinson disease.

In summary, present data provide evidence that the partial correlation of fcMRI data may be used to study the interactions of human BG when subjects are not performing voluntary movements, and to identify the modification of these interactions during the execution of particular tasks. This experimental approach even proved to be suitable to study complex closed-loop networks which, as occurs with the BGmC, present multiple structural and functional interactions between their components. The BGmC showed a generalized change of the functional connectivity of its center with aging, an effect observed during both the motion and the no-motion time-intervals. These changes may be at the basis of the movement and posture deterioration observed in age-related neurodegenerative disorders such as Parkinson's disease. New studies in aged people with particular motor handicaps are necessary to understand which BG interaction is involved in each of these problems. A similar study could be performed in Parkinson's patients with slowness movements (bradykinesia) or with a deterioration of the automatic activities which are necessary to maintain body posture.

DATA AVAILABILITY STATEMENT

The original contributions presented in the study are included in the article/supplementary material, further inquiries can be directed to the corresponding author/s.

ETHICS STATEMENT

The studies involving human participants were reviewed and approved by an Institutional Review Board (Human Studies Committee-La Laguna University). The patients/participants provided their written informed consent to participate in this study.

AUTHOR CONTRIBUTIONS

CR-S was involved in the planning and execution of the study, in the recording of data, and in the manuscript review. IM was involved in the execution of the study. MR was involved in the planning of the study, analysis and interpretation of data, and in the manuscript review. All authors contributed to the article and approved the submitted version.

FUNDING

This work was supported by the Center for Networked Biomedical Research in Neurodegenerative Diseases (CIBERNED; 2021/02), Madrid, Spain, and the Foundation Curemos el Parkinson, La Coruña, Spain.

REFERENCES

Agyapong-Badu, S., Warner, M., Samuel, D., and Stokes, M. (2016). Measurement of ageing effects on muscle tone and mechanical properties of rectus femoris and biceps brachii in healthy males and females using a novel hand-held myometric device. *Arch. Gerontol. Geriatr.* 62, 59–67. doi: 10.1016/j.archger.2015.09.011

Alexander, G. E., Delong, M. R., and Strick, P. L. (1986). Parallel organization of functionally segregated circuits linking basal ganglia and cortex. *Annu. Rev. Neurosci.* 9, 357–381. doi: 10.1146/annurev.ne.09.030186.002041

Baudrexel, S., Witte, T., Seifried, C., Von Wegner, F., Beissner, F., Klein, J. C., et al. (2011). Resting state fMRI reveals increased subthalamic nucleus-motor cortex connectivity in Parkinson's disease. *Neuroimage* 55, 1728–1738. doi: 10.1016/j.neuroimage.2011.01.017

Behler, A., Kassubek, J., and Muller, H. P. (2021). Age-related alterations in DTI metrics in the human brain-consequences for age correction. *Front. Aging Neurosci.* 13:682109. doi: 10.3389/fnagi.2021.682109

Bhagat, Y. A., and Beaulieu, C. (2004). Diffusion anisotropy in subcortical white matter and cortical gray matter: changes with aging and the role of CSF-suppression. *J. Magn. Reson. Imaging* 20, 216–227. doi: 10.1002/jmri.20102

Biswal, B., Yetkin, F. Z., Haughton, V. M., and Hyde, J. S. (1995). Functional connectivity in the motor cortex of resting human brain using echo-planar MRI. *Magn. Reson. Med.* 34, 537–541. doi: 10.1002/mrm.1910340409

Cox, S. R., Ritchie, S. J., Tucker-Drob, E. M., Liewald, D. C., Hagenaars, S. P., Davies, G., et al. (2016). Ageing and brain white matter structure in 3,513 UK Biobank participants. *Nat. Commun.* 7:13629. doi: 10.1038/ncomms13629

De Groot, M., Ikram, M. A., Akoudad, S., Krestin, G. P., Hofman, A., Van Der Lugt, A., et al. (2015). Tract-specific white matter degeneration in aging: the Rotterdam Study. *Alzheimers Dement* 11, 321–330. doi: 10.1016/j.jalz.2014.06.011

Delong, M., and Wichmann, T. (2009). Update on models of basal ganglia function and dysfunction. *Parkinsonism Relat. Disord.* 15(Suppl. 3), S237–240. doi: 10.1016/S1353-8020(09)70822-3

Delong, M. R. (1990). Primate models of movement disorders of basal ganglia origin. *Trends Neurosci.* 13, 281–285. doi: 10.1016/0166-2236(90)90110-V

Fair, D. A., Schlaggar, B. L., Cohen, A. L., Miezin, F. M., Dosenbach, N. U., Wenger, K. K., et al. (2007). A method for using blocked and event-related fMRI data to study "resting state" functional connectivity. *Neuroimage* 35, 396–405. doi: 10.1016/j.neuroimage.2006.11.051

Ferreira, L. K., and Busatto, G. F. (2013). Resting-state functional connectivity in normal brain aging. *Neurosci. Biobehav. Rev.* 37, 384–400. doi: 10.1016/j.neubiorev.2013.01.017

Fjell, A. M., and Walhovd, K. B. (2010). Structural brain changes in aging: courses, causes and cognitive consequences. *Rev. Neurosci.* 21, 187–221. doi: 10.1515/REVNEURO.2010.21.3.187

Fox, M. D., and Raichle, M. E. (2007). Spontaneous fluctuations in brain activity observed with functional magnetic resonance imaging. *Nat. Rev. Neurosci.* 8, 700–711. doi: 10.1038/nrn2201

Fox, M. D., Snyder, A. Z., Vincent, J. L., Corbetta, M., Van Essen, D. C., and Raichle, M. E. (2005). The human brain is intrinsically organized into dynamic, anticorrelated functional networks. *Proc. Natl. Acad. Sci. USA*. 102, 9673–9678. doi: 10.1073/pnas.0504136102

Gopinath, K., Ringe, W., Goyal, A., Carter, K., Dinse, H. R., Haley, R., et al. (2011). Striatal functional connectivity networks are modulated by fMRI resting state conditions. *Neuroimage* 54, 380–388. doi: 10.1016/j.neuroimage.2010.07.021

Greicius, M. D., Krasnow, B., Reiss, A. L., and Menon, V. (2003). Functional connectivity in the resting brain: a network analysis of the default mode hypothesis. *Proc. Natl. Acad. Sci. USA*. 100, 253–258. doi: 10.1073/pnas.0135058100

Hampson, M., Driesen, N., Roth, J. K., Gore, J. C., and Constable, R. T. (2010). Functional connectivity between task-positive and task-negative brain areas and its relation to working memory performance. *Magn. Reson. Imaging.* 28, 1051–1057. doi: 10.1016/j.mri.2010.03.021

Hellmers, S., Izadpanah, B., Dasenbrock, L., Diekmann, R., Bauer, J. M., Hein, A., et al. (2018). Towards an automated unsupervised mobility assessment for older people based on inertial TUG measurements. *Sensors (Basel)* 18:3310. doi: 10.3390/s18103310

Hoover, J. E., and Strick, P. L. (1993). Multiple output channels in the basal ganglia. *Science* 259, 819–821. doi: 10.1126/science.7679223

Lehericy, S., Benali, H., Van De Moortele, P. F., Pelegrini-Issac, M., Waechter, T., Ugurbil, K., et al. (2005). Distinct basal ganglia territories are engaged in early and advanced motor sequence learning. *Proc. Natl. Acad. Sci. USA*. 102, 12566–12571. doi: 10.1073/pnas.0502762102

Marchand, W. R., Lee, J. N., Suchy, Y., Garn, C., Johnson, S., Wood, N., et al. (2011). Age-related changes of the functional architecture of the cortico-basal ganglia circuitry during motor task execution. *Neuroimage* 55, 194–203. doi: 10.1016/j.neuroimage.2010.12.030

Mathys, C., Hoffstaedter, F., Caspers, J., Caspers, S., Sudmeyer, M., Grefkes, C., et al. (2014). An age-related shift of resting-state functional connectivity of the subthalamic nucleus: a potential mechanism for compensating motor performance decline in older adults. *Front. Aging Neurosci.* 6, 178. doi: 10.3389/fnagi.2014.00178

Obeso, I., Casabona, E., Rodriguez-Rojas, R., Bringas, M. L., Macias, R., Pavon, N., et al. (2017). Unilateral subthalamotomy in Parkinson's disease: cognitive, psychiatric and neuroimaging changes. *Cortex* 94, 39–48. doi: 10.1016/j.cortex.2017.06.006

Obeso, J. A., Rodriguez-Oroz, M. C., Rodriguez, M., Macias, R., Alvarez, L., Guridi, J., et al. (2000). Pathophysiologic basis of surgery for Parkinson's disease. *Neurology* 55, S7–12.

Parent, A., and Hazrati, L. N. (1995). Functional anatomy of the basal ganglia. I. The cortico-basal ganglia-thalamo-cortical loop. *Brain Res. Brain Res. Rev.* 20, 91–127. doi: 10.1016/0165-0173(94)00007-C

Power, J. D., Mitra, A., Laumann, T. O., Snyder, A. Z., Schlaggar, B. L., and Petersen, S. E. (2014). Methods to detect, characterize, and remove motion artifact in resting state fMRI. *Neuroimage* 84, 320–341. doi: 10.1016/j.neuroimage.2013.08.048

Riecker, A., Grodd, W., Klose, U., Schulz, J. B., Groschel, K., Erb, M., et al. (2003). Relation between regional functional MRI activation and vascular reactivity to carbon dioxide during normal aging. *J. Cereb Blood Flow. Metab.* 23, 565–573. doi: 10.1097/01.WCB.0000056063.25434.04

Rodriguez, M., Morales, I., Rodriguez-Sabate, C., Sanchez, A., Castro, R., Brito, J. M., et al. (2014). The degeneration and replacement of dopamine cells in Parkinson's disease: the role of aging. *Front. Neuroanat.* 8:80. doi: 10.3389/fnana.2014.00080

Rodriguez, M., Rodriguez-Sabate, C., Morales, I., Sanchez, A., and Sabate, M. (2015). Parkinson's disease as a result of aging. *Aging. Cell.* 14, 293–308. doi: 10.1111/acel.12312

Rodriguez-Rojas, R., Carballo-Barreda, M., Alvarez, L., Guridi, J., Pavon, N., Garcia-Maeso, I., et al. (2018). Subthalamotomy for Parkinson's disease: clinical outcome and topography of lesions. *J. Neurol. Neurosurg. Psychiatry* 89, 572–578. doi: 10.1136/jnnp-2017-316241

Rodriguez-Sabate, C., Llanos, C., Morales, I., Garcia-Alvarez, R., Sabate, M., and Rodriguez, M. (2015). The functional connectivity of intralaminar thalamic nuclei in the human basal ganglia. *Hum. Brain. Mapp.* 36, 1335–1347. doi: 10.1002/hbm.22705

Rodriguez-Sabate, C., Morales, I., Sanchez, A., and Rodriguez, M. (2017a). The multiple correspondence analysis method and brain functional connectivity: its application to the study of the non-linear relationships of motor cortex and Basal Ganglia. *Front. Neurosci.* 11:345. doi: 10.3389/fnins.2017.00345

Rodriguez-Sabate, C., Sabate, M., Llanos, C., Morales, I., Sanchez, A., and Rodriguez, M. (2017b). The functional connectivity in the motor loop of human basal ganglia. *Brain Imaging Behav.* 11, 417–429. doi: 10.1007/s11682-016-9512-y

Sala-Llonch, R., Bartres-Faz, D., and Junque, C. (2015). Reorganization of brain networks in aging: a review of functional connectivity studies. *Front. Psychol.* 6:663. doi: 10.3389/fpsyg.2015.00663

Seidler, R. D., Bernard, J. A., Burutolu, T. B., Fling, B. W., Gordon, M. T., Gwin, J. T., et al. (2010). Motor control and aging: links to age-related brain structural, functional, and biochemical effects. *Neurosci. Biobehav. Rev.* 34, 721–733. doi: 10.1016/j.neubiorev.2009.10.005

Sun, J., Tong, S., and Yang, G. Y. (2012). Reorganization of brain networks in aging and age-related diseases. *Aging. Dis.* 3, 181–193.

Takakusaki, K. (2017). Functional neuroanatomy for posture and gait control. *J. Mov. Disord.* 10, 1–17. doi: 10.14802/jmd.16062

Takakusaki, K., Oohinata-Sugimoto, J., Saitoh, K., and Habaguchi, T. (2004). Role of basal ganglia-brainstem systems in the control of postural muscle tone and locomotion. *Prog. Brain Res.* 143, 231–237. doi: 10.1016/S0079-6123(03)43023-9

Taniwaki, T., Okayama, A., Yoshiura, T., Togao, O., Nakamura, Y., Yamasaki, T., et al. (2007). Age-related alterations of the functional interactions within the basal ganglia and cerebellar motor loops *in vivo*. *Neuroimage* 36, 1263–1276. doi: 10.1016/j.neuroimage.2007.04.027

Tomasi, D., Shokri-Kojori, E., and Volkow, N. D. (2016). High-resolution functional connectivity density: hub locations, sensitivity, specificity, reproducibility, and reliability. *Cereb Cortex* 26, 3249–3259. doi: 10.1093/cercor/bhv171

Tomasi, D., and Volkow, N. D. (2010). Functional connectivity density mapping. *Proc. Natl. Acad. Sci. USA*. 107, 9885–9890. doi: 10.1073/pnas.1001414107

Uddin, L. Q., Kelly, A. M., Biswal, B. B., Xavier Castellanos, F., and Milham, M. P. (2009). Functional connectivity of default mode network components: correlation, anticorrelation, and causality. *Hum. Brain. Mapp.* 30, 625–637. doi: 10.1002/hbm.20531

Van Dijk, K. R., Hedden, T., Venkataraman, A., Evans, K. C., Lazar, S. W., and Buckner, R. L. (2010). Intrinsic functional connectivity as a tool for human connectomics: theory, properties, and optimization. *J. Neurophysiol.* 103, 297–321. doi: 10.1152/jn.00783.2009

Walhovd, K. B., Westlye, L. T., Amlien, I., Espeseth, T., Reinvang, I., Raz, N., et al. (2011). Consistent neuroanatomical age-related volume differences across multiple samples. *Neurobiol. Aging.* 32, 916–932. doi: 10.1016/j.neurobiolaging.2009.05.013

Wang, Q., Xu, X., and Zhang, M. (2010). Normal aging in the basal ganglia evaluated by eigenvalues of diffusion tensor imaging. *Am. J. Neuroradiol.* 31, 516–520. doi: 10.3174/ajnr.A1862

Woodhull-Mcneal, A. P. (1992). Changes in posture and balance with age. *Aging (Milano)* 4, 219–225. doi: 10.1007/BF03324095

Xiao, T., Zhang, S., Lee, L. E., Chao, H. H., Van Dyck, C., and Li, C. R. (2018). Exploring age-related changes in resting state functional connectivity of the amygdala: from young to middle adulthood. *Front. Aging Neurosci.* 10:209. doi: 10.3389/fnagi.2018.00209

Yin, H. H. (2017). The basal Ganglia in action. *Neuroscientist*. 23:299–313. doi: 10.1177/1073858416654115

Zhang, D., Snyder, A. Z., Fox, M. D., Sansbury, M. W., Shimony, J. S., and Raichle, M. E. (2008). Intrinsic functional relations between human cerebral cortex and thalamus. *J. Neurophysiol.* 100, 1740–1748. doi: 10.1152/jn.90463.2008

Zhang, D., Snyder, A. Z., Shimony, J. S., Fox, M. D., and Raichle, M. E. (2010). Noninvasive functional and structural connectivity mapping of the human thalamocortical system. *Cereb. Cortex.* 20, 1187–1194. doi: 10.1093/cercor/bhp182

Conflict of Interest: The authors declare that the research was conducted in the absence of any commercial or financial relationships that could be construed as a potential conflict of interest.

Publisher's Note: All claims expressed in this article are solely those of the authors and do not necessarily represent those of their affiliated organizations, or those of the publisher, the editors and the reviewers. Any product that may be evaluated in this article, or claim that may be made by its manufacturer, is not guaranteed or endorsed by the publisher.

frontiers in Human Neuroscience

ORIGINAL RESEARCH
published: 03 March 2022
doi: 10.3389/fnhum.2022.786853

Verbal Training Induces Enhanced Functional Connectivity in Japanese Healthy Elderly Population

Fan-Pei Gloria Yang[1,2,3], Tzu-Yu Liu[1,2†], Chih-Hsuan Liu[1,2†], Shumei Murakami[3] and Toshiharu Nakai[3,4]*

[1] Department of Foreign Languages and Literature, National Tsing Hua University, Hsinchu, Taiwan, [2] Center for Cognition and Mind Sciences, National Tsing Hua University, Hsinchu, Taiwan, [3] Department of Radiology, Graduate School of Dentistry, Osaka University, Suita, Japan, [4] Institute of NeuroImaging and Informatics, Obu, Japan

This study employs fMRI to examine the neural substrates of response to cognitive training in healthy old adults. Twenty Japanese healthy elders participated in a 4-week program and practiced a verbal articulation task on a daily basis. Functional connectivity analysis revealed that in comparison to age- and education-matched controls, elders who received the cognitive training demonstrated increased connectivity in the frontotemporal regions related with language and memory functions and showed significant correlations between the behavioral change in a linguistic task and connectivity in regions for goal-oriented persistence and lexical processing. The increased hippocampal connectivity was consistent with previous research showing efficacious memory improvement and change in hippocampal functioning. Moreover, the increased intra-network connectivity following cognitive training suggested an improved neural differentiation, in contrast to the inter-network activation pattern typical in the aging brain. This research not only validates the relationship of functional change in the frontal and temporal lobes to age-associated cognitive decline but also shows promise in turning neural change toward the right direction by cognitive training.

Keywords: fMRI, aging, connectivity, plasticity, hippocampus, rsfMRI = resting state fMRI

OPEN ACCESS

Edited by:
Jessica A. Turner, Georgia State University, United States

Reviewed by:
Takashi Tsukiura, Kyoto University, Japan
Kheng Seang Lim, University of Malaya, Malaysia
Ahmad Nazlim Bin Yusoff, Universiti Kebangsaan Malaysia, Malaysia

****Correspondence:***
Fan-Pei Gloria Yang
fbyang@gmail.com

† These authors have contributed equally to this work

Specialty section:
This article was submitted to Brain Health and Clinical Neuroscience, a section of the journal Frontiers in Human Neuroscience

Received: *30 September 2021*
Accepted: *11 January 2022*
Published: *03 March 2022*

Citation:
Yang F-PG, Liu T-Y, Liu C-H, Murakami S and Nakai T (2022) Verbal Training Induces Enhanced Functional Connectivity in Japanese Healthy Elderly Population. Front. Hum. Neurosci. 16:786853. doi: 10.3389/fnhum.2022.786853

INTRODUCTION

With the increasing aging population around the globe and the lack in effective treatment in dementia, measures to intervene cognitive decline are urgently needed. Cognitive training is one of the strategies that has shown some promise in the retention of cognitive functions for healthy elders and elders at risk for mild cognitive impairments (MCI) (Ball et al., 2002; Belleville, 2008; Valenzuela and Sachdev, 2009; Mowszowski et al., 2010; Rosen et al., 2011). Additionally, studies have suggested that enriching mental activities could moderate the deterioration process as healthy elders participating in social and cognitive activities were less likely to develop MCI and eventually converted to dementia (Wilson et al., 2002; Verghese et al., 2003, 2006; Prince et al., 2013). A recent review on non-pharmaceutical interventions based on 13 reviews or meta-analyses published from 2010 to 2019 reported that cognitive interventions focusing on memory or language skills, executive functions, social interactions, etc. were effective for maintaining or improving cognitive functions in older adults regardless of their cognitive status (Sanjuan et al., 2020). This raises the question of which type of language-based training is effective on older adults who are cognitively normal.

The transmission deficit hypothesis (TDH) has pointed out that the change in linguistic competence is asymmetric in aging, with comprehension relatively preserved and production strongly affected (Burke and Shafto, 2004). Behavioral evidence has shown that word retrieval problem in healthy aging is due to a failure in the complete retrieval of the phonology of the target word, instead of generalized slowing (Shafto et al., 2007). In another study using event-related potential (ERP) and visual evoked potential (VEP), healthy young and older adults performed an implicit picture-naming task while making a segmental or syllabic decision in a Go/No-go paradigm. The older adults showed longer latencies in both behavioral judgment and ERP amplitudes in response to phonological stimuli. In contrast, there was no latency difference between the young and old groups regarding the VEP stimuli. The authors concluded that age-associated delay was only specific to the phonological system and proposed that the practice of phonological skills might improve general linguistic abilities in older adults (Neumann et al., 2009). This study hypothesizes that a linguistic task focusing on articulatory skills will improve general linguistic abilities for two reasons. First, appropriate articulation calls for awareness of linguistic constituents, which are fundamentals for proper word and sentence production. Second, articulatory practice will activate the cortices and connectivity related to phonological retrieval, which has been reported to be the cause of production difficulty and word retrieval problem commonly seen in older adults (Shafto et al., 2007).

The temporal regions, particularly the medial portions, including the hippocampus, were most commonly impacted by neurodegeneration, as studies of MCI and early Alzheimer's disease (AD) have consistently revealed hippocampus atrophy (Braak and Braak, 1996; Kordower et al., 2001; Scheff et al., 2006). The hippocampus is related to conscious memory recollection, and the hippocampal lesions are associated with memory deficits in MCI and AD (Cohen and Squire, 1981; Tulving, 2002). Improvements in memory and change in hippocampal functioning could suggest alterations in the disease progression of MCI and AD. Therefore, interventions leading to the functional change in the hippocampus might be considered as an effective strategy for retention of cognitive reserve in successful aging. This study predicts the change in the functional connectivity in the hippocampus and sensory-motor regions after articulation training, as the training task taps into the cortices associated with movement and verbal memory. The frontal lobe is also anticipated to show improved connectivity as most previous studies have revealed frontal involvement when cognitive interventions are effective (Sanjuan et al., 2020).

Cognitive neuroscience of aging has addressed the relationship between cognitive function performance with global and local functional activations in the brain. The increased bilateral, mostly prefrontal involvement has been consistently reported in healthy old adults, while other regions either showed decreased or increased activations relative to those in young adults, as discussed in a review (Park and Reuter-Lorenz, 2009). The localized activation difference from the young adults was often interpreted as compensation or degeneration, with conflicting results by different experimental manipulations. Such inconsistency used to be attributed to the paradigm or task demand, with a weak foundation for the argument reasoning. This problem suggested that the investigation of isolated regions in the brain may not suffice to understand the neural change associated with age-induced decline. Therefore, there has been a support for the examination of network connectivity for interacting regions to elucidate the neural bases underlying altered cognitive functions in aging (Antonenko and Floel, 2014).

Functional connectivity (FC) between brain regions reveals the degree of synchronization or temporal correlations of activities in them. It reflects the quality of information transfer among brain regions, which could be achieved by direct white matter pathways or indirect connections through multiple regions (Fox and Raichle, 2007). Previous research has related hyper- and hypo-connectivity in older adults compared with young adults to decreased cognitive functions (Antonenko and Floel, 2014). Various techniques, such as electroencephalography, magnetoencephalography, and functional magnetic resonance imaging (fMRI), have been employed to study functional connectivity (Buldu et al., 2011; Ferreira and Busatto, 2013; Freitas et al., 2013). FC has been analyzed by means of correlational (Fox and Raichle, 2007), non-linear (Buldu et al., 2011), and graph-theoretical approaches (Meunier et al., 2009). This study focuses on the resting-state fMRI connectivity, similar to those in the review of FC approaches (Ferreira and Busatto, 2013), using the inter-regional correlational approach.

MATERIALS AND METHODS

Participants

Twenty healthy elders (mean age = 69.7, *SD* = 4.2, 8 women) participated in the cognitive training group, and 20 age-matched

TABLE 1 | Baseline scores for the clinical and demographic characteristics of the control and cognitive training groups.

	Training (*n*=20)	Control (*n*=20)		
Characteristics[a]			***F (df)***	***p*-value**
Age, years	69.7 (4.2)	70.3 (3.6)	0.5107 (1, 39)	0.479092
Education, years	12.8 (2.5)	11.9 (2.1)	0.3635 (1, 39)	0.550059
WAISS III Vocabulary (Raw score)	31.5 (10.1)	33.4 (10.2)	0.9614 (1, 39)	0.3328781
WAISS III Vocabulary (Scaled score)	11.8 (2.7)	12.5 (2.5)	0.7404 (1, 39)	0.3947919
MMSE (total raw, /30)	29.0 (1.5)	29.4 (0.8)	0.0068 (1, 39)	0.934701
GDS (total raw, /30)	2.1 (2.3)	0.9 (1.2)	0.0071 (1, 39)	0.9332796
H.N. Handedness Test	97.0 (9.5)	99.5 (2.4)	1.3315 (1, 39)	0.255561
Characteristics[b]			**x^2**	***p*-value**
Gender, female (% of total subjects)	8 (20)	10 (25)	0.4	0.5270893

[a]Data reported as mean (SD); [b]Data reported as number (%). MMSE, Mini-Mental State Examination. GDS, Geriatric Depression Scale.

The whole study lasted 5 weeks. During the training period (Day 2–Day 27), participants were instructed to complete the verbal articulation task by reading 40 sentences (10 for each condition) 10 times as fast and accurately as possible. The training time lasted 20–25 min/day, with a 1-day break after the 3-day training.

controls (mean age = 70.3, *SD* = 3.6, 10 women) enrolled in this study. As shown in **Table 1**, there was no significant difference between the training and control groups in the education (training group mean = 12.8, *SD* = 2.5; control group mean = 11.9, *SD* = 2.1), WAIS III Vocabulary Scaled Score (training group mean = 11.8, *SD* = 2.7; control group mean = 12.5, *SD* = 2.5), Mini-Mental State Examination (MMSE) (training group mean = 29.0, *SD* = 1.5; control group mean = 29.4, *SD* = 0.8), geriatric depression scale (GDS) (training group mean = 2.1, *SD* = 2.3; control group mean = 0.9, *SD* = 1.2), and H.N. Handedness Test (training group mean = 97.0, *SD* = 9.5; control group mean = 99.5, *SD* = 2.4).

Procedure

The study procedure is illustrated in **Figure 1**. After healthy elders were recruited, they were randomly assigned to the training group or control group. The training group was offered explanations of behavioral measurements and scans and the training program, including the training stimuli, program duration, and practice frequency. All the 20 elders agreed to complete the program and were allocated to individual training sessions. The participants assigned to the control group were provided with explanations of behavioral measurements and scans. All of them agreed to participate in the study. Within the 28-day period of the study, research assistants made phone calls to inquire about their willingness to stay in the study and keep elders motivated by encouraging them. No elders dropped out of the study. Behavioral and scan data of all subjects collected on days 1 and 28 were analyzed.

At baseline (Day 1), all participants underwent scanning, including MPRAGE (6 min), resting-state fMRI (7 min), and DTI (8 min). Later, they completed a standardized battery of neuropsychological tests including the verbal fluency test (5 min), Stroop task (10 min), Bochumer Matrices Test (BOMAT)

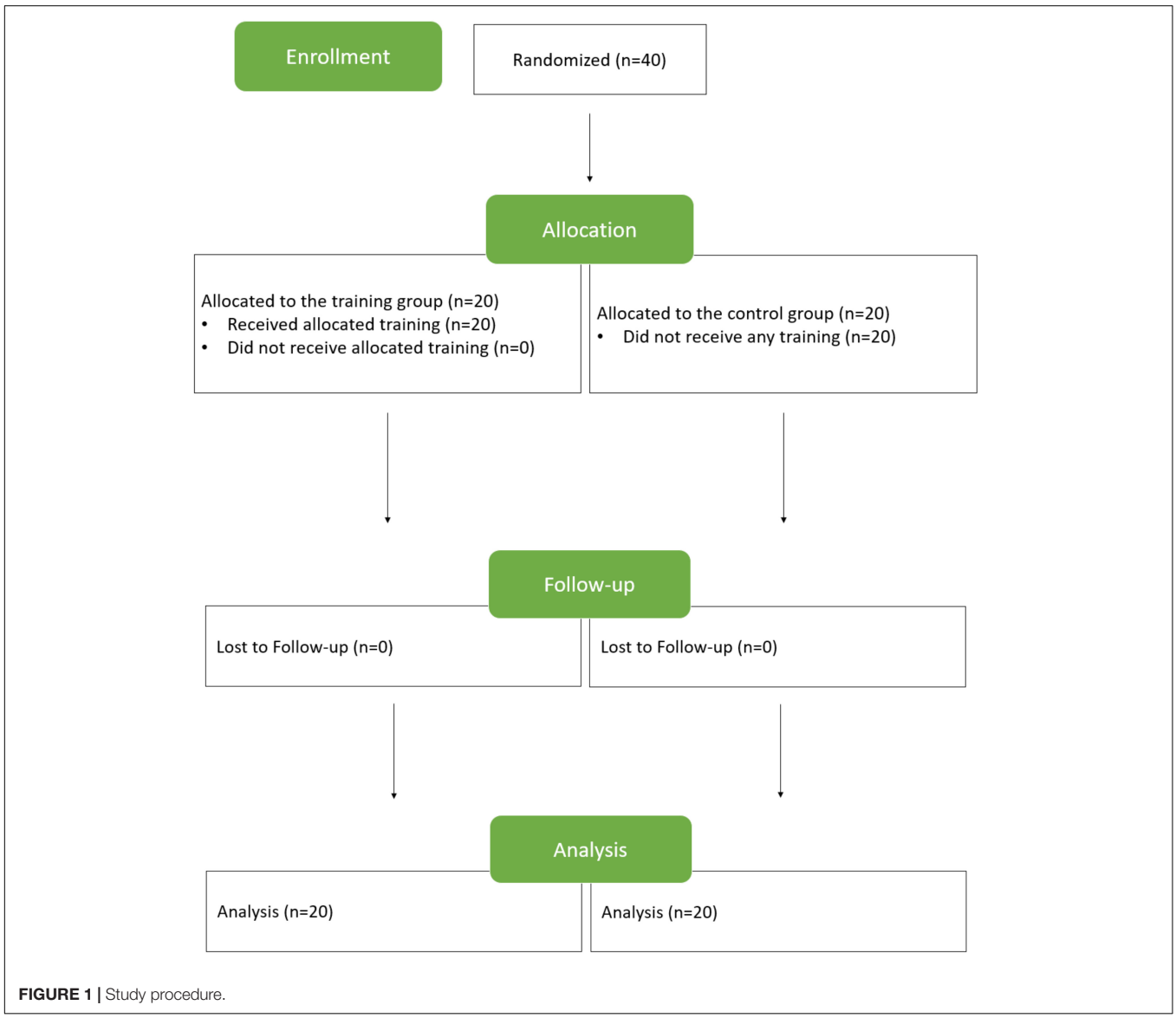

FIGURE 1 | Study procedure.

(15 min), WAIS-III digit span (backward only, 5 min), WAIS-III digit symbol (5 min), MMSE (10 min), GDS (3 min), H.N. Handedness (3 min), and a sentence reading task (10 min). The sentences used in the sentence reading task were categorized by sensicality and difficulty into four types: easy non-sensical sentences, difficult non-sensical sentences, easy meaningful sentences, and difficult meaningful sentences. Participants were asked to read 10 items in each type, 40 items in total. Durations of reading four types of sentences were documented for all subjects.

During the period of training, from Days 2 to 27, participants were instructed to complete the verbal articulation of 40 sentences (10 for each condition). They were required to read aloud each sentence 10 times as fast and accurately as possible, with the reading being recorded. The training time lasted 20–25 min/day, with a 1-day break after the 3-day training. Furthermore, participants were checked whether they performed the task properly by phone every 4 days. On Day 28, all participants underwent the scans, neuropsychological battery testing, and the sentence-reading task. The timing arrangement for behavioral tests, sentence reading tasks, rsfMRI, and verbal articulation training is represented in **Figure 2**.

Verbal Articulation Training

There is evidence showing that the articulation rate and articulation stability are affected in aging (Tremblay et al., 2019). Particularly, aging is associated with an increase in the duration and duration variability of speech utterances in a number of tasks, such as syllable and non-word reading (Tremblay and Deschamps, 2016; Tremblay et al., 2017, 2018), and non-word repetition (Sadagopan and Smith, 2013). This study employs verbal articulation training as the intervention for two reasons. First, the training is expected to improve the articulation in elders, which they have already experienced difficulties in and might feel frustrated within daily life. Second, the practice of articulation skills is anticipated to influence the performance of other linguistic tasks, as previous studies proposed that failure in phonological retrieval led to other linguistic difficulties, such as word retrieval difficulties and delayed response (Burke and Shafto, 2004; Shafto et al., 2007; Shafto and Tyler, 2014), and suggested that elders might benefit from the training of phonological skills (Neumann et al., 2009).

The psychometric properties of the verbal articulation training included comprehension, language, memory, or articulation functions. The stimuli of the verbal articulation training contained four sets of sentences. The first set was difficult-to-articulate sentences with real words. The second set was an easy-to-articulate sentence with real words. The third set was a difficult-to-articulate sentence with pseudowords. The final set was an easy-to-articulate sentence with pseudowords. The definition of difficult or easy to articulate was determined by the consonants which were late or early acquired by Japanese children. To exclude any confounding factors, the syntactic structure, morae number, word familiarity, and word imageability were matched across the four conditions. All sentences were presented in the order of Subject-Adjective-Object-Verb. Words, such as wa, no, and wo appearing in sentences, were case markers for syntactic features. A typical example for the first set of training stimuli was シホは 私費の 施設を 保守する "Shiho protects a private facility." An example for the second set was マキは 棚の 刀を 磨く "Maki polishes a sword on the shelf." In the third and final sets with pseudowords, the sentences also followed an order of Subject-Adjective-Object-Verb with easy or difficult-to-articulate consonants. **Table 2** illustrates the weekly training schedule with training and break days.

Image Acquisition

Images were acquired in a 3 Tesla MR scanner (TIM Trio, Siemens, Erlangen, Germany) with a 12-channel head coil in National Center for Geriatrics and Gerontology. A gradient-echo echo planar imaging (EPI) sequence was used for

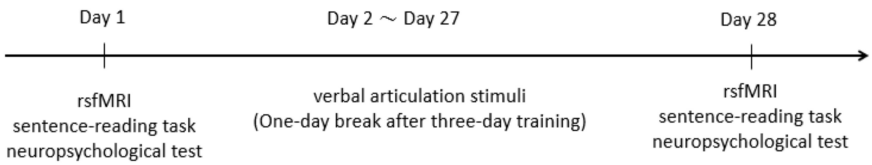

FIGURE 2 | Timing diagram of the scans and stimulus delivery.

TABLE 2 | The training schedule.

	Wed/Sat	Thu/Sun	Fri/Mon	Sat/Tue	Sun/Wed	Mon/Thu	Tue/Fri
Week 1	fMRI-1 Behav-1	Train-1	Train-2	Train-3 (call)		Train-4	Train-5
Week 2	Train-6 (call)		Train-7	Train-8	Train-9 (call)		Train-10
Week 3	Train-11	Train-12 (call)		Train-13	Train-14	Train-15 (call)	
Week 4	Train-16	Train-17	Train-18 (call)		Train-19	Train-20	Train-21 (call)
Week 5	fMRI-2 Behav-2						

functional images to measure blood-oxygen level-dependent (BOLD) contrast with the following parameters: repetition time (TR) = 3,000 ms, echo time (TE) = 30 ms, flip angle = 90°, field of view (FOV) = 192 mm, voxel size = 3 × 3 mm, slice thickness = 3 mm, and 39 axial slices with 0.75 mm gaps. A T2-weighted image (TR = 5,920 ms, TE = 95 ms, flip angle = 150°, FOV = 192 mm, voxel size = 0.8 × 0.8 mm, slice thickness = 3 mm, and 39 axial slices with 0.75-mm gaps). For anatomical references, a high-resolution T1-weighted 3D MPRAGE scan covering the whole brain (TR = 2,500 ms, TE = 2.63 ms, flip angle = 7°, FOV = 256 mm, and isotropic voxels 1 × 1 × 1 mm) was obtained for all participants.

Resting-State Functional Magnetic Resonance Imaging Processing

We used the CONN functional connectivity toolbox (version 16.a),[1] in conjunction with SPM12 (Wellcome Department of Cognitive Neurology, London, United Kingdom),[2] to perform all preprocessing steps (using default preprocessing pipeline of CONN) and subsequent statistical analyses. In this preprocessing pipeline, raw functional images were slice-time corrected, realigned (motion-corrected), unwrapped, and coregistered to the MPRAGE image of each subject in accordance with standard algorithms.

Denoising pipeline of CONN employed linear regression to estimate and remove potential confounding factors for each voxel for each subject and functional run/session and then used temporal band-pass filtering to remove temporal frequencies below 0.008 Hz or above 0.09 Hz to focus on slow frequency fluctuations. Potential confounding factors included noise components from cerebral white matter and cerebrospinal areas (Behzadi et al., 2007), estimated subject-motion parameters (Friston et al., 1996), identified outlier scans or scrubbing (Power et al., 2014), constant and first-order linear session effects, and constant task effects (Whitfield-Gabrieli and Nieto-Castanon, 2012). To minimize the BOLD variability caused by head motion, 12 potential noise components were defined from the estimated subject-motion parameters, with 3 translation parameters, 3 rotation parameters, and their associated first-order derivatives.

Images were then normalized to Montreal Neurological Institute coordinate space, spatially smoothed (8-mm full-width at half maximum), and resliced to 2 × 2 × 2 mm voxels. The regions of interest (ROIs) in this study were derived from a freely available ROI atlas defined by correlated activation patterns.[3] All ROIs provided by the atlas were used for analysis.

Functional Connectivity Measures and Statistical Analysis

For the calculation of FC, we used the ROI-to-ROI measure, which characterizes the connectivity between all pairs of ROIs among a predefined set of regions. The level of connectivity is represented by an ROI-to-ROI (PRC) matrix, in which each element is defined as the Fisher-transformed bivariate correlation coefficient between a pair of ROI BOLD time series:

$$r(i,j) = \frac{\int R_i(t)R_j(t)dt}{\left(\int R_i^2(t)dt \int R_j^2(t)dt\right)^{1/2}} \quad (1)$$

$$Z(i,j) = \tanh^{-1}(r(i,j)) \quad (2)$$

where r is a matrix of correlation coefficients, R is the BOLD time series within each ROI, and Z is the RRC matrix of Fisher-transformed correlation coefficients.

The reading time difference of the sentence-reading task of each subject was also added as 2nd level covariates. This yielded the brain maps demonstrating the correlation between the reading time and the post-functional > pre-functional connectivity. All group-level results were corrected for multiple comparisons (false discovery rate, FDR) ($p < 0.05$) within the CONN toolbox.

In studying the effect of training on the performance of the sentence-reading task, we conducted a three-way ANOVA test on reading speed of the verbal training group. The effects and interactions of three factors were examined, namely, training, sensicality of sentences, and difficulty of sentences. **Table 3** shows the analysis of speed (duration) in reading sentences and the effects of training. In comparing the change of neuropsychological battery after 28 days in the training and control groups, we simply subtracted the 2nd measurement from the 1st measurement of these tests in two groups, respectively, and performed an F test on the subtraction difference between the two measurements.

RESULTS

Behavioral Measures

The treatment effect was investigated with the sentence-reading task, neuropsychological battery, and questionnaire data by the

TABLE 3 | ANOVA of speed in reading sentences.

	Df	Sum sq	Mean sq	*F*-value	*p*-value
Training[a]	1	571,451,416	571,451,416	2633.989	<0.001***
Sensicality[b]	1	62,990,103	62,990,103	290.340	<0.001***
Difficulty[c]	1	1,231,336	1,231,336	5.6756	0.022*
Training: Sensicality	1	111,891,968	111,891,968	515.7434	<0.001***
Training: Difficulty	1	23,562	23,562	0.1086	0.741
Sensicality: Difficulty	1	6,770	6,770	0.0312	0.860
Training: Sensicality: Difficulty	1	1,478,534	1,478,534	6.8150	0.009**

[a] *Pretraining and post-training.*
[b] *Non-sensical and meaningful sentences.*
[c] *Easy and difficult sentences.*
*$p < 0.05$; **$p < 0.01$; ***$p < 0.005$.*

[1] https://www.nitrc.org/projects/conn
[2] http://www.fil.ion.ucl.ac.uk/spm
[3] http://findlab.stanford.edu/functional_ROIs.html

F-test. As shown in **Table 3**, the ANOVA of reading non-sensical and meaning sentences revealed significant main effects of training ($p < 0.001$), sensicality ($p < 0.001$), and difficulty ($p = 0.022$) and interactions of training × sensicality ($p < 0.001$) and training × sensicality × difficulty ($p = 0.009$). The differences of the neuropsychological battery in the baseline and follow-up between the control and training groups did not reach significance between groups (cf. **Supplementary Table 1**).

Post-functional Pre-functional Connectivity Change

The regions showing significant connectivity ($p < 0.05$, uncorrected) are represented in **Figure 3** and **Table 4**. The color in the node circles represents the connectivity intensity, and the size of the node suggests the degree of hubness of the node, with the bigger size being the hub with a larger number of connections to other nodes. The edges are the lines connecting nodes, which represent the connectivity among ROIs. As shown in **Figure 3**, all the ROIs demonstrated a similar level of intensity. The ROIs with increased connectivity were mostly right-lateralized within the fronto-temporal network, e.g., the middle frontal gyrus, the inferior frontal gyrus opercularis, the hippocampus, parahippocampal gyrus, and the temporo-occipital part of the inferior temporal gyrus. These ROIs belong to the language and memory networks. The language network ROIs included the right inferior frontal gyrus opercularis and inferior temporal gyrus. The memory network ROIs consisted of the right hippocampus, right parahippocampal gyrus, and temporoparietal cortex. The temporal ROIs also exhibited connectivity with the left precentral gyrus, visual cortices, and the left inferior cingulate gyrus.

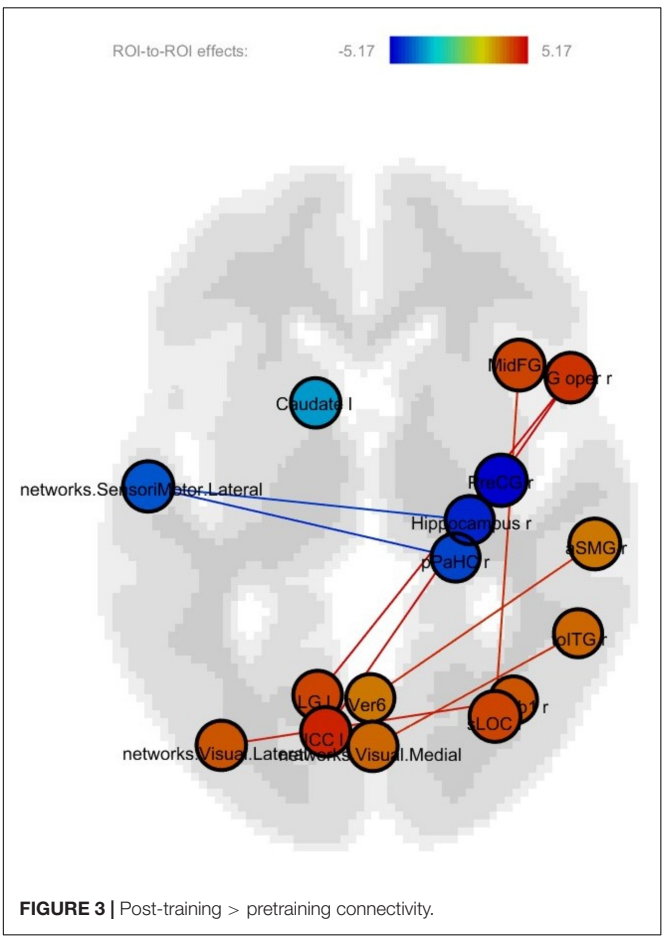

FIGURE 3 | Post-training > pretraining connectivity.

TABLE 4 | Post-training > pretraining connectivity statistics.

Analysis Unit	*F*-value (df)	*p*-unc	*p*-FDR
Hippocampus r	3.20 (4.16)	**0.0413**	0.4503
Cereb1 r	6.03 (4.16)	**0.0037**	0.1656
MidFG r	2.1 (4.16)	0.1276	0.6345
IFG oper r	1.47 (4.16)	0.2561	0.6718
Caudate l	2.15 (4.16)	0.1218	0.6345
PreCG r	1.03 (4.16)	0.4198	0.7462
Networks.SensoriMotor.Lateral l	2.08 (4.16)	0.1317	0.6345
aSMG l	1.51 (4.16)	0.2467	0.6718
pPaHC r	3.18 (4.16)	**0.0421**	0.4503
tolTG r	3.63 (4.16)	**0.0275**	0.4503
LG l	3.77 (4.16)	**0.0242**	0.4503
Ver 6	1.35 (4.16)	0.2939	0.6718
sLOC r	1.91 (4.16)	0.1587	0.6345
ICC l	4.57 (4.16)	**0.0119**	0.3181
Networks.Visual.Medial r	7.09 (4.16)	**0.0018**	0.1656
Networks.Visual.Lateral l	1.32 (4.16)	0.3066	0.6718

Hippocampus r, the right hippocampus; Cereb1 r, the right cerebellum 1; MidFG r, the right middle frontal gyrus; IFG oper r, the right inferior frontal gyrus opercularis; Caudate l, the left caudate; networks.SensoriMotor.Lateral l, the left lateral motor cortex; PreCG r, the right precentral gyrus; aSMG l, the left anterior supramarginal gyrus; pPaHC r, the right parahippocampal gyrus; tolTG r, the right temporo-occipital part of inferior temporal gyrus; LG l, the left lingual gyrus; Ver 6, Vermis 6; sLOC r, the right superior lateral occipital cortex; ICC l, the left inferior cingulate cortex; networks.Visual.Medial r, the right medial visual cortex; networks.Visual.Lateral l, the left lateral visual cortex. The bold values indicate p < 0.05.

Correlation Between Functional Connectivity and Reading Speed of the Sentence Reading Task

Figures 4A–D show correlations between connectivity intensity and change in reading speed of the sentences without FDR correction. In this analysis, the behavior-function correlation was calculated by using the change of reading speed as a covariate in the computation of the regional intensity of each ROI and connectivity between ROIs. The nodes in color were the ROIs whose intensities correlated with the behavioral change, and the edges were the ROI-to-ROI connectivity showing correlations with the behavioral change. The frontal pole-planum temporal connectivity significantly correlated with the post-training > pre-training reading speed difference of the difficult non-sensical and easy non-sensical sentences ($p < 0.05$, FDR-corrected). There was an additional frontal pole-anterior superior temporal gyrus connectivity significantly correlated with the difficult non-sensical sentences ($p < 0.05$, FDR-corrected). There were no significant correlations after FDR correction between FC and the reading speed difference of easy and difficult meaningful sentences.

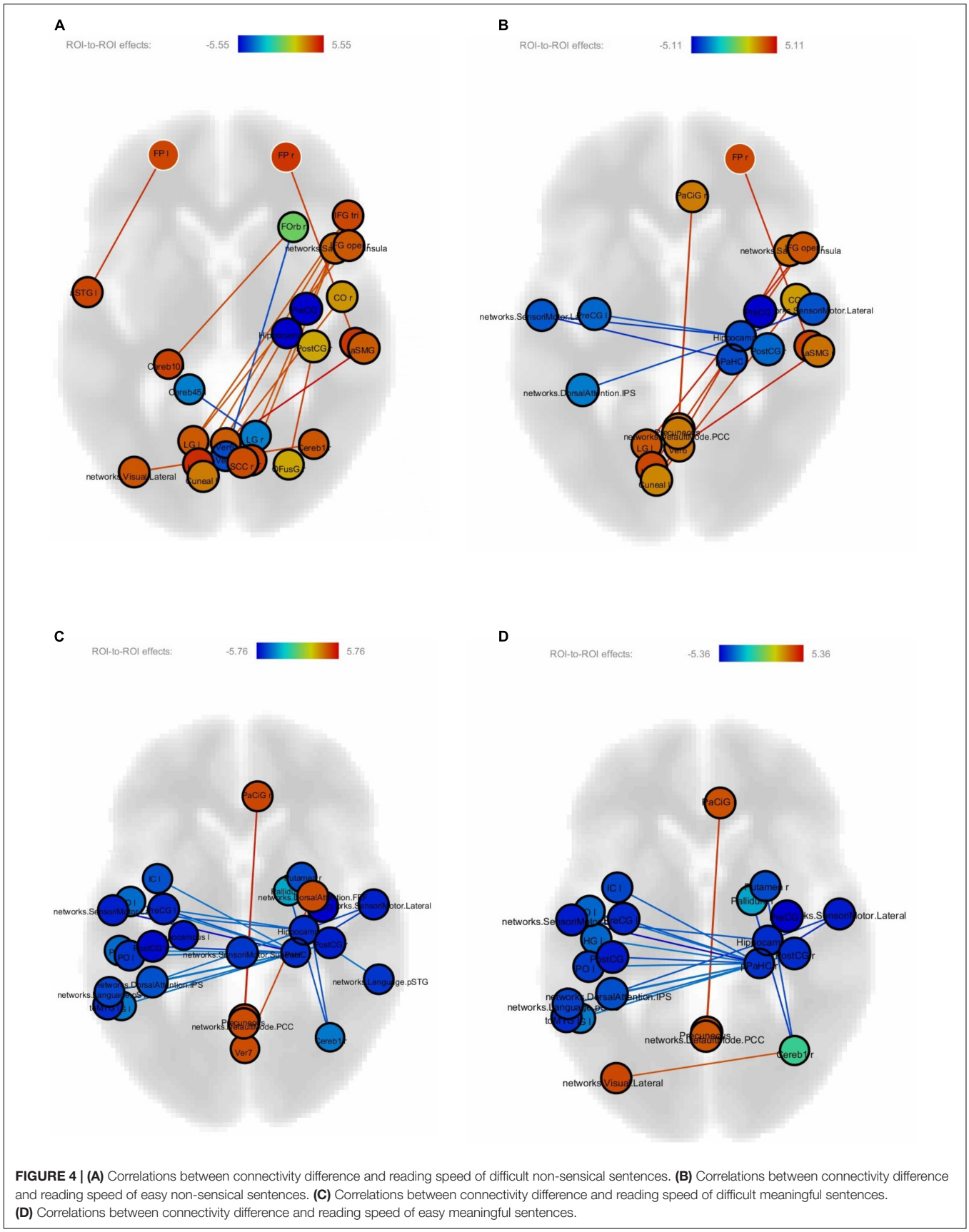

FIGURE 4 | (A) Correlations between connectivity difference and reading speed of difficult non-sensical sentences. **(B)** Correlations between connectivity difference and reading speed of easy non-sensical sentences. **(C)** Correlations between connectivity difference and reading speed of difficult meaningful sentences. **(D)** Correlations between connectivity difference and reading speed of easy meaningful sentences.

DISCUSSION

Although the reading speed of the sentence reading task has been shown to be affected by training, the scores of neuropsychological battery before and after training in the cognitive training group did not reach statistical significance. Neither did the pre- and post-change between the control and training groups reveal significant differences (**Supplementary Table 1**). A potential reason could be the lack of intensity in a simple task in this study. According to reviews and meta-analysis of interventions that have proven to be more effective in improving general functioning, the intervention programs have the following characteristics: (1) a minimum of 10 weeks of treatment with two sessions per week, (2) session length of 60–90 min, (3) interventions for healthy aging in a group format, (4) study follow-ups included, (5) several cognitive skills worked on at the same time, (6) inclusion of other components related to quality of life, (7) employment of personal, internal, or external strategies, and (8) inclusion of measurements of daily functioning (Sanjuan et al., 2020). The articulation task is a relatively simple task that does not include other components related to the quality of life, such as decreasing depression level and improvement of sleep quality, as suggested in the review research. An articulation task is not a challenging task that requires the assistance of internal or external strategies. Additionally, the training program in this research was in individual format and lacked group dynamics that could boost motivations and confidence to apply the skills to daily life functioning. Consequently, the linguistic improvement resulting from articulation training could not be translated to other behavior measured by the neuropsychological battery.

In contrast, the fMRI connectivity analysis revealed prominently increased connectivity in the ROIs within the language and memory networks in the frontal and temporal lobes after training. The temporal ROIs also exhibited connectivity with the left precentral gyrus, visual cortices, and the left inferior cingulate gyrus. The pathological change in the medial temporal lobe (MTL) has been found to be strongly associated with neurodegeneration in elders (Braak and Braak, 1996; Kordower et al., 2001; Scheff et al., 2006). Research has also reported an association of higher life-span cognitive activity with a reduced rate of hippocampal atrophy in elders at risk for dementia (Valenzuela et al., 2008). Studies that employed active training for healthy elders and effectively slowed down the progression to MCI have shown that training was most efficacious in improving memory (Verghese et al., 2003, 2006; Norrie et al., 2011; Rosen et al., 2011; Prince et al., 2013; Diamond et al., 2015). The enhanced hippocampal connectivity in this study is in accordance with previous research that revealed increased hippocampal activations in elders with MCI after cognitive training (Rosen et al., 2011).

The increased connections of the hippocampus to the cerebellum also suggested enhanced communications to achieve cognitive functions, as previous research has demonstrated a functional link between the cerebellum and hippocampus in humans to facilitate the cognitive aspects of navigation (Igloi et al., 2015). In a previous study, the task-based analyses using 787 subjects from the human connectome project showed that the cerebellar cortex was engaged in language, working memory, movement, social, and emotional task processing (Guell et al., 2018a). In this research, the cerebellum lobule showed increased connectivity with the temporal lobe, which is consistent with the observation that the non-motor processing lobule in the cerebellum supports a cognitive function that is left-lateralized, i.e., language (Guell et al., 2018b; Schmahmann et al., 2019).

Notably, in this study, there was right-lateralized increased connectivity within the frontotemporal network (**Figure 3**). This suggested that the effectiveness of the training was manifested in enhanced communications among the frontotemporal language regions (i.e., the inferior frontal gyrus opercularis and inferior temporal gyrus) and temporal memory regions (i.e., the hippocampus and parahippocampal gyrus) in the right hemisphere. Prior fMRI studies on healthy aging have generally reported spread instead of localized functional activations in elders relative to young controls (Salami et al., 2012; Spreng and Schacter, 2012). Inter-network connectivity or activations seem to suggest detrimental effects caused by age-related inefficiency, which is consistent with neural dedifferentiation in the aging brain (Park and Reuter-Lorenz, 2009; Antonenko and Floel, 2014; Geerligs et al., 2014). The increased intra-network connectivity following cognitive training in this research could serve as evidence for improved neural differentiation. This also provides a solid foundation for the rationale of turning neural change toward the right direction by cognitive training.

The correlation between FC in the frontal pole and improved performance of the sentence reading task suggested the important role of frontal involvement in driving the task success as a result of articulation training. Recent research has shown that the structural properties of the frontal pole cortex contain information that can differentiate participants with high goal-directed persistence from those with low persistence, regardless of task domains, such as cognitive, language, and motor learning (Hosoda et al., 2020). They also found that participants with high persistence exhibited experience-dependent neuroplastic changes in the frontal pole after completing language and motor learning tasks. The increased connectivity between the frontal pole and planum temporale, which is a region typically involved in auditory processing (Nakada et al., 2001) and lexical processing (Bookheimer, 2002), could also represent the post-training neural plasticity in the fontal pole to complete the task involving auditory and lexical processes. Additionally, the anterior superior temporal gyrus has been reported to be related to sentence processing (Mellem et al., 2016). The connectivity between the anterior superior temporal gyrus and the frontal pole might suggest the training-induced persistence in reading difficult non-sensical sentences.

Regarding maintenance of training effects, previous research has reported that sustained benefits of cognitive interventions were verified in healthy elders for periods of 2 months (Chiu et al., 2017) to 5 years (Kelly et al., 2014) after treatment. The sustainability of the effects also relied on subsequent practices of the training stimuli, similar to any kind of skills. The study follow-ups are crucial for not only maintenance of the effects but also translation of the skills to general functioning (Sanjuan et al., 2020). This study did not follow up with the participants

after the study was completed. Our future study will take into consideration long-term follow-ups and measurements of sustained treatment effects.

CONCLUSION

This study utilizes a simple verbal articulation task for cognitive training in Japanese healthy adults. In comparison to age- and education-matched controls, elders who received the articulation training demonstrated significantly increased connectivity in the right frontotemporal regions, with extended connectivity from temporal regions to cerebellum and visual cortices. The increased hippocampal connectivity was consistent with previous research showing efficacy in intervening cognitive decline and change in hippocampal functioning. Moreover, the increased intra-network connectivity following cognitive training suggested an improved neural differentiation, in contrast to the dedifferentiation pattern in the aging brain. Although the training was simply relative to programs used in other cognitive training studies, the fMRI connectivity analysis showed patterns suggesting a promising functional change in the frontal and temporal regions that are associated with goal-oriented persistence, as well as language and memory functions.

DATA AVAILABILITY STATEMENT

The original contributions presented in the study are included in the article/**Supplementary Material**, further inquiries can be directed to the corresponding author/s.

ETHICS STATEMENT

The studies involving human participants were reviewed and approved by IRB of National Center for Geriatrics and Gerontology. The patients/participants provided their written informed consent to participate in this study.

AUTHOR CONTRIBUTIONS

F-PY analyzed the data and wrote the manuscript. T-YL and C-HL assisted in the preparation of tables and figures and the organization of references. TN helped in designing the task and organized data collection. SM provided opinions on the results of verbal training from the perspective of oral functions and worked with TN to supervise the collaborative research and review the manuscript draft. All authors contributed to the article and approved the submitted version.

FUNDING

This research was supported by the Japan Society for the Promotion of Science (JSPS) under Grants-in-Aid for Scientific Research (KAKENHI #15H03104 and 19H04025] and the Taiwan Ministry of Education Grant (108J0054RT).

ACKNOWLEDGMENTS

We would like to acknowledge the contribution of Sachiko Kiyama, Ph.D. for designing the verbal training task and supporting data collection.

SUPPLEMENTARY MATERIAL

The Supplementary Material for this article can be found online at: https://www.frontiersin.org/articles/10.3389/fnhum.2022.786853/full#supplementary-material

REFERENCES

Antonenko, D., and Floel, A. (2014). Healthy aging by staying selectively connected: a mini-review. *Gerontology* 60, 3–9. doi: 10.1159/000354376

Ball, K., Berch, D. B., Helmers, K. F., Jobe, J. B., Leveck, M. D., Marsiske, M., et al. (2002). Effects of cognitive training interventions with older adults: a randomized controlled trial. *JAMA* 288, 2271–2281. doi: 10.1001/jama.288.18.2271

Behzadi, Y., Restom, K., Liau, J., and Liu, T. T. (2007). A component based noise correction method (CompCor) for BOLD and perfusion based fMRI. *Neuroimage* 37, 90–101. doi: 10.1016/j.neuroimage.2007.04.042

Belleville, S. (2008). Cognitive training for persons with mild cognitive impairment. *Int. Psychogeriatr.* 20, 57–66. doi: 10.1017/S104161020700631X

Bookheimer, S. (2002). Functional MRI of language: new approaches to understanding the cortical organization of semantic processing. *Annu. Rev. Neurosci.* 25, 151–188. doi: 10.1146/annurev.neuro.25.112701.142946

Braak, H., and Braak, E. (1996). Evolution of the neuropathology of Alzheimer's disease. *Acta Neurol. Scand. Suppl.* 165, 3–12. doi: 10.1111/j.1600-0404.1996.tb05866.x

Buldu, J. M., Bajo, R., Maestu, F., Castellanos, N., Leyva, I., Gil, P., et al. (2011). Reorganization of functional networks in mild cognitive impairment. *PLoS One* 6:e19584. doi: 10.1371/journal.pone.0019584

Burke, D. M., and Shafto, M. A. (2004). Aging and language production. *Curr. Dir. Psychol. Sci.* 13, 21–24. doi: 10.1111/j.0963-7214.2004.01301006.x

Chiu, H. L., Chu, H., Tsai, J. C., Liu, D., Chen, Y. R., Yang, H. L., et al. (2017). The effect of cognitive-based training for the healthy older people: a meta-analysis of randomized controlled trials. *PLoS One* 12:e0176742. doi: 10.1371/journal.pone.0176742

Cohen, N. J., and Squire, L. R. (1981). Retrograde amnesia and remote memory impairment. *Neuropsychologia* 19, 337–356. doi: 10.1016/0028-3932(81)90064-6

Diamond, K., Mowszowski, L., Cockayne, N., Norrie, L., Paradise, M., Hermens, D. F., et al. (2015). Randomized controlled trial of a healthy brain ageing cognitive training program: effects on memory, mood, and sleep. *J. Alzheimers Dis.* 44, 1181–1191. doi: 10.3233/JAD-142061

Ferreira, L. K., and Busatto, G. F. (2013). Resting-state functional connectivity in normal brain aging. *Neurosci. Biobehav. Rev.* 37, 384–400. doi: 10.1016/j.neubiorev.2013.01.017

Fox, M. D., and Raichle, M. E. (2007). Spontaneous fluctuations in brain activity observed with functional magnetic resonance imaging. *Nat. Rev. Neurosci.* 8, 700–711. doi: 10.1038/nrn2201

Freitas, C., Farzan, F., and Pascual-Leone, A. (2013). Assessing brain plasticity across the lifespan with transcranial magnetic stimulation: why, how, and what is the ultimate goal? *Front. Neurosci.* 7:42. doi: 10.3389/fnins.2013.00042

Friston, K. J., Williams, S., Howard, R., Frackowiak, R. S., and Turner, R. (1996). Movement-related effects in fMRI time-series. *Magn. Reson. Med.* 35, 346–355. doi: 10.1002/mrm.1910350312

Geerligs, L., Maurits, N. M., Renken, R. J., and Lorist, M. M. (2014). Reduced specificity of functional connectivity in the aging brain during task performance. *Hum. Brain Mapp.* 35, 319–330. doi: 10.1002/hbm.22175

Guell, X., Gabrieli, J. D. E., and Schmahmann, J. D. (2018a). Triple representation of language, working memory, social and emotion processing in the cerebellum: convergent evidence from task and seed-based resting-state fMRI analyses in a single large cohort. *Neuroimage* 172, 437–449. doi: 10.1016/j.neuroimage.2018.01.082

Guell, X., Schmahmann, J. D., Gabrieli, J., and Ghosh, S. S. (2018b). Functional gradients of the cerebellum. *Elife* 7:e36652. doi: 10.7554/eLife.36652

Hosoda, C., Tsujimoto, S., Tatekawa, M., Honda, M., Osu, R., and Hanakawa, T. (2020). Plastic frontal pole cortex structure related to individual persistence for goal achievement. *Commun. Biol.* 3:194. doi: 10.1038/s42003-020-0930-4

Igloi, K., Doeller, C. F., Paradis, A. L., Benchenane, K., Berthoz, A., Burgess, N., et al. (2015). Interaction between hippocampus and cerebellum crus I in sequence-based but not place-based navigation. *Cereb. Cortex* 25, 4146–4154. doi: 10.1093/cercor/bhu132

Kelly, M. E., Loughrey, D., Lawlor, B. A., Robertson, I. H., Walsh, C., and Brennan, S. (2014). The impact of cognitive training and mental stimulation on cognitive and everyday functioning of healthy older adults: a systematic review and meta-analysis. *Ageing Res. Rev.* 15, 28–43. doi: 10.1016/j.arr.2014.02.004

Kordower, J. H., Chu, Y., Stebbins, G. T., DeKosky, S. T., Cochran, E. J., Bennett, D., et al. (2001). Loss and atrophy of layer II entorhinal cortex neurons in elderly people with mild cognitive impairment. *Ann. Neurol.* 49, 202–213. doi: 10.1002/1531-8249(20010201)49:2<202::aid-ana40>3.0.co;2-3

Mellem, M. S., Jasmin, K. M., Peng, C., and Martin, A. (2016). Sentence processing in anterior superior temporal cortex shows a social-emotional bias. *Neuropsychologia* 89, 217–224. doi: 10.1016/j.neuropsychologia.2016.06.019

Meunier, D., Achard, S., Morcom, A., and Bullmore, E. (2009). Age-related changes in modular organization of human brain functional networks. *Neuroimage* 44, 715–723. doi: 10.1016/j.neuroimage.2008.09.062

Mowszowski, L., Batchelor, J., and Naismith, S. L. (2010). Early intervention for cognitive decline: can cognitive training be used as a selective prevention technique? *Int. Psychogeriatr.* 22, 537–548. doi: 10.1017/S1041610209991748

Nakada, T., Fujii, Y., Yoneoka, Y., and Kwee, I. L. (2001). Planum temporale: where spoken and written language meet. *Eur. Neurol.* 46, 121–125. doi: 10.1159/000050784

Neumann, Y., Obler, L. K., Gomes, H., and Shafer, V. (2009). Phonological vs sensory contributions to age effects in naming: an electrophysiological study. *Aphasiology* 23, 1028–1039. doi: 10.1080/02687030802661630

Norrie, L. M., Diamond, K., Hickie, I. B., Rogers, N. L., Fearns, S., and Naismith, S. L. (2011). Can older "at risk" adults benefit from psychoeducation targeting healthy brain aging? *Int. Psychogeriatr.* 23, 413–424. doi: 10.1017/S1041610210001109

Park, D. C., and Reuter-Lorenz, P. (2009). The adaptive brain: aging and neurocognitive scaffolding. *Annu. Rev. Psychol.* 60, 173–196. doi: 10.1146/annurev.psych.59.103006.093656

Power, J. D., Mitra, A., Laumann, T. O., Snyder, A. Z., Schlaggar, B. L., and Petersen, S. E. (2014). Methods to detect, characterize, and remove motion artifact in resting state fMRI. *Neuroimage* 84, 320–341. doi: 10.1016/j.neuroimage.2013.08.048

Prince, M., Bryce, R., Albanese, E., Wimo, A., Ribeiro, W., and Ferri, C. P. (2013). The global prevalence of dementia: a systematic review and metaanalysis. *Alzheimers Dement.* 9, 63.e2–75.e2. doi: 10.1016/j.jalz.2012.11.007

Rosen, A. C., Sugiura, L., Kramer, J. H., Whitfield-Gabrieli, S., and Gabrieli, J. D. (2011). Cognitive training changes hippocampal function in mild cognitive impairment: a pilot study. *J. Alzheimers Dis.* 26(Suppl. 3), 349–357. doi: 10.3233/JAD-2011-0009

Sadagopan, N., and Smith, A. (2013). Age differences in speech motor performance on a novel speech task. *J. Speech Lang. Hear. Res.* 56, 1552–1566. doi: 10.1044/1092-4388(2013/12-0293)

Salami, A., Eriksson, J., and Nyberg, L. (2012). Opposing effects of aging on large-scale brain systems for memory encoding and cognitive control. *J. Neurosci.* 32, 10749–10757. doi: 10.1523/JNEUROSCI.0278-12.2012

Sanjuan, M., Navarro, E., and Calero, M. D. (2020). Effectiveness of cognitive interventions in older adults: a review. *Eur. J. Investig. Health Psychol. Educ.* 10, 876–898. doi: 10.3390/ejihpe10030063

Scheff, S. W., Price, D. A., Schmitt, F. A., and Mufson, E. J. (2006). Hippocampal synaptic loss in early Alzheimer's disease and mild cognitive impairment. *Neurobiol. Aging* 27, 1372–1384. doi: 10.1016/j.neurobiolaging.2005.09.012

Schmahmann, J. D., Guell, X., Stoodley, C. J., and Halko, M. A. (2019). The Theory and Neuroscience of Cerebellar Cognition. *Annu. Rev. Neurosci.* 42, 337–364. doi: 10.1146/annurev-neuro-070918-050258

Shafto, M. A., and Tyler, L. K. (2014). Language in the aging brain: the network dynamics of cognitive decline and preservation. *Science* 346, 583–587. doi: 10.1126/science.1254404

Shafto, M. A., Burke, D. M., Stamatakis, E. A., Tam, P. P., and Tyler, L. K. (2007). On the tip-of-the-tongue: neural correlates of increased word-finding failures in normal aging. *J. Cogn. Neurosci.* 19, 2060–2070. doi: 10.1162/jocn.2007.19.12.2060

Spreng, R. N., and Schacter, D. L. (2012). Default network modulation and large-scale network interactivity in healthy young and old adults. *Cereb. Cortex* 22, 2610–2621. doi: 10.1093/cercor/bhr339

Tremblay, P., and Deschamps, I. (2016). Structural brain aging and speech production: a surface-based brain morphometry study. *Brain Struct. Funct.* 221, 3275–3299. doi: 10.1007/s00429-015-1100-1

Tremblay, P., Deschamps, I., Bedard, P., Tessier, M. H., Carrier, M., and Thibeault, M. (2018). Aging of speech production, from articulatory accuracy to motor timing. *Psychol. Aging* 33, 1022–1034. doi: 10.1037/pag0000306

Tremblay, P., Poulin, J., Martel-Sauvageau, V., and Denis, C. (2019). Age-related deficits in speech production: from phonological planning to motor implementation. *Exp. Gerontol.* 126:110695. doi: 10.1016/j.exger.2019.110695

Tremblay, P., Sato, M., and Deschamps, I. (2017). Age differences in the motor control of speech: an fMRI study of healthy aging. *Hum Brain Mapp.* 38, 2751–2771. doi: 10.1002/hbm.23558

Tulving, E. (2002). Episodic memory: from mind to brain. *Annu. Rev. Psychol.* 53, 1–25. doi: 10.1146/annurev.psych.53.100901.135114

Valenzuela, M. J., Sachdev, P., Wen, W., Chen, X., and Brodaty, H. (2008). Lifespan mental activity predicts diminished rate of hippocampal atrophy. *PLoS One* 3:e2598. doi: 10.1371/journal.pone.0002598

Valenzuela, M., and Sachdev, P. (2009). Can cognitive exercise prevent the onset of dementia? Systematic review of randomized clinical trials with longitudinal follow-up. *Am. J. Geriatr. Psychiatry* 17, 179–187. doi: 10.1097/JGP.0b013e3181953b57

Verghese, J., LeValley, A., Derby, C., Kuslansky, G., Katz, M., Hall, C., et al. (2006). Leisure activities and the risk of amnestic mild cognitive impairment in the elderly. *Neurology* 66, 821–827. doi: 10.1212/01.wnl.0000202520.68987.48

Verghese, J., Lipton, R. B., Katz, M. J., Hall, C. B., Derby, C. A., Kuslansky, G., et al. (2003). Leisure activities and the risk of dementia in the elderly. *N. Engl. J. Med.* 348, 2508–2516. doi: 10.1056/NEJMoa022252

Whitfield-Gabrieli, S., and Nieto-Castanon, A. (2012). Conn: a functional connectivity toolbox for correlated and anticorrelated brain networks. *Brain Connect.* 2, 125–141. doi: 10.1089/brain.2012.0073

Wilson, R. S., Mendes De Leon, C. F., Barnes, L. L., Schneider, J. A., Bienias, J. L., Evans, D. A., et al. (2002). Participation in cognitively stimulating activities and risk of incident Alzheimer disease. *JAMA* 287, 742–748. doi: 10.1001/jama.287.6.742

Conflict of Interest: The authors declare that the research was conducted in the absence of any commercial or financial relationships that could be construed as a potential conflict of interest.

Publisher's Note: All claims expressed in this article are solely those of the authors and do not necessarily represent those of their affiliated organizations, or those of the publisher, the editors and the reviewers. Any product that may be evaluated in this article, or claim that may be made by its manufacturer, is not guaranteed or endorsed by the publisher.

frontiers in Human Neuroscience

ORIGINAL RESEARCH
published: 07 March 2022
doi: 10.3389/fnhum.2022.787413

Foreign Language Learning in Older Adults: Anatomical and Cognitive Markers of Vocabulary Learning Success

Manson Cheuk-Man Fong[1,2]*, *Matthew King-Hang Ma*[3], *Jeremy Yin To Chui*[1], *Tammy Sheung Ting Law*[1], *Nga-Yan Hui*[1], *Alma Au*[4] *and William Shiyuan Wang*[1,2,3]*

[1] Research Centre for Language, Cognition, and Neuroscience, Department of Chinese and Bilingual Studies, The Hong Kong Polytechnic University, Kowloon, Hong Kong SAR, China, [2] Research Institute for Smart Ageing, The Hong Kong Polytechnic University, Kowloon, Hong Kong SAR, China, [3] Department of Electronic Engineering, The Chinese University of Hong Kong, Hong Kong, Hong Kong SAR, China, [4] Department of Applied Social Science, The Hong Kong Polytechnic University, Kowloon, Hong Kong SAR, China

OPEN ACCESS

Edited by:
Toshiharu Nakai,
Osaka University, Japan

Reviewed by:
Giovanna Bubbico,
University of Studies G. d'Annunzio Chieti and Pescara, Italy
Olga Kepinska,
University of Vienna, Austria
Eri Nakagawa,
National Institute for Physiological Sciences (NIPS), Japan

***Correspondence:**
Manson Cheuk-Man Fong
cmmfong@polyu.edu.hk
William Shiyuan Wang
wsywang@polyu.edu.hk

Specialty section:
This article was submitted to Speech and Language, a section of the journal Frontiers in Human Neuroscience

Received: 30 September 2021
Accepted: 08 February 2022
Published: 07 March 2022

Citation:
Fong MC-M, Ma MK-H, Chui JYT, Law TST, Hui N-Y, Au A and Wang WS (2022) Foreign Language Learning in Older Adults: Anatomical and Cognitive Markers of Vocabulary Learning Success. Front. Hum. Neurosci. 16:787413. doi: 10.3389/fnhum.2022.787413

In recent years, foreign language learning (FLL) has been proposed as a possible cognitive intervention for older adults. However, the brain network and cognitive functions underlying FLL has remained largely unconfirmed in older adults. In particular, older and younger adults have markedly different cognitive profile—while older adults tend to exhibit decline in most cognitive domains, their semantic memory usually remains intact. As such, older adults may engage the semantic functions to a larger extent than the other cognitive functions traditionally considered the most important (e.g., working memory capacity and phonological awareness). Using anatomical measurements and a cognitive test battery, the present study examined this hypothesis in twenty cognitively normal older adults (58–69 years old), who participated in a two-month Italian learning programme. Results showed that the immediate learning success and long-term retention of Italian vocabularies were most consistently predicted by the anatomical measures of the left pars orbitalis and left caudal middle frontal cortex, which are implicated in semantic and episodic memory functions. Convergent evidence was also found based on the pattern of cognitive associations. Our results are consistent with a prominent role of semantic and episodic memory functions in vocabulary learning in older learners.

Keywords: foreign language learning, vocabulary learning, structural MRI, FreeSurfer, pars orbitalis, caudal middle frontal cortex, semantic memory, episodic memory

1. INTRODUCTION

1.1. Foreign Language Learning in Older Adults

In foreign language learning (FLL) research, older adults have been an understudied population (Mackey and Sachs, 2012), which may be caused by the increased difficulty in picking up a new language after the "critical period" (Lenneberg, 1967; Hartshorne et al., 2018, see also Wang, 2018). However, there has been a recent change in attitude, due in part to a series of pioneering studies on the effect of lifelong bilingualism on brain structures and cognitive functions (Bialystok et al., 2007; Luk et al., 2011; Costa and Sebastián-Gallés, 2014; Olsen et al., 2015) and on the neuroplasticity induced by intensive FLL in younger adults (Wong and Perrachione, 2007; Mårtensson et al., 2012; Stein et al., 2012; Zatorre, 2013; Qi et al., 2019).

Relative to older monolinguals, older bilinguals were reported to have greater protection against dementia, better inhibition function, and improved executive control (Bialystok et al., 2007; van den Noort et al., 2019). The bilingual advantage has also been reported for other cognitive domains, e.g., episodic and verbal memory (Schroeder and Marian, 2012; Grant et al., 2014, but see Paap et al., 2015). Neurally, the correlates of bilingual experiences have been studied using many anatomical segmentation tools (Li et al., 2014; Hämäläinen et al., 2018; Maschio et al., 2019). Using a technique known as surface-based morphometry (SBM; Fischl and Dale, 2000; Winkler et al., 2010; Luders et al., 2012), early acquisition of two languages is found to be associated with larger surface area in the left pars opercularis of the inferior frontal gyrus (IFG) and right superior temporal gyrus (STG), while late acquisition is associated with increased mean curvature in the left STG (Hämäläinen et al., 2018). Bilingualism-induced neural differences have also been demonstrated using related anatomical measures such as sub-cortical volumes (DeLuca et al., 2019b) or gray matter density (Abutalebi et al., 2015), obtained by volume-based morphometry and voxel-based morphometry. For example, an expansion of the thalamus was observed for individuals with greater immersion in the second language (Pliatsikas et al., 2017; Deluca et al., 2019a).

As for learning-induced neuroplasticity in younger adults, five months of intensive FLL was sufficient to bring about increases in gray matter volume in the left IFG and left anterior temporal lobe (Stein et al., 2012). Intensive vocabulary learning in young interpreters was found to promote increases in cortical thickness across various regions in the left-lateralized language network, including left middle frontal gyrus, IFG, and STG, along with increased volume in the bilateral hippocampus (Mårtensson et al., 2012). Consistent with the classroom-based learning above, a recent experimental work based on either the picture–word association or virtual reality as the FLL paradigm revealed both structural and functional changes in younger adults, including increased cortical thickness over both the core language areas in the left hemisphere and many regions in the right hemisphere (Legault et al., 2019a). In another study, increased brain volume was found in the right hippocampus (Bellander et al., 2016).

Taken together, the findings on the bilingual advantage and learning-induced neuroplasticity have raised the possibility to use FLL as a non-pharmacological means for promoting successful aging in older adults (Antoniou et al., 2013; Antoniou and Wright, 2017; Ware et al., 2017; Klimova, 2018; Pfenninger and Polz, 2018; Klimova and Pikhart, 2020). Consistent with this conjecture, a few studies reported cognitive improvements in older learners after intensive FLL (Bak et al., 2016; Bubbico et al., 2019; Wong et al., 2019). For example, improvement in global cognition was found following six months of individual computer-based cognitively stimulating activities, including FLL and cognitive games (Wong et al., 2019). In another study, older learners also showed significant improvement in global cognition, along with increased resting-state functional connectivities (RSFCs) between posterior cingulate cortex and three right-hemispheric regions, including right IFG, right superior frontal gyrus, and left superior parietal lobule (Bubbico et al., 2019). This interesting finding suggests that the right-hemisphere homologs of the left-hemisphere language areas may provide "scaffolding" in the early phase of second language learning, before a right-to-left shift occurs (Yang et al., 2015; Qi and Legault, 2020). Despite the positive findings above, results have been mixed, with a few studies reporting no improvement for all cognitive skills examined (Ware et al., 2017; Berggren et al., 2020), some degree of enhancement that was however not significantly different from that of a control group (Valis et al., 2019), or neither learning-induced anatomical nor behavioral changes (Nilsson et al., 2021).

1.2. Neurocognitive Bases of Foreign Language Learning

To account for the neuroplastic changes or cognitive gains that could be driven by FLL in older adults, an understanding about the neurocognitive bases of FLL is essential, because the learning-induced changes in a brain region likely arise due to its increased recruitment over the learning programme (Wong et al., 2007). Toward this end, some prominent neuroanatomical models of language (e.g., Ullman, 2001a, 2004; Hickok and Poeppel, 2007) have provided the guiding theoretical framework. In the declarative–procedural model (DP model; Ullman, 2001a, 2004), the declarative memory (comprising semantic and episodic memory), as subserved by a cortical–hippocampal system (Mcclelland et al., 1995; Eichenbaum, 2000), is posited to be involved for learning words. In contrast, the procedural memory, as subserved by the insula and basal ganglia (especially the striatum), is recruited in phonological and rule-based grammar learning. Functional activation and connectivities studies have been central to the quest for the neurocognitive bases of FLL (e.g., Mestres-Missé et al., 2008; Abutalebi and Green, 2016; Bakker-Marshall et al., 2021, for a recent review, see Qi and Legault, 2020). However, one source of information that could not be understated is individual differences—the focus of the present article. Traditionally, they are sometimes considered as "noise" that may obscure the effect of interest. Nonetheless, they have proved reliable for linking brain functions and cognitive behavior (e.g., Kanai and Rees, 2011; Chiarello et al., 2013).

In FLL research, individual differences in brain functions are posited to put strong constraints on the learning success (Zatorre, 2013; Li and Grant, 2016). Previous behavioral and neural findings have suggested that phonological skills, such as phonological short-term memory (PSTM) and phonological awareness, are the determining factors of language learning success (Papagno et al., 1991; Baddeley et al., 1998; Koda, 1998; Linck et al., 2014; Gillon, 2017). Corroborating evidence has been found in both classroom-based and laboratory-based studies with younger learners, for phonemic learning (Golestani and Zatorre, 2009; Silbert et al., 2015; Fuhrmeister and Myers, 2021), lexical tone learning (Wong and Perrachione, 2007; Chandrasekaran et al., 2010), and artificial grammar learning (Yang and Li, 2012; Kepinska et al., 2017). In agreement with the view that PSTM plays a crucial role in FLL, functional connectivity or activation studies have reported an association between FLL success and regions important for phonological processing, e.g., left precentral gyrus (Veroude et al., 2010), left

supramarginal gyrus (SMG; Veroude et al., 2010; Sliwinska et al., 2012), and left posterior STG (e.g., Wong et al., 2007). Also, consistent with the hypothesis that phonological awareness plays a critical role in language learning success, individual variation in learning outcomes can be predicted by individual variation in baseline sensitivity to non-lexical pitch patterns (Wong et al., 2007).

Of special interest to the present study are the anatomical associations with learning performance. For example, the success in linguistic pitch learning or direction discrimination were predicted by the volume of left Mescal's gyrus (Wong et al., 2008) and by the cortical thickness of the right hemispheric homolog of the Broca's area (Novén et al., 2019). In the study by Legault et al. (2019a), reviewed in the last section, the FLL performance was associated with the cortical thickness of right IFG in the picture–word group, and with the cortical thickness of right inferior parietal lobe in the VR group. The emphasis of phonological skills has extended to sub-cortical regions. Recent empirical works (Legault et al., 2019a) and theoretical papers (Abutalebi and Green, 2007; Li et al., 2014) have highlighted the roles of the striatum—comprising caudate nucleus and putamen—in phonological learning. For example, the caudate nucleus is involved in phonemic fluency (rather than semantic fluency; Grogan et al., 2009) and procedural memory (Ullman, 2004), while the putamen has been implicated in articulatory planning and detecting phonological errors (e.g., Abutalebi and Green, 2007).

While the emphasis on phonological skills in previous studies is understandable, in light of the DP model, it is surprising that the roles played by semantic and verbal episodic memory have seldom been tested in neural research on FLL. Since the DP model was initially proposed, functional imaging and neurological studies have established that semantic functions are supported by a widespread network that includes the ventrolateral prefrontal cortex, anterior temporal lobe, middle temporal gyrus, etc. (Patterson et al., 2007; Binder et al., 2009; Ralph et al., 2017), along with sub-cortical regions like the thalamus. In addition to being a main relay station of sensory information, the thalamus may also play an important role in language production by selecting lexical and semantic representations (Abutalebi and Green, 2016), by virtue of its connection with the left IFG (Ford et al., 2013). The episodic memory is subserved by the hippocampus and its surrounding medial temporal lobe structures (including the entorhinal cortex and the parahippocampal gyrus), along with the prefrontal cortex (e.g., Breitenstein et al., 2005). The hippocampus is well-known for its role in transforming short-term memory to long-term memory, while the entorhinal cortex and the parahippocampal gyrus are implicated during the processing of object/event information and spatial-temporal context, respectively (Eichenbaum et al., 2012). Another study also reported that the entorhinal cortex reflects elementary memory processes related to novelty detection, while the parahippocampus is more involved in the formation and subsequent reactivation of the memory (Daselaar et al., 2004). A few recent studies have reported evidence that supports a role of hippocampus in younger adults in FLL (Kepinska et al., 2017, 2018). For example, the connectivity of the hippocampus and Broca's area was implicated during the acquisition of a novel grammar (Kepinska et al., 2018).

There are reasons that the brain networks and cognitive mechanisms could be different in older learners, which could result in different learning outcomes (Service and Craik, 1993; Glass et al., 2012; Ingvalson et al., 2017). To start with, older adults had poorer speech discrimination for phonemes and pitch (Shen et al., 2016), which may promote the use of alternative strategies in vocabulary learning. Due to lower working memory capacity (Service and Craik, 1993; Mackey and Sachs, 2012), they may also rely less on rote memorization. In addition, the inhibition function is generally in decline (Hasher et al., 1991, but see Veríssimo et al., 2021), making it difficult for them to retrieve the L2 word because it is more difficult for them to suppress the L1 word. In contrast, older adults often have better crystallized knowledge (e.g., world and vocabulary knowledge) than younger adults (Salthouse, 2012; Hartshorne and Germine, 2015). It is plausible that declarative memory may play a crucial role in older learners (Ullman, 2001b). For example, they may take advantage of their better semantic knowledge to remember the vocabularies as a chunk (e.g., by forming a story to connect the words being learnt), or to proactively derive semantic associations for use as retrieval cues in episodic memory recall. However, individual differences studies on FLL in older adults have remained scarce, and even fewer have examined the neural correlates of FLL in older adults. To our knowledge, one such study has focused on vocabulary learning, and it suggested that the hippocampal volume and the associative memory ability prior to language learning are robust predictors of vocabulary proficiency at the end of training (Nilsson et al., 2021). Another study showed that the artificial grammar learning performance was influenced by structural and functional connectivity of the Broca's area and its right hemisphere homolog (Antonenko et al., 2012).

1.3. The Present Study

The present study investigates the neurocognitive factors that influence the immediate learning success and long-term retention of the vocabularies during an intensive FLL programme, based on a group of Cantonese-speaking Hong Kong older learners aged 58–69, all of whom were familiar with English as a second language. Italian was chosen as the target language due to its highly regular grapheme–phoneme correspondence, its use of the Latin alphabet, the unfamiliarity with the language by the general population in Hong Kong, and the popularity of Italy as a tourist destination. By design, while both vocabulary and basic grammar rules were taught throughout the learning programme, a stronger emphasis was put on the vocabulary since it plays a fundamental role in both spoken and written language comprehension across all stages of learning (Yum et al., 2014). Also, older learners may be less motivated in learning a new language in its entirety, and they may only wish to learn the essential vocabularies for simple communications and travels (Antoniou et al., 2013; Pfenninger and Polz, 2018). Our main hypothesis is that, for foreign vocabulary learning in older adults, both semantic and episodic memory are more strongly associated with the learning success than phonological skills. To examine this hypothesis, two groups

of analyses were conducted, using MRI and cognitive data to predict the immediate learning success and long-term retention.

The first group of analyses (MRI analysis) comprised a *cortical analysis* and a complementary *sub-cortical analysis*. For the cortical analysis, using SBM, four cortical morphological measures (cortical thickness, cortical surface area, cortical volume, and mean curvature) were extracted over a broad range of regions of interest (ROIs); these measures were then used as predictors to test the associations of each ROI with the in-class performances and the final test scores. The ROIs were selected because they have consistently been found to support semantic memory (Patterson et al., 2007; Lau et al., 2008; Binder et al., 2009; Ralph et al., 2017), have exhibited learning-induced neuroplasticity (Lee et al., 2007; Stein et al., 2012; Li et al., 2014), have previously been associated with second language learning performance in general (Ullman, 2016; Tagarelli et al., 2019), or are part of the language control network (Abutalebi and Green, 2007). Although language processing is strongly left-lateralized in the brain, the right hemisphere is also heavily engaged for learning a second language (Hosoda et al., 2013; Bubbico et al., 2019; Qi et al., 2019; Chen et al., 2021). Thus, the homologous areas in both hemispheres were included as ROIs. Our hypothesis would be supported if the cortical measures of the brain regions centrally involved in semantic functions (pars orbitalis and temporal pole) or episodic memory (caudal middle frontal cortex and entorhinal cortex) are more associated with learning performance than those that underlie phonological functions (precentral gyrus and SMG).

For the *sub-cortical analysis*, sub-cortical volume measures were used to predict in-class and final test scores. Due to our relatively small sample size and the already extended set of cortical regions examined, exploration was limited to four ROIs: hippocampus, thalamus, caudate nucleus, and putamen. This analysis complemented the cortical analysis in providing further evidence consistent with the main hypothesis. For example, if the hippocampal volume was associated with learning performance, it would strengthen the view that the episodic memory is associated with FLL in older adults.

In the second group of analyses (*cognitive analysis*), a broad range of cognitive and phonological measures, derived from a cognitive and phonological test battery, were used as the predictors of language learning performance. Behavioral support for our main hypothesis would be obtained if the semantic function score (semantic fluency and picture naming) and verbal episodic memory score (Hong Kong List Learning test) are more important predictors of the learning outcomes than phonological function scores (phonological discrimination and awareness).

2. MATERIALS AND METHODS

2.1. Participants

A group of 25 older learners aged 58–69 were initially enrolled into the Italian learning programme. They were native Cantonese speakers, had no known neurological disorders and normal/correct-to-normal vision. All of them had limited exposure to Italian, had visited Italy for no more than a month, and had at least 6 years of prior experience in learning English. The cohort was recruited *via* the Institute of Active Aging, Hong Kong Polytechnic University. Hong Kong version of Montreal Cognitive Assessment (Wong et al., 2009) was used to confirm that they were cognitively normal (mean = 27.9, *SD* = 1.7). The attendance for the intensive Italian learning programme was high, with 21 of 25 participants completing all the 21 possible visits. There were four drop-outs midway through the programme, including three who completed 5 visits and one who completed 10 visits. One female participant was left-handed (handedness = −60) according to the Edinburgh inventory (Oldfield, 1971); only the remaining 20 participants were included in the present analysis. Their mean age, education, and HK-MoCA were 63.7 (SD = 2.9, range = 58.6–69.3), 15.2 (SD = 3.1, range = 11–21), and 27.8 (SD = 1.7, range = 25–30), respectively. All procedures were approved by the Ethical Review Committee, Hong Kong Polytechnic University. Written signed informed consent was obtained from all participants. They were reimbursed HKD 800 for their participation.

2.2. Study Description

The participants individually attended an intensive Italian vocabulary learning programme (**Figure 1**). The whole programme comprised an introductory lesson (visit 1), ten computerized vocabulary lessons (visits 3–4, 6–7, 9–10, 12–13, and 15–16), four revisions sessions (visit 8, 11, 14, 17), an Italian final test (visit 18), and a range of tests arranged at various points of the programme. These included an MRI session (visit 2), initial-learning phase cognitive tests (visit 5), initial-learning phase phonological tests (at the beginning of visits 3, 4, and 6), post-learning phase phonological tests (visits 18–19), post-learning phase cognitive tests (visit 20), and a debriefing session (visit 21; see **Supplementary Section S1**). The MRI, phonological, and cognitive testing were not conducted right at the beginning, for two reasons. (1) In reality, many language learners have some degree of knowledge of the target foreign language before proceeding to take a formal course. The introductory session serves to provide a more uniform experience prior to the MRI visit. Also, the introductory session gave them a taste of learning a new foreign language and offered a buffer period for them to commit to participating in the structural MRI session and the subsequent intensive Italian learning programme, which would likely reduce the dropout rate. (2) Upon enrolling to the study, most participants were anxious and most motivated to start learning Italian. As such, arranging too many tests that are unrelated to Italian learning right at the beginning would likely be seen as non-ideal arrangement from the learner's view, which might increase the dropout rate. Hence, the phonological and cognitive testing were not arranged immediately after the MRI session, but they were spread over sessions 3–5 as a compromise, especially because it was not our primary goals to investigate learning-induced cognitive gains. Overall, the whole programme can be divided into three phases—initial learning (visits 1–5), intensive-learning (visits 6–17), and post-learning (visits 18–21). The division of visits 1–17 into two phases was an arbitrary one, but the main difference was that a variety of tests were throughout the initial learning stage, while a revision session was arranged every two lessons only during the intensive-learning phases. Also, there was more separation between visits in the initial-learning phase

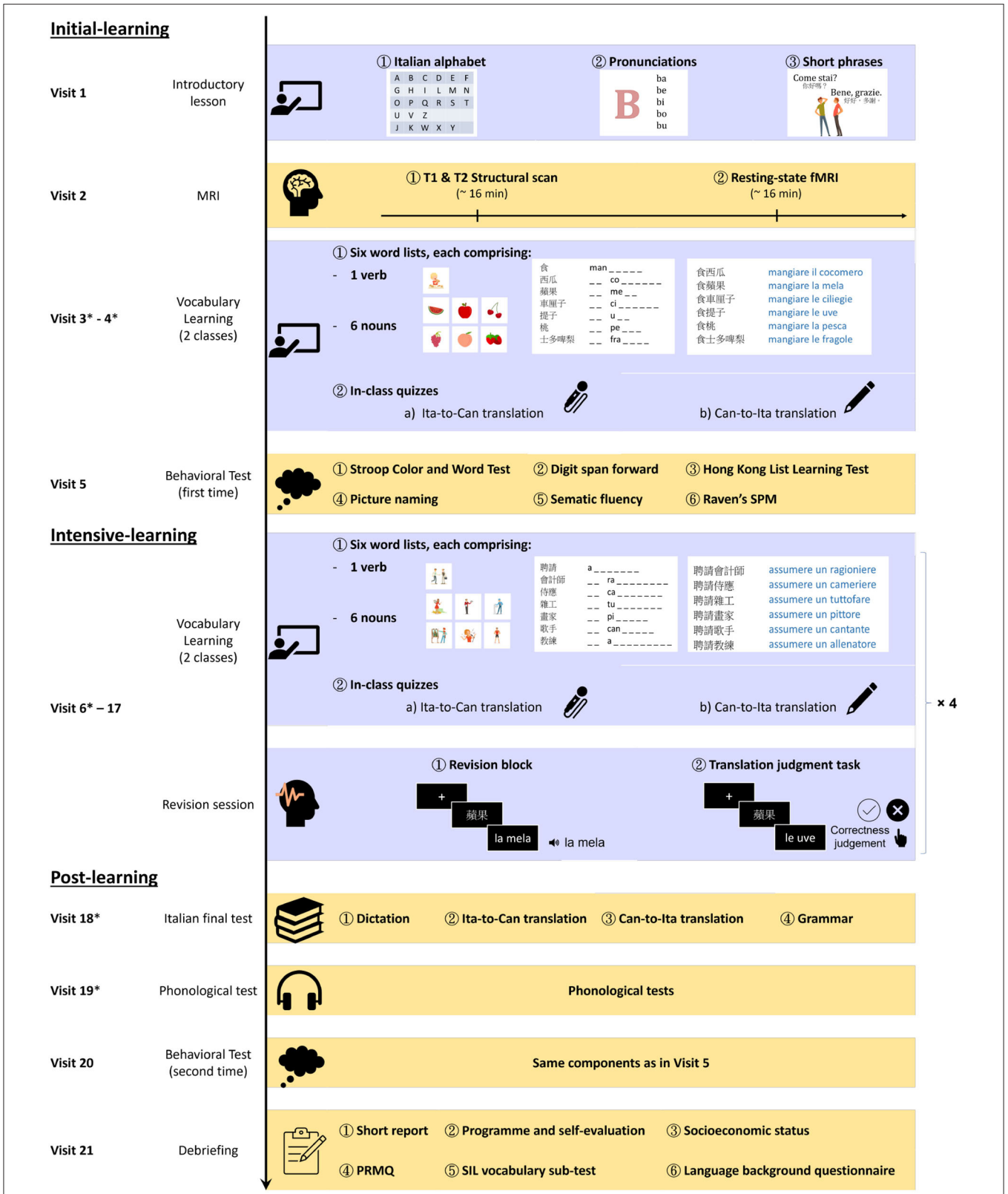

FIGURE 1 | Italian learning programme. The whole programme was divided into three phases—initial-learning (visits 1–5), intensive-learning (visits 6–17), and post-learning (visits 18–21). In the initial- and intensive-learning phases, six word lists were taught per vocabulary lesson, each comprising a verb and six nouns. After two vocabulary lessons, there was a revision session. Such a cycle of three sessions was repeated four times during the learning programme (hence × 4 in the figure). Asterisks (*) were used to indicate the visits during which phonological tests were administered (see main text).

(4.5 days on average, $SD = 1.1$ days) than in intensive-learning (3.2 days, $SD = 0.7$ days), due to scheduling difficulties. The completion time of the first twenty visits of the programme was 68.9 days on average ($SD = 11.6$ days). The details for each component are laid out below in the following sections: Italian vocabulary learning programme, MRI protocol, and behavioral test battery.

2.3. Italian Vocabulary Learning Programme

2.3.1. Introductory Lesson

Each participant attended a 1.5-h introductory Italian lesson, in which they watched a custom-made video under the direction of an experimenter. There were three main parts in the video: Italian alphabet, Italian sounds, and Italian short phrases. Sixteen syllable identification questions were given as homework.

2.3.2. Computerized Vocabulary Lessons

Each computerized vocabulary learning lesson was about 120 min long. The goal of each lesson was to learn six word lists, each comprising a transitive verb (e.g., *mangiare*, "to eat") and six matching nouns (e.g., *la mela*, "an apple.") Thus, over the course of ten vocabulary lessons, there were 60 word lists in total, comprising 60 verbs and 360 nouns (see **Supplementary Table 1**, for the complete list of Italian words used, along with their Cantonese and English translation). In constructing these word lists, control measures were taken so that any systematic changes in the learning performance over time would not be due to confounding factors like the inherent difficulties of the Italian word lists or their Cantonese counterparts. In particular, because Italian words with a larger number of syllables or letters would likely be more difficult to remember, 5 groups of 12 word lists were constructed, with each group being the study materials for two consecutive classes. Across all pairs of groups, the verbs and nouns were matched separately in number of syllables (verbs: $ps > 0.14$, nouns: $ps > 0.10$) and letters (verbs: $ps > 0.32$; nouns: $ps > 0.14$). The Cantonese translation of the word list were also matched in the number of Chinese characters (verbs: $ps > 0.10$; nouns: $ps > 0.07$) and strokes (verbs: $ps > 0.28$; nouns: $ps > 0.12$). The stimulus matching was not conducted by lesson, because, due to the non-arbitrary pairing of the verbs and nouns, it was exceedingly difficult to create 10 groups that are matched in all four variables. Dividing by week also provided a better match in terms of the structure of the whole programme, in that, during the intensive-learning phase, the vast majority of older adults had two lessons per week, and a revision session was arranged every two lessons. By using week rather than lesson as a measurement unit, each in-class score is the average over two lessons, which should have lower measurement noise compared to that derived using only one lesson. For more details about the stimulus matching and construction, see **Supplementary Section S1** and **Supplementary Table S1**. The teaching materials were delivered based on a custom-made E-Prime 3.0 script.

For each word list, the participant first learnt the verb through a picture depicting the verb and by listening to its pronunciation three times. Next, the participant learnt the six nouns through clicking on the corresponding pictures to listen to their pronunciations. Each picture could be clicked three times, before it would vanish on-screen. The order and pace of learning were self-determined. The participant was then given a chance to read aloud the seven words, upon hearing the pronunciation of each word. Next, they completed a fill-in-the-blank exercise on paper, in which they should spell all the seven words learnt. They were asked to check their own answer directly afterwards. The participant then listened to the pronunciation of the six verb-noun phrases (e.g., *mangiare la mela*, meaning "to eat an apple") for three times each, before continuing with the next word list. The learning of each list usually took 15–20 min. After learning all six word lists, a short quiz was given at the end of each lesson. They were given as much time as they wish before the short quiz. The fill-in-the-blank and the quiz were included to promote memory consolidation and to assess immediate learning success, respectively.

There were two parts in the quiz: Italian-to-Cantonese and Cantonese-to-Italian translation (*abbr.* Ita-to-Can and Can-to-Ita thereafter). In either part, all 36 phrases learnt were tested, with each verb and noun would be tested six times or once, respectively. In Ita-to-Can, the participants read a verb-noun phrase (e.g., *mangiare la mela*) on screen and listened to its pronunciation, and they were asked to orally translate the phrase into Cantonese. The maximum score for this part was $36 \times 2 = 72$. In Can-to-Ita, the participants were given a paper-and-pen test, and they should write down the Italian translation of Cantonese verb-noun phrases. The order of the phrases was pseudorandomized, with no more than two consecutive phrases sharing the same verb. No feedback about the correct answer was given. For simplicity, participants were asked to write down the taught form of article (definite or indefinite) for the nouns in Can-to-Ita. However, the article was not scored because there was more than one possible grammatically correct choices, and their distinction was only learnt gradually; thus the maximum score remained as 72. As such, the grammatical use of the article was only scored in the final test.

In addition, six pages of handouts (one word list per page) showing the concepts learnt in pictorial form were given at the end of each lesson, on which the participants should copy the Italian words, either immediately or at home. Though the lexical consolidation process would be influenced by the number of times that participants revised the Italian vocabularies, the notes were essential for the effectiveness of the lessons. Also, although these lessons put more emphasis on vocabulary building, basic grammatical components and rules (including gender, singular and plural forms, article, present tense, adjective, numerals, and possessive adjective) were also taught, through four handouts and corresponding homework exercises, distributed at the end of lesson 1, 6, 8, and 10. Participants attended four revision sessions in total, each time following the completion of two vocabulary sessions. Results for the revision sessions, which involved electroencephalogram recordings, will be reported in a separate paper (under preparation).

2.3.3. Italian Final Test

An 1.5-h Italian test comprising four different parts—dictation, Ita-to-Can, Can-to-Ita, and grammar—was administered about one week after the final vocabulary lesson. In the first three parts, the words were uniformly sampled across the ten vocabulary

learning lessons. The first three parts were delivered using E-Prime 3.0, while the grammar test was an open-note, paper-and-pen test. For dictation, 60 nouns (including the article, e.g., il gesso, "the chalk") were presented aurally at a rate of 15 s / item. Participants were asked to dictate each word on an answer sheet. The nouns would be repeated at a rate of 5 s / item, during which they could check and change their answers. Each correct spelling of the article and noun was worth half a point. The procedures for Ita-to-Can and Can-to-Ita translation were the same as those for the vocabulary lessons, except that there were only 30 verb-noun phrases here. While there were 30 questions in each test, the maximum score of Ita-to-Can was $30 \times 2 = 60$ because participants were asked to translate one Italian verb-noun phrase into one Cantonese verb and one Cantonese noun; the Cantonese verb and noun accounted for a point each. The maximum score of Can-to-Ita was $30 \times 3 = 90$ because participants were asked to translate one Cantonese verb-noun phrase into a verb, an article, plus a noun. For the grammar test, the questions were multiple-choice questions with either two or four choices; correspondingly, each question was worth two or four marks. The distribution of points approximately matched the relative emphasis in the grammatical notes. For the details of the final test, see **Supplementary Section S1** and **Supplementary Table S2**.

2.3.4. Measures of Immediate Learning Success and Language Retention

The participants' performance in each lesson was summarized by means of two scores: Ita-to-Can translation (maximum: 42) and Can-to-Ita translation (maximum: 42). For the final test, the maximum for dictation, Ita-to-Can, Can-to-Ita, and grammar were 60, 60, 90, and 180, respectively. Partial credit was not given; the Italian spellings or Cantonese words should be produced entirely.

2.4. MRI Protocol

2.4.1. Structural MRI

The MRI session was arranged after the introductory lesson. All patients were scanned with a Signa Premier 3T scanner (GE Healthcare, USA), located at the MRI Unit, Department of Radiology, University of Hong Kong. A head coil with forty-eight channels was used. High-resolution T1-weighted structural scans were acquired using a T1-weighted sequence known as 3D Gradient-Echo BRAin VOlume (BRAVO; TR 7.3 ms, TE 3 ms, TI 900 ms, flip angle 8°, $1 \times 1 \times 1$ mm^3 voxels, TA = 5 min 42 s, FOV $= 256 \times 256 \times 376$ mm^3). T2 and resting-state fMRI data were also acquired, but they were not analyzed for the present paper. The total acquisition time was about 35 min.

2.4.2. Extraction of Anatomical Measures

The T1 data were analyzed using FreeSurfer 7.2.0 `recon-all` segmentation pipeline (Fischl, 2012). The automatic pipeline started with various pre-processing steps, including motion correction, skull-stripping, removal of non-brain tissues, and intensity normalization. The pipeline then proceeded with both surface-based morphometry (SBM) and volume-based morphometry.

Regarding the SBM part, a mesh model was constructed for the cortical surface, comprising an inner white matter surface that separated gray matter (GM) and white matter (WM) and an outer pial surface that separated GM and cerebrospinal fluid (Fischl and Dale, 2000). The surface models were then inflated, and co-registered to the `fsaverage` template. Desikan-Killiany cortical parcellation (aparc.annot) was adopted for cortical segmentation (Desikan et al., 2006). For each cortical ROI (**Figure 2**), four measures were extracted based on the surface models by summing/averaging across the vertices of the mesh: cortical thickness (the mean distance between the white and pial surface), cortical surface area (the sum of areas, measured at the white surface), cortical volume (the total volume of the gray matter that lies between the white and pial surface), and mean curvature (the average degree of cortical gyrification) (Winkler et al., 2010; Luders et al., 2012). Our rationale for using all four cortical measures was three-fold. (1) They have all been implicated in either language learning or cognition in general. (2) As a group, they would multivariately explain a larger percent of variance in the learning performance than they would individually, given that they likely encapsulate complementary information (e.g., Winkler et al., 2010; Yang et al., 2016). For example, there is only a weak correlation between cortical thickness and cortical surface area (Winkler et al., 2010). (3) These measures also have different developmental trajectories across the lifespan (Hogstrom et al., 2013), differential associations with cognitive functions (Gautam et al., 2015; Chung et al., 2017; Green et al., 2018; Tadayon et al., 2020) or even genetic factors (Grasby et al., 2020). For example, not only were individual differences in cortical thickness and cortical surface area ascribed to largely different genetic factors, but these factors also exert their influences in different developmental stages (Grasby et al., 2020).

The volume-based morphometry involves a non-linear volumetric registration to the FreeSurfer atlas, with the structural labeling being performed using a Gaussian Classifier Atlas (GCA; Fischl et al., 2002). For each sub-cortical ROI (**Figure 2**), the sub-cortical volume was extracted as the single measure.

2.5. Behavioral Test Battery

2.5.1. Cognitive Test Battery

A neuropsychological test battery comprising six standard cognitive tests was conducted, with the language of instruction being the native language of the participants (Cantonese). These tests included the Stroop Color and Word Test (Golden and Freshwater, 1978; Fong et al., 2020), digit span forward, Hong Kong List Learning Test (HKLLT; Chan and Kwok, 1998), picture naming (Bates et al., 2003; Fong et al., 2020), semantic fluency (Fong et al., 2021), and Raven's Standard Progressive Matrices (Raven and Court, 1998), and they were administered after three Italian learning lessons and one week post-learning. These tests assess processing speed, inhibition, short-term memory, verbal episodic memory, semantic knowledge, and matrix reasoning, respectively (**Table 1**). This battery was administered at the fifth visit (initial-learning phase) and the twentieth visit (post-learning phase) to assess the learning-induced cognitive gains, except for the possible use of two

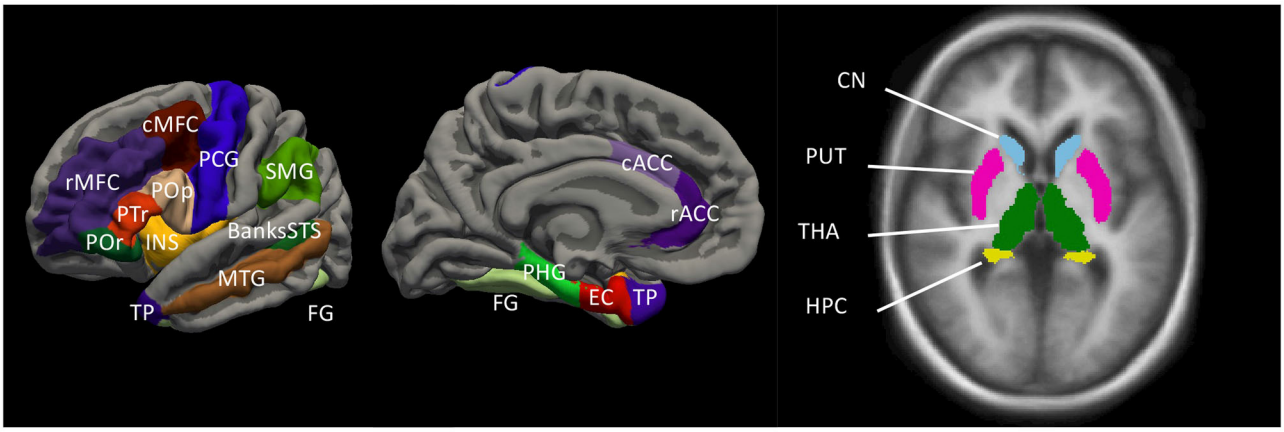

Cortical ROIs			
Rostral middle frontal cortex	rMFC	Supramarginal gyrus	SMG
Caudal middle frontal cortex	cMFC	Middle temporal gyrus	MTG
Pars opercularis	POp	Rostral anterior cingulate	rACC
Pars triangularis	PTr	Caudal anterior cingulate	cACC
Pars orbitalis	POr	Fusiform gyrus	FG
Temporal pole	TP	Parahippocampal gyrus	PHG
Insula	INS	Entorhinal cortex	EC
Precentral gyrus	PCG	Banks of the Superior Temporal Sulcus	BanksSTS
Sub-cortical ROIs			
Thalamus	THA	Hippocampus	HPC
Caudate nucleus	CN	Putamen	PUT

FIGURE 2 | Cortical and sub-cortical regions of interest (ROIs).

TABLE 1 | Measures of behavioral test performance.

Task	Cognitive function or phonological skill	Detail
Stroop Color and Word Test	Processing speed	Average number of correct responses in 45 s across the word and color sub-tasks
	Inhibition function	Number of correct responses in the color-word sub task, divided by the processing speed measure above
Digit span forward	Phonological STM	The maximum memory load reached (test continued if 2 of 3 questions were correct at a given load; half a point would be added in case of a single correct answer)
Hong Kong List Learning Test	Verbal episodic memory	Number of memory items retrieved after 30 min
Picture naming task	Naming latency	The average latency of correct answers
Semantic fluency	Semantic memory	Average number of responses across 16 semantic categories
Raven's SPM	Matrix reasoning	Standardized number of correct responses
Cantonese discrimination	Cantonese perceptual skill	Number of correct answers (Max: 41)
Cantonese Spoonerism	Cantonese phonological awareness	Number of correct answers (Max: 30)
English discrimination	English perceptual skill	Number of correct answers (Max: 38)
English Spoonerism	English phonological awareness	Number of correct answers (Max: 30)
Italian discrimination	Italian perceptual skill	Number of correct answers (Max: 35)
Italian Spoonerism	Italian phonological awareness	Number of correct answers (Max: 30)

different versions of tests to minimize training effects. Details of this battery can be found in **Supplementary Section S2** and **Supplementary Tables S3–S5**.

2.5.2. Phonological Test Battery

Two phonological tests (discrimination and Spoonerism) each were run for all three languages—Cantonese (L1), English (L2), and Italian (L3). For the discrimination task, participants heard four auditory stimuli in succession in each trial (*c.f.* Koda, 1998). Three of the stimuli shared the same segmental or suprasegmental feature (in the case of Cantonese tone), with the fourth not sharing the feature in question. The number of blocks and trials for each language examined was different, due to the different number of distinctive segmental and suprasegmental feature in each language. The Cantonese discrimination task was divided into three blocks, in which the feature in question was initial consonant (25 trials), vowel (10 trials), and tone (6 trials), respectively. The English discrimination task was

divided into two blocks, in which the feature in question was initial consonant (26 trials) and vowel (12 trials). The Italian discrimination task was divided into two blocks, in which the feature in question was also initial consonant (25 trials) and vowel (10 trials). For Spoonerism, participants listened to a pair of words in succession. Their task was to swap the initial consonant of the two words. There were 15 trials in all three versions. The test would be terminated if the participants failed to score any point in three consecutive trials. The Cantonese and English tests were arranged on visits 3 and 4 (one per visit, order counterbalanced), and together in visit 19 (order counterbalanced). The Italian tests were arranged on visits 5 and 18. More details of this battery can be found in **Supplementary Section S3** and **Supplementary Tables S6–S9**.

2.6. Linear Mixed-Effects Modeling

Linear mixed-effects (LME) models were constructed to test our main hypothesis that semantic and episodic memory functions play a major role in language learning in older learners. First, baseline demographic models (baseline models thereafter) were constructed for each of the three scores (in-class Ita-to-Can, in-class Can-to-Ita, and final test). In each baseline model, in addition to either Week (for the in-class Ita-to-Can or Can-to-Ita) or TestPart (for the final test), three demographic variables (age, years of education, and gender) were included as fixed-effects predictors, while participants were included as a random-effects variable.

Next, two groups of analyses were conducted, each involving comparisons between the full model(s) of interest against the corresponding baseline models. The first analysis comprised both a cortical and a complementary sub-cortical analysis. In the cortical analysis, the surface-based morphological measures were used as predictors to test the neural associations with the in-class performances and the final test scores. The regions of interest (ROIs), illustrated in **Figure 2**, comprised the Broca's area (pars opercularis and pars triangularis), the regions supporting semantic memory (pars orbitalis, temporal pole, and middle temporal gyrus) and episodic memory (caudal and rostral middle frontal cortex, entorhinal cortex, and parahippocampal gyrus), as well as regions important for phonological processing (SMG, precentral gyrus, banks of superior temporal sulcus), procedural memory (insula), language switching (caudal and rostral anterior cingulate), and orthographical processing (fusiform gyrus). For each ROI, a full model was constructed that include all the predictors in the baseline model, four anatomical measures of the ROI, and the interactions between each anatomical measure with either Week or TestPart. Likelihood ratio tests were used to evaluate whether the full model of each ROI represented an improvement over the baseline model. Multiple comparisons were corrected using the false discovery rate (FDR) procedure. If a significant interaction was found, *post hoc* trend analysis was conducted to reveal how the degree of association of each anatomical measure with the language learning performance was modulated by Week or TestPart. In the sub-cortical analysis, the sub-cortical volumes were used to predict the in-class and final test scores. The eight regions of interest (ROIs) included the hippocampus, thalamus, caudate nucleus, and putamen on both hemispheres. For each ROI, a full model was constructed using the sub-cortical volume of the ROI and its interaction with either Week or TestPart. The subsequent likelihood ratio tests were FDR-corrected.

In the second group of analyses—cognitive analysis—the cognitive predictors, derived from the neuropsychological data, were included as the additional predictors for modeling the three scores (Bonferroni correction was applied). For each model, backward elimination was conducted to yield the final model.

TABLE 2 | Summary statistics of the scores for the in-class quizzes (Ita-to-Can and Can-to-Ita) and the final test.

Score (%)	*Mean*	*SD*	*Min*	*Max*
InClass-Ita-to-Can	71.8	20.4	26.7	93.5
InClass-Can-to-Ita	41.1	22.5	6.2	73.0
FinalTest-Dictation	59.5	17.1	30.0	91.7
FinalTest-Ita-to-Can	80.2	21.4	36.7	100
FinalTest-Can-to-Ita	56.4	27.7	16.7	96.7
FinalTest-Grammar	92.9	5.9	78.9	100

2.7. Cognitive and Phonological Skill Comparisons Between Initial- and Post-learning

For completeness, we tested the changes in cognitive functions and phonological skills incurred between the initial- and post-learning, despite the lack of a control group to assess whether the changes were due to repetition effects or induced by language learning. For each cognitive/phonological measure, a pairwise Wilcoxon signed rank test (two-tailed) was conducted with FDR-correction.

3. RESULTS

3.1. Italian Learning Performances

Table 2 shows the summary statistics for the mean performance for the two in-class quizzes (Ita-to-Can and Can-to-Ita) and the final test, which were used as indices for immediate learning success and language retention, respectively. **Figure 3** illustrates the overall in-class learning performance across the five weeks; the verb and noun components were separately plotted to reflect the structure of the in-class quizzes, although only the overall learning performance was selected for statistical analysis. To test whether the improvement was significant across the five weeks, a linear mixed-effects model was fitted for each in-class quiz, using the demographic variables for predicting the performance (**Table 3**). In both cases, the main effect of Week was significant, $ps < 0.001$. For Ita-to-Can, *post hoc* pairwise comparisons with Tukey's correction showed that the performance for week 1 was significantly worse than all other weeks, while that for week 5 was significantly better than all other weeks, with no differences among Week 2–4 being significant. For Can-to-Ita, the *post hoc* pairwise comparisons

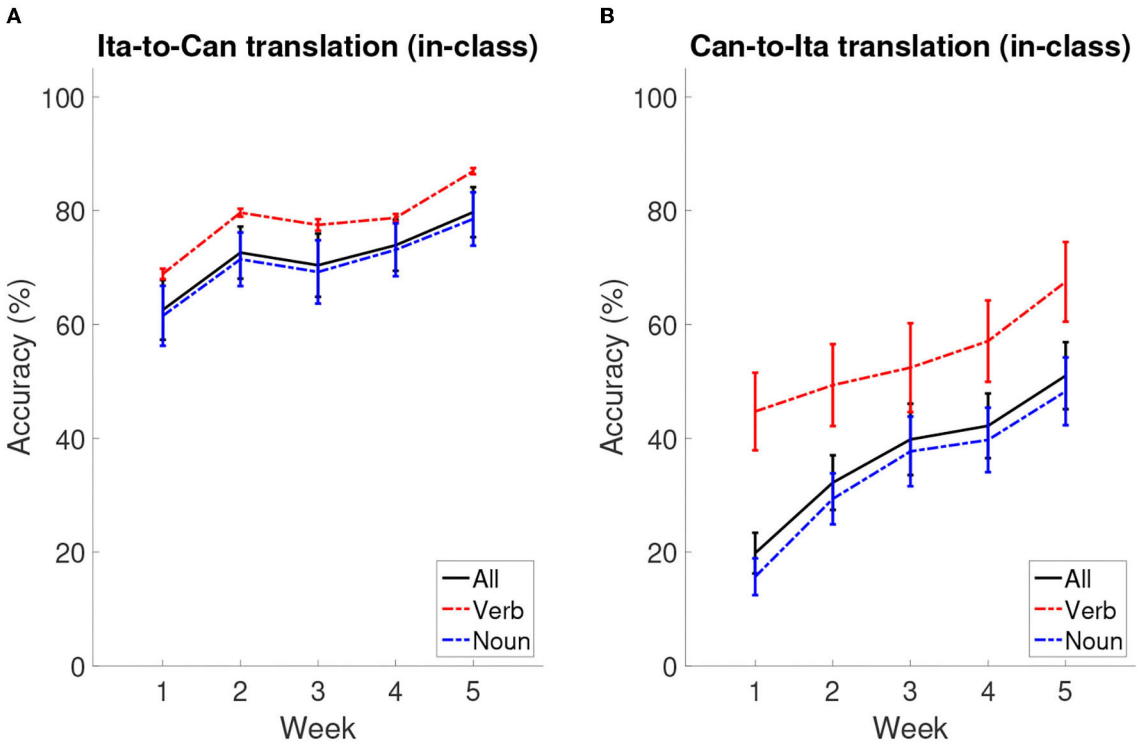

FIGURE 3 | Learning curves across the five weeks. **(A)** The accuracy of Ita-to-Can translation across weeks. **(B)** The accuracy of Can-to-Ita translation across weeks. Solid lines: overall in-class learning performance as a function of week; dotted lines: the scores for the verb and noun components, separately plotted to reflect the structure of the in-class quizzes. The error bars represent standard error means.

TABLE 3 | Demographic models for the in-class quizzes (Ita-to-Can and Can-to-Ita) and the final test.

Score	*Term*	*SumSq*	*MeanSq*	*NumDF*	*DenDF*	*F*	*p*	
Ita-to-Can	Week	3156.37	789.09	4	80.0	19.83	< 0.001	***
	Age	29.23	29.23	1	20.0	0.73	0.402	ns
	Education	25.39	25.39	1	20.0	0.64	0.434	ns
	Gender	21.36	21.36	1	20.0	0.54	0.472	ns
Can-to-Ita	Week	4726.65	1181.66	4	80.0	20.64	< 0.001	***
	Age	68.48	68.48	1	20.0	1.20	0.287	ns
	Education	43.20	43.20	1	20.0	0.75	0.395	ns
	Gender	0.59	0.59	1	20.0	0.01	0.920	ns
FinalTest	TestPart	18082.02	6027.34	3	60.0	41.41	< 0.001	***
	Age	307.16	307.16	1	20.0	2.11	0.162	ns
	Education	119.81	119.81	1	20.0	0.82	0.375	ns
	Gender	132.84	132.84	1	20.0	0.91	0.351	ns

****, p <0.001, **, p <0.01, *, p <0.05, †, marginal, ns, non-significant.*

indicated that the improvements over two weeks or more were all significant, although the improvement between successive weeks was only significant going from Week 1 to 2. These results suggested that the participants were generally able to learn an increasing number of Italian words across the five weeks.

For the final test, the participants were able to dictate 59.5% of the Italian words, backward translate 80.2% of Italian words into Cantonese verbally, forward translate 56.4% of Cantonese words into Italian in written form, and achieve a score of 92.9% for grammar. It is worth noting that the first three parts were closed-note tests while participants were allowed to refer to the notes in the grammar part, which likely accounts for the higher grammar score. In the baseline model, the main effect of TestPart was significant, $p < 0.001$. *Post hoc* pairwise comparisons showed that the test score significantly

differed across the four parts, except between dictation and Can-to-Ita.

3.2. MRI Results

3.2.1. Surface-Based Cortical Measures and Brain Volume Measures

The four cortical anatomical measures (thickness, surface area, volume, and mean curvature) and the sub-cortical volumes were extracted for all cortical and sub-cortical ROIs (see **Supplementary Section S4** and **Supplementary Tables S10**, **S11**). In general, the cortical measures of the same ROI were strongly correlated, suggesting a high degree of redundancy in the measures. Despite the expected shared variance among the predictors, the associations with the learning performances could be best captured multivariately by the whole set of parameters. Therefore, all four predictors were included in testing the associations of the ROI with Italian learning performances. Special considerations were taken in interpreting the coefficients of the predictors (see section 3.2.2).

3.2.2. Cortical Predictors of Learning Performance

LME modeling was conducted on the in-class and final test scores. **Table 4** summarizes the cortical ROIs at which the anatomical parameters were sensitive to the learning performance (for the results at all the ROIs tested, see **Supplementary Tables S12**, **S14**, and **S16**). For transparency, the marginally significant associations (FDR-corrected $p < 0.10$) and all other associations with uncorrected $p < 0.05$ were also tabulated. Due to the strong correlations among the four predictors, sequential regression was applied to transform the original predictors into four adjusted predictors (more precisely, the most important predictor, determined by the chi-square test, was kept unchanged; in other words, only three predictors were transformed). In this way, the same amount of variance was explained by these adjusted predictors and the original predictors, with the advantage of improved interpretability of the predictors. Type III sums of squares procedure was conducted to estimate each fixed-effect term, including the main effects and the four interaction terms (**Supplementary Tables S13**, **S15**, and **S17**). *Posthoc* trend analysis was conducted on the significant interactions using the Satterthwaite method for estimating degrees of freedom. For in-Class Ita-to-Can score, after FDR correction for multiple comparisons, the baseline model was only marginally improved by the anatomical measures of four ROIs: (1) left pars orbitalis, $p = 0.052$; (2) left caudal middle frontal cortex, $p = 0.075$; (3) right insula, $p = 0.075$; and (4) left entorhinal, $p = 0.082$ (see **Supplementary Section S5**, for the follow-up analyses on each ROI).

The prediction of in-class Can-to-Ita performance was significantly improved by the cortical anatomical measures of seven ROIs. For (1) left pars orbitalis, the performance was significantly associated with adjusted curvature, $t = 3.03$, $p = 0.007$, and adjusted area, $t = -2.35$, $p = 0.029$. Week × adjusted area was significant, with the negative association being significant only for Week 3–5, and that the association was significantly larger in magnitude in Week 5 than both Weeks 1 and 2 (**Figure 4A**). Week × adjusted volume was also significant. Although the association was non-significant in all weeks, there were subtle pairwise differences in the strength of association across different weeks. For (2) right pars orbitalis, Week × adjusted volume was significant, but the *post hoc* trend analysis revealed no significant association. Like left pars orbitalis, the interaction was due to subtle pairwise differences in the strength of association across different weeks. For conciseness, only significant associations were reported thereafter. For (3) right insula, the performance was significantly predicted by adjusted volume, $t = 4.10$, $p < 0.001$, adjusted area, $t = -3.95$, $p < 0.001$, and adjusted curvature, $t = -2.58$, $p = 0.018$. Week × adjusted volume was significant, with the association being significant in all five weeks; the interaction was due to the significantly larger association strength in the final two weeks (Weeks 4 and 5) than Week 2. For (4) right caudal anterior cingulate cortex, both Week × adjusted area and Week × adjusted curvature were significant, but none of the association was significant in any of the weeks. For (5) left entorhinal cortex, the performance was significantly associated with adjusted thickness, $t = 3.62$, $p = 0.001$, and adjusted curvature, $t = -5.16$, $p < 0.001$. There was a significant Week × adjusted curvature, which was due to the much more negative association in Week 5 than in both Week 1 and 2. For (6) left caudal middle frontal cortex, there was significant association between Can-to-Ita performance with adjusted curvature $t = 2.75$, $p = 0.013$, and with adjusted thickness $t = 2.48$, $p = 0.022$. Week × adjusted thickness was significant, which was attributed to the fact that the association was significant only for Week 3–5. For (7) right middle temporal gyrus, Week significantly interacted with adjusted area and adjusted volume. However, the association between performance and neither measure was significant in any of the weeks. For an understanding about the subtle changes in association across weeks, readers may refer to **Figure 4B**. Apart from the seven ROIs above, the baseline model was marginally improved at five additional ROIs (left pars triangularis, left temporal pole, right pars triangularis, right entorhinal cortex, and right banks of STS).

For final test, significant associations of the test score with the cortical measures were found for nine ROIs. For (1) right entorhinal cortex, there was significant positive association between final test score and adjusted curvature, $t = 3.06$, $p = 0.006$, adjusted thickness, $t = 2.56$, $p = 0.019$, and adjusted area, $t = 2.12$, $p = 0.047$. TestPart × adjusted volume was significant, as the adjusted volume was negatively associated with only the two translation scores (Ita-to-Can, and Can-to-Ita). TestPart also interacted with adjusted curvature, which was positively associated with the first three parts (Dictation, Ita-to-Can, and Can-to-Ita), and adjusted thickness, which had the same association pattern except that its association with Dictation was only marginally significant. For (2) left pars orbitalis, the test score was significantly predicted by adjusted volume, $t = 3.15$, $p = 0.005$. The interaction between TestPart and adjusted volume was also significant, meaning that the association between the test score and adjusted area was modulated across different parts. For (3) left banks of STS, the test score was significantly and negatively associated with adjusted thickness, $t = -2.63$, $p = 0.016$. There were significant interactions

TABLE 4 | Cortical ROIs showing significant associations with the Italian learning performance.

Score	Region	*AIC*	*BIC*	*logLik*	*r2m*	*r2c*	χ^2	*df*	*p* (unc)	*p* (FDR)	
Ita-to-Can	L pars orbitalis	742.99	821.14	−341.49	0.67	0.94	43.75	20	0.002	0.052	†
	R insula	747.47	825.63	−343.74	0.75	0.93	39.26	20	0.006	0.075	†
	L caudalmiddlefrontal	747.91	826.07	−343.96	0.63	0.94	38.82	20	0.007	0.075	†
	L entorhinal	749.27	827.42	−344.63	0.58	0.94	37.46	20	0.010	0.082	†
	R parsorbitalis	751.16	829.31	−345.58	0.33	0.94	35.58	20	0.017	0.110	ns
	L parstriangularis	751.90	830.06	−345.95	0.59	0.93	34.83	20	0.021	0.112	ns
	L middletemporal	754.23	832.38	−347.11	0.49	0.94	32.51	20	0.038	0.163	ns
	R rostralmiddlefrontal	754.50	832.65	−347.25	0.53	0.93	32.23	20	0.041	0.163	ns
	R entorhinal	755.31	833.46	-347.65	0.42	0.94	31.43	20	0.050	0.177	ns
Can-to-Ita	L parsorbitalis	739.46	817.62	−339.73	0.60	0.96	79.54	20	< 0.001	< 0.001	***
	R parsorbitalis	773.79	851.94	−356.89	0.36	0.94	45.22	20	0.001	0.016	*
	R insula	775.95	854.10	−357.97	0.72	0.92	43.05	20	0.002	0.019	*
	R caudalanteriorcingulate	776.55	854.71	−358.28	0.32	0.94	42.45	20	0.002	0.019	*
	L entorhinal	778.46	856.61	−359.23	0.70	0.92	40.55	20	0.004	0.027	*
	L caudalmiddlefrontal	779.93	858.08	−359.96	0.56	0.93	39.08	20	0.007	0.035	*
	R middletemporal	781.39	859.55	−360.70	0.33	0.94	37.61	20	0.010	0.045	*
	L parstriangularis	782.35	860.51	−361.18	0.47	0.93	36.65	20	0.013	0.052	†
	L temporalpole	782.89	861.04	−361.44	0.64	0.92	36.11	20	0.015	0.053	†
	R parstriangularis	784.01	862.16	−362.00	0.30	0.94	34.99	20	0.020	0.064	†
	R entorhinal	785.88	864.03	−362.94	0.49	0.93	33.13	20	0.033	0.089	†
	R bankssts	785.97	864.12	−362.98	0.41	0.93	33.04	20	0.033	0.089	†
Final test	R entorhinal	659.81	719.36	−304.91	0.75	0.86	48.06	16	< 0.001	0.001	**
	L parsorbitalis	665.77	725.32	−307.89	0.71	0.86	42.10	16	< 0.001	0.006	**
	L bankssts	668.01	727.57	−309.01	0.69	0.86	39.86	16	0.001	0.009	**
	R fusiform	668.87	728.42	−309.43	0.74	0.83	39.01	16	0.001	0.009	**
	L supramarginal	672.66	732.22	−311.33	0.70	0.84	35.21	16	0.004	0.024	*
	L precentral	673.41	732.96	−311.70	0.67	0.85	34.47	16	0.005	0.025	*
	L parstriangularis	674.62	734.17	−312.31	0.67	0.84	33.26	16	0.007	0.031	*
	L rostralmiddlefrontal	676.83	736.38	-313.41	0.68	0.83	31.05	16	0.013	0.048	*
	L caudalmiddlefrontal	676.87	736.43	−313.44	0.70	0.82	31.00	16	0.013	0.048	*
	R supramarginal	677.77	737.32	−313.89	0.65	0.84	30.10	16	0.017	0.056	†

*p(unc), uncorrected p, p(FDR), FDR-corrected p. ***, p <0.001, **, p <0.01, *, p <0.05, †, marginal, ns, non-significant.*

of TestPart with adjusted thickness (which was significantly and negatively associated with translation scores) and adjusted area (which was marginally and negatively associated with both translation scores). For (4) right fusiform gyrus, the test score was significantly predicted by adjusted thickness, $t = -4.59$, $p < 0.001$. TestPart × adjusted thickness was significant: adjusted thickness was negatively associated with the scores in the first three parts. For (5) left SMG, the test score was positively associated with adjusted volume, $t = 2.21$, $p = 0.039$, and negatively associated with adjusted area, $t = -2.33$, $p = 0.030$. TestPart × adjusted area was also significant, with the negative association being significant for both translation scores. For (6) left precentral gyrus, TestPart interacted with both adjusted thickness and adjusted curvature, with the thickness being significantly associated with the two translation scores, while adjusted curvature was only significantly associated with Can-to-Ita. For (7) left pars triangularis, the test score was significantly predicted by adjusted volume, $t = 2.52$, $p = 0.021$. TestPart × adjusted volume and TestPart × adjusted curvature were significant, with both adjusted volume and curvature being positively contributing to the two translation scores. For (8) left caudal middle frontal cortex, the test score was significantly predicted by adjusted curvature, $t = 3.16$, $p = 0.005$. TestPart also interacted with adjusted curvature and adjusted area, with the adjusted curvature being positively associated with the test scores for the first three parts, and the adjusted area negatively associated with the two translation scores. For (9) left rostral middle frontal cortex, the test score was significantly and positively associated with adjusted volume, $t = 2.19$, $p = 0.041$, and with adjusted curvature, $t = 2.11$, $p = 0.047$. TestPart × adjusted curvature was significant, with the curvature being positively associated with the two translation scores. Marginal improvement over the baseline model was observed at one additional ROI (right SMG). For each ROI above, the representative interaction term was illustrated in **Figure 5**.

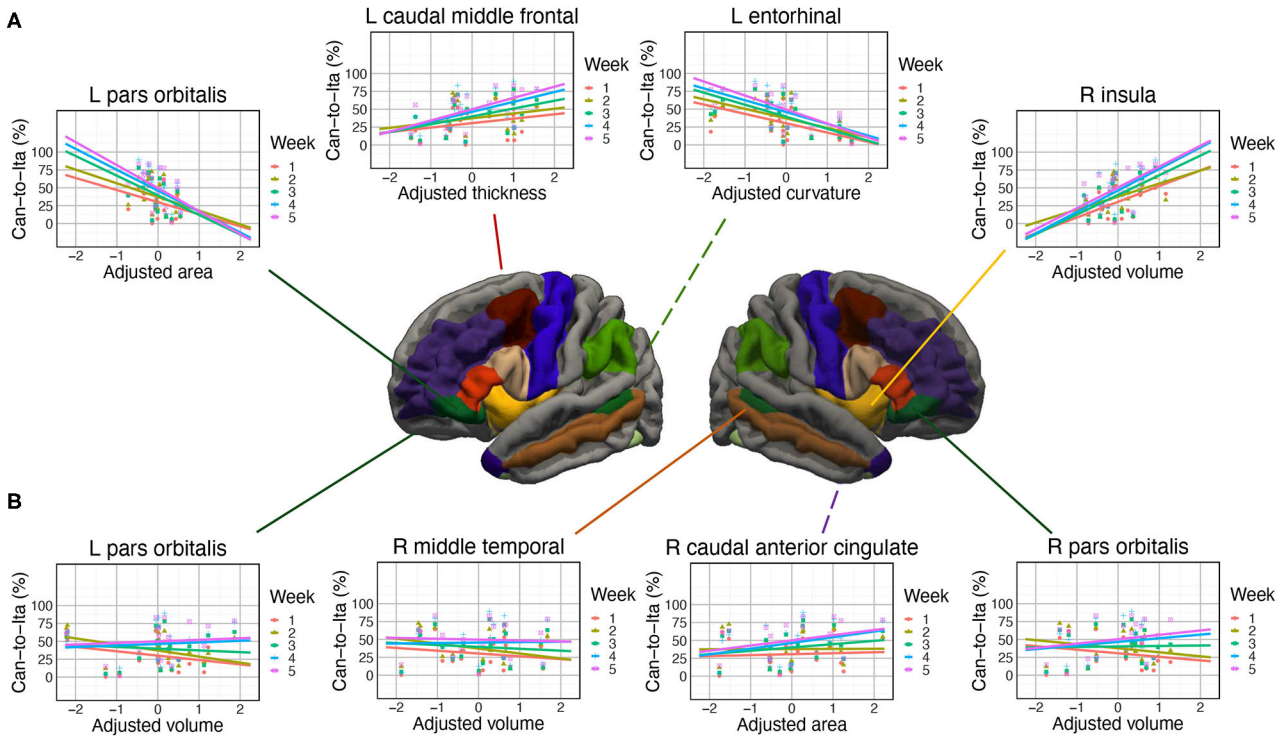

FIGURE 4 | Associations of the in-class Can-to-Ita score with the cortical measures. **(A)** Significant associations at left pars orbitalis, left caudal middle frontal cortex, left entorhinal cortex, and right insula. **(B)** Subtle modulations in the degree of association between final test scores with the cortical measures, found at left pars orbitalis, right middle temporal gyrus, right caudal anterior cingulate, and right pars orbitalis.

3.2.3. Sub-cortical Volumetric Predictors of Learning Performance

The contributions of sub-cortical regions were also examined using sub-cortical volumes, normalized by the intracranial volume (ICV). None of the normalized sub-cortical volumes could significantly improve the two baseline models for the in-class vocabulary learning performances: Ita-to-Can, all uncorrected p's > 0.13, Can-to-Ita, all uncorrected p's > 0.16. For the final test score, the baseline model was significantly improved by two predictors, namely, the sub-cortical volume of left and right thalamus (**Table 5**). For left thalamus, the interaction TestPart × normalized volume was significant, $F(3, 60) = 4.29$, $p = 0.008$, due to the positive association of normalized volume with the scores in two parts: Ita-to-Can, $t = 2.24$, $p = 0.031$, and Can-to-Ita, $t = 2.35$, $p = 0.024$. For right thalamus, the interaction TestPart × normalized volume was significant, $F(3, 60) = 3.74$, $p = 0.016$, due to the significant positive associations of normalized volume with Can-to-Ita, $t = 2.73$, $p = 0.009$ and Ita-to-Can, $t = 2.43$, $p = 0.019$. There was only a weak indication for an association with the sub-cortical volume of right hippocampus (uncorrected $p = 0.09$).

3.3. Cognitive and Phonological Associations

3.3.1. Correlations Among the Cognitive and Phonological Predictors

Figure 6 shows the correlations among the cognitive and phonological predictors. In general, there were high correlations among the three phonological discrimination scores (average $r = 0.58$, range $= 0.45 - 0.76$) and among the three Spoonerism scores (average $r = 0.52$, range $= 0.47 - 0.56$), but relatively low correlations across these measures. This pattern of correlation supported our a priori choice of selecting only one measure each of phonological discrimination and of Spoonerism for representing phonological skills. Given the non-phonological nature of the Chinese writing system, the majority of the older learners were unfamiliar with the phonetic system used in Cantonese. Consequently, the English phonological discrimination and Spoonerism scores were selected as the phonological predictors.

3.3.2. Cognitive Models: Predictors of In-class and Final Test Performances

One of the three baseline models was significantly improved by the cognitive predictors: Can-to-Ita, $AIC = 789.83$, $BIC = 933.11$, $logLik = -339.91$, $\chi^2 = 79.18$, $DF = 45$, uncorrected $p = 0.001$, corrected $p = 0.004$. Backward elimination was applied to yield the final model (**Table 6**). The performance was positively associated with HKLLT ($t(20) = 4.8$, $p < 0.001$), Raven's SPM ($t(20) = 4.33$, $p < 0.001$), English Spoonerism ($t(20) = 3.28$, $p = 0.004$), semantic fluency ($t(20) = 3.05$, $p = 0.006$), and processing speed ($t(20) = 2.49$, $p = 0.022$), and as expected, negatively associated with picture naming latency ($t(20) = -6.53$, $p < 0.001$), but it was also negatively associated with digit span forward ($t(20) = -6.34$, $p < 0.001$) and inhibition ($t(20) = -5.90$, $p < 0.001$). The positive

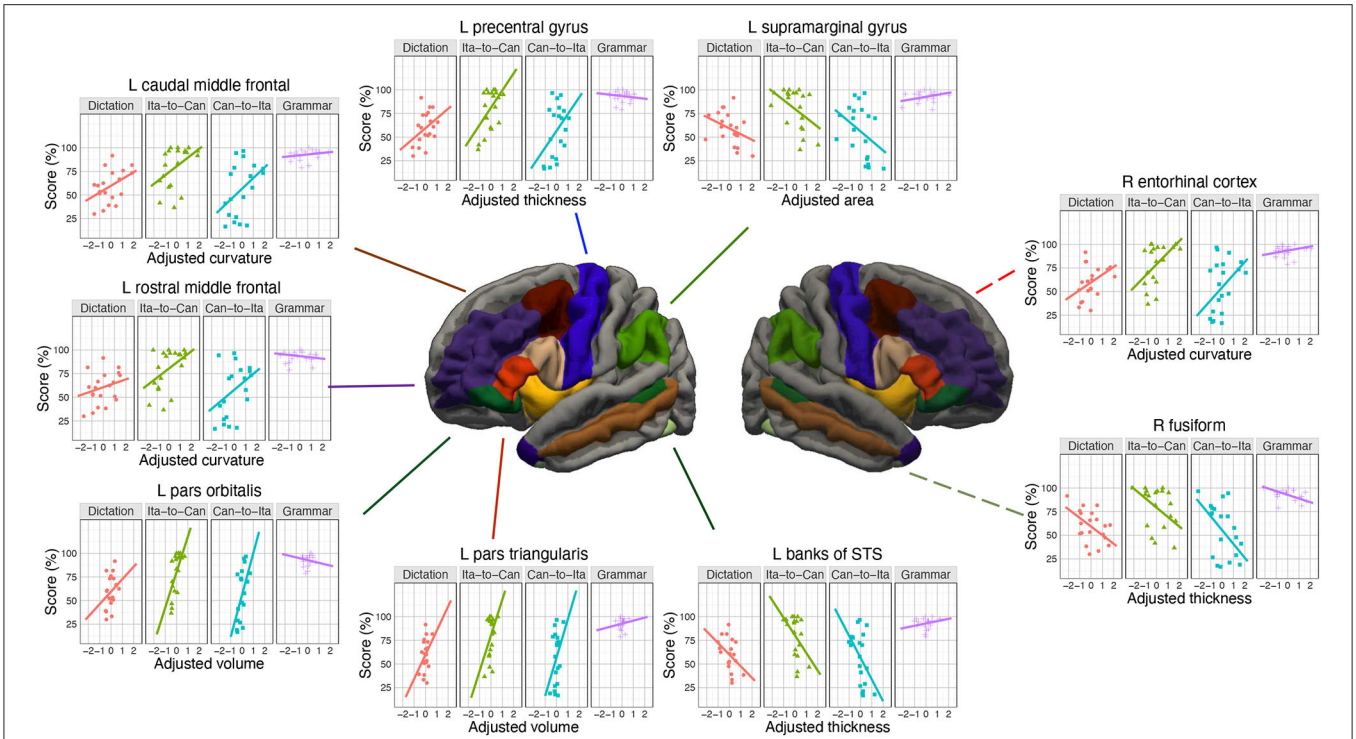

FIGURE 5 | Associations of the final test score with the cortical measures. A more left-dominant network was implicated, with seven left hemisphere regions showing significant associations with the final test score when compared to only two right hemisphere regions.

TABLE 5 | Sub-cortical ROIs showing significant associations with the final test scores.

Region	*AIC*	*BIC*	*logLik*	*r2m*	*r2c*	χ^2	*Df*	*p* (unc)	*p* (FDR)	
L thalamus	669.78	700.75	−321.89	0.58	0.80	14.09	4	0.007	0.036	*
L caudate	683.15	714.11	−328.57	0.51	0.76	0.73	4	0.948	0.948	ns
L putamen	680.32	711.29	−327.16	0.54	0.77	3.55	4	0.470	0.626	ns
L hippocampus	679.81	710.78	−326.91	0.53	0.77	4.06	4	0.397	0.626	ns
R thalamus	670.33	701.30	−322.17	0.59	0.80	13.54	4	0.009	0.036	*
R caudate	682.64	713.60	−328.32	0.53	0.76	1.24	4	0.872	0.948	ns
R putamen	679.95	710.91	−326.97	0.54	0.77	3.93	4	0.416	0.626	ns
R hippocampus	675.83	706.80	-324.92	0.56	0.78	8.04	4	0.090	0.240	ns

p(unc), uncorrected p, p(fdr), FDR-corrected p.
****, p <0.001, **, p <0.01, *, p <0.05, †, marginal, ns, non-significant.*

associations and the negative association with picture naming latency are illustrated in **Figures 7A–E**. In addition, Week × processing speed was also significant, $F(4, 80) = 4.07$, $p = 0.005$. This interaction effect was due to the general increase in the association of processing speed with the learning performance across time (**Figure 7F**), reaching statistical significance in Week 4 ($t(20) = 2.26$, $p = 0.029$) and Week 5 ($t(20) = 4.09$, $p < 0.001$).

For in-class Ita-to-Can, the improvement over the baseline model did not survive the correction, $AIC = 774.01$, $BIC = 917.30$, $logLik = -332.01$, $\chi^2 = 62.72$, $DF = 45$, uncorrected $p = 0.041$, corrected $p = 0.124$. The same held for the baseline model of the final test, $AIC = 696.15$, $BIC = 803.34$, $logLik = -303.08$, $\chi^2 = 51.72$, $DF = 36$, $p = 0.043$. However, backward elimination was applied to explore the most important predictor(s). For the in-class Ita-to-Can, the exploratory analysis revealed a significant Lesson × HKLLT interaction; the trend analysis revealed marginally significant positive associations in week 1 ($t(80) = 2.05$, $p = 0.052$) and week 3 ($t(80) = 1.86$, $p = 0.076$). For the final test, it was positively associated with semantic fluency ($t(20) = 2.18$, $p = 0.041$).

3.4. Cognitive Comparison Between the Initial-Learning vs. Post-learning Phase

Pairwise Wilcoxon signed rank tests revealed marginally shorter picture naming latency, $p = 0.057$, with an effect size (King et al.,

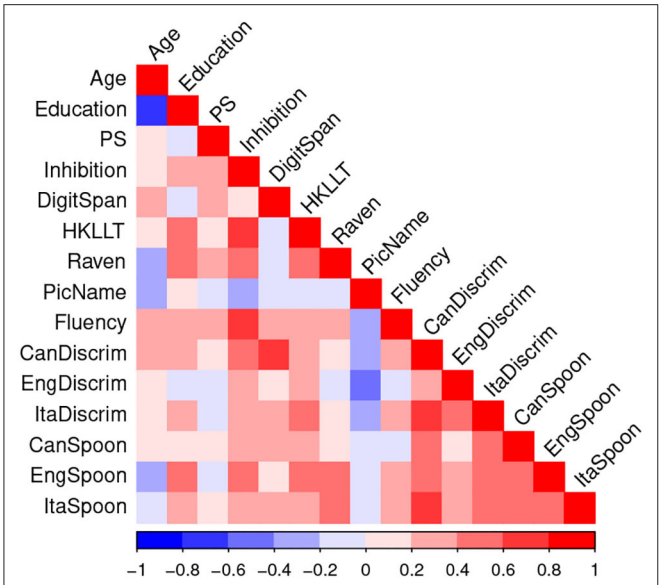

FIGURE 6 | Correlation matrix among demographic, cognitive, and phonological measures at the initial-learning phase.

2011) of $r_c = -0.67$, marginally better Raven score ($p = 0.057$, $r_c = 0.67$) and HKLLT ($p = 0.094$, $r_c = 0.67$). There were also marginally higher Italian discrimination score, $p = 0.057$, $r_c = 0.67$, as well as higher scores in the two Cantonese tests: CanDiscrim, $p = 0.094$, $r_c = 0.57$, and CanSpoon, $p = 0.094$, $r_c = 0.62$ (**Table 7**). However, due to the lack of a control group, it is unclear whether the change arose due to repetition effect or it was truly induced by intensive vocabulary learning.

4. DISCUSSION

4.1. Semantic, Episodic, and Phonological Associations With Vocabulary Learning

Taking an individual-differences approach, the present study used both anatomical and cognitive measurements to investigate the basis of FLL in older adults, focusing on whether semantic and episodic memory play an especially important role in vocabulary learning within this special group of language learners.

In support of the hypothesis that semantic functions are important for older language learners, the left pars orbitalis, which is central to semantic control (Sabb et al., 2007; Binder et al., 2009; Ralph et al., 2017) by virtue of its white matter pathway (uncinate fasciculus) to the semantic hub in the temporal pole (Harvey et al., 2013), was found to be associated with the performance in the in-class quiz and the final test. In particular, its adjusted curvature was positively associated with the in-class Can-to-Ita performance while its adjusted volume was significantly associated with the first three parts of the final test (dictation, Ita-to-Can, and Can-to-Ita). This suggests that high-performing learners tend to have higher adjusted curvature and volume in left pars orbitalis. To our knowledge, the importance of the left pars orbitalis has seldom been reported in previous works in which the learner group comprised mostly younger adults, even though a whole-brain analysis was conducted in these studies (e.g., Bellander et al., 2016). Instead, it is generally understood that the anatomical measures of the left IFG, as the seat of the Broca's area, are sensitive to language processes and bilingualism. For example, its gray matter volume was positively correlated with L2 performance (Mårtensson et al., 2012; Stein et al., 2012). Its cortical thickness was also larger for bilinguals that acquired their L2 in late childhood (8–13 years) than in early childhood (4–7 years) (Klein et al., 2014). Our finding is consistent with this general understanding, but further suggests that the pars orbitalis is especially associated with both immediate and long-term vocabulary retention. It is worth noting that the left temporal pole has barely failed to reach statistical significance in predicting in-class Can-to-Ita (FDR-corrected $p = 0.053$), which would have provided another piece of convergent evidence.

In support of the hypothesis that episodic memory is also important for older language learners, associations with the performance of both the in-class quiz and the final test were found at the left caudal middle frontal cortex. In particular, the mean curvature of the left caudal frontal cortex was consistently positively associated with the learning performance, including the in-class Can-to-Ita score regardless of week and the first three parts of the final test. By comparison, the adjusted thickness only significantly predicted the in-class Can-to-Ita over Weeks 1–3 while the adjusted cortical surface area was negatively associated with the two translation scores in the final test. In the literature, the left caudal middle frontal cortex is known to be associated with semantic strategies (Kirchhoff et al., 2014; Yu et al., 2018), referential encoding strategies (Yang et al., 2013), self-initiated elaborative encoding strategies (Husa et al., 2017), and working memory (Petrides et al., 1993). The present finding suggests that better-performing older learners might have employed a variety of encoding strategies in vocabulary learning. The present result corroborated with two previous works. Yang et al. (2015) reported that the middle frontal cortex was more active in successful learners in a tone discrimination task. The authors suggested that the higher level of activation was associated with the path between middle frontal gyrus and inferior parietal lobe, where lexical knowledge was automatically activated and sent to middle frontal gyrus. Another study found that the cortical thickness of MFG was increased after FLL (Legault et al., 2019b). Apart from the left caudal middle frontal cortex, converging evidence was also found in the left entorhinal cortex, which is implicated in the episodic processing of object/event information in relation to the context (Eichenbaum et al., 2012). Specifically, the in-class Can-to-Ita performance was positively associated with its cortical thickness.

In contrast, for regions that are especially important for phonological processing, they were associated with only long-term retention. Specifically, the left precentral gyrus is important for phonological working memory, serving as a locus for phonological rehearsal (Veroude et al., 2010; Novén et al., 2019), while the left SMG is known to play important role in phonological processing skills (Veroude et al., 2010;

TABLE 6 | Cognitive models for the in-class Ita-to-Can and Can-to-Ita scores and for the final test, obtained after backward elimination of the full models.

Score	*Term*	*SumSq*	*MeanSq*	*NumDF*	*DenDF*	*F*	*p*	
Ita-to-Can ‡	Age	71.22	71.22	1	20.0	2.15	0.158	ns
	Gender	0.24	0.24	1	20.0	0.01	0.933	ns
	Education	2.23	2.23	1	20.0	0.07	0.798	ns
	Week	3156.37	789.09	4	80.0	23.87	< 0.001	***
	HKLLT	75.30	75.30	1	20.0	2.28	0.147	ns
	Week:HKLLT	539.17	134.79	4	80.0	4.08	0.005	**
Can-to-Ita	Age	139.41	139.41	1	20.0	2.93	0.102	ns
	Gender	410.31	410.31	1	20.0	8.62	0.008	**
	Education	19.29	19.29	1	20.0	0.41	0.532	ns
	Week	4726.65	1181.66	4	80.0	24.84	< 0.001	***
	PS	295.42	295.42	1	20.0	6.21	0.022	*
	Inhibition	1655.79	1655.79	1	20.0	34.80	< 0.001	***
	DigitSpan	1912.07	1912.07	1	20.0	40.19	< 0.001	***
	HKLLT	1095.99	1095.99	1	20.0	23.04	< 0.001	***
	PicName	2028.22	2028.22	1	20.0	42.63	< 0.001	***
	Fluency	441.17	441.17	1	20.0	9.27	0.006	**
	Raven	893.03	893.03	1	20.0	18.77	< 0.001	***
	EngSpoon	511.33	511.33	1	20.0	10.75	0.004	**
	Week:PS	773.63	193.41	4	80.0	4.07	0.005	**
FinalTest ‡	Age	892.65	892.65	1	20.0	6.13	0.022	*
	Gender	478.92	478.92	1	20.0	3.29	0.085	†
	Education	6.57	6.57	1	20.0	0.05	0.834	ns
	TestPart	18082.02	6027.34	3	60.0	41.41	< 0.001	***
	Fluency	693.43	693.43	1	20.0	4.76	0.041	*

‡*The likelihood ratio test comparing the baseline and full model of the in-class Ita-to-Can score was non-significant after Bonferroni correction; the result tabulated here was obtained to explore the cognitive predictors of the in-class Ita-to-Can performance (see main text).*
***, p <0.001, **, p <0.01, *, p <0.05, †, marginal, ns, non-significant.*

Sliwinska et al., 2012). In partial support to the hypothesis that phonological skills play a role in learning success, for left precentral gyrus, its adjusted thickness and curvature were significantly or marginally associated with the two translation tasks in the final test. The adjusted volume of left SMG was positively associated with the final test score in general, while the adjusted area was negatively associated with the scores in the two translation scores of the final test. The lack of associations of in-class scores with the precentral gyrus and left SMG associations, coupled with the presence of such associations with left pars orbitalis and left caudal middle frontal gyrus, is consistent with our hypothesis that the semantic and episodic memory functions play a more important role for FLL in older adults.

We speculate that semantic and episodic memory processes would be especially needed for intensive vocabulary learning; they are involved, for example, in strategically and proactively generating idiosyncratic semantics-based mnemonics (Thomas and Wang, 1996; Khoii and Sharififar, 2013) or referential encoding strategies for the new words (Turk et al., 2015). Suppose the learner is not confident that they can directly retrieve the meaning of *la mela* ("the apple,") a possible cue for retrieval could be the semantic category "fruit," which could in turn be encoded in terms of the learner's native language. Referential encoding strategies may also be relevant, as the learner could encode the contextual information, e.g., the noun "la mela" was learnt within the word list associated with the verb *mangiare* ("to eat") or it was the first word in the first list. Having such cues facilitates the word recall during the in-class translation quizzes. Learners who used these cues may also tend to have better performance in long-term retention, even though the learners no longer need such strategies after many weeks of consolidation.

The cognitive associations reported are consistent with the putative reasons for the strong association of the FLL performance with the left pars orbitalis and left caudal middle frontal cortex discussed above. Across the three cognitive models, only semantic fluency and the delayed recall in the Hong Kong List Learning Test (HKLLT), as measures of semantic retrieval and verbal episodic memory functions, were significant predictors in more than one final models. Specifically, HKLLT significantly contributed to the two in-class scores but not the final test; this pattern suggested that verbal episodic memory is more associated with the immediate learning than long-term language retention performance. In contrast, semantic fluency significantly predicted both in-class Can-to-Ita and the final test. Thus, the evidence suggested that semantic fluency was associated with both immediate learning

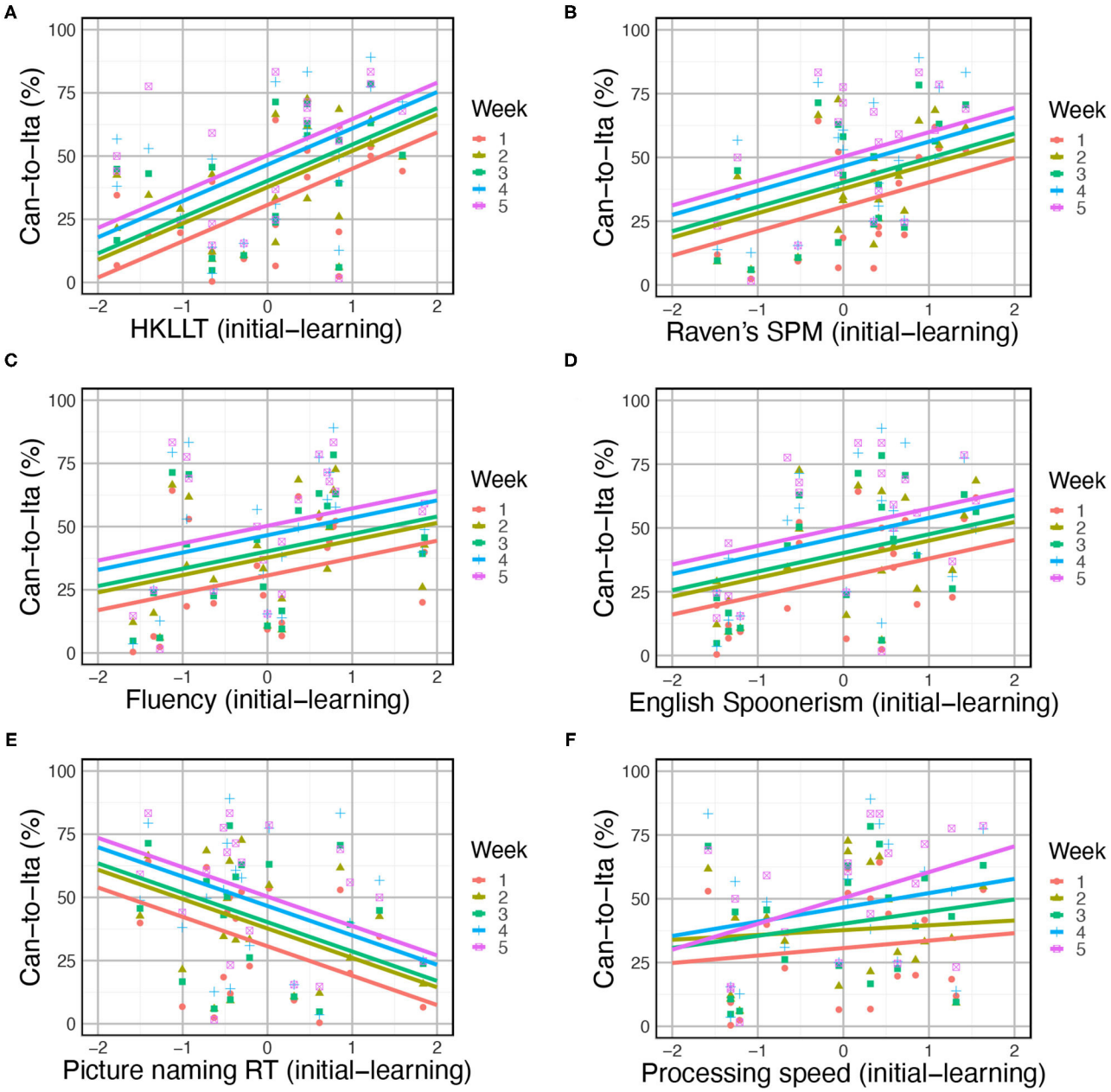

FIGURE 7 | Modulation of in-class Can-to-Ita score by cognitive predictors, including **(A)** HKLLT, **(B)** Raven's SPM, **(C)** semantic fluency, **(D)** English Spoonerism, **(E)** picture naming, and **(F)** processing speed. Each point represents the score of one participant at a certain week, and the solid lines are the fitted data based on the LME models.

and long-term retention. One reason that semantic fluency was not significant for predicting in-class Ita-to-Can is that controlled semantic retrieval ability, as captured by the semantic fluency task, has a strong association with the use of semantic associations and strategies. During vocabulary learning, most learners tend to be able to make a direct association of the L2 (Italian) word with the L1 (Cantonese) word, as reflected by a relatively high performance of the Ita-to-Can task in the present study. In contrast, they were much less accurate in the Can-to-Ita task, indicating that they had difficulty in recalling the same association in the reverse direction, i.e., from the L1 (Cantonese) word to the L2 (Italian) word. Such asymmetry has been a point of emphasis in modeling the acquisition of foreign vocabulary, e.g., the parasitic model of vocabulary acquisition (Ecke, 2015). Due to the relative difficulty in Can-to-Ita, the task is subject to a greater use of mnemonic strategies for retrieval. The stronger association of semantic fluency with Can-to-Ita than with Ita-to-Can suggests that

TABLE 7 | Comparisons of cognitive and phonological scores between initial- and post-learning phases.

Test	Initial-learning			Post-learning			r_c	*p*(unc)	*p*(FDR)	
	Mean	SD	Range	Mean	SD	Range				
Cognitive										
PS	75.5	9.5	(60.5, 91)	76.3	9.7	(61, 93)	0.26	0.313	0.452	ns
Inhibition	0.46	0.09	(0.27, 0.60)	0.46	0.06	(0.36, 0.57)	−0.10	0.729	0.729	ns
DigitSpan	9.1	1.6	(5.5, 11.5)	9.2	1.3	(7.5, 12.5)	0.19	0.571	0.710	ns
HKLLT	11.8	2.7	(7, 16)	12.8	2.6	(8, 16)	0.67	0.043	0.094	†
Raven	0.67	0.97	(−1.89, 2.05)	1.22	0.95	(−0.98, 2.40)	0.67	0.009	0.057	†
PicName	1358.7	221	(1026.4, 1821.9)	1247	276.2	(853.8, 1946.9)	−0.67	0.007	0.057	†
Fluency	12.6	2.6	(8.5, 17.3)	12.7	2.6	(8.3, 16.8)	0.14	0.601	0.710	ns
Phonological										
CanDiscrim	19.6	7.6	(7, 35)	22.3	6.7	(11, 39)	0.57	0.036	0.094	†
EngDiscrim	21	5.3	(8, 29)	23.2	5.9	(5, 29)	0.42	0.111	0.206	ns
ItaDiscrim	14.9	4.9	(6, 25)	16.9	5.4	(6, 26)	0.67	0.013	0.057	†
CanSpoon	4.1	6.4	(0, 23)	7.5	8.5	(0, 28)	0.62	0.031	0.094	†
EngSpoon	10.8	7.3	(0, 22)	11.8	7.4	(0, 24)	0.12	0.685	0.729	ns
ItaSpoon	5.2	5.5	(0, 19)	6	6.9	(0, 24)	0.32	0.224	0.364	ns

r_c, effect size of the Wilcoxon signed rank test, p(unc), uncorrected p, p(FDR), FDR-corrected p.
****, p <0.001, **, p <0.01, *, p <0.05, †, marginal, ns, non-significant.*

semantic retrieval strategies could have been utilized more in the Can-to-Ita task.

Besides HKLLT and semantic fluency, the remaining cognitive measures were kept in at most only one model, namely, in-class Ita-to-Can. In addition to processing speed, which is known to be a general deciding factor of the performance of older adults across domains (Salthouse, 1996), the in-class Ita-to-Can was associated with faster picture naming latency and better Raven's SPM. In contrast, in terms of phonological function measures, while EngSpoon contributed positively to in-class Can-to-Ita, the opposite was true for digit span forward (an index of phonological STM), suggesting that phonological function measures do not necessarily contribute positively. The inhibition function, measured using Stroop Color and Word Test, was also negatively to the learning performance.

Taken together, the anatomical and cognitive models of the learning performance were consistent with our main hypothesis that both semantic and episodic memory functions are prominently implicated in older adults. Phonological skills were also implicated, but their associations with learning performance were not as consistently observed.

4.2. Differential Hemispheric Associations in Immediate and Long-Term Retention

Beyond our main hypothesis, the present results could also be viewed from another perspective, in that there were interesting differences in the global pattern of anatomical associations between immediate learning and long-term retention (see **Figures 4**, **5**). As discussed above, the left pars orbitalis and left caudal middle frontal cortex were the only two regions that consistently showed associations with the performance in both immediate learning (Can-to-Ita) and long-term retention. All other regions were only associated with the performance of either the in-class Can-to-Ita or the final test score.

For the in-class Can-to-Ita performance, there were five such regions: left entorhinal cortex, right insula, right pars orbitalis, right caudal anterior cingulate, right middle temporal gyrus. Among them, significant anatomical associations with Can-to-Ita performance were found at left entorhinal cortex (see section 4.1) and right insula. The insula is known to be involved in procedural memory and rule-based learning (Ullman, 2001a, 2004; Yang and Li, 2012). In the present study, the in-class Can-to-Ita score was positively associated with the adjusted volume of the right insula but negatively associated with its adjusted surface area and curvature. In contrast to the right insula, the remaining three right hemisphere regions only showed some subtle changes in the association strength with the in-class Can-to-Ita score, in the sense that while the association was non-significant in any of the five weeks, the magnitude of such association varied significantly across weeks. Taken together, the significant association of right insula and the significant modulation of association over the other three right hemisphere regions suggest that the right hemisphere is implicated in the initial-learning phase. Such right hemisphere associations above added to the literature that reported some associations of the right hemisphere with FLL performance (Hosoda et al., 2013) or bilingualism-induced neuroplasticity (Bubbico et al., 2019; Maschio et al., 2019; Legault et al., 2019b), although the precise roles should be tested using online functional MRI tasks.

For long-term language retention, beyond left pars orbitalis and left caudal middle frontal cortex, seven regions were additionally associated with the final test results: left precentral gyrus (see section 4.1), left SMG (see section 4.1), left pars

triangularis, left rostral middle frontal cortex, left banks of superior temporal sulcus, right fusiform gyrus, and right entorhinal cortex. In other words, a more left-dominant network was implicated in long-term vocabulary retention, with seven left hemisphere regions showing significant associations with the final test score when compared to only two right hemisphere regions. Also, unlike the subtle right-hemispheric associations with in-class Can-to-Ita, all regions here showed significant associations with individual test scores. For the left hemisphere, the inclusion of left pars triangularis was not surprising, given that it is a part of the Broca's area. The left rostral middle frontal cortex has been implicated in language learning (Sheppard et al., 2012; Novén et al., 2019), while the left banks of superior temporal sulcus is known to reflect verbal intelligence and receptive language functions in children (Li et al., 2020). For the right hemisphere, the right fusiform gyrus is well-known for its role in object recognition (as opposed to word recognition for the left fusiform gyrus), while the right entorhinal cortex was especially important for long-term memory consolidation (Haist et al., 2001; Piefke et al., 2003).

Overall, while the best anatomical predictor of immediate success was found on semantics-associated (the left pars orbitalis) and episodic memory-related regions (left caudal middle frontal gyrus and the left entorhinal cortex), there were significant association with the right insula and some subtle changes in association with the right pars orbitalis, right rostral anterior cingulate, and right middle temporal gyrus over the course of learning. The increased left-lateralization in the association pattern of the final test scores was consistent with the view that the right-hemisphere homologs of the left-hemisphere language areas may provide "scaffolding" in the early phase of FLL, before a right-to-left shift occurs (Yang et al., 2015; Qi and Legault, 2020).

4.3. The Anatomical Associations of Sub-cortical Regions

In previous works, increased hippocampal volume was observed in Swedish individuals studying Italian (Bellander et al., 2016). The hippocampal volume was also a good predictor of the achieved vocabulary proficiency (Nilsson et al., 2021). Apart from the hippocampus, the striatum has been highlighted in previous works (Ullman, 2004; Abutalebi and Green, 2007; Li et al., 2014; Legault et al., 2019a). However, instead of the hippocampus and striatum, our results showed that the thalamus has stronger association with long-term vocabulary retention, with the cortical volumes of the bilateral thalami showing positive associations with the final test scores. The thalamus is implicated in language production by selecting lexical and semantic representations (Abutalebi and Green, 2016), and an expansion of thalamus is associated with greater second language immersion (Pliatsikas et al., 2017; Deluca et al., 2019a). The present finding added to the literature showing that the structural parameters of thalamus are sensitive to aspects of FLL, although the underlying reasons for the associations should be investigated further.

For hippocampus, we observed some degree of association of the right hippocampal volume with the Can-to-Ita test score, but the association did not survive the FDR correction. Indeed, while the role of hippocampus in associative memory, especially in various learning and recall paradigms, is well-established in patient populations in the neurological literature (Suzuki, 2008), direct associations of hippocampal volume with associative memory have not been consistently found in cognitively normal older adults (Becker et al., 2015; Zheng et al., 2017). Finally, for striatum, the sub-cortical volumes were significantly associated with none of the three learning measures. One possibility is that these structures are non-unitary in functions. A finer-grained atlas may be necessary to reveal the associations.

4.4. Conclusion and Limitations

Previous studies have suggested that structural associations could provide valuable information for inferring functional associations (Kanai and Rees, 2011; Chiarello et al., 2013). In the present study, significant associations with vocabulary learning performances were consistently found for the left pars orbitalis and left caudal middle frontal cortex. These results suggest that the individual variations in structural morphometry of the prefrontal lobe are strongly associated with language learning success in older adults, considering that the prefrontal lobe is known to be involved in many "higher" cognitive skills such as language, reasoning, and planning (Wood and Grafman, 2003). In particular, the structural brain and cognitive models were consistent with our main hypothesis that semantic and episodic memory functions likely play an important role in language learning in older adults, with the regions most implicated with these functions being prominently represented in the overall pattern of associations. It should be noted that the present study had not explicitly tested what cognitive processes were involved during learning, given that an online design was not employed. Indeed, an alternative account for the association pattern observed is that the surface-based morphological features and the cognitive predictors are good indices of language aptitude, as previous studies suggested (e.g., Novén et al., 2019). Which could be a parsimonious and alternative explanation why these measures could significantly predict the FLL performance. Nonetheless, language aptitude also has multiple components that are differentially associated with cognitive functions, which could provide a more domain-general account of the anatomical associations with learning performance.

Our research complemented previous works that put a stronger focus on the acquisition of other linguistic elements such as phonology (Wong and Perrachione, 2007) and grammar (Yang and Li, 2012). However, due to the absence of a young learner group in the present study, no conclusion could be drawn regarding the relative contributions of semantic functions in FLL across older and younger adults. On the other hand, the majority of the studies thus far were on younger learners, and the role of the left pars orbitalis and left caudal middle frontal gyrus have seldom been reported. In this respect, the present findings suggest that semantic functions could play a more important role in older adults, although this hypothesis should be re-examined with online experimental designs.

Also, a strength of the present study was that objective measures of learning performance were collected throughout the Italian vocabulary learning protocol. Such longitudinal data play a crucial role in the sensitivity of the present analysis in revealing the anatomical markers of learning performance, despite our relatively modest sample size. In addition, by incorporating different surface-based measures into our univariate LME models, we successfully revealed a relatively consistent pattern of significant brain–learning associations. Where an association was found, the adjusted cortical volume was consistently a positive predictor of learning performance, with only one exception found at the fusiform gyrus. Similarly, the adjusted curvature of the regions involved was a strong positive predictor of learning performance, with only two exceptions found for the left entorhinal cortex and the right insula. In contrast, the adjusted area was consistently a negative predictor of the learning performance, without any exception. Adjusted thickness showed the least consistent pattern, being a positive predictor at four ROIs but a negative predictor at two ROIs.

The present work was limited in several ways. First, the MRI scans were not acquired at the beginning of the Italian learning programme but after an introductory Italian lesson of 90 min, to acclimate the learners with a more uniform experience with the target language prior to the scanning. Previous studies have shown that measurable changes in diffusion MRI indices could be induced by short-term intervention of 45 min (Tavor et al., 2020) or 120 min (Sagi et al., 2012). Structural changes were found after 20 days of language learning (Legault et al., 2019b), with some even estimating that only 2 h of training could bring about structural changes in the brain (Park and Bischof, 2013). However, considering that such structural changes may not be long-lasting, and the neuroplasticity of older adults' brains are lower than younger adults' (e.g., Freitas et al., 2011), it is unlikely that a 1.5-h lesson could significantly influence the anatomical measures extracted, to a point that their associations with learning performance would change qualitatively. Secondly, we acknowledge that from the experimenter's perspective, it would have been best to arrange the cognitive and phonological tests prior to the introductory Italian lesson. However, at the beginning of the programme, most participants were anxious and most motivated to start learning Italian. As such, arranging the prolonged testing of about 3.5 h that are not directly related to learning Italian could be seen as a non-ideal arrangement from the learner's perspective, which could lower their engagement in the programme, leading to an increased dropout rate. Because it was not our primary goal to investigate the learning-induced cognitive gains, a compromise was made to spread the cognitive and phonological tests over visits 3 to 6. Considering that a cognitive gain or an improvement of phonological skills could have already incurred following the 90-min introductory lesson and the 2-h vocabulary lessons in the initial-learning phase, we acknowledge that our decision to delay these assessments could have led to an underestimation of the cognition gains or phonological skill improvements reported. Finally, no post-learning MRI scan was conducted, such that any learning-related neuroplasticity could not be tested. The lack of a younger group also precluded any formal hypothesis testing on the differential brain–learning associations between young and older learners. These issues will be addressed in our next round of data collection.

DATA AVAILABILITY STATEMENT

The raw data supporting the conclusions of this article will be made available by the authors, without undue reservation.

ETHICS STATEMENT

The studies involving human participants were reviewed and approved by Institutional Review Board, The Hong Kong Polytechnic University. The patients/participants provided their written informed consent to participate in this study.

AUTHOR CONTRIBUTIONS

MF, AA, and WW contributed to the conception and grant application of the study. MF and TL implemented the Italian learning protocol in the present study. MF, JC, TL, MM, and N-YH were involved in data collection and data transcription. MF and MM analyzed the data and wrote the manuscript. MF, MM, and WW contributed to the interpretation of the results. All authors contributed to the article and approved the submitted version.

FUNDING

This research was partially supported by HKRGC-GRF grant 15606119 and Dean's Reserve from the Faculty of Humanities, The Hong Kong Polytechnic University, both awarded to WW. The article processing charge was supported by the Research Institute for Smart Aging (RISA), The Hong Kong Polytechnic University.

ACKNOWLEDGMENTS

The present analysis was conducted partially on the computer clusters offered by the University Facility of Big Data Analytics (UBDA) of the Hong Kong Polytechnic University. We thank two undergraduate student assistants (Kristy Wong and Sabrina Wong) for their assistance in data transcription. We also thank Joseph Tse of the MRI Unit, Department of Diagnostic Radiology, The University of Hong Kong, for scheduling and administrating our MRI sessions.

SUPPLEMENTARY MATERIAL

The Supplementary Material for this article can be found online at: https://www.frontiersin.org/articles/10.3389/fnhum.2022.787413/full#supplementary-material

REFERENCES

Abutalebi, J., and Green, D. (2007). Bilingual language production: the neurocognition of language representation and control. *J. Neurolinguist.* 20, 242–275. doi: 10.1016/J.JNEUROLING.2006.10.003

Abutalebi, J., and Green, D. W. (2016). Neuroimaging of language control in bilinguals: neural adaptation and reserve. *Bilingualism Lang. Cogn.* 19, 689–698. doi: 10.1017/S1366728916000225

Abutalebi, J., Guidi, L., Borsa, V., Canini, M., Rosa, P. A. D., Parris, B. A., et al. (2015). Bilingualism provides a neural reserve for aging populations. *Neuropsychologia* 69, 201–210. doi: 10.1016/J.NEUROPSYCHOLOGIA.2015.01.040

Antonenko, D., Meinzer, M., Lindenberg, R., Witte, A. V., and Flöel, A. (2012). Grammar learning in older adults is linked to white matter microstructure and functional connectivity. *NeuroImage* 62, 1667–1674. doi: 10.1016/J.NEUROIMAGE.2012.05.074

Antoniou, M., Gunasekera, G. M., and Wong, P. C. M. (2013). Foreign language training as cognitive therapy for age-related cognitive decline: a hypothesis for future research. *Neurosc. Biobehav. Rev.* 37, 2689–2698. doi: 10.1016/J.NEUBIOREV.2013.09.004

Antoniou, M., and Wright, S. M. (2017). Uncovering the mechanisms responsible for why language learning may promote healthy cognitive aging. *Front. Psychol.* 8, 2217. doi: 10.3389/FPSYG.2017.02217

Baddeley, A., Gathercole, S., and Papagno, C. (1998). The phonological loop as a language learning device. *Psychol. Rev.* 105, 158–173. doi: 10.1037/0033-295X.105.1.158

Bak, T. H., Long, M. R., Vega-Mendoza, M., and Sorace, A. (2016). Novelty, challenge, and practice: the impact of intensive language learning on attentional functions. *PLOS ONE* 11, e0153485. doi: 10.1371/JOURNAL.PONE.0153485

Bakker-Marshall, I., Takashima, A., Fernandez, C. B., Janzen, G., McQueen, J. M., and Hell, J. G. V. (2021). Overlapping and distinct neural networks supporting novel word learning in bilinguals and monolinguals. *Bilingualism Lang. Cogn.* 24, 524–536. doi: 10.1017/S1366728920000589

Bates, E., D'Amico, S., Jacobsen, T., Székely, A., Andonova, E., Devescovi, A., et al. (2003). Timed picture naming in seven languages. *Psychonomic Bull. Rev.* 10, 344–380. doi: 10.3758/BF03196494

Becker, N., Laukka, E. J., Kalpouzos, G., Naveh-Benjamin, M., Bäckman, L., and Brehmer, Y. (2015). Structural brain correlates of associative memory in older adults. *NeuroImage* 118, 146–153. doi: 10.1016/J.NEUROIMAGE.2015.06.002

Bellander, M., Berggren, R., Märtensson, J., Brehmer, Y., Wenger, E., Li, T. Q., et al. (2016). Behavioral correlates of changes in hippocampal gray matter structure during acquisition of foreign vocabulary. *NeuroImage* 131, 205–213. doi: 10.1016/J.NEUROIMAGE.2015.10.020

Berggren, R., Nilsson, J., Brehmer, Y., Schmiedek, F., and Lövdén, M. (2020). Foreign language learning in older age does not improve memory or intelligence: Evidence from a randomized controlled study. *Psychol. Aging* 35, 212–219. doi: 10.1037/pag0000439

Bialystok, E., Craik, F. I., and Freedman, M. (2007). Bilingualism as a protection against the onset of symptoms of dementia. *Neuropsychologia* 45, 459–464. doi: 10.1016/J.NEUROPSYCHOLOGIA.2006.10.009

Binder, J. R., Desai, R. H., Graves, W. W., and Conant, L. L. (2009). Where is the semantic system? a critical review and meta-analysis of 120 functional neuroimaging studies. *Cereb. Cortex* 19, 2767–2796. doi: 10.1093/CERCOR/BHP055

Breitenstein, C., Jansen, A., Deppe, M., Foerster, A. F., Sommer, J., Wolbers, T., et al. (2005). Hippocampus activity differentiates good from poor learners of a novel lexicon. *NeuroImage* 25, 958–968. doi: 10.1016/J.NEUROIMAGE.2004.12.019

Bubbico, G., Chiacchiaretta, P., Parenti, M., di Marco, M., Panara, V., Sepede, G., et al. (2019). Effects of second language learning on the plastic aging brain: Functional connectivity, cognitive decline, and reorganization. *Front. Neurosci.* 13, 423. doi: 10.3389/fnins.2019.00423

Chan, A., and Kwok, I. (1998). *Hong Kong List Learning Test (HKLLT): Manual and Preliminary Norms.* (Department of Psychology, The Chinese University of Hong Kong, Hong Kong).

Chandrasekaran, B., Sampath, P. D., and Wong, P. C. M. (2010). Individual variability in cue-weighting and lexical tone learning. *J. Acoust. Soc. America* 128, 456. doi: 10.1121/1.3445785

Chen, L., Wu, J., Hartwigsen, G., Li, Z., Wang, P., and Feng, L. (2021). The role of a critical left fronto-temporal network with its right-hemispheric homologue in syntactic learning based on word category information. *J. Neurolinguist.* 58, 100977. doi: 10.1016/J.JNEUROLING.2020.100977

Chiarello, C., Vazquez, D., Felton, A., and Leonard, C. M. (2013). Structural asymmetry of anterior insula: behavioral correlates and individual differences. *Brain Lang.* 126, 109–122. doi: 10.1016/J.BANDL.2013.03.005

Chung, Y. S., Hyatt, C. J., and Stevens, M. C. (2017). Adolescent maturation of the relationship between cortical gyrification and cognitive ability. *NeuroImage* 158, 319–331. doi: 10.1016/J.NEUROIMAGE.2017.06.082

Costa, A., and Sebastián-Gallés, N. (2014). How does the bilingual experience sculpt the brain? *Nat. Rev. Neurosci.* 15, 336–345. doi: 10.1038/nrn3709

Daselaar, S. M., Veltman, D. J., and Witter, M. P. (2004). Common pathway in the medial temporal lobe for storage and recovery of words as revealed by event-related functional MRI. *Hippocampus* 14, 163–169. doi: 10.1002/HIPO.10158

DeLuca, V., Rothman, J., Bialystok, E., and Pliatsikas, C. (2019a). Redefining bilingualism as a spectrum of experiences that differentially affects brain structure and function. *Proc. Natl. Acad. Sci.* 116, 7565–7574. doi: 10.1073/PNAS.1811513116

Deluca, V., Rothman, J., and Pliatsikas, C. (2019b). Linguistic immersion and structural effects on the bilingual brain: a longitudinal study. *Bilingualism Lang. Cogn.* 22, 1160–1175. doi: 10.1017/S1366728918000883

Desikan, R. S., Ségonne, F., Fischl, B., Quinn, B. T., Dickerson, B. C., Blacker, D., et al. (2006). An automated labeling system for subdividing the human cerebral cortex on MRI scans into gyral based regions of interest. *NeuroImage* 31, 968–980. doi: 10.1016/J.NEUROIMAGE.2006.01.021

Ecke, P. (2015). Parasitic vocabulary acquisition, cross-linguistic influence, and lexical retrieval in multilinguals. *Bilingualism Lang. Cogn.* 18, 145–162. doi: 10.1017/S1366728913000722

Eichenbaum, H. (2000). A cortical–hippocampal system for declarative memory. *Nat. Rev. Neurosci.* 1, 41–50. doi: 10.1038/35036213

Eichenbaum, H., Sauvage, M., Fortin, N., Komorowski, R., and Lipton, P. (2012). Towards a functional organization of episodic memory in the medial temporal lobe. *Neurosci. Biobehav. Rev.* 36, 1597–1608. doi: 10.1016/J.NEUBIOREV.2011.07.006

Fischl, B. (2012). Freesurfer. *NeuroImage* 62, 774–781. doi: 10.1016/J.NEUROIMAGE.2012.01.021

Fischl, B., and Dale, A. M. (2000). Measuring the thickness of the human cerebral cortex from magnetic resonance images. *Proc. Natl. Acad. Sci.* 97, 11050–11055. doi: 10.1073/PNAS.200033797

Fischl, B., Salat, D. H., Busa, E., Albert, M., Dieterich, M., Haselgrove, C., et al. (2002). Whole brain segmentation: automated labeling of neuroanatomical structures in the human brain. *Neuron* 33, 341–355. doi: 10.1016/S0896-6273(02)00569-X

Fong, M. C.-M., Hui, N. Y., Fung, E. S.-W., Ma, M. K.-H., Law, T. S.-T., Wang, X., et al. (2020). Which cognitive functions subserve clustering and switching in category fluency? generalisations from an extended set of semantic categories using linear mixed-effects modelling. *Quart. J. Exp. Psychol.* 73, 2132–2147. doi: 10.1177/1747021820957135

Fong, M. C.-M., Law, T. S. T., Ma, M. K.-H., Hui, N. Y., and Wang, W. S. (2021). Can inhibition deficit hypothesis account for age-related differences in semantic fluency? Converging evidence from Stroop color and word test and an ERP flanker task. *Brain Lang.* 218, 104952. doi: 10.1016/J.BANDL.2021.104952

Ford, A. A., Triplett, W., Sudhyadhom, A., Gullett, J., McGregor, K., FitzGerald, D. B., et al. (2013). Broca's area and its striatal and thalamic connections: A diffusion-MRI tractography study. *Front. Neuroanatomy* 7, 8. doi: 10.3389/FNANA.2013.00008

Freitas, C., Perez, J., Knobel, M., Tormos, J. M., Oberman, L., Eldaief, M., et al. (2011). Changes in cortical plasticity across the lifespan. *Front. Aging Neurosci.* 3, 5. doi: 10.3389/FNAGI.2011.00005

Fuhrmeister, P., and Myers, E. B. (2021). Structural variation in the temporal lobe predicts learning and retention of non-native speech sounds. *Lang. Cogni. Neurosci.* 37, 63–79. doi: 10.1080/23273798.2021.1944658

Gautam, P., Anstey, K. J., Wen, W., Sachdev, P. S., and Cherbuin, N. (2015). Cortical gyrification and its relationships with cortical volume, cortical thickness, and cognitive performance in healthy mid-life adults. *Behav. Brain Res.* 287, 331–339. doi: 10.1016/J.BBR.2015.03.018

Gillon, G. T. (2017). *Phonological Awareness: From Research To Practice, 2nd edn.* (New York: Guilford Publications).

Glass, B. D., Chotibut, T., Pacheco, J., Schnyer, D. M., and Maddox, W. T. (2012). Normal aging and the dissociable prototype learning systems. *Psychol. Aging* 27, 120–128. doi: 10.1037/A0024971

Golden, C., and Freshwater, S. (1978). *Stroop Color and Word Test*. Chicago, IL: Stoelting.

Golestani, N., and Zatorre, R. J. (2009). Individual differences in the acquisition of second language phonology. *Brain Lang.* 109, 55–67. doi: 10.1016/J.BANDL.2008.01.005

Grant, A., Dennis, N. A., and Li, P. (2014). Cognitive control, cognitive reserve, and memory in the aging bilingual brain. *Front. Psychol.* 5, 1401. doi: 10.3389/FPSYG.2014.01401

Grasby, K. L., Jahanshad, N., Painter, J. N., Colodro-Conde, L., Bralten, J., Hibar, D. P., et al. (2020). The genetic architecture of the human cerebral cortex. *Science* 367, 6484. doi: 10.1126/science.aay6690

Green, S., Blackmon, K., Thesen, T., DuBois, J., Wang, X., Halgren, E., et al. (2018). Parieto-frontal gyrification and working memory in healthy adults. *Brain Imag. Behav.* 12, 303–308. doi: 10.1007/S11682-017-9696-9

Grogan, A., Green, D. W., Ali, N., Crinion, J. T., and Price, C. J. (2009). Structural correlates of semantic and phonemic fluency ability in first and second languages. *Cereb. Cortex* 19, 2690–2698. doi: 10.1093/CERCOR/BHP023

Haist, F., Gore, J. B., and Mao, H. (2001). Consolidation of human memory over decades revealed by functional magnetic resonance imaging. *Nat. Neurosci.* 4, 1139–1145. doi: 10.1038/nn739

Hämäläinen, S., Joutsa, J., Sihvonen, A. J., Leminen, A., and Lehtonen, M. (2018). Beyond volume: A surface-based approach to bilingualism-induced grey matter changes. *Neuropsychologia* 117, 1–7. doi: 10.1016/J.NEUROPSYCHOLOGIA.2018.04.038

Hartshorne, J. K., and Germine, L. T. (2015). When does cognitive functioning peak? the asynchronous rise and fall of different cognitive abilities across the life span. *Psychol. Sci.* 26, 433–443. doi: 10.1177/0956797614567339

Hartshorne, J. K., Tenenbaum, J. B., and Pinker, S. (2018). A critical period for second language acquisition: Evidence from 2/3 million english speakers. *Cognition* 177, 263–277. doi: 10.1016/J.COGNITION.2018.04.007

Harvey, D. Y., Wei, T., Ellmore, T. M., Hamilton, A. C., and Schnur, T. T. (2013). Neuropsychological evidence for the functional role of the uncinate fasciculus in semantic control. *Neuropsychologia* 51, 789–801. doi: 10.1016/J.NEUROPSYCHOLOGIA.2013.01.028

Hasher, L., Stoltzfus, E. R., Zacks, R. T., and Rypma, B. (1991). Age and inhibition. *J. Exp. Psychol. Learn. Memory Cogn.* 17, 163–169. doi: 10.1037//0278-7393.17.1.163

Hickok, G., and Poeppel, D. (2007). The cortical organization of speech processing. *Nat. Rev. Neurosci.* 8, 393–402. doi: 10.1038/nrn2113

Hogstrom, L. J., Westlye, L. T., Walhovd, K. B., and Fjell, A. M. (2013). The structure of the cerebral cortex across adult life: Age-related patterns of surface area, thickness, and gyrification. *Cereb. Cortex* 23, 2521–2530. doi: 10.1093/CERCOR/BHS231

Hosoda, C., Tanaka, K., Nariai, T., Honda, M., and Hanakawa, T. (2013). Dynamic neural network reorganization associated with second language vocabulary acquisition: a multimodal imaging study. *J. Neurosci.* 33, 13663–13672. doi: 10.1523/JNEUROSCI.0410-13.2013

Husa, R. A., Gordon, B. A., Cochran, M. M., Bertolin, M., Bond, D. N., and Kirchhoff, B. A. (2017). Left caudal middle frontal gray matter volume mediates the effect of age on self-initiated elaborative encoding strategies. *Neuropsychologia* 106, 341–349. doi: 10.1016/j.neuropsychologia.2017.10.004

Ingvalson, E. M., Nowicki, C., Zong, A., and Wong, P. C. M. (2017). Non-native speech learning in older adults. *Front. Psychol.* 8, 148. doi: 10.3389/FPSYG.2017.00148

Kanai, R., and Rees, G. (2011). The structural basis of inter-individual differences in human behaviour and cognition. *Nat. Rev. Neurosci.* 12, 231–242. doi: 10.1038/nrn3000

Kepinska, O., de Rover, M., Caspers, J., and Schiller, N. O. (2017). On neural correlates of individual differences in novel grammar learning: an fMRI study. *Neuropsychologia* 98, 156–168. doi: 10.1016/J.NEUROPSYCHOLOGIA.2016.06.014

Kepinska, O., de Rover, M., Caspers, J., and Schiller, N. O. (2018). Connectivity of the hippocampus and Broca's area during acquisition of a novel grammar. *NeuroImage* 165, 1–10. doi: 10.1016/J.NEUROIMAGE.2017.09.058

Khoii, R., and Sharififar, S. (2013). Memorization versus semantic mapping in l2 vocabulary acquisition. *ELT J.* 67, 199–209. doi: 10.1093/ELT/CCS101

King, B. M., Rosopa, P., and Minium, E. W. (2011). *Statistical Reasoning in the Behavioral Sciences*, 6th Edn, vol. 394 (Hoboken, NJ: J. Wiley & Sons).

Kirchhoff, B. A., Gordon, B. A., and Head, D. (2014). Prefrontal gray matter volume mediates age effects on memory strategies. *NeuroImage* 90, 326–334. doi: 10.1016/J.NEUROIMAGE.2013.12.052

Klein, D., Mok, K., Chen, J. K., and Watkins, K. E. (2014). Age of language learning shapes brain structure: A cortical thickness study of bilingual and monolingual individuals. *Brain Lang.* 131, 20–24. doi: 10.1016/J.BANDL.2013.05.014

Klimova, B. (2018). Learning a foreign language: A review on recent findings about its effect on the enhancement of cognitive functions among healthy older individuals. *Front. Hum. Neurosci.* 12, 305. doi: 10.3389/FNHUM.2018.00305

Klimova, B., and Pikhart, M. (2020). Current research on the impact of foreign language learning among healthy seniors on their cognitive functions from a positive psychology perspective–a systematic review. *Front. Psychol.* 11, 765. doi: 10.3389/FPSYG.2020.00765

Koda, K. (1998). The role of phonemic awareness in second language reading. *Second Lang. Res.* 14, 194–215. doi: 10.1191/026765898676398460

Lau, E. F., Phillips, C., and Poeppel, D. (2008). A cortical network for semantics: (de)constructing the n400. *Nat. Rev. Neurosci.* 9, 920–933. doi: 10.1038/nrn2532

Lee, H., Devlin, J. T., Shakeshaft, C., Stewart, L. H., Brennan, A., Glensman, J., et al. (2007). Anatomical traces of vocabulary acquisition in the adolescent brain. *J. Neurosci.* 27, 1184–1189. doi: 10.1523/JNEUROSCI.4442-06.2007

Legault, J., Fang, S. Y., Lan, Y. J., and Li, P. (2019a). Structural brain changes as a function of second language vocabulary training: Effects of learning context. *Brain Cogn.* 134, 90–102. doi: 10.1016/J.BANDC.2018.09.004

Legault, J., Grant, A., Fang, S. Y., and Li, P. (2019b). A longitudinal investigation of structural brain changes during second language learning. *Brain Lang.* 197, 104661. doi: 10.1016/J.BANDL.2019.104661

Lenneberg, E. H. (1967). *The Biological Foundations of Language* (New York: Wiley). doi: 10.1080/21548331.1967.11707799

Li, P., and Grant, A. (2016). Second language learning success revealed by brain networks. *Bilingualism Lang. Cogn.* 19, 657–664. doi: 10.1017/S1366728915000280

Li, P., Legault, J., and Litcofsky, K. A. (2014). Neuroplasticity as a function of second language learning: anatomical changes in the human brain. *Cortex* 58, 301–324. doi: 10.1016/J.CORTEX.2014.05.001

Li, T., McCorkle, G. S., Williams, D. K., Badger, T. M., and Ou, X. (2020). Cortical morphometry is associated with neuropsychological function in healthy 8-year-old children. *J. Neuroimag.* 30, 833–842. doi: 10.1111/JON.12754

Linck, J. A., Osthus, P., Koeth, J. T., and Bunting, M. F. (2014). Working memory and second language comprehension and production: A meta-analysis. *Psychonomic Bull. Rev.* 21, 861–883. doi: 10.3758/S13423-013-0565-2

Luders, E., Kurth, F., Mayer, E. A., Toga, A. W., Narr, K. L., and Gaser, C. (2012). The unique brain anatomy of meditation practitioners: alterations in cortical gyrification. *Front. Hum. Neurosci.* 6, 34. doi: 10.3389/FNHUM.2012.00034

Luk, G., Bialystok, E., Craik, F. I. M., and Grady, C. L. (2011). Lifelong bilingualism maintains white matter integrity in older adults. *J. Neurosci.* 31, 16808–16813. doi: 10.1523/JNEUROSCI.4563-11.2011

Mårtensson, J., Eriksson, J., Bodammer, N. C., Lindgren, M., Johansson, M., Nyberg, L., et al. (2012). Growth of language-related brain areas after foreign language learning. *NeuroImage* 63, 240–244. doi: 10.1016/J.NEUROIMAGE.2012.06.043

Mackey, A., and Sachs, R. (2012). Older learners in SLA research: a first look at working memory, feedback, and L2 development. *Lang. Learn.* 62, 704–740. doi: 10.1111/J.1467-9922.2011.00649.X

Maschio, N. D., Fedeli, D., Sulpizio, S., and Abutalebi, J. (2019). The relationship between bilingual experience and gyrification in adulthood: A cross-sectional surface-based morphometry study. *Brain Lang.* 198, 104680. doi: 10.1016/J.BANDL.2019.104680

Mcclelland, J. L., Mcnaughton, B. L., and O'reilly, R. C. (1995). Why there are complementary learning systems in the hippocampus and neocortex: Insights

from the successes and failures of connectionist models of learning and memory. *Psychol. Rev.* 102, 419–457. doi: 10.1037/0033-295X.102.3.419

Mestres-Missé, A., Càmara, E., Rodriguez-Fornells, A., Rotte, M., and Münte, T. F. (2008). Functional neuroanatomy of meaning acquisition from context. *J. Cogn. Neurosci.* 20, 2153–2166. doi: 10.1162/JOCN.2008.20150

Nilsson, J., Berggren, R., Garzón, B., Lebedev, A. V., and Lövdén, M. (2021). Second language learning in older adults: effects on brain structure and predictors of learning success. *Front. Aging Neurosci.* 13, 666851. doi: 10.3389/FNAGI.2021.666851

Novén, M., Schremm, A., Nilsson, M., Horne, M., and Roll, M. (2019). Cortical thickness of broca's area and right homologue is related to grammar learning aptitude and pitch discrimination proficiency. *Brain Lang.* 188, 42–47. doi: 10.1016/J.BANDL.2018.12.002

Oldfield, R. C. (1971). The assessment and analysis of handedness: The Edinburgh inventory. *Neuropsychologia* 9, 97–113. doi: 10.1016/0028-3932(71)90067-4

Olsen, R. K., Pangelinan, M. M., Bogulski, C., Chakravarty, M. M., Luk, G., Grady, C. L., et al. (2015). The effect of lifelong bilingualism on regional grey and white matter volume. *Brain Res.* 1612, 128–139. doi: 10.1016/J.BRAINRES.2015.02.034

Paap, K. R., Johnson, H. A., and Sawi, O. (2015). Bilingual advantages in executive functioning either do not exist or are restricted to very specific and undetermined circumstances. *Cortex* 69, 265–278. doi: 10.1016/J.CORTEX.2015.04.014

Papagno, C., Valentine, T., and Baddeley, A. (1991). Phonological short-term memory and foreign-language vocabulary learning. *J. Mem. Lang.* 30, 331–347. doi: 10.1016/0749-596X(91)90040-Q

Park, D. C., and Bischof, G. N. (2013). The aging mind: neuroplasticity in response to cognitive training. *Dialogues Clin. Neurosci.* 15, 109. doi: 10.31887/DCNS.2013.15.1/DPARK

Patterson, K., Nestor, P. J., and Rogers, T. T. (2007). Where do you know what you know? the representation of semantic knowledge in the human brain. *Nat. Rev. Neurosci.* 8, 976–987. doi: 10.1038/nrn2277

Petrides, M., Alivisatos, B., Meyer, E., and Evans, A. C. (1993). Functional activation of the human frontal cortex during the performance of verbal working memory tasks. *Proc. Natl. Acad. Sci.* 90, 878–882. doi: 10.1073/PNAS.90.3.878

Pfenninger, S. E., and Polz, S. (2018). Foreign language learning in the third age: A pilot feasibility study on cognitive, socio-affective and linguistic drivers and benefits in relation to previous bilingualism of the learner. *J. Eur. Second Lang. Assoc.* 2, 1. doi: 10.22599/JESLA.36

Piefke, M., Weiss, P. H., Zilles, K., Markowitsch, H. J., and Fink, G. R. (2003). Differential remoteness and emotional tone modulate the neural correlates of autobiographical memory. *Brain* 126, 650–668. doi: 10.1093/BRAIN/AWG064

Pliatsikas, C., DeLuca, V., Moschopoulou, E., and Saddy, J. D. (2017). Immersive bilingualism reshapes the core of the brain. *Brain Struct. Funct.* 222, 1785–1795. doi: 10.1007/S00429-016-1307-9

Qi, Z., Han, M., Wang, Y., de los Angeles, C., Liu, Q., Garel, K., et al. (2019). Speech processing and plasticity in the right hemisphere predict variation in adult foreign language learning. *NeuroImage* 192, 76–87. doi: 10.1016/J.NEUROIMAGE.2019.03.008

Qi, Z., and Legault, J. (2020). Neural hemispheric organization in successful adult language learning: is left always right? *Psychol. Learn. Motivation Adv. Res. Theory* 72, 119–163. doi: 10.1016/BS.PLM.2020.02.004

Ralph, M. A. L., Jefferies, E., Patterson, K., and Rogers, T. T. (2017). The neural and computational bases of semantic cognition. *Nat. Rev. Neurosci.* 18, 42–55. doi: 10.1038/nrn.2016.150

Raven, J. C., and Court, J. H. (1998). *Raven's Progressive Matrices and Vocabulary Scales*, vol. 759. (Oxford, UK: Oxford Pyschologists Press).

Sabb, F. W., Bilder, R. M., Chou, M., and Bookheimer, S. Y. (2007). Working memory effects on semantic processing: priming differences in pars orbitalis. *NeuroImage* 37, 311–322. doi: 10.1016/J.NEUROIMAGE.2007.04.050

Sagi, Y., Tavor, I., Hofstetter, S., Tzur-Moryosef, S., Blumenfeld-Katzir, T., and Assaf, Y. (2012). Learning in the fast lane: New insights into neuroplasticity. *Neuron* 73, 1195–1203. doi: 10.1016/J.NEURON.2012.01.025

Salthouse, T. (2012). Consequences of age-related cognitive declines. *Ann. Rev. Psychol.* 63, 201–226. doi: 10.1146/ANNUREV-PSYCH-120710-100328

Salthouse, T. A. (1996). The processing-speed theory of adult age differences in cognition. *Psychol. Rev.* 103, 403–428. doi: 10.1037/0033-295X.103.3.403

Schroeder, S. R., and Marian, V. (2012). A bilingual advantage for episodic memory in older adults. *J. Cogn. Psychol.* 24, 591–601. doi: 10.1080/20445911.2012.669367

Service, E., and Craik, F. I. (1993). Differences between young and older adults in learning a foreign vocabulary. *J. Memory Lang.* 32, 608–623. doi: 10.1006/JMLA.1993.1031

Shen, J., Wright, R., and Souza, P. E. (2016). On older listeners' ability to perceive dynamic pitch. *J. Speech Lang. Hearing Res.* 59, 572. doi: 10.1044/2015_JSLHR-H-15-0228

Sheppard, J. P., Wang, J. P., and Wong, P. C. (2012). Large-scale cortical network properties predict future sound-to-word learning success. *J. Cogn. Neurosci.* 24, 1087. doi: 10.1162/JOCN_A_00210

Silbert, N. H., Smith, B. K., Jackson, S. R., Campbell, S. G., Hughes, M. M., and Tare, M. (2015). Non-native phonemic discrimination, phonological short term memory, and word learning. *J. Phonetics* 50, 99–119. doi: 10.1016/J.WOCN.2015.03.001

Sliwinska, M. W., Khadilkar, M., Campbell-Ratcliffe, J., Quevenco, F., and Devlin, J. T. (2012). Early and sustained supramarginal gyrus contributions to phonological processing. *Front. Psychol.* 3, 161. doi: 10.3389/FPSYG.2012.00161

Stein, M., Federspiel, A., Koenig, T., Wirth, M., Strik, W., Wiest, R., et al. (2012). Structural plasticity in the language system related to increased second language proficiency. *Cortex* 48, 458–465. doi: 10.1016/J.CORTEX.2010.10.007

Suzuki, W. A. (2008). Associative learning signals in the brain. *Progr. Brain Res.* 169, 305–320. doi: 10.1016/S0079-6123(07)00019-2

Tadayon, E., Pascual-Leone, A., and Santarnecchi, E. (2020). Differential contribution of cortical thickness, surface area, and gyrification to fluid and crystallized intelligence. *Cereb. Cortex* 30, 215–225. doi: 10.1093/CERCOR/BHZ082

Tagarelli, K. M., Shattuck, K. F., Turkeltaub, P. E., and Ullman, M. T. (2019). Language learning in the adult brain: a neuroanatomical meta-analysis of lexical and grammatical learning. *NeuroImage* 193, 178–200. doi: 10.1016/J.NEUROIMAGE.2019.02.061

Tavor, I., Botvinik-Nezer, R., Bernstein-Eliav, M., Tsarfaty, G., and Assaf, Y. (2020). Short-term plasticity following motor sequence learning revealed by diffusion magnetic resonance imaging. *Hum. Brain Map.* 41, 442–452. doi: 10.1002/HBM.24814

Thomas, M. H., and Wang, A. Y. (1996). Learning by the keyword mnemonic: Looking for long-term benefits. *J. Exp. Psychol. Appl.* 2, 330–342. doi: 10.1037/1076-898X.2.4.330

Turk, D. J., Gillespie-Smith, K., Krigolson, O. E., Havard, C., Conway, M. A., and Cunningham, S. J. (2015). Selfish learning: the impact of self-referential encoding on children's literacy attainment. *Learn. Inst.* 40, 54–60. doi: 10.1016/J.LEARNINSTRUC.2015.08.001

Ullman, M. T. (2001a). The neural basis of lexicon and grammar in first and second language: the declarative/procedural model. *Bilingualism Lang. Cogn.* 4, 105–122. doi: 10.1017/S1366728901000220

Ullman, M. T. (2001b). A neurocognitive perspective on language: the declarative/procedural model. *Nat. Rev. Neurosci.* 2, 717–726. doi: 10.1038/35094573

Ullman, M. T. (2004). Contributions of memory circuits to language: the declarative/procedural model. *Cognition* 92, 231–270. doi: 10.1016/J.COGNITION.2003.10.008

Ullman, M. T. (2016). The declarative/procedural model: A neurobiological model of language learning, knowledge, and use. In eds G. Hickok, and S. L. Small, *Neurobiol. Lang.* Elsevier, p. 953–968. doi: 10.1016/B978-0-12-407794-2.00076-6

Valis, M., Slaninova, G., Prazak, P., Poulova, P., Kacetl, J., and Klimova, B. (2019). Impact of learning a foreign language on the enhancement of cognitive functions among healthy older population. *J. Psycholinguist. Res.* 48, 1311–1318. doi: 10.1007/S10936-019-09659-6

van den Noort, M., Struys, E., Bosch, P., Jaswetz, L., Perriard, B., Yeo, S., et al. (2019). Does the bilingual advantage in cognitive control exist and if so, what are its modulating factors? a systematic review. *Behav. Sci.* 9, 27. doi: 10.3390/BS9030027

Veríssimo, J., Verhaeghen, P., Goldman, N., Weinstein, M., and Ullman, M. T. (2021). Evidence that ageing yields improvements as well as declines across attention and executive functions. *Nat. Hum. Behav.* 6, 97-110. doi: 10.1038/s41562-021-01169-7

Veroude, K., Norris, D. G., Shumskaya, E., Gullberg, M., and Indefrey, P. (2010). Functional connectivity between brain regions involved in learning words of a new language. *Brain Lang.* 113, 21–27. doi: 10.1016/J.BANDL.2009.12.005

Wang, W. S.-Y. (2018). Critical periods for language: Comment on "Rethinking foundations of language from a multidisciplinary perspective" by T. Gong et al. *Phys. Life Rev.* 26–27, 179–183. doi: 10.1016/J.PLREV.2018.09.002

Ware, C., Damnee, S., Djabelkhir, L., Cristancho, V., Wu, Y.-H., Benovici, J., et al. (2017). Maintaining cognitive functioning in healthy seniors with a technology-based foreign language program: a pilot feasibility study. *Front. Aging Neurosci.* 9, 42. doi: 10.3389/FNAGI.2017.00042

Winkler, A. M., Kochunov, P., Blangero, J., Almasy, L., Zilles, K., Fox, P. T., et al. (2010). Cortical thickness or grey matter volume? the importance of selecting the phenotype for imaging genetics studies. *NeuroImage* 53, 1135–1146. doi: 10.1016/J.NEUROIMAGE.2009.12.028

Wong, A., Xiong, Y. Y., Kwan, P. W., Chan, A. Y., Lam, W. W., Wang, K., et al. (2009). The validity, reliability and clinical utility of the hong kong montreal cognitive assessment (HK-MoCA) in patients with cerebral small vessel disease. *Dementia Geriatric Cogn. Dis.* 28, 81–87. doi: 10.1159/000232589

Wong, P. C. M., Ou, J., Pang, C. W. Y., Zhang, L., Tse, C. S., Lam, L. C. W., et al. (2019). Language training leads to global cognitive improvement in older adults: a preliminary study. *J. Speech Lang. Hearing* 62, 2411–2424. doi: 10.1044/2019_JSLHR-L-18-0321

Wong, P. C. M., and Perrachione, T. K. (2007). Learning pitch patterns in lexical identification by native english-speaking adults. *Appl. Psycholinguist.* 28, 565–585. doi: 10.1017/S0142716407070312

Wong, P. C. M., Perrachione, T. K., and Parrish, T. B. (2007). Neural characteristics of successful and less successful speech and word learning in adults. *Hum. Brain Map.* 28, 995–1006. doi: 10.1002/HBM.20330

Wong, P. C. M., Warrier, C. M., Penhune, V. B., Roy, A. K., Sadehh, A., Parrish, T. B., et al. (2008). Volume of left heschl's gyrus and linguistic pitch learning. *Cereb. Cortex* 18, 828–836. doi: 10.1093/CERCOR/BHM115

Wood, J. N., and Grafman, J. (2003). Human prefrontal cortex: processing and representational perspectives. *Nat. Rev. Neurosci.* 4, 139–147. doi: 10.1038/nrn1033

Yang, D. Y., Beam, D., Pelphrey, K. A., Abdullahi, S., and Jou, R. J. (2016). Cortical morphological markers in children with autism: a structural magnetic resonance imaging study of thickness, area, volume, and gyrification. *Mol. Autism* 7, 11. doi: 10.1186/S13229-016-0076-X

Yang, J., Gates, K. M., Molenaar, P., and Li, P. (2015). Neural changes underlying successful second language word learning: An fMRI study. *J. Neurolinguist.* 33, 29–49. doi: 10.1016/J.JNEUROLING.2014.09.004

Yang, J., and Li, P. (2012). Brain networks of explicit and implicit learning. *PLOS ONE* 7, e42993. doi: 10.1371/JOURNAL.PONE.0042993

Yang, W., Liu, P., Cui, Q., Wei, D., Li, W., Qiu, J., et al. (2013). Directed forgetting of negative self-referential information is difficult: an fMRI study. *PLOS ONE* 8, e75190. doi: 10.1371/JOURNAL.PONE.0075190

Yu, Q., McCall, D. M., Homayouni, R., Tang, L., Chen, Z., Schoff, D., et al. (2018). Age-associated increase in mnemonic strategy use is linked to prefrontal cortex development. *NeuroImage* 181, 162–169. doi: 10.1016/J.NEUROIMAGE.2018.07.008

Yum, Y. N., Midgley, K. J., Holcomb, P. J., and Grainger, J. (2014). An ERP study on initial second language vocabulary learning. *Psychophysiology* 51, 364–373. doi: 10.1111/PSYP.12183

Zatorre, R. J. (2013). Predispositions and plasticity in music and speech learning: Neural correlates and implications. *Science* 342, 585–589. doi: 10.1126/SCIENCE.1238414

Zheng, Z., Li, R., Xiao, F., He, R., Zhang, S., and Li, J. (2017). Sex matters: hippocampal volume predicts individual differences in associative memory in cognitively normal older women but not men. *Front. Hum. Neurosci.* 11, 93. doi: 10.3389/FNHUM.2017.00093

Conflict of Interest: The authors declare that the research was conducted in the absence of any commercial or financial relationships that could be construed as a potential conflict of interest.

Publisher's Note: All claims expressed in this article are solely those of the authors and do not necessarily represent those of their affiliated organizations, or those of the publisher, the editors and the reviewers. Any product that may be evaluated in this article, or claim that may be made by its manufacturer, is not guaranteed or endorsed by the publisher.

frontiers | Frontiers in Aging

REVIEW
published: 26 April 2022
doi: 10.3389/fragi.2022.848219

Developments in Deep Brain Stimulators for Successful Aging Towards Smart Devices—An Overview

Angelito A. Silverio[1,2]* *and Lean Angelo A. Silverio*[3]

[1]Department of Electronics Engineering, University of Santo Tomas, Manila, Philippines, [2]Research Center for the Natural and Applied Sciences, University of Santo Tomas, Manila, Philippines, [3]Department of Neurological Surgery, Davao Doctor's Hospital, Davao, Philippines

This work provides an overview of the present state-of-the-art in the development of deep brain Deep Brain Stimulation (DBS) and how such devices alleviate motor and cognitive disorders for a successful aging. This work reviews chronic diseases that are addressable via DBS, reporting also the treatment efficacies. The underlying mechanism for DBS is also reported. A discussion on hardware developments focusing on DBS control paradigms is included specifically the open- and closed-loop "smart" control implementations. Furthermore, developments towards a "smart" DBS, while considering the design challenges, current state of the art, and constraints, are also presented. This work also showcased different methods, using ambient energy scavenging, that offer alternative solutions to prolong the battery life of the DBS device. These are geared towards a low maintenance, semi-autonomous, and less disruptive device to be used by the elderly patient suffering from motor and cognitive disorders.

Keywords: intervention for motor disorder, deep brain stimulation, DBS mechanism and hardware, open-loop DBS control, closed-loop DBS control, smart DBS

OPEN ACCESS

Edited by:
Toshiharu Nakai,
Osaka University, Japan

Reviewed by:
Tai Tran,
Ho Chi Minh City Medicine and Pharmacy University, Vietnam
Sabato Santaniello,
University of Connecticut, United States
Satomi Chiken,
National Institute for Physiological Sciences (NIPS), Japan

***Correspondence:**
Angelito A. Silverio
aasilverio@ust.edu.ph

Specialty section:
This article was submitted to Interventions in Aging, a section of the journal Frontiers in Aging

Received: *04 January 2022*
Accepted: *15 March 2022*
Published: *26 April 2022*

Citation:
Silverio AA and Silverio LAA (2022) Developments in Deep Brain Stimulators for Successful Aging Towards Smart Devices—An Overview. Front. Aging 3:848219. doi: 10.3389/fragi.2022.848219

CLINICAL APPLICATIONS OF DEEP BRAIN STIMULATION FOR CHRONIC DISEASES

Deep brain stimulation (DBS) has developed during the past decades as a remarkable treatment option for several different disorders replacing ablative procedures (Lyons, 2011). There is a continuous expansion of the range of applications for deep brain stimulation (DBS) surgery since the initial observation of controlling or suppressing tremor with high frequency (130 Hz) thalamic ventralis intermedius (Vim) stimulation (Benabid, et al., 1996). With FDA approval, DBS has then been used for the therapy and management of certain chronic diseases such as Parkinson's disease (PD) (Schupbach, et al., 2005; Koller, et al., 2000; Tani, et al., 2014), refractory or drug-resistant epilepsy (Salanova et al., 2015), dystonia (Hu & Stead, 2014), refractory essential tremors (ET) (Lyons & Pahwa, 2008), and dementia in Alzheimer's disease (AD) and PD (Lv, et al., 2018).

Parkinson's disease is an idiopathic, chronic, progressive and degenerative movement disorder that primarily affects the elderly caused by the progressive loss of striatal dopaminergic neurons in the substantia nigra (SNr) (DeMaagd and Philip, 2015). This upsets the balance between the direct and the indirect cortico-basal ganglia-thalamo-cortical (CBGTC) loop leading to its characteristic motor symptoms such as bradykinesia, resting tremors in several parts of the body, rigidity, and postural instability. Parkinson's disease was uncommon before 50 years of age after which a notable

increase in its prevalence with age was observed and peaked between 85 and 89 years (1·7% for men; 1·2% for women) and decreased after that age (GBD 2016 Parkinson's Disease Collaborators, 2018). Up to 76–94% of PD patients appear levodopa-induced motor complications such as dyskinesia were considered for DBS therapy (Tran, et al., 2018).

Chronic epilepsy is a prevalent disorder that may be associated with significant abnormalities in cognition, brain structure, and psychiatric health that progress in some patients by middle age. It is associated with an increased prevalence of lifestyle factors associated with abnormal cognitive aging and dementia (Herman et al., 2008) and is characterized by spontaneous recurrent seizures and affects around 60 million patients worldwide, with 40% having drug-resistant epilepsy (DRE) (Engel, 2016). Prevalence of active epilepsy of idiopathic or secondary nature, for both genders, increased with age, with peaks at ages 5–9 years and at ages older than 80. The global age-standardized rate of disability adjusted life years (DALY) for idiopathic epilepsy was 182.6 for a population of 100,000 (GBD 2016 Epilepsy Collaborators, 2019). DALY is a summary measure of health loss defined by the sum of years of life lost (YLL). YLL peaked at age under 5 years and at ages of 15–19 years which then decreased progressively with age (GBD 2016 Epilepsy Collaborators, 2019). The years of living with disease (YLD) peaked at 5–9 years of age, decreased until 40–49 years, and increased progressively to the oldest age group (GBD 2016 Epilepsy Collaborators, 2019).

Dystonia is generally defined as a type of movement disorder with manifestations such as sustained or intermittent muscle contractions causing abnormal, often repetitive, movements, postures, or both. Dystonic movements are typically patterned and twisting, and may be tremulous. Dystonia is often initiated or worsened by voluntary action and associated with overflow muscle activation. This disorder was later classified by a consensus on movement disorders along two axes: clinical characteristics, including age at onset, body distribution, temporal pattern and associated features (additional movement disorders or neurological features); and etiology, which includes nervous system pathology and inheritance (Albanese, et al., 2013). Dystonia is poorly controlled solely by medication using anticholinergic drugs, dopamine modulators, pharmacologic agents, etc. Deep brain stimulation revolutionized its symptomatic treatment (Jankovic, 2013).

Tremor is generally defined as an involuntary, rhythmic, oscillatory movement of a body part. The original consensus criteria for classifying tremor disorders were published by the International Parkinson and Movement Disorder Society in 1998. A more updated criteria was later developed by Bhatia and others (Bhatia, et al., 2018) to account for subsequent advances in ET, tremor associated with dystonia, and other monosymptomatic and indeterminate tremors. The revised consensus statement classifies tremors along axes: clinical characteristics which includes historical features (age at onset, family history, and temporal evolution), tremor characteristics (body distribution, activation condition), associated signs (systemic, neurological), and laboratory tests (electrophysiology, imaging); and etiology (acquired, genetic, or idiopathic). Action tremors are classified as neurodegenerative (Aging-related tremors), and non-neurodegenerative (Essential tremors). Essential tremors constitute minor neurological findings such as mild cerebellar abnormalities which may either be hereditary (60–80%) and sporadic (20–40%) (Deuschl et al., 2015). Meanwhile, ARTs manifest as decline of aging parameters, including a change of cognition, activities of daily living, and reduction of strength and thereby a faster aging (Deuschl et al., 2015).

Dementia is the loss of cognitive functioning—thinking, remembering, and reasoning. One form of dementia is Alzheimer's disease (AD) which is caused by changes in the brain, including abnormal buildups of proteins, known as amyloid plaques and tau tangle that aggravate with age. (https://www.nia.nih.gov/health/what-is-dementia). **Table 1** summarizes these including the target section of the brain.

EFFICACY OF DEEP BRAIN STIMULATION FOR THE MANAGEMENT AND TREATMENT OF CHRONIC DISEASES

Parkinson's Disease

For the past several years, DBS has been established as a highly-effective therapy for advanced PD (Groiss et al., 2009), with options for treating PD symptoms continually expanding (Fox, et al., 2018). Based on an extensive evidence-based review conducted by the International Parkinson and movement disorder society, it was concluded that bilateral STN and GPi DBS are clinically useful for motor fluctuations and for dyskinesia when administered in tandem with the standard medications (Fox, et al., 2018).

On one retrospective analysis of the medical records of 400 consecutive patients who underwent DBS implantation, a 10-years survival rate of 51% for patients with PD has been reported using Kaplan-Meier estimation and multivariate regression utilizing Cox proportional hazards modeling (Hitti et al., 2019). The study results suggest that DBS provides durable symptomatic relief and allows many PD individuals to maintain activities of daily living (ADLs) over long-term follow-up exceeding 10 years. Meanwhile, a review paper and meta-analysis of eight eligible randomized control trials (RCTs) (n = 1,189) by Bratsos, et al. (2018), comparing the efficacy of DBS and best medical therapy (BMT) has shown that DBS provided more significant improvements based on the following outcome measures: Unified Parkinson's disease Rating Scale (UPDRS), quality of life (QoL) using the Parkinson's disease Questionnaire (PDQ-39), levodopa equivalent dose (LED) reduction, and rates of serious adverse events (SAE).

Epilepsy

Deep brain stimulation has shown significant seizure frequency reduction on patients with drug-resistant epilepsy (DRE) across different age groups based from several independent studies as summarized in one review (Zangiabadi et al., 2019). In one follow up study investigating the long term efficacy of the clinical trial that involved the Stimulation of the Anterior Nucleus of the Thalamus for Epilepsy (SANTE), a median percent seizure

TABLE 1 | Chronic diseases and corresponding DBS target sites.

disease	Target	References
Parkinson's disease	GPi, STN, (PPN)	Deuschl et al., 2013; Deep Brain Stimulation for Parkinson's Disease Study Group, 2001
Chronic Epilepsy	Cerebellum, CN, STN, hippocampus, CM, CC, LoC, MB)	Bergey et al., 2015; Fisher et al., 2010
Primary Dystonia	GPi, (STN)	Ostrem et al., 2011; Vidailhet et al., 2007
Essential Tremor	Vim, (STN)	Zhang et al., 2010; Blomstedt et al., 2010
Alzheimer's disease	NBM, fornix	Laxton et al. (2010)

Abbreviations: GPi, globus pallidus internus; STN, subthalamic nucleus; PPN, pedunculopontine nucleus; CN, caudate nucleus; CM, centromedian nucleus of the thalamus; CC, corpus callosum; LoC, locus coeruleus; MB, mammillary bodies; Vim, ventral intermediate nucleus of the thalamus; NBM, nucleus basalis of Meynert.

reduction from the baseline for year one and year five was reported to be 41 and 69%, respectively (Salanova et al., 2015). Wille et al. (2011) reported 30—100% seizure reduction on five adult patients with progressive myoclonic epilepsy (PME) upon application of chronic high-frequency deep-brain stimulation.

Dystonia

In one study comparing DBS with sham stimulation in a randomized, controlled clinical trial of 40 patients with primary segmental or generalized dystonia, it was shown that DBS has resulted in a higher movement score from baseline using the Burke–Fahn–Marsden Dystonia Rating Scale (Kupsch et al., 2006). The efficacy of continuous bilateral GPi-DBS was assessed on a prospective, controlled, multi-center study of 22 patients with primary generalized dystonia (Vidailhet et al., 2005). It was shown that after 3, 6, and 12 months of continuous bilateral GPi-DBS, dystonia motor symptoms were ameliorated by 47, 51, and 55%, respectively. Motor function has improved by 34, 42, and 44% at 3, 6, and 12 months, respectively based on the Burke-Fahn-Marsden Dystonia Rating Scale (BFMDRS). It was further shown that chronic bilateral pallidal stimulation is an efficient treatment option for patients with cervical dystonia who do not benefit from conservative treatment (e.g. local botulinum toxin injections) (Krauss, 2007); furthermore, there were significant improvements in dystonic posture and movements, reduced pain caused by dystonia and lesser related disabilities. Ostreem and Starr (2008) collated the different clinical trials on the application of DBS for dystonia treatment and has shown that, in general, significant improvement is manifested on patients with primary dystonia using BFMDRS.

Alzheimer's Disease

A review paper by Luo, et al. (2021), summarized 30 recent studies on the application of DBS to AD, 16 of which included actual clinical trials. On two independent studies, the memory of AD patients improved with the rate of cognitive decline decreased accompanied by an increase in cerebral glucose metabolism (Laxton et al., 2010; Smith et al., 2012). Other studies have also shown that the nutritional status of AD patients remained stable, and the rate of hippocampal atrophy slowed down after 1 year of DBS (Noreik et al., 2015; Sankar et al., 2015).

Tremors

It was found that thalamic DBS is a safe and effective therapy in patients with essential tremor followed for up to 13 years based on the assessment done by Baizbal-Carvallo (2014). Here, 13 male patients (Age: 47 – 88 years) treated with DBS for essential tremor for at least 8 years were evaluated in the 'on' and 'off' state using the Fahn–Tolosa–Marin tremor rating scale, and their medical records were reviewed to assess complications related to this therapy. DBS provided a functional improvement of 31.7% in the 'on' state; furthermore, a total non-blinded improvement in the tremor rating scale of 39% was observed in the 'on' state. Meanwhile, on an observer blinded study of 20 patients with ET by Paschen et al., 2019, ventralis intermedius (ViM) DBS showed significant improvement over the non-stimulated condition based on the Tremor Rating Scale. However, it was further observed that Vim DBS loses efficacy over the long term (e.g. 10 years) for cases with medically refractory severe ET.

Side Effects of DBS

Most DBS side effects can be understood as a result of current spreading into brain regions adjacent to the target area. Some of its common side effects include spastic muscle contractions, uni- or bilateral gaze deviation, autonomic side effects, *paresthesia*, speech impairment, *dyskinesia*, gait impairment and postural instability, acute neuropsychiatric side effects, depression, Impulse Control Disorders (ICD), and cognitive side effects (Koeglsperger et al., 2019).

MECHANISMS OF DEEP BRAIN STIMULATION

Although DBS significantly reduces motor symptoms, limits drug-induced side effects, improves performance of activities of daily living, and enhances quality of life (Halpern et al., 2007), the corresponding physiological mechanisms are not fully explained (Montgomery and Gale, 2008). Several hypotheses offer an explanation on its mechanism namely: blockade depolarization, synaptic inhibition, desynchronization of abnormal oscillatory neuronal activity and antidromic activation (Li et al., 2014).

The blockade depolarization mechanism has been verified on an *in vitro* setup where high frequency stimulation can cause sustained depolarization of neural membranes by inactivating sodium channels and increasing potassium currents preventing the initiation or propagation of action potentials (Beurrier et al., 2001; Magariños-Ascone et al., 2002).

DBS is said to inhibit neuronal activity by reducing the firing rate of the neurons at the stimulated site similar to that of reversible lesion in ablative surgery (Herrington et al., 2016). This inhibitory activity was observed in normal awake monkeys

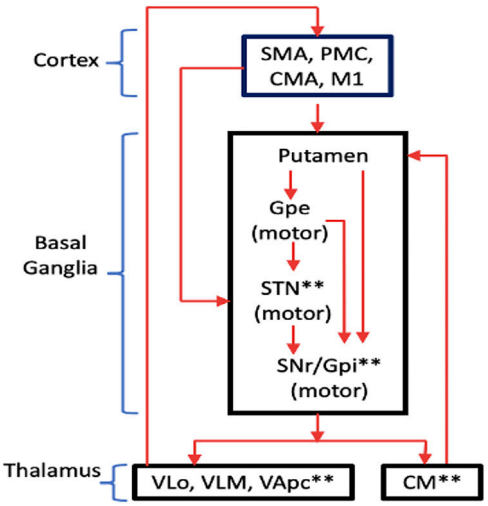

FIGURE 1 | Motor circuit of the CBGTC showing the segregated sub-circuits. The targets of current DBS treatments are labeled with asterisks (*). Abbreviations: SMA, supplementary motor area; PMC, premotor cortex; CMA, cingulate motor area; M1, primary motor cortex; Gpe, globus pallidus externa; SNr, substantia nigra pars reticulata; Gpi, globus pallidus internus VLo, ventrolateral nucleus of thalamus, pars oralis; VLm, ventrolateral nucleus of thalamus, pars medialis; VApc, ventral anterior nucleus of thalamus, pars parvocellularis. (redrawn from Wichmann and Delong., 2011).

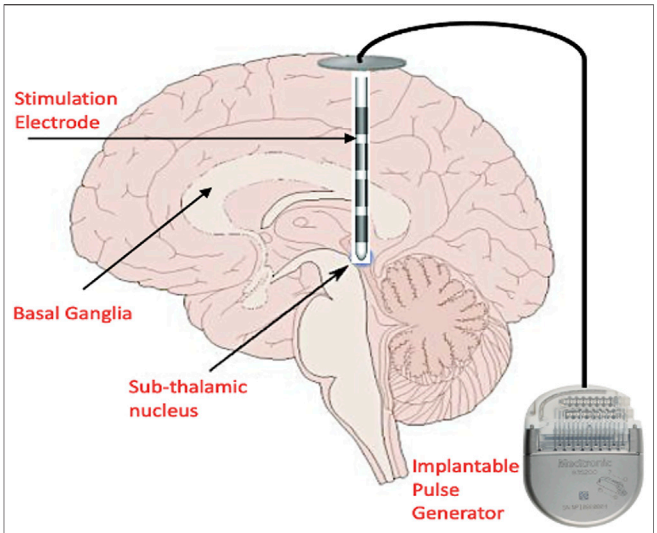

FIGURE 2 | Conventional DBS setup showing the placement of the stimulation electrodes in the basal ganglia and sub-thalamic nucleus. The Implantable Pulse Generator (IPG) is placed in the sub-clavicular space, and extension wires are tunneled subcutaneously to connect the intracranial electrodes and IPG. The IPG is programmed remotely by the physician. (This figure indicates only cortical biomarkers and is a simplified diagram).

where single-pulse stimulation of the GPi evoked brief inhibition in neighboring globus pallidus internus (GPi) neurons, mediated by the gamma-aminobutyric acid type A (GABA-A) receptors, while high-frequency stimulation of the GPi completely inhibited spontaneous firings of GPi neurons by activation of GABA-A and GABA-B receptors (Chiken and Nambu, 2013). This inhibitory activity was also observed intraoperatively on actual PD patients administered with STN-DBS (Filali et al., 2004; Welter et al., 2004), GPi-DBS (Dostrovsky et al., 2000; Lafreniere-Roula et al., 2010) and SNr-DBS (Lafreniere-Roula et al., 2010).

DBS is also said to be disrupting the abnormal flow of information in the cortico-basal ganglia-thalamocortical circuits (CBGTCs) during pathological conditions (Chiken and Nambu, 2016). Here, DBS activates axon terminals in the stimulated nucleus thereby inducing the release of inhibitory (GABA) and excitatory glutamate (Glu) neurotransmitters that dissociates the inputs and outputs in the stimulated nucleus. GABA is an amino acid released into the post-synaptic terminals of neurons that functions as the primary inhibitory neurotransmitter for the central nervous system (CNS). GABA causes hyperpolarization and inhibits neuronal activity. Glu, on the other hand, is an excitatory neurotransmitter. The neurotransmitter dopamine in the basal ganglia serves as the agent that modulates the functions of the striatum, the external and internal segment of the globus pallidus (GPe and GPi, respectively), the subthalamic nucleus (STN), and the substantia nigra pars compacta and reticulata (SNc and SNr, respectively) (Rommelfanger & Wichmann, 2010). The input and output nuclei of the basal ganglia are connected through two main pathways, i.e., the monosynaptic GABAergic "direct" pathway and polysynaptic "indirect" pathway. The latter involves GABAergic projections from the striatum to GPe and from GPe to the STN, as well as excitatory glutamatergic projections from the STN to GPe, GPi, and SNr. It was shown recently that nigrostriatal dopamine neurons inhibit striatal projection neurons by releasing a neurotransmitter that activates GABA-A receptors extending also to the mesolimbic afferents (Tritsch et al., 2014). Meanwhile, dopamine released from the striatum is also implicated in the modulation of learning and neuronal plasticity through processes such as long-term depression (LTD) or potentiation (LTP), acting at glutamatergic synapses (Pawlak and Kerr, 2008; Flajolet, et al., 2008). The balance between inhibitory neuronal transmission via GABA and excitatory neuronal transmission via glutamate is essential for proper cell membrane stability and neurologic function (https://www.ncbi.nlm.nih.gov/books/NBK526124/).

The basal ganglia consist of massive parallel and largely closed cortical-subcortical circuits, in which information is sent from different cortical areas to spatially separate domains of the basal ganglia where they are processed, and then returned to the frontal cortical area of origin via the thalamus (Wichmann and Delong, 2011). Based from the known functionalities of the cortical region, different CBGTCs may be classified as "motor," "oculomotor," "prefrontal," (or "associative") and "limbic" circuits. Each CBGTC is understood to consist of so-called "segregated" sub-circuits where the effect of DBS may be identified. Wichmann and Delong, 2011 showed an intuitive diagram of the motor circuit with its corresponding segregated sub-circuits as well as the DBS targets (**Figure 1**). Movement

TABLE 2 | Typical DBS parameter settings.

Parameter	Value	References
Mode	• Constant Current (CC) • Constant Voltage (CV)	Fleming et al. (2020) Stanlaski et al. (2012)
Amplitude	• CC: 0–3 mA • CV: 1–3.5 V • CV: 1–10 V	Fleming et al. (2020) Stanlaski et al. (2012) Wu et al. (2021)
Frequency	• Low Frequency (LF) - 60–80 Hz - 20–45 Hz • High Frequency (HF) - 130–185 Hz	Su et al. (2018) Baizabal-Carvallo and Alonso-Juerez, (2016) Santaniello et al., 2011 Su et al. (2018)
Pulse Width	60–210 ms	Moro et al., 2002; O'Suilleabhain et al., 2003; Rizzone et al., 2001; Volkmann et al., 2002
Pattern of Stimulus	• Monophasic - charge imbalanced • Biphasic - charge imbalanced - charge balanced - passive - active - symmetric - asymmetric	Parastarfeizabadi and Kouzani, (2017)

disorders, such as PD, dystonia and Tourette's Syndrome (TS), are caused by dysfunctions in the motor circuit.

CONVENTIONAL OPEN-LOOP CONTROL DEEP BRAIN STIMULATION

Harmsen and others (Harmsen, et al., 2020) consolidated the current state of affairs in the clinical trials for DBS registered in the Clinical-Trials.org database. The trials spanned 28 different disorders across 26 distinct brain targets, with almost 40% of trials being for conditions other than movement disorders. For addressing movement disorders, DBS is administered by implanting electrodes into any of the basal ganglia nuclei namely: GPi and STN (Halpern et al., 2007) and delivering pulses of preset amplitude, frequency, duration and polarity from an Implantable Pulse Generator (IPG) (**Figure 2**). Some of the typical DBS parameters used in disease management and therapy are summarized in **Table 2**.

Successful DBS depends on properly set stimulus parameters, including pulse width, frequency, and amplitude alongside with the proper electrode positioning (Su et al. (2018)). Determination of the optimal stimulation parameters is vital: to improve clinical efficacy; to minimize side effects; to maximize the battery life; and to evaluate the dose-response relationship between stimulation parameters and clinical effects. In one study by Obeso, et al. (2001), the final mean stimulus parameter settings that provided the highest efficacy to treat PD symptoms were 3V, 82 μs, and 152 Hz for STN-DBS, and 3.2 V, 125 μs, and 162 Hz for GPi-DBS. For the treatment of epilepsy, common DBS parameters are ≥100 Hz at 1–10 V for ANT stimulation for refractory temporal lobe epilepsy, ≥ 130 Hz at 1–5 V for hippocampus and STN stimulation for refractory temporal lobe epilepsy, tens to high frequency stimulation at 1–10 V for stimulation of centromedian nucleus (CMN) of the thalamus for generalized tonic-clonic seizures (Wu et al., 2021).

When finding the optimal DBS settings, the pulse width and frequency are initially kept constant at 60 μs and 130 Hz, respectively with gradual increase of stimulation amplitude in steps of 0.1–0.5 V or 0.1–0.5 mA until the safe treatment margin is obtained (Volkmann et al., 2006). Once the leads have been implanted stereotactically or via a surgical robot, each ring contact is tested in a monopolar configuration with the electrode as negative (cathode) and the IPG as positive (anode). Each of the rings or segments of the electrode are set to have the same stimulation intensity and are fired in unison (Volkmann et al., 2006). The mode of stimulation, either constant current (CC) or constant voltage (CV), has its corresponding pros and cons. CC stimulation provides a more precise control independent of brain tissue–electrode interface impedance variations but wastes significant amount of power and therefore reduces battery life, whereas, CV stimulation provides the reverse (Lettieri et al., 2015). The interface impedance tends to reduce post-operatively at an average rate of 73 Ω/year (Satzer et al., 2014). A recommended safe charge density limit of 30 mC/cm^2 is normally considered in the selection of DBS parameters. Charge density is calculated by dividing the product of the voltage and the pulse width by the product of the impedance and the geometric surface area of the electrode (Kuncel and Gril, 2004).

The lack of understanding on the DBS mechanism makes the setting of stimulation parameters quite cumbersome. Several experimental studies, centered on PD, demonstrated that motor symptoms depend nonlinearly on the frequency and amplitude of stimulation (Moro et al., 2002; Moreau et al.,

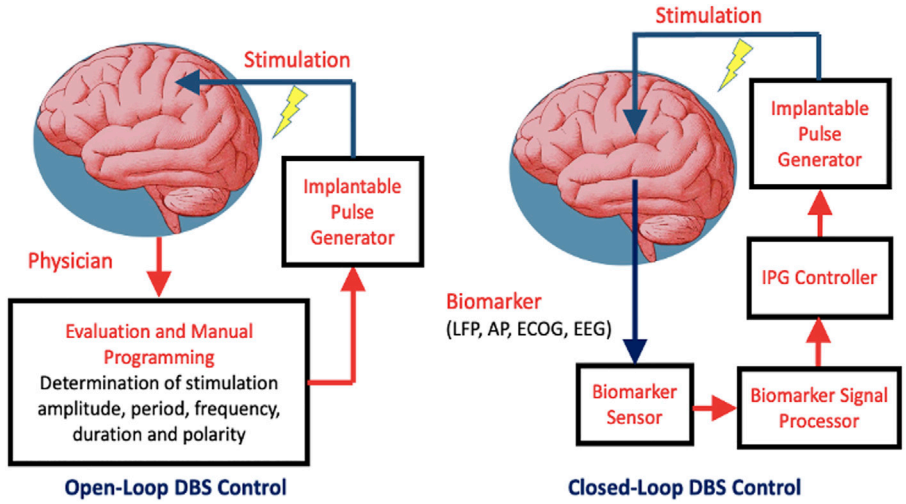

FIGURE 3 | Two types of DBS control: open-loop and closed-loop. Abbreviations: IPG–implantable pulse generator; LFP–local field potential; AP–Action Potential; ECOG–Electrocorticography; EEG - Electroencephalography.

2008). Verification of DBS effects, i.e. STN-DBS for PD, is normally done by assessing rigidity, bradykinesia or (rest) tremor, and axial symptoms (Koeglsperger et al., 2019). Also, selected items from the Unified Parkinson's disease Rating Scale (UPDRS) UPDRS or the Motion Disorder Society UPDRS (MDS-UPDRS) scale are used to assess the therapeutic effect and to document effects in a systematic manner.

To optimize therapy, a balance between maximal clinical improvement and minimal stimulation-induced side effects is being achieved through the adjustment of active electrode contacts, stimulus frequency, amplitude, and pulse duration (Mayo Clinic, 2017). This, however, is largely an ad hoc process that relies on clinical expertise and does not totally equate to optimal outcomes (Santaniello et al., 2011). Furthermore, the selection of parameters has important implications for power consumption, and thus the battery life of the implantable pulse generator (Santaniello et al., 2011; Parastarfeizabadi and Kouzani, 2017).

Conventional open-loop DBS involves the programming of the stimulation parameters based on the present condition of the patient. This is an iterative process in which stimulation parameters are adjusted to maximize therapeutic benefits while minimizing side effects (Morishita et al., 2013). However, the efficacy of these therapeutic parameters normally deteriorates over time due to disease progression, interactions between the host environment and the electrode, and lead migration (Grahn et al., 2014). Optimization of its efficacy is commonly achieved by multiple post-operative visits where the stimulation parameters are adjusted until the desired therapeutic effects are achieved with minimal adverse effects (Grahn et al., 2014). Risk factors abounding this process involve suboptimal outcomes, infections, device failure, and lead removal or repositioning (Frizon et al., 2019).

As a resolve, development of closed-loop control systems that can respond to variative neurochemical environments, tailoring DBS therapy to individual patients, is paramount for improving the therapeutic efficacy. This device is generally called "Smart DBS" because it is able to adapt dynamically to the condition of the patient and deliver the optimal electrical stimulation semi-autonomously (with minimal intervention) or autonomously.

CLOSED-LOOP CONTROLLED DEEP BRAIN STIMULATION—"SMART" DBS

In a closed-loop DBS control, the clinical state of the patient is quantified periodically in order to adjust the stimulation parameters for optimal treatment while reducing stimulation induced side-effects (Fleming et al., 2020). The corresponding block diagrams of the DBS with open-loop and closed-loop controls are shown in **Figure 3**.

The DBS with closed-loop control consists of the neurofeedback loop where the stimulation is controlled either on/off or adaptively depending on the characteristics of a particularly biomarker. Such biomarker arises in lieu of a specific pathological condition. This loop is composed of biomarker sensor, signal processor, IPG controller and IPG device. Meanwhile, the DBS with open-loop control relies on the stimulation parameters programmed by the physician. Adaptive control involves dynamic adjustment of the stimulation parameters in response to the extent of the biomarker stimuli. In the presence of extensive pathological biomarkers, stimulation is prolonged with either its amplitude or frequency increased to deliver more stimulation energy, and vice versa. Meanwhile, to save on power, stimulation is deactivated whenever the preset biomarker threshold is not reached. Thresholding could either be singular or dual. The latter tends to be perform better in the presence of noise and offsets.

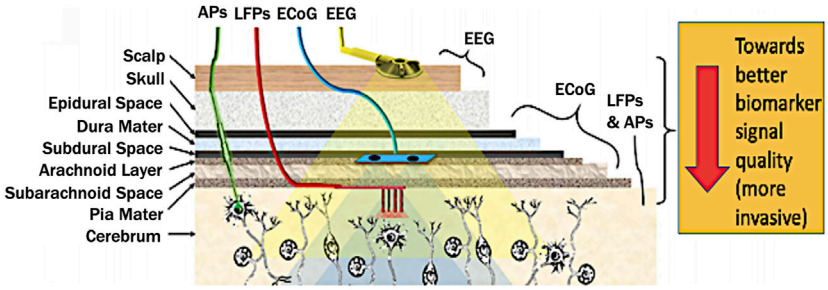

Biomarker	Frequency Range	Spatial Resolution
Local Field Potentials	~ 1 to 500 Hz	~ 0.5 – 1 mm
Action Potentials	~ 100 to 8 kHz	~ 0.1 – 0.2 mm
ECoG	~ 1 to 500 Hz	~ 1 – 5 mm
EEG	~ 1 to 100 Hz	~ 3 – 9 cm

FIGURE 4 | Brain biomarkers for closed-loop DBS stimuli (top figure adapted from Parastarfeizabadi and Kouzani, 2017). Abbreviations: LFP–local field potential; AP–Action Potential; ECOG–Electrocorticography; EEG - Electroencephalography.

CHOICE OF THE BIOMARKER FOR CLOSED-LOOP DBS CONTROL

To implement an autonomous or Smart DBS, the proper biomarker has to be identified. Several candidates have been considered in literature namely: electroencephalographs (EEG) (Abdelhalim et al., 2013), electrocortigraphs (ECoG) (Thomas and Jobst, 2015), Local Field Potentials (LFPs) (Abosch et al., 2012; Stanslaski et al., 2012; Little et al., 2013; Priori et al., 2013) and action potentials (Rosin et al., 2011) (**Figure 4**).

By considering the spatial resolution, proximity to the brain, and localization, LFPs are considered the most potent biomarker (Abosch et al., 2012; Little et al., 2013; Priori et al., 2013). Another key advantage is that LFPs can be directly recorded from the stimulation electrodes also achieving long-term stability at the electrode-tissue interface (Little and Brown, 2012). Meanwhile, other closed-loop control for DBS involved wearable sensors for detecting hand tremor (Sarikhani et al., 2019), and inertial measurement units (IMUs) for gait freezing (Bikias et al., 2021). However, for a fully implanted system which reduces the risk of infection, brain-based signals hold more ground since such system can be made in proximity with the stimulation electrodes.

The LFP is a summation signal of excitatory and inhibitory dendritic potentials from many neurons about the recording site. These are potentials generated in the extracellular space by propagation of APs through axons reflecting neuronal processes occurring within a local region around electrode in the neuronal extracellular space (Kajikawa and Schroeder, 2011). These have a spatial resolution of ~0.5–1 mm (Schwartz et al., 2006), and frequency range covering ~1–500 Hz with an amplitude of ~200 μV (Einevoll et al., 2013).

It was observed that the energy signature of specific waves in the LFP signal, particularly the pathological beta waves (13—35 Hz), are directly related to abnormal brain activity associated to Parkinson's disease (Rosin et al., 2011; Hariz, 2014; Hosain et al., 2014; Müller and Robinson, 2018). Hence, most works explore the energy of these waves as the biomarker for a potential closed-loop control DBS (Parastarfeizabadi and Kouzani, 2017; Müller and Robinson, 2018).

CLOSED-LOOP CONTROL SCHEMES

Several controller models have been developed theoretically (Santaniello et al., 2011; Fleming et al., 2020). The controller of Santinello et al. (2011), was based on a recursively identified autoregressive model (ARX) of the relationship between the stimulation input and LFP output. It resulted to excellent performances in tracking the reference (tremor free) spectral features of the LFP through selective changes in the theta (2–7 Hz), alpha (7–13 Hz), and beta (13–35 Hz) frequency ranges, which is better than a static controller approach. In the work of Fleming et al. (2020), various closed-loop control algorithms *in silico* have been modeled incorporating extracellular DBS electric field, antidromic and orthodromic activation of STN afferent fibers, LFPs at non-stimulating contacts of the DBS electrode and temporal variation beta-band activity within the cortico-basal ganglia-thalamo cortical loop. The performances of various control modes such as on/off, dual threshold, proportional (P) and proportional-integral (PI) have been verified computationally, with PI yielding the optimum output in terms of power consumption and mean error in modulating the pathological DBS frequency. Meanwhile, the work of Molina, et al., 2021 demonstrated a closed loop DBS approach using bilateral GPi DBS implantation to address levodopa-responsive PD symptoms with open-loop stimulation, and PPN DBS to serve as feedback for the treatment of medication

refractory Freezing of Gait (FoG). The primary outcome of the study was a 40% improvement in medication-refractory FoG in 60% of subjects at 6 months when "on".

HARDWARE IMPLEMENTATIONS OF SMART DBS

There have been several works that implemented the closed loop control either on an on-board module (Parastarfeizabadi et al., 2016; Parastarfeizabadi and Kouzani, 2017) or on a system-on-chip (Rhew et al., 2014; Wu et al., 2017; Wang et al., 2021). On-board module implementation involves the use of commercially available electronic components, microcontroller and digital signal processing modules. System-on-chip (SoC) implementations constitute miniaturized version of the DBS circuit blocks thereby providing a better form factor and less intrusive deployment than the on-board module.

On-Board Module Smart DBS

A miniature closed loop deep brain stimulation device has been developed using dual energy thresholding for the on/off control (Parastarfeizabadi et al., 2016). The device incorporated pre- and post-amplifiers achieving 113 dB of gain, bandpass filter centered around 0.7–50 Hz, and a pulse generator, driven by a pico-power microcontroller unit, that provides on-demand stimulation current pulses of 90 μs duration, frequency 130 Hz, and amplitude 200 μA. Another work extended the DBS functionality to accommodate other diseases into one module (Parastarfeizabadi et al., 2016). This involved the neural sensor, a controller with a feature extractor, a 4×4 disease classifier using fuzzy logic, and a control strategy, and a neural stimulator. The front-end has a gain range of 50–100 dB, dual bandwidth of 7–45 Hz and 200–1000 Hz for the extraction of five biomarkers namely: five alpha, beta, sG, HFO, and spikes. The overall module dissipates 35 mW of power.

SoC-Based Smart DBS Developments

System on Chip developments of the closed-loop DBS control have also proliferated. One work built a viable closed loop DBS SoC that utilizes logarithmic processing for the control and adaptation of stimulation currents based on detected low-frequency brain field signals (Rhew et al., 2014). Such method contributed to power savings while maintaining a wide dynamic range. Their system records and processes neural signals using four low-noise neural amplifier (LNA) channels, a multiplexed logarithmic ADC, and two high-pass and two low-pass digital logarithmic filters. A logarithmic domain digital signal processor (DSP) and PI-controller controls eight current stimulator channels and enables closed-loop stimulation. The SoC also incorporates an RF transceiver, a clock generator, and a power harvester. The overall SoC, implemented on CMOS 0.18 μm technology, has an overall area of 4 mm^2 while consuming a total power of 468 μW for recording and processing neural signals, for stimulation, and for two-way wireless communication. Another SoC has been developed that incorporates a wireless power supply via an inductive link, a wireless interface, an adaptive high voltage tolerant stimulator, a bio-signal processor for seizure detection, and an 8-channel EEG acquisition unit (Wu et al., 2017). The acquisition unit consists of auto-reset capacitive-coupled instrumentation amplifiers (ARCCIA), band-pass filters, V-to-I programmable gain amplifiers, a multiplexer, a transimpedance amplifier (TIA), and a 10-bit DMSAR (Delta-Modulated Successive Approximation Register ADC). Its acquisition unit has achieved a Noise Efficiency Factor (NEF) of 1.77 with an input referred noise of 5.23μVrms, a stimulation current of 30 μA, and a standby power of 2.8 mW.

An 8-channel closed-loop neuromodulation SoC with 2-level seizure classification has been developed (Wang et al., 2021). It consists of a capacitive-coupled instrument amplifier (CCIA) at the analog front-end with a feedback-based common-mode (CM) cancellation circuit that suppresses large-scale CM interferences. Meanwhile, the stimulation artefacts are suppressed by a mixed signal loop. An auto-zero based pre-charge path boosts the input impedance, while the electrode DC offset is canceled by a DC servo loop with very-large and accurate time constant. The analog front-end chip occupies an area of 2.32 mm^2 accompanied by a DSP with an area of 3.51 mm^2. The CCIA can suppress 1.5-Vpp CM interference, and has achieved an accurate high-pass corner frequency as low as 0.1 Hz and an input impedance greater than 2.2 GΩ. The overall classifier achieves 97.8% sensitivity and consumes only 1.16-μW average power.

Another work on closed loop DBS control involved the two novel control algorithms for stimulator triggering namely: detection of gait arrhythmicity and logistic-regression model for the detection of gait freezing. Such controls were validated on a benchtop model in conjunction with a closed-loop DBS system by responding to real-time human subject kinematic and pre-recorded data from leg-worn inertial sensors from a participant with Parkinson's disease. A novel control policy algorithm that changes neurostimulator frequency in response to the kinematic inputs has also been incorporated (O'Day et al., 2020). Another non-LFP based DBS control uses the hand tremors as input stimulus to trigger the implanted DBS module. Here, two sites of the basal ganglia (BG) namely the subthalamic nucleus (STN) and globus pallidus internus (GPi) are simultaneously controlled via stimulation using intelligent single input interval type-2 fuzzy logic (iSIT2-FL) combined with non-integer sliding mode control (SMC) (Gheisarnejad et al., 2020). On another work, neural sensing of movement (using chronically implanted cortical electrodes) was used to enable or disable stimulation for tremor. Therapeutic stimulation is delivered only when the patient is actively using their effected limb, thereby reducing the total stimulation applied, and potentially extending the lifetime of surgically implanted batteries (Herron et al., 2017).

Commercially Available IPG Devices for DBS

Meanwhile, there exist some commercially available IPG devices for DBS with closed loop control features that have been successfully deployed clinically. One of which is the Activa™ RC + S system (Medtronic, Inc.) which records electrophysiological signals from the implanted DBS electrodes and offers inertial measurements (Hell et al., 2019). A more recent DBS system called the Percept™ PC platform (Medtronic, Inc.)

TABLE 3 | Commercially available IPG devices.

Device	Frequency	Pulsewidth	Mode	Ampltiude (Joohi, 2021)	Feature	Application
Medtronic Activa™ PC (Paff et al., 2020)	2–250 Hz	60–450 μs	CC or CV	0–25.5 mA 0–10.5 V	conditionally safe with MRI	Bilateral STN and Gpi Stimulation for PD, Unilateral Thalamic Stimulation for Ets,Unilateral or Bilateral stimulation of the Gpi or STN for treatment of chronic, drug refractory segmental or generalized dystonia
Medtronic Activa™ RC (Paff et al., 2020)					dual channel, rechargeable, conditionally safe with MRI	
Medtronic Activa™ SC (Paff et al., 2020)	3–250 Hz				single channel, conditionally safe with MRI	
Medtronic Percept™ PC (Joohi, 2021)	2–250 Hz	20–450 μs	CC	0–25.5 mA	closed loop feature (using local field potential as biomarker)	
Abbott Infinity 5 (Paff et al., 2020)	2–240 Hz	20–500 μs	CC	0–12.75 mA	dual channel	Bilateral STN and GPi stimulation for PD and for bilateral thalamic stimulation for ETs
AbbottInfinity 7 (Paff et al., 2020)						
Boston Scientific Vercise PC (Paff et al., 2020)	2–255 Hz	20–450—μs	CC	0.1–20 mA	dual channel	Bilateral STN stimulation for PD
Boston Scientific Vercise RC (Paff et al., 2020)			CC		dual channel, rechargeable	
Boston Scientific Gevia (Paff et al., 2020)					dual channel, rechargeable, conditionally safe with MRI	
PINS Medical G102 (Paff et al., 2020)	2–250 Hz	30–450—μs	CC or CV	0–25 mA; 0–10 V	dual channel, remote wireless programming	PD, tremor, dystonia (Joohi, 2021)
PINS Medical G102R (Paff et al., 2020)					dual channel, rechargeable, remote wireless programming	
PINS Medical G101A (Paff et al., 2020)					single channel, remote wireless programming	
SceneRay 1180	1–1600 Hz	60–960 μs	—	—	dual channel remote wireless programming	—
Neuropace (Joohi, 2021)	1–333 Hz	40–1000 μs	CC	0–12.0 mA	closed loop feature (responsive neurostimulation), rechargeable (Shaikhouni, et al., 2015)	Drug-Resistant Epilepsy (DRE)

TABLE 4 | Efficacy of some commercial IPG devices based on independent clinical studies.

Device	Study design	Disease	Test subjects	Efficacy	Scoring
Medtronic Activa PC + S (Molina, et al., 2021)	Interventional (clinical trial), single group assignment	Medication-refractory Freezing of Gait (FoG) in PD	5	40% improvement at 60% of the subjects after 6 months	FOGQ, PDQ-39 (Peto et al., 1998), GFQ (Giladi et al., 2000), ABC (Powell and Myers, 1995, UPDRS) (Fahn and Elton, 1987)
Boston Scientific™ (Moro, et al., 2010)	Nonrandomized, prospect, blinded, multi-center	PD	51	45.4% (STN), 20% (GPi)	UPDRS III
Boston Scientific™ Vercise System (Follett, et al., 2010)	Multi-center, randomized, blinded	PD	bilateral STN: 147; bilateral Gpi: 152	25.3% improvement in UPDRS III; improvement in 6 of 8 subscales	UPDRS III
Abbot St. Jude Medical INFINITY™ (Okun, et al., 2012)	Multi-center, randomized, blinded	PD	136	39% on the baseline UPDRS III scores improvement	UPDRS III
Medtronic Kinetra and Soletra (Schuepbach, et al., 2013)	Interventional (clinical trial), randomized, parallel assignment	PD	251	QoL improvement by 7.8 points	PDQ-39, UPDRS-II, III and VI

FOGQ, Freezing of Gait Questionnaire; GFQ, Gait and Falls Questionnaire; ABC, Activities Specific Balance Confidence Scale; PDQ, Parkinson's disease Quality of Life Questionnaire, Unified Parkinson's disease Rating Scale (UPDRS).

incorporates "brainsense" technology utilizing LFP signals for refining therapeutic stimulation, symptoms tracking and correlation to neurophysiologic characteristics (Shahed, 2021). The Neuropace device has demonstrated responsive neurostimulation (RNS) and has been utilized for the treatment of drug-resistant epilepsy (DRE) (Shaikhouni, et al., 2015). A summary of the commercially available IPG devices for DBS is presented in **Table 3** (Paff et al., 2020; Joohi, 2021; Shaikhouni, et al., 2015). It is noticeable that there are advancements in the features of IPGs such as rechargeability of the battery; multiplicity of the channels; wireless programmability and closed loop feedback. Meanwhile the efficacy of some of these commercial devices based on independent clinical studies are summarized in **Table 4**.

DESIGN CONSIDERATIONS FOR SMART DBS IMPLEMENTATION

Since the LFP signal is about 50–500 μV (Einevoll et al., 2013), the analog front-end that extracts the LFP should have low input-referred noise within the bandwidth of interest. However, solid state devices tend to generate a lot of noise especially in the frequency range of the biopotential signal which normally covers 0.5 Hz to 1 kHz (Ha et al., 2021; Parastarfeizabadi and Kouzani, 2017) The dominant noise in this spectrum is the flicker (1/f) noise which may be attributed to the crystal defects within the silicon material and silicon–oxide interface. The input referred rms noise voltages should be within <10 μVrms (Parastarfeizabadi and Kouzani, 2017). Corollary to this specification is the target signal-noise ratio (SNR) at the output of the AFE. An SNR of >40 dB is necessary to imply an intelligible signal. On the interface between the AFE and the tissue, several non-idealities exist namely: parasitic electrode impedance, ambient noise such as electromagnetic interference and power supply hum. To reduce these, the AFE should have a high common-mode rejection ratio (CMRR). This is defined as the ratio of the gain in the intensity of the intelligent signal (biopotential signal) over the gain of the common-mode signals resulting from the interface non-idealities and noise. A differential gain of >80 dB and a CMRR of >100 dB are considered typically for an AFE (Arlotti et al., 2016). The AFE should be able to reject large transients at the input and should accommodate a wide input dynamic range to prevent saturating its inputs. This is very essential since the DBS leads are shared for delivering the stimulation pulses and for extracting the LFPs. The AFE should be able to block the stimulation pulses while it is able to amplify the LFPs.

The stimulator should be programmable in amplitude (voltage/current), frequency, and in duration and phase. Different combinations of these parameters have been extensively used in clinical practice for different cases similar to PD. Generally, the stimulator should only be activated at defined intervals either based on demand (as in a closed loop case) or pre-programmed. This is to save battery life. A potential alternative or support unit for the embedded battery is an *in vivo* or a subcutaneous energy harvester. Several mechanisms for this have been explored in literature constituting mechanical energy, radio frequency, ultrasound, and thermal (Shi et al., 2018; Zhao et al., 2020; Zou et al., 2021). One work demonstrated the potential of harvesting ambient mechanical energy from pressure fluctuations in the CSF within the lateral ventricles of the brain (Beker et al., 2017). In general, the harvester should be designed to have the maximum efficiency possible and should be positioned where there are maximum physical stimuli while having minimal coupling loss. Other key considerations for developing these harvesters would be material biocompatibility, packaging, form factor, efficiency, and site practicality. For maximum power transfer, the harvester's transducer should also be properly matched with the impedance of the front-end power scavenging electronics of the implantable device.

Finally, the overall power dissipation of a neural implant should be constrained so as not to cause any irreversible damage due to excessive current density and heating at the vicinity of the leads. To date, the power consumption of neural implants is within the range of 30 μW to 25 mW (Zhao et al., 2020), with most power attributed to the stimulator or to the wireless transceiver link.

Another aspect to consider in implementing a low maintenance DBS device is the need for supplemental energy sources that offer semi-perpetual charging with lower cost than present rechargeable devices. A typical rechargeable battery for DBS can support the device for a period of 9 years with an approximate long-term cost of care savings of $60,900 by considering lesser replacement surgeries, lesser number of clinical appointments and hospital visits, lesser need for preoperative planning, and lesser time off from work (Hitti et al., 2018). However, despite these advantages, a study conducted by (Khaleeq et al., 2019) showed that almost two thirds of patients with DBS, especially those who have a socially active and independent lifestyle, preferred the non-rechargeable IPG over the rechargeable ones. The choice is majorly because of convenience and concern about forgetting to recharge the battery. Furthermore, rechargeable DBS devices are more expensive than the non-rechargeable ones. According to the study of (Qiu et al., 2021), patients with less financial capabilities tend to choose the non-rechargeable DBS devices.

CONCLUSION

In this overview paper, we have presented the efficacies of DBS therapy for diseases that aggravate with age based on independent clinical trials. We have also presented the current state of the art in DBS instrumentation, specifically the additive features of IPGs that cater for ease of use, monitoring, programmability and closed-loop control. Meanwhile, while such advancements are already on the market, innovation towards making the DBS therapy more stand-alone, semi-autonomous, and having smaller form factors are still underway. These specifically point to the developments in system-on-chip (SoC) implementations for closed loop control or "smart" DBS. This work detailed the future prospects of SoC-based DBS technology that tend to provide more freedom of movement and lesser intervention while highlighting its technical constraints and design

challenges collated from technical literature. These can serve as guide for developing low maintenance DBS systems with an aim of improving the QoL of elderly patients.

AUTHOR CONTRIBUTIONS

AS, serves as the corresponding author. AS wrote the hardware part of this research as well as the design considerations for developing a DBS system and the energy scavenging mechanism. LAS, served as the consultant of this work. He also co-wrote the medical part specifically the pathophysiology of Parkinson's disease and DBS treatment.

FUNDING

Department of Science and Technology - Philippine Council for Health Research and Development and The University of Santo Tomas - Faculty of Engineering.

REFERENCES

Abdelhalim, K., Jafari, H. M., Kokarovtseva, L., Velazquez, J. L. P., and Genov, R. (2013). 64-Channel UWB Wireless Neural Vector Analyzer SOC with a Closed-Loop Phase Synchrony-Triggered Neurostimulator. *IEEE J. Solid-state Circuits* 48, 2494–2510. doi:10.1109/jssc.2013.2272952

Abosch, A., Lanctin, D., Onaran, I., Eberly, L., Spaniol, M., and Ince, N. F. (2012). Long-term Recordings of Local Field Potentials from Implanted Deep Brain Stimulation Electrodes. *Neurosurgery* 71, 804–814. doi:10.1227/neu.0b013e3182676b91

Albanese, A., Bhatia, K., Bressman, S. B., Delong, M. R., Fahn, S., Fung, V. S. C., et al. (2013). Phenomenology and Classification of Dystonia: a Consensus Update. *Mov Disord.* 28 (7), 863–873. doi:10.1002/mds.25475

Arlotti, M., Rossi, L., Rosa, M., Marceglia, S., and Priori, A. (2016). An External Portable Device for Adaptive Deep Brain Stimulation (aDBS) Clinical Research in Advanced Parkinson's Disease. *Med. Eng. Phys.* 38, 498–505. doi:10.1016/j.medengphy.2016.02.007

Baizabal-Carvallo, J. F., and Alonso-Juarez, M. (2016). Low-frequency Deep Brain Stimulation for Movement Disorders. *Parkinsonism Relat. Disord.* 31, 14–22. doi:10.1016/j.parkreldis.2016.07.018

Baizabal-Carvallo, J. F., Kagnoff, M. N., Jimenez-Shahed, J., Fekete, R., and Jankovic, J. (2014). The Safety and Efficacy of Thalamic Deep Brain Stimulation in Essential Tremor: 10 Years and beyond. *J. Neurol. Neurosurg. Psychiatry* 85, 567–572. doi:10.1136/jnnp-2013-304943

Beker, L., Benet, A., Meybodi, A. T., Eovino, B., Pisano, A. P., and Lin, L. (2017). Energy Harvesting from Cerebrospinal Fluid Pressure Fluctuations for Self-Powered Neural Implants. *Biomed. Microdevices* 19, 32. doi:10.1007/s10544-017-0176-1

Benabid, A. L., Pollak, P., Gao, D., Hoffmann, D., Limousin, P., Gay, E., et al. (1996). Chronic Electrical Stimulation of the Ventralis Intermedius Nucleus of the Thalamus as a Treatment of Movement Disorders. *J. Neurosurg.* 84 (2), 203–214. doi:10.3171/jns.1996.84.2.0203

Bergey, G. K., Morrell, M. J., Mizrahi, E. M., Goldman, A., King-Stephens, D., Nair, D., et al. (2015). Long-term Treatment with Responsive Brain Stimulation in Adults with Refractory Partial Seizures. *Neurology* 84 (8), 810–817. doi:10.1212/WNL.0000000000001280

Beurrier, C., Bioulac, B., Audin, J., and Hammond, C. (2001). High-frequency Stimulation Produces a Transient Blockade of Voltage-Gated Currents in Subthalamic Neurons. *J. Neurophysiol.* 85, 1351–1356. doi:10.1152/jn.2001.85.4.1351

Bhatia, K. P., Bain, P., Bajaj, N., Elble, R. J., Hallett, M., Louis, E. D., et al. (20182018). Consensus Statement on the Classification of Tremors. From the Task Force on Tremor of the International Parkinson and Movement Disorder Society. *Mov Disord.* 33 (1), 75–87. doi:10.1002/mds.27121

Bikias, T., Iakovakis, D., Hadjidimitriou, S., Charisis, V., and Hadjileontiadis, L. J. (2021). DeepFoG: An IMU-Based Detection of Freezing of Gait Episodes in Parkinson's Disease Patients via Deep Learning. *Front. Robot. AI* 8, 537384. doi:10.3389/frobt.2021.537384

Blomstedt, P., Sandvik, U., and Tisch, S. (2010). Deep Brain Stimulation in the Posterior Subthalamic Area in the Treatment of Essential Tremor. *Mov. Disord.* 25 (10), 1350–1356. doi:10.1002/mds.22758

Bratsos, S. P., Karponis, D., and Saleh, S. N. (2018). Efficacy and Safety of Deep Brain Stimulation in the Treatment of Parkinson's Disease: A Systematic Review and Meta-Analysis of Randomized Controlled Trials. *Cureus* 10 (10), e3474. doi:10.7759/cureus.3474

Chiken, S., and Nambu, A. (2013). High-frequency Pallidal Stimulation Disrupts Information Flow through the Pallidum by GABAergic Inhibition. *J. Neurosci.* 33 (6), 2268–2280. doi:10.1523/JNEUROSCI.4144-11.2013

Chiken, S., and Nambu, A. (2016). Mechanism of Deep Brain Stimulation. *Neuroscientist* 22 (3), 313–322. doi:10.1177/1073858415581986

DeMaagd, G., and Philip, A. (2015). Parkinson's Disease and its Management: Part 1: Disease Entity, Risk Factors, Pathophysiology, Clinical Presentation, and Diagnosis. *P T* 40 (8), 504–532.

Deuschl, G., Paschen, S., and Witt, K. (2013). Clinical Outcome of Deep Brain Stimulation for Parkinson's Disease. *Handb Clin. Neurol.* 116, 107–128. doi:10.1016/B978-0-444-53497-2.00010-3

Deuschl, G., Petersen, I., Lorenz, D., and Christensen, K. (2015). Tremor in the Elderly: Essential and Aging-Related Tremor. *Mov Disord.* 30 (10), 1327–1334. doi:10.1002/mds.26265

Dostrovsky, J. O., Levy, R., Wu, J. P., Hutchison, W. D., Tasker, R. R., and Lozano, A. M. (2000). Microstimulation-induced Inhibition of Neuronal Firing in Human Globus Pallidus. *J. Neurophysiol.* 84, 570–574. doi:10.1152/jn.2000.84.1.570

Einevoll, G. T., Kayser, C., Logothetis, N. K., and Panzeri, S. (2013). Modelling and Analysis of Local Field Potentials for Studying the Function of Cortical Circuits. *Nat. Rev. Neurosci.* 14, 770–785. doi:10.1038/nrn3599

Engel, J., Jr. (2016). What Can We Do for People with Drug-Resistant Epilepsy? *Neurology* 87, 2483–2489. doi:10.1212/wnl.0000000000003407

Fahn, S., Elton, R., and Members of the UPDRS Development Committee (1987). The Unified Parkinson's Disease Rating Scale. In: *Recent Developments in Parkinson's Disease*. Editors S. Fahn, C.D. Marsden, D.B. Calne, and M. Goldstein Vol. 2 (Florham Park: McMellam Health Care Information), 153–163.

Filali, M., Hutchison, W. D., Palter, V. N., Lozano, A. M., and Dostrovsky, J. O. (2004). Stimulation-induced Inhibition of Neuronal Firing in Human Subthalamic Nucleus. *Exp. Brain Res.* 156, 274–281. doi:10.1007/s00221-003-1784-y

Fisher, R., Salanova, V., Witt, T., Worth, R., Henry, T., Gross, R., et al. (2010). Electrical Stimulation of the Anterior Nucleus of Thalamus for Treatment of Refractory Epilepsy. *Epilepsia* 51 (5), 899–908. doi:10.1111/j.1528-1167.2010.02536.x

Flajolet, M., Wang, Z., Futter, M., Shen, W., Nuangchamnong, N., Bendor, J., et al. (2008). FGF Acts as a Co-transmitter through Adenosine A2A Receptor to Regulate Synaptic Plasticity. *Nat. Neurosci.* 11, 1402–1409. doi:10.1038/nn.2216

Fleming, J. E., Dunn, E., and Lowery, M. M. (2020). Simulation of Closed-Loop Deep Brain Stimulation Control Schemes for Suppression of Pathological Beta Oscillations in Parkinson's Disease. *Front. Neurosci.* 14, 166. doi:10.3389/fnins.2020.00166

Follett, K. A., Weaver, F. M., Stern, M., Hur, K., Harris, C. L., Luo, P., et al. (2010). Pallidal versus Subthalamic Deep-Brain Stimulation for Parkinson's Disease. *N. Engl. J. Med.* 362 (22), 2077–2091. doi:10.1056/NEJMoa0907083

Fox, S. H., Katzenschlager, R., Lim, S.-Y., Barton, B., de Bie, R. M. A., Seppi, K., et al. (2018). International Parkinson and Movement Disorder Society Evidence-Based Medicine Review: Update on Treatments for the Motor Symptoms of Parkinson's Disease. *Mov Disord.* 33 (8), 1248–1266. doi:10.1002/mds.27372

Frizon, L. A., Nagel, S. J., May, F. J., Shao, J., Maldonado-Naranjo, A. L., Fernandez, H. H., et al. (2019). Outcomes Following Deep Brain Stimulation lead Revision or Reimplantation for Parkinson's Disease. *J. Neurosurg.* 130, 1841–1846. doi:10.3171/2018.1.jns171660

GBD 2016 Parkinson's Disease Collaborators (2018). Global, Regional, and National Burden of Parkinson's Disease, 1990-2016: A Systematic Analysis for the Global Burden of Disease Study 2016. *The Lancet. Neurology*, 17 (11), 939–953. doi:10.1016/S1474-4422(18)30295-3

GBD 2016 Epilepsy Collaborators (2019). Global, Regional, and National Burden of Epilepsy, 1990–2016: A Systematic Analysis for the Global Burden of Disease Study 2016. *The Lancet. Neurology*, 18, 357–375. doi:10.1016/S1474-4422(18)30454-X

Gheisarnejad, M., Faraji, B., Esfahani, Z., and Khooban, M.-H. (2020). A Close Loop Multi-Area Brain Stimulation Control for Parkinson's Patients Rehabilitation. *IEEE Sensors J.* 20 (4), 2205–2213. doi:10.1109/JSEN.2019.2949862

Giladi, N., Shabtai, H., Simon, E. S., Biran, S., Tal, J., and Korczyn, A. D. (2000). Construction of Freezing of Gait Questionnaire for Patients with Parkinsonism. *Parkinsonism and Related disorders*, 6 (3), 165–170. doi:10.1016/s1353-8020(99)00062-0

Grahn, P. J., Mallory, G. W., Khurram, O. U., Berry, B. M., Hachmann, J. T., Bieber, A. J., et al. (2014). A Neurochemical Closed-Loop Controller for Deep Brain Stimulation: toward Individualized Smart Neuromodulation Therapies. *Front. Neurosci.* 8, 169. doi:10.3389/fnins.2014.00169

Groiss, S. J., Wojtecki, L., Südmeyer, M., and Schnitzler, A. (2009). Deep Brain Stimulation in Parkinson's Disease. *Ther. Adv. Neurol. Disord.* 2 (6), 20–28. doi:10.1177/1756285609339382

Ha, S., Kim, C., Wang, H., Chi, Y. M., Mercier, P .P., and Cauwenberghs, G. (2021). Chapter 6 - Low-power Integrated Circuits for Wearable Electrophysiology. In "*Wearable Sensors - Fundamentals, Implementation and Applications*" (2nd ed.) (Elsevier, Academic Press). 2021. 163–199.

Halpern, C., Hurtig, H., Jaggi, J., Grossman, M., Won, M., Baltuch, G., et al. (2007). Deep Brain Stimulation in Neurologic Disorders. *Parkinsonism Relat. Disord.* 13, 1–16. doi:10.1016/j.parkreldis.2006.03.001

Hariz, M. (2014). Deep Brain Stimulation: New Techniques. *Parkinsonism Relat. Disord.* 20 (Suppl. 1), S192–S196. doi:10.1016/s1353-8020(13)70045-2

Harmsen, I. E., Elias, G. J. B., Beyn, M. E., Boutet, A., Pancholi, A., Germann, J., et al. (2020). Clinical Trials for Deep Brain Stimulation: Current State of Affairs. *Brain Stimulation* 13, 378–385. doi:10.1016/j.brs.2019.11.008

Hell, F., Palleis, C., Mehrkens, J. H., Keoglsperger, T., and Bötzel, K. (2019). Deep Brain Stimulation Programming 2.0: Future Perspectives for Target Identification and Adaptive Closed Loop Stimulation. *Front. Neurol.* 10, 314. doi:10.3389/fneur.2019.00314

Hermann, B. P., Jones, J. E., Sheth, R., Koehn, M., Becker, T., Fine, J., et al. (2008). Growing up with Epilepsy: A Two-Year Investigation of Cognitive Development in Children with New Onset Epilepsy. *Epilepsia*, 49 (11), 1847–1858. doi:10.1111/j.1528-1167.2008.01735.x

Herrington, T. M., Cheng, J. J., and Eskandar, E. N. (2016). Mechanisms of Deep Brain Stimulation. *J. Neurophysiol.* 115, 19–38. doi:10.1152/jn.00281.2015

Herron, J. A., Thompson, M. C., Brown, T., Chizeck, H. J., Ojemann, J. G., and Ko, A. L. (2017). Cortical Brain-Computer Interface for Closed-Loop Deep Brain Stimulation. *IEEE Trans. Neural Syst. Rehabil. Eng.* 25 (11), 2180–2187. doi:10.1109/TNSRE.2017.2705661

Hitti, F. L., Ramayya, A. G., McShane, B. J., Yang, A. I., Vaughan, K. A., and Baltuch, G. H. (2019). Long-term Outcomes Following Deep Brain Stimulation for Parkinson's Disease. *J. Neurosurg.* 132, 205–210. doi:10.3171/2018.8.JNS182081

Hitti, F. L., Vaughan, K. A., Ramayya, A. G., McShane, B. J., and Baltuch, G. H. (2018). Reduced Long-Term Cost and Increased Patient Satisfaction with Rechargeable Implantable Pulse Generators for Deep Brain Stimulation. *J. Neurosurg.* 131, 799–806. doi:10.3171/2018.4.JNS172995

Hosain, M. K., Kouzani, A., and Tye, S. (2014). Closed Loop Deep Brain Stimulation: an Evolving Technology. *Australas. Phys. Eng. Sci. Med.* 37, 619–634. doi:10.1016/j.fmre.2021.05.00210.1007/s13246-014-0297-2

Hu, W., and Stead, M. (2014). Deep Brain Stimulation for Dystonia. *Transl Neurodegener* 3 (1), 2. doi:10.1186/2047-9158-3-2

Jankovic, J. (2013). Medical Treatment of Dystonia. *Mov Disord.* 28 (7), 1001–1012. doi:10.1002/mds.25552

Joohi, J. S. (2021) Device Profile of the Percept PC Deep Brain Stimulation System for the Treatment of Parkinson's Disease and Related Disorders. *Expert Rev. Med. Devices*. 18 (4), 319–332. doi:10.1080/17434440.2021.1909471

Kajikawa, Y., and Schroeder, C. E. (2011). How Local Is the Local Field Potential? *Neuron* 72, 847–858. doi:10.1016/j.neuron.2011.09.029

Khaleeq, T., Hasegawa, H., Samuel, M., and Ashkan, K. (2019). Fixed-life or Rechargeable Battery for Deep Brain Stimulation: Which Do Patients Prefer? *Neuromodulation: Technol. Neural Interf.* 22 (4), 489–492. doi:10.1111/ner.12810

Koeglsperger, T., Palleis, C., Hell, F., Mehrkens, J. H., and Bötzel, K. (2019). Deep Brain Stimulation Programming for Movement Disorders: Current Concepts and Evidence-Based Strategies. *Front. Neurol.* 10, 410. doi:10.3389/fneur.2019.00410

Koller, W. C., Pahwa, P. R., Lyons, K. E., and Wilkinson, S. B. (2000). Deep Brain Stimulation of the Vim Nucleus of the Thalamus for the Treatment of Tremor. *Neurology* 55 (12 Suppl. 6), S29–S33.

Krauss, J. K. (2007). Deep Brain Stimulation for Treatment of Cervical Dystonia. *Acta Neurochirurgica. Suppl.* 97 (Pt 2), 201–205. doi:10.1007/978-3-211-33081-4_22

Kuncel, A. M., and Grill, W. M. (2004). Selection of Stimulus Parameters for Deep Brain Stimulation. *Clin. Neurophysiol.* 115 (11), 2431–2441. doi:10.1016/j.clinph.2004.05.031

Kupsch, A., Benecke, R., Müller, J., Trottenberg, T., Schneider, G.-H., Poewe, W., et al. (2006). Pallidal Deep-Brain Stimulation in Primary Generalized or Segmental Dystonia. *N. Engl. J. Med.* 355, 1978–1990. doi:10.1056/NEJMoa063618

Lafreniere-Roula, M., Kim, E., Hutchison, W. D., Lozano, A. M., Hodaie, M., and Dostrovsky, J. O. (2010). High-frequency Microstimulation in Human Globus Pallidus and Substantia Nigra. *Exp. Brain Res.* 205 (2), 251–261. doi:10.1007/s00221-010-2362-8

Laxton, A. W., Tang-Wai, D. F., McAndrews, M. P., Zumsteg, D., Wennberg, R., Keren, R., et al. (2010). A Phase I Trial of Deep Brain Stimulation of Memory Circuits in Alzheimer's Disease. *Ann. Neurol.* 68 (4), 521–534. doi:10.1002/ana.22089

Lettieri, C., Rinaldo, S., Devigili, G., Pisa, F., Mucchiut, M., Belgrado, E., et al. (2015). Clinical Outcome of Deep Brain Stimulation for Dystonia: Constant-Current or Constant-Voltage Stimulation? A Non-Randomized Study. *Eur. J. Neurol.* 22 (6), 919–926. doi:10.1111/ene.12515

Li, Q., Qian, Z.-M., Arbuthnott, G. W., Ke, Y., and Yung, W.-H. (2014). Cortical Effects of Deep Brain Stimulation. *JAMA Neurol.* 71 (1), 100–103. doi:10.1001/jamaneurol.2013.4221

Little, S., and Brown, P. (2012). What Brain Signals Are Suitable for Feedback Control of Deep Brain Stimulation in Parkinson's Disease? *Ann. New York Acad. Sci.* 1265, 9–24. doi:10.1111/j.1749-6632.2012.06650.x

Little, S., Pogosyan, A., Neal, S., Zavala, B., Zrinzo, L., Hariz, M., et al. (2013). Adaptive Deep Brain Stimulation in Advanced Parkinson Disease. *Ann. Neurol.* 74, 449–457. doi:10.1002/ana.23951

Luo, Y., Sun, Y., Tian, X., Zheng, X., Wang, X., Li, W., et al. (2021). Deep Brain Stimulation for Alzheimer's Disease: Stimulation Parameters and Potential Mechanisms of Action. *Front. Aging Neurosci.* 13, 619543. doi:10.3389/fnagi.2021.619543

Lv, Q., Du, A., Wei, W., Li, Y., Liu, G., and Wang, X. P. (2018). Deep Brain Stimulation: A Potential Treatment for Dementia in Alzheimer's Disease (AD) and Parkinson's Disease Dementia (PDD). *Front. Neurosci.* 12, 360. doi:10.3389/fnins.2018.00360

Lyons, K. E., and Pahwa, R. (2008). Deep Brain Stimulation and Tremor. *Neurotherapeutics* 5 (2), 331–338. doi:10.1016/j.nurt.2008.01.004

Lyons, M. K. (2011). Deep Brain Stimulation: Current and Future Clinical Applications. *Mayo Clinic Proc.* 86 (7), 662–672. doi:10.4065/mcp.2011.0045

Mayo Clinic (2017). *Deep Brain Stimulation for Movement Disorders*. Available at https://www.mayoclinic.org/medical-professionals/neurology-neurosurgery/news/dbs-for-movement-disorders/mac-20429733.

Magariños-Ascone, C., Pazo, J. H., Macadar, O., and Buño, W. (2002). High-Frequency Stimulation of the Subthalamic Nucleus Silences Subthalamic Neurons: A Possible Cellular Mechanism in Parkinson's Disease. *Neuroscience* 115 (4), 1109–1117. doi:10.1016/s0306-4522(02)00538-9

Molina, R., Hass, C. J., Cernera, S., Sowalsky, K., Schmitt, A. C., Roper, J. A., et al. (2021). Closed-Loop Deep Brain Stimulation to Treat Medication-Refractory

Freezing of Gait in Parkinson's Disease. *Front. Hum. Neurosci.* 15. doi:10.3389/fnhum.2021.633655

Montgomery, E. B., and Gale, J. T. (2008). Mechanisms of Action of Deep Brain Stimulation (DBS). *Neurosci. Biobehavioral Rev.* 32, 388–407. doi:10.1016/j.neubiorev.2007.06.003

Moreau, C., Defebvre, L., Destee, A., Bleuse, S., Clement, F., Blatt, J. L., et al. (2008). STN-DBS Frequency Effects on Freezing of Gait in Advanced Parkinson Disease. *Neurology* 71, 80–84. doi:10.1212/01.wnl.0000303972.16279.46

Morishita, T., Fayad, S. M., Goodman, W. K., Foote, K. D., Chen, D., Peace, D. A., et al. (2014). Surgical Neuroanatomy and Programming in Deep Brain Stimulation for Obsessive Compulsive Disorder. *Neuromodulation: Technol. Neural Interf.* 17, 312–319. doi:10.1111/ner.12141

Moro, E., Esselink, R. J. A., Xie, J., Hommel, M., Benabid, A. L., and Pollak, P. (2002). The Impact on Parkinson's Disease of Electrical Parameter Settings in STN Stimulation. *Neurology* 59, 706–713. doi:10.1212/wnl.59.5.706

Moro, E., Lozano, A. M., Pollak, P., Agid, Y., Rehncrona, S., Volkmann, J., et al. (2010). Long-term Results of a Multicenter Study on Subthalamic and Pallidal Stimulation in Parkinson's Disease. *Mov. Disord.* 25 (5), 578–586. doi:10.1002/mds.22735

Müller, E. J., and Robinson, P. A. (2018). Suppression of Parkinsonian Beta Oscillations by Deep Brain Stimulation: Determination of Effective Protocols. *Front. Comput. Neurosci.* 12, 98. doi:10.3389/fncom.2018.00098

Noreik, M., Kuhn, J., Hardenacke, K., Lenartz, D., Bauer, A., Bührle, C. P., et al. (2015). Changes in Nutritional Status after Deep Brain Stimulation of the Nucleus Basalis of Meynert in Alzheimer's Disease - Results of a Phase I Study. *J. Nutr. Health Aging* 19, 812–818. doi:10.1007/s12603-015-0595-8

O'Day, J. J., Kehnemouyi, Y. M., Petrucci, M. N., Anderson, R. W., Herron, J. A., and Bronte-Stewart, H. M. (2020). "Demonstration of Kinematic-Based Closed-Loop Deep Brain Stimulation for Mitigating Freezing of Gait in People with Parkinson's Disease," in 2020 42nd Annual International Conference of the IEEE Engineering in Medicine & Biology Society (EMBC), Montreal, QC, July 20 - 24, 2020, 3612–3616. doi:10.1109/EMBC44109.2020.9176638

O'Suilleabhain, P. E., Frawley, W., Giller, C., and Dewey, R. B. (2003). Tremor Response to Polarity, Voltage, Pulsewidth and Frequency of Thalamic Stimulation. *Neurology* 60, 786–790. doi:10.1212/01.wnl.0000044156.56643.74

Deep-Brain Stimulation for Parkinson's Disease Study GroupObeso, J. A., Olanow, C. W., Rodriguez-Oroz, M. C., Krack, P., Kumar, R., and Lang, A. E. (2001). Deep-brain Stimulation of the Subthalamic Nucleus or the Pars Interna of the Globus Pallidus in Parkinson's Disease. *N. Engl. J. Med.* 345 (13), 956–963. doi:10.1056/NEJMoa000827

Obeso, J. A., Obeso, J. A., Olanow, C. W., Rodriguez-Oroz, M. C., Krack, P., Kumar, R., et al. (2001). Deep-brain Stimulation of the Subthalamic Nucleus or the Pars Interna of the Globus Pallidus in Parkinson's Disease. *N. Engl. J. Med.* 345, 956–963. doi:10.1056/NEJMoa000827

Okun, M. S., Gallo, B. V., Mandybur, G., Jagid, J., Foote, K. D., Revilla, F. J., et al. (2012). Subthalamic Deep Brain Stimulation with a Constant-Current Device in Parkinson's Disease: an Open-Label Randomised Controlled Trial. *Lancet Neurol.* 11 (2), 140–149. doi:10.1016/s1474-4422(11)70308-8

Ostrem, J. L., Racine, C. A., Glass, G. A., Grace, J. K., Volz, M. M., Heath, S. L., et al. (2011). Subthalamic Nucleus Deep Brain Stimulation in Primary Cervical Dystonia. *Neurology* 76, 870–878. doi:10.1212/wnl.0b013e31820f2e4f

Ostrem, J. L., and Starr, P. A. (2008). Treatment of Dystonia with Deep Brain Stimulation. *Neurotherapeutics* 5 (2), 320–330. doi:10.1016/j.nurt.2008.01.002

Paff, M., Loh, A., Sarica, C., Lozano, A. M., and Fasano, A. (2020). Update on Current Technologies for Deep Brain Stimulation in Parkinson's Disease. *Jmd* 13 (3), 185–198. doi:10.14802/jmd.20052

Parastarfeizabadi, M., and Kouzani, A. Z. (2017). Advances in Closed-Loop Deep Brain Stimulation Devices. *J. Neuroengineering Rehabil.* 14, 79. doi:10.1186/s12984-017-0295-1

Parastarfeizabadi, M., Kouzani, A. Z., Gibson, I., and Tye, S. J. (2016). "A Miniature Closed-Loop Deep Brain Stimulation Device," in 2016 38th Annual International Conference of the IEEE Engineering in Medicine and Biology Society (EMBC), 1786–1789. doi:10.1109/EMBC.2016.7591064

Paschen, S., Forstenpointner, J., Becktepe, J., Heinzel, S., Hellriegel, H., Witt, K., et al. (2019). Long-term Efficacy of Deep Brain Stimulation for Essential Tremor. *Neurology* 92 (12), e1378–e1386. doi:10.1212/WNL.0000000000007134

Pawlak, V., and Kerr, J. N. D. (2008). Dopamine Receptor Activation Is Required for Corticostriatal Spike-timing-dependent Plasticity. *J. Neurosci.* 28 (10), 2435–2446. doi:10.1523/jneurosci.4402-07.2008

Peto, V., Jenkinson, C., and Fitzpatrick, R. (1998). PDQ-39: A Review of the Development, Validation and Application of a Parkinson's Disease Quality of Life Questionnaire and its Associated Measures. *J. Neurol.* 245 Suppl 1, S10–S14. doi:10.1007/pl00007730

Priori, A., Foffani, G., Rossi, L., and Marceglia, S. (2013). Adaptive Deep Brain Stimulation (aDBS) Controlled by Local Field Potential Oscillations. *Exp. Neurol.* 245, 77–86. doi:10.1016/j.expneurol.2012.09.013

Powell, L. E., and Myers, A. M. (1995). The Activities-Specific Balance Confidence (ABC) Scale. *J. Gerontol. A Biol. Sci. Med. Sci.* 50A (1), M28–M34. doi:10.1093/gerona/50a.1.m28

Qiu, X., Peng, T., Lin, Z., Zhu, K., Wang, Y., Sun, B., et al. (2021). Fixed-Life or Rechargeable Battery for Deep Brain Stimulation: Preference and Satisfaction in Chinese Patients with Parkinson's Disease. *Front. Neurol.* 12, 668322. doi:10.3389/fneur.2021.668322

Rhew, H.-G., Jeong, J., Fredenburg, J. A., Dodani, S., Patil, P. G., and Flynn, M. P. (2014). A Fully Self-Contained Logarithmic Closed-Loop Deep Brain Stimulation SoC with Wireless Telemetry and Wireless Power Management. *IEEE J. Solid-state Circuits* 49 (10), 2213–2227. doi:10.1109/JSSC.2014.2346779

Rizzone, M., Lanotte, M., Bergamasco, B., Tavella, A., Torre, E., Faccani, G., et al. (2001). Deep Brain Stimulation of the Subthalamic Nucleus in Parkinson's Disease: Effects of Variation in Stimulation Parameters. *J. Neurol. Neurosurg. Psychiatry* 71, 215–219. doi:10.1136/jnnp.71.2.215

Rommelfanger, K. S., and Wichmann, T. (2010). Extrastriatal Dopaminergic Circuits of the Basal Ganglia. *Front. Neuroanat.* 4, 139. doi:10.3389/fnana.2010.00139

Rosin, B., Slovik, M., Mitelman, R., Rivlin-Etzion, M., Haber, S. N., Israel, Z., et al. (2011). Closed-loop Deep Brain Stimulation Is superior in Ameliorating Parkinsonism. *Neuron* 72, 370–384. doi:10.1016/j.neuron.2011.08.023

Salanova, V., Witt, T., Worth, R., Henry, T. R., Gross, R. E., Nazzaro, J. M., et al. (2015). Long-term Efficacy and Safety of Thalamic Stimulation for Drug-Resistant Partial Epilepsy. *Neurology* 84 (10), 1017–1025. doi:10.1212/WNL.0000000000001334

Sankar, T., Chakravarty, M. M., Bescos, A., Lara, M., Obuchi, T., Laxton, A. W., et al. (2015). Deep Brain Stimulation Influences Brain Structure in Alzheimer's Disease. *Brain Stimul* 8, 645–654. doi:10.1016/j.brs.2014.11.020

Santaniello, S., Fiengo, G., Glielmo, L., and Grill, W. M. (2011). Closed-Loop Control of Deep Brain Stimulation: A Simulation Study. *IEEE Trans. Neural Syst. Rehabil. Eng.* 19 (1), 15–24. doi:10.1109/TNSRE.2010.2081377

Sarikhani, P., Miocinovic, S., and Mahmoudi, B. (2019). "Towards Automated Patient-specific Optimization of Deep Brain Stimulation for Movement Disorders," in 2019 41st Annual International Conference of the IEEE Engineering in Medicine and Biology Society (EMBC), 6159–6162. doi:10.1109/EMBC.2019.8857736

Satzer, D., Lanctin, D., Eberly, L. E., and Abosch, A. (2014). Variation in Deep Brain Stimulation Electrode Impedance over Years Following Electrode Implantation. *Stereotact Funct. Neurosurg.* 92, 94–102. doi:10.1159/000358014

Schuepbach, W. M. M., Rau, J., Knudsen, K., Volkmann, J., Krack, P., Timmermann, L., et al. (2013). Neurostimulation for Parkinson's Disease with Early Motor Complications. *N. Engl. J. Med.* 368, 610–622. doi:10.1056/NEJMoa1205158

Schupbach, W. M., Chastan, N., Welter, M. L., Houeto, J. L., Mesnage, V., Bonnet, A. M., et al. (2005). Stimulation of the Subthalamic Nucleus in Parkinson's Disease: a 5-year Follow-Up. *J. Neurol. Neurosurg. Psychiatry* 76, 1640–1644. doi:10.1136/jnnp.2005.063206

Schwartz, A. B., Cui, X. T., Weber, D. J., and Moran, D. W. (2006). Brain-controlled Interfaces: Movement Restoration with Neural Prosthetics. *Neuron* 52, 205–220. doi:10.1016/j.neuron.2006.09.019

Shahed, J. (2021). Device Profile of the Percept PC Deep Brain Stimulation System for the Treatment of Parkinson's Disease and Related Disorders. *Expert Rev. Med. Devices* 18 (4), 319–332. doi:10.1080/17434440.2021.1909471

Shaikhouni, A., Deogaonkar, M., and Rezai, A. (2015). "Surgical Treatment for Epilepsy," in *Epilepsy and Brain Tumors* (Cambridge: Academic Press), 133–141. doi:10.1016/b978-0-12-417043-8.00009-2

Shi, B., Li, Z., and Fan, Y. (2018). Implantable Energy-Harvesting Devices. *Adv. Mater.* 30, e1801511. doi:10.1002/adma.201801511

Smith, G. S., Laxton, A. W., Tang-Wai, D. F., McAndrews, M. P., Diaconescu, A. O., Workman, C. I., et al. (2012). Increased Cerebral Metabolism After 1 Year of Deep Brain Stimulation in Alzheimer Disease. *Arch. Neurol.* 69 (9), 1141–1148. doi:10.1001/archneurol.2012.590

Stanslaski, S., Afshar, P., Peng, C., Giftakis, J., Stypulkowski, P., Carlson, D., et al. (2012). Design and Validation of a Fully Implantable, Chronic, Closed-Loop Neuromodulation Device with Concurrent Sensing and Stimulation. *IEEE Trans. Neural Syst. Rehabil. Eng.* 20, 410–421. doi:10.1109/tnsre.2012.2183617

Su, D., Chen, H., Hu, W., Liu, Y., Wang, Z., Wang, X., et al. (2018). Frequency-dependent Effects of Subthalamic Deep Brain Stimulation on Motor Symptoms in Parkinson's Disease: a Meta-Analysis of Controlled Trials. *Scientific Rep.* 8 (1), 14456. doi:10.1038/s41598-018-32161-3

Tani, N., Morigaki, R., Kaji, R., and Goto, S. (2014). "Current Use of Thalamic Vim Stimulation in Treating Parkinson's Disease," in *A Synopsis of Parkinson's Disease* (London, UK: IntechOpen). doi:10.5772/57105

Thomas, G. P., and Jobst, B. C. (2015). Critical Review of the Responsive Neurostimulator System for Epilepsy. *Med. Devices* 8, 405–411. doi:10.2147/MDER.S62853

Tran, T. N., Vo, T., Frei, K., and Truong, D. D. (2018). Levodopa-induced Dyskinesia: Clinical Features, Incidence, and Risk Factors. *J. Neural Transm.* 125 (8), 1109–1117. doi:10.1007/s00702-018-1900-6

Tritsch, N. X., Oh, W. J., Gu, C., and Sabatini, B. L. (2014). Midbrain Dopamine Neurons Sustain Inhibitory Transmission Using Plasma Membrane Uptake of GABA, not Synthesis. *eLife* 3, e01936. doi:10.7554/eLife.01936

Vidailhet, M., Vercueil, L., Houeto, J.-L., Krystkowiak, P., Benabid, A.-L., Cornu, P., et al. (2005). Bilateral Deep-Brain Stimulation of the Globus Pallidus in Primary Generalized Dystonia. *N. Engl. J. Med.* 352 (5), 459–467. doi:10.1056/NEJMoa042187

Vidailhet, M., Vercueil, L., Houeto, J. L., Krystkowiak, P., Lagrange, C., Yelnik, J., et al. (2007). Bilateral, Pallidal, Deep-Brain Stimulation in Primary Generalised Dystonia: a Prospective 3 Year Follow-Up Study. *Lancet Neurol.* 6, 223–229. doi:10.1016/s1474-4422(07)70035-2

Volkmann, J., Herzog, J., Kopper, F., and Deuschl, G. (2002). Introduction to the Programming of Deep Brain Stimulators. *Mov. Disord.* 17 Suppl 3, S181–S187. doi:10.1002/mds.10162

Volkmann, J., Moro, E., and Pahwa, R. (2006). Basic Algorithms for the Programming of Deep Brain Stimulation in Parkinson's Disease. *Mov Disord.* 21 (Suppl. 14), S284–S289. doi:10.1002/mds.20961

Wang, Y., Luo, H., Chen, Y., Jiao, Z., Sun, Q., Dong, L., et al. (2021). A Closed-Loop Neuromodulation Chipset with 2-level Classification Achieving 1.5-Vpp CM Interference Tolerance, 35-dB Stimulation Artifact Rejection in 0.5ms and 97.8%-Sensitivity Seizure Detection. *IEEE Trans. Biomed. Circuits Syst.* 15, 802–819. doi:10.1109/TBCAS.2021.3102261

Welter, M. L., Houeto, J. L., Bonnet, A. M., Bejjani, P. B., Mesnage, V., Dormont, D., et al. (2004). Effects of High-Frequency Stimulation on Subthalamic Neuronal Activity in Parkinsonian Patients. *Arch. Neurol.* 61, 89–96. doi:10.1001/archneur.61.1.89

Wichmann, T., and Delong, M. R. (2011). Deep-Brain Stimulation for Basal Ganglia Disorders. *Basal ganglia* 1 (2), 65–77. doi:10.1016/j.baga.2011.05.001

Wille, C., Steinhoff, B. J., Altenmüller, D. M., Staack, A. M., Bilic, S., Nikkhah, G., et al. (2011). Chronic High-Frequency Deep-Brain Stimulation in Progressive Myoclonic Epilepsy in Adulthood-Rreport of Five Cases. *Epilepsia.* 52 (3), 489–496. doi:10.1111/j.1528-1167.2010.02884.x

Wu, C., Cheng, C.-H., Yang, Y.-H. O., Chen, C.-G., Chen, W.-M., Ker, M.-D., et al. (2017). "Design Considerations and Clinical Applications of Closed-Loop Neural Disorder Control SoCs," in 2017 22nd Asia and South Pacific Design Automation Conference (ASP-DAC), 295–298. doi:10.1109/ASPDAC.2017.7858337

Wu, Y-C., Liao, Y-S., Yeh, W-H., Liang, S-F., and Shaw, F-Z. (2021). Directions of Deep Brain Stimulation for Epilepsy and Parkinson's Disease. *Front. Neurosci.* 15, 671. doi:10.3389/fnins.2021.680938

Zangiabadi, N., Ladino, L. D., Sina, F., Orozco-Hernández, J. P., Carter, A., and Téllez-Zenteno, J. F. (2019). Deep Brain Stimulation and Drug-Resistant Epilepsy: A Review of the Literature. *Front. Neurol.* 10, 601. doi:10.3389/fneur.2019.00601

Zhang, K., Bhatia, S., Oh, M. Y., Cohen, D., Angle, C., and Whiting, D. (2010). Long-term Results of Thalamic Deep Brain Stimulation for Essential Tremor. *J. Neurosurg.* 112 (6), 1271–1276. doi:10.3171/2009.10.JNS09371

Zhao, J., Ghannam, R., Htet, K. O., Liu, Y., Law, M.-K., Rou, V. A. L., et al. (2020). Self-Powered Implantable Medical Devices: Photovoltaic Energy Harvesting Review. *Adv. Health Care Mater.* 9, 2000779. doi:10.1002/adhm.202000779

Zou, Y., Bo, L., and Li, Z. (2021). Recent Progress in Human Body Energy Harvesting for Smart Bioelectronic System- Review. *Fundam. Res.* 1 (3), 364–382. doi:10.1016/j.fmre.2021.05.002,

Conflict of Interest: The authors declare that the research was conducted in the absence of any commercial or financial relationships that could be construed as a potential conflict of interest.

Publisher's Note: All claims expressed in this article are solely those of the authors and do not necessarily represent those of their affiliated organizations, or those of the publisher, the editors and the reviewers. Any product that may be evaluated in this article, or claim that may be made by its manufacturer, is not guaranteed or endorsed by the publisher.

Advantages of publishing in Frontiers

OPEN ACCESS
Articles are free to read for greatest visibility and readership

FAST PUBLICATION
Around 90 days from submission to decision

HIGH QUALITY PEER-REVIEW
Rigorous, collaborative, and constructive peer-review

TRANSPARENT PEER-REVIEW
Editors and reviewers acknowledged by name on published articles

Frontiers
Avenue du Tribunal-Fédéral 34
1005 Lausanne | Switzerland

Visit us: www.frontiersin.org
Contact us: frontiersin.org/about/contact

REPRODUCIBILITY OF RESEARCH
Support open data and methods to enhance research reproducibility

DIGITAL PUBLISHING
Articles designed for optimal readership across devices

FOLLOW US
@frontiersin

IMPACT METRICS
Advanced article metrics track visibility across digital media

EXTENSIVE PROMOTION
Marketing and promotion of impactful research

LOOP RESEARCH NETWORK
Our network increases your article's readership